

Editors: Snježana Mihalić Arbanas and Željko Arbanas

Landslide and Flood Hazard Assessment



CROATIAN
LANDSLIDE
GROUP

Landslide and Flood Hazard Assessment

Snježana Mihalić Arbanas • Željko Arbanas
Editors

Landslide and Flood Hazard Assessment

Proceedings of the
1st Regional Symposium on Landslides
in the Adriatic-Balkan Region
with the
3rd Workshop of the Croatian-Japanese Project
'Risk Identification and Land-Use Planning
for Disaster Mitigation of
Landslides and Floods in Croatia'

Croatian Landslide Group

Faculty of Mining, Geology and Petroleum Engineering
of the University of Zagreb

Faculty of Civil Engineering of the University of Rijeka

Editors

Snježana Mihalić Arbanas
Faculty of Mining, Geology and Petroleum Engineering
University of Zagreb
Zagreb, Croatia

Željko Arbanas
Faculty of Civil Engineering
University of Rijeka
Rijeka, Croatia

Editorial Board

Biljana Abolmasov
Faculty of Mining and Geology, University of Belgrade,
Serbia

Željko Arbanas
Faculty of Civil Engineering, University of Rijeka, Croatia

Primož Banovec
Faculty of Civil and Geodetic Engineering, University of
Ljubljana, Slovenia

Milorad Jovanovski
Faculty of Civil Engineering, Ss. Cyril and Methodius
University, Skopje, Macedonia

Barbara Karleuša
Faculty of Civil Engineering, University of Rijeka, Croatia

Marko Komac
Geological Survey of Slovenia, Ljubljana, Slovenia

Boris Kompare
Faculty of Civil and Geodetic Engineering, University of
Ljubljana, Slovenia

Janko Logar
Faculty of Civil and Geodetic Engineering, University of
Ljubljana, Slovenia

Matej Maček
Faculty of Civil and Geodetic Engineering, University of
Ljubljana, Slovenia

Hideaki Marui
Research Institute for Natural Hazards and Disaster
Recovery, Niigata University, Niigata, Japan

Snježana Mihalić Arbanas
Faculty of Mining, Geology and Petroleum Engineering,
University of Zagreb, Croatia

Matjaž Mikoš
Faculty of Civil and Geodetic Engineering, University of
Ljubljana, Slovenia

Ylber Muceku
Institute of Geosciences, Energy, Water and Environment,
Polytechnics University of Tirana, Albania

Nevenka Ožanić
Faculty of Civil Engineering, University of Rijeka, Croatia

Ana Petkovšek
Faculty of Civil and Geodetic Engineering, University of
Ljubljana, Slovenia

Boštjan Pulko
Faculty of Civil and Geodetic Engineering, University of
Ljubljana, Slovenia

Kyoji Sassa
International Consortium on Landslides and Kyoto
University, Kyoto, Japan

Alexander Strom
Geodynamics Research Centre – branch of JSC “Hydroproject
Institute”, Moscow, Russia

Fawu Wang
Research Center on Natural Disaster Reduction, Shimane
University, Matsue, Japan

Robert Župan
Faculty of Geodesy, University of Zagreb, Croatia

A CIP catalogue record for this book is available in the Online Catalogue of the National and University Library in Zagreb as 895370.

ISBN 978-953-6923-26-7, ISBN 978-953-6923-27-4 (eBook) - Faculty of Mining, Geology and Petroleum Engineering of the University of Zagreb
ISBN 978-953-6953-43-1, ISBN 978-953-6953-44-8 (eBook) - Faculty of Civil Engineering of the University of Rijeka

Published by: Faculty of Mining, Geology and Petroleum Engineering, University of Zagreb and Faculty of Civil Engineering, University of Rijeka

For publisher: Zoran Nakić and Aleksandra Deluka Tibljaš

Cover design: Studio 2M d.o.o.

Issued: December 2014, 250 copies

Foreword

Exposure of people, economic assets and social infrastructures to small and large-scale landslides caused disasters in the past and poses considerable risk to our society over the world. Even this year, a large-scale landslide triggered by heavy rainfalls claimed a toll of 2700 on May 2nd, 2014 in Badakhstan, Afganistan. On August 20th, 2014 in Hiroshima, Japan, a local and heavy rainfall (rainfall intensity for three hours was historically the largest in this area) triggered small and rapid landslides which killed 74 people in the urban area. Climate change intensifies the frequency and magnitude of heavy rainfall and triggers landslides in many countries. The Adriatic-Balkan region is in the landslide hot spot zone where both landslide triggering factors of rainfall and earthquakes are active, and slopes are steep due to tectonic movement.

The International Consortium on Landslides (ICL) was established in 2002. It is an international non-governmental and non-profit scientific organization promoting landslide research and capacity development for the benefit of society and the environment. ICL created the International Programme on Landslides (IPL) with regards to the 2006 Tokyo Action Plan which is jointly managed by the IPL Global Promotion Committee. The Members of IPL-GPC are all members of ICL and ICL-Supporting organizations (UNESCO, WMO, FAO, UNISDR, UNU, ICSU, WFEO and IUGS).

ICL applied for a SATREPS (Science and Technology Research Partnership for Sustainable Development) program funded by the Japan Science and Technology Agency (JST) and the Japan International Cooperation Agency (JICA) to implement a joint project between Croatia and Japan in 2008. The budget was approved and ICL has started a new IPL project "IPL-161 Risk identification and land-use planning for disaster mitigation of landslides and floods in Croatia" from 2009. This project is very successful in research, capacity development and social implementation. To develop this initiative in the Adriatic-Balkan region, the Adriatic-Balkan Network of ICL (coordinator: Snježana Mihalić Arbanas; co-coordinators: Željko Arbanas and Biljana Abolmasov) was established in 2012 following the ICL Strategic plan 2012-2021. The 1st Regional Symposium on Landslides in the Adriatic-Balkan Region was organized by the Croatian Landslide Group (from the Faculty of Mining, Geology and Petroleum Engineering of the University of Zagreb and Faculty of Civil Engineering of the University of Rijeka) on March 6th-9th, 2013 in Zagreb, Croatia. The book "Landslide and Flood Hazard Assessment" represents the proceedings of the 1st Regional Symposium on Landslides in the Adriatic-Balkan Region together with the 3rd Workshop of the Croatian-Japanese SATREPS Project "Risk Identification and Land-Use Planning for Disaster Mitigation of Landslides and Floods in Croatia".

I am deeply appreciative of all members of the organization committee of this successful regional symposium, the editors of this book, and JST and JICA for funding these initiatives. I would request all partners to support the further development of the Adriatic-Balkan Network of ICL and the successful organization of the 2nd Regional Symposium on Landslides in the Adriatic-Balkan Region to be held in Belgrade, Serbia on May 14th-16th, 2015.



A handwritten signature in black ink that reads "Kyoji Sassa". The signature is written in a cursive, flowing style.

Kyoji Sassa
Executive Director of
the International Consortium on Landslides
Kyoto, Japan

Preface

Throughout the Adriatic-Balkan Region, people continue to experience dangerous landslides and floods in response to unfavorable hydrometeorological events. These threats require the evaluation of potential hazards and the application of the appropriate countermeasures based on research. Landslide and flood research is an interdisciplinary field that primarily encompasses scientists from geomorphology, engineering geology, hydrology, hydrogeology, geotechnical and hydrotechnical engineering in collaboration with researchers from such fields as geodesy, geophysics, and many others.

This book contains most of the papers presented at the 1st Regional Symposium on Landslides in the Adriatic-Balkan Region entitled 'Landslide and Flood Hazard Assessment' with the 3rd Workshop of the Croatian-Japanese SATREPS FY2008 Project 'Risk Identification and Land-Use Planning for Disaster Mitigation of Landslides and Floods in Croatia'. The symposium was held in Zagreb, Croatia from March 6th to 9th, 2013. A wide range of landslide topics are presented in the Workshop and Symposium sessions that include landslide mapping, landslide investigation, landslide monitoring, landslide hazard and risk assessment, and landslide stabilization and remediation measures.

This collection of papers covers recent case histories, theoretical advances, laboratory and field-testing, and design methods beneficial to practitioners, researchers and other professionals. The proceedings reflect the ongoing response of researchers and practitioners from Bosnia and Herzegovina, Croatia, Japan, Macedonia, Romania, the Russian Federation, Serbia, Slovenia, Switzerland, the United Kingdom and Vietnam.

We are using this opportunity to express our gratitude to the Japan International Cooperation Agency (JICA), Japan Agency for Science and Technology (JST) and Ministry of Science, Education and Sports of the Republic of Croatia for financing the scientific joint-research bilateral Croatian-Japanese project 'Risk Identification and Land-Use Planning for Disaster Mitigation of Landslides and Floods in Croatia'. Regional scientific cooperation was initiated and developed through the Project Workshops held in Dubrovnik in 2010 and in Rijeka in 2011 and finally resulted in the organization of this Symposium. We would also like to extend our appreciation to the Symposium and Workshop Organizing Committee, the government of the City of Zagreb, as well as to Croatian-Japanese Project member institutions for supporting the organization of the Symposium.

We would like to thank all authors and participants for sharing their ideas and results in the area of landslide and flood research. We wish to acknowledge the help from all the reviewers in advising and refining the contributions.

Snježana Mihalić Arbanas

Željko Arbanas

S. Mihalić A.

Arbanas Z.



Contents

Workshop Sessions

Landslide Investigation and Monitoring

Manual of Transportable Ring Shear Apparatus ICL-1	1
Maja Oštrić, Kyoji Sassa, Kristijan Ljutić, Martina Vivoda, Bin He, Kaoru Takara	

Manual of LS-RAPID Numerical Simulation Model for Landslide

Teaching and Research	5
Bin He, Kyoji Sassa, Osamu Nagai, Kaoru Takara	

Application of Integrated Landslide Simulation Model LS-Rapid

to the Kostanjek Landslide, Zagreb, Croatia	11
Karolina Gradiški, Kyoji Sassa, Bin He, Željko Arbanas, Snježana Mihalić Arbanas, Martin Krkač, Predrag Kvasnička, Maja Oštrić	

Mineralogical Composition of the Kostanjek Landslide Sediments and its Possible Influence on the Sliding and Swelling Processes

.....	17
Jasmina Martinčević, Snježana Mihalić Arbanas, Sanja Bernat, Martin Krkač, Željko Miklin, Laszlo Podolszki	

Analysis of Water Fluctuation Dynamics in the Wider Area of the Kostanjek Landslide.....

.....	23
-------	----

Martin Krkač, Josip Rubinić, Jakov Kalajžić

The Kostanjek landslide - Monitoring System Development and Sensor Network.....

..... 27
Martin Krkač, Snježana Mihalić Arbanas, Osamu Nagai, Željko Arbanas, Kristijan Špehar

Geographic Information System of the Kostanjek Landslide: Integration of Real-time GNSS Monitoring Data with Other Sensor Data

.....	33
-------	----

Martina Baučić, Snježana Mihalić Arbanas, Martin Krkač

Remote Monitoring of a Landslide Using an Integration of GPS, TPS and Conventional Geotechnical Monitoring Methods

.....	39
-------	----

Željko Arbanas, Vedran Jagodnik, Kristijan Ljutić, Martina Vivoda, Sanja Dugonjić Jovančević, Josip Peranić

The Grohovo Landslide Monitoring System - Experiences from 18 Months Period of Monitoring System Operating

.....	45
-------	----

Kristijan Ljutić, Vedran Jagodnik, Martina Vivoda, Sanja Dugonjić Jovančević, Željko Arbanas

Rockfall Monitoring by Terrestrial Laser Scanning - Case Study of the Rock Cliff at Duće, Croatia.....

.....	51
-------	----

Goran Vlastelica, Predrag Mišćević, Hiroshi Fukuoka

Landslide Mapping and Susceptibility Assessment

Overview of Historical Landslide Inventories of the Podsljeme Area	57
---	----

Laszlo Podolszki, Snježana Mihalić Arbanas, Željko Arbanas, Željko Miklin, Jasmina Martinčević

Derivation of Historical Land Cover Map Based on Digital Orthophoto Images of the Zagreb Area

.....	63
-------	----

Nikola Belić, Snježana Mihalić Arbanas, Darko Šiško, Dubravko Gajski

Shallow Landslide Susceptibility Mapping Using SINMAP in Zagreb Hilly Area, Croatia

.....	67
-------	----

Chunxiang Wang, Snježana Mihalić Arbanas, Hideaki Marui, Naoki Watanabe, Gen Furuya

Deterministic Landslide Susceptibility Analyses Using LS-Rapid Software	73
Sanja Dugonjić Jovančević, Osamu Nagai, Kyoji Sassa, Željko Arbanas	
Slope Movements and Erosion Phenomena in the Dubračina River Basin: A Geomorphological Approach	79
Sanja Bernat, Petra Đomlija, Snježana Mihalić Arbanas	
Landslide Occurrence Prediction in the Rječina River Valley as a Base for an Early Warning System	85
Martina Vivoda, Sanja Dugonjić Jovančević, Željko Arbanas	
Analysis of Historical Landslide Information from the Area of the City of Zagreb and Primorsko-Goranska County	91
Snježana Mihalić Arbanas, Sanja Bernat, Slađan Fabijanović, Željko Arbanas	
 Flash Floods and Debris Flows	
Hydrologic Data Analysis for the Grohovo Landslide Area	97
Elvis Žic, Ivana Sušanj, Igor Ružić, Nevenka Ožanić, Yosuke Yamashiki	
Analysis of Flash Flood Occurred at Slani Potok Catchment, Croatia	107
Ivana Sušanj, Nevenka Ožanić, Yosuke Yamashiki	
Validation Study of Debris Flow Movement – Laboratory Experiments and Numerical Simulation	111
Elvis Žic, Yosuke Yamashiki, Shota Kurokawa, Shigeo Fujiki, Nevenka Ožanić, Nenad Bičanić	
Mošćenička Draga Early Warning Systems Development Using Machine Learning	117
Igor Ružić, Nevenka Ožanić, Čedomir Benac	
Involving the Public in Flash Flood and Erosion Mitigation	121
Nevena Dragičević, Barbara Karleuša, Nevenka Ožanić	
Citizens’ Awareness and Preparedness for Disasters in Zagreb, Croatia	127
Naoko Kimura, Yosuke Yamashiki, Ivica Kisić	
Seasonal Changes of CO₂ Emissions in Tillage Induced Agroecosystem	131
Darija Bilandžija, Željka Zgorelec, Ivica Kisić, Milan Mesić, Aleksandra Jurišić, Ivana Šestak	

Symposium Sessions

Landslide Investigation, Modeling, Remediation and Monitoring	
Triggering Mechanism of Shallow Landslides on the Northeast Rim of Mt. Aso Caldera, Japan, in July 2012.....	135
Hufeng Yang, Fawu Wang, Yasuhiro Mitani, Tomokazu Sonoyama	
Sliding Causes and Triggering Mechanisms at the Bogatići Landslide	141
Sabid Zekan, Nedim Suljić	
Instability Phenomena and Mitigation Measures in the Area of the Cluj Ethnographic Museum.....	147
Silvaş George-Cătălin	
Instabilities of Open Pit Cut Slopes: Case Study from the Torine Quarry in Croatia.....	153
Mirko Grošić, Sanja Bernat, Željko Arbanas, Snježana Mihalić Arbanas, Igor Matjašić, Damir Vidović	
Experimental Study on the Motion Mechanism of Submarine Landslides and the Impact Force on Communication Cables.....	159
Yohei Kuwada, Fawu Wang, Tomokazu Sonoyama, Mitsuki Honda	

Ramina Landslide from a Natural Hazard to Remediation	165
Josif Josifovski, Spasen Gjorgjevski, Bojan Susinov	
Rockfall Hazard Management on Traffic Facilities in Croatia	171
Dalibor Udovič, Željko Arbanas, Snježana Mihalić Arbanas, Mirko Grošić	
Landslide and Debris Flow Barriers at A83 Rest and be Thankful in Scotland	177
Vjekoslav Budimir, Corinna Wendeler	
Monitoring and Warning Tool for Landslide Risk Prevention	183
Cristian Marunteanu, Mihaela Roca	
The Analysis of Landslide Umka Dynamics Based on Automated GNSS Monitoring	187
Biljana Abolmasov, Marko Pejić, Vladimir Šušić	
Landslides in Vietnam and the JICA - JST Joint Research Project for Landslide Disaster Reduction	193
Khang Quang Dang, Kyoji Sassa, Do Minh Duc, Dinh Van Tien	
 Landslide Hazard Mapping: Inventories, Susceptibility, Hazard and Risk	
Landslide Database on the Road Network in Serbia	199
Svetozar Milenković, Milovan Jotić, Vladeta Vujančić, Branko Jelisavac	
Program of the Landslide Database Development of the Republic of Srpska	203
Cvjetko Sandić, Koviljka Leka	
Landslide Inventory Map of the Republic of Macedonia: Statistics and Description of Main Historical Landslide Events	207
Igor Peshevski, Milorad Jovanovski, Blagoja Markoski, Silvana Petrusheva, Bojan Susinov	
The Instability Phenomena along the Coasts of the Kvarner Area (NE Adriatic Sea)	213
Čedomir Benac, Petra Đomlija, Martina Vivoda, Renato Buljan, Dražen Navratil	
Landslides Hazard Maps for Mures County Central Area, Romania	219
Emilia Elena Milutinovici, Simona Corlateanu, Daniel Mihailescu, Raul Iacobescu	
Landslide Hazard Forecast in Slovenia – MASPREM	225
Marko Komac, Jasna Šinigoj, Mateja Jemec Auflič, Magda Čarman, Matija Krivic	
On Perspectives of Semi-Automated Landslide Assessment	231
Miloš Marjanović, Snežana Zečević, Irena Basarić	
Exposure of Inhabitants, Buildings and Different Types of Infrastructure to Potential Landslides in Case of Selected Municipalities in Slovenia	237
Tina Peternel, Mateja Jemec Auflič, Marko Komac, Jasna Šinigoj, Matija Krivic	
The Preliminary Damage Assessment of Properties Based on Massive Appraisal Maps	241
Branislav Bajat, Milan Kilibarda, Milutin Pejović, Mileva Samardžić Petrović	
Rockslides and Rock Avalanches in the Kokomeren River Valley (Kyrgyz Tien Shan)	245
Alexander Strom	
 Flash Floods and Debris Flows	
Torrential Check Dams as Debris-Flow Sources	251
Jošt Sodnik, Andrej Kryžanowski, Manica Martinčič, Matjaž Mikoš	
Hydraulics of Stratified Two-Layer Flow in Rječina Estuary	257
Nino Krvavica, Vanja Travaš, Nenad Ravlić, Nevenka Ožanić	
 Author Index	 263

Manual of Transportable Ring Shear Apparatus ICL-1

Maja Oštrić⁽¹⁾, Kyoji Sassa⁽²⁾, Kristijan Ljutić⁽³⁾, Martina Vivoda⁽³⁾, Bin He⁽⁴⁾, Kaoru Takara⁽⁴⁾

1) Kyoto University, Graduate School of Engineering, Kyoto, Japan, ostric.maja@gmail.com

2) International Consortium on Landslides, Kyoto, Japan

3) University of Rijeka, Faculty of Civil Engineering, Rijeka, Croatia

4) Kyoto University, Disaster Prevention Research Institute, Kyoto, Japan

Abstract A new Croatia-Japan Joint Project “Risk identification and land-use planning for disaster mitigation of landslides and floods in Croatia” was initiated in 2009. A new transportable undrained ring shear apparatus, ICL-1, was designed for laboratory soil test and landslide simulation test as a part of Project activities. The aim of ICL-1 was to develop much inexpensive and transportable undrained ring shear apparatus to be used in different counterpart organizations with a standard electricity available anywhere. To make this apparatus effectively and practically used in Croatia and also in other countries, a detailed manual has been made based on the experiences of students and researchers invited from Croatia to Japan. This paper introduces the manual including the concept, design and construction of this apparatus as well as test procedures and data analysis.

Keywords ring shear apparatus, landslides, laboratory test

Introduction

None of the laboratory shear tests used for measurement of peak strength (triaxial, direct shear tests) is suitable for determination of the residual shear strength because they can produce only limited displacement along a failure surface. As a result, a ring shear apparatus was developed to evaluate both the peak and residual shear strengths. Its main advantage is that it can continuously shear the soil in one direction until almost unlimited shearing displacement (Bishop et al. 1971).

First ring shear devices were initially developed in the early 1930's by a number of independent researchers including Grunner and Haefeli, Hafaali, Tiedemann and Hvorslev (Hvorslev 1939). Most of the early devices are described and reviewed in the papers of Hvorslev and Bishop (Hvorslev 1939, Bishop et al. 1971). Hvorslev's device was the first to force shearing of the specimen on a predefined plane located at the separation of the upper and lower confining rings. Today, there are several ring shear apparatuses available but the two most widely used are the apparatus based upon the Imperial College and

Norwegian Geotechnical Institute concept (Bishop et al. 1971) and the Bromhead ring shear apparatus (Bromhead 1979).

However, almost all previously mentioned apparatuses were unable to perform undrained shearing tests and they all used a conventional shear-speed control motor, without possibility to provide shear-stress loading. Sassa and his colleagues have developed seven designs of ring shear apparatus since 1984. (Sassa et al. 2004). DPRI series of ring shear apparatuses (DPRI-3, 4, 5, 6 and 7) have capability of shear stress-controlled tests which enables simulation of both monotonic and dynamic loadings (real seismic waves or sine wave form) under undrained conditions.

Some of the apparatuses in the series have also pore-pressure-control test to simulate the ground water rise in the slope and/ or displacement control. Due to all those capabilities, the ring shear apparatus is not used only as the basic soil test, to measure shear resistance as a parameter, but also as a landslide simulation test that can reproduce the stress and pore pressure acting on a potential sliding surface. Compared to previous apparatus (DPRI-1 to 7), the new apparatus ICL-1 (Fig. 1) has smaller dimensions and higher performances (Table 1). It can keep undrained condition up to 1 MPa of pore water pressure and load normal stress up to 1 MPa. This makes it suitable for investigation of large - scale and deep-seated landslides.

ICL-1 (Fig. 1) was donated to Croatia in July 2012. In order to make the apparatus effectively and practically used in Croatia, Croatian students and researchers have been invited to Japan to learn to work with it. For that purpose, a detailed manual has been prepared (Fig. 2).

Based on their experiences, the manual was improved and supplementary material prepared. The content of the Manual is described in the following text. The chapters that describe the cleaning and maintaining of the apparatus are not presented here.

Concept of the ring shear apparatus

The undrained ring-shear apparatus simulates the formation of the landslide shear surface and the following post-failure motion and observes the consequence of

Table 1 Features of new Ring Shear Apparatus, ICL-1, compared with the previous versions of DPRI- 6 and 7 (modified from Sassa et al. 2004).

AUTHOR	Sassa (1997) DPRI-6	Sassa (2004) DPRI-7	Sassa (2011) ICL-1
Inner diameter (cm)	25.0	27.0	10.0
Outer diameter (cm)	35.0	35.0	14.0
Max. height of sample (cm)	15.0	11.5	5.2
Ratio max. height/width	3.0	2.88	2.6
Shear area (cm ²)	471.24	389.56	75.36
Max. normal stress (kPa)	3,000	500	1,000
Max. shear speed (cm/sec)	224.0	300.0	5.4
Cyclic torque control testing (max. frequency)	5 Hz	5 Hz	1.0 Hz
Undrained testing and pore pressure monitoring	Yes	Yes	Yes
Max. data acquisition rate (readings/sec)	200	1,000	1,000
Max pore water pressure	400-600	400-600	1,000



Figure 1 Transportable Ring Shear Apparatus, ICL-1 with its Instrument box, Monitoring box and Control box.

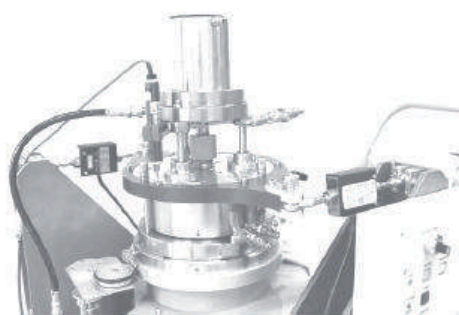
mobilized shear resistance, as well as the post-failure shear displacement and generated pore-water pressure.

Samples are taken from the layer in which a previous landslide occurred, or the layer in which a sliding surface can be formed in the future. The sample is set in the ring shear box which is divided in a static upper half and a rotary lower half. All stresses acting on the potential sliding surface; normal and shear stresses due to gravity, seismic stress due to seismic shaking as well as generated pore pressures, can be reproduced in the shear box. When stresses are high enough to trigger sample failure, a shear surface will develop within the shear box, and the rotary lower half of the shear box will start turning.

During the process of shear failure development and

TRANSPORTABLE RING SHEAR APPARATUS - ICL 1

Manual



Text: Oštrić Maja
Vivoda Martina
Ljutić Kristijan

Kyoto, 2012.

Figure 2 Cover Page of the Manual of Transportable Ring Shear Apparatus, ICL-1.

subsequent post-failure motion, resulting excess pore pressure build up, mobilized shear resistance, and shear displacement during and after seismic or cyclic loading are monitored by load cells and displacement sensor (Fig. 3).

Structure and control system

The structure of undrained dynamic loading ring shear apparatus is shown in Figure 3.

Vertical load is given by pulling the central axis instead of large and tall loading frame used in the previous apparatus. This enabled decreasing the size of the apparatus and increasing the upper limit of undrained capability. Normal stress is given by another servo-control motor through oil piston and is monitored by the load cell N (Fig. 3).

The shear stress is given by a servo-control motor either by shear stress-control, speed-control or displacement-control. The shear stress acting on the shear surface is monitored by a pair of shear load cells (S₁ and S₂ on Fig. 3).

The gap of the upper shear box and the lower shear box is automatically controlled by the third servo-motor through an oil piston. Gap control system, enable prevention of leakage of water and sample during shearing.

Pore pressure generated in the shear zone is monitored by a pore pressure transducer P (Fig. 3) connected to a gutter extending around the whole circumference of the inner wall of the outer and upper ring. The gutter is covered by two metal filters and a felt cloth filter.

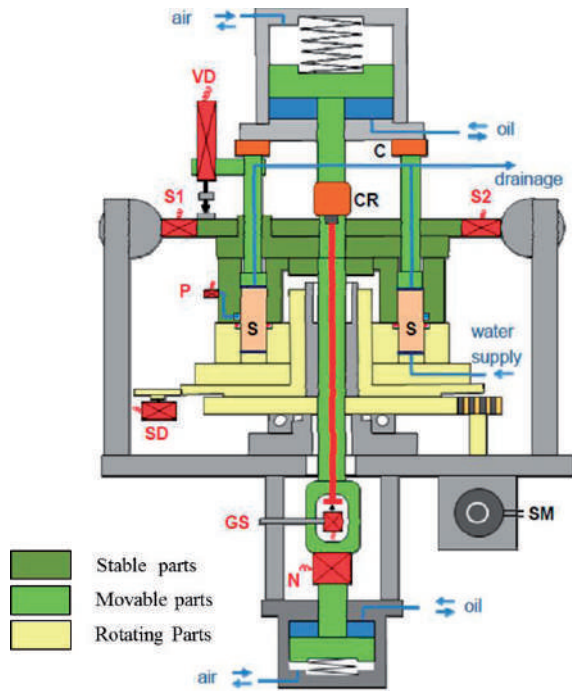


Figure 3 Mechanical structure of the apparatus (S- Specimen, CR- Connection Ring, C- Connection, N- Load cell for Normal Stress; S1, S2- Load cell for shear resistance; P- Pore pressure transducer; GS- Gap sensor; VD- Vertical Displacement; SD- Shear Displacement).

Testing procedure

Samples used for tests can be dry or fully saturated and different procedures are used. Both procedures are described in the Manual. Both procedures could be summarized in several main steps.

Gap adjustment and shear box assembling

First, the gap value should be adjusted to avoid leakage of water and sample, by applying vertical load of 0.8-1 kN. When the gap of the upper and the lower shear box is adjusted, it should be kept constant during the test.

Saturation

In the case of dry sample preparation, first, the sample is poured into the shear box and then saturated with CO₂ and de-aired water.

In the case of wet sample placement, shear box without sample is filled with CO₂ and de-aired water. After that, prepared sample (saturated by de-aired water during night) is slowly placed in shear box.

After that water circulation can start to enable full water saturation of the specimen. The water circulation process is kept at a very slow rate.

B_D checking

The saturation of sample is then checked by measuring B_D value that for fully saturated samples should be greater than 0.95. B_D is a pore pressure parameter in direct shear state, related to the degree of saturation that was proposed by Sassa (1988) as:

$$B_D = \Delta u / \Delta \sigma \quad [1]$$

where Δu and $\Delta \sigma$ are increments of pore pressure and normal stress, respectively.

Consolidation

After sample is fully saturated, the initial stress state should be created. The sample is normally consolidated under pre-decided normal and shear stress, in drained condition.

Shearing

After consolidation, shearing can start. Soil sample can be sheared in drained, undrained or partially drained conditions. Drainage is allowed by keeping the upper valve open while undrained condition is maintained by keeping the valves closed.

The shear stress is given by a servo-control motor either by shear stress-control, speed-control or displacement-control. The use of Speed Control Test or Stress Control Test depends on the purpose of the test. Speed Control Test is usually used to obtain soil parameters and Stress Control test is used for simulating landslide. Pore Pressure Control Test can also be done in ICL-1 apparatus.

Data analysis

Ring shear tests data are controlled and recorded in Control box, using software application Portable ring shear apparatus - Data acquisition and control developed by Marui Co. There are both sensor and test values in output file, but only test values in the data analysis are used. Preparation of data is made using Excel and visualization is made using KaleidaGraph.

Figures 4 and 5 are showing the results of undrained speed control tests conducted on the ground samples from Croatian landslides, Grohovo and Kostanjek. Total stress path (TSP) is shown in blue line and effective stress path (ESP) in red line. From undrained speed control test results, basic parameters (peak, mobilized and apparent friction angle, cohesion) as well as steady state normal and shear stress of soil samples were obtained.

Figure 4 shows the stress path of the undrained speed control test conducted on Kostanjek landslide for initial normal stress of 1000 kPa and constant shear speed of 0.002 cm/sec. Failure occurred when failure line was

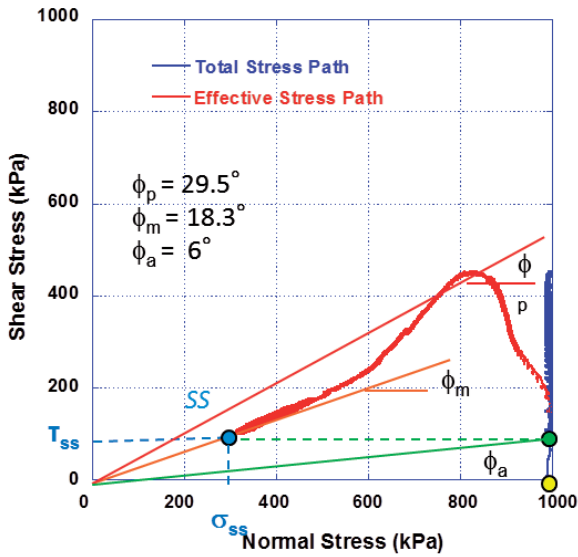


Figure 4 Stress Path of Undrained Speed Control Test on saturated shale sample from Kostanjek landslide ($B_D=0.95$; initial dry density: 1.53 g/cm^3 , specific gravity, $G_s=2.78$).

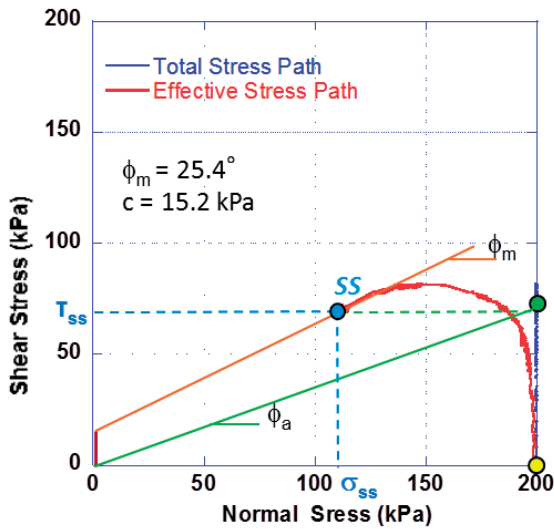


Figure 5 Stress Path of Undrained Speed Control Test on saturated clayey sample from Grohovo landslide ($B_D=0.95$; initial dry density: 1.59 g/cm^3 , specific gravity, $G_s=2.66$).

reached, at peak friction angle, $\phi_p=29.5^\circ$. Mobilized friction angle is $\phi_m=18.3^\circ$ and apparent friction angle $\phi_a=6^\circ$. We assumed cohesion is zero.

Figure 5 shows the stress path of the undrained speed control test conducted on Grohovo landslide for initial normal stress of 200 kPa and constant shear speed of 0.002 cm/sec. Stress path that seems to have reached the failure line and moved down along the failure line. In this test, the peak failure line was not observed. The straight line fitting the stress path gave values of the friction angle as 25.4° , cohesion as 15.2 kPa and apparent friction angle, $\phi_a=20.4^\circ$.

Summary and conclusion

The paper has presented the Manual of the Transportable Ring Shear Apparatus that was prepared for the use and training of Croatian students. The concept of the ring shear, as well as its structure and testing procedure are described in detail.

Beside its use for determination of soil parameters, ring shear apparatus can be used as a landslide simulation test.

In order to simulate natural landslide conditions different types of tests can be conducted: undrained cyclic or seismic stress-control tests in order to simulate dynamic loading and earthquake induced landslides or naturally drained pore pressure control tests for simulation of groundwater level rise during rainfall.

Undrained speed controlled tests are usually conducted as basic soil tests for obtaining basic parameters. In this paper we showed the result of the undrained speed-controlled tests conducted on ground samples from Croatian landslides. These tests were conducted as a part of Croatian students training that resulted in improvement of the Manual.

Acknowledgments

The help of Prof. Arbanas and Prof. Mihalić Arbanas are highly appreciated. Also, the help of Master student Hendy Setiawan and all the engineers of Marui & Co., Ltd. Osaka, Japan who enabled numerous improvements and modifications of the apparatus. Laboratory work was part of a total of 4 months Trainees Programme of Croatian students, financed by JICA and JST budget. The design and construction of the ring shear apparatus ICL-1, was conducted under the support of SATREPS Programme (Science and Technology Research Partnership for Sustainable Development) and International Programme on Landslides (IPL-161 “Risk identification and land-use planning for disaster mitigation of landslides and floods in Croatia”).

References

- Bishop A W, Green G E, Garge V K, Andersen A, Brown J D (1971) A New Ring Shear Apparatus and its Application to the Measurement of Residual Strength, *Géotechnique*, 21(1): 273–328.
- Bromhead E N (1979) A Simple Ring Shear Apparatus, *Ground Engineering*, 12 (5): 40–44.
- Hvorslev M J (1939) Torsion Shear Tests and Their Place in the Determination of Shearing Resistance of Soils, *Proceedings of the American Society of Testing and Materials*, 39: 999–1022.
- Sassa K, Fukuoka H, Wang G H, Ishikawa N (2004) Undrained Dynamic Loading Ring Shear Apparatus and its Application to Landslide Dynamics, *Landslides*, 1(1): 7–19.

Manual of LS-RAPID Numerical Simulation Model for Landslide Teaching and Research

Bin He⁽¹⁾, Kyoji Sassa⁽²⁾, Osamu Nagai⁽²⁾, Kaoru Takara⁽¹⁾

1) Kyoto University, Disaster Prevention Research Institute, Kyoto, Japan

2) International Consortium of Landslides, Kyoto, Japan

Abstract LS-RAPID is user-friendly landslide simulation software based on the program, “Integrated Landslide Simulation Model”, produced by Kyoji Sassa (International Consortium on Landslides). It can assess the initiation and motion of landslides triggered by earthquakes, rainfall or the combined effects of rainfall and earthquakes. It is the first simulation model to reproduce the initiation process and the runout process from stable state until deposition within the same model. The model is based on the key parameters; the shear resistance at the steady state, the peak friction angle, cohesion, the shear displacements at peak and the onset of steady state, the lateral pressure ratio with physical meaning, which can be measured or estimated from experiments. It uses a visual interface which enables the user to input topography parameters, sliding surface parameters, and parameters of soil characteristics to simulate results in 3D. It is designed to be easily operated by both experienced and first time users. The latest one, Version 2.03 Beta10, has been developed in 2013. Currently, it has been used in different cases of landslides, including large scale submarine landslides, urban long travel landslides, and subaerial megalandslides triggered by earthquake and heavy rainfall. In this paper, the English manual of LS-RAPID numerical simulation model is introduced. Firstly, the detailed steps about how to use LS-RAPID are described based on an example of the simple slope landslide. The procedures of generating LS-RAPID format topographical DEM data, creating sliding surface topography using ellipsoidal method, defining the soil parameters, setting the landslide simulation conditions and viewing the 2D or 3D results of landslide results have been introduced. Then, four cases studies including Leyte Landslide (Philippines), Suruga Bay Landslide (Japan), Grohovo Landslide (Croatia), and Kostanjek Landslide (Croatia) are described. Core parts of the manual are introduced in this paper.

Keywords LS-RAPID, landslide, manual, simulation

Introduction

The LS-RAPID system is an application designed for Microsoft Windows based on the program, “Landslide

Motion Simulation”, produced by Dr. Kyoji Sassa (International Consortium on Landslides). The software uses a visual interface which enables the user to input topography parameters, sliding surface parameters, and parameters of soil characteristics to simulate results in 3D. It is designed to be easily operated by both experienced and first time users.

The latest one, Version 2.03 Beta10, has been developed in 2013. Currently, it has been used in different cases of landslides, including large scale submarine landslides, urban long travel landslides, and subaerial megalandslides triggered by earthquake and heavy rainfall. In this paper, the English manual of LS-RAPID numerical simulation model is introduced. Firstly, the detailed steps about how to use LS-RAPID are described based on an example of the simple slope landslide. The procedures of generating LS-RAPID format topographical DEM data, creating sliding surface topography using ellipsoidal method, defining the soil parameters, setting the landslide simulation conditions and viewing the 2D or 3D results of landslide results have been introduced. The four cases studies including Leyte Landslide (Philippines), Suruga Bay Landslide (Japan), Grohovo Landslide (Croatia), and Kostanjek Landslide (Croatia) are described. Core parts of the manual are introduced in this paper.

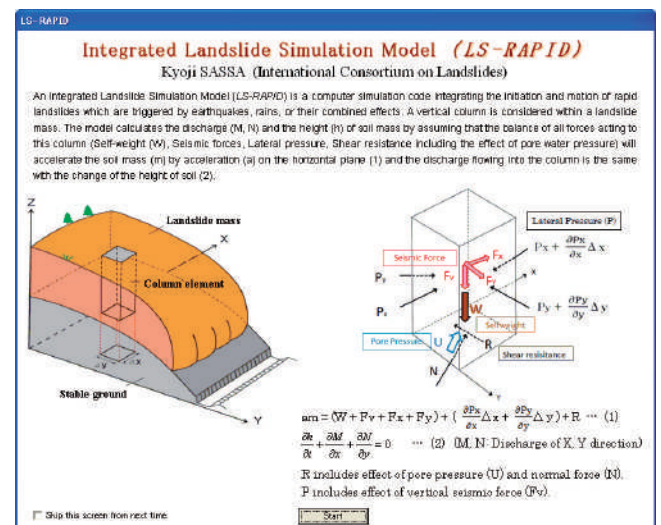


Figure 1 Interface of the Landslide simulation model: LS-RAPID.

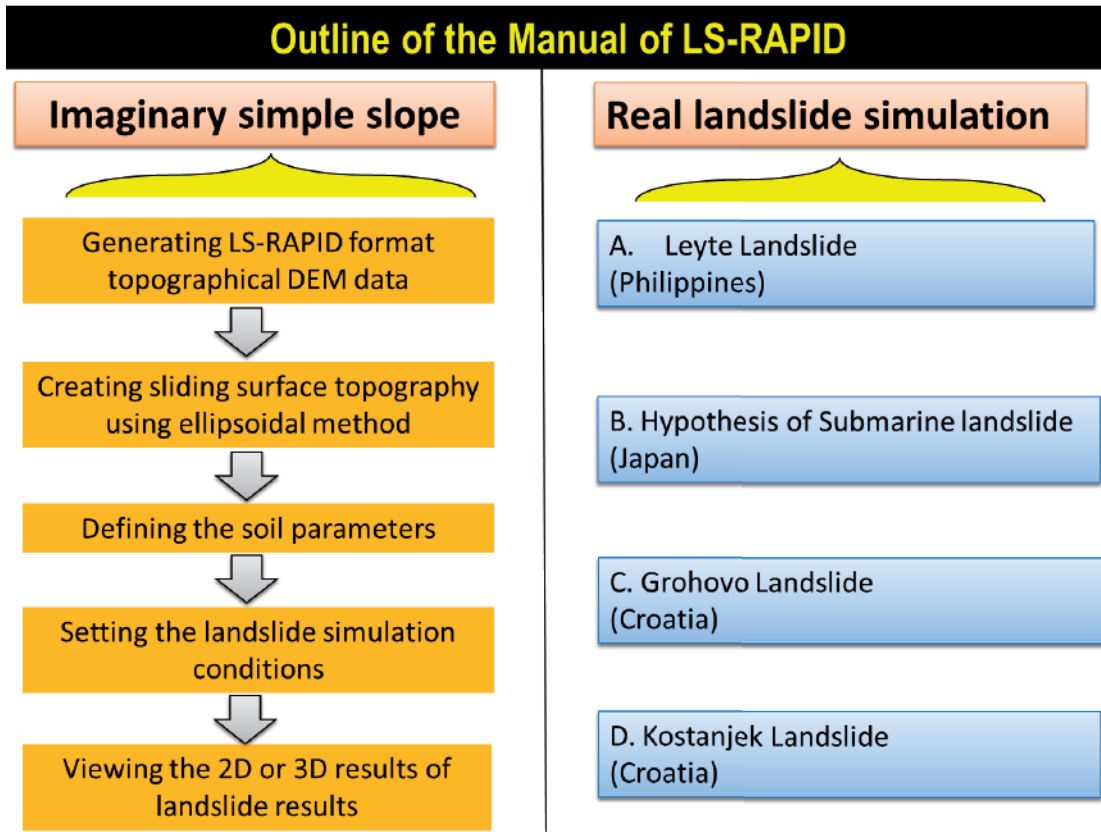


Figure 2 Outline of the LS-RAPID manual.

Framework of the manual

The outline of the manual of LS-RAPID is shown in Figure 2. Firstly, the detailed procedures on how to generate LS-RAPID format topographical DEM data, creating sliding surface topography, defining soil parameters, setting the landslide simulation conditions, and viewing the 2D or 3D results of landslide results are given for an imaginary simple slope landslide simulation.

Then, the real landslide simulations are provided for four case studies, i.e. Leyte landslide (Philippines), Hypothesis of submarine landslide (Japan), Grohovo landslide (Croatia), Kostanjek (Croatia). The detailed description for these four real landslide simulation are included in this manual.

Figure 3 shows the simulation flow chart for landslide simulation using LS-RAPID. This flow chart is same for the imaginary simple slope landslide simulation and the four real landslide simulation case studies.

Main procedures in the manual

Topography edition

Generally DEMs are provided with a text file (X,Y,Z) including Latitude, Longitude and Elevation. To input the DEM data for LS-Rapid simulation, text file (X,Y,Z) should be converted to the elevation mesh data in

advance. The accompanying software (DEMmake) is available to convert a text file to elevation mesh data. When the program is started and a new document is created, there will be no topography data or settings for simulation. In the manual, the section of “Topography edition” explains the initial settings required to view topography. It is impossible to load and edit the text file if parameters other than those listed in the manual are modified. If the Control Point needs to be edited manually, the tab needed to be edited can be selected and the “Control Point” radio button will be chosen. If the Mesh data needs to be edited manually, the Mesh Data radio button can be selected to start editing the mesh values. If there is already a text file for the Mesh data, from the [File] menu the [Load Text Data File] [Load (Slope Surface · Sliding Surface · Sliding Mass Thickness) Mesh data] can be selected and the appropriate file can be chosen.

If the Mesh data of the Slope Surface is already created, the Sliding Surface can be built using the ellipsoidal parameter. An ellipsoidal sliding surface can be created by setting the longitudinal section of the landslide on the left side of this dialog box. Once the starting and ending points are entered, the corresponding longitudinal section will appear on the right side of the dialog box. After setting the longitudinal section, the passing points of the sliding surface can be set. By setting

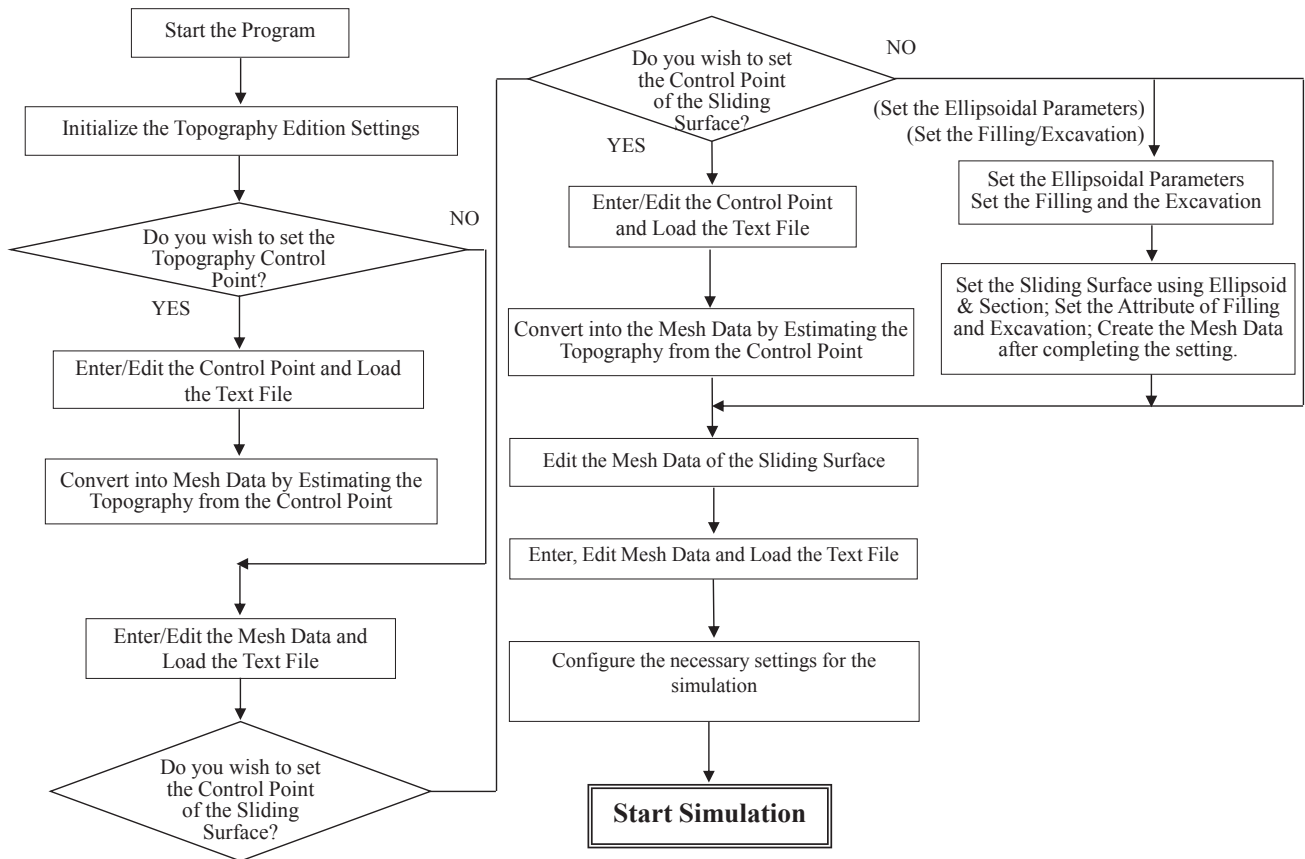


Figure 3 Simulation Flow Chart for landslide simulation using LS-RAPID.

the passing points, the crossing section which passes through the center of the passing points will appear. The left part of the screen will display the position information. When the center point of the ellipsoid are entered, the ellipsoid will be displayed on the longitudinal section. Similar to the longitudinal section, the passing point and the center point of the ellipsoid on the crossing section can also be set. The crossing point can be set between the sliding surface, the slope, and the X-coordinate of the center point of the ellipsoid. The cross point of the two sections and the elevation of the center of ellipsoid are already determined on the crossing section. If there is a subsection, the ellipsoidal subsection can be created. Once the mesh data of the slope surface is provided, the sliding surface and the original topography before triggering land sliding can be created by using the function of "Recovery of the ground surface".

After running the recovery process, the slope surface of the current settings will become the sliding surface. The source area created by [filling] in the menu of [Recovery of the ground surface] will become a new slope surface. If only the recovery of deposition area needs to be processed by [excavation] in the menu of [Recovery of the ground surface], the elevations of the sliding surface and the slope surface will be the same. In this case, the

range of the original slope surface will be deleted.

Once creating the geographical features of both the slope surface and the sliding surface are finished, the distribution of the unstable mass height can be seen. In the distribution, the delineation of elements such as "landslide source area" and "volume enlargement area" can be specified.

Setting the simulation

After creating the mesh data representing the geographical features of the slope surface and the sliding surface, the necessary settings for the simulation can be configured.

In the LS-RAPID system, various patterns of land sliding simulation can be set. In "Initiation + Motion + Expansion", the power of the pore pressure and the seismic loading as the induction of landslide can be set. The starting time of the induction of landslide can also be determined.

In the landslide simulation, the seismic waveform based on the model seismic waveform as well as actual observation data by the initiation simulation of inducement of seismic loading can be set. The manual describes the steps for setting the seismic waveform based on actual observed data. In the landslides

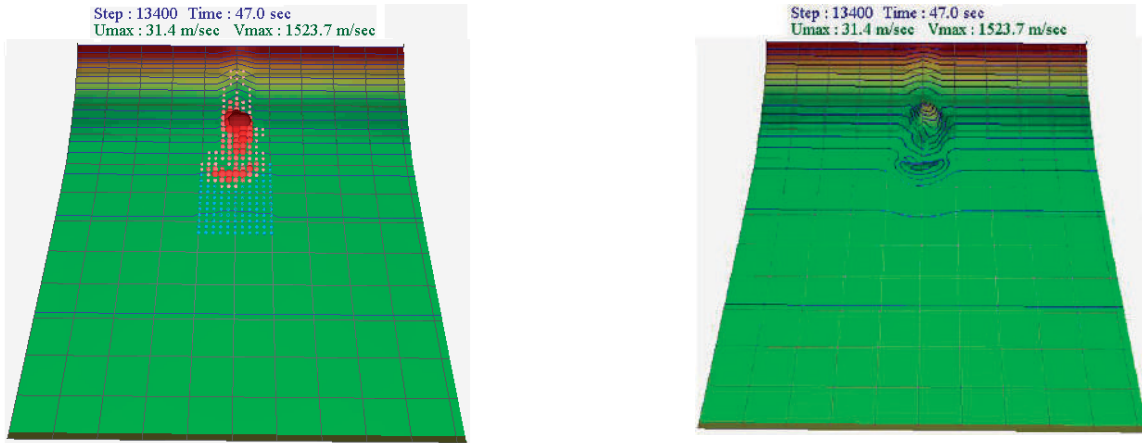


Figure 4 Left: an illustration of the ellipsoid. Right: the mass thickness expanded three times.

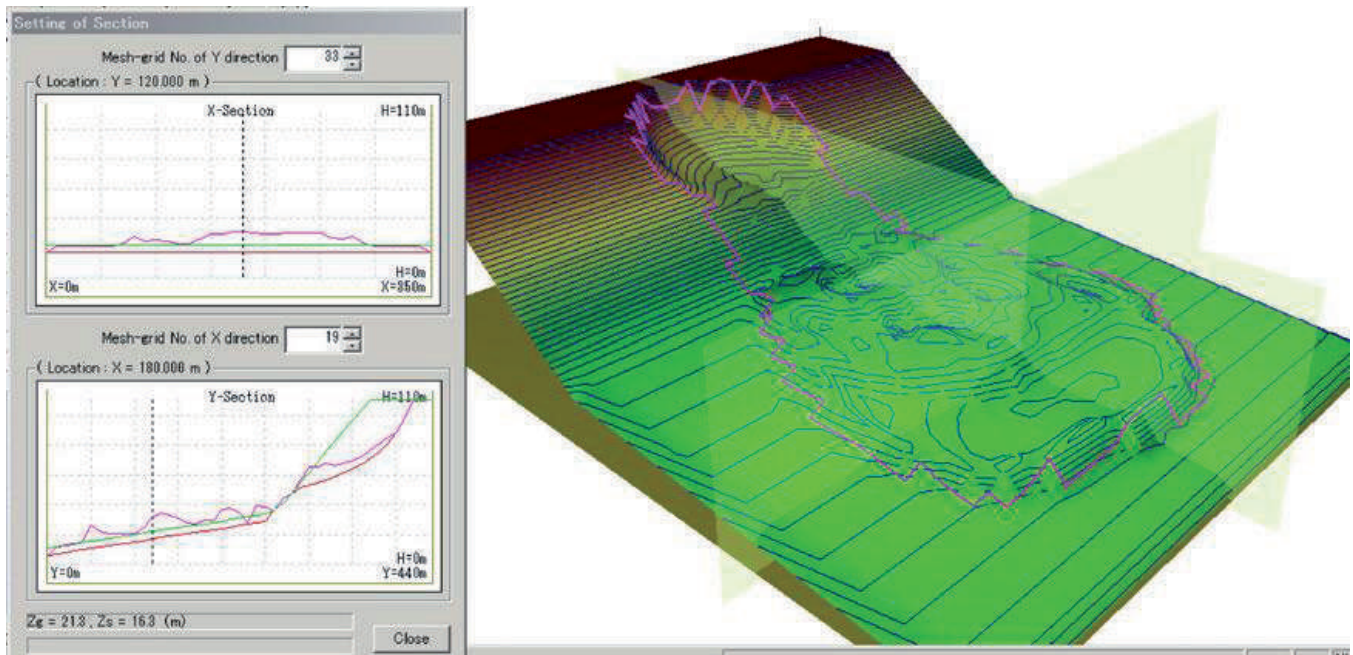


Figure 5 The simulation result for the simple imaginary slope. Left: cross sections of X and Y axis. Right: landslide area.

simulation, the motion process degree using a specified time step can be adjusted.

In the manual, the output settings for the landslide simulation are also described. While and after simulating, the generated output screen of JPEG or AVI file can be selected for either the 3D view area or the application area. When select the application area as the output range, if it is not able to properly output the screen, then the 3D view can be changed instead.

Run simulation and results analysis

From the [Execute] menu and [Start Simulation], the model can be launched to run. From the menu of [Output of arbitrary section profile], the window where

the section layout can be set, will be seen as necessary. Enter the starting and the ending points of the cross section, the cross section can be displayed. The cross section profile can be displayed based on the specified values of the section coordinates. The coordinate values of the cross sections of the slope surface and the sliding surface corresponding to the above cross section profile can also be displayed.

Operation guide using a simple slope as example

The imaginary simple slope landslide is presented in the manual as an example to show how to conduct the simulation with the basic steps. The performance of each

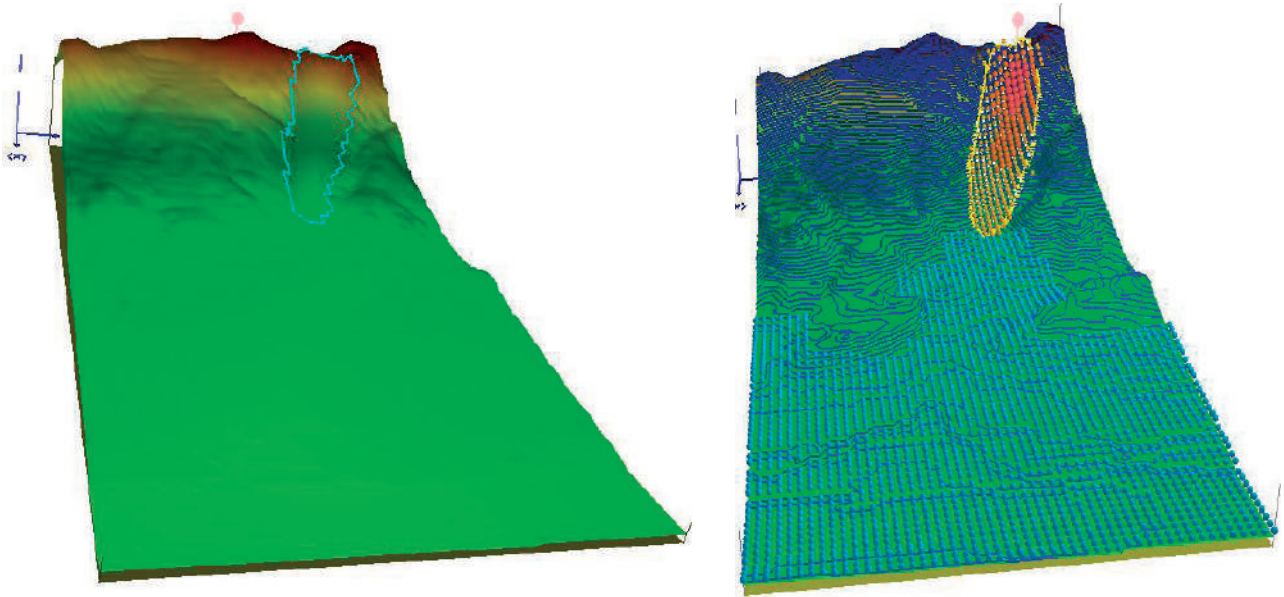


Figure 6 Left: an illustration of the ellipsoid. Right: an illustration of mass distribution in the elevation edit area.

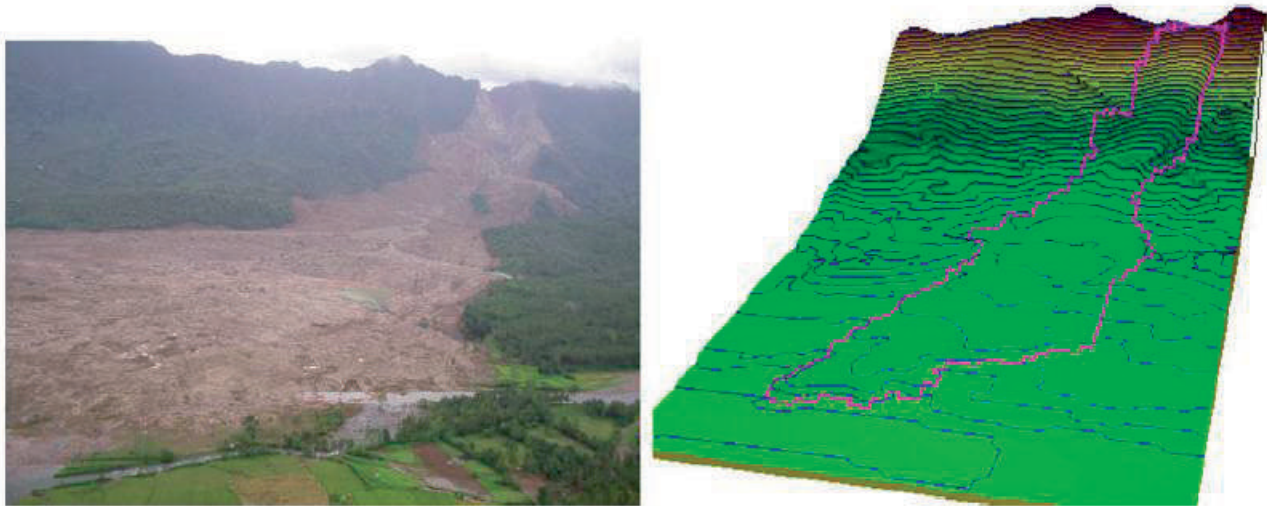


Figure 7 Air photo and the results of the LS-RAPID computer simulation of the Leyte landslide.

process of LS-RAPID is examined by applying it to this simple imaginary slope. The imaginary slope is composed of three parts of slope; a flat ground in the top, a steep slope in the middle and a gentle slope in the bottom. The area of simulation is 350 m wide and 440 m long, the size of mesh is 10 m, the maximum vertical depth of landslide is 40.53 m, the total landslide volume is 231,300 m³. The landslide body was created in a form of ellipsoid shown in Figure 4.

The initiation process by pore pressure increase on the initiation of rapid landslides is firstly examined. The border between rapid landslide and no movement is then examined by earthquake loading in addition to pore pressure ratio. Figure 5 shows one example of the

simulation results for the simple imaginary slope. The cross section of X and Y axis can be depicted, respectively. The dynamic animation of the simulation process can also be output as video and picture files.

Four examples in different conditions

The real landslide simulations are provided for four case studies, i.e. Leyte landslide (Philippines), Hypothesis of submarine landslide (Japan), Grohovo landslide (Croatia), Kostanjek (Croatia).

As for the Leyte landslide, which was a rapid and long-traveling landslide, occurred on 17 February 2006 in

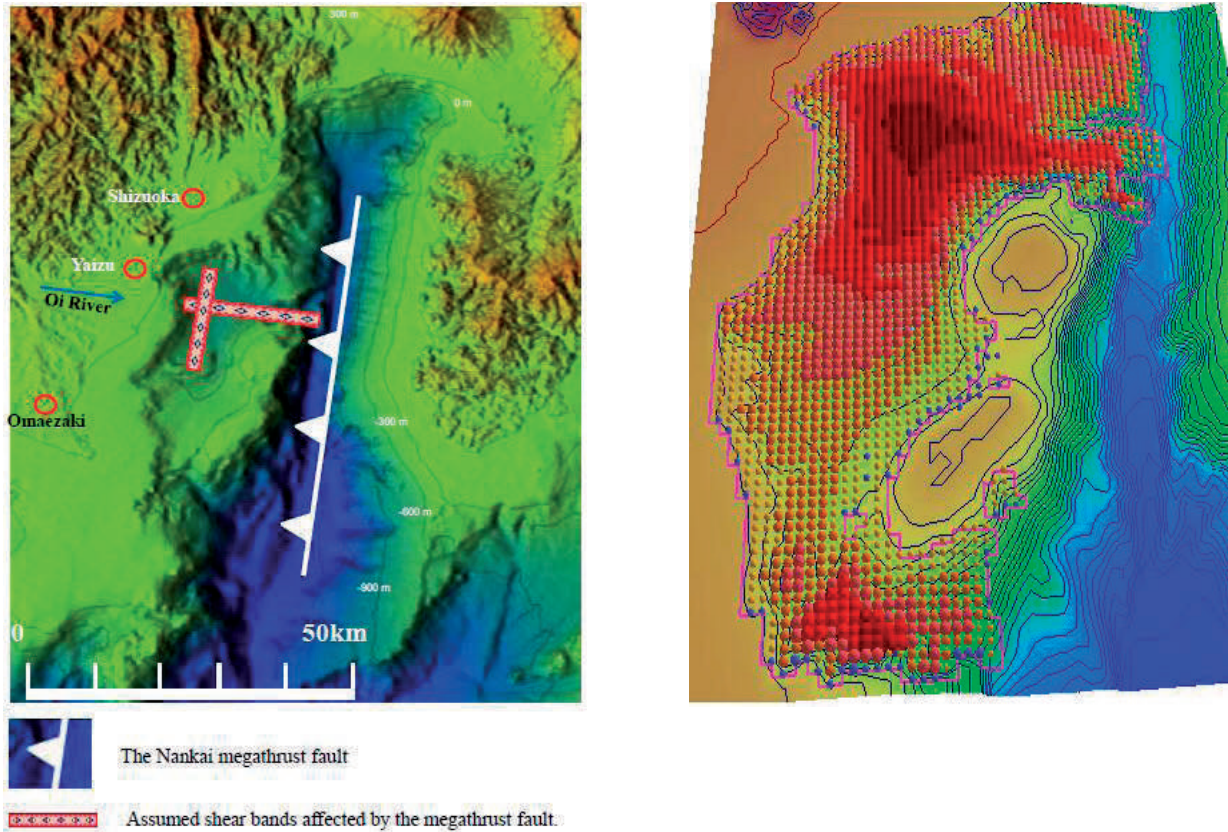


Figure 8 Left: assumption of fracture zones in Senoumi. Right: landslide simulation result by the Tohoku earthquake record.

the southern part of Leyte Island (Philippines), it caused 154 confirmed fatalities and 990 people missing in the debris. Figure 6 shows an illustration of the ellipsoid and mass distribution in the elevation edit area. In Figure 7 it can be seen that the major parts of landslide distribution are well reproduced. The secondary debris flow and muddy water spreads to the leftward in the photo and in field observations.

As for the hypothesis of submarine landslide simulation, Figure 8 (left) shows the assumption of fracture zones in Senoumi. The deep sea floor in the blue colour is called as Suruga Trough. Figure 8 (right) shows the landslide simulation result by the Tohoku earthquake record. The results show that the feature, created by LS-RAPID using the parameters of volcanic ash, was most similar to the Senoumi in depth and extent.

As for the two landslide simulation, i.e. Grohovo landslide and Kostanjek landslide in Croatia, they will be presented in the same volume of this book.

The detailed procedure of the above four examples are described in the manuals of LS-RAPID. The datasets and parameters for running the landslide model are also included in the manuals. The users can open and modify the topography, soil parameters for their study.

Acknowledgments

We are grateful for the support provided by the Kyoto University Global COE program “Sustainability/Survivability Science for a Resilient Society Adaptable to Extreme Weather Conditions”, the JSPS Grant-in-Aid for Young Scientists (B) (KAKENHI Wakate B, 90569724), and the Science and Technology Research Partnership for Sustainable Development Programme (SATREPS) of the Japan Science and Technology Agency (JST) and the Japan International Cooperation Agency (JICA).

References

- He B, Sassa K, Ostric M, Takara K, Yamashiki Y (2011) Effects of parameters in landslide simulation model LS-RAPID on the dynamic behaviour of earthquake-induced rapid landslides. In C. Margottini et al. (eds.), *Landslide Science and Practice*, vol. 3, pp 119-125.
- Sassa K (1988) Special lecture: the geotechnical model for the motion of landslides. *Proceedings of the 5th International Symposium on Landslides, Lausanne*, vol.1, pp 33–52
- Sassa K, Nagai O, Solidum R, Yamazaki Y, Ohta H (2010) An integrated model simulating the initiation and motion of earthquake and rain induced rapid landslides and its application to the 2006 Leyte landslide. *Landslides* 7–3:219–236
- Sassa K, He B, Miyagi T, Ostric M, Baba T, Nagai O, Furumura T, Konagai K, Kaneda Y, Yamashiki Y (2011) A possible submarine megaslide in Suruga bay in Japan -An interpretation of Senoumi (Stony flower sea) bathymetric feature. *Landslides*, 9(4), 439-455.

Application of Integrated Landslide Simulation Model LS-Rapid to the Kostanjek Landslide, Zagreb, Croatia

Karolina Gradiški⁽¹⁾, Kyoji Sassa⁽²⁾, Bin He⁽³⁾, Željko Arbanas⁽⁴⁾, Snježana Mihalić Arbanas⁽¹⁾, Martin Krkač⁽¹⁾, Predrag Kvasnička⁽¹⁾, Maja Oštrić⁽⁵⁾

1) University of Zagreb, Faculty of Mining, Geology and Petroleum Engineering, Zagreb, Croatia, +385 1 5535 898

2) International Consortium on Landslides, Kyoto, Japan

3) Kyoto University, Disaster Prevention Research Institute, Kyoto, Japan

4) University of Rijeka, Faculty of Civil Engineering, Rijeka, Croatia

5) Kyoto University, Graduate School of Engineering, Kyoto, Japan

Abstract This paper describes numerical modeling of the Kostanjek landslide using the LS-Rapid software. The analyses using the LS-Rapid software were made for two different triggering factors i.e. excess of pore water pressure, and combination of pore water pressure excess and earthquake occurrence, and it was applied at two different landslide cases. In the first case, the LS-Rapid software was used to re-examine the landslide model for the Kostanjek landslide reported by Ortolan (1996), Mihalinec and Stanić (1991) and Stanić and Nonveiller (1996). In the second case, LS-Rapid was used to confirm the Kostanjek landslide model in which the sliding surfaces are initially developed through the soil mass. During the initial shearing, the excess pore pressure is often generated during the landslide activations by triggering factors and the post failure-motion of the landslide. The strength parameters used in these analyses were derived from tests in undrained ring shear apparatus carried out by Oštrić et al. (2012 a,b). It is expected that the results of the Kostanjek Landslide simulation using LS-Rapid software and parameters obtained from undrained tests carried out in ring shear apparatus would give realistic results and would help for better understanding of the Kostanjek landslide behavior.

Keywords Kostanjek landslide, LS-RAPID, slope stability

Introduction

The Kostanjek Landslide is located in the western part of the City of Zagreb, in residential area at the base of the southwestern slope of the Medvednica Mt. It was initially activated in 1963 by mining and excavation in two open pit mines. Massive blasting and excavation in the foot of the slope caused slope movements in an area of 1.2 square kilometers. Landslide velocities have been changing in last 50 years, from landslide activation until today, in range from extremely slow to very slow.

Historical landslide model and slope stability analysis

Engineering geological model according to Ortolan (1996)

Ortolan (1996) proposed engineering geological landslide model on the basis of geotechnical investigations mainly carried out in the period 1988-1989 and this landslide model is in use until today. According to this model there exist three slip surfaces at different depths. The maximum depth of the deepest slip surface is about 90 m; the depth of the intermediate slip surface is 65 m, while the superficial slip surface is about 50 m deep (Fig. 1). The total volume of the displaced landslide mass amounts to approx. $32.6 \times 10^6 \text{ m}^3$, while it is about $12.8 \times 10^6 \text{ m}^3$ for the intermediate slip surface and about $7 \times 10^6 \text{ m}^3$ for the shallowest slip surface. Slip surfaces are subparallel; they are predisposed by the bedding planes in the rock mass (Ortolan and Pleško 1992).

The landslide geometry, the state of pore pressure on sliding surface and shear resistance parameters were determined from the results of field and laboratory investigations. The 3D engineering geological model of the Kostanjek landslide (Ortolan 1996) is presented on the Fig. 1.

Hydrogeological conditions at the area of the Kostanjek landslide were determined based on the data of permeability tests and piezometric level measurements in the exploration boreholes (KS-2, KS-2', KS-3, KS-4, KS-5, KS-6 and KS-7) from the period 1988-1994. In some piezometers (KS-6 and KS-7 placed on the east and south-east part of landslide body) the water pressure level is above the surface, and in all of them it is close to the ground surface. The yearly precipitation in the region averages 1,000 mm, partly in the form of snow, which causes rising of ground water level in the spring, when soil becomes saturated to the surface (Stanić and Nonveiller 1996).

Geotechnical properties of the materials in the landslide body were determined from laboratory test of the undisturbed soil samples taken from the boreholes in

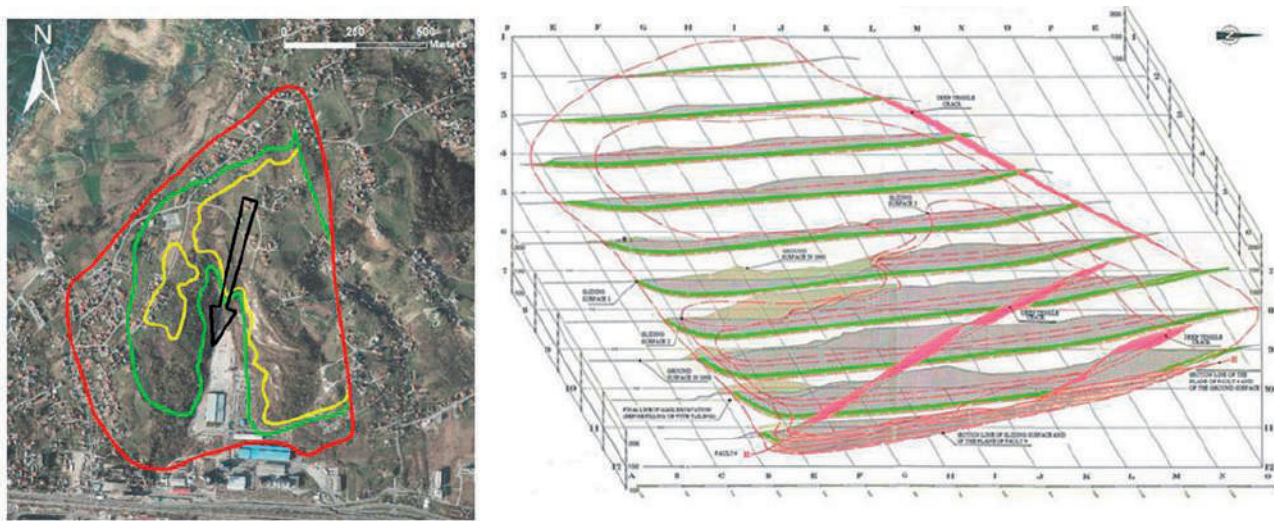


Figure 1 Engineering geological model according to Ortolan (1996). Left: landslide contours of the Kostanjek landslide (red line –the deepest sliding surface landslide contour; green line –the intermediate sliding surface landslide contour; yellow line –the superficial sliding surface landslide contour). Right: 3D engineering geological model of the Kostanjek landslide.

Table 1 Physical and mechanical soil properties (Stanić and Nonveiller 1996).

Parameter	Pannonian Clayey-limely marl	Thin clay layers	Sarmatian Varved layers	Laminated silty marl
WL (%)	33.5-81.5	77.5-94.5	54.9-143.0	40.0-105.5
WP (%)	14.1-41.6	30.0-42.2	31.5-126.7	13.8-62.9
IP (%)	19.5-27.5	43.1-54.8	16.3-28.3	17.3-42.6
AC class	-	CI/CH	MH	CI/CH
ρ (g/cm ³)	1.75	2.15	1.22-1.59	1.39-2.18
ρ_s (g/cm ³)	2.60	2.83	2.32-2.50	2.36-2.78
ρ_d (g/cm ³)	1.25	1.80	0.71-1.09	0.82-1.78
Φ_d (°)	27.5-35	-	23-28	23-28
c_d (KPa)	0-40	-	6-40	6-40
Φ_r (°)	-	7-8	8-20	8-20
c_r (KPa)	-	0	0	0
q_u (KPa)	500-5000	-	-	-

the Lower Pannonian, Upper Pannonian and Sarmatian deposits, especially from the varved Sarmatian deposits (i.e. thinly laminated alteration of carbonate and clayey layers) in which the deepest sliding plane was developed (Stanić and Nonveiller 1996). The following laboratory tests were carried out: grain size distribution and soil classification, unconfined soil strength, shear strength in drained slow tests in triaxial tests and in the direct shear tests, and the residual shear strength in a ring shear apparatus. The results of these tests are shown in Table 1.

The results of shear strength tests, which were verified in the stability analyses show that under the given geometric setting and hydrogeological conditions, the residual shear strength defined by the parameters $c_r=0$, $\phi=9^\circ$, brings the slide to a stable condition with a factor of safety FoS=1.0.

Stability analysis according to Stanić and Nonveiller (1996)

The stability analyses of the Kostanjek landslide were presented by Mihalinec and Stanić (1991), Stanić and Nonveiller (1996) and Stanić and Nonveiller (1995). For the given landslide model they have presented a 3D solution for the analysis of slope slides. The sliding body is divided into elements, each of which is defined by representative cross-section (Fig. 2). The resisting and active forces, and the 2D safety factors are computed for all cross-sections, and they form, along with the width of the elements, the necessary data for the computation of the 3D safety factor.

The 2D analyses were carried out by the Spencer slice method (Spencer 1967), using the software SSTAB1 which was modified to enable the computation of the input data for the 3D analysis (Stanić and Nonveiller 1996). The data required for the compatibility check and 3D effects (transversal inclination and width of element, computational length of section, shear strength parameters on the vertical contacts, average depth of groundwater on the slip surface) are added to the input data for selected cross-sections (2D FoS, resisting forces, active forces, weight of the elements) (Stanić and Nonveiller 1996). The results of the computation obtained for the geometry of the marl excavation in quarry in 1988 are shown on Figure 2.

According to Stanić and Nonveiller (1996), the differences between the maximum and minimum 2D safety factors are caused by much higher pore pressures on the right part of the slide and a deficit of mass at the toe in the central part. The stability analyses for slope geometry from 1963 gave the safety factor of 1.17, which confirmed that the start of slide was caused by excavation in quarry.

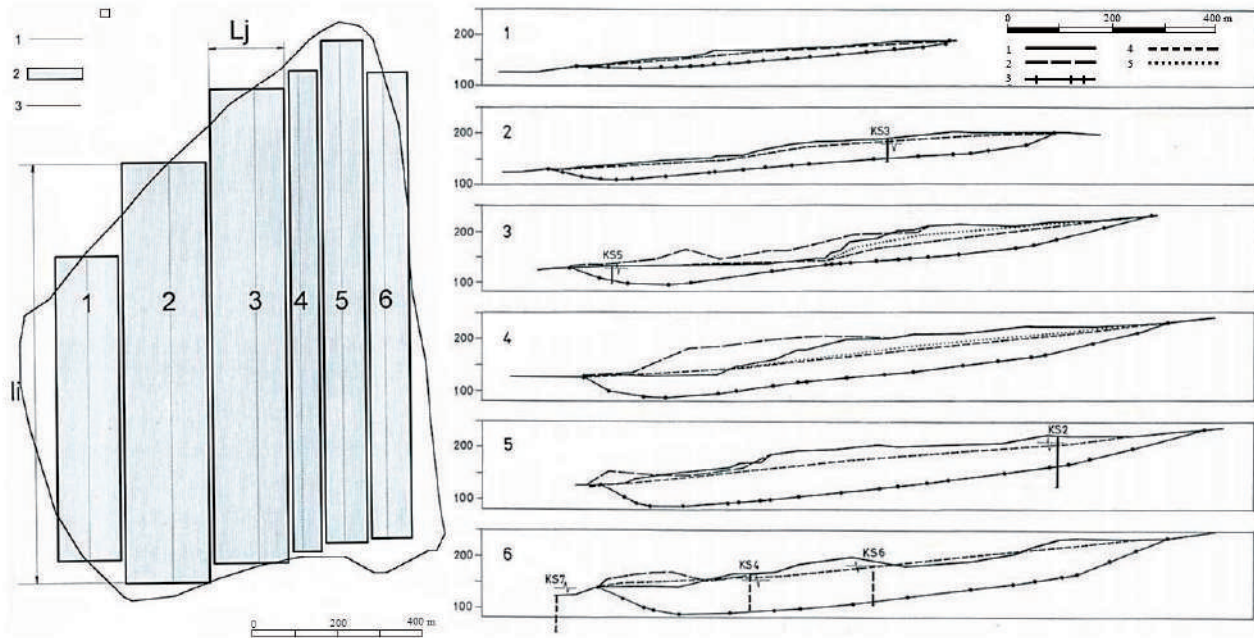


Figure 2 Stability computation of the Kostanjek slide according to Stanić and Nonveiller (1996). Left: plan view of analyzed landslide and elements used in the analysis (1 - computational cross-sections; 2 - elements; 3 - landslide contour). Right: cross-sections used in the computation (1 - ground surface in 1988; 2 - ground surface in 1963; 3 - deep slide surface; 4 - groundwater level in 1963; 5 - groundwater level in 1988).

Stanić and Nonveiller (1966) concluded that possible causes for the landslide activation may be extremely high pore pressures and/or the dynamic effects caused by the excavation of marl by mass blasting. The critical acceleration which brings the computed safety factor to $FoS = 1$ amounts to $a_{crit} = 0.014$ g, which corresponds to the order of magnitude of the acceleration caused by mass blasting.

Stability analysis using LS-RAPID software

About LS-RAPID software

The Integrated Landslide Simulation Model (LS-RAPID) is simulation software that has been developed to assess the initiation and motion of landslides triggered by earthquakes, rainfalls or the combined effects of rainfalls and earthquakes (Sassa 2010). The software has following characteristics (Sassa 2010):

- It is the first simulation model to reproduce the initiation process and the run out process from stable state until deposition within the same model.
- It is the simulation model based on the key parameter, shear resistance at the steady state with physical meaning, which can be measured or estimated from experiments.
- Landslide can be triggered by seismic loading either using real seismic record or simple cyclic waves under a certain pore water pressure (pore pressure ratio) within LS-RAPID.

- The model can simulate the entrainment of unstable deposits along the run out path, which increases landslide volume and hazard area.

- The model can reproduce “Progressive failure phenomenon”. This phenomenon manifests when weak zones subjected by higher pore pressure will firstly fail and the failure area will expand around the initial failure zone, then finally a whole landslide mass will start to move.

- The basic equation of LS-RAPID is established on the assumption in which all potential energy is consumed as the frictional energy at the sliding surface. However, the landslide mass may lose kinetic energy during collision of sub-masses within a landslide mass, momentum transfer to engulfed materials and the movement passing over vertical gaps/falls, horizontal bent or other not-smooth ground surface. The model incorporates a non-frictional energy loss function only for a specific mesh and a specific time step by the threshold values of extraordinary velocity or/and thickness.

The basic concept of LS-RAPID simulation model is presented on Figure 3. A vertical imaginary column is considered within a moving landslide mass. The forces acting on the column are the following: (1) self-weight of column (W), (2) seismic forces (vertical seismic force F_v , horizontal x-y direction seismic forces F_x and F_y), (3) lateral pressure acting on the side column walls (P), (4) shear resistance acting on the bottom (R), (5) normal stress acting on the bottom (N), (6) pore pressure acting on the bottom (U).

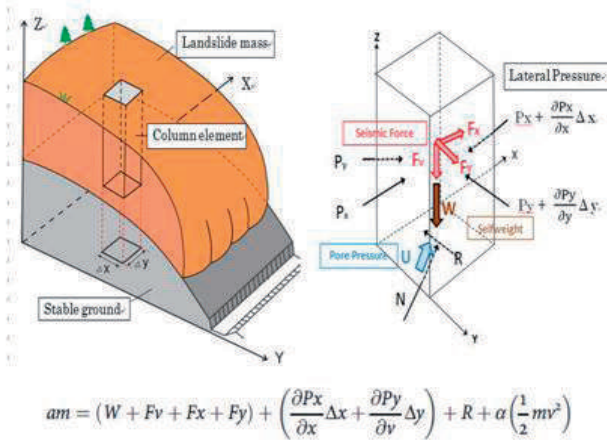


Figure 3 Basic principles of LS-RAPID (Sassa et al. 2010)

The landslide mass (m) will be accelerated by the acceleration (a) given by the sum of the following forces: driving forces (self weight + seismic forces) + lateral pressure ratio + shear resistance + non-frictional energy consumption in a column (Sassa et al. 2010). Described LS-RAPID software is used for stability analyses of the Kostanjek landslide.

Input data for Analysis

The Kostanjek landslide is a complex landslide with a deficit of a mass in the middle part of the landslide body and with slip surface inclined to the south-southeast. As it is aforementioned, slip surface reaches maximum

Table 2 Soil parameters used for stability analysis using

Soil Parameters	Value	Unit
Lateral Pressure ratio (k)	0.6	-
Friction angle inside landslide mass (Φ_i)	18.3	°
Friction angle during motion (Φ_m)	18.3	°
Steady state shear resistance (τ_{ss})	150	kPa
Pore pressure generation rate (B_{ss})	0.95	-
Peak friction angle at sliding surface (Φ_p)	29.5	°
Peak cohesion at sliding surface (c_p)	0.1	kPa
Total unit weight of the mass (γ_t)	20	kN/m ³
Unit weight of water (γ_w)	9.81	kN/m ³
Cohesion inside mass (c_i)	0.1	kPa
Cohesion at sliding surface during motion (c_m)	0.1	kPa
Shear displacement at the start of strength reduction	25	mm

depth of the 90 m in the southeastern part of the landslide body. Topography input data were created by combining Digital Elevation Model (DEM) data 5x5 m resolution and geodetic survey data with 1x1 m resolution. For creating the slip surface position, the structural-tectonic map presented by Ortolan (1996) was used.

The same slip surface topography data were used in stability analysis presented by Stanić and Nonveiller (1995, 1996). The topography of ground surface and slip surface is presented on Figure 4A. Slope stability analyses were also conducted for ellipsoidal slip surface, shown on Figure 4B. The biggest difference between this two sliding surface models is on the eastern part of the sliding body.

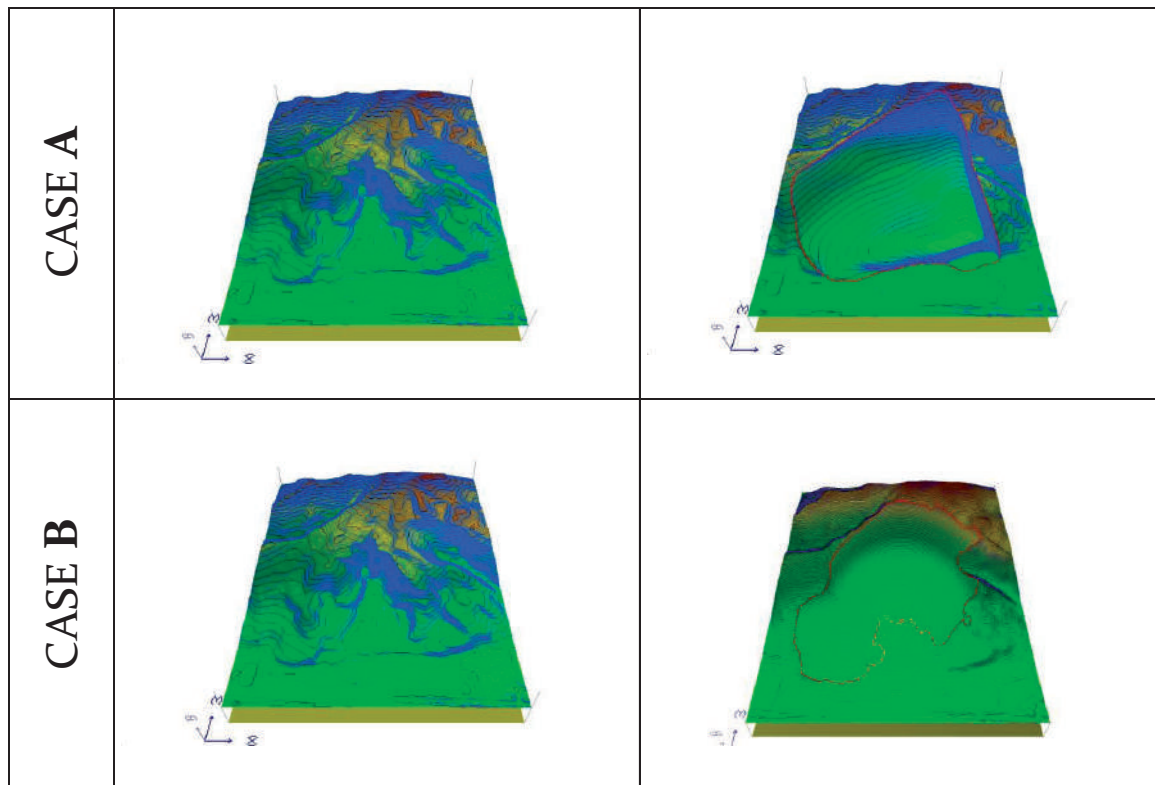


Figure 4 Topography and sliding surface for Case A (Ortolan’s model) and Case B (Ellipsoidal sliding surface).

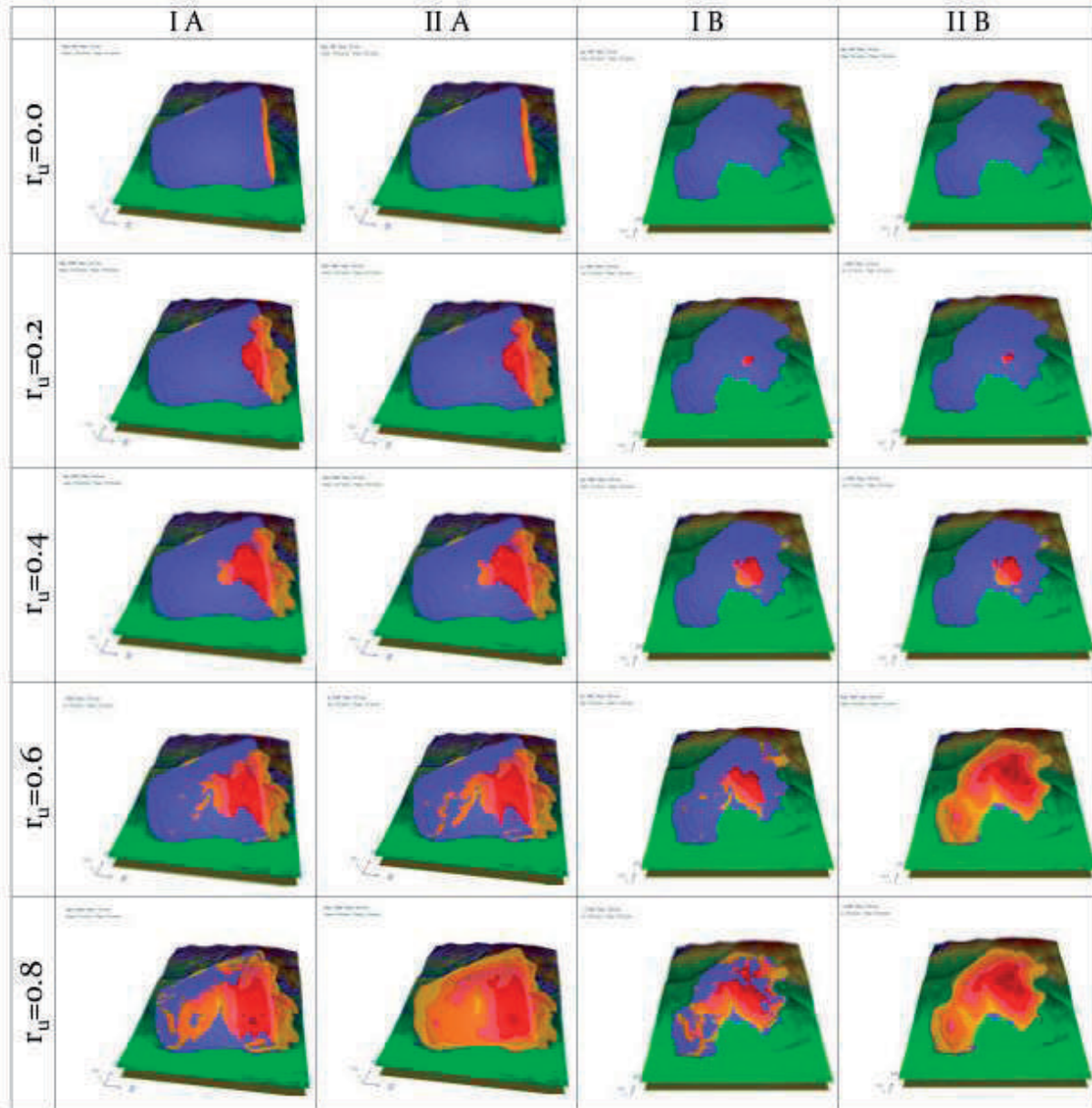


Figure 5 Results of the analysis for two different cases: Case A (Ortolan's model) and Case B (Ellipsoidal sliding surface).

Ellipsoidal slip surface was used to check how the different shape of the sliding body affect the results of slope stability within LS-RAPID software.

Parameters used for these two analyses (case A and case B) were the same and they were determined from undrained test of samples in ring shear apparatus. The test was performed on sample taken from artificial outcrop, i.e. abandoned mining cut placed in the central part of landslide body, assumed as a position of the deepest slip surface at the depth of around 65 m (Oštrić et al. 2012a, 2012b). Soil parameters used for these analyses are already presented in Table 2.

For the both analyses, two different landslide triggering factors were examined. In the cases IA and IB the triggering factor was pore water pressure and in the cases IIA and IIB the triggering factors were pore water pressure and dynamic loading. In the cases IA and IB pore pressure ratio (r_u) was set as a fluctuating value and it was increased from 0.0 to 0.8. For the dynamic loading the real earthquake loadings were used with maximum acceleration of $a_{max}=0.344 \text{ cm/s}^2$. Results of the analyses are presented on the figure 5.

The blue zones represent soil columns stable or with moving velocity less than 0.04 m/s. Red zones show columns with velocity values greater than 0.04 m/s.

Results

According to the results of the analysis, the eastern and central parts of the landslide are more unstable than the western part of the landslide. This corresponds to the results of the historical slope stability analysis from 1995 and 1996 performed by Stanić and Nonveiller.

The eastern part of the deepest slip surface according to Ortolan (1996) is inclined steeply to the surface which seems unrealistic. This element cause the significant difference in the analyses results obtained using the Ortolan's model and ellipsoidal slip surface. It should be necessary to carry out additional field investigations to verify this part and overall geometry of the slip surface(s).

The earthquake with maximal acceleration of 0.344 cm/s^2 will cause movements of overall defined landslide body.

The velocities analyzed by LS-RAPID are much higher than measured in the field. It could be caused by the fact that the LS-RAPID software was primarily developed for rapid motion landslide analyses and the motions of the Kostanjek landslide are very slow to slow.

The soil strength parameters used in the analyses are based on the ring shear test results on the samples taken from the ground surface. Before the next phase of analyses, it should be necessary to conduct testing on the samples taken from appropriate depths which correspond to the slip surface position.

References

- Mihalinec Z, Stanić B (1991) Procedure of 3D slope stability. *Građevinar*. 43: 441-447. (In Croatian)
- Ortolan Ž (1996) Development of 3D engineering geological model of deep landslide with multiple sliding surfaces (Example of the Kostanjek Landslide) PhD thesis. Faculty of Mining, Geology and Petroleum Engineering, University of Zagreb, Zagreb. (In Croatian)
- Ortolan Ž, Pleško J (1992) Repeated photogrammetric measurements at shaping geotechnical models of multi-layer landslides. *Rudarsko-geološko-naftni zbornik*. 4:51-58.
- Oštrić M, Ljutić K, Krkač M, Setaiwan H, He B, Sassa K (2012) Undrained Ring Shear Test Performed on Samples from Kostanjek and Grohovo Landslide. *Proceeding of the 10th Anniversary of ICL*, January 2012, Kyoto, Japan.
- Oštrić M, Ljutić K, Krkač M, Sassa K, He B, Takara K, Yamashiki Y (2012) Portable Ring Shear Apparatus and its Application on Croatian Landslides. *Disaster Prevention Research Institute Annuals*. B 55: 57-65.
- Sassa K (2010) Integrated Landslide simulation model LS-RAPID Operation Manual. ICL, Godai Kaihatsu Corporation.
- Sassa K, Nagai O, Solidum R, Yamazaki Y, Ohta H (2010) An integrated model simulating the initiation and motion of earthquake and rain induced rapid landslides and its application to the 2006 Leyte landslide. *Landslides*. 7: 219-236.
- Spencer E (1967) A Method of Analysis of the Stability of Embankments Assuming Parallel Inter-Slice Forces. *Geotechnique*. 17(1): 11-26.
- Stanić B, Nonveiller E (1995) Large scale landslide in Kostanjek area. *Građevinar*. 47(4): 201-209. (In Croatian)
- Stanić B, Nonveiller E (1996) The Kostanjek landslide in Zagreb. *Engineering Geology*. 42: 269-283.

Mineralogical Composition of the Kostanjek Landslide Sediments and its Possible Influence on the Sliding and Swelling Processes

Jasmina Martinčević⁽¹⁾, Snježana Mihalić Arbanas⁽²⁾, Sanja Bernat⁽²⁾, Martin Krkač⁽²⁾, Željko Miklin⁽¹⁾, Laszlo Podolszki⁽¹⁾

1) Croatian Geological Survey, Zagreb, Croatia, Sachsova 2, +385 1 6160 727

2) University of Zagreb, Faculty of Mining, Geology and Petroleum Engineering, Zagreb, Croatia

Abstract One of a key point in the investigation and interpretation of landslides is the role of mineralogical and geochemical composition of sediment in physical and mechanical properties of soils, as well as its influence on sensitivity of landslide material to swelling and sliding. The objective of this paper is to present a mineralogical composition of sediments from the Kostanjek landslide area, aimed at interpretation of influence of its mineralogical and geochemical composition to sliding and swelling processes, especially regarding to clay minerals species like smectite clays. The analyses were performed on 17 samples collected from 100 m deep borehole B-1 drilled in the central part of the Kostanjek landslide in which the four lithological groups differ: engineering soil (Quaternary); massive marls (Upper Pannonian); marls intercalated with limestone, (Lower Pannonian); thinly laminated marls, also known as “Tripoli” sediments or tripolite (Lower Pannonian – Sarmatian). Samples K₁ – K₃ represent engineering soil, coarse to fine grained. Samples K₄ – K₁₁ represent massive marls while sample K₁₂ represent the marls between limestone intercalations. Samples K₁₃ – K₁₇ represent thinly laminated clays recognized in two forms: flat laminated and wavy laminated. The analysis was performed by X-ray powder diffraction method on random and oriented mounts of air dried material, after glycol treatment and heating to 400°C and 550°C. The results of x-ray diffraction analyses represent a bulk composition of each sediment group. Predominant are sheet silicates, followed by carbonates and quartz. Dolomite and pyrite occur in some samples at trace levels. Among clay minerals the most abundant is smectite component (50–70 w %) which is susceptible to swelling. Namely, because of its characteristic structure, in interaction with circulating solution in soil, smectite clays increase the volume of crystal lattice and thus have a negative impact on shear strength parameters, which can result in the appearance of swelling or sliding.

Keywords landslides, swelling, sliding, clay minerals, smectite, x-ray diffraction, Kostanjek landslide

Introduction

The Kostanjek landslide is the largest landslide at the area of south – western hilly zone of Medvednica Mt. and it belongs to urbanized area of the City of Zagreb. It is activated in 1963 due to massive uncontrolled blasting for mining purposes and excavation in a marl quarry at the foot of the hills (Mihalić and Arbanas 2012).

Engineering geological model of the Kostanjek was developed by Ortolan (1996) and it was used as a base for design of remedial measures. According to this model, Kostanjek landslide is a complex landslide with three sliding surfaces (Vrsaljko et al. 2011): (1) sliding surface with maximum depth of 50 meters along lithological contact between thickly bedded (massive marls) and thinly bedded marls in Upper Pannonian deposits; (2) sliding surface with maximum depth of 65 meters along thin layer of clay in thinly bedded marls in Upper Pannonian deposits; and (3) sliding surface with maximum depth of 90 meters along the contact between thinly laminated clayey marls and coarse grained rocks in Sarmatian deposits. This model was based on the correlation of data from four boreholes placed inside landslide body. The main criteria which were used to define described model were identification of stratigraphical units and plasticity index of engineering soils from borehole cores.

One of the key points in the investigation and interpretation of landslides is the role of mineralogical composition in physical and mechanical properties of soils, and sensitivity of landslide materials to swelling and sliding. Therefore, the aim of this paper was study of mineralogical composition of sediments from the Kostanjek landslide which is one of the pilot areas in the framework of the Croatian–Japanese joint research project on “Risk Identification and Land – Use Planning for Disaster Mitigation of Landslides and Floods in Croatia” described in Mihalić and Arbanas (2012).

Planned research will encompass the following: (a) review of existing data, (b) mineralogical analyses, (c) chemical analyses, (d) interpretation of analytical results, and (e) correlation of mineralogical compositions with physical and mechanical properties of soils and

rocks. This paper also presents existing data from investigation carried out by Balen (1975) and Slovenec (1989), as well as results of mineralogical analysis performed in 2012 on 17 samples from B-1 borehole.

Study area

Geological settings

The Kostanjek landslide is developed in Upper and Middle Miocene sediments (Fig. 1). They are characterized by great vertical and lateral lithological diversity, and they are composed mostly of marls, as well as gravels, clays and limestone which belong to clastic-carbonate succession. Miocene sediments are covered by Plio-Quaternary gravely-silty and clayey sediments with variable thickness in the top part (0-10 m). Miocene clastic-carbonate succession lies transgressively on Triassic carbonate sediments (limestone, dolomites).

In the framework of the Croatian - Japanese project, a new 100 m deep borehole B-1 was drilled in 2012 in the central part of the Kostanjek area. In the borehole core the following groups of material types have been identified: engineering soils (0 - 10.20 meters) of Quaternary age; massive marls (10.20 - 46.65 meters) of Upper Pannonian age; marl intercalated with limestone (46.65 - 54.10 meters) of Lower Pannonian age; and thinly laminated clay also known as "Tripoli" sediments (54.10 - 100 meters) of Sarmatian age. Relative geological ages are defined on the basis of zonal fossils, among them the most frequent are molluscs, foraminifera and ostracods (Vrsaljko et al. 2011).

The Miocene deposits of Medvednica hilly zone belong to the south - western marginal belt of the Pannonian Basin System (PBS) which was part of the central Paratethys (Kovačić 2004). Mineralogical composition of sediments at the area of the Kostanjek

landslide is a result of their sedimentary history within PBS. Grizelj et al. (2007) explained that sedimentation of Upper Miocene deposits usually started by deposition of Lower Pannonian Croatica Beds on the Sarmatian beds in a littoral zone of the low-salinity lake. Croatica Beds are represented by alternation of thinly-bedded clayey limestones and calcite-rich marls. The Upper Pannonian Banatica Beds, represented by massive marls, were continuously deposited on the Croatica Beds within the deep sedimentation basin (Kovačić 2004; Grizelj et al. 2007). These deposits are covered by Plio-Quaternary siliciclastic sediments deposited in small fresh-water lakes, swamps or rivers (Pavelić et al. 2003; Grizelj et al. 2007).

Historical data

According to results of geotechnical investigations from 1963 (Pehnc 1967), swelling of the unloaded marl layers exposed by the excavation was identified as a possible cause of the damages. Several years later, in 1976, Nonveiller analyzed the incurred movements and concluded that the displacements could not be caused by swelling (Stanić and Nonveiller 1996). Excavation in the quarry was stopped in 1988 after mining activities were identified as the main triggering factors of the landslide (Stanić and Nonveiller 1996).

The Kostanjek landslide model developed by Ortolan in 1996 (Ortolan 1996), was developed on the basis of geotechnical investigations which can be summarized as follows: engineering geological mapping from 1984; exploratory drilling 1988; geophysical investigations in boreholes from 1988 and seismic reflection survey performed in 1989. On the basis of geological and paleontological investigations of samples from borehole core, Ortolan (1996) assumed that the deepest sliding surface is developed in deposits of Sarmatian age.

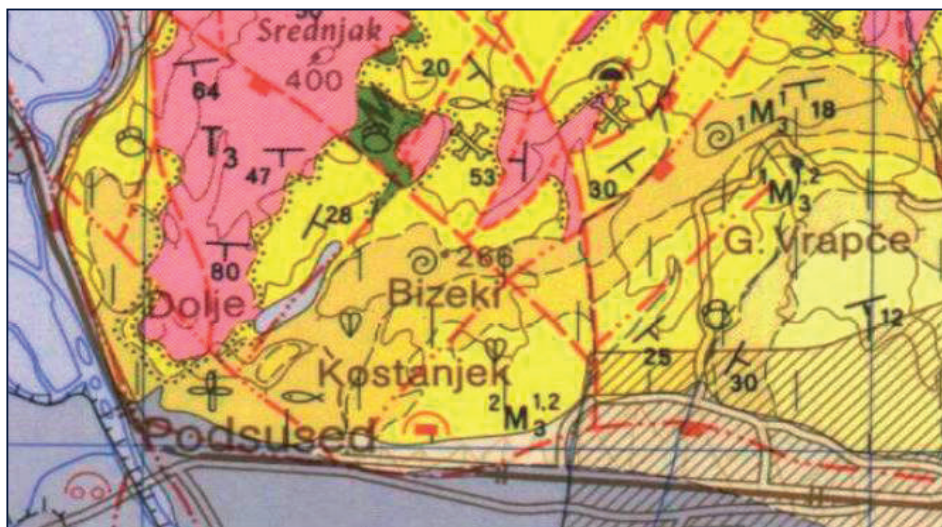


Figure 1 Base Geological Map (OGK, Zagreb Sheet; Šikić et al. 1972) of south - western part of Medvednica Mt. Original scale is 1:100,000.

During engineering geological and geotechnical investigations in seventies and eighties of the last century, Balen et al. (1975) and Slovenec (1989) performed mineralogical analysis of samples from marl quarry in the toe of the landslide body.

Through the microscopic observations of thin sections Balen et al. (1975) recorded two types of sample texture: (1) marl with homogenous texture; and (2) marls with visible alternation of white and gray thin layers. White layers are enriched on carbonate component, while gray layers are enriched on clay minerals. First type of marl is equivalent to Lower Pannonian marls (type 3) while second one is equivalent to Sarmatian thinly laminated clays (type 4). The marl samples consist of 57 – 83 w% of calcite component and 17 – 43 w% of insoluble residue.

According to Slovenec (1989) x-ray diffraction pattern of insoluble residue revealed the presence of clay minerals as main component and feldspar, pyrite, muscovite, garnet, hematite as minor constituents.

Mineralogical analyses performed in 2012

Material and methods

A new borehole (B-1) with total depth of 100 m was drilled in 2012 in the framework of the Croatian – Japanese joint research. On the basis of lithological and stratigraphical characteristics, core sediments were grouped in four recognizable units: (1) engineering soil of Quaternary age (0-10.20 m); (2) massive marls of Upper Pannonian age (10 – 46.65 m); (3) marl intercalated with limestone of Lower Pannonian age (46.65-54.10 m); and (4) thinly laminated clay also known as “Tripoli” sediments of Sarmatian age (54.10-100 m).

Seventeen samples were collected from each geological unit, represented by Figure 2:

- Samples K₁ – K₃ represent Holocene engineering soil, coarse to fine grained.
- Samples K₄ – K₁₁ represent Upper Pannonian massive marls.
- Sample K₁₂ represents Lower Pannonian marls.
- Samples K₁₃ – K₁₇ represent various rock types of Sarmatian age: K₁₃ – limestone; K₁₄ – laminated clayey marl; K₁₅ - clayey marl; K₁₆ and K₁₇ – laminated siltstone.

Lower Pannonian marls were well studied by Balen (1975) and Slovenec (1989).

Mineralogical analyses were performed in the laboratory of the Croatian Geological Survey by X-ray powder diffraction method on random and oriented mounts of air dried material, after glycol treatment, heating to 400°C and 550°C using a PANalytical X-ray diffractometer X'Pert PRO equipped with Cu tube with the following conditions: 40 kV, 40 mA, primary beam divergence 1/4° and continuous step scan (0.02°2θ/s). The “RockJock” quantification software (Eberl 2003) was used for data processing.

SAMPLE	DEPTH (m)	SEDIMENT UNITS	STRATIGRAPHY
K1	2,5	engineering soil; fine grained to coars grained	Quaternary
K2	3,5		
K3	6,2		
K8	27,7	massive marls	Upper Pannonian
K9	33,4		
K10	37,7		
K11	43,5		
K12	51,3	marls interclated with limeston	Lower Pannonian
K13	58,5	thinly laminated clays known as "Tripoli" sediments	Sarmatian
K14	61,9		
K15	65,7		
K16	70,6		
K17	75,8		

Figure 2 List of samples analyzed in 2012.

Results

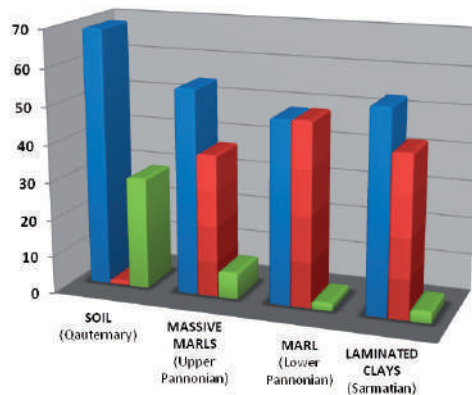
Results obtained by interpretation of X-ray diffraction patterns are: quantitative mineral composition (w%) of the whole rock (Tab. 1) and semi-quantitative content of clay minerals in a fraction <2 μm of insoluble residue (Tab. 2).

Table 1 Quantitative mineral composition (w%) of whole rock made by X-ray powder diffraction of samples from each geological unit according to the procedure of sample preparation described by Schultz (1964).

Sample	Clay	Calcite	Quartz	Feldspar	Dolomite
K1	78,8	-	12,9	8,3	-
K2	65,5	-	22,0	12,4	-
K3	61,8	4,0	19,6	14,5	-
K4	57,0	33,1	9,9	-	-
K5	62,0	24,7	8,3	5,0	-
K6	49,4	44,6	2,9	3,1	-
K7	51,6	42,9	1,8	3,5	-
K8	64,6	31,2	4,2	-	-
K9	48,5	43,6	7,0	-	-
K10	56,1	41,7	2,2	-	-
K11	51,9	44,8	3,3	-	3,1
K12	49,3	49,0	1,8	-	-
K13	43,2	55,4	1,4	-	-
K14	52,6	44,0	3,3	-	-
K15	35,9	63,5	0,5	-	-
K16	81,7	11,1	4,7	-	6,5
K17	55,3	40,0	4,8	-	-

Table 2 Semi – quantitative content of clay minerals in the <2 μm fraction of insoluble residue. The analyses were made by X-ray powder diffraction according to the procedure of sample preparation described by Schultz (1964). Explanation: **** - dominant (60-100%), *** - abundant (30-60%), ** - considerable (10-30%), * - subordinate, ~ - traces (<1%)

Sample	Illite and/or muscovite	Chlorite	Kaolinite	Smectite
K1	**	~	*	***
K2	**	~	*	***
K3	**	~	*	***
K4	**	~	*	***
K5	**	~	*	**
K6	**	~	*	***
K7	*	*	*	***
K8	**	*	*	***
K9	**	*	*	***
K10	*	*	*	***
K11	*	*	*	***
K12	*	*	*	***
K13	*	*	*	***
K14	**	*	*	**
K15	*	~	*	**
K16	***	*	*	***
K17	**	*	*	**



	SOIL (Quaternary)	MASSIVE MARLS (Upper Pannonian)	MARL (Lower Pannonian)	LAMINATED CLAYS (Sarmatian)
CLAY MINERALS	69	55	49	54
CALCITE	1	38	49	43
QTZ, FDS, DOL AND AMORPH. COMPONENT	30	7	2	3

Figure 3 Distribution of main mineral components in each sediment unit through the depth (in w%).

Discussion and conclusion

According to data obtained in laboratory it is visible that almost all samples contain the same mineral species, but in significantly different quantities. Through the all samples clay minerals are predominant component, except in Lower Pannonian marls where content of clay minerals is equal with content of calcite component. In engineering soil a content of calcite is very low because it is dissolved during the processes of weathering, but it shows an increasing trend with depth. Except calcite, the most common mineral components in the silty fraction are quartz and feldspar. Dolomite is present only in samples K11 (Upper Pannonian massive marls) and K16 (Sarmatian laminated siltstone).

Results of calculated average mass fraction of main mineral components in each geological unit were presented in Figure 3.

Among clay minerals predominant is smectite component and its content is almost constant with a depth (Fig. 4). Except smectite clays in samples are present also kaolinite, chlorite, illite and muscovite. Their content varies with a depth (Tab. 2).

Because of the characteristic structure of smectite clays, in the interaction with circulating solution in soil, they incorporate the large cations, even entire molecules that increase a volume of crystal lattice (Fig. 5). This property of smectite clays can have a negative impact on shear strength parameters which can result in the appearance of swelling and sliding events.

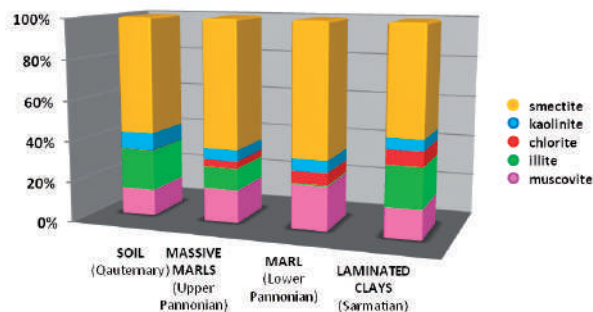


Figure 4 Proportion of clay minerals in each sedimentary unit.

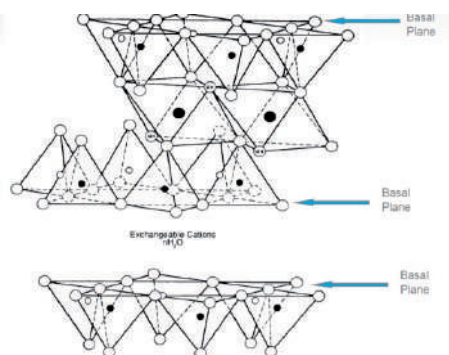


Figure 5 Schematic sketch of the structure of smectite according to Grim (1968). It is composed of layers made up of two silica tetrahedral sheets and one central alumina octahedral sheet. Between two layers is a large space in which can enter a large molecules (H₂O, organic molecules).

As a next step in research we plan to analyze in what extent the smectite is active. Therefore, the plan is to perform some chemical analyses, including the cation exchange capacity (CEC) of above mentioned sediments. The obtained chemical and mineralogical data will be compared with results of testing of physical-mechanical properties.

References

- Balen I, Tišljarić J, Majer V (1975) Petrographic characteristics of marl from Podsused area on the southwestern slopes of Medvednica Mt. *Geološki vjesnik*. 28: 167-172. (In Croatian)
- Eberl D D (2003) User's guide to RockJock -- a program for determining quantitative mineralogy from powder X-ray diffraction data. Open-File Report 03-78. U.S. Geological Survey. 55p.
- Grim R E (1968) *Clay Mineralogy*, 2nd ed. McGraw-Hill, New York. 464p.
- Grizelj A, Tibljaš D, Kovačić M (2007) Mineralogy and geochemistry of Upper Miocene pelitic sediments of the Zagorje Basin (Croatia): Implication for evolution of the Pannonian Basin. *Geologica Carpathica*. 58(3): 263-276.
- Kovačić M (2004) Sedimentology of the Upper Miocene deposits from the southwest part of the Pannonian Basin. PhD thesis, Faculty of Natural Science, University of Zagreb, Zagreb, Croatia. 203p. (In Croatian)
- Mihalić S, Arbanas Ž (2012) The Croatian–Japanese Joint Research Project on Landslides: Activities and Public Benefits. Sassa K et al. (eds), *Landslides: Global Risk Preparedness*, Springer, Verlag, Germany. (DOI 10.1007/978-3-642-22087-6_24). 335-351.
- Ortolan Ž (1996) Development of 3D engineering geological model of deep landslide with multiple sliding surfaces (Example of the Kostanjek Landslide). PhD thesis, Faculty of Mining, Geology and Petroleum Engineering, University of Zagreb, Zagreb, Croatia. 236p. (In Croatian)
- Pavelić D, Avanić R, Kovačić M, Vrsaljko D, Miknić M (2003) Stages in the evolution of the Miocene North Croatian Basin (Pannonian Basin System). Vlahović I and Tišljarić I (eds), *Field trip guidebook of the 22nd IAS Meeting of Sedimentology – Opatija 2003*, HGI, Zagreb, Croatia. 153-182.
- Pehnek V (1967) Damages of factory buildings due to marl expansion. *Građevinar*. 19(6): 197-201. (In Croatian)
- Schultz L G (1964) Quantitative interpretation of mineralogical composition from X-ray and chemical data for the Pierre Shale. U.S. Geological Survey Professional Paper 391-C. 38p.
- Slovenec D (1989) Mineralogical characteristics of sediments from "SLOBODA" cement factory in Podsused. Faculty of Mining, Geology and Petroleum Engineering, University of Zagreb, Zagreb, Croatia. 56p. (In Croatian)
- Stanić B, Nonveiller E (1996) The Kostanjek landslide in Zagreb. *Engineering Geology*. 42: 269-283.
- Šikić K, Basch O, Šimunić A (1972) Basic geological map in the scale 1:100,000, Zagreb Sheet L33-80. Geološki zavod, Zagreb, Savezni geološki zavod, Beograd. (In Croatian)
- Vrsaljko D, Mihalić S, Bošnjak M, Krkač M (2011) Lithostratigraphical investigations of the Kostanjek Landslide wider area: review of existing data and planned activities. Proceedings of the 2nd Workshop of the Project on Risk Identification and Land-Use Planning for Disaster Mitigation of Landslides and floods, 15-17 December 2011. Rijeka, Croatia. pp. 9-13.

Analysis of Water Fluctuation Dynamics in the Wider Area of the Kostanjek Landslide

Martin Krkač⁽¹⁾, Josip Rubinić⁽²⁾, Jakov Kalajžić⁽¹⁾

1) University of Zagreb, Faculty of Mining, Geology and Petroleum Engineering, Zagreb, Croatia, Pierottijeva 6, +385 98 968 2171

2) University of Rijeka, Faculty of Civil Engineering, Rijeka, Croatia

Abstract At the Kostanjek landslide in Zagreb, an initial monitoring system with geotechnical, geodetic and hydrological monitoring equipment was established in 2011. The objective of this paper is a description of the hydrological monitoring system, a presentation of monitored data (rainfall, discharge and water levels) for one and a half year period (November 2011 - February 2013) and an analysis of water level fluctuations. The analyses of hydrological data have shown that regime of water fluctuations in wider area of the Kostanjek landslide is stable and that displacement measured with extensometers coincides with higher degree of water saturation in underground.

Keywords hydrological monitoring, hydrological analysis, rainfall, discharge, landslide displacement

Introduction

The Kostanjek landslide is the biggest landslide in Republic of Croatia with a total volume of $32 \times 10^6 \text{ m}^3$. In the frame of the Croatian-Japanese scientific project on 'Risk Identification and Land-Use Planning for Disaster Mitigation of Landslides and Floods in Croatia' (2009-2014), in the wider area of the Kostanjek landslide, an initial hydrological monitoring, with the purpose of evaluation of hydrological characteristics and its relationship to landslide displacement, was established in 2011.

Hydrological monitoring encompassed rainfall and water fluctuation measurements. Rainfall was measured continuously with a tipping bucket rain gauge placed in the central part of the landslide. Water fluctuations in superficial streams were measured periodically as a discharge with a current meter and continuously as a water level with water level sensors. Water fluctuations were measured at two locations: (i) superficial stream at the exit of the abandoned transportation tunnel in the central part of the landslide; and (ii) Dolje Stream spring in the Bizek Quarry, approximately one kilometer north from the landslide.

In 2012, hydrological monitoring becomes more comprehensive. Two additional water level sensors for continuous measuring of water levels were installed in

two domestic wells with the purpose of measurement of the groundwater level in the shallowest aquifer.

Monitoring data and analysis

Rainfall data

Rainfall data at the Kostanjek landslide have been collecting from September 2011. They were compared to rainfall data from the Grič meteorological station, which presents the major meteorological station in Zagreb, with continuous measurements since 1861. The meteorological station Grič is located about 9 kilometers east from the Kostanjek landslide and it is situated in a similar geomorphologic environment: (i) at the toe part of southern slopes of the Medvednica Mountain; (2) at a similar altitude (157 m a.s.l.) to the altitude of the rain gauge installed at the Kostanjek landslide (200 m a.s.l.). Figs 1 and 2 present comparison of data from the rain gauge at the Kostanjek landslide and the Grič meteorological station. It shows similar rainfall regime for 2012, with coefficient of determination for daily records of 0.85. The total rainfall for the period of 16 months was 812.7 mm at the Grič station and 809.0 mm at the Kostanjek monitoring site.

According to the historical data for the period of last 52 years from the Grič meteorological station (1960-2012), the last three years (2010-2012) are characterized with atypical hydrological conditions because of the maximal annual rainfall in 2010 (1,155.1 mm) and the minimum annual rainfall in 2011 (520.8 mm). The average rainfall for 51 years (1962-2012) is 874.4 mm.

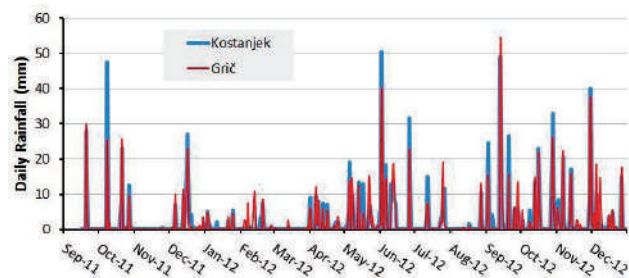


Figure 1 Daily rainfall for the period September 2011-December 2012 recorded at the Grič meteorological station and at the Kostanjek landslide, using rain gauge.

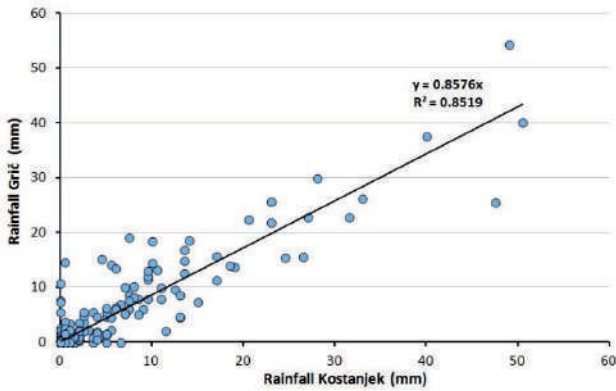


Figure 2 Correlation between rainfalls measured at Grič and Kostanjek, for the period September 2011-December 2012.

Autocorrelation analyses of annual rainfall data recorded at the Grič meteorological station indicates that dry and wet years do not occur as successive and prolonged periods, but they usually exchange cyclically (Fig. 3).

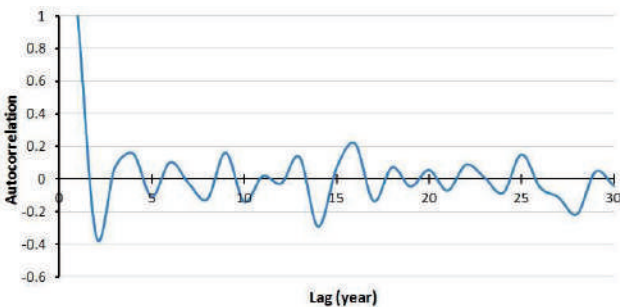


Figure 3 Autocorrelation of annual rainfall (1962-2012) at the Grič meteorological station.

Water levels and discharge measured at outflow weirs

Weirs and water level sensors in the superficial streams at the entrance of the abandoned tunnel and in spring of the Dolje Stream were installed in November 2011. Fig. 4 shows locations of hydrological sensors and extensometers.

The tunnel, which passes through the landslide body, was constructed at the beginning of 1970' and was used for transportation of limestone from the Bizek Quarry to the marl quarry, near the cement factory. Construction of the tunnel changed the drainage conditions of the area, redirecting the flow towards the drainage channel in the tunnel which is the lowest drainage base of the surrounding area (Krkač et al. 2012).

The Dolje Spring is located approximately 1 kilometer north from the top part of the Kostanjek landslide. Superficial water flows from the spring towards the southwest as the Dolje Stream. The Dolje Stream is of special interest because it is mainly recharged from karst aquifer and it partly recharges groundwater which drains through the abandoned tunnel (Krkač et al. 2012).

Water level at the Dolje Spring varies in a range from 50 to 250 mm. It reacts relatively fast and shows large oscillations related to rainfall. However, water level

at the entrance of the abandoned tunnel shows very small oscillations, only up to 20 mm (Fig. 5).

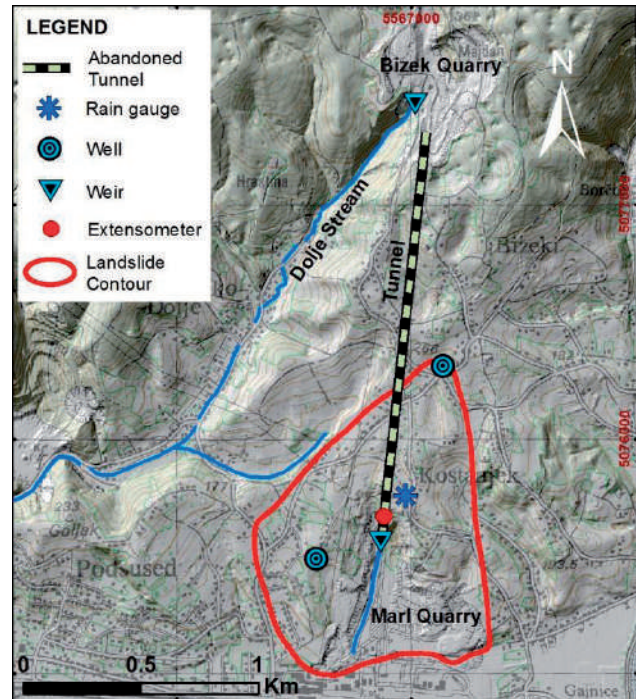


Figure 4 Locations of hydrology monitoring equipment at the wider area of the Kostanjek landslide.

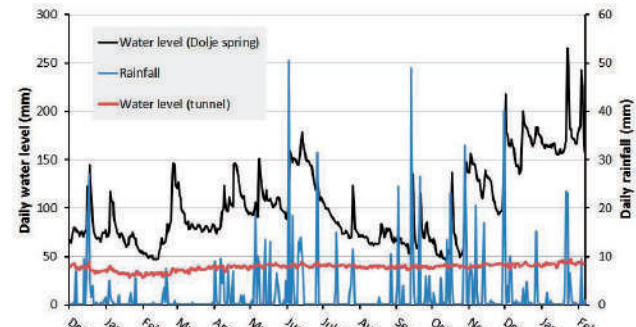


Figure 5 Daily water levels at the tunnel entrance and Dolje Spring compared to the rainfall data measured in central part of the Kostanjek landslide (December 2011 - February 2013).

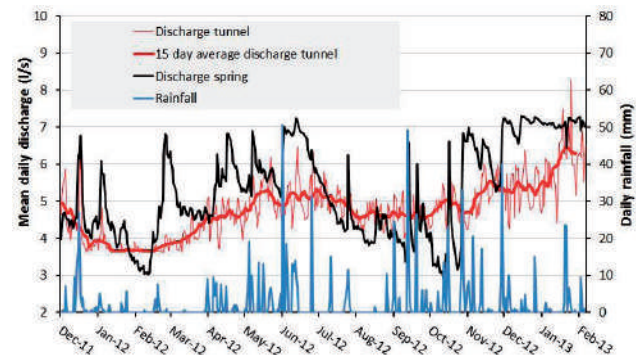


Figure 6 Daily discharges at the tunnel entrance and Dolje Spring compared to rainfall data measured at the central part of Kostanjek landslide (December 2011 - February 2013).

The relationship between water levels and discharge was established on the basis of several measurements of discharge with a standard current meter. Daily discharges at the weirs located at the entrance of the abandoned tunnel and in the Dolje Spring are presented in Fig. 6. Similar to water levels, it is possible to notice larger and faster oscillation of discharge at the Dolje Spring, between 3 and 7.3 l/s. The maximum measured discharge at the Dolje Spring was from 16th to 19th December 2012. It was related to the rainy period of two months, with the total rainfall quantity of 222 mm. A high water wave with the maximum of 6.8 l/s, appears on the Dolje Spring in February 2012, as a consequence of snow melting.

Abrupt daily oscillations of discharge data from the tunnel entrance are a consequence of the water level sensor errors. To present more realistic discharge data, we used 15-day average values. The discharge at the tunnel entrance varies from 3.6 to 6.8 l/s. The highest value of the discharge was measured on 21th and 22th of January 2013, approximately one month after the maximum discharge on the Dolje Spring. A slow reaction of discharge to rainfall at the tunnel entrance is probably related to a weak communication with surface water and longer transportation of groundwater.

From discharge data of the Dolje Spring, two most important periods of recession were extracted: (i) winter 2011/12; and (ii) summer 2012 (Fig. 7). According to the curves, winter dry period was more intensive than summer dry period, which is not usual in continental climate of Croatia. According to Krešić (1991), recession coefficient (α) obtained from a recession curve of aquifer discharge (Maillet 1905), indicates that aquifer of the Dolje Spring is relatively fractured and open to water transport and water communication.

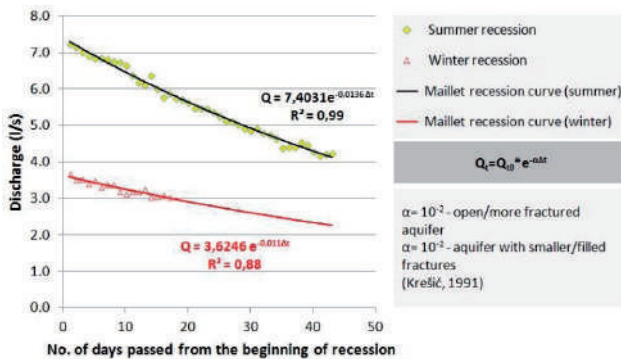


Figure 7 Mailet recession curve of aquifer discharge for Dolje Spring.

Because of small discharge fluctuations and erroneous oscillations, caused by imprecision of the measuring device, it was not possible to extract characteristic recession periods for the tunnel entrance.

Autocorrelation analyses of water discharges (Fig. 8) were also performed to identify memory effect of the catchment area which influences the water fluctuations on the Dolje Spring and in the tunnel. For usually adopted 0.2 criteria (Mangin 1984), spring and

tunnel shows relatively long (60 to 70 days) memory effect of related aquifer. Autocorrelation function also indicates cyclic exchange of dry and wet periods of approximately 250 days.

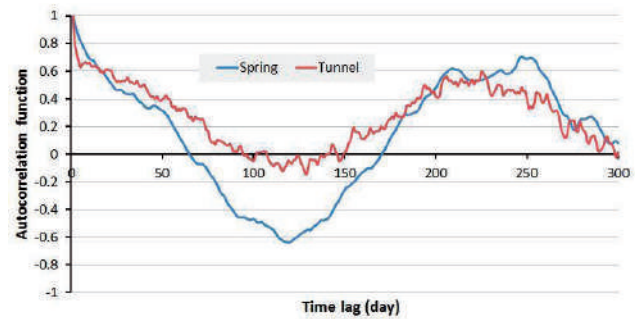


Figure 8 Autocorrelation graph of daily discharge at Dolje Spring and abandoned tunnel entrance for the period November 2011 - February 2013.

Groundwater levels in domestic wells

Because of project dynamic and absence of boreholes with piezometers, initial continuous water level measurements started in two domestic wells with no or occasional usage. One monitored well is located near main scarp of landslide in Bizek II St. and the other is located west from abandoned open marl pit in Vodopijijn Breg St. (Fig. 4). Water level depths for both wells show similar patterns, but well in Vodopijijn Breg St. shows much stronger influence to daily rainfall and greater oscillation of groundwater depth (13-21 m), while well in Bizek II, in monitored period shows only 4 meter of difference between minimum and maximum water level.

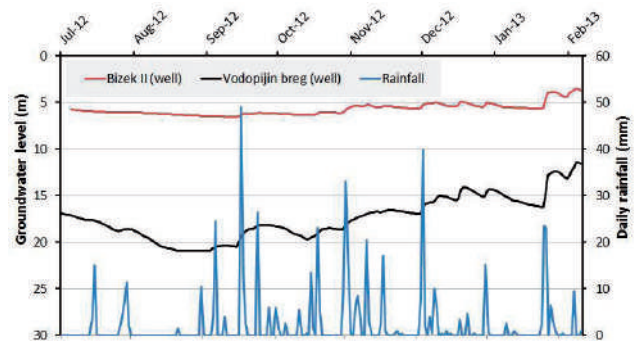


Figure 9 Daily groundwater levels of the wells in Vodopijijn Breg St. and Bizek II St. for period July 2012 - February 2013.

Autocorrelation analyses of water levels for 6 months period (July 2012 to February 2013) were performed to identify memory effect of the catchment which influences the water levels in wells. For adopted 0.2 criteria, autocorrelation function shows longer period of memory effect (around 90 days) than it is on the Dolje Spring and the tunnel entrance. The 90-day memory effect also indicates relatively stable aquifer, with slow reactions to rainfall. Because of short measuring period it was not possible to determine evidence of cyclic exchange of dry and wet periods.

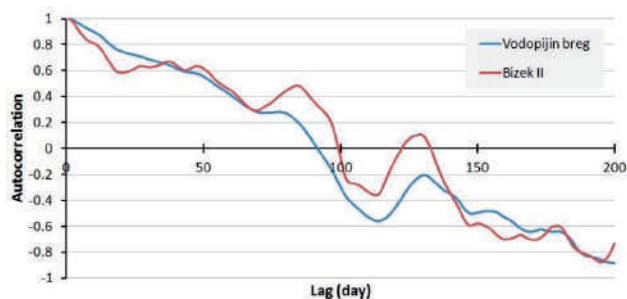


Figure 10 Autocorrelation graph of daily water level of wells in Vodopijin Breg St. and Bizek II St. for period July 2012 - February 2013.

Comparison of landslide displacement and discharge data

Final analysis of data was made to compare hydrology data with landslide displacement data obtained from extensometer in the abandoned tunnel (Fig. 4). The extensometer was installed in March 2011, about 60 m from the entrance and it measures displacement between two points: stable part of tunnel, north from the damaged zone and landslide body, south from damaged zone. Damaged zone of the tunnel Ortolan (1996) interpreted as a zone of sliding surface.

For comparison of data it was used modular data of cumulative rainfall, cumulative displacement, discharge of water at tunnel entrance and discharge of water at the Dolje Spring (Fig. 11). It is possible to notice that first measured period of displacement in the tunnel corresponds to the peak of discharge at Dolje Spring, shortly after period of significant rainfalls in May and June 2012. Second period of progressive displacement (November 2012 to February 2013) corresponds to second and third peak of discharge at the Dolje Spring together with simultaneous increase of discharge at the tunnel. The peak of tunnel discharge series occurred approximately one month after the peak of the Dolje Spring coinciding to greatest amount of displacement and also corresponding to previous analyses of groundwater discharge, e.g., slower reaction of aquifer to rainfall. This data also indicate that landslide displacement is result of groundwater fluctuations related to deep underground.

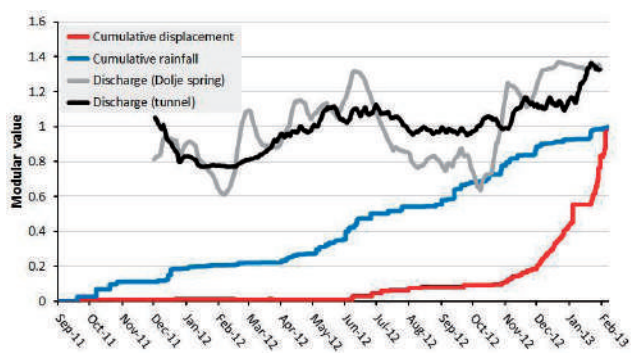


Figure 11 Comparison between modular rainfall, discharge and landslide displacement values.

Conclusions

According to the available historical data (1996 - 2012) from meteorological station Grič, described hydrological measurements were carried out during atypical hydro-meteorological period. Extremely wet 2010 (1,155.1 mm) and extremely dry 2011 (520.8 mm) were followed by relatively dry 2012 with extremely wet period at the end of the year. Results of hydrological monitoring and performed analyses at the Kostanjek landslide and at the Grič meteorological station, for the period from November 2011 to February 2012, confirmed similarity between rainfall regime in the Kostanjek landslide area and wider area.

Fluctuations of water levels and dynamics of discharge at the abandoned tunnel entrance and Dolje Spring measured periodically with current meter and continuously with water level sensors indicate stable hydrological regime, especially in deeper aquifers. Analysis of dynamic of water level fluctuations in domestic wells also indicates aquifer with stable hydrological regime, with relatively slow changes, especially at the well in Bizek II St., which is at higher altitude (242 m a.s.l.) than the well in Vodopijin Breg St. (178 m a.s.l.), but shows smaller amplitudes of water fluctuations.

Displacement in the abandoned tunnel, monitored by an extensometer, coincides with greater amounts of water in deeper aquifer after long periods of intensive rains. These data indicate that groundwater fluctuations in deeper aquifer have influence on landslide displacement.

Acknowledgments

The authors would like to thank Croatian Meteorological and Hydrological Service for rainfall data from the meteorological station Grič.

References

- Krešić N (1991) Quantitative karst hydrogeology with elements of groundwater protection. Beograd, Naučna knjiga. 192p. (In Serbian)
- Krkač M, Rubinić J, Mihalić S (2012) Landslide Kostanjek - analyses of groundwater discharge as a basis for the new hydrological monitoring. Proceedings of the 2nd Project Workshop on the monitoring and analyses for disaster mitigation of landslides, debris flow and floods, 15-17 December 2011. Rijeka 2012, Croatia. pp. 17-20.
- Maillet E (1905) Essais d'hydraulique souterraine et fluviale. Herman et Cie, Paris. 218p.
- Mangin A (1984) Pour une meilleure connaissance des systèmes hydrologiques a partir des analyses corrélatoire et spectrale. Journal of Hydrology. 67: 25-43.
- Ortolan Ž (1996) Development of 3D engineering geological model of deep landslide with multiple sliding surfaces (Example of the Kostanjek Landslide). PhD thesis. Faculty of Mining, Geology and Petroleum Engineering, University of Zagreb, Zagreb, Croatia. 236p. (In Croatian)

The Kostanjek Landslide - Monitoring System Development and Sensor Network

Martin Krkač⁽¹⁾, Snježana Mihalić Arbanas⁽¹⁾, Osamu Nagai⁽²⁾, Željko Arbanas⁽³⁾, Kristijan Špehar⁽⁴⁾

1) University of Zagreb, Faculty of Mining, Geology and Petroleum Engineering, Zagreb, Croatia, Pierottijeva 6, +385 1 5535 896

2) International Consortium on Landslides, Kyoto, Japan

3) University of Rijeka, Faculty of Civil Engineering, Rijeka, Croatia

4) University of Zagreb, Faculty of Natural Science, Zagreb, Croatia

Abstract Kostanjek landslide is the largest landslide in the Republic of Croatia. It is located in the western part of the City of Zagreb, in residential area at the base of the south western slope of Mt. Medvednica. Investigation of this landslide is one of the objectives of the Japanese-Croatian five-year (2009-2014) scientific joint-research project 'Risk Identification and Land-Use Planning for Disaster Mitigation of Landslides and Floods in Croatia'. The aim of investigation is to check and improve existing landslide model and to establish landslide monitoring system aimed at landslide risk mitigation. A comprehensive, real time monitoring system was designed during the period of 2010 and 2011, installation of equipment started in October 2011, while the completion of works will be finished during the 2013. Monitoring system consist of geodetic, geotechnical, seismological and hydrological equipment. Geodetic equipment includes 15 GNSS stations, geotechnical equipment includes 9 extensometers at five different locations and one 100 m borehole with inclinometer casing. Pore pressure gauges will be installed in borehole during 2013, at the central part of landslide, at three different levels. Seismological monitoring consists of 7 accelerometers installed at five different locations. Hydrological equipment consist of two weirs with water level sensors for measuring discharge, rain gauge and two water level sensors installed in two domestic wells. Aim of this paper is to present design of planned monitoring system, what has been done so far and to present initial monitoring data from installed equipment.

Keywords Kostanjek landslide, monitoring system

Introduction

Kostanjek landslide extends over an area of approximately 1 km², occupying territory of 'Sloboda' cement factory at the south (toe), open marl pit (middle part) and inhabited area (western and eastern flanks and crown at the north). First instabilities were observed in the period 1963-1964 and were intensified during the 1966

when numerous cracks have occurred at industrial facilities and private buildings as a consequence of subsiding and uplifting of the terrain. The most comprehensive geotechnical investigations of Kostanjek landslide were carried out in the period 1988-1989. Based on the results of these investigations an engineering geological model of the Kostanjek landslide was interpreted (Ortolan 1996). According to this model, the width of the displaced mass and the width of the rupture surface are 1.116 km, the total length of the landslide, the length of displaced mass and the length of rupture surface are 1.43 km, while the maximum depth of the displaced mass and the maximum depth of rupture surface are 90 m. The total volume of moving mass is approximately 32x10⁶ m³.

Cumulative horizontal displacements were interpreted from aerial photos and from measurements of stabilized geodetic points. According to the photo interpretation of aerial stereo pairs from 1963, 1979, 1981, 1985 and 1988, the horizontal displacements of the ground surface in the period 1963-1988 were in range 3-6 m (Ortolan and Pleško 1992). Ortolan and Pleško (1992) interpreted differences in displacement of the landslide surface (determined on approximately 110 points) by movement on two additional slip surfaces at the depths of 65 m and 50 m, which are subparallel to the deepest sliding surface. Horizontal displacements were considered as representative for the total displacements because of the low angle of the sliding surface (average 5°). Limitation of measurements on stabilized geodetic points is that measuring campaigns were carried out during relatively short periods and with different sets of geodetic points, i.e. measuring campaigns were carried out in the periods 1966-1976, 1973-1976, 1978-1979, 1988-2001, 1998-1999, 2009-2010, 2010-2012. From these data it is not possible to obtain total displacement data so as displacement rates for the landslide since its activation, but only partial data for different periods. Horizontal component of displacement measured on 35 geodetic points during period 2010-2012 was 6-92 mm (Županović et al. 2012) which indicate that landslide is still active.

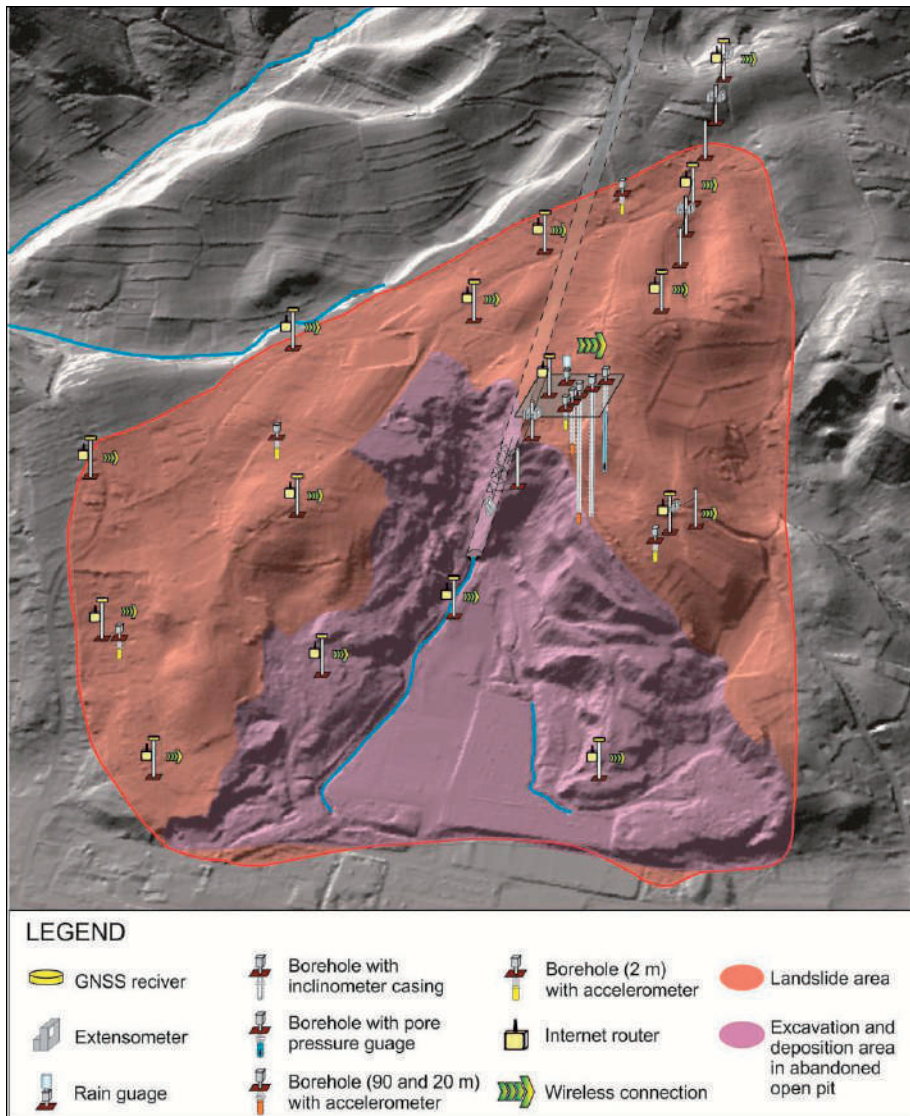


Figure 1 Sensor network at the Kostanjek landslide area established in the frame of scientific joint research of the Croatian-Japanese SATREPS project.

Based on the joint research in the frame of Croatian-Japanese project, the monitoring system of the Kostanjek landslide was designed to include a number of different types of instruments communicating in near-real time with a data transmission to the on-line centre located at the Faculty of Mining, Geology and Petroleum Engineering, University of Zagreb (UNIZG-RGNF). The system, whose conceptual design was outlined by Nagai et al. (2011), is meant to improve or influence public safety, public education, scientific research, and university education. The sensor network installed at the Kostanjek landslide area encompasses approximately 40 sensors for the monitoring of landslide movement and landslide causal factors. Fig. 1 provides the layout of the sensor network which is currently installed or is under installation at the Kostanjek landslide.

Sensors for displacement measurement

The sensors for displacement measurements provide a reliable data stream on a year-round basis and measure easily interpretable parameters of the superficial and subsurface movements. The displacement measurement sensor network includes 15 Global Navigation Satellite System (GNSS) receivers, 9 extensometers and 1 inclinometer.

A Trimble GNSS monitoring system consists of fifteen double-frequency NetR9 TI-2 GNSS reference stations with Zephyr Geodetic 2 GNSS antennas (Fig. 2a) installed on each of GNSS reference points. GNSS receivers are fixed to 4 meter high poles with 1 meter deep reinforced foundations (Fig. 2b). All monitoring stations are supplied with electricity from public network. Receivers collect GNSS raw data and deliver this

data in real-time, over communication lines (using routers), to Trimble 4D Control software (T4DC) installed on an application/data server in a data center at UNIZG-RGNF. GNSS receivers provide data on absolute positions of surficial points with precisions in the range of cm to mm.

The locations of GNSS receivers (Fig. 1) can be grouped as follows: above the landslide crown, i.e. outside the landslide area to check the assumption that

this area is stable (1 GNSS receiver); near the top of the abandoned slope cuts (4 GNSS receivers); inside of the abandoned open pit mine (3 GNSS receivers); along the western and north-western landslide border (5 GNSS receivers); and in northern part of landslide (2 GNSS). To be able to calculate very precise coordinates of 15 GNSS reference stations at the landslide area, the system needs at least one GNSS reference stations outside of the landslide zone.

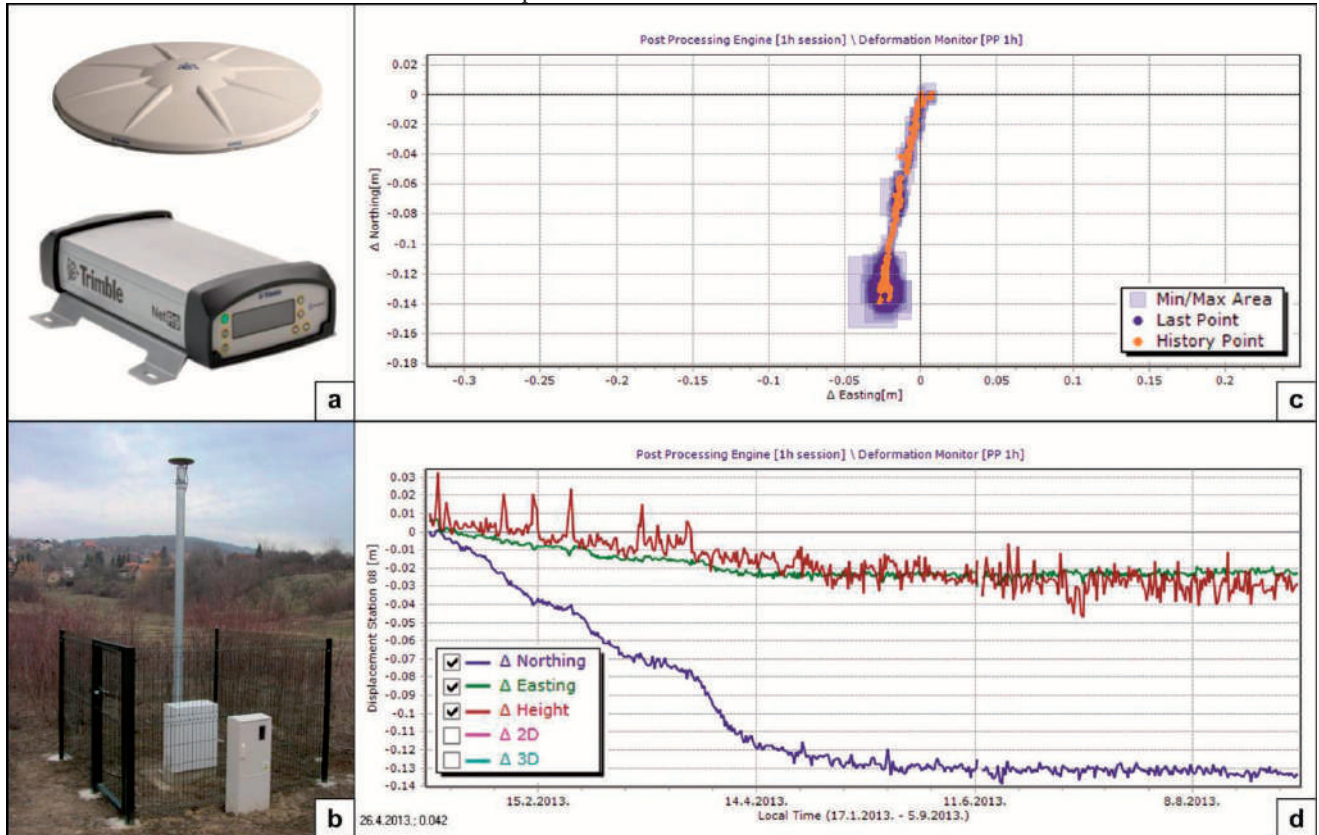


Figure 2 Trimble GNSS landslide monitoring system: (a) GNSS reference receiver NetR9 TI-2 GNSS and Zephyr Geodetic 2 antenna; (b) one of the GNSS monitoring locations with antenna at the top of 4 meter pole; (c) diagram showing direction of sliding of GNSS located in the centre of landslide; (d) diagram showing displacement components (easting, northing, vertical) of GNSS located in the centre of landslide.

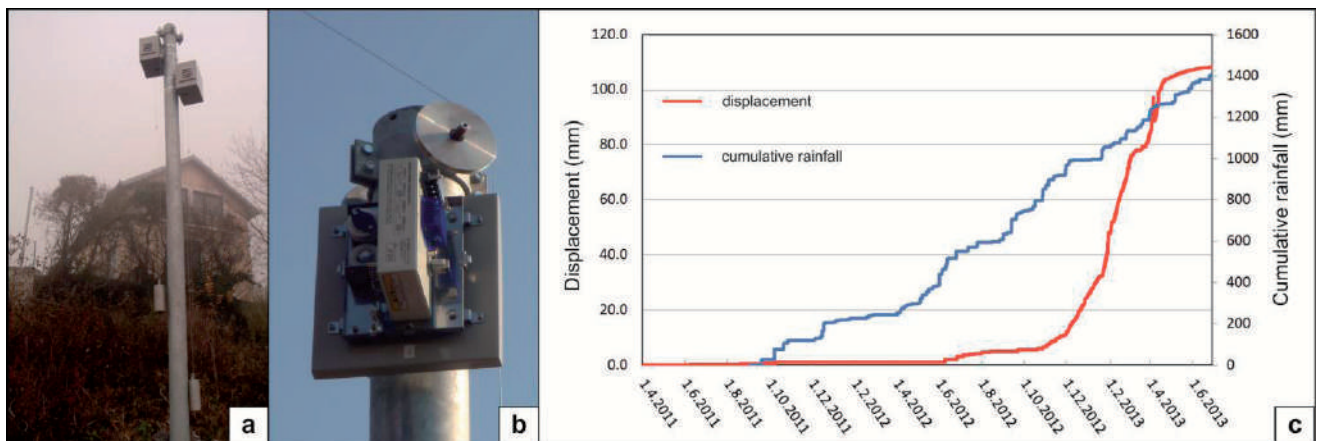


Figure 3 Osasi landslide monitoring system: (a,b) extensometers at the top of 4 meter pole; (c) diagram of extensometer displacement data compared to cumulative rainfall data obtained from rain gauge.

For that purpose, the system is using data from a permanent GNSS reference station in Gornji Stupnik (16th GNSS reference station), which is 7 km away from Kostanjek. T4DC monitoring software installed on an application/data server collects GNSS raw data and synchronizes, calculates and adjusts the collected data. It analyses measurement results, and it has capability to operate an alarm. One hour post processed data from the GNSS receiver in the central part of landslide are presented in Figures 2c and 2d.

The long- and short-span wire extensometers, type NetLG-501E Osasi, provide data on absolute deformation with submillimetre-level precision. Five long-span extensometers are placed from the top of the most stable point above the landslide, perpendicular to the main scarp, and in the direction of sliding. One short-span extensometer is placed perpendicular to the left landslide flank, where a scarp with steep displacement is clearly visible. Two long-span extensometers are installed to cross the crown of an artificial steep slope where the highest magnitude of displacement is expected. One

short-span extensometer is installed in the underground, in a tunnel which crosses the sliding surface. Extensometers with data loggers are fixed on 4 meter high poles (Fig. 3a,b) with reinforced foundations and some are on the same poles as the GNSS antennas. Data collection from extensometers is manual, but data transfer using routers is currently underway.

One inclinometer casing is installed in a 100 m deep vertical borehole in the middle of the landslide for measurements of the inclination of the pipe by a high-precision probe. The depth of the present-day major active shear surface is at 62.5 m (determined on the basis of two measurements, in May 2012 and February 2013). There is also some evidence of shallower sliding in the same borehole, at an approximate depth of 30 m. The deeper sliding surface is considered very important for the appraisal of future scenarios of the evolution of mass movement. Registered cumulative movement in last 8 months is approximately 4 cm (Fig. 4b).

Sensors for hydrological measurement

Sensors for hydrological measurements are necessary to provide background data that are useful in the interpretation of displacement measurement results, in terms of causes of sliding. The planned hydrological measurement sensors include a rain gauge and a meteorological station (rain, wind, temperature, barometric pressure). The rain gauge has been installed in the middle part of the landslide, at the central monitoring station, since 2011 (Fig. 4a). Work is currently underway to purchase a meteorological station. The data recorded from these sensors is being used to correlate observed displacements with meteorological changes.

Two outflow weirs, at the mouth of the abandoned tunnel (Fig 5) and on a spring outside the landslide area, and three water level sensors (two in domestic wells and one in a borehole) are installed to assess delays in superficial and groundwater discharge and pore pressure after precipitation. Initial measurements and

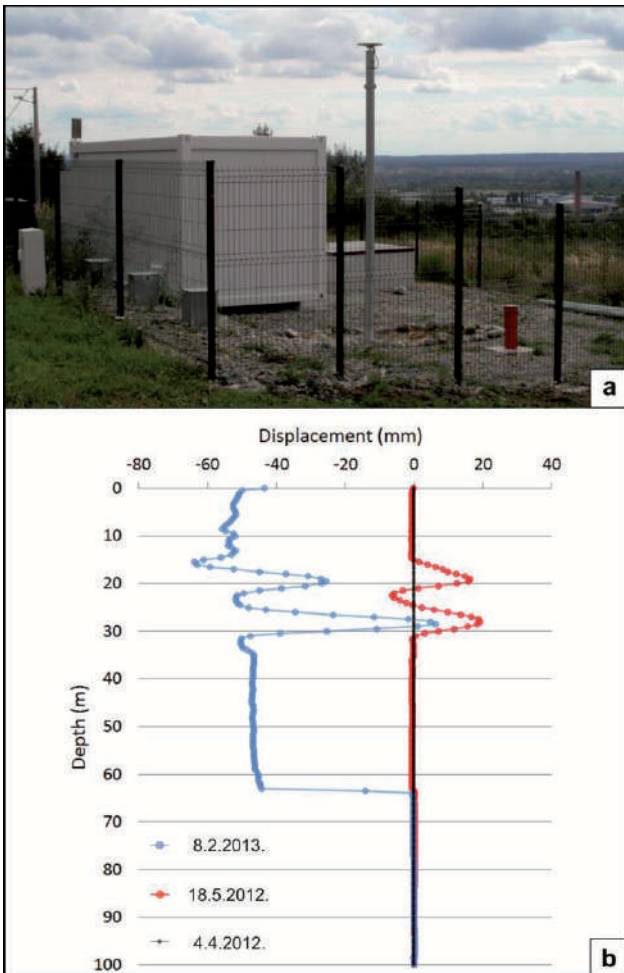


Figure 4 (a) Central monitoring station at Kostanjek landslide with container, rain gauge (upper left corner of container), GNSS antenna (on the 4 meter pole) and inclinometer (lower right); and (b) inclinometer data.



Figure 5 Entrance of the tunnel with outflow weir.

observations of hydrological conditions are presented in Krkač et al. (2011, 2014).

The purchase of three piezometers (pore pressure gauges) is currently underway to measure pore pressure and groundwater levels at two depths inside the landslide mass and one below the landslide. All hydrological sensors have a power supply from batteries because of their low power consumption. Until now, data collections have been manual, but data transfer using routers is currently underway.

Sensors for geophysical measurement

The geophysical measurement sensor network encompasses seven accelerometers installed inside the landslide area for the purpose of (i) monitoring local micro-earthquake activity in the landslide area; (ii) monitoring regional earthquake activity, including strong motion; and (iii) monitoring of any ground tremors associated with the landslide, including possible ground inclination. This is a low cost and hi-fidelity broad-band monitoring system consisting of three-component MEMS accelerometer and three-channel autonomous broadband digital recorders with GPS to keep accurate synchronization between each other. A Seismic Source DAQ3-3 3CH high-fidelity digital logger with accurate GPS clocking enables continuous recording (Fig. 7c), with data harvesting by the attached USB memory every three weeks.

Three accelerometers (Colibrays SF1500S.A) modified and adjusted for borehole installation (Fig. 6a) are installed in three boreholes at the central monitoring station in the middle part of the landslide: one is in 90 m deep borehole below the sliding surface; one is in a 20 m deep borehole inside the landslide body; and one is in a shallow borehole near the surface. Four accelerometers (Colibrays SF3000L, Fig. 6b) are installed near the surface, in shallow boreholes at depths of approximately 1.5 m. They are spatially arranged to cover all parts of the landslide area that are supposed to be separate landslide bodies: the upper part of the landslide, the left (eastern) landslide flank and the adjacent valley with shallow creeping phenomena.

Conclusion

Movements of the Kostanjek landslide cause, on a yearly basis, damage to private houses and infrastructure. Moreover, a very attractive city area of abandoned cement factory has been situated near the toe of the landslide over the last 50 years, which has prevented development of this part of the city.

The monitoring system of Kostanjek landslide is designed to measure changes in conditions that affect the potential for a reactivation of sliding and to provide early warning of extreme conditions to authorities responsible for emergency preparedness. The public education role of the landslide monitoring system involves raising the level of awareness of the general public regarding hazardous sliding and its potential impacts. The scientific research role of the system is to provide long-term monitoring data that can be used to gain a better understanding of the mechanisms associated with landslide in hard soil-soft rock (Pannonian and Sarmatian marl), and to advance the development of technology in landslide monitoring. Finally, a monitoring system that is housed at the UNIZG-RGNF has the potential to increase the educational potential of the University of Zagreb, and thereby benefit the national educational capacities.

The Kostanjek landslide monitoring system is almost completely finished with the installation of monitoring equipment. The next stage of system setup is the establishment of automated data transmission from almost all of 40 sensors. So far, the data transmission is set up for 15 GNSS sensors. In order to integrate the data from all sensors in the Geographic Information System (GIS), a customized GIS application is currently under development (Baučić et al. 2014).

Further activities related to monitoring system encompass forecasting of potential landslide failure in the periods of landslide reactivation. At first, the forecasting can be based on the Fukuzono (1985) method of inverse velocities and the Saito (1969) method of tertiary creep using data from extensometers and GNSS sensors. After a longer period of monitoring, data analysis should enable an estimation of the relationship between landslide causal factors and landslide displacement rates. This relationship will be used for the establishment

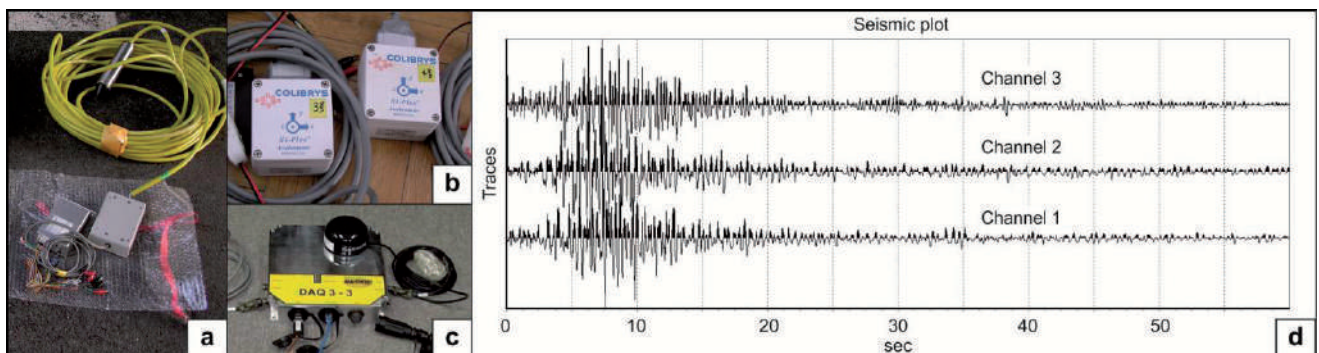


Figure 6 Geophysical monitoring system: (a) modified Colibrays SF1500S.A accelerometer for deep borehole; (b) Colibrays SF3000L accelerometer for shallow borehole; (c) data acquisition unit Seismic Source DAQ3-3 3CH with GPS; (d) seismogram.

of the threshold values for the early warning system.

Final activities at the Kostanjek landslide are related to warning and response and it should be implemented in collaboration with the following Zagreb City offices: (1) Emergency Management Office of the Zagreb City which deals with protecting activities against natural hazards; and (2) Zagreb City Office for Physical Planning, Construction of the City, Utility Services and Transport which deals with landslides remediation.

Acknowledgments

Results presented herein have been obtained with the financial support from JST/JICA's SATREP Program (Science and Technology Research Partnership for Sustainable Development). Ministry of Science, Education and Sports of the Republic of Croatia have been financing preparatory and installation works. City Office for Physical Planning, Construction of the City, Utility Services and Transport, City of Zagreb enabled and financed supply of the system with electricity from public network. These supports are gratefully acknowledged.

We would like to express our very great appreciation to the company Geomatika- Smolčak Ltd. for sponsoring the Kostanjek landslide monitoring system development with consultations during the planning and development of the system. Our special thanks are extended to our colleague Ms. Sanja Bernat for their support in the site and cabinet work.

Authors want to thank the Emergency Management Office of the City of Zagreb for continuous collaboration. We are also thankful to the City Office for the Strategic Planning and Development of the City, City of Zagreb for enabling us use digital data, orthophoto maps and LiDAR DEM.

We wish to thank numerous citizens and the City of Zagreb for their contribution to this project, by enabling use of private and City's land for measurement stations establishment.

References

- Baučić M, Mihalić Arbanas S, Krkač M (2014) Geographic information system of landslide Kostanjek: Integration of real-time GNSS monitoring data with other sensor data. Proceedings of the 1st Regional Symposium on Landslides in the Adriatic-Balkan Region, 6-9 March 2013. Croatian Landslide Group, Zagreb, Rijeka, Croatia. (in press)
- Fukuzono T (1985) A new method for predicting the failure time of a slope. Proceedings of IVth ICFL. Japan. pp. 145-150.
- Krkač M, Rubinić J, Mihalić S (2011) Kostanjek Landslide - analyses of groundwater discharge as a basis for the new hydrological monitoring. Proceedings of the 2nd Workshop of the Project Risk Identification and Land-Use Planning for Disaster Mitigation of Landslides and Floods in Croatia, 15-17 December 2011. Rijeka, Croatia. pp. 17-20.
- Krkač M, Rubinić J, Kalajžić J (2014) Analysis of water fluctuation dynamics in the wider area of the Kostanjek landslide. Proceedings of the 1st Regional Symposium on Landslides in the Adriatic-Balkan Region, 6-9 March 2013. Croatian Landslide Group, Zagreb, Rijeka, Croatia. (in press)
- Nagai O, Krkač M, Mihalić S (2011) Introduction of one of methods to predict failure time of a slope widely used in Japan and application to the Kostanjek Landslide. Proceedings of the 2nd Workshop of the Project Risk Identification and Land-Use Planning for Disaster Mitigation of Landslides and Floods in Croatia, 15-17 December 2011. Rijeka, Croatia. pp. 46-50.
- Ortolan Ž (1996) Development of 3D engineering geological model of deep landslide with multiple sliding surfaces (Example of the Kostanjek Landslide). PhD thesis. Faculty of Mining, Geology and Petroleum Engineering, University of Zagreb, Zagreb. 236p. (In Croatian)
- Ortolan Ž, Pleško J (1992) Repeated photogrammetric measurements at shaping geotechnical models of multi-layer landslides. Rudarsko-geološko-naftni zbornik. 4: 51-58.
- Saito M (1969) Forecasting time of slope failure by tertiary creep. Proceedings of the 7th International Conference on Soil Mechanics and Foundation Engineering, Vol. 2. Mexico City, Mexico. pp. 677-683.
- Županović Lj, Opačić K, Bernat S (2012) Determination displacements of landslides Kostanjek with relative static method. Ekscentar. 15: 46-53. (In Croatian)

Geographic Information System of the Kostanjek Landslide: Integration of Real-time GNSS Monitoring Data with other Sensor Data

Martina Baučić⁽¹⁾, Snježana Mihalić Arbanas⁽²⁾, Martin Krkač⁽²⁾

1) University of Split, Faculty of Civil Engineering, Architecture and Geodesy, Split, Croatia; Geodata d.o.o. Split, Croatia, Kopolica 62, +385 21 490497

2) University of Zagreb, Faculty of Mining, Geology and Petroleum Engineering, Zagreb, Croatia

Abstract The Kostanjek landslide monitoring system consists of more than 40 sensors permanently installed at the more than 20 locations in the field: (1) sensors for displacement measurement (GNSS receivers, short- and long-span extensometers); (2) sensors for hydrological measurements (rain gauge, outflow weirs, water level sensors, piezometers); and (3) sensors for geophysical measurements (accelerometers). This paper shortly presents concept of the Geographic information system (GIS) of Kostanjek landslide which has been developing with the primary objective: integration of real-time GNSS monitoring data with other sensor data. To integrate and visualize GNSS monitoring data, GIS is connected to MS SQL database and it reads GNSS data, transferred to server via communication devices. A new MS SQL database has been created for storing measurement data, and new application has been developed for import and geolocating data which are transferred to server manually. To integrate and visualize sensor data, GIS is connected to sensor database in MS SQL database. The GIS functions are realized using ESRI ArcGIS software. An ArcGIS comprehensive map is created and it shows topographic data, landslide features, GNSS monitoring data and sensor data. The users can use all the ArcGIS functions for creating their own maps and analyze data. The main advantage of data integration into one GIS system is to enable consistent and reliable framework for long-term archiving of all types of data which will be used in further analyses.

Keywords Kostanjek landslide, landslide monitoring system, monitoring data integration, GNSS, GIS

Introduction

The Kostanjek landslide is located on the south hills of Medvednica Mt. in western part of the Zagreb city. It has an estimated volume of up to 32.6 Mm³ and is slow

moving landslide moving at a velocity of up to 44 cm/year, which was maximum velocity reached in the period 1974-1976 according to Ortolan (1996). Catastrophic failure of the landslide mass would endanger urbanized area with total size 1,2 km². Because of the size of the moving landslide mass, remedial engineering measures are prolonged for 50 years till now. Consequently, the landslide risk must be managed by implementing an effective early warning system based on long-term continuous landslide monitoring (Bazin 2012). A major monitoring and early warning program were begun at the Kostanjek landslide in 2011 in the frame of the scientific joint-research bilateral Croatian-Japanese SATREPS FY2008 project (Mihalić and Arbanas 2013).

Monitoring can be generally defined as the systematic repetition of observations of a particular object or area (Fig. 1). Landslide monitoring in particular comprises a number of different tasks that will influence the choice of the optimal technique which can be applied to landslide detection, fast characterization, rapid mapping and long-term monitoring (Stumpf et al. 2011). The objective of Kostanjek landslide monitoring is long-term monitoring which implies processing data for retrieving deformation patterns and time series. Long-term monitoring of the Kostanjek landslide is necessary, because it was identified as active landslide in the last 50 years (in 1963) and repeated activity in the future has to be anticipated. Long-term monitoring of the Kostanjek landslide is required to: i) implement an early warning system; ii) to validate the kinematic model formulated for the landslide 17 years ago (Ortolan 1996); iii) to check the effectiveness of the stabilization or other remedial measures and, once they will be applied.



Figure 1 Definition of monitoring as the systematic repetition of observations (Stumpf et al. 2011).

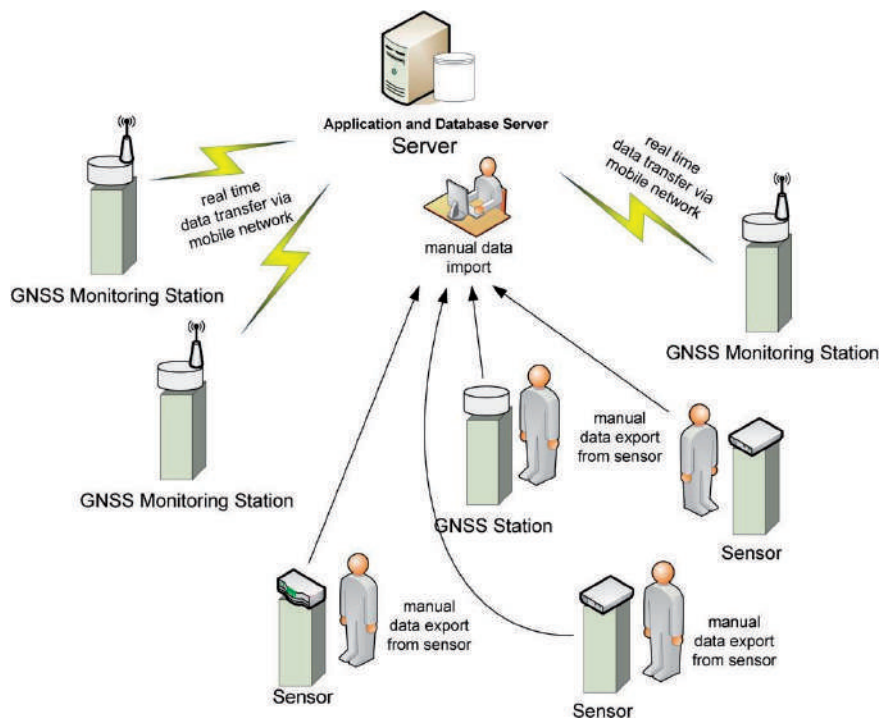


Figure 2 GNSS monitoring and sensor data transfer to server.

The Kostanjek landslide monitoring system has been establishing from 2011. Assessments over large landslide area (total size of the Kostanjek landslide is 1,2 km²) require consequently the installation of networks composed of many instruments, and the accomplishment of a field work in which many traditional measures are performed at many discrete points. According to the list of 15 European landslides for which real data collection and analysis is established (published in Baron et al. 2012), this site belongs to 3 the biggest one. The core of the monitoring system consists of 15 GNSS reference stations (dual frequency), 9 long- and short-span wire extensometers, 1 inclinometer, 4 vertical wire extensometers, 3 piezometers in one borehole up to 70 meters deep, 1 rain gauge, 3 water level sensors and 5 accelerometers (Mihalić Arbanas et al. 2013). Among observations using instruments installed at the landslide site, there are numerous periodical monitoring of ground water level in wells, discharge measurement in superficial streams etc. (Krkač et al. 2014). As a result, the costs and the time needed to gather the required amount of data may increase dramatically. Moreover, the possibility to focus on data that show signs of activity (e.g., places of larger displacements or increased velocities etc.) can be crucial for practical applicability of the system.

This paper summarizes the concept of the geographic information system (GIS) of Kostanjek landslide which has been developed with the primary objective of integration of real-time GNSS monitoring data with other sensor data. There are 15 GNSS monitoring stations with real-time data transfer to server,

and more than 20 sensors with manual data transfer (Fig. 2). The server for landslide data and applications resides at Faculty of Mining, Geology and Petroleum Engineering in Zagreb. The prerequisite for integration was to establish GIS connection to GNSS monitoring data and to store, read and geolocate measurements data from all sensors.

Geographic information system of Kostanjek landslide

At first, the broader information system architecture has been designed. The main users, functions and subsystems are identified. The main groups of users are: Faculty of Mining, Geology and Petroleum Engineering in Zagreb, local government (Emergency Management Office of the City of Zagreb and City Office for Physical Planning, Construction of the City, Utility Services and Transport) and regional government (National Protection and Rescue Directorate of the Republic of Croatia), contracted companies and scientific public. The four subsystems are: GNSS monitoring, Sensor data, GIS and Alerting. The identified GIS subsystem functions are: storing geodata, integrating and visualizing geodata from other subsystems, geo-analyzing, preparing views and downloads.

GNSS monitoring subsystem

The GNSS monitoring subsystem consists of 15 GNSS monitoring stations installed at 15 fixed poles at the Kostanjek landslide area of 1,2 km². The GNSS monitoring stations are equipped with communication devices for

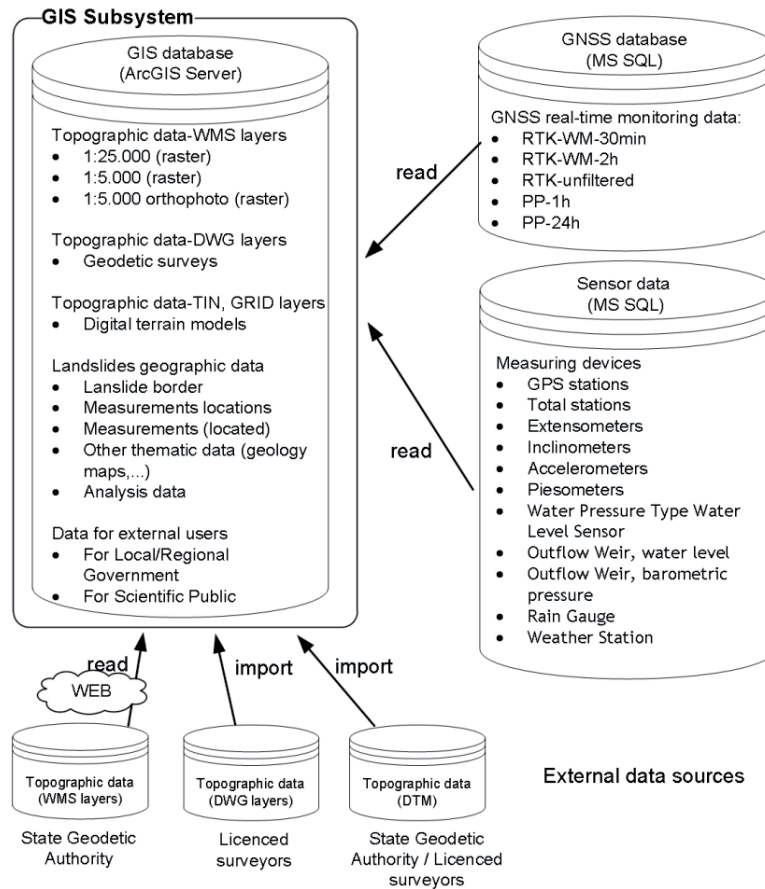


Figure 3 GIS layers.

automated data transfer to server (Fig. 3). MS SQL database and complex Trimble T4D monitoring software reside on server. T4D manages with GNSS data in SQL database and performs GNSS station set-up, data collection, transfer, storage, processing, analyze, viewing and alarming.

Today, the following measurements are present in the GNSS Monitoring Subsystem:

- RTK, unfiltered
- RTK, filtered (weighted mean 30 min)
- RTK, filtered (weighted mean 2 hours)
- Post-processing 1 hour
- Post-processing 24 hours.

The GNSS Monitoring Subsystem allows changes and adding of new types of processed GNSS data. To integrate and visualize GNSS data, GIS is connected to MS SQL database and it reads GNSS data.

Sensor data subsystem

Sensor data subsystem contains different types of measurements coming from geodetic, geotechnical and hydrological sensors covering more than 50 locations at the area of the Kostanjek landslide: 37 stable geodetic points temporarily measured by GNSS; 9 extensometers, 1

inclinometer, 7 accelerometers, 4 water level sensors and 1 rain gauge.

Data are stored in sensor specific device (e.g. data logger, memory card), and using sensor specific data format and structure (e.g. CSV file format). Measurements data is now exported from the sensor manually, by copying file from sensor data logger or memory card to server.

To enable data integration and GIS connection to sensor data, various sensors data formats and structures are converted in one data model of standard relational database. There are three main entities in the data model: sensor, location and measurement. Therefore, a new MS SQL database has been created for storing sensor data, and an application has been developed for import and geolocating. To integrate and visualize sensor data, GIS is connected to sensor database in MS SQL database.

Geographic information subsystem

The main GIS functions are:

- storing landslide geographic and geolocated data
- integrating and visualizing topographic, landslide, GNSS monitoring and sensor data, by showing on map in common geographic reference system

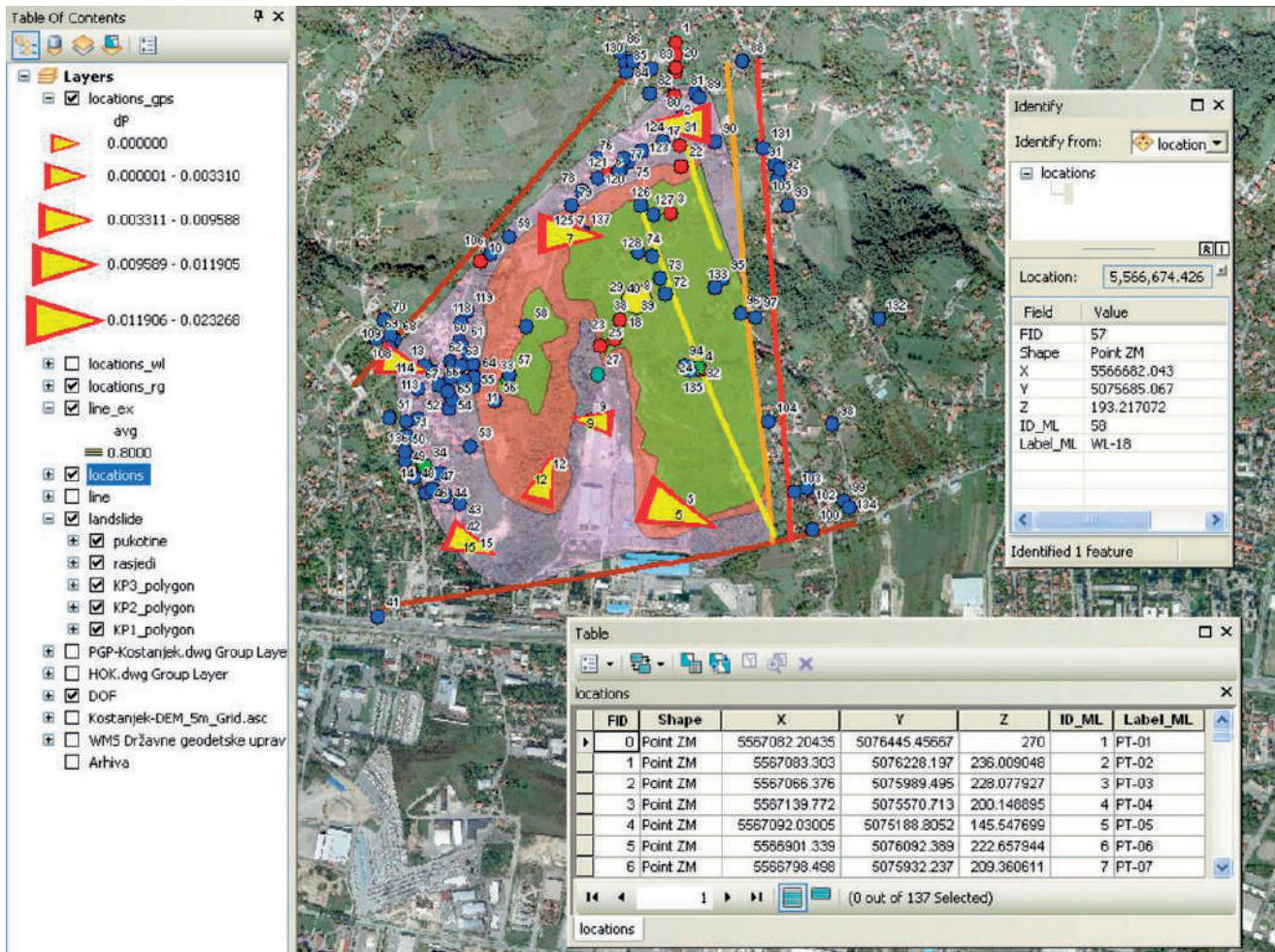


Figure 4 ArcGIS map.

- geoanalyze landslide data
- preparing views and downloads for users (via e-services).

An initial GIS database is created and stored on server. The GIS layers are shown on Figure 4. The GIS subsystem functions are realized using ESRI ArcGIS software. An ArcGIS map is created and it shows topographic data, landslide features, GNSS monitoring data and other measurements data. The users can use all the ArcGIS functions for creating their own maps and analyze geodata.

Achievements

In this paper, the development of GIS of landslide Kostanjek has been described. GNSS and other sensor data are integrated and visualized. Data from various sensors in specific data structures are now stored in one data model in MS SQL database.

The improvement of existing system will be to automatically transfer data from the sensors to the server. Thus, the system will have access to real time sensors

data what is crucial for implementation of an effective early warning system. In order to achieve this it is necessary to add communications equipment to each sensor, and to install an application to server that will import and store measurements in a database.

The effort described here has proved all the complexity of collecting different types of data for landslide characterization and monitoring. There are also additional types of data collected from time to time (e.g., seasonally) by sampling in the field (e.g., water level measurement, chemical and mineralogical content of water, rock and soil etc.). Here, we coped only with data and all its heterogeneity. As Kandawasvika (2009) stated: 'The major problem is how to integrate or manage simultaneously these various, heterogeneous sensors within that single application space'.

The main advantage of data integration into one GIS system is to enable consistent and reliable framework for long-term archiving of all types of data which will be used in further analyses. Most of monitoring parameters of the Kostanjek landslide monitoring system can be grouped as follows: slope movement / deformation / activity (displa-

cement); hydrologic properties (ground water level/pore-water pressure, water balance, inflow and outflow, surface flow; surface and subsurface water quality); external triggers (meteorological conditions and seismicity/earthquakes).

We hope that we will continue with analysis. Landslides are dynamic features of reality, and as such require advanced models of spatiotemporal data, spatiotemporal analysis and spatiotemporal reasoning.

Acknowledgments

Results presented herein have been obtained with the financial support from JST/JICA's SATREPS Program (Science and Technology Research Partnership for Sustainable Development). This support is gratefully acknowledged. We would like to express our very great appreciation to the company Geomatika- Smolčak Ltd., Trimble Germany and Geodata Ltd. for consultations during the planning and development of the system. Our special thanks are extended to our colleagues Mr. Nenad Smolčak, Ms. Daniela Koch and Mrs. Daniela Staničić for their support during the work.

References

- Baroň I, Supper R, Ottowitz D (2012) Report on evaluation of mass movement indicators. SafeLand deliverable D4.6. Geological Survey of Austria. Vienna, Austria. 382p.
- Bazin S (2012) SafeLand guidelines for landslide monitoring and early warning systems in Europe - Design and required technology. Geophysical Research Abstracts, Vol 14, EGU2012-1347-2, EGU General Assembly.
- Kandawasvika A (2009) On Interoperable Management of Multi-Sensors in Landslide Monitoring Applications. PhD thesis, The Universität der Bundeswehr München, Germany.
- Mihalić S, Arbanas Ž (2013) The Croatian–Japanese Joint Research Project on Landslides: Activities and Public Benefits. In Sassa K et al (eds). Landslides: Global Risk Preparedness, Springer-Verlag. (ISBN: 978-3-642-22086-9). pp. 335-351.
- Mihalić Arbanas S, Arbanas Ž, Krkač M (2013) TXT-tool 2.385-1.2 A comprehensive landslide monitoring system: The Kostanjek landslide, Croatia. In Sassa K et al (eds). ICL Landslide Teaching Tool, ICL, Kyoto, Japan. (ISBN: 978-4-9903382-2-0). pp. 158-168.
- Krkač M, Rubinić J, Kalajžić J (2014) Analysis of water fluctuation dynamics in the wider area of the Kostanjek landslide. Proceedings of the 1st ICL ABN Regional Symposium on Landslides, 6-9 March 2013. Croatian Landslide Group, Zagreb, Rijeka, Croatia. (in press)
- Ortolan Ž (1996) Development of 3D engineering geological model of deep landslide with multiple sliding surfaces (Example of the Kostanjek Landslide). PhD thesis, Faculty of Mining, Geology and Petroleum Engineering, University of Zagreb, Zagreb, Croatia. (In Croatian)
- Stumpf A, Kerle N, Malet JP (2011) Guidelines for the selection of appropriate remote sensing technologies for monitoring different types of landslides. SafeLand deliverable D4.4. Faculty for Geo-information Science and Earth Observation – ITC and University of Twente, United Nations University. Netherland. 91p.

Remote Monitoring of a Landslide Using an Integration of GPS, TPS and Conventional Geotechnical Monitoring Methods

Željko Arbanas⁽¹⁾, Vedran Jagodnik⁽¹⁾, Kristijan Ljutić⁽²⁾, Martina Vivoda⁽¹⁾, Sanja Dugonjić Jovančević⁽¹⁾, Josip Peranić⁽¹⁾

1) University of Rijeka, Faculty of Civil Engineering, Rijeka, Croatia, Radmile Matejčić 3, zeljko.arbanas@gradri.uniri.hr

2) 4D Monitoring Ltd, Milčetići, Milčetići 20, Croatia

Abstract Case studies of monitored complex landslides presented in scientific papers are numerous but, owing to variability of landslide types and behavior, goals of investigation, field conditions and the ongoing technological development of monitoring sensors, no standardized approach regarding the setting up of a monitoring system can be adopted as an universally solution. The monitoring results should provide a basis for develop and validate confidential numerical models and adequate hazard management. There are a lot of examples used in landslides practice those used different techniques and different devices (sensors) to monitor landslides activity. The use of multiple devices (sensors) at same points and for the same purpose (equipment fusion) should be very useful to guarantee redundancy of measurements that can prevent loss of data if one instrument fails. Selection of the same position for different type of monitoring devices (sensors) will also enable spatial correlation of measurement data on the landslide surface and trough the landslide profile. Using of geodetical and geotechnical equipment fusion in combination with hydrological monitoring equipment, which should be consisted of pore pressure gauges and pluviometer or/and weather station, enable reconstruction of the relationship between rainfalls, groundwater level and appropriate landslide behavior as a basis for an early warning system establishment. In beginning of the an early warning system establishment, the most important step is to link device measurement and possible failure mechanism and consequences those should following the sliding occurrence (the landslide risk). Based on presumptions described before, an advanced comprehensive monitoring system was designed and applied on the Grohovo Landslide. The crucial role in equipment (and sensor fusion) selection had scientific requirements and the equipment fusion request was based on consideration of possible ranges of monitored values and sensors precision. Establishment of an early warning system and defining of alarm thresholds should be based on existing cognition of the Grohovo Landslide behavior so as on collected comprehensive monitoring data. The focus of the early warning system establishment at the Grohovo Landslide must be on effective device combination (equipment fusion) results

with respect to device malfunction detecting and reduction of false alarms in the future. Reliability of an early warning system is dependent on the weakest link in the system. The weakest link in the Grohovo monitoring system is power supply and data transmitting from the field PC to the control room at the Faculty of Civil Engineering University of Rijeka. In this paper the main ideas and advances of the monitoring equipment fusion so as weaknesses of the monitoring system at the Grohovo Landslide will be presented. Based on 18 months period of measurement results the weaknesses of existing monitoring system were located and necessary improvements are analyzed and partially involved. Without these improvements, the future early warning system will be vulnerable and reliability of the system will be too low to use it as a practical application.

Keywords landslide, monitoring system, sensor, sensor fusion, early warning system

Introduction

Landslides are, by definition, characterized by movement. Landslide movement monitoring expressed via ground surface displacements and deformation of the landslide body related to sliding can be accomplished using different types of monitoring systems and techniques. Comprehensive monitoring systems include different type of techniques and equipment (sensors) and a selection of measurement instrumentation and methods or the planning and design of a desirable monitoring system depends on the movement types and deformation as well as on the role and purpose of the monitoring campaign (Savvaidis 2003). The monitoring system should be suitable, the instrumentation should be installed at the correct locations and extend below the sliding zone, and the collected data should be regular, accurate, reliable, usable, and submitted to the users in a timely manner. Establishment of landslide monitoring system requires an adequate design and plan of installation and operating. Dunncliff (1988) stated: 'Every instrument on a project should be selected and placed to assist with answering a specific question; if there is no question, there should be no instrumentation'.



Figure 1 Aerial view at the Grohovo Landslide, May 2011.

The Grohovo Landslide, located outside of the City of Rijeka, Croatia, was chosen as a pilot area for comprehensive integrated real-time monitoring system development in the frame of Croatian-Japanese joint research project “Risk identification and Land-Use Planning for Disaster Mitigation of Landslides and Floods in Croatia” initiated in 2009 (Mihalić and Arbanas 2013). The Grohovo Landslide is the largest active landslide along the Croatian part of the Adriatic coast and it is located on the north-eastern slope of the Rječina River Valley. Slopes of the Rječina River Valley are prone to sliding and there are numerous documented landslides occurred in the wider area of the Grohovo Landslide in the recent history (Arbanas et al. 2010). The last complex retrogressive reactivated landslide occurred in December 1996, after 100 year of dormant period and about 3.0×10^6 m³ moved down the slope and buried the Rječina riverbed (Benac et al. 2005) (Fig.1).

The comprehensive monitoring system was designed and the most of monitoring instrumentation was installed from March 2011 to November 2012. The first 18 months of monitoring system operating resulted with significant cognitions related to the system behavior (Arbanas et al. 2012a) and pointed on weaknesses and deficiencies of the system those should be solved to ensure regular, accurate, reliable, usable measurement data necessary for any landslide behavior analysis.

The Grohovo Landslide Monitoring System

The comprehensive monitoring system at the Grohovo Landslide is consisted of geodetic and geotechnical monitoring (Arbanas et al. 2012a,b). Geodetic monitoring includes geodetic surveys using a robotic total station that measures positions of 25 prisms and displacement measurements of GPS receivers (9 rovers and 1 master unit). The robotic total station and the GPS master unit are located in a relatively stable area, on the top of the opposite slope. The monitoring master unit consists of the robotic total station TM30 Leica, single frequency GPS master unit GMX901 Leica (combined receiver and

antenna), meteorological sensor and web cam. Equipment for the geotechnical monitoring includes vertical inclinometers, long and short-span wire extensometers, pore pressure gauges and weather station. Pore pressure gauges (four pieces), inclinometers (two inclinometer casings) and vertical extensometers (four pieces) are installed at two main monitoring points inside the central part of the landslide body. Wire extensometers (12 long span extensometers and three short span) are installed from the Rječina riverbed to the limestone mega-blocks at the top of the slope and over open cracks in limestone mega-blocks at the landslide crown. All monitoring equipment will be connected in one system with continuous monitoring, collect the data at the master field unit and field PC workstation and export the data to the central computer unit located at the Faculty of Civil Engineering, University of Rijeka. In the next step establishment of an early warning system for possible landslide reactivation and assessment of landslide risk, based on the monitoring results would be carried out (Arbanas et al. 2010, 2012c).

The monitoring master field unit and field PC workstation at the Veli Vrh location are powered using the hybrid mini power plant consisted of 1 KW 6 solar panels and 500 W windmill connected in the integrated power system that can produce about 1,5 kW of electrical energy in peak production constructed nearby the monitoring master unit. GPS rovers located in the landslide body are powered by one pair of solar panels.

Data from a geodetic equipment (GPS, robotic total station) continuously collected through the landslide's local Wi-Fi network into the SQL database installed on the field PC workstation at the Veli Vrh location, which is wirelessly (by UMTS mobile data connection) connected to the main PC unit at the Faculty of Civil Engineering. Such a data acquisition ensures continuous data collection and processing using System Anywhere software. Geotechnical part of the devices (long and short span wire extensometers, pore water pressure gauges, rain gauge) will be included in the same integrated system during 2013. All data collected from geotechnical monitoring equipment should be directly downloaded from data loggers or directly measured in the field. Field trips for data downloading should be well planned and organized, taking into account all the necessary details to ensure successful data collection (weather conditions, tools, accessories, batteries etc.). Collected data from geotechnical monitoring devices are less frequently available and cannot presents an actual overview of landslide behavior necessary for establishment of an early warning system.

Integration of GPS, TPS and conventional geotechnical monitoring methods

Case studies of monitored complex landslides presented in scientific papers are numerous but, owing to

variability of landslide types and behavior, goals of investigation, field conditions and the ongoing technological development of monitoring sensors, no standardized approach regarding the setting up of a monitoring system can be adopted as an universally solution. Comprehensive monitoring systems have been established on numerous landslides throughout the world and certain of them are described in detail, that is, the Ancona Landslide (Cotecchia 2006), Corvara Landslide (Corsini et al. 2005), Tessina Landslide (Angeli et al. 2000; Tarchi et al. 2003; Hervas et al. 2003; Petley et al. 2005), and Valoria Landslide (Bertacchini et al. 2009) in Italy; the Gradenbach deep-seated mass movement (Brückl et al. 2006) in Austria; the Åknes rockslide (Blikra 2012) in Norway; the rockslide at Turtle Mountain (Froese et al. 2012) in Canada; and the Grohovo Landslide (Arbanas et al. 2012a, Benac et al. 2011) in Croatia. The monitoring results should provide a basis for develop and validate confidential numerical models and adequate hazard management. There are a lot of examples used in landslides practice those used different techniques and different devices (sensors) to monitor landslides activity. The use of multiple devices (sensors) at same points and for the same purpose (equipment fusion) should be very useful to guarantee redundancy of measurements that can prevent loss of data if one instrument fails. Selection of the same position for different type of monitoring

devices (sensors) will also enable spatial correlation of measurement data on the landslide surface and trough the landslide profile. Using of geodetical and geotechnical equipment fusion in combination with hydrological monitoring equipment, which should be consisted of pore pressure gauges and pluviometer or/and weather station, enable reconstruction of the relationship between rainfalls, groundwater level and appropriate landslide behavior as a basis for early warning system establishment. In beginning of the an early warning system establishment, the most important step is to link device measurement and possible failure mechanism and consequences those should following the sliding occurrence (the landslide risk).

Based on previously described presumptions, an advanced comprehensive monitoring system was designed and applied on the Grohovo landslide. Previously described remote monitoring of the landslide using an integration of GPS, TPS and conventional geotechnical monitoring methods is established using different combination of sensor fusion. The crucial role in equipment (and sensor fusion) selection had scientific requirements and the equipment fusion request was based on consideration of possible ranges of monitored values and sensors precision. The positions of sensors in the landslide are presented on Figure 2, while the list of sensor is presented in Table 1.

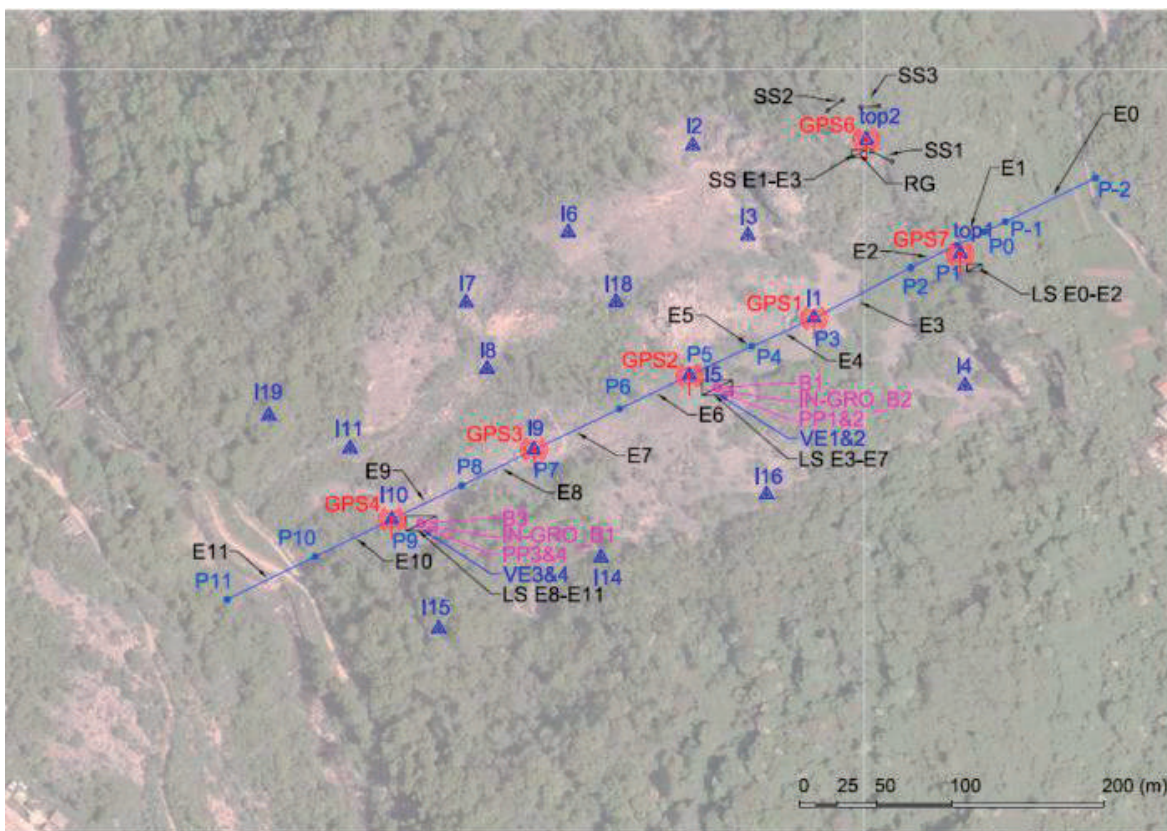


Figure 2 Installed sensors at the Grohovo Landslide: GPS - GPS rover; I - prism; E - long span wire extensometer, P - extensometer pole; SS -short span extensometer; B - position of borehole; IN - inclinometer casing in borehole; VE - vertical extensometer in borehole; PP - pore pressure gauge in borehole; LS -long span extensometer data logger; RG - rain gauge.

Table 1 Installed geodetical and geotechnical monitoring sensors (equipment) integrated in the Grohovo Landslide Monitoring System.

Sensor	Label	Number	Monitoring Techniques
GPS Rover	GPS	9	Geodetical Monitoring
TPS Prism	I	25	
Long Span Wire Extensometer	E	12	Geotechnical Monitoring
Short Span Wire Extensometer	SS	3	
Vertical Wire Extensometer	VE	4	
Inclinometer Casing	IN	2	
Pore pressure Gauge	PP	4	
Rain Gauge	RG	1	

The main monitoring points are established in the central part of the landslide where the most of purchased geotechnical sensors were installed in fusion with geodetical sensors. At two locations (B1 and B3, Fig. 2) 23 and 25m depth inclinometer casings were installed in with coring drilled boreholes. Along the inclinometer casing two wire extensometers were installed related to two orthogonal casing axes. In inclinometer nearby borehole two pore pressure gauges, one above one below the slip surface, were installed. At the same location the extensometer pole with geodetic prism and GPS receiver at the top of the pole is constructed. Long span extensometer wires were connected to the pole linked in continuous extensometers' line over the landslide. The view at the main monitoring point B3 in the landslide is presented on Figure 2, while the list of sensors in fusion and sensor roles in the monitoring system are presented in Table 2.

Table 2 Installed geodetical and geotechnical monitoring sensors (equipment) in fusion at the B3 control point in the Grohovo Landslide Monitoring System.

Position	Sensor	Label	Measuring
B3	GPS Rover	GPS4	Global position at the surface
	TPS Prism	I10	Relative position at the surface
	2 Long Span Wire Extensometer	E9, E10	Relative deformation at the surface
	2 Vertical Wire Extensometer	VE3, VE4	Deformation of inclinometer casing
	Inclinometer Casing	INGRO B3	Horizontal deformation through the landslide profile
	2 Pore pressure Gauges	PP3, PP4	Pore pressures above and below slip surface



Figure 3 GPS rover and prism at the top of the pole and solar panel installation at the control point B3 in the Grohovo Landslide. Concrete box is round up construction for geotechnical monitoring equipment protection with inclinometer casing, vertical extensometers and pore pressure gauges inside (Arbanas et al. 2012a).

This integration enables correlation of measurement data on the landslide surface movements, measuring absolute and relative position of the control points using GPS and TPS with the movements in the landslide profile using measurement data obtained by inclinometers and vertical wire extensometers. Including the control points in the extensometers' line installed from the pole located below the landslide foot to the limestone mega-blocks at the landslide crown, positioning of the other extensometer poles in extensometers' line was enabled. Based on this fusion and integration of data from all extensometers in extensometers' line, the assessment of surface landslide deformation is possible. Data obtained from previously described equipment fusion in combination with hydrological monitoring data obtained from pore pressure gauges and pluviometer or/and weather station (installed outside of this particular equipment fusion) enables reconstruction of relationships between rainfalls, pore pressures and correspondent landslide behavior as a basis for landslide behavior prediction and an early warning system establishment.

Other sensor fusions in the monitoring system were established in relatively simple control combinations of GPS rovers and TPS prisms so as interpolation of GPS rovers and TPS prisms in long span wire extensometers' line.

Experiences obtained from 18 month measurement time period were needed for understanding relation between disturbing effects and their causes (Arbanas et al. 2012a,c,d) and procedures for equipment calibrating and effects of weather impacts on measurements

accuracy eliminating were established. An important role in understanding of disturbing effects and their causes had control effects which were arising from established correlations measured collected data obtained from integrated sensors in fusion.

Establishment of the Grohovo Landslide Early Warning System

Establishment of an early warning system and defining of alarm thresholds should be based on existing cognition of the Grohovo Landslide behavior so as from collected comprehensive monitoring data. The focus of an early warning system establishment at the Grohovo Landslide should be on effective monitoring sensor and equipment results with respect to device malfunction detecting and reduction of possible false alarms. The current state of the established monitoring system still not enables sufficiently long continuous series of monitoring data that would be ensured establishment of spatial, physical and phenomenological correlations on those a reliable prediction of the Grohovo Landslide behavior can be accepted. An important step in the system improvement by removing of system weaknesses and stabilization of the system should be conducted and continuous series of monitoring data should be ensured, especially for the period from September to end of March when the most of landslide occurrences in the past have been appeared.

Reliability of an early warning system is dependent on the weakest link in the system. The weakest link in the presently established Grohovo Landslide Monitoring System is power supply and data transmitting from the field PC, where all field data are collecting, to the control room at the Faculty of Civil Engineering University of Rijeka. Major part of the installed equipment is powered using solar panels power supply systems. The hybrid mini power plant consisted of 1 KW 6 solar panels and 500 W windmill connected in an integrated power system that can produce about 1,5 kW of electrical energy was designed and constructed near the monitoring master unit. GPS rovers located in the landslide body are powered by one pair of solar panels (Fig. 3). The hybrid mini power plant is not able to produce enough electric energy to keep working PC workstation, robotic total station, GPS master unit, weather station, web camera and wireless network communication system continuously during the late autumn and winter, especially during a series of cloudy days. Short daylight period and unfavorable sun position don't enable producing enough electric energy in this period while the existing windmill was seriously damaged in extreme gusts of the wind. The power supply system should be significantly improved to ensure enough electric energy in any weather conditions and year period.

Wi-Fi network used to transfer data from the equipment in the landslide area to the field PC workstation, as well as the UMTS data transfer to the

control center at the Faculty of Civil Engineering have been proved as stable and reliable.

Considering a landslide hazard in the monitored area of the Grohovo Landslide in the frame of an early warning system establishment it is necessary to:

- Identify real hazard of further sliding and possible direct and indirect threats;
- Identify possible movements and landslide widening with high hazard;
- Select appropriate equipment relating to position in the field and measurement accuracy as a competent equipment to startup an alarm and
- Define critical limit values (criteria values) that would indicate a new sliding appearance and start up an alarm (Arbanas et al. 2012c).

Based on results of conducted analyses the following positions of further movement and related threats are identifying:

1. Reactivated landslide in the landslide foot - Threat: Reactivated landslide cause covering of the Rječina River channel and forming a landslide dam and a lake behind it. After dam collapsing, the water wave will cause fatalities and serious damages in the City of Rijeka situated downstream the Rječina River. Related motoring sensors: sensors in fusion at monitoring point B3; lower part of extensometers' line.

2. Widening of the landslide to the Valići dam and occurrences of new landslides around Valići Lake - Threat: Filling the Valići Lake with a sliding mass causing water wave that can cause fatalities and serious damages at the Valići dam in the City of Rijeka situated downstream the Rječina River. Related motoring sensors: sensors (prisms) outside of the landslide body; sensors (GPS, prisms) at the Valići dam.

3. Retrogressive development of the landslide to the landslide crown - Threat: Widening of the landslide and destabilizing carbonate mega-blocks on the limestone scarps and endangering the Kačani and Ilovik villages located at the top of the slope. Related motoring sensors: sensors in fusion at monitoring point B1; upper part of extensometers' line; short span extensometers over the cracks; sensors (GPS, prisms) at the landslide crown.

Critical values for different levels of for startup of the alarm will be defined based on analyses of monitoring results obtained in the period after final equipment adjustment and elimination of weather influences on monitoring results. All measured critical values that would start up of the alarm, should be controlled using equipment in fusion. Analogues measured values or less effective and time consuming field check are necessary to confirm alarm start up for all alert levels.

Conclusions

The reactivated complex Grohovo Landslide was chosen as the pilot area for comprehensive integrated real-time monitoring system development in the frame of

Croatian-Japanese joint research project “Risk identification and Land-Use Planning for Disaster Mitigation of Landslides and Floods in Croatia”. The comprehensive monitoring system consisted of geodetical and geotechnical monitoring equipment was designed and monitoring equipment was installed during 2011 and 2012. The most of sensors in the system are integrated and at same points and for the same purpose (equipment fusion) to guarantee redundancy of measurements that can prevent loss of data if one instrument fails. Sensors fusion also enables spatial correlation of measurement data on the landslide surface and trough the landslide profile and in combination with hydrological monitoring equipment enables reconstruction of the relationship between rainfalls, groundwater level and appropriate landslide behavior as a basis for early warning system establishment. The weakest link in the presently established Grohovo Landslide Monitoring System is the power supply. The existing power supply system is not able to produce enough electric energy to keep working the master monitoring unit in the field and wireless network communication system continuously during the late autumn and winter period and it should be significantly improved to produce enough electric energy in any weather conditions and year period.

Acknowledgments

Equipment presented herein has been obtained with the financial support from JST/JICA's SATREPS Program (Science and Technology Research Partnership for Sustainable Development). This support is gratefully acknowledged.

References

- Angeli M-G, Pasuto A, Silvano S (2000) A critical review of landslide monitoring experiences. *Engineering Geology*, 55, 133–147.
- Arbanas Ž, Benac Č, Dugonjić S (2010) Dynamic and Prediction of future behavior of the Grohovo Landslide. In Proc. 1st Workshop of the Project Risk identification and Land-Use Planning for Disaster Mitigation of Landslides and Floods in Croatia, 22-24 November 2010, Dubrovnik, Croatia (in press).
- Arbanas Ž, Sassa K, Marui H, Mihalić S (2012a) Comprehensive monitoring system on the Grohovo Landslide, Croatia. In Proc. 11th International and 2nd North American Symposium on Landslides: Landslides and Engineered Slopes: Protecting Society through Improved Understanding, June 2-8, 2012. Banff, Canada, pp. 1441-1447.
- Arbanas Ž, Jagodnik V, Ljutić K, Dugonjić Jovančević S, Vivoda M (2012b) Establishment of the Grohovo Landslide monitoring system. In: Proc. 2nd Workshop of the Project Risk identification and Land-Use Planning for Disaster Mitigation of Landslides and Floods in Croatia: Monitoring and analyses for disaster mitigation of landslides, debris flow and floods, University of Rijeka, pp. 29-32.
- Arbanas Ž, Vivoda M, Jagodnik V, Dugonjić Jovančević S, Ljutić K (2012c) Consideration of early warning system on the Grohovo Landslide. In: Proc. 2nd Workshop of the Project Risk identification and Land-Use Planning for Disaster Mitigation of Landslides and Floods in Croatia: Monitoring and analyses for disaster mitigation of landslides, debris flow and floods, University of Rijeka, pp. 51-54.
- Arbanas Ž, Dugonjić Jovančević S, Ljutić K, Vivoda M, Jagodnik V (2012d) Initial results of the Grohovo Landslide monitoring. In: Proc. 2nd Workshop of the Project Risk identification and Land-Use Planning for Disaster Mitigation of Landslides and Floods in Croatia: Monitoring and analyses for disaster mitigation of landslides, debris flow and floods, University of Rijeka, pp. 33-36.
- Benac Č, Arbanas Ž, Jurak V, Oštrić M, Ožanić N (2005) Complex landslide in the Rječina River valley (Croatia): origin and sliding mechanism. *Bulletin of Engineering Geology and the Environment*. 64(4): 361-371.
- Benac Č, Dugonjić S, Vivoda M, Oštrić M, Arbanas Ž (2011) A complex landslide in the Rječina Valley: results of monitoring 1998-2010. *Geologia Croatica*. 64(3): 239-249.
- Bertacchini E, Capitani A, Capra A, Castagnetti C, Corsini A, Dubbini M, Ronchetti F (2009) Integrated surveying system for landslide monitoring, Valoria landslide (Apennines of Modena, Italy). In Proceedings of the FIG Working Week 2009, Surveyors Key Role in Accelerated Development, Eilat, Israel. International Federation of Surveyors (FIG), pp. 1-11.
- Blikra L S (2012) The Åknes rockslide, Norway. In J J Clague and D Stead (Eds), *Landslides – Types, Mechanisms and Modeling*, Cambridge, UK. Cambridge University Press, pp. 323-334.
- Brückl E, Brunner F K, Kraus K (2006) Kinematics of a deep - seated landslide derived from photogrammetric, GPS and geophysical data. *Engineering Geology*. 88: 149-159.
- Corsini A, Pasuto A, Soldati M, Zannoni A (2005) Field monitoring of the Corvara landslide (Dolomites, Italy) and its relevance for hazard assessment. *Geomorphology*. 66: 149-165.
- Cotecchia V (2006) The Second Hans Cloos Lecture. Experience drawn from the great Ancona landslide of 1982. *Bulletin of Engineering Geology and the Environment*. 65: 1-41.
- Dunnicliff J (1988) *Geotechnical instrumentation for monitoring field performance*. New York, NY: John Wiley and Sons.
- Froese C R, Charrière M, Humair F, Jaboyedoff M, Pedrazzini A (2012) Characterization and management of rockslide hazard at Turtle Mountain, Alberta, Canada. In J J Clague and D Stead (Eds), *Landslides – Types, Mechanisms and Modeling*, Cambridge, UK. Cambridge University Press, pp. 310-322.
- Hervas J, Barredo J I, Rosin P L, Pasuto A, Mantovani F, Silvano S (2003) Monitoring landslides from optical remotely sensed imagery: the case history of Tessina landslide, Italy. *Geomorphology*. 54(1-2): 63-75.
- Mihalić S, Arbanas Ž (2013) The Croatian-Japanese joint research project on landslides: activities and public benefits. *Landslides: Global Risk Preparedness*. Sassa K, Rouhban B, Briceño S, McSaveney M, He B (eds). Heidelberg: Springer. pp. 333-349.
- Petley D N, Mantovani F, Bulmer M H, Zannoni A (2005) The use of surface monitoring data for the interpretation of landslide movement patterns. *Geomorphology*. 66: 133-147.
- Savvaidis P D (2003) Existing landslide monitoring systems and techniques. In Proc. of the Conference from Stars to Earth and Culture, In honor of the memory of Professor Alexandros Tsoumis Thessaloniki, Greece: The Aristotle University of Thessaloniki, pp. 242-258.
- Tarchi D, Casagli N, Fanti R, Leva D D, Luzi G, Pasuto A, Pieraccini M, Silvano S (2003) Landslide monitoring by using ground-based SAR interferometry: an example of application to the Tessina landslide in Italy. *Engineering Geology*. 68: 15-30.

The Grohovo Landslide Monitoring System - Experiences from 18 Months Period of Monitoring System Operating

Kristijan Ljutić⁽¹⁾, Vedran Jagodnik⁽²⁾, Martina Vivoda⁽²⁾, Sanja Dugonjić Jovančević⁽²⁾, Željko Arbanas⁽²⁾

1) 4D Monitoring Ltd, Milčetići, Croatia, Milčetići 20, kristijan.ljusic@4d-monitoring.com

2) University of Rijeka, Faculty of Civil Engineering, Rijeka, Croatia

Abstract The Grohovo Landslide, the largest active landslide along the Croatian part of the Adriatic coast, is located on the north-eastern slope of the Rječina River Valley. In 2009, the Croatian-Japanese research joint project “Risk identification and Land-Use Planning for Disaster Mitigation of Landslides and Floods in Croatia” was initiated and the Grohovo Landslide was chosen as a pilot area for a monitoring system development. A comprehensive monitoring system was designed, consisted of geodetical and geotechnical monitoring equipment. Installation was started in March 2011 and, in a major part, completed till the end of 2011. This integrated monitoring system generally can be divided in two major parts: geodetical consisted of GPS system (9 rovers and 1 master unit), and robotic total station with 24 geodetical prisms; and geotechnical consisted of pore pressure gauges, inclinometers and extensometers. Establishment of the monitoring system was carried out in stages according to monitoring equipment purchasing process and equipment delivery. Installation of inclinometer casings and pore pressure gauges was started in March 2011 while foundations and poles for long span extensometers were completed in May 2011. Main part of geodetical monitoring equipment was installed in July 2011. After monitoring system was powered up and turned on, several problems in equipment functioning were observed and equipment readjustment was carried out until the end of November 2011. Observations from geodetic prisms with robotic total station and GPS system are collected and processed in the automated integrated monitoring system software. During the first 18 months of monitoring system operating, the equipment calibration, system improvement and maintenance took considerable part of the system establishment. Seasonal meteorological and atmospherical conditions significantly influenced on monitoring equipment and results. Extreme temperatures during late June and whole July 2012 influenced in uneven bending deformation of the main pillar which affected on total station position and leaning and, consequently, on its measurements. While solar panel system power supplies at the landslide are sufficient for GPS rovers, the hybrid power system consisted of 1 KW solar panels and 500 W windmill located at the Veli Vrh location, during

the late autumn and winter is not able to efficiently produce enough electric energy for main monitoring station consisted of PC workstation, robotic total station, main GPS unit, web camera and wireless network system to work continuously. However, collected measurement data are sufficient for observing the landslide in whole period, because of their consistent data trends and correlation between different data sets. In this paper the problems related to the installation and working of the system are described, as well as solutions those should improve the system for successful continuous work.

Keywords landslide, monitoring system, calibration, maintenance

Introduction

The Grohovo Landslide, the largest active landslide along the Croatian part of the Adriatic coast, is located on the north-eastern slope of the Rječina River Valley outside of the City of Rijeka. It was noted that during 19th and 20th centuries considerable instabilities on the Rječina Valley slopes occurred. The last complex retrogressive reactivated landslide was activated in December 1996, after long dormant period and about 3.0×10^6 m³ moved down the slope and buried the Rječina river-bed (Benac et al. 2005) (Fig.1).

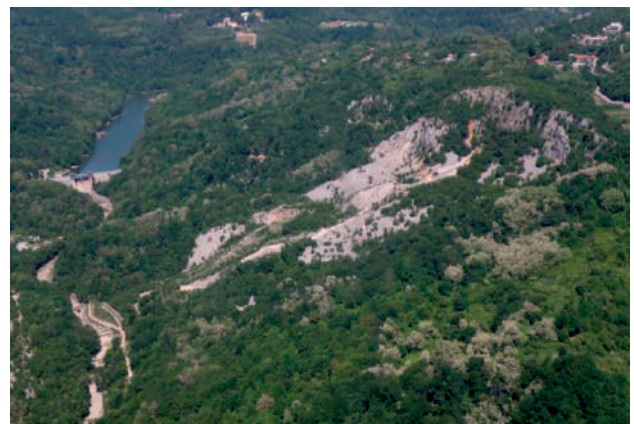


Figure 1 Aerial view at the Grohovo Landslide, May 2011.

In 2009 the Croatian-Japanese joint research project “Risk identification and Land-Use Planning for Disaster Mitigation of Landslides and Floods in Croatia” was initiated and the Grohovo Landslide was chosen as a pilot area for comprehensive integrated real-time monitoring system development (Mihalić and Arbanas 2013).

The comprehensive monitoring system at the Grohovo Landslide was designed to consist of geodetic and geotechnical monitoring (Arbanas et al. 2012a). Geodetic monitoring includes geodetic surveys with a robotic total station and displacement measurements of GPS points (9 rovers and 1 master unit). Equipment for the geotechnical monitoring includes vertical inclinometers, long span and short span wire extensometers, pore pressure gauges and weather station. Pore pressure gauges (four pieces), inclinometers (two inclinometer casings) and vertical wire extensometers (four pieces) are installed at two locations inside the central part of the landslide body. Wire extensometers (12 long span extensometers and three short span) are installed from the Rječina riverbed to the limestone mega-blocks at the top of the slope and over open cracks in limestone mega-blocks. All monitoring equipment will be connected in one system with continuous monitoring and export of the data to a central computer unit located at the Faculty of Civil Engineering, University of Rijeka. It was planned to establish an early warning system for possible landslide occurrence and assessment of landslide risk, based on the monitoring results (Arbanas et al. 2010, 2012b).

Major part of the installed equipment is powered using solar panels power supply systems. The hybrid mini power plant consisted of 1 KW 6 solar panels and 500 W windmill connected in an integrated power system that can produce about 1,5 kW of electrical energy in peak production was designed and constructed at the Veli Vrh location near the monitoring master unit (Fig. 2). GPS rovers located in the landslide body are powered by one pair of solar panels (Fig. 3).



Figure 2 Mini power plant at the Veli Vrh location consisted of 1 KW 6 solar panels and 500 W windmill.



Figure 3 GPS rover and solar panel installation. Concrete box is round up construction for geotechnical monitoring equipment protection (Arbanas et al. 2012a).

After installed part of monitoring system was powered up and turned on, several problems in equipment functioning were observed and equipment re-adjustment was carried out until the end of November 2011 (Arbanas et al. 2012c,d). Observations of geodetic prisms with robotic total station and measurements of GPS rovers are collected and processed in the automated integrated monitoring system software. Installation of long span extensometers was completed until the end of 2011, while the short span extensometers, vertical extensometers and pore water pressure data loggers were installed during 2012. Geotechnical part of the equipment (long and short span extensometers, pore water pressure gauges, rain gauge) will be included in the same integrated system during 2013.

Maintenance, adjustment and calibration of the system

The first 12 months period of monitoring data collection was needed for understanding relation between disturbing effects and their causes (Arbanas et al. 2012a,d) and procedures for equipment calibrating and effects of weather impacts on measurements accuracy eliminating were established. Seasonal meteorological and atmospheric conditions also influenced on constructional elements of the monitoring system. Extremely high temperatures during late June and whole July 2012 influenced on non-uniform warming of concrete main pillar with total station and caused uneven bending deformation of the pillar which affected on total station's absolute position and unacceptable leaning with final consequences in measurements' accuracy. After more

than 20 days of daily peak air temperature higher than 40°C, total station was inclined out of its compensator's range, and the measurements should be stopped. Therefore, total station had to be reinstalled and repositioned to absolute zero balance, as it was originally installed one year before.

These accidents pointed on necessity of a thermal insulation applying to the main pillar before necessary calibration of the robotic total station. Thermal insulation consisted of 1 cm thick timber panels mounted above 1 cm of thick Styrofoam layer was applied during August 2012 (Fig. 4). After thermal insulation was applied and calibration of the total station was completed, TPS measurements were started again.

Results of further TPS measurements were conducted without interferences caused by thermal influence of main pillar behavior. According to the measurement results obtained from the bi-axis clinometer installed on the main pillar, pillar inclinations caused by pillar warming are drastically reduced after thermal insulation applying (Fig. 5), which generally ensured continuous total station's measurement cycles.



Figure 4 Concrete main pillar housing for robotic total station on the top at the Veli Vrh location before insulation is applied (left) and after thermal insulation is applied (right).

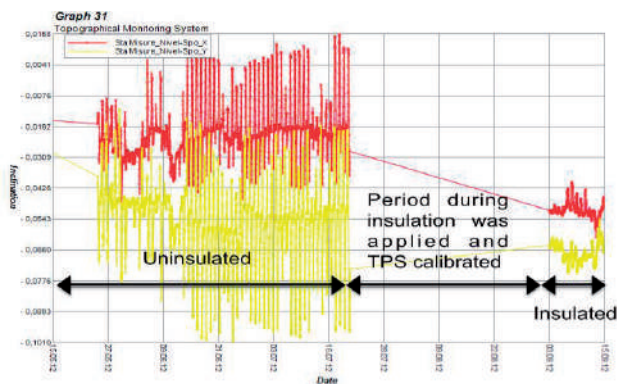


Figure 5 Measured inclinations obtained bi-axis clinometer installed on the main pillar at the Veli Vrh location before and after thermal insulation applying.

Windmill, as a part of hybrid mini power plant located at the Veli Vrh location, suffered several damages due to extreme wind Bora (Fig. 6). Wind Bora is changeable wind and blows in gusts and can reach speeds up to 200 km/h at the Veli Vrh location. It is most common during the winter from November to the end of March. After every particular damage occurred, repair and strengthening of weak parts was applied. Although reparations resulted in a slightly better windmill's resistance and performances, it couldn't be expected that it can survive extreme wind speeds occurring in that area in long term monitoring period in the future. Because of this reason, a new windmill model should be purchased, which could survive wind speed up to 200 km/h.

While the solar panel supply system produce sufficient electric energy for the GPS rovers located in the landslide, the hybrid mini power plant consisted of 1 KW solar panels and 500 W wind mill located at the Veli Vrh location is not able to produce enough electric energy to keep working PC workstation, robotic total station, GPS master unit, weather station, web camera and wireless network communication system continuously during the late autumn and winter, especially during a series of cloudy days. Short daylight period and unfavorable sun position don't enable producing and accumulating enough electric energy in this period. Bora and sirocco as dominated winds can be very efficient in windmill's production but wind's activity is not permanent energy source. The power production module (MPPT) is connected to the monitoring PC workstation at the site in order to enable remote monitoring of a power production and consumption at the monitoring main unit (Fig. 7). This solution gives possibility for decision to turn of particular part of the monitoring system or the entire system when the power accumulation in the battery system is too low and avoid complete battery drainage and related damages.



Figure 6 Damages on the windmill caused by bora. Red arrows are showing the damaged wind tail vane and head of the rotor.

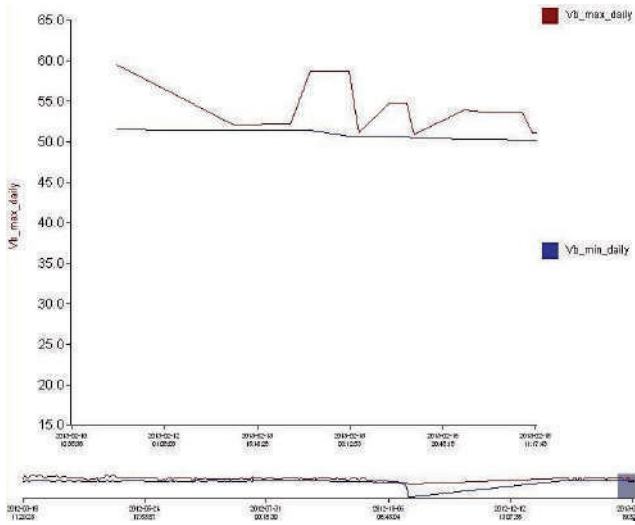


Figure 7 Power production diagram showing minimal (Vb min) and maximal (Vb max) battery voltage during day and night.

Wi-Fi network used to transfer data from the equipment in the landslide area to the field PC workstation, as well as the UMTS data transfer from the field PC workstation to the control center at the Faculty of Civil Engineering have been proved as very stable and reliable but the data transmitting system is also dependent on previously described power supply.

Minor adverse effects on the system working were caused by vegetation growth that can results in interruption of direct visibility from the total station to several prisms located in the forested part of the landslide and contact of tree branches and extensometers' wire. Therefore, vegetation cutting should be periodically carried out from spring to autumn to avoid described obstructions and ensure continuous data collection.

Monitoring results

The monitoring system at the Grohovo Landslide is consisted of geodetic and geotechnical monitoring. Equipment for the geotechnical monitoring (vertical inclinometers, long and short-span extensometers, pore pressure gauges, and weather station) is not included into the wireless network data transfer, approach to the data collection, as well as its processing, is completely different than for automated geodetical monitoring. All data collected from geotechnical monitoring equipment should be directly downloaded from data loggers or directly measured in the field. Field trips for data downloading should be well planned and organized, taking into account all the necessary details to ensure successful data collection (weather conditions, tools, accessories, batteries etc.). Collected data from geotechnical monitoring equipment are less frequently available and cannot present an actual overview of landslide behavior.

Inclinometer data would presents the best overview of movements at the slip surface and related profile.

Totally 5 inclinometer's casings are installed (two in 2012 and three in 1998). Measurement results are closely accordant to the results and assumptions described by Benac et al. (2005, 2011) with clearly visible deformations at the slip surface occurred at the depth of 6 m., with total deformation in direction along the slope (A-Axis) of about a 1 cm per year (Fig. 8).

Surface deformations are clearly presented by wire extensometer measurements' result. Figure 9 represents measurements from the long span wire extensometer E01 installed over the landslide main scarp with total extension of about 2 cm from the start of measurements.

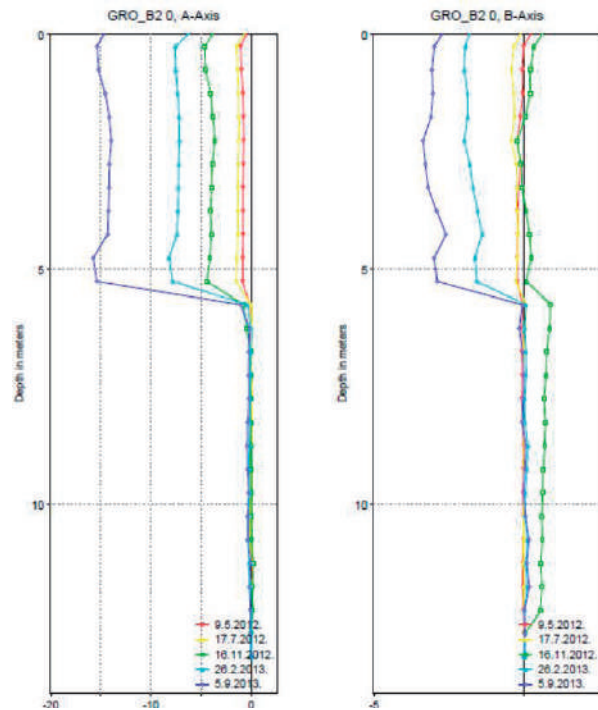


Figure 8 Inclinometer measurements at borehole B2 showing cumulative displacements of inclinometer casing in two axis.

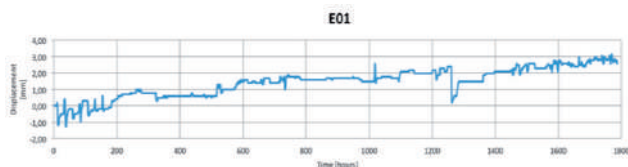


Figure 9 Measurements from long span wire extensometer E01.

Data from a geodetic equipment (GPS, TPS) are continuously collected through the landslide's local Wi-Fi network into the SQL database installed on the field PC workstation at the Veli Vrh location, which is wirelessly (by UMTS mobile data connection) connected to the main PC unit at the Faculty of Civil Engineering. Such a data acquisition ensures continuous data collection and processing using System Anywhere software (Fig 10). During designing and installation of monitoring equipment different types of monitoring equipment were installed on same locations. Selection of same position for different type of monitoring equipment enables spatial

correlation of measurement data on the landslide surface and trough the landslide profile and reconstruction of data in a case when part of equipment is failed (Arbanas et al. 2012). Figure 11 presents measurements' data from GPS2 (both 1h and 24h cycle) and prism I5 installed at same position showing a typical example of the dataset obtained from a continuous real time monitoring system. Marked time periods with measurements data missing are caused with some of previously described

interruption in monitoring process. Despite the data series are missing, it is easy to reconstruct them based on established correlations and consistent trends. In combination with hydrological monitoring equipment, which consists of pore pressure gauges and pluviometer, it would be possible to reconstruct relationship between rainfalls, groundwater level and appropriate landslide behavior as a basis for an early warning system establishment.

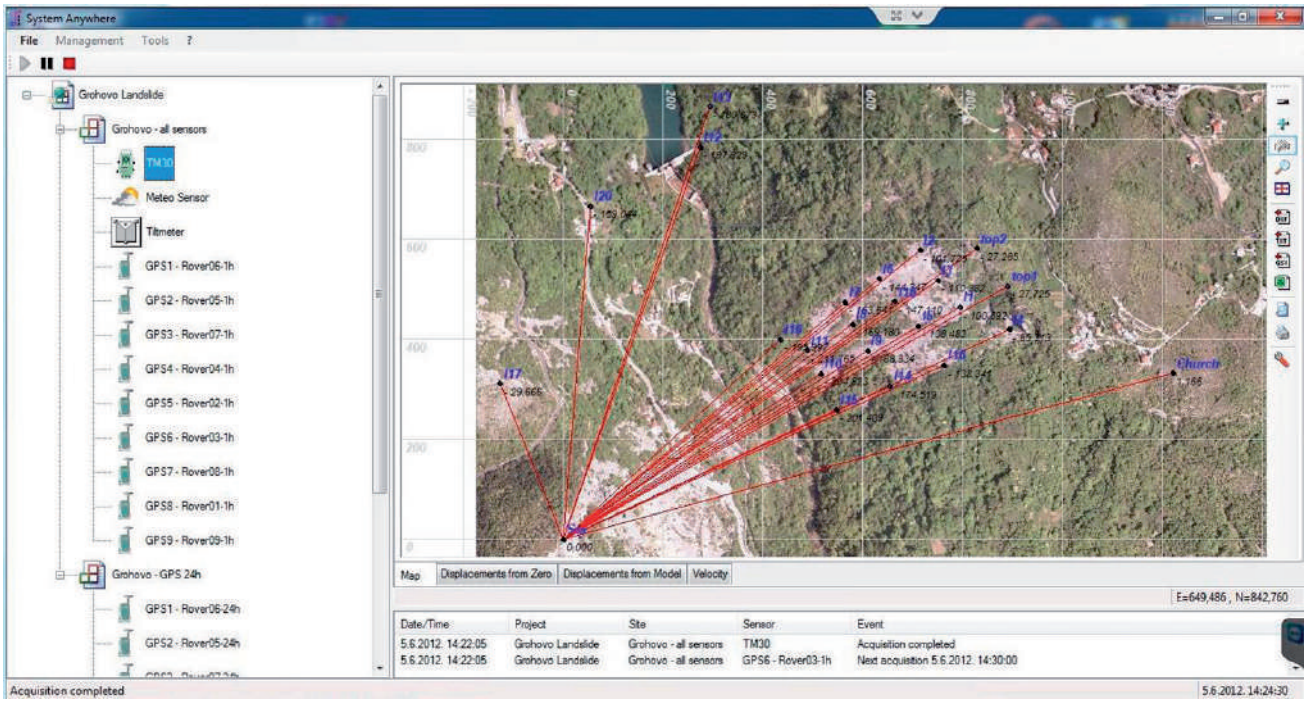


Figure 10 Screen of System Anywhere software used for GPS and TPS measurement data presentation from SQL database collection.

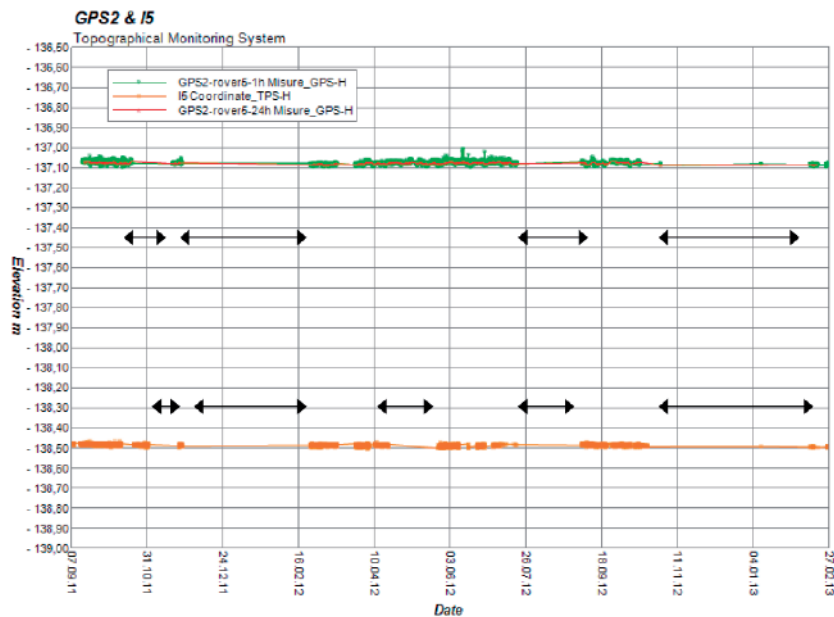


Figure 11 Measurements data from GPS2 (both 1h and 24h cycle) and prism I5. Time periods where data series are missing are marked with black arrows.

Conclusions

The Grohovo Landslide was chosen as a pilot area for comprehensive integrated real-time monitoring system development in the frame of Croatian-Japanese joint research project “Risk identification and Land-Use Planning for Disaster Mitigation of Landslides and Floods in Croatia” initiated in 2009. The comprehensive monitoring system was designed to consist of geodetic and geotechnical monitoring and monitoring equipment was installed during 2011 and 2012. The first 12 months period of monitoring data collection was needed for understanding relations between disturbing effects and their causes and procedures for equipment calibrating and effects of weather impacts on measurements accuracy eliminating were established. Seasonal extreme meteorological and atmospheric conditions also had significant influences on constructional elements of the monitoring system, especially high temperatures during summer and strong winds during winter period. After comprehensive monitoring system installation, the maintenance, adjustment and calibration of monitoring equipment have important role in the efficiency, reliability and accuracy of the operation of the system. Taking into consideration all previously described issues, about two years’ time period would be necessary to complete adjustment and calibrating of the system while the maintenance of the system should be intensive during all its working life.

Acknowledgments

Equipment presented herein has been obtained with the financial support from JST/JICA’s SATREPS Program (Science and Technology Research Partnership for Sustainable Development). This support is gratefully acknowledged.

References

- Arbanas Ž, Benac Č, Dugonjić S (2010) Dynamic and Prediction of future behavior of the Grohovo Landslide. In Proc. 1st Workshop of the Project Risk identification and Land-Use Planning for Disaster Mitigation of Landslides and Floods in Croatia, 22-24 November 2010, Dubrovnik, Croatia (in press).
- Arbanas Ž, Sassa K, Marui H, Mihalić S (2012a) Comprehensive monitoring system on the Grohovo Landslide, Croatia. In Proc. 11th International and 2nd North American Symposium on Landslides: Landslides and Engineered Slopes: Protecting Society through Improved Understanding, June 2-8, 2012. Banff, Canada, pp. 1441-1447.
- Arbanas Ž, Vivoda M, Jagodnik V, Dugonjić Jovančević S, Ljutić K (2012b) Consideration of early warning system on the Grohovo Landslide. In: Proc. 2nd Workshop of the Project Risk identification and Land-Use Planning for Disaster Mitigation of Landslides and Floods in Croatia: Monitoring and analyses for disaster mitigation of landslides, debris flow and floods, University of Rijeka, pp. 51-54.
- Arbanas Ž, Jagodnik V, Ljutić K, Dugonjić Jovančević S, Vivoda M (2012c) Establishment of the Grohovo Landslide monitoring system. In: Proc. 2nd Workshop of the Project Risk identification and Land-Use Planning for Disaster Mitigation of Landslides and Floods in Croatia: Monitoring and analyses for disaster mitigation of landslides, debris flow and floods, University of Rijeka, pp. 29-32.
- Arbanas Ž, Dugonjić Jovančević S, Ljutić K, Vivoda M, Jagodnik V (2012d) Initial results of the Grohovo Landslide monitoring. In: Proc. 2nd Workshop of the Project Risk identification and Land-Use Planning for Disaster Mitigation of Landslides and Floods in Croatia: Monitoring and analyses for disaster mitigation of landslides, debris flow and floods, University of Rijeka, pp. 33-36.
- Benac Č, Arbanas Ž, Jurak V, Oštrić M, Ožanić N (2005) Complex landslide in the Rječina River valley (Croatia): origin and sliding mechanism. Bulletin of Engineering Geology and the Environment. 64(4): 361-371.
- Benac Č, Dugonjić S, Vivoda M, Oštrić M, Arbanas Ž (2011) A complex landslide in the Rječina Valley: results of monitoring 1998-2010. Geologia Croatica. 64(3): 239-249.
- Mihalić S, Arbanas Ž (2013) The Croatian–Japanese joint research project on landslides: activities and public benefits. Landslides: Global Risk Preparedness. Sassa K, Rouhban B, Briceño S, McSaveney M, He B (eds). Heidelberg: Springer. pp. 333-349.

Rockfall Monitoring by Terrestrial Laser Scanning - Case Study of the Rock Cliff at Duće, Croatia

Goran Vlastelica⁽¹⁾, Predrag Mišćević⁽¹⁾, Hiroshi Fukuoka⁽²⁾

1) University of Split, Faculty of Civil Engineering, Architecture and Geodesy, Split, Croatia, Matice hrvatske 15, +385 21 303 388

2) Kyoto University, Disaster Prevention Research Institute, Kyoto, Japan

Abstract A rock cliff face at Luka location in Duće area affected by small rockfalls and large block detachment has been monitored using a ground-based remote sensing apparatus: Terrestrial Laser Scanner (TLS). Three datasets of the slope were acquired from September 2011 to February 2013 in an on-going project. The geomorphological evolution of the rock face, in terms of volume and frequency of potential rockfall, large block movement and erosion process on marly part of the slope was studied by comparison of sequential datasets. As a method of confirming large block movement, from November 2012 additional measurement of relative displacements of rock cracks on the cliff top were made. So far, in a four month interval, movement of large block via crack displacement was not detected.

Keywords breccia, flysch, TLS, spectrometer, monitoring, displacement detection, rockfall

Introduction

Dalmatia region in Croatia has dozens of registered active rockfall zones. Virtually the whole area along main coastal road from the city of Split to town of Omiš is a potential danger zone. Every year, in periods after heavy rain and/or considerable low air temperature, many sudden rockfalls in these areas are recorded (Fig. 1).

As long as effective preventive measures are not taken, rockfalls in this area will continue to be the

primary threat for inhabitants and community infrastructure. Unfortunately, stabilizing and managing the entire area without localizing potential threats would require considerable funding which private owners and local communities cannot afford, so more suitable method for forecasting and detecting potential rockfalls is needed (Mišćević et al. 2010).

Most studies on landslide forecasting use point-based instruments of measurement (e.g. differential Global Positioning System, extensometers, total stations, etc.) to monitor displacements (Zvelebil and Moser 2001, Crosta and Agliardi 2003, Rose and Hungr 2007). These instruments, despite their accuracy, have a certain disadvantage - low density of points. Since the precise location of the moving areas is often unknown, a method of detecting the portions of a slope affected by displacement is still required. The possibility to acquire topographic datasets with high accuracy and spatial resolution, using laser, optical and/or radar technologies, mounted on terrestrial, aerial and/or satellite instruments is currently opening up new ways to visualize, model and interpret surface processes (Abellan et al. 2010). However, sometimes a combination of these methods (with the TLS high resolution and point-based instruments high precision) is preferred.

TLS Optech ILRIS-3D was used in this study for the detection and spatial prediction of rockfall and tracking of erosion processes at the Luka location (Duće area, Dalmatia, Croatia, Fig. 2).



Figure 1 Detached block under the rock cliff at Luka location, Duće area (February 2007, Photo: Ante Čizmić / Cropix).



Figure 2 Rock cliff at Luka location, Duće area. (Photo: Ante Čizmić / Cropix).

Study area

Duće area is situated on the east Adriatic coastline, approximately 20 kilometers south-east of the city of Split. This area has many registered landslide and rockfall zones, however the Luka location is one of the most noticed and most dangerous. Slope over Luka location is made of Eocene flysch, which is covered by a relatively thin and hard layer of breccia (Fig. 3).



Figure 3 South-east view of the rock cliff at Luka location. Slope is made of Eocene flysch with layer of breccia marked by black arrow. Larger detached blocks are marked with red arrows.

Main component of flysch is marl, a rock material which is prone to weathering when submitted to atmospheric agents (Mišćević and Vlastelica 2011). Surface formed of weaker marl is deteriorated and eroded with rain as a result of weathering. A layer of a harder breccia remains and in time starts to form "cantilevers" on the slope. With the development and elongation of joints in these "cantilevers", parts of breccia become instable and start to fall off as large blocks (Fig. 3,4). From an engineering geological aspect failure mechanism can be characterized as translational or rotational descent of blocks of competent rock upon an incompetent base (Poisel and Eppensteiner 1988).



Figure 4 Middle part of the rock cliff at Luka location. Large subducted block is marked with arrow.

From a hydrogeological aspect, alongside surface erosion, another triggering factor of block detachment is breccia's high porosity. Water seeps through cracks all the way to the weaker marl layers thus additionally weakening the material.

Some prevention measures were made on one of the blocks (Fig. 5), using steel cables and anchorages. However, despite the efforts to secure it, the block was deemed highly dangerous to the inhabitants under the slope and therefore removed.

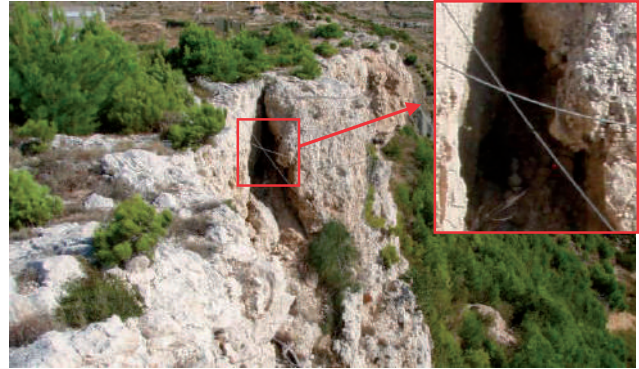


Figure 5 Middle part of the rock cliff. Block that was stabilized by steel cables and anchorages (removed March 2012).

Materials and methods

Terrestrial laser scanner (TLS)

This instrument is also known as a Ground based LiDAR (Light Detection and Ranging system). In this study an ILRIS-3D with enhanced range mode was used. This is a well-known technique of geodetic surveying which has been used often in the last five years (for some basic explanation of application see Pesci et al. 2009; Abell'an et al. 2010; Vlastelica et al. 2012 etc.).

Maximum declared range for ILRIS-3D-ER is 1,700 meters at 80% reflectivity or 650 meters at 10% surface reflectivity, which is more than enough for the purpose of monitoring the Duće area. Range and other specifications are shown in Table 1.

Table 1 Specification of ILRIS-3D-ER

Parameter	ILRIS-3D-ER
Range 80% reflectivity	1700m
Range 10% reflectivity	650m
Laser repetition rate	2500 to 3500 Hz
Raw range accuracy	7mm @ 100m
Field of view	40°x40°
Minimum step size	0.001146°
Maximum density	2cm @ 1000m
Rotational speed	0.001 to 20°/sec
Beam diameter	22mm @ 100m
Laser wavelength	1535 nm

Accuracy of scanning is a function of range, angle of incidence, surface roughness and reflectivity. Considering that ILRIS has a wavelength close to water bands in the atmosphere, data acquisition during rainy or foggy days may be inaccurate. Weather in this area is usually favorable so this limitation didn't pose any problems.

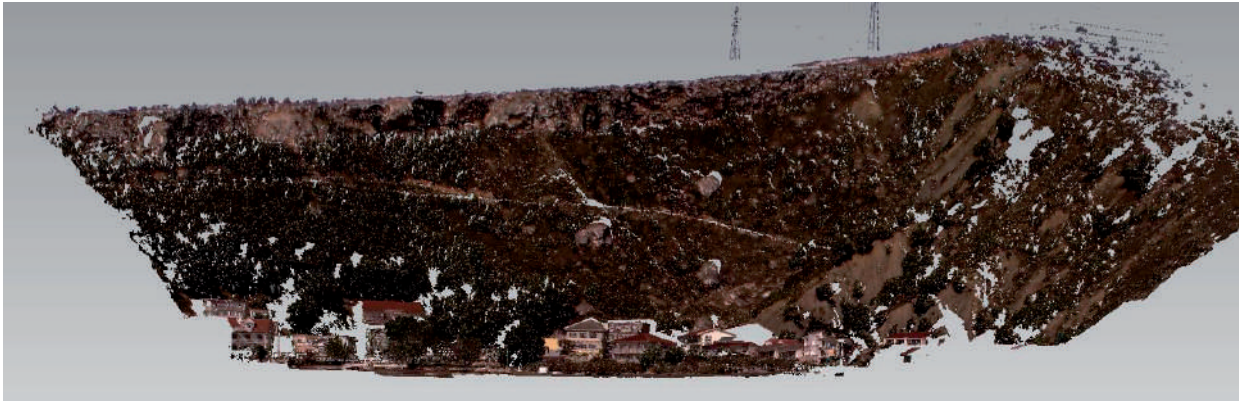


Figure 6 Colored cloud of points of the study area in Luka location.

Data acquisition by TLS

The reference dataset (referred to as reference point cloud) was acquired in 2012/04/15. All datasets were acquired from two stations: local marina breakwater (mean distance from the cliff app 250 meters), and from the bottom of the slope (app 100 meters). Used point spacing at both stations was 4 cm at mean distance. From these sites, occluded portions of the cliff area were minimized, allowing for the alignment and merging in a single cloud of points (Fig. 6), and from it creating a final 3D model.

Data acquisition was repeated 2012/08/31, 2012/11/10 and 2013/02/22. Also, a scan that was previously made in 2011/09/27 when TLS was partially malfunctioned is used.

PolyWorks v12.0 from InnovMetric is the main software used for the visualization, alignment and comparison of the point clouds.

Rock cracks displacements measurement

As a method of confirmation of large block movement, additional monitoring of relative displacements of three major rock cracks on the cliff top (Fig. 7) was made. Basic information about these cracks is shown in Table 2.

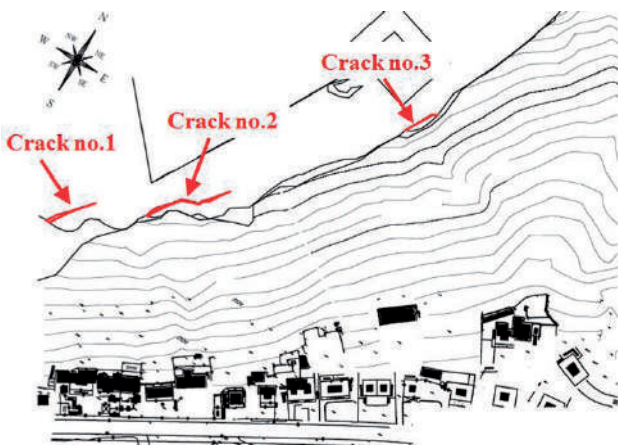


Figure 7 Three major rock cracks on the top of the rock cliff at Luka location.

Comparison of sequential scans

Temporal differences of the terrain were detected by comparing sequential datasets. Comparison is made as follows:

1. reference point cloud acquisition,
2. construction of the surface of reference,
3. temporal acquisition of additional point clouds,
4. alignment of these datasets with surface of reference
5. comparison between surface of reference and point cloud datasets,
6. calculation of the differences for dataset comparison.

This methodology is described in detail by Rosser et al. (2005) and Lim et al. (2006).

Table 2 Basic information about three major cracks on the top of the rock cliff at Luka location.

Crack no.	Number of points monitored	Length (m)	Depth (m)	Width (m)	Distance from edge (m)
1	T1-T4	~ 23	~ 8,0	0,5-1,0	3,5-5,0
2	T5-T8	~ 45	> 4,5	0,3-0,5	7,0-11,0
3	T9-T13	~ 20	filled	~ 0,1	3,0-3,5

Monitoring started in November 2012 at total 13 points (T1-T13) along cracks on the cliff top (Fig. 8), and it will be repeated every time when the data by TLS is collected.

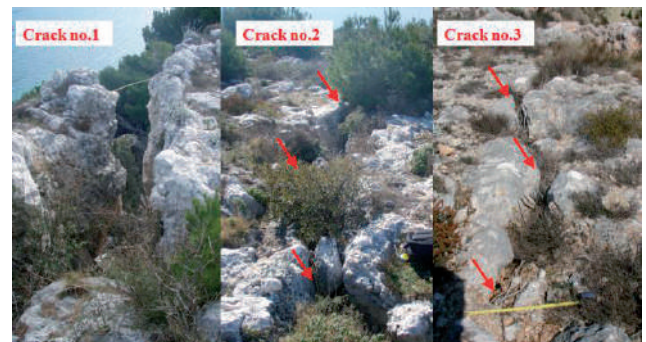


Figure 8 Photos of the three major cracks on the top of the rock cliff at Luka location.

Points are stabilized on both sides of the crack using quick drying cement and metal pins. Measurement is carried out with simple metal measurement tape. So far, in a four month interval, movement of large block via crack displacement was not detected.

Spectrometer

Spectrometer is an instrument used to measure properties of light over a specific portion of the electromagnetic spectrum, typically used in spectroscopic analysis to identify materials (Butler et al. 1995). The variable measured is most often the light's intensity. In this case study field spectroradiometer TerraSpec 4 Hi-Res (ASD Inc., USA) with wavelength range from 350 to 2500 nm was used. Wavelength range and other specifications are shown in Table 3.

All preliminary tests were made at Faculties Geomechanical laboratory (Fig. 9). Focus of these tests was on determining reflectance of materials at study location.

Also, some tests were made on marl samples which are submitted to simulated weathering and changes are tracked via visual or statistical analysis of reflectance.



Figure 9 TerraSpec 4 Hi-Res spectroradiometer (ASD Inc., USA).

Table 3 Specification of spectroradiometer TerraSpec 4 Hi-Res

Parameter	TerraSpec 4 Hi-Res
Full Spectral Range	350-2500 nm
Resolution	3 nm @ 700 nm and 6 nm @ 1400/2100 nm
Scanning time	100 milliseconds
Wavelength reproducibility	0.1 nm
Wavelength accuracy	0.5 nm
Channels	2151

Results

Fig 10 shows a sequential comparison of 2011/09/27 and 2012/04/15 TLS datasets. As it was previously mentioned large block shown in Figure 5 was removed in-between this two scans. Difference shown by this comparison corresponds with the measured block size in the field.

In Figure 11 a more detailed image of the block is shown. When observed more closely, right to the big block, a smaller block can also be noticed. When the scale of comparison is changed from a maximum of 4 meters to 1.5 meters, the actual block size can be more clearly detected. Both blocks were removed after only one scan therefore any deformation prior to their removal could not be detected.

Preliminary tests using spectroradiometer were also made. Main goal of these tests was to determine reflectance of materials at study location. In Figure 12 it

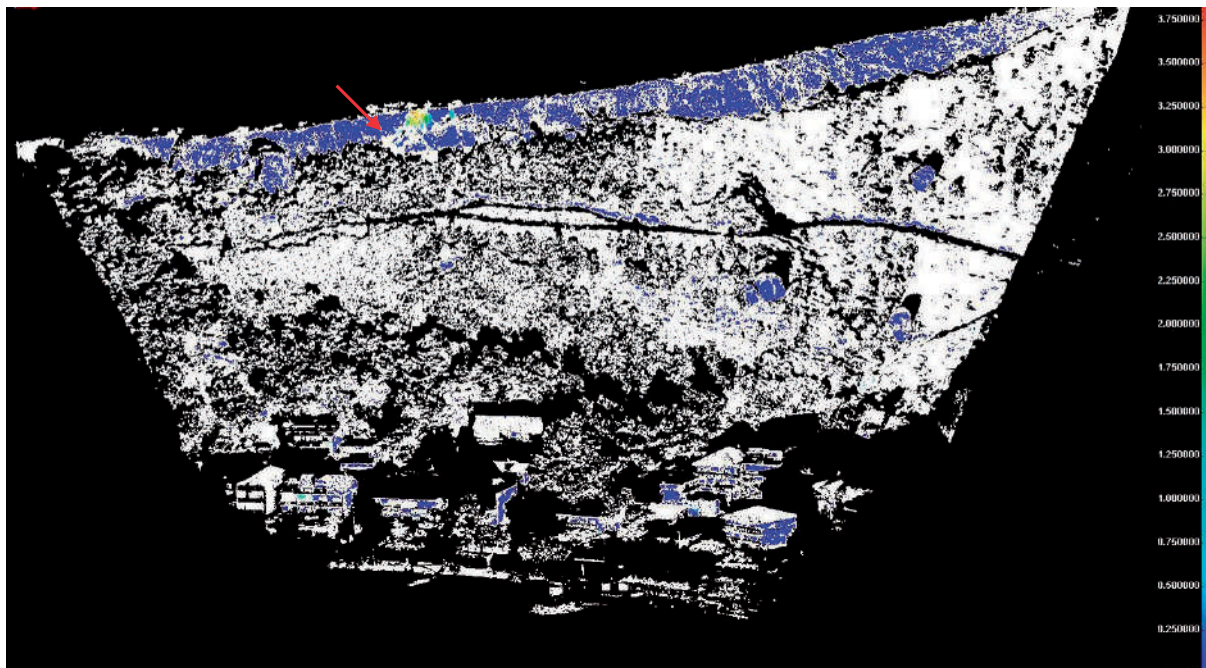


Figure 10 Comparison of 2011/09/27 and 2012/04/15 TLS datasets.

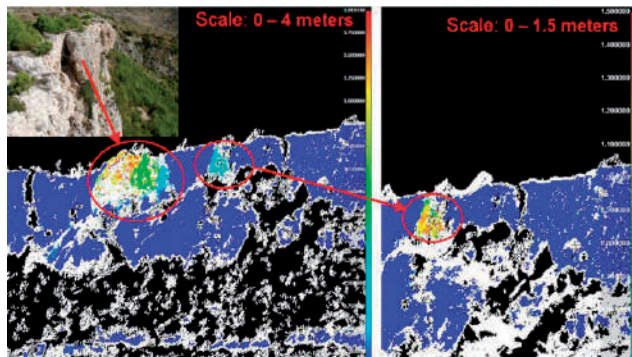


Figure 11 Detail of the removed block from comparison of 2011/09/27 and 2012/04/15 TLS datasets.

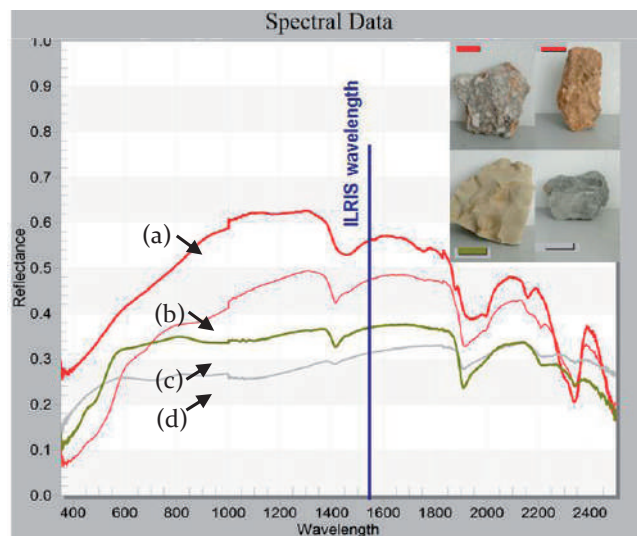


Figure 12 Reflectance of materials from which the study area consists of: (a) grey surface of breccia at the cliff, (b) red surface breccia, (c) grey marl and (d) light brown marl.

can be noticed that grey surface of breccia from which the most of the cliff surface consists has highest surface reflectance at a wavelength on which the ILRIS operates. It is almost double the reflectance of the grey marl and light brown marl from which the lower part of the slope consists.

Considering that ILRIS-3D has a range of 650 meters at 10% reflectivity (Tab. 1), obtaining results at maximum distance of 400 meters should not be a problem. This is confirmed by the results obtained at the site. In Fig 10 it can be clearly seen that the data is obtained at every part of target slope, except in occluded areas.

Conclusions

The usage of TLS is certainly the way to deepen our understanding of rockfall phenomena. For this study ILRIS-3D with enhanced range mode is used. At this stage small displacements in the rock cliff were not detected, however neither have any rockfalls occur from the start of monitoring.

An example of a large block removal was used to test the methodology of comparing sequential datasets. The differences starting from 10 cm up to 4 m between two scans are clearly observed. With these results the morphology of the slope, block size and shape can be obtained very precisely and which can then be used in rockfall analysis. To detect smaller displacements, data acquired from standpoints closer to the cliff shall be used for future analysis. Also, the amount of acquired data in future scans should be increased by using multiple scan pattern repeat, thus providing more accurate data.

Acknowledgments

The authors would like to thank everyone involved in Japanese-Croatian project: Risk Identification and Land-Use Planning for Disaster Mitigation of Landslides, Japan Science and Technology Agency - JST, Japan International Cooperation Agency - JICA and Ministry of Science, Education and Sport of Republic of Croatia.

References

Abellan A, Calvet J, Vilaplana J M, Blanchard E (2010) Detection and spatial prediction of rockfalls by means of terrestrial laser scanner monitoring. *Geomorphology*. 119(3-4): 162-171.

Butler L R P, Laqua K (1995) Nomenclature, symbols, units and their usage in spectrochemical analysis-IX. Instrumentation for the spectral dispersion and isolation of optical radiation (IUPAC Recommendations). *Pure Appl. Chem.* 67(10): 1725-1744.

Crosta G B, Agliardi F (2003) Failure forecast for large rock slides by surface displacement measurements. *Can Geotech J.* 40: 176-191.

Miščević P, Vlastelica G (2011) Durability Characterization of Marls from the Region of Dalmatia, Croatia. *Geotechnical and geological engineering*. 29(5): 771-781.

Miščević P, Smailbegović A, Vlastelica G (2010) Investigation proposal: Rockfalls in Omiš and Duće areas. 1st Workshop on Risk Identification and Land-Use Planning for Disaster Mitigation of Landslides and Floods in Croatia, Dubrovnik.

Pesci A, Casula G, Loddo F, Bianchi M G, Teza G (2009) Optech Ilris-3d Terrestrial Laser Scanner: Short User Guide. Technical report, 24 pp., at: <http://www.earth-Prints.org/handle/2122/5207>

Poisel R, Eppensteiner W (1988) A Contribution to the Systematics of Rock Mass Movements. In: *Proc. of 5th Int. Symp. Landslides Lausanne, Vol. 2: 1353-1357.*

Rose N D, Hungr O (2007) Forecasting potential rock slope failure in open pit mines using the inverse-velocity method. *Int J Rock Mech Min Sci.* 44: 308-320.

Rosser N J, Dunning S A, Lim M, Petley D N (2005) Terrestrial laser scanning for quantitative rock fall hazard assessment. *Landslide risk management*, edited by: Hungr O, Fell R, Couture R, Eberhardt E, Balkema, Rotterdam, paper 091.

Vlastelica G, Miščević P, Fukuoka H, Smailbegović A (2012) First Experience with Ground Based LiDAR in Omiš and Duće Areas. Second Project Workshop of the Monitoring and Analyses for Disaster Mitigation of Landslides, Debris Flow and Floods. Rijeka: Faculty of Civil Engineering University of Rijeka. pp. 37-41.

Zvebil J, Moser M (2001) Monitoring based time-prediction of rock falls: three case-histories. *Phys Chem Earth (B).* 26: 159-167.

Overview of Historical Landslide Inventories of the Podsljeme Area in the City of Zagreb

Laszlo Podolszki⁽¹⁾, Snježana Mihalić Arbanas⁽²⁾, Željko Arbanas⁽³⁾, Željko Miklin⁽¹⁾, Jasmina Martinčević⁽¹⁾

1) Croatian Geological Survey, Zagreb, Croatia, Sachsova 2, +385 1 6144 701

2) University of Zagreb, Faculty of Mining, Geology and Petroleum Engineering, Zagreb, Croatia

3) University of Rijeka, Faculty of Civil Engineering, Rijeka, Croatia

Abstract Data about landslides at the hilly area of the Zagreb city (Podsljeme area), was systematically collected three times in last 50 years. In this paper three geomorphological historical landslide inventories are shortly presented together with framework studies ordered by local City government aimed at landslide risk management. Quantitative comparison of inventories was made by comparing main characteristics of landslide maps and size of recorded landslides. Examples from certain locations were also selected to show overlapping of mapped landslide contours. It is evident that, despite using the same landslide identification method, landslide contours in all three inventories vary significantly primarily as a consequence of subjectivity of interpretations inherent to identification of landslide borders by reconnaissance ground surveys in large scale.

Keywords geomorphological landslide inventory, historical information, Podsljeme area, City of Zagreb

Introduction

Constant growth of population in the Zagreb city has been resulting in increasing urbanization. Southern foothill of Medvednica Mt. placed inside borders of the City of Zagreb (known as Podsljeme) is especially attractive as a residential area and, consequently it is prone to development of slope instabilities, mostly in the form of soil slides. Landslides have been occurring in this area as a result of geomorphological conditions and adverse human activities such as: cutting without adequate support systems, improper drainage systems, creation of dumps of very loose waste, etc. Simplified geological map of this area, derived by generalization of the Basic geological maps in the scale 1:100,000, Zagreb Sheet (Šikić 1972) and Ivanić Grad Sheet (Basch 1976) is shown on Fig. 1. In the period from 1967 to 2007 City authorities invested in three studies aimed at preparation of landslide inventory maps: Šikić (1967); Polak et al. (1979); and Miklin et al. (2007).

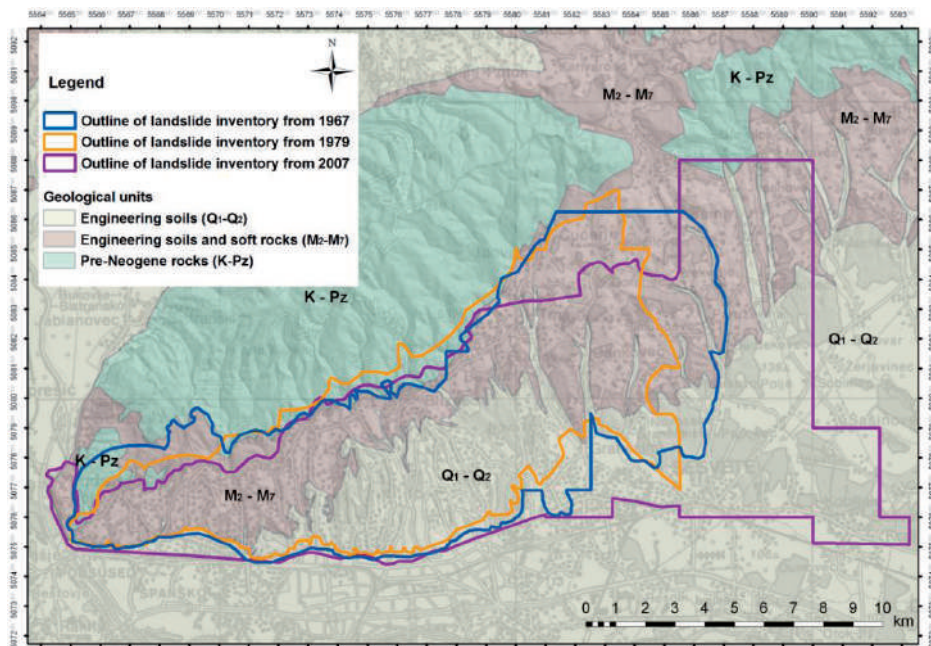


Figure 1 Simplified geological map of the area of Medvednica Mt. with outlines of three historical landslide inventories from 1967 (Šikić 1967), 1979 (Polak et al. 1979) and 2007 (Miklin et al. 2007).

Description of historical landslide inventories of the Podsljeme Area

Landslide inventory from 1967

Historical landslide inventory map from 1967 was created in the framework of the study entitled 'Engineering geological study of Zagreb and wider area' (Šikić 1967). The study encompassed urbanized part of hilly Podsljeme area which total size is approximately 125 km² (Fig. 1). The study resulted in analogue maps in the scale 1:10,000: engineering geological map with landslide inventory map and landslide susceptibility map.

Landslide inventory was compiled by systematic field mapping on the base topographic maps in the scale 1:10,000. Landslides are classified as active, inactive and sliding phenomena and falls. Maps also depict unstable zones described as follows: unstable zones with active landslide, unstable zones with inactive and fossil landslides, unstable slopes and falls. Besides landslides, phenomena of linear erosion were also mapped. Totally, there are 535 landslide phenomena and unstable zones. Fig. 2a shows landslide inventory map with five zones of slope angles (0-5°, 5-10°, 10-20°, 20-30°, >30°) and lithological map. Lithology was mapped using engineering geological units created on the basis of rock/soil characteristics. Descriptive data about all instabilities are given in phenomena/zone forms.

Figure 2b shows landslide susceptibility map with three zones: stable areas without registered instability phenomena, conditionally stable slopes and conditionally unstable slopes with landslides. Landslide susceptibility was assessed by heuristic method using direct mapping in which slope angles and relative density of landslides and unstable zones were evaluated. Zonation method was subjective evaluation of landslide susceptibility according to the following criteria used for delineation of zones:

- Stable areas without instability phenomena and terrains with slope angles less than 10° (green color),

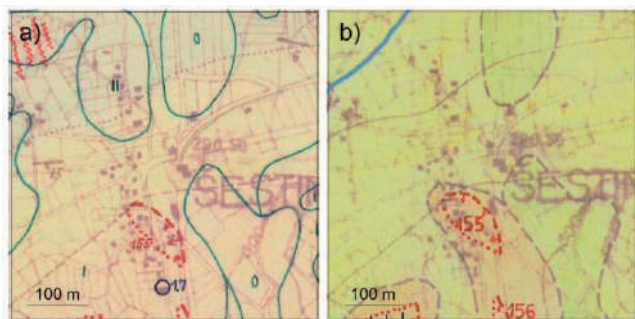


Figure 2 Segments of landslide maps from the study 'Engineering geology of Zagreb north and south' (Šikić 1967) for the area of Šestine: a) engineering geological map in the original scale 1:10,000 with portray of landslide no. 155 and outlines of zones of slope angles depicted by green lines and labels with the following meanings: 0=0-5°, I=5-10°, II=10-20°, III=20-30°, IV=>30°; and b) landslide susceptibility map in the original scale 1:10,000 with red landslide contours. Yellow color depicts conditionally stable slopes; orange color depicts conditionally unstable slopes.

- Conditionally stable areas and terrains with slope angles in a range of 10-20° (yellow color),
- Conditionally unstable areas with instability phenomena and terrains with slope angles greater than 20° (orange color), and
- Unstable areas with active instability phenomena (orange color).

The study was made by team of experts from Croatian Geological Survey. Systematic field work was carried out from 1963 to 1967. There are numerous locations on the map without identified contours of individual landslides. For such areas, maps depict larger zones interpreted as unstable.

Landslide inventory from 1979

Historical landslide inventory map from 1979 was created in the framework of the study entitled 'Lithology and categorization according to slope stability of Medvednica Mt. hills at the area of the Zagreb City' (Polak et al. 1979). The study encompassed urbanized part of southern and southeastern hills of Medvednica Mt. which total size is approximately 105 km² (Fig. 1). The study resulted in analogue maps in the scale 1:10,000: lithological map with landslide inventory and landslide susceptibility map.

Landslide inventory was compiled by systematic field mapping on the base topographic maps in the scale 1:10,000, partially by visual analysis of aerial photographs and on the basis of archive information from geotechnical reports. Landslides are classified as active, inactive and creeping sliding phenomena and falls. Landslides were mapped on the basis of visible features, such as main scarp, lateral scarps (flanks) and accumulation of displaced material in toe part of landslide. Inventory map also depict linear erosion phenomena, excavations, fills, uncontrolled disposals, taluses and swamps. Totally, there are 812 landslide phenomena (406 active landslides, 294 inactive landslides, 112 creeping phenomena) and 58 taluses. Groups of small landslides are mostly depicted by one large contour. Figure 3a shows landslide inventory map with lithological cartographic units in the background of landslide contours. Very short descriptive data about all instabilities are given in the accompanying report. Lithology was mapped in the form of simplified geological units derived from Basic geological map in the scale 1:100,000 (Šikić et al. 1972, Basch 1976).

Figure 3b shows landslide susceptibility map with four zones: zone I - stable areas composed of alluvial deposits in which there is no possibility for development of instability phenomena; zone II - zones with rare small landslides caused by anthropogenic activities; zone III - zones with large and deep landslides; zone IV - zones of unfavorable natural conditions regarding slope stability (e.g., erosion, steep slopes etc.). For all zones, general possibilities for construction are also described. Landslide susceptibility was assessed by heuristic method using direct mapping, mainly on the basis of landslide densities.



Figure 3 Segments of landslide maps from the study 'Lithology and categorization according to slope stability of Medvednica Mt. hills at the area of the Zagreb City' (Polak et al. 1979) for the area of Završje: a) lithological map in the original scale 1:10,000 with portray of landslides of which three are active (landslides no. 1,19, 1,21, 1,28), and three are inactive (landslides no. 2,133, 2,134, 2,142); and b) landslide susceptibility map in the original scale 1:10,000. A dotted area is category II – moderately stable slopes; and stripped areas is category III – moderately unstable slopes.

The study was made by team of experts from the company 'Geotehnika-Geoexpert', based on the extensive field work and data from archive of geotechnical documentation. There are also locations without identified contours. For such areas, maps depict larger zones interpreted as zones of small landslides.

Landslide inventory from 2007

Historical landslide inventory map from 2007 was created in the framework of the study entitled 'Detailed engineering geological map of the Podsljeme urbanized zone in the scale 1:5,000, DIGK – Phase I' (Miklin et al. 2007). The study encompassed urbanized part of southern and southeastern hills of Medvednica Mt. as well as neighboring eastern areas with small settlements. Total size of the study area was approximately 175 km² (Fig. 1). The study resulted in cartographic database in Geographic information system (GIS) with the following data types: geological and hydrogeological units in the scale 1:25,000; engineering geological units in the scale 1:5,000; landslide contours; linear erosion phenomena; boreholes (existing from geotechnical reports and shallow boreholes drilled in the framework of this study); sampling points for laboratory analysis (chemical, mineralogical, geomechanical); dug wells used for ground water level measurements. All the data are presented in the form of four digital maps: geological map (Fig. 4a) and hydrogeological map in the scale of 1:25,000 (Fig. 4b); engineering geological map with landslide inventory in the scale of 1:5,000 (Fig. 4c); slope map with resolution of 25x25 m (Fig. 4d).

Landslide inventory was compiled by systematic field mapping on the base topographic maps in the scale 1:5,000 and on the basis of collected achieve information, from geotechnical documentation. Landslides are classified as active, inactive and stabilized. Unreliable landslide contours are depicted by broken lines.

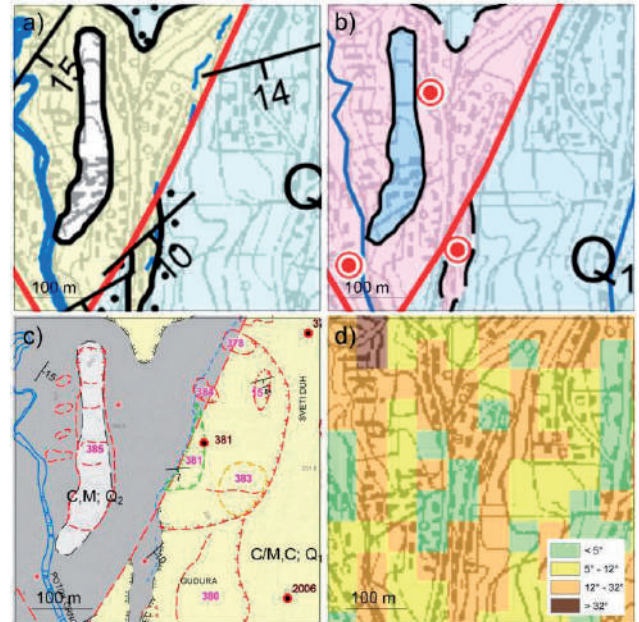


Figure 4 Segments of maps from the study 'Detailed engineering geological map of the Podsljeme urbanized zone in the scale 1:5,000, DIGK – Phase I' (Miklin et al. 2007) for the area between Črnomerac creek and Sv. Duh Street: a) geological map in the original scale 1:25,000 with portray of stratigraphical units and structural-geological symbols (e.g., geological contacts, faults and bedding orientation); b) hydrogeological map in the original scale 1:25,000 with portray of hydrogeological units and dug wells in the form of red dots; c) engineering geological map in the original scale 1:5,000 with portray of landslide contours of which seven are active (landslides no. 15, 378, 380, 384, 385), one is inactive (landslide no. 383) and one is stabilized (landslide no. 381); (d) slope map with resolution of 25x25 m.

Inventory map also depict linear erosion phenomena. Totally, there are 707 landslide phenomena (265 active landslides, 244 inactive landslides, 14 stabilized landslides, 184 potential landslides) and 266 erosion phenomena. According to landslide type, there are: 538 sliding phenomena, 11 creeping to sliding phenomena, 15 creeping to flow phenomena, 14 falls, 114 creeping phenomena and 15 instability phenomena of undefined type. Fig. 4c shows landslide inventory map with lithological cartographic units in the background of landslide contours. Descriptive data about all instabilities are given in landslide forms. Lithology was mapped in the form of engineering geological units derived on the basis of field mapping in the large scale. Thickness of superficial deposits in range of 0.2-2.0 m is presented by zones with striped patterns.

The study was ordered by the administration of the City of Zagreb responsible for construction, for the purpose of landslide inventory mapping and landslide susceptibility mapping in large scale (1:5,000). Planned application of landslide maps was definition of restrictions and conditions for constructions related to slope stability. The landslide map was made by team of two engineering geologist from Croatian Geological

Survey. The systematic field work was carried out from 2005 to 2007. Besides landslide contours of individual landslides, map also depict contours of larger unstable zones, where it was not possible to identify landslide borders. The most reliable landslide contours are those taken from geotechnical investigation reports. Updating of landslide inventory map by replacing landslide contours with more realistic once have started in 2011.

Comparison of landslide inventories

Extensive qualitative comparison of the three landslide inventories from the Podsljeme area in the City of Zagreb was given in Podolszki (2014). Two analyzed landslide inventories were prepared by the engineering geologists from the Croatian Geological Survey: Šikić (1967) in the scale 1:10,000 and Miklin et al. (2007) in the scale 1:5,000. Landslide inventory Polak et al. (1979) was prepared by engineering geologists and geotechnical engineers from the company Geotehnika-Geoexpert. Summarized comparison of main characteristics of three inventories is presented in Table 1. Landslide maps from 1979 were part of the Physical Plan of the City of Zagreb (PPGZ) until 2001. In 2009, the local government of the City of Zagreb adopted landslide inventory map from 2007 as part of the PPGZ.

Common characteristic of all existing landslide inventories prepared at the area of the City of Zagreb is that they are geomorphological historical inventories derived on the basis of extensive field mapping in large scale (1:5,000-1:10,000) with limited use of data from geotechnical documentation. Inventories from 1967 and 1979 were prepared only for urbanized part of the City of Zagreb; inventory from 2007 also encompassed area of small settlements inside border of the City. Two older landslide inventory maps were published as analog maps with lithological mapping unit in the background of landslide contours. The newest landslide inventory map from 2007 was produced in the form of GIS cartographic data base with the same concept of presentation of lithological map as background information. Landslide forms containing information about individual landslides

are part of landslide inventories from 1967 and 2007. On the basis of landslide inventory map, landslide susceptibility maps were derived in 1967 and 1979 using heuristic approach and direct mapping. In both cases, assessment was made mainly on the basis of landslide density, presence of other erosion phenomena and slope angles of the terrain.

Table 2 presents total number of mapped landslides, landslide densities and total landslide area in all three historical inventories. Number of landslides varies from 535 to 812, landslide densities vary from 4.28 to 7.73 landslides per km² and from 6.3 to 11.7%, total landslide area vary from 7.9 to 20.5 square kilometers.

Table 2 Comparison of landslide data from inventories from the hilly area of Medvednica Mt. at the area of the City of Zagreb.

	Inventory from 1967 (Šikić 1967)	Inventory from 1979 (Polak et al. 1979)	Inventory from 2007 (Miklin et al. 2007)
Total number of landslides	535	812	707
Landslide density	4.28 landslides/km ²	7.73 landslides/km ²	4.04 landslides/km ²
	6.3%	8.7%	11.7%
Total landslide area	7.9 km ²	9.1 km ²	20.5 km ²

Comparison of data about landslide size

This paragraph presents results of analysis of landslide size made by comparison of frequency-area distributions of 535 landslides from inventory from 1967, 812 landslides from inventory from 1979 and 707 landslides from inventory from 2007. Non-cumulative distributions of three analyzed landslide inventories were constructed in the form of histograms of landslide areas. Histograms were constructed by dividing the intervals covered by the data values of landslide areas into equal sub-intervals, known as “logarithmic bins” (bins of constant width in logarithmic coordinates) and using linear coordinates to display the obtained frequencies (Guzzetti 2006). Table 3 presents comparison of results interpreted from non-cumulative frequency-area histograms in log-linear coordinates of all three available inventories.

Table 1 Comparison of three geomorphological landslide inventories from the hilly area of Medvednica Mt., City of Zagreb.

Main characteristics		Inventory from 1967 (Šikić 1967)	Inventory from 1979 (Polak et al. 1979)	Inventory from 2007 (Miklin et al. 2007)
LANDSLIDE MAP CHARACTERISTICS	Map usage time	12 years (1967-1979)	Part of PPGZ 22 years (1979-2001)	Currently part of PPGZ (2009-today)
	Study area total size	125 km ²	105 km ²	175 km ²
	Landslide map type	Analogue map in the scale 1:10,000	Analogue map in the scale 1:10,000	Digital GIS map in the scale 1:5,000
	Base maps	Lithological map	Lithological map	Lithological map
	Other landslide maps prepared in the same study	Landslide susceptibility map (scale 1:10,000)	Landslide susceptibility map (scale 1:10,000)	/
SOURCE OF LANDSLIDE DATA	Main landslide identification techniques	Field mapping in large scale	Field mapping in large scale	Field mapping in large scale
	Other sources of landslide data	Historical data from geotechnical reports	Historical data from geotechnical reports Aerial photographs	Historical data from geotechnical reports
	Landslide classification	Landslide activity	Landslide activity	Landslide activity
	Landslide descriptions	Landslide forms	Short textual descriptions	Landslide forms and digital data base

Table 3 Comparison of landslide areas from three analyzed geomorphological historical inventories on the basis of non-cumulative frequency-area histograms.

	Inventory from 1967 (Šikić 1967)	Inventory from 1979 (Polak et al. 1979)	Inventory from 2007 (Miklin et al. 2007)
Minimum landslide size	607 m ²	454 m ²	284 m ²
Maximum landslide size	506,932 m ²	289,501 m ²	927,168 m ²
Range of landslide areas with maximum frequency	5,012 to 6,310 m ²	3,981 to 5,012 m ²	7,943 to 10,000 m ²
Maximum frequency of landslides in one log-bin (number, percentage)	76 (14%)	86 (11%)	55 (8%)

Comparison of the three geomorphological historical inventories shows that maximum area of identified landslides is the smallest in inventory from 1979 (landslide area of 289,501 m²), followed by maximum landslide area from inventory from 1967 (landslide area of 506,932 m²) and the largest landslide area from inventory from 2007 (landslide area of 927,168 m²). Ranges of landslide areas with maximum frequency also differ among inventories as follows: the smallest landslide areas were determined in the inventory from 1979 (landslide area of 3,981-5,012 m²) and the largest in the inventory from 2007 (7,943-10,000 m²). Frequency of landslides outside representative most frequent ranges of landslide areas are as follows:

- 121 landslides (23%) are smaller than 5,012 m² and 338 landslides (63%) are larger than 6,310 m² in the inventory from 1967;
- 326 landslides (40%) are smaller than 3,981 m² and 400 landslides (49%) are larger than 5,012 m² in the inventory from 1979;
- 256 landslides (36%) are smaller than 7,943 m² and 396 landslides (56%) are larger than 10,000 m² in the inventory from 2007.

Comparison of landslide contours on particular locations

In the following paragraphs landslide contours from all three historical inventories are compared for three locations in the City of Zagreb: the area of the Kostanjek landslide activated in 1963; area between the open pit Grmoščica and Ilica St.; and area around Jelenovac creek.

Figure 5a shows the area of the Kostanjek landslide at the landslide susceptibility map from 1967 with depicted landslide contours. There are nine landslides (landslide areas of 5,401-32,790 m²) registered at the artificial slopes of the open pit marl and on the urbanized slopes in its vicinity. Figure 5b shows landslide contours from the inventory from 1979 in which two landslides (landslide areas of 11,887 and 18,192 m²) were registered at the artificial slopes of the open pit marl. Figure 5c shows landslide contour from the inventory from 2007 of the

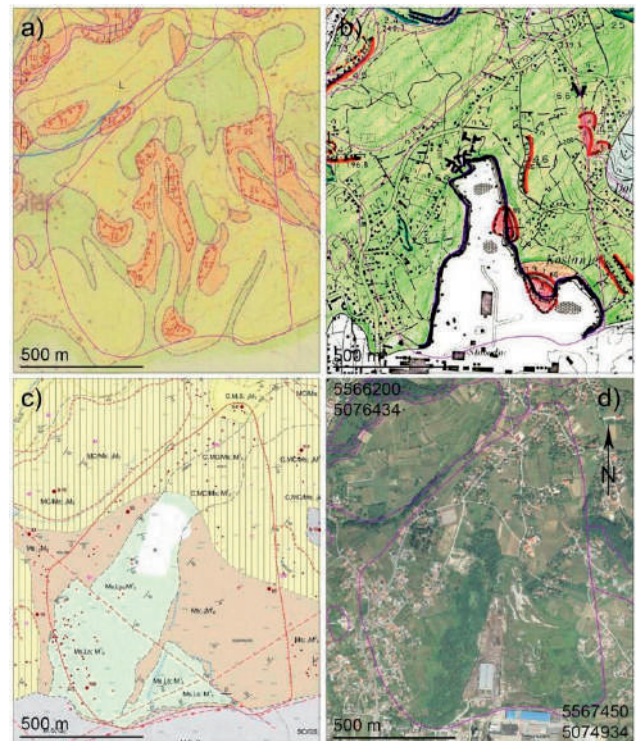


Figure 5 Landslide contours at the area of the Kostanjek landslide in Podsused-Vrapče depicted on analyzed landslide inventory maps: (a) landslide susceptibility map with landslide contours from 1967 (Šikić 1967); (b) landslide inventory map from 1979 (Polak et al. 1979); (c) landslide inventory map from 2007 (Miklin et al. 2007); (d) orthophoto map from 2007. Purple lines in 5a, 5b and 5d depict landslide contours of the Kostanjek landslide from the newest landslide inventory from 2007.

Kostanjek landslide interpreted according to detailed geotechnical investigations from 1989 (landslide area of 927,168 m²) as well as one big landslide (landslide area of 244,895 m²) on the north-western side of the Kostanjek landslide. Figure 5d is orthophoto map from 2007.

Figure 6a shows part of the area of the Grmoščica open pit and the area between open pit and Ilica St. at the landslide susceptibility map from 1967 with depicted landslide contours of only one small landslide (landslide area of 5,857 m²). Figure 6b shows landslide contours from the inventory from 1979 in which one bigger landslide (landslide area of 39,548 m²) with the direction of movement toward SE is registered. Figure 6c shows one landslide contour (14,542 m²) inside abandoned open pit and one inactive (stabilized) landslide (landslide area of 28,491 m²) interpreted in existing geotechnical report. Figure 6d is orthophoto map from 2007.

Figure 7a shows the area of the Jelenovac creek at the landslide susceptibility map from 1967 with depicted contour of one big active landslide (landslide area of 73,642 m²) on the western side of the creek. Figure 7b shows few landslide contours from the inventory from 1979 in which one inactive landslide (landslide area of 22,730 m²) and one active landslide (landslide area of

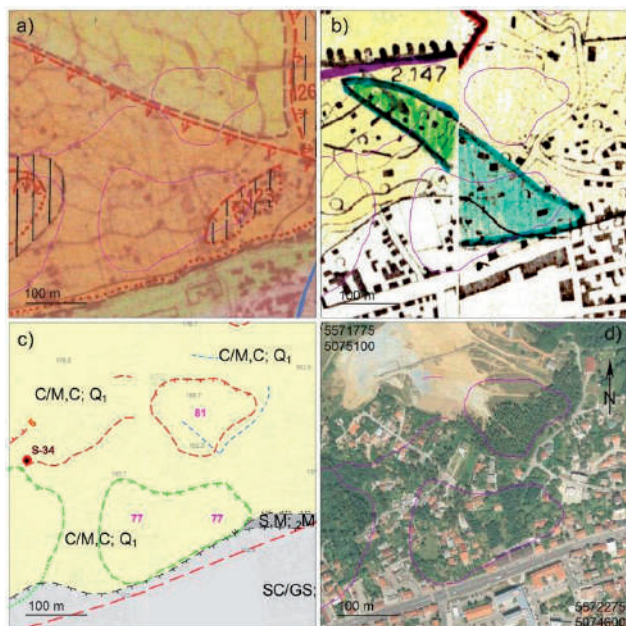


Figure 6 Landslide contours at the area south-east from the Grmošćica open pit in Črnomerec (Zagreb city) depicted on analyzed landslide inventory maps: (a) landslide susceptibility map with landslide contours from 1967 (Šikić 1967); (b) landslide inventory map from 1979 (Polak et al. 1979); (c) landslide inventory map from 2007 (Miklin et al. 2007); (d) orthophoto map from 2007. Purple lines in 6a, 6b and 6d depict landslide contours from the newest landslide inventory from 2007.

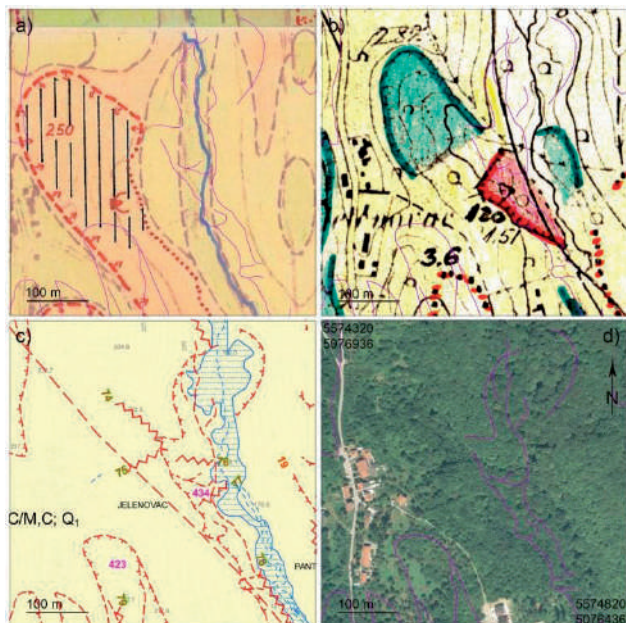


Figure 7 Landslide contours at the area of the Jelenovac creek in Črnomerec (Zagreb city) depicted on analyzed landslide inventory maps: (a) landslide susceptibility map with landslide contours from 1967 (Šikić 1967); (b) landslide inventory map from 1979 (Polak et al. 1979); (c) landslide inventory map from 2007 (Miklin et al. 2007); (d) orthophoto map from 2007. Purple lines in 7a, 7b and 7d depict landslide contours from the newest landslide inventory from 2007.

10,348 m²) are registered on the western side of the creek and one small inactive landslide (landslide area of 5,999 m²) is on eastern side of the creek. Figure 7c shows one active landslide from 2007 (landslide no. 434 with landslide area of 18,847 m²) on western side of the creek and numerous linear erosion phenomena. Figure 7d is orthophoto map from 2007.

Conclusions

Qualitative comparison of the three historical geomorphological landslide inventories from the urbanized hilly Podsljeme area of the City of Zagreb shows that there are significant differences in number of identified landslides as well as in its size. Consequently, landslide densities among different inventories vary for almost 100% if it is expressed in number of landslides per square kilometer (4.04 landslides/km² in the inventory from 2007 versus 7.73 landslides/km² in the inventory from 1979). Similarly, very large differences in landslide densities are between densities expressed in percentage of total landslide area in the total study area (6.3% in the inventory from 1967 versus 11.7% in the inventory from 2007). On the basis of analysis of maximum frequencies of landslide areas it is evident the following: 51% of landslides from landslide inventory from 1979 are smaller than 3,981 m²; 37% of landslides from landslide inventory from 1967 are smaller than 5,012 m²; and 44% of landslides from landslide inventory from 2007 are smaller than 7,943 m². Larger landslide areas and smaller number of landslide contours are indicator of mapping of larger unstable zones instead of individual landslide borders. Performed qualitative comparison of historical inventories enables evaluation of overall quality of criteria adopted during the process of landslide mapping.

References

- Basch O (1976) Basic geological map in scale of 1:100,000, Ivanić Grad Sheet. Geological Survey, Zagreb. (In Croatian)
- Guzzetti F (2006) Landslide hazard and risk assessment. PhD Thesis, Mathematisch-Naturwissenschaftlichen Fakultät der Rheinischen Friedrich-Wilhelms-Universität, University of Bonn, Bonn, Germany.
- Miklin Ž, Mlinar Ž, Brkić Ž, Hećimović I, Dolić M (2007) Report of the project 'Detailed engineering geological map of Podsljeme urban area in scale of 1:5.000 (DIKG-Phase I)'. Croatian Geological Survey, Zagreb. (In Croatian)
- Polak K, Klemar M, Nejkova M, Radošević N, Stepan Z, Miroslav M, Križanić Z (1979) Report of the study 'Lithology and categorization according to slope stability of Medvednica Mt. hills at the area of the Zagreb City.' Geotehnika-Geoexpert, Zagreb. 102p. (In Croatian)
- Podolszki L (2014) Stereoscopic analysis of landslides and landslide susceptibility on the southern slopes of the Medvednica Mt. PhD Thesis, Faculty of Mining, Geology and Petroleum Engineering, University of Zagreb, Zagreb, Croatia. (In Croatian)
- Šikić K, Basch O, Šimunić A (1972) Basic geological map in scale of 1:100,000, Zagreb Sheet. Geological Survey, Zagreb. (In Croatian)
- Šikić V (1967). Report of the study 'Engineering geological study of Zagreb and wider area'. Geol Survey, Zagreb. 131p. (In Croatian)

Derivation of Historical Land Cover Map Based on Digital Orthophoto Images of the Zagreb Area

Nikola Belić⁽¹⁾, Snježana Mihalić Arbanas⁽²⁾, Darko Šiško⁽³⁾, Dubravko Gajski⁽⁴⁾

1) Associate Researcher, Letinčićeva St. 34 HR-10000, Zagreb, Croatia, nik.belic@gmail.com

2) University of Zagreb, Faculty of Mining, Geology and Petroleum Engineering, Zagreb, Croatia

3) City of Zagreb, City Office for the Strategic Planning and Development, Zagreb, Croatia

4) University of Zagreb, Faculty of Geodesy, Zagreb, Croatia

Abstract Land cover map was made based on digital orthophoto images of Zagreb area from the year of 2007 which were used as input data. Automated supervised classification method was applied, with the use of open source software MultiSpec and GRASS GIS. Classification results were processed using combination of raster algorithms in GRASS GIS. Resulting land cover map (with 3 classes: urban areas, high vegetation areas and low vegetation areas) was compared with the official land use map of the City of Zagreb. Both maps were also compared with landslide inventory map to calculate landslide frequency in different land cover and land use types.

Keywords land cover map, land use map, automated supervised classification, digital orthophoto images, MultiSpec, GRASS GIS, City of Zagreb

Introduction

The objective of the research was to develop a historical land cover map with the emphasis on using open source GIS software and the existing input data which are available in the City Office for the Strategic Planning and Development of the City. Digital orthophoto images from 2007 were selected for the analysis performed at the research area which total size is 121.5 km².

Research area is located in hilly area of the Medvednica Mt. and it is chosen to cover test area for landslide mapping inside pilot area of the Croatian-Japanese SATREPS FY2008, as it is described in Ferić et al. (2012). Figure 1 depicts whole pilot area (with total size of 180 km²) and its relative position inside administrative boundaries of the City of Zagreb and in urbanized part named Zagreb city. Figure 2 depicts test area as well as its basic morphological characteristics: altitude and slope orientation.

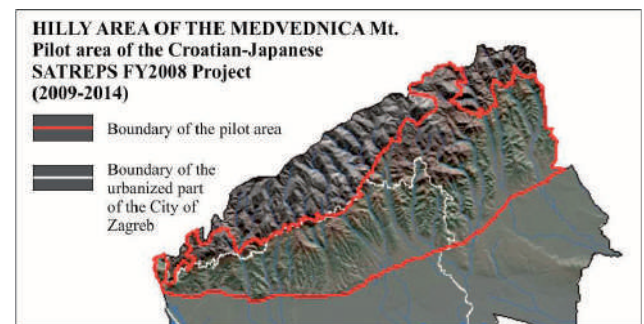


Figure 1 Pilot area (marked red) of the Croatian-Japanese SATREPS FY2008 project encompasses whole hilly area of the Medvednica Mt located inside administrative area of the City of Zagreb (Mihalić et al. 2012).

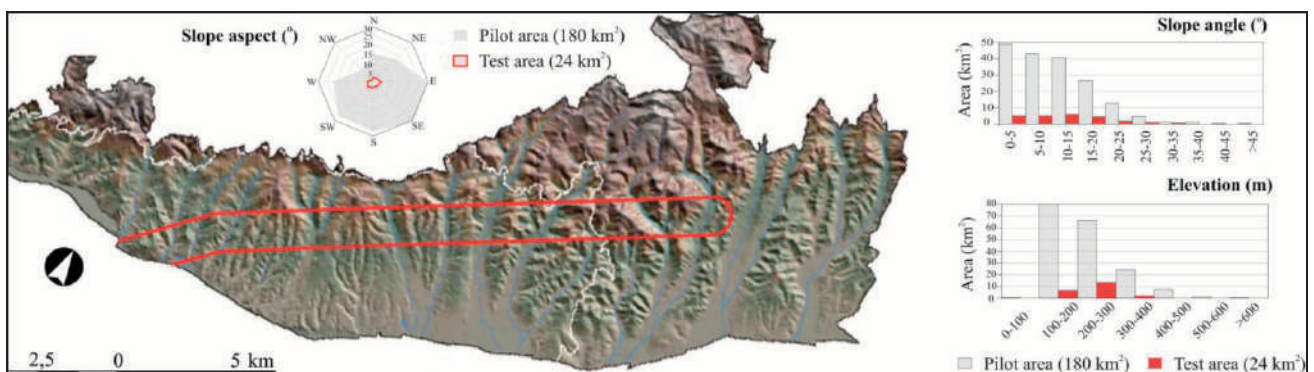


Figure 2 Map derived from the Digital Elevation Model 25 m x 25 m (DEM) of the Croatian-Japanese SATREPS FY2008 project's pilot area. The test area (marked red) covers 24 km² and it is located inside the pilot area which total size is 180 km² (Ferić et al. 2012).

The research area is covered by 18 digital orthophoto images in scale 1:5,000. Land cover map was derived using automated supervised classification in MultiSpec and GRASS GIS software with maximum likelihood and SMAP (Sequential Maximum A Posteriori) option. Additional processing of the classification results was necessary to obtain more reliable data.

Input data

Digital orthophoto images of Zagreb area from 2007 were used as an input data. The scale of orthophoto images was 1:5,000, the resolution was 6,000 x 4,500 pixels, and spatial resolution was 0.25 square meters per pixel. For the research purposes, resolution was decreased to 3,000 x 2,250 pixels, and spatial resolution was changed to 1 square meter per pixel.

Each of the 18 orthophoto images covers the area of 6.75 square kilometers and the total area amounts to 121.5 square kilometers. The images consist of RGB channels (Red, Green and Blue) with absence of NIR (Near Infra - Red) channel. Using the NIR channel would increase NDVI (Normalized Difference Vegetation Index), which would improve classification results for the green channel, and differentiation of vegetation cover type.

Data analysis

MultiSpec software

MultiSpecWin32 software (developed by Prof. David Landgrebe and Larry Beihl at Purdue University in Indiana, US) is the system used for interactive analysis of multispectral satellite (Landsat) and space hyperspectral image data and aerial photographs of the Earth (AVIRIS), and also has important applications in the processing of digital images in medicine (Biehl and Landgrebe 2011).

Figure 3 shows the classification procedure in MultiSpec. First step is the determination of 'Training' and 'Test' fields in the original image which are used for

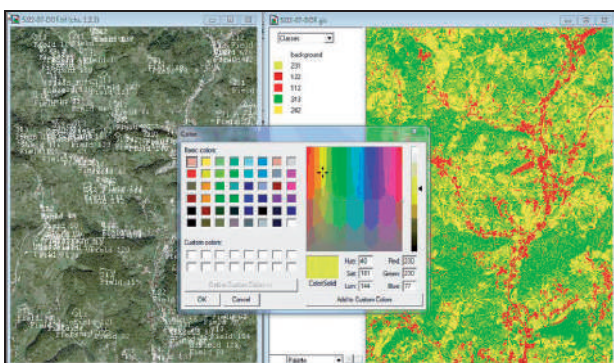


Figure 3 Classification in MultiSpec; determination of 'Training' and 'Test' fields in the original image (left), classification results (right) and editing class color (center).

classification. Next step is choosing classification type; Maximum Likelihood or SMAP (Sequential Maximum A Posteriori). Final step is editing classification results, by changing color and text. Results were shown visually and numerically in the confusion matrix for each image. Visual results, presented in Fig. 3 as classification results, did not express clear distinction of land cover classes. Consequently, they needed to be additionally processed using GRASS GIS. Automated supervised classification followed by additional processing was performed on whole area of each of 18 digital orthophoto images (18*6.75 km²) and on the area clipped by border of the project test area (24 km²).

GRASS GIS software

GRASS software (Geographic Resources Analysis Support System) is an open source GIS, originally developed by the US Army (1982-1995). Since 1997 it is developed by an international team of scientists and experts gathered in the OSGeo (Open Source Geospatial Foundation), a non-profit organization whose mission is the promotion and development of geospatial technologies and data (GRASS GIS 2011).

Classification procedure in GRASS GIS is similar to the one in MultiSpec. First step is to develop a 'signaturefile' (Fig. 4A) in the original image, by drawing polygons that represent different area types, i.e., classes. Signaturefile is used to create 'ground truth training map' (Fig. 4B) by adding values to the selected areas, which allows building an attribute table used for classification. In the process, there is an option of choosing Maximum Likelihood or SMAP classification. The result (Fig. 4C) needs to be edited by changing color and text, and additionally processed using raster processing modules.

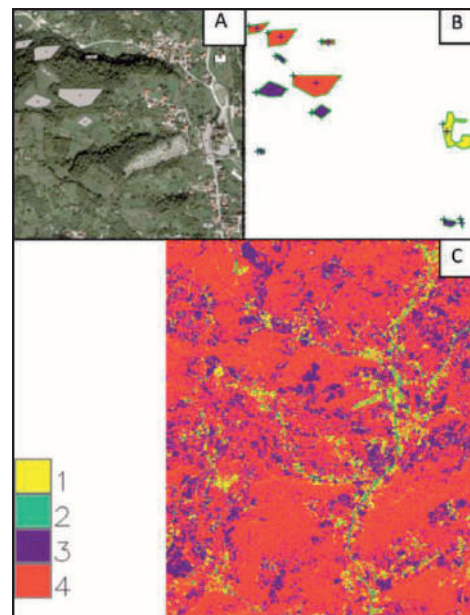


Figure 4 Classification in GRASS GIS; (A) development of 'signaturefile', (B) creating ground truth training map, and (C) the result.

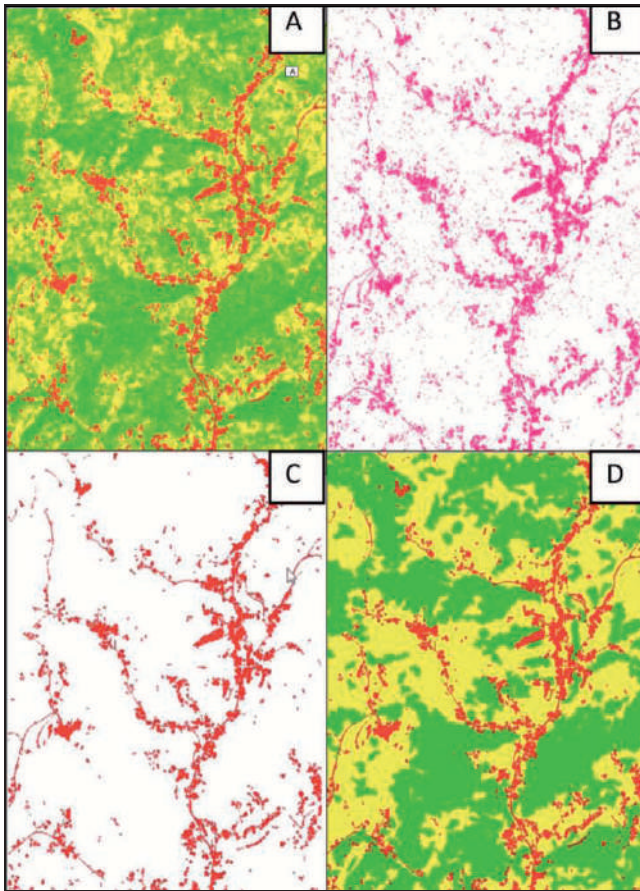


Figure 5 Processing in GRASS GIS: (A) original result derived by automated classification, (B) extracted bitmap file for class 1 – urban areas, (C) bitmap file for class 1 after processing by GRASS GIS, and (D) the resulting map with three separate processed classes.

Due to software imperfection, within one class value, pixels with other class values were scattered. This problem was solved with a combination of different raster processing algorithms in GRASS GIS. The key was to process each class separately, as a bitmap file.

Series of derivative maps created during processing procedure in GRASS GIS is illustrated in Figure 5. The original result of automated classification (Fig. 5A) is used to extract separate bitmap files for all classes, for example class 1 – urban areas (Fig. 5B). Further processing of particular class was done using combinations of raster algorithms, for example `r.reclass`, `r.reclass area`, `r.grow` and `r.null`. Final land cover map with three classes (Fig. 5D) is result of merging three separately processed bitmap files.

The same procedure was applied to whole area of each of 18 digital orthophoto images (18*6.75 km²) and to the area clipped by border of the project test area (24 km²). The classification nomenclature and color RGB values for classes used for the map production, with minor adjustments, are taken from the Corine Land Cover classification (Croatian Environment Agency 2011).

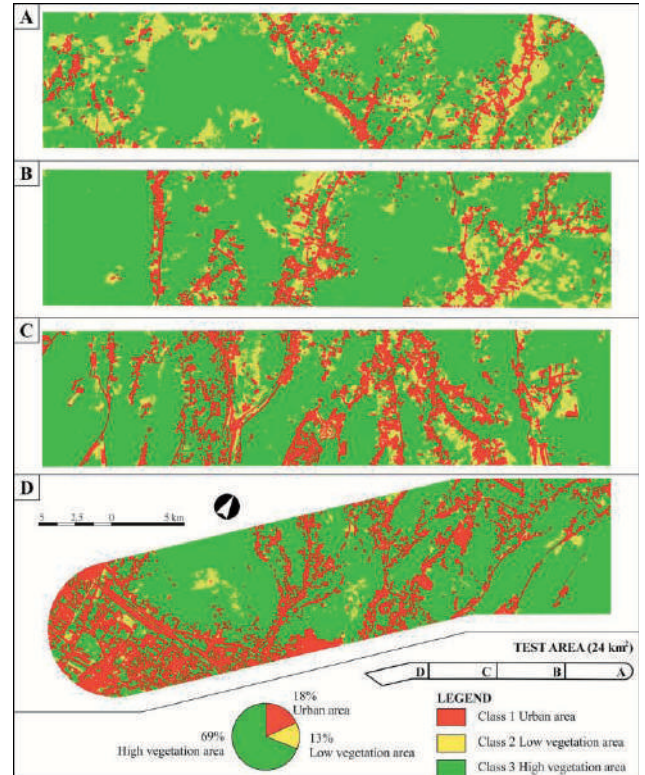


Figure 6 Historical land cover map based on digital orthophoto images of the Zagreb Area. The diagram shows representation of land cover classes: 18% of class 1, 13% of class 2, and 69% of class 3.

Results

Historical land cover map

The result of the research was the historical land cover map from 2007 based on automated supervised classification and processing of the digital orthophoto images in the scale 1:5,000 for the area of the 121,5 km². Fig. 6 shows historical land cover map for the project's test area of 24 km². Both maps consist of three classes: class 1 - urban areas, class 2 - low vegetation areas, and class 3 - high vegetation areas. The diagram shows relative representation of classes in the whole test area: 18% for urban areas; 13% for low vegetation areas; and 69% for high vegetation areas.

Application of historical land cover maps in landslide hazard and risk analysis

Derived historical land cover map from 2007 and land use map from 2012 were compared with landslide inventory map from 2010 to calculate landslide frequency in different land cover and land use types. Landslide inventory map (Ferić et al. 2012), derived on the basis of visual classification of airborne LiDAR DEM scanned in April 2010, was used as an input data for landslide frequencies.

Table 1 shows relative frequency of landslides in land use classes where 78% landslides are in forest areas and 12% landslides are in arable land. Table 2 shows relative frequency of landslides in land cover classes where 88% landslides are in high vegetation areas, and 6.58% in low vegetation areas.

Table 1 Landslide area in classes of land use map from 2012.

Category	Percentage (%)	Area (m ²)
2100A - residential and mixed objects	1	2,988
2200 - outbuildings	0	99
2400 - other facilities	0	1,268
4100 - road traffic	1	2,497
5100A - arable land – ploughed land	0	714
5100B - arable land - meadows	5	18,086
5100C - arable land - orchards and vineyards	7	24,648
5100F – forest land - forest	78	262,270
5100G – forest land - thickets	1	4,471
5300D - yards	6	19,329
5300F – developed area - graveyard	0	346
Total area:		336,716

Table 2 Landslide area in classes of land cover map from 2007.

Class	Percentage (%)	Area (m ²)
1 – urban areas	5,37	18,067
2 – low vegetation areas	6,58	22,158
3 – high vegetation areas	88,05	296,484
Total area:		336,709

Conclusions

Land cover map was created on the basis of digital orthophoto images of Zagreb area from the year of 2007. Historical orthophoto images in the scale 1:5,000 were used as input data for automated supervised classification in MultiSpec and GRASS GIS software with maximum likelihood and SMAP (Sequential Maximum A Posteriori) option followed by additional processing to improve classification results. The advantage of using automated classification instead of semi-automated or manual classification is the overall speed of map derivation process. Disadvantage is relatively small number of classes in a resulting map which is caused due to the absence of NIR channel. Further advantage of the used approach is availability of this kind of historical data (i.e., orthophoto images from different historical period of the City of Zagreb), which enables derivation of historical

land cover maps. The use of open source software is also important for financial feasibility of recommended type of analysis of historical data.

The automated supervised classification method of orthophoto images is somewhat less precise, but its simplicity and performance speed, and mostly financial justifiability are highly advantageous. The semi-automated classification of airborne LiDAR derived images is more expensive, but on the other hand, more precise.

Resulting land cover map (with 3 classes: urban areas, high vegetation areas and low vegetation areas) was compared with the official land use map of the City of Zagreb (which depicts 23 classes of land use types) derived on the basis of semi-automated classification of airborne LiDAR DEM scanned in March 2012. The objective was to evaluate quantitatively quality of classification.

Spatial analysis shows that more than 80% landslide area is placed in high vegetation zones (forest), which implies necessity of use of landslide data before planning changes of land use types (e.g. deforestation).

Acknowledgments

We kindly thank to the City Office for the Strategic Planning and Development of the City for providing digital orthophoto images and land use data.

References

- Beihl L, Landgrebe D (2011). MultiSpec – A Freeware Multispectral Image Data Analysis System. URL: <https://engineering.purdue.edu/~biehl/MultiSpec/> [Last accessed: 8 July 2011].
- Croatian Environment Agency (2010). Land Cover and Land Use Database – CORINE Land Cover. URL: <http://www.azo.hr/CORINELandCoverCLC> [Last accessed: 28 March 2013].
- Ferić P, Mihalić S, Krkač M (2012). Visual mapping of landslides from LiDAR imagery, Zagreb, Croatia. 2nd Project Workshop on Risk Identification and Land-Use Planning for Disaster Mitigation of Landslides and Floods, Rijeka (Croatia), 15-17 November 2011, pp 132 - 135.
- GRASS GIS (2011). The World Leading Free Software GIS. URL: <http://www.grass.fbk.eu> [Last accessed: 18 February 2013].
- Mihalić S, Bernat S, Hamasaki E, Gerber N (2012). Historical landslides in the City of Zagreb (Croatia): Analysis of existing data. 2nd Project Workshop on Risk Identification and Land-Use Planning for Disaster Mitigation of Landslides and Floods, Rijeka (Croatia), 15-17 November 2011, pp 124 - 127.

Shallow Landslide Susceptibility Mapping Using SINMAP in Zagreb Hilly Area, Croatia

Chunxiang Wang⁽¹⁾, Snježana Mihalić Arbanas⁽²⁾, Hideaki Marui⁽¹⁾, Naoki Watanabe⁽¹⁾, Gen Furuya⁽³⁾

1) Niigata University, Research Institute for Natural Hazards and Disaster Recovery, Niigata, Japan

2) University of Zagreb, Faculty of Mining, Geology and Petroleum Engineering, Zagreb, Croatia

3) Toyama Prefectural University, Faculty of Engineering, Toyama, Japan

Abstract This study was carried out to map the landslide susceptibility of the hilly area of Medvednica Mt. located in the northwestern part of the City of Zagreb, Croatia. Landslides in this region are mostly shallow movements of superficial deposits along contacts with fresh deposits of soil and cause significant economic losses by damaging houses and the urban infrastructure. The method used here is the deterministic slope stability analysis model SINMAP which is developed by Pack et al. (2005). SINMAP is a raster based slope stability predictive tool based on coupled hydrological-infinite slope stability model. This approach applies to shallow translational landslide phenomena controlled by shallow ground water convergence. The input data required for this model are: (i) inventory of past landslides in a point vector format, (ii) Digital Elevation Model (DEM) of the study area, (iii) geotechnical data such as soils strength properties, thickness of soil above the failure plane, and (iv) hydrological data such as soils hydraulic conductivity and the rainfall amount. Because the geotechnical and hydrological data are highly variable in both, space and time, the method does not require numerically precise input and accepts ranges of values that represent this uncertainty. The major output of this model is the stability index grid theme, which can be used as a landslide susceptibility map. The results also provided statistical summary of slope stability index for the study area facilitating the data interpretation. Three different rainfall recharge scenarios are considered: 50 mm/day, 100 mm/day and 150 mm/day. The landslide susceptibility map which is developed in this study is also compared with two landslide inventory maps.

Keywords shallow landslide, susceptibility mapping, landslide inventory, SINMAP

Introduction

The City of Zagreb is located in northwest Croatia in the western part of the Pannonian Basin. The urbanized area is located below the forest region of Medvednica Mt. to the north and extends to the flood plain of the Sava River

in the south. Approximately 40% of the urban area is located in hilly areas in which landslides are the main geological hazard. Landslides in the hilly area of Zagreb are mostly small and shallow movements of superficial deposits along contacts with fresh deposits of soil (Mihalić and Arbanas 2013). Despite this, landslides cause significant economic losses by damaging houses and the urban infrastructure.

The hilly area of Medvednica Mt., which covers about 180 km², is the pilot area of Japanese-Croatian scientific joint-research project 'Risk Identification and Land-Use Planning for Disaster Mitigation of Landslides and Floods in Croatia'. The study area of approximate size of 45 km² is part of the hilly area of Medvednica Mt. Figure 1 shows the digital elevation model of the study area.

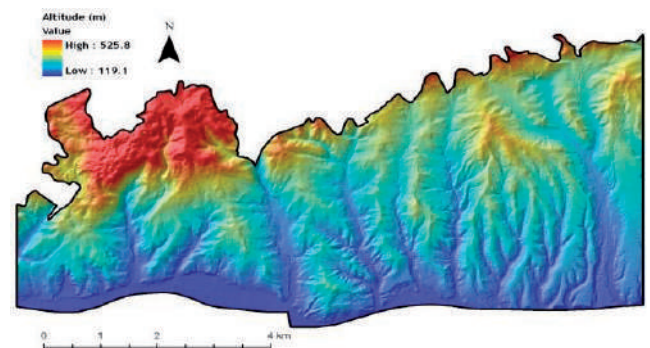


Figure 1 Digital elevation model of the study area.

The most frequent triggering factor of landslides is rainfall. The objectives of the study are to map the shallow landslide susceptibility using SINMAP model considering 3 different precipitation scenarios and to compare landslide susceptibility map generated by this study with the two landslide inventory maps: (1) the landslide inventory from 1979 (Polak et al. 1979); 2) the landslide inventory derived in 2012 by interpretation of stereo-pairs of aerial photos from 1998 accompanied by landslide evaluation using AHP (Analytical Hierarchy Process) method (Hamasaki and Miyagi 2012).

The infinite-slope stability model SINMAP

The SINMAP (Stability INDEX MAPping) methodology is based upon the infinite-slope stability model that balances the destabilizing components of gravity and the restoring components of friction and cohesion on a failure plane parallel to the ground surface with edge effects neglected. The details of the SINMAP model are available in Pack et al. (2005). The summary of the SINMAP modeling approach is provided in the following sections.

The SINMAP developed by Pack et al. (2005) is based on a combination of an infinite-slope stability model and a hydrological model used to define a stability index (*SI*) (Eq. 1), which is defined as the probability of a stable slope, assuming a uniform distribution of the parameters on the uncertainty margins; this index ranges from 0 (unstable) to 1 (stable).

$$FS = \frac{C + \cos\theta \left[1 - \min\left(\frac{Ra}{T \sin\theta}, 1\right) r \right] \tan\varphi}{\sin\theta} \quad [1]$$

where: $C=(C_r + C_s)/(h\rho_s g)$ is the combined cohesion of roots and soil made dimensionless relative to the perpendicular soil thickness; h is soil thickness, perpendicular to the slope; $r = \rho_w/\rho_s$ is the water to soil density ratio; θ is the angle of the slope ($^\circ$); and φ is the angle of internal friction ($^\circ$). The relative wetness which is expressed as Eq. 2 is incorporated into SINMAP.

$$w = \min\left(\frac{Ra}{T \sin\theta}, 1\right) \quad [2]$$

The ratio R/T is the ratio of the steady-state recharge (r) (m/hour) and the soil transmissivity (t , m^2 /hour). The specific area of the basin, “ a ”, is defined by the surface area in relation to the contour length of the unit (m^2/m). A value of 1 indicates that any excess above this limit will be assigned to one surface flow that flows over the soil surface.

SINMAP is utilized in the study for modeling the rainfall-triggered shallow landslides at a regional scale and allows uncertainty in the three variables (C , $\tan\varphi$, and R/T) through the specification of upper and lower boundaries. These boundaries define uniform probability distributions over which these parameters are assumed to vary at random. Denoting $R/T=x$, $\tan\varphi=t$, and the uniform distributions with upper and lower boundaries as $C\sim U(C_1, C_2)$, $x\sim U(x_1, x_2)$, and $t\sim U(t_1, t_2)$, the probability is evaluated over the distributions of C , x , and t . The smallest C and t (C_1 and t_1) together with the largest x (x_2) defines the worst-case (most conservative) scenario under the assumed uncertainty (variability) in the parameters. Areas under this worst-case scenario where the factor of safety (FS) is greater than 1 are, according to this model, unconditionally stable. For areas

where the minimum FS is less than 1, there is a probability of failure. This is a spatial probability due to the uncertainty (spatial variability) in C , $\tan\varphi$ and T . In these regions with $FS_{min} < 1$, SI is defined as $SI = \text{Prob}(FS > 1)$. The best-case scenario is when $C=C_2$, $x=x_1$, and $t=t_2$. In the case that $FS_{max} < 1$, then $SI = \text{Prob}(FS > 1) = 0$.

Classification of stability index values (SI) and descriptive terms for the stability of shallow landslides assessed using SINMAP is given in Table 1.

Table 1 SINMAP stability index (SI) classification.

Stability index values (SI)	Classification
$SI > 1.5$	Stable
$1.5 > SI > 1.25$	Moderately stable
$1.25 > SI > 1.0$	Quasi-stable
$1.0 > SI > 0.5$	Lower threshold
$0.5 > SI > 0.0$	Upper threshold
$0.0 > SI$	Defended

Data processing

In order to use the SINMAP methodology to derive a shallow landslides susceptibility map for the study area, several steps are accomplished, starting with selection of input data, which depends on the available digital elevation model (DEM) and landslide inventory, and ending by the presentation of final result, which is a definition of grid theme that divides the study area into several zones depending on the stability index.

A topographical map of the study area is a 5x5 m resolution DEM shown in Figure 1. For calibration purposes, the landslides inventory map is needed. In this study, two landslide inventory maps are used. One is a historical landslide inventory map compiled on the basis of field mapping and published in 1979 by Polak et al. (1979). The second is a geomorphological inventory derived by interpretation of stereo pairs of aerial photographs in the frame of the Japanese-Croatian SATREPS FY2008 project (Hamasaki and Miyagi 2012).

Nearly 52-year-long daily rainfall record from 1961–2012 was used to determine rainfall magnitude for the study area. The maximum precipitation was 95.8 mm/day recorded in August 4, 1989, and the cumulative precipitation for seven days period was 134 mm recorded in November, 1962.

Hydrological data are included into the model in the form of a wetness index (T/R) parameter. According to the SINMAP Manual (Pack et al. 2005), the parameter (T/R) is considered as the length of hill slope required to develop saturation in the critical wet period. T is the transmissivity or the vertical integral of the hydraulic conductivity of soil zone and is determined by $T=(ks)\times h$, where ks is the hydraulic conductivity or the permeability of the soils and h is the thickness of the soil above the failure surface. Hydraulic conductivity of the weathered surface zone is $10^{-5} \sim 10^{-3}$ m/second.

Table 2 Parameters values used for the study area.

Case	Dimensionless cohesion		Friction angle (°)		Recharge (mm/day)	T/R (meter)	
	L	U	L	U		L	U
1	0.1	0.7	10	30	50	345	1.382
2	0.1	0.7	10	30	100	172	691
3	0.1	0.7	10	30	150	115	460

L = Lower bound value; U = Upper bound value

Cohesion index and internal friction angle of soils are the geotechnical parameters included into the model. Cohesion index is the relative contribution of soil and root cohesive forces combined to slope stability. In this study, the failure surface is assumed to be below the root zone. Therefore, only cohesive strength of soil (Cs) was considered.

Rainfall was chosen as the most frequent triggering factors of landslides. The three different rainfall recharge scenarios are considered: 50 mm/day, 100 mm/day and 150 mm/day.

Table 2 shows parameters values used for the study area in the City of Zagreb.

Results

Using the 5x5 m DEM and the input parameters listed in Tab. 2, the SINMAP model was used to derive a stability index map. The SI distribution maps of the three different rainfall recharge scenarios are shown in Figures 2-4, respectively.

The percentage of area classified as unstable were about: 48% for rainfall intensity of 50 mm/day; 64% for rainfall intensity of 100 mm/day; and 67% for rainfall intensity of 150 mm/day. Upper threshold of the stability index covers 0.27%, 0.35%, and 0.45%, respectively. Rainfall recharge decreases the safety factor over time. These maps are very useful for identifying where and when the critical slope with high landslide susceptibility can be expected.

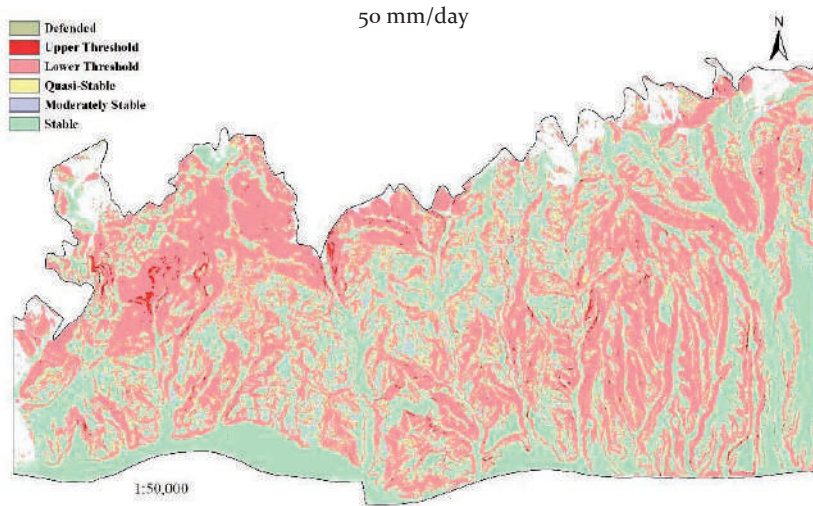


Figure 2 Slope stability index with for precipitation scenario of 50 mm/day.

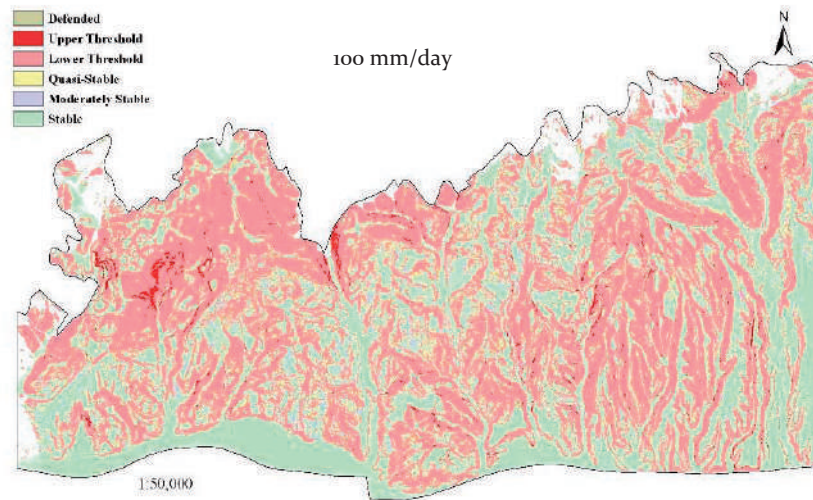


Figure 3 Slope stability index with for precipitation scenario of 100 mm/day.

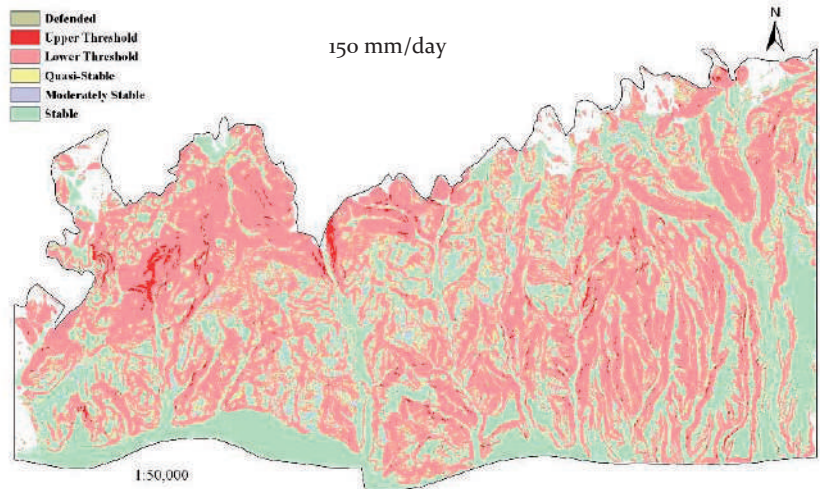


Figure 4 Slope stability index with for precipitation scenario of 150 mm/day.

Figure 5 shows the slope stability index map with for precipitation scenario of 150 mm/day overlain by the landslide inventory map from 1979 (Polak et al. 1979). There are 94 landslides in this historical inventory and 64 of this fall within the lower stability classes. Figure 6 shows the slope stability index map with for precipitation

scenario of 150 mm/day overlain by the geomorphological landslide inventory map derived on the basis of the photogrammetric analysis of stereo-pairs of aerial photographs from 1998. There are 142 landslides and 101 landslides fall within the lower stability classes.

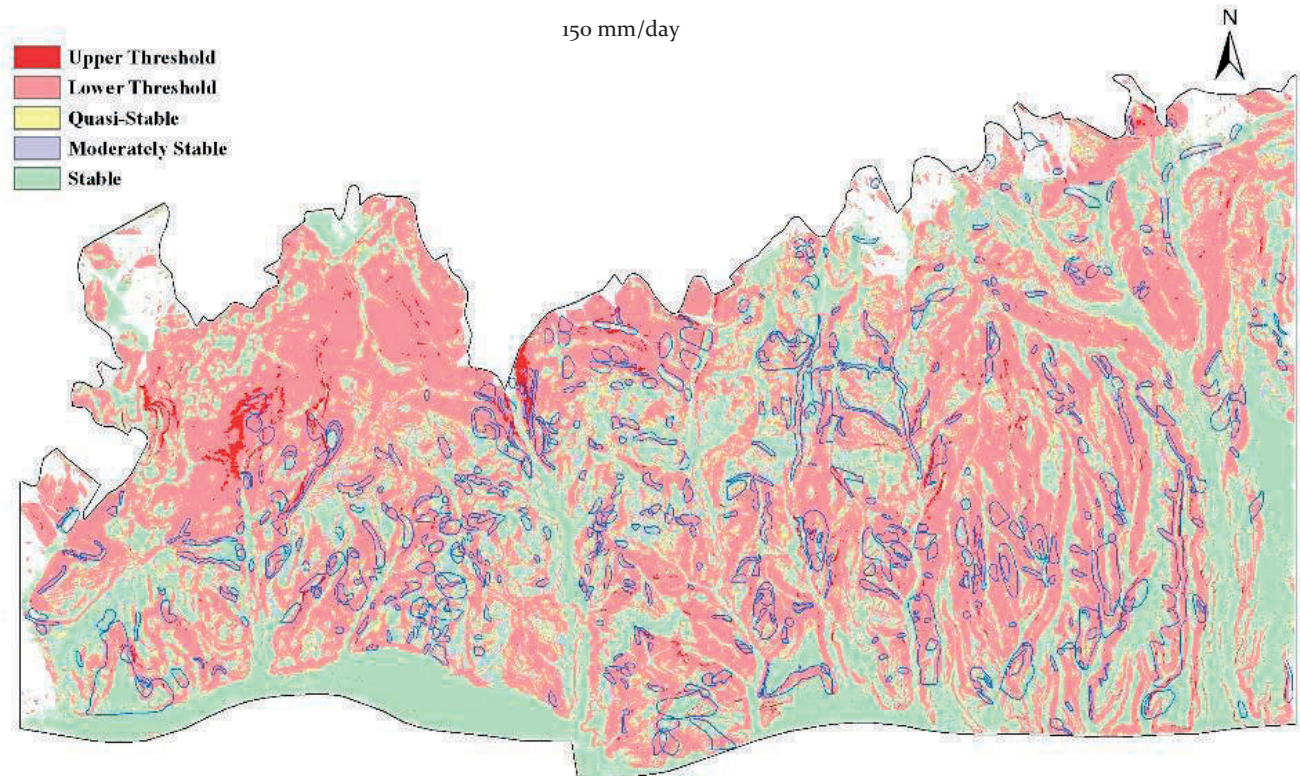


Figure 5 Slope stability index map with for precipitation scenario of 150 mm/day overlain by the historical landslide inventory from 1979 (Polak et al. 1979).

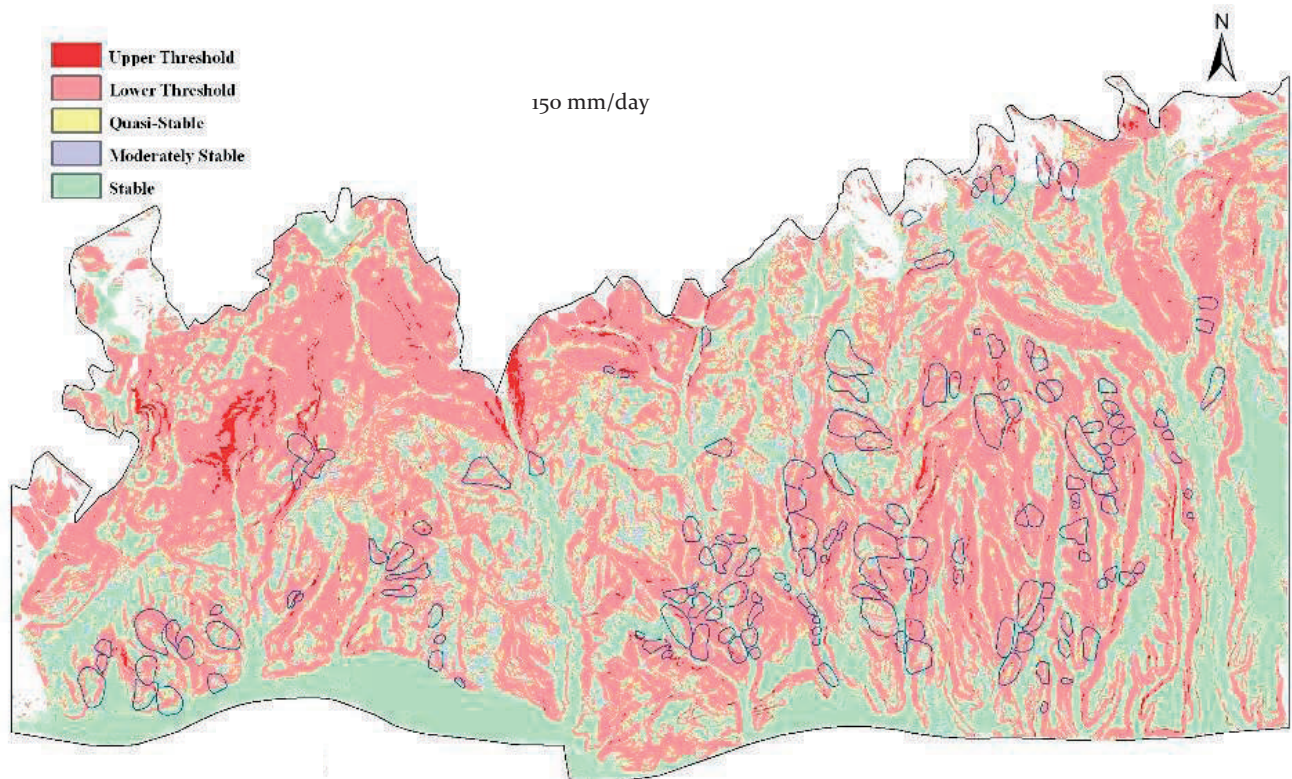


Figure 6 Slope stability index map with for precipitation scenario of 150 mm/day overlain by the geomorphological landslide inventory based on interpretation of stereo-pairs of aerial photographs taken in 1998 (Hamasaki and Miyagi 2012).

Conclusions

The deterministic slope stability model SINMAP was used to assess the susceptibility of slopes to shallow landslides in the study area of the hilly area of Medvednica Mt., under daily rainfall with three different scenarios. The percentage of area classified as unstable are 48%, 64%, 67% for 3 different rainfall 50 mm/day, 100 mm/day and 150 mm/day respectively. There is no significant difference for unstable area between 100 mm/day and 150 mm/day. From the rainfall data of the period of 52 years, the maximum precipitation is 95.8 mm/day. Therefore, the results derived on the basis of 100 mm/day can be satisfactory for the shallow landslide susceptibility map for the study area. The natural causative factors such as lithology, thickness of soil layer, slope angle range, hydrology, and landforms are reasonably represented in the SINMAP model. Therefore, it is reasonable to assume that this model can be utilized as a tool for identification of landslide hazard zones in the study area. The preliminary results could be regarded as a good reference

for preparation of landslide hazard map and land use guidelines which are objectives of the Japanese-Croatian joint research project.

References

- Hamasaki E, Miyagi T (2012) Report of Japanese-Croatian joint project "Risk Identification and Land-Use Planning for Disaster Mitigation of Landslides and Floods in Croatia". Niigata University, Japan. (In Japanese)
- Mihalić S, Arbanas Ž (2013) The Croatian–Japanese Joint Research Project on Landslides: Activities and Public Benefits. Sassa K et al. (eds), *Landslides: Global Risk Preparedness*, Springer, Verlag, Germany. (DOI 10.1007/978-3-642-22087-6_24). pp. 335-351.
- Pack R T, Tarboton D G, Goodwin C N, Prasad A (2005) SINMAP 2. A Stability Index Approach to Terrain Stability Hazard Mapping, technical description and users guide for version 2.0. Utah State University, U.S. 65p.
- Polak K, Klemar M, Nejkova M, Radošević N, Stepan Z, Miroslav M, Križanić Z (1979) Lithology and landslide susceptibility zonation of the hilly area of Medvednica Mt. at the area of the Zagreb city. Technical report. Geotehnika-Geoexpert, Zagreb. 102p. (In Croatian)

Deterministic Landslide Susceptibility Analyses Using LS-Rapid Software

Sanja Dugonjić Jovančević⁽¹⁾, Osamu Nagai⁽²⁾, Kyoji Sassa⁽²⁾, Željko Arbanas⁽¹⁾

1) University of Rijeka, Faculty of Civil Engineering, Rijeka, Croatia, Radmile Matejčić 3, +385 51 265934

2) International Consortium on Landslides, Kyoto, Japan

Abstract This paper presents the landslide susceptibility analyses on flysch slopes in Istra, Croatia, performed using deterministic three dimensional analyses in LS-Rapid software. The area of investigation is in the Pazin Paleogene Flysch Basin in the northeastern part of the Istrian Peninsula. Using deterministic approach in landslide hazard and risk analysis includes gathering of fundamental data about geometry, soil strength parameters, cover thickness and groundwater level, as well as the application of numerical models in safety factor calculation. LS-Rapid uses 3D models for simulation of progressive failure phenomena, developed to assess the sliding initiation and activation of landslides triggered by earthquake, rainfall or their combination. Detail distribution of pore pressures or the groundwater level inside the slope is taken into account through the pore pressure ratio r_u , which gradually increases until the failure appearance in a certain part of the slope. If this approach is applied on the wider area, in which is possible to define the relative position of sliding surface, it is possible to obtain the values of the critical pore pressure ratio that causes conditions in which failures occur in a specific parts of the investigation area. Connecting the critical pore pressure ratio with distribution of rainfall it is possible to obtain the landslide susceptibility and landslide hazard. The model was validated through the interpretation of stereopairs and engineering geological mapping, and the results have shown that landslides inside the zones that in model were characterized as highly susceptible, occurred in the nearest of farthest past.

Keywords landslide susceptibility, deterministic analyses, LS-Rapid, triggering factor, pore pressure ratio

Introduction

One of the key objectives of the Japanese-Croatian Project ‘Risk Identification and Land-Use Planning for Disaster Mitigation of Landslides and Floods in Croatia’ within the Working Group 3 (WG3) is landslide susceptibility zonation and hazard mapping of the investigation areas. Landslide susceptibility is function of the present slope stability (expressed through the safety factor), together with the existence and activity of

triggering factors which cause increasing of active forces or decreasing of strength and, consequently, landslide activation.

Deterministic approach, using LS-Rapid software has been applied on the flysch area in Istria, Croatia. This area is in the Pazin Paleogene Flysch Basin in the northeastern part of the Istrian Peninsula which stretches from Trieste Bay in the west to the Učka Mountain in the east (Fig. 1). This area is formed of flysch units and, because of their gray color, is called Gray Istria. Types of landslides that generally occurred in the area are rotational and translational type landslides, as well as rock falls and debris flow.

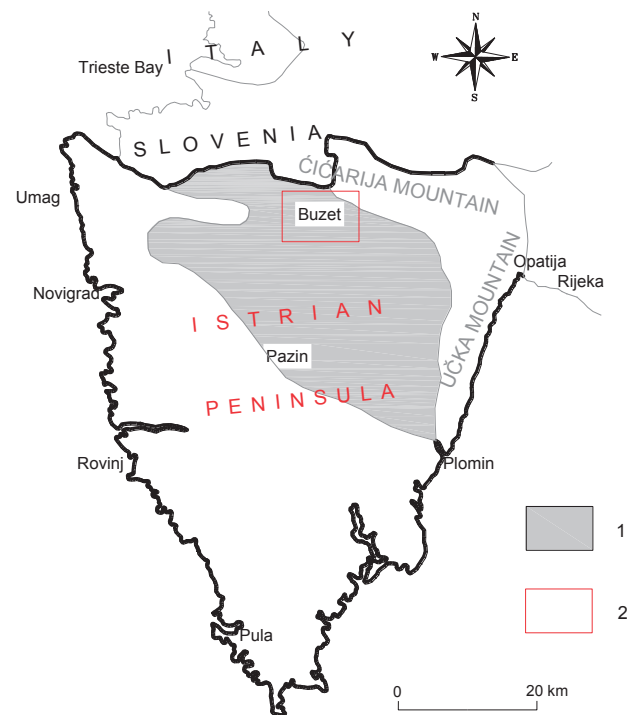


Figure 1 Simplified map of the Istrian Peninsula: 1 Flysch Basin, 2 The analysed area around the City of Buzet.

According to the well-known and widely applied principle “The past and the present are keys to the future” (Varnes 1984, Carrara et al. 1995), it is assumed that new landslide occurrences on the flysch slopes will appear in

morphological, geological, hydrogeological and geotechnical conditions that are similar to the conditions of recent landslide occurrences (Dugonjić et al. 2008, Dugonjić Jovančević and Arbanas 2012).

From the previous investigations performed in the flysch area of Gray Istria following conditions that predispose future landslides on flysch slopes can be listed as follows: 1. geological conditions in which the clayey superficial deposit is present over the flysch bedrock on a slope with suitable inclination and kinematic conditions for sliding; 2. conditions that allow the admission of a corresponding amount of water from higher parts of the slope; 3. conditions in which the inclination of the almost-impermeable flysch bedrock retaining the groundwater at the location or in the direction of the groundwater flows is close to the slope inclination; and 4. conditions in which the slope is exposed to a sufficiently long, continuous period of rainfall with corresponding infiltration. The fourth condition is the main triggering factor for the activation of landslides on the flysch slopes of Gray Istria, and is important to landslide susceptibility and hazards assessment as well as mitigation measures and risk management (Dugonjić Jovančević and Arbanas 2012).

Deterministic approach in landslide hazard and risk analyses

The use of deterministic models in landslide hazard analyses has not the pretention to calculate in an absolute and precise way the safety factor at each site in the terrain. The high spatial variability of geotechnical parameters is serious limitation of this model. The final stage in deterministic landslide hazard zonation consists of the calculation of failure probability maps to convert factor of safety maps into failure probability maps.

Using deterministic approach in landslide hazard and risk analysis includes gathering of fundamental data about geometry, soil strength parameters, cover thickness and groundwater level, as well as the application of numerical models in safety factor calculation. Such an approach is often used in geotechnical engineering in slope stability analysis for common engineering problems. Most common is the one-dimensional deterministic model, and one of the mostly used methods inside its framework is stability analysis of infinite slope. Accuracy and reliability of safety factor calculation in each model are defined by the level of field investigations at the location, accuracy of the input data and understanding of the stress history. Detailed study of the whole area can give relatively accurate input parameters for the model, but is hard and demanding work. In some cases, heterogeneous areas are simplified and the gained input parameters are extrapolated to a wider area than the investigated location. These are basic limitations of the deterministic model.

Using of Geographic Information System (GIS) can facilitate deterministic as well as probabilistic geotechnical approach, as part of landslide hazard assessment methodology. However, high accuracy in data preview inside GIS cannot replace high impropriety in the assessment of the failure probability which is result of the wrong selection of the geotechnical model or inappropriate failure mechanism. Two dimensional and three dimensional deterministic analyses currently cannot be performed inside GIS, yet the data are being exported in some external software for 2D and 3D slope stability analyses and then restored in GIS as a results preview tool. That is applicable on a very small investigation area with huge amount of available information, where the data conversion between software presents the highest challenge.

Application of LS- Rapid software on the investigation area in Istria, Croatia

Theoretical background of LS- Rapid software

LS-Rapid software uses three dimensional models for simulation of progressive failure phenomena, developed to assess the sliding initiation and activation of landslides triggered by earthquake, rainfall or their combination. LS-Rapid aims to combine the process of landslide initiation and process of sliding mass movement (dynamic analysis), including the process of the sliding mass volume enlargement on the sliding path (Sassa et al. 2010). This model is based on the key parameter - shear resistance in the steady state which can be measured or established by soil laboratory testing. The software offers the recommended values for the input parameters in case when no detail data of the investigation area are available. The basic concept of simulation is based on the analysis of the forces acting on a vertical column inside the moving mass (Fig. 2).

Increase in pore pressure during the rainfall affects the development of the sliding surface and initiation of

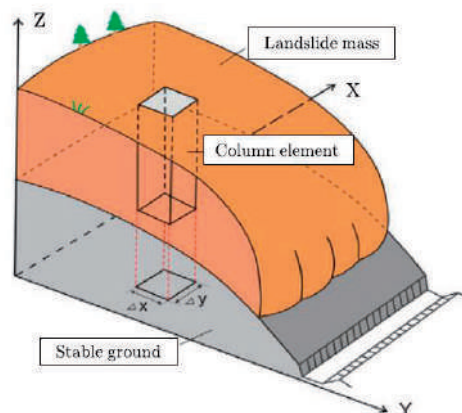


Figure 2 Column element inside the moving landslide mass (Sassa et al. 2010).

the landslide. In similar way it is possible to use LS-Rapid in seismic analyses to establish landslide susceptibility and landslide hazard caused by earthquake motions.

General features of the analysed area

Landslides in Gray Istria usually occur on the contact of the bedrock and colluvial soil deposit. This layer is product of soil formed in various mechanical processes of bedrock weathering. The instabilities are usually caused by heavy rainfall and/or human activity that significantly change the slope geometry and/or assists in leading and retaining surface water in the sliding zone (Arbanas et al. 2007).

The geological fabric of Istria today is a result of repeated tectonic deformations from the Cretaceous in addition to the intensive processes of erosion and accumulation. Sediments have nearly subhorizontal layers, except for the contacts with the Ćićarija Mountain range in the northeast and the Učka Mountain in the east, where the flysch rock mass was significantly deformed during tectonic activities (Dugonjić Jovančević and Arbanas 2012).

In a typical situation, the flysch bedrock is covered by quaternary deposits, except the isolated areas where the erosion is more expressed. This is particularly evident on the southwestern margin of the Ćićarija Mountain, at the foot of the cliffs, where the coarse-grained fragments have mixed with the silty clay materials from the flysch rock mass weathering zone (Arbanas et al. 2006). Two zones of different hydraulic conductivity can be recognized in the geological profile: the clayey and silty superficial deposit with low hydraulic conductivity and the fresh rock mass in the flysch bedrock, which can be considered to be completely impermeable. Systems of vertical fissures and joints in marls and sandstones allow easy infiltration and flow of groundwater from the upper part of the slope. Deeper, slightly weathered and fresh siltstone layers act as watertight zones, causing the draining of groundwater along the fissure-joint system running down the slope. After long rainy periods, the

joint system cannot completely drain the infiltrated water, resulting in the rise of the groundwater level in the vertical joints and a subsequent increase in pore pressures (Arbanas et al. 2010, Dugonjić Jovančević and Arbanas 2012).

Geological profiles of the studied landslides mainly consist of flysch bedrock (of Paleogene age) covered by a clayey colluvium and/or residual soil. It appears that nearly all of the studied landslides were caused by a longer rainy period and water infiltration, which caused a rise in the groundwater level, a pore water pressure increase and a decrease in strength on the slip surface from total to effective values.

Characteristics of the performed LS-Rapid model

The depth of the potential failure surface and the groundwater table, the two main factors in landslide hazard zonation, are very difficult to map in the field. They were determined from the existing data collected during the investigation works performed for remedial work designs of few landslides in the area and extrapolated on the wider area.

The effect of earthquake on slope stability was not taken into account in this analysis because the area is not seismically active. Other triggering factors, such as snow melting and climate change were also not significant for this area. The main triggering factor of the past and present landslides in the area is rainfall.

Rainfall is hydrological trigger which can be defined as decrease in shear strength on the potential sliding surface due to the increase in pore water pressure as result of rainfall infiltration and percolation (Terlien 1996, 1998). Rainfall is more evident and instantaneous than other natural processes which act gradually and trough decades, as for example erosion. Daily amount of rainfall is an instant trigger while the antecedent rainfall involves the progressive weakening of materials. Combination of both factors gives the triggering threshold for landslides.

Table 1 Values for soil parameters in LS-Rapid model: (*) after Sassa et al. 2010.

Item	Lower case (*)	Upper case(*)	Probable case(*)	Value used in the model
Friction angle during motion at sliding surface (φ_m) and coefficient ($\tan \varphi_m$)	25° ($\tan \varphi_m=0.466$)	35° ($\tan \varphi_m=0.700$)	30° ($\tan \varphi_m=0.577$)	25°
Peak friction angle at sliding surface (φ_p) and coefficient ($\tan \varphi_p$)	33° ($\tan \varphi_p=0.649$)	38° ($\tan \varphi_p=0.781$)	35° ($\tan \varphi_p=0.700$)	32°
Friction angle inside landslide mass (φ_i) and coefficient ($\tan \varphi_i$)	20° ($\tan \varphi_i=0.364$)	30° ($\tan \varphi_i=0.577$)	25° ($\tan \varphi_i=0.466$)	28°
Steady state shear resistance at sliding surface (τ_{ss})	5 kPa	50 kPa	20 kPa	60 kPa
Cohesion inside mass (C_i)	0.1 kPa	0.5 kPa	0.2 kPa	3 kPa
Cohesion at sliding surface during motion (C_m)	0.1 kPa	0.5 kPa	0.2 kPa	5 kPa
Peak cohesion at sliding surface (C_p)	2 kPa	200 kPa	10-100 kPa	10 kPa

In the simulation model of the Buzet area (Fig. 3) soil strength parameters from the performed 2D back stability analyses and some laboratory testing from the similar flysch locations were used. For the parameters with no investigation background recommended values (Sassa et al. 2010) were used (Tab. 1).

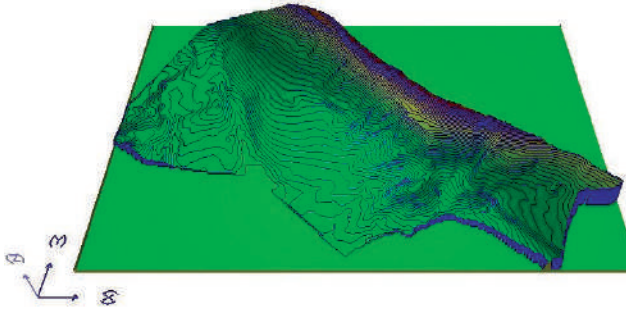


Figure 3 Simulation model of Buzet area in LS-Rapid software, mesh 30 m.

Performed model covers the matrix 205x143 in x and y direction. The height of 50m above the sea level has been given to the area outside the analysed polygon, because the model demands the rectangular mesh. Due to this reason all instability processes occurring on the polygon edges can be considered unreal and cannot be taken into account.

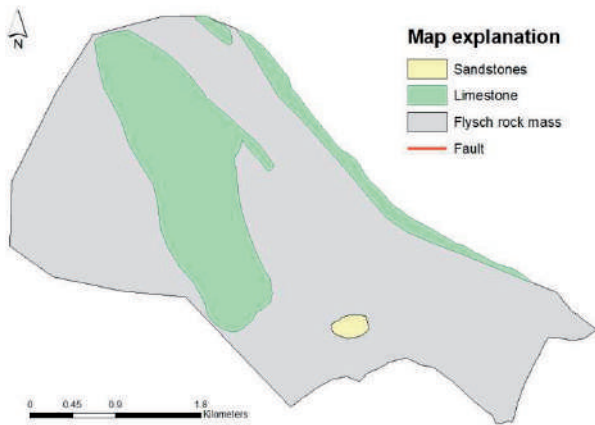


Figure 4 Simplified geological map of the analysed area.

Some geological units (Fig. 4) inside the area (limestone and sandstones) have no cover thickness. There are no results of the stability analyses in these areas, because the possibility of sliding is negligible. Based on the former investigation works the average cover thickness is 10m. According to the performed back stability analyses on landslides in the flysch area of Gray Istria, the unit weight of mass is $\gamma=20 \text{ kN/m}^3$, cohesion inside the mass $c_i =3 \text{ kPa}$ and the cohesion at sliding surface during motion $c_m=5 \text{ kPa}$. The friction angles are given also based on the back analyses.

Other parameters used values from the similar materials or recommended values (Tab. 1). Pore water pressure generation and the apparent friction angle are affected by the degree of saturation. Parameter of pore-pressure generation B_{ss} is defined in the undrained ring shear test ($B_{ss}=1.0$ at full saturation, $B_{ss}=0.0$ at dry state). The apparent friction angle $\phi_a = \phi_m$ in the dry state, ϕ_a is the lowest at full saturation and in between at partial saturation (Sassa et al. 2010). The rate of excess pore-pressure generation used in this analysis is $B_{ss}=0.5$, and lateral pressure ratio is $k=0.35$

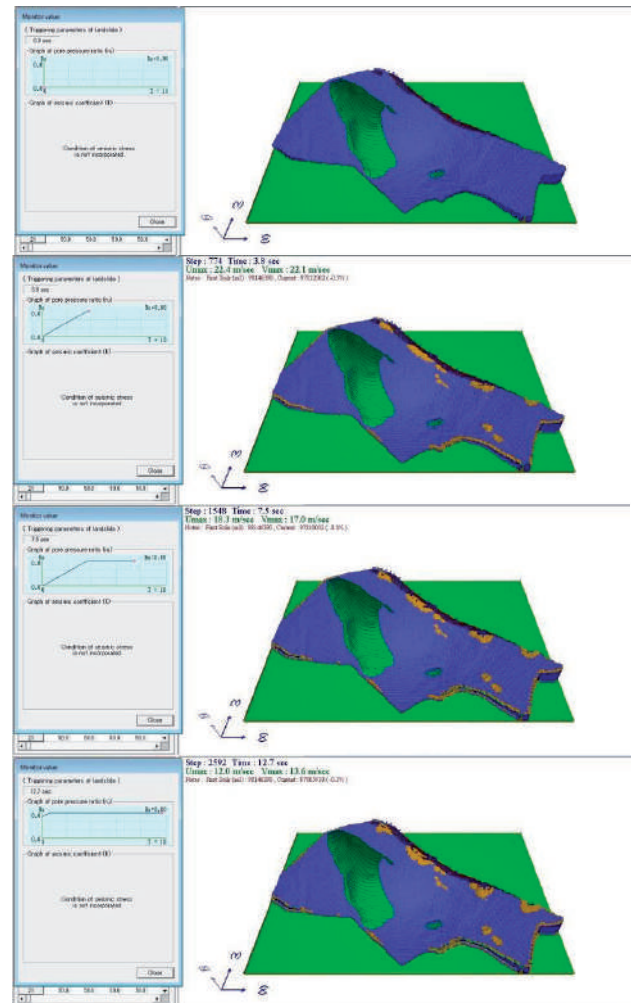


Figure 5 Gradual increase of pore pressure ratio (r_u) from value 0.0 to value 0.60 and its influence on the stability shown in LS-Rapid simulation model for landslide susceptibility in Buzet area: blue- stable areas, orange- instable areas.

The pore pressure ratio r_u increases from 0.0 to 0.60 in the time period that is corresponding to 30 days. Pore pressure ratio is calculated as relation between pore pressure and the geostatic stress at specific depth. Value $r_u=0.6$ is reached when complete superficial deposit is saturated and the groundwater level reaches the ground surface. It is considered as the main trigger of landslide

occurrence because the seismic forces are not considered due to the low seismicity in the area. The results have been set to calculate stability every 24h inside 1 month period. The gradual increase of the r_u and its influence on the 3D stability analyses are shown in Figure 5. From the results of the analyses it can be seen that the r_u reaches the full value of 0.60 inside the period of 9 days, after what its value remains constant. The stable areas are shown in blue colour, while the unstable, orange areas increase progressively due to the pore pressure increase and afterwards, when it remains constant ($r_u=0.60$).

The regional analysis unlike the analysis of one specific landslide location is less precise and more indicative. According the deterministic model in LS-Rapid it can be concluded that critical area for landslide appearance is the fault zone (Figure 4) in the north-eastern part of the analysed area. Part of the terrain northeast from this critical zone is formed in the limestone rock mass of the Čičarija Mountain range, where very steep, often vertical slope angles prevail, so the sliding in these zones can be excluded. Southwest from the critical zone considerably gentle slopes formed in flysch rock mass proceed. Sliding in these areas is occasional, but exists, what is also visible in the model.

Discussion and conclusions

Results of the performed analyses have shown that LS-Rapid can be used as a powerful tool in deterministic analyses in landslide prediction, susceptibility and landslide hazard assessment. Deterministic model performed in LS-Rapid provided the critical area for landslide appearance which corresponds to the real conditions in the slope.

The validation of the model was carried out by interpretation of stereopairs and engineering geological mapping (Fig. 6). It was concluded that landslides inside the zones that in model were characterized as highly

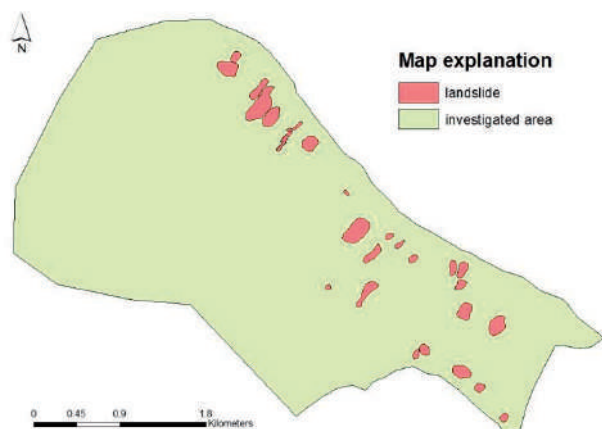


Figure 6 Existing landslides in Buzet area.

susceptible, occurred in the nearest of farthest past. In other words, it can be concluded that the results of performed analyses confirmed that LS-Rapid, except for the detailed analysis of slope stability at one specific location, can also be used for the landslide hazard assessment on wider area. Another conclusion is that the performed analyses using LS-Rapid are more accurate and give more reliable results than alternative methods used in deterministic landslide hazard analyses.

Acknowledgments

Acknowledgments to the International Consortium of Landslides for the disposition of the LS-Rapid software. Explanations and training course, as well as guidance and support during this analysis were ensured in the frame of the Croatian-Japanese SATREPS FY2008 Project.

References

- Arbanas Ž, Benac Č, Jurak V (2006) Causes of debris flow formation in flysch area of North Istria, Croatia, In: Lorenzini G, Brebbia CA, Emmanoueloudis DE (eds.) *Monitoring, Simulation, Prevention and Remediation of Dense and Debris Flows*, WIT Transaction on Ecology and the Environment. 90: 283-292.
- Arbanas Ž, Grošič M, Goršič D, Griparić B (2007) Landslides remedial works on small roads of Istria. In: Raus B (ed) *Proceedings of the 4th Croatian Roads Congress*, Croatian Road Society-Via Vita, Zagreb, 38p. (In Croatian)
- Arbanas Ž, Mihalić S, Grošič M, Dugonjić S, Vivoda M (2010) Brus Landslide, translational block sliding in flysch rock mass. In: *Rock Mechanics in Civil and Environmental Engineering. Proceedings of the European Rock Mechanics Symposium*, CRC Press/Balkema, London, 635-638.
- Carrara A, Cardinali M, Guzzetti F, Reichenbach P (1995) GIS technology in mapping landslide hazard. In: Carrara, A., Guzzetti, F. (Eds.), *Geographical Information Systems in Assessing Natural Hazards*. Kluwer Academic Publishers, 135-175.
- Dugonjić S, Arbanas Ž, Benac Č (2008) Assessment of landslide hazard on flysch slopes, *Proceedings of 5th Slovenian Geotechnical Symposium and 9. Šuklje's day*, 12-14 June 2008, Nova Gorica, Slovenia, 263-272.
- Dugonjić Jovančević S, Arbanas Ž (2012) Recent landslides on the Istrian Peninsula, Croatia. *Natural hazards*. 62(3): 1323-1338.
- Sassa K, Nagai O, Solidum R, Yamazaki Y, Ohta H (2010) An integrated model simulating the initiation and motion of earthquake and rain induced rapid landslides and its application to the 2006 Leyte landslide, *Landslides*. 7(3): 219-236.
- Terlien MTJ (1996) *Modelling spatial and temporal variations in rainfall-triggered landslides*. ITC Publ. 32, Enschede, Netherlands, 50p.
- Terlien M T J (1998) The determination of statistical and deterministic hydrological landslide-triggering thresholds, *Environmental Geology*. 35 (2-3): 124-130.
- Varnes D J (1984) *Landslide hazard zonation: A review of Principles and Practice*, Natural Hazards 3, UNESCO, Paris.

Slope Movements and Erosion Phenomena in the Dubračina River Basin: A Geomorphological Approach

Sanja Bernat⁽¹⁾, Petra Đomlija⁽²⁾, Snježana Mihalić Arbanas⁽¹⁾

1) University of Zagreb, Faculty of Mining, Geology and Petroleum Engineering, Zagreb, Croatia, Pierottijeva 6

2) University of Rijeka, Faculty of Civil Engineering, Rijeka, Croatia

Abstract This paper presents results of mapping of active geomorphological processes at the area of the Dubračina River Basin. Regarding to geological settings, geomorphological features and hydrological conditions, different landform units were outlined and are characterized by typical types of slope movement and erosion phenomena. Remote sensing represents a valuable tool for the identification and mapping of active geomorphological processes for the whole investigated area. Available remote sensing data for the Dubračina River Basin were stereopairs of aerial photographs from 2006 and high resolution DEM derived from the airborne LiDAR survey conducted in March 2012. Visual interpretation of aerial photographs and LiDAR imagery was undertaken with the aim to derive landform classification map presenting different landform units with typical types of slope movement and erosion phenomena. It is evident that each landform unit has its unique type of hazardous active geomorphological processes. Presented analysis will be used as a base for development of a methodology for multihazard inventory map preparation of the Dubračina River Basin.

Keywords landform map, active geomorphological processes, slope movement, erosion, Dubračina River Basin

Introduction

The Dubračina River Basin is situated in western Croatia in the Primorsko-Goranska County near the City of Crikvenica (Fig. 1a). The basin covers an area of 43.5 km² and it is mostly rural with six settlements and 11,882 residents. The current land use includes 38 km² of forest and semi-natural areas, 3 km² of agricultural land and 2 km² of artificial surfaces (roads and buildings) (Mihalić and Arbanas 2013).

The main geological hazards in the Dubračina River Basin are represented by several types of active geomorphological processes: different types of slope movements and local occurrences of excessive (accelerated) erosion (Fig. 1b). These represent causes of significant economical losses by damaging roads, facilities, houses and watercourses. In 2009, the Croatian-Japanese joint research project “Risk identification and

Land-Use Planning for Disaster Mitigation of Landslides and Floods in Croatia” was initiated and the Dubračina River Basin was chosen as a pilot area for landslide inventory mapping, mapping of landslide causal factors for landslide susceptibility and hazard analysis and zonation, derivation of hazard maps for use in the systems of land-use planning and civil protection and the development of guidelines for the application of susceptibility and hazard maps.

This study provides an overall review of active geomorphological processes which are characteristic for each landform unit type, identified by the visual inspection of available remote sensing data. The results will serve for establishing the methodology for preparation of multihazard inventory map of the area of the Dubračina River Basin. Multihazard inventory map will present different geological hazards of varying magnitude, frequency and area of its influence. This type of map will be the most appropriate for practical use because of comprehensive portrayal of hazardous natural phenomena. Contrary, using individual maps to portray information on each hazard type can be cumbersome and confusing for planners and decision-makers because of their combined effects at the particular locations.

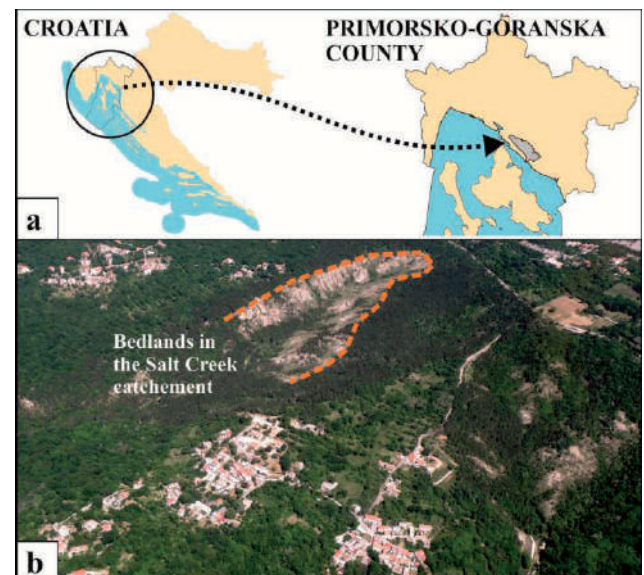


Figure 1 (a) Geographical location of Dubračina River Basin; (b) Photograph of excessive erosion in the Salt Creek sub-basin.

Overview of study area

The Dubračina River Basin represents a lower part of the elongated unique morphostructural unit Rječina Valley – Bakar Bay – Vinodol Valley. The central part of the Vinodol Valley, which belongs to the Dubračina river catchment area, is about 13 km long and 1.5-5 km wide and stretches parallel to the Adriatic coast in the northwest-southeastern direction. The Vinodol valley has an asymmetrical cross section in this part with a prominently longer northeastern and shorter southwestern slope. The Dubračina riverbed is mostly situated on the littoral ridge (Benac et al. 2010).

Basic morphological features of the study area are presented in Fig. 2a. Elevations in the Dubračina river basin range from 5 to 922 m a.s.l.: 44% of the basin area is lower than 200 m a.s.l.; 25% of the area is in a range from 200 to 400 m a.s.l.; 15% of the area is in a range from 400 to 600 m a.s.l.; and 14% of the area is in a range from 600 to 800 m a.s.l. Only 2% of the investigated area is higher than 800 m a.s.l.. Along its northeastern border, the valley is surrounded by steep carbonate cliffs whose peaks reach 922 m a.s.l.. The ridge peaks on the southwestern side reach 357 m a.s.l. and the valley bottom is at 30 m a.s.l.. Maximal slope angle reaches 88°. The prevailing slope angles (58%) in the Dubračina River Basin are in range between 5° and 20°, with an average angle of 16.2°. They are present in the middle part of the basin. Slope angles are significantly higher in the northeastern part of the valley, respectively in the area of steep carbonate cliffs.

Generalized geological map, showing main stratigraphical units, is presented in Fig. 2b. Map was prepared by the Croatian Geological Survey in 2007, but it is still unpublished. In the study area, the oldest rocks are Cretaceous platform limestone. Together with Paleogene foraminiferous limestone, they present karstified carbonate rock mass which covers 55% of the basin area. Carbonate rocks compose terrains along NE and SW borders of the valley. Only small portion (2%) of NE part of the basin is composed of transitional deposits of Paleogene, built of marls and limestone in alternation. The clearly marked rocky scarps represent the rim of the karstic plateau at the top of the NE slopes (Benac et al. 2010). Flysch complex (i.e., siliciclastic rock mass) of Middle Eocene age is predominantly composed of pelitic intervals, with subordinate sandstones and biocalcudites both containing significant amounts of siliciclastic detritus (Aljinović et al. 2010). Flysch bedrock crops out only in the area of the Salt Creek (Slani Potok in Croatian) catchment which presents 1% of the basin area. Great part of the study area (36%) is covered by slope deposits, representing heterogeneous products of physical, mechanical and chemical weathering of carbonate and siliciclastic rock mass. Quaternary fluvial deposits (7% of the area) are situated in the lowest parts of the valley and represent the mixture of mostly gravelly sediments originating from carbonate background and sporadically sandstone outcrops, with various amounts of silt and clay. Fossiliferous conglomerates and sandstones (equivalent of Late Eocene/Oligocene Promina

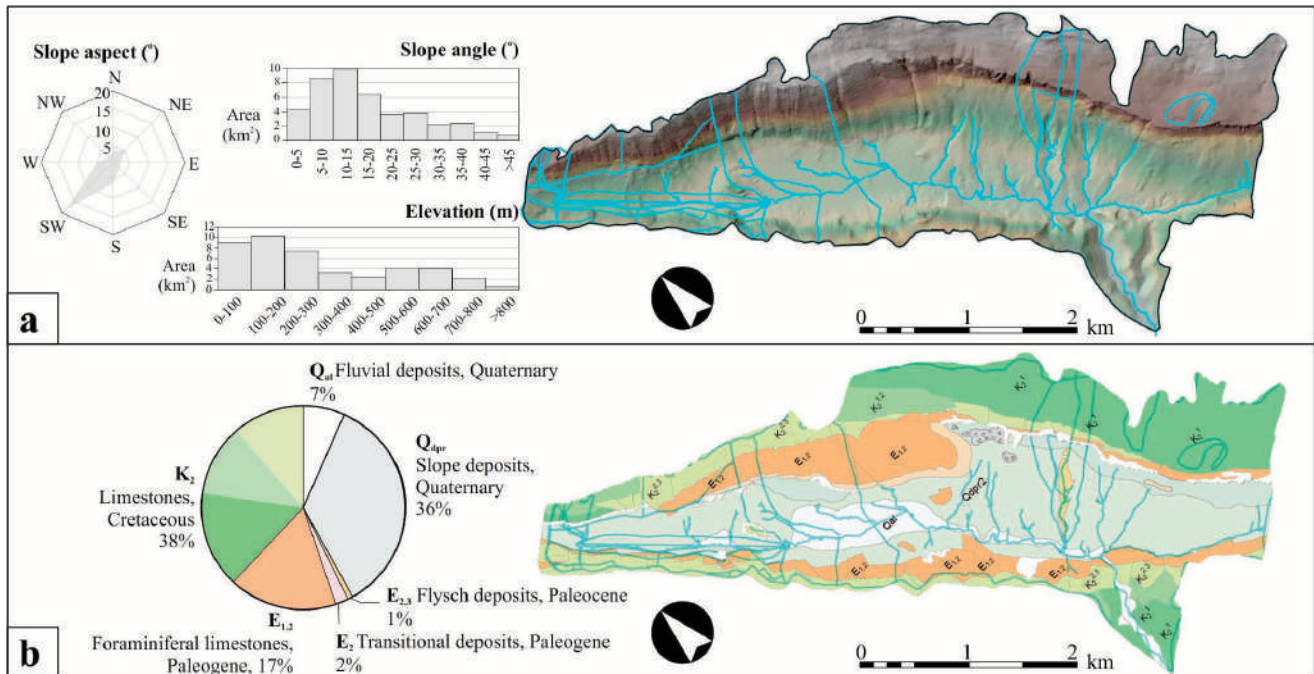


Figure 2 (a) Elevation map derived from the 5-m resolution DEM. Histograms show the distribution of elevation and slope angle computed from the DEM. Rose diagram shows the distribution of slope aspect (in km²); (b) Geological map showing the main stratigraphical units. Original scale of the geological map is 1:25,000. Geological map was prepared by the Croatian Geological Survey in 2007 for Croatian Waters and it is still unpublished.

formation), breccias (equivalent to the Late Eocene/Oligocene Jelar formation) and Quaternary talus breccias have also been determined and are described in Blašković (1983) and in Blašković and Tišljar (1983).

Flysch deposits that crop out in the area of Salt Creek catchment are characterized by excessive erosion (Aljinović et al. 2010) which results in formation of badlands and this erosion phenomena is associated with intensive sliding and creeping processes. As a result, the flysch deposits are not currently in the original position, but exhibit a chaotic appearance with overturned, fragmented and deformed beds. Such unusually intense erosion, significant for the area of Salt Creek catchment, represents a unique phenomenon within the Dinaridic flysch domain and has been investigated by Jurak et al. (2002, 2003, 2005, 2006), Mileusić et al. (2004) and Benac et al. (2005). Its cause has been related to the crystallization of the sodium mineral thenardite due to the dispersive effect of the sodium on clay particles derived from pelitic flysch intervals and due to expansion of thenardite during its transformation into a decahydrate (Aljinović et al. 2010).

Due to its distinctive morphology, Blašković (1999) describes the Vinodol Valley as a syncline of very complex internal structure. Middle Eocene flysch deposits, of which this tectonic structure is mostly composed of, are found in a central part of syncline, compressed by the Early-Middle Eocene and Upper Cretaceous limestone. Contacts between the flysch deposits and the carbonate rock mass are mainly tectonic, i.e., fault contacts. Several fault systems, that controlled the evolution of the Vinodol Valley morphology, have variable kinematic features that change along directions of their strike and dip, merging into reverse or over-thrust structures (Blašković 1997). Blašković (1999) explained that in this way, a narrow valley with a NW-SE strike is formed. The Late Eocene limestone breccia and Quaternary deposits have a patchy occurrence in the valley, where talus breccias occurred as a product of tectonic activity and were deposited underneath the steep cliffs.

Due to the underlying geological conditions, in the parts of the Dubračina River Basin with the presence of low permeable clastic deposits, the surface hydrological network is formed (Rubinić and Ožanić 2010). In the Dubračina River Basin, the main surface flow is the Dubračina River with length of 15.16 km. Several left tributary flows, present in the middle and the southeastern part of the basin, generally are of torrential type: Ričina Tribaljska; Pećica; Kostelj; Slani Potok (Salt Creek in English); Malenica; Kučina; Mala Dubračina. Due to the relatively high slope angles of the terrain, these periodical torrential flows can often be very intensive during the periods of heavy rainfalls. The most significant among them is the Salt Creek torrent, with the most powerful erosional potential. At the same time, the formation of many small springs in the basin area can also be significant (Rubinić and Ožanić 2010).

Landform classification map of the Dubračina River Basin

The mapping of active geomorphological processes at the area of investigation was performed on the basis of identification of geomorphological features which are characteristic for particular types of geomorphological phenomena. Because of complexity of geological settings and variability of morphological conditions in the Dubračina River Basin, it was necessary to identify and to delineate geomorphological units. Determination of homogeneous landforms was performed as a first step of analysis. The criteria adopted for the differentiation of landforms of specific genetic type were the overall appearance (morphography), the shape/surface geometry (morphometry), the underlying geology, relief forming processes and association of morphological forms.

The main geological hazards in the Dubračina River Basin are represented by several types of active geomorphological processes: different types of slope movements (i.e., gravitational processes) and occurrences of excessive erosion in the Salt Creek catchment (Aljinović et al. 2010). These active processes cause significant economic losses primarily by damaging roads, facilities, houses and watercourses. In the present study, landform classification map of the Dubračina River Basin provides an overall view of the identified different landform units and identified active and historical geomorphological processes. Regarding to the geomorphological approach in the landslide mapping to generate a landslide inventory, but also in mapping of all other active geomorphological processes and geological hazards, landform classification map represents the first and important step towards an effective landslide susceptibility and hazard analysis and zonation. Therefore, landform classification map is recognized as a very valuable base map for natural hazards management which would help in various types of planning and development activities.

Since the large part of the study area is heavily accessible, possibilities for field mapping in large scale are very limited. Because of that, capturing data by application of remote sensing techniques plays an important role in the process of identification and mapping of active geomorphological processes in large scale. Available remote sensing data for the Dubračina River Basin were stereo-pairs of aerial photographs from 2006 in scale 1:20,000 and high resolution DEM derived from the airborne LiDAR survey conducted in March 2012. The landform units were distinguished and outlined primarily based on the interpretation of stereo-pairs of aerial photographs. On the other hand, aerial photographs in medium scale did not enable precise identification of historical and active geomorphological phenomena. After identification of landform units, geomorphological phenomena were recognized and determined using topographic maps derived from the high resolution DEM obtained by airborne LiDAR survey.

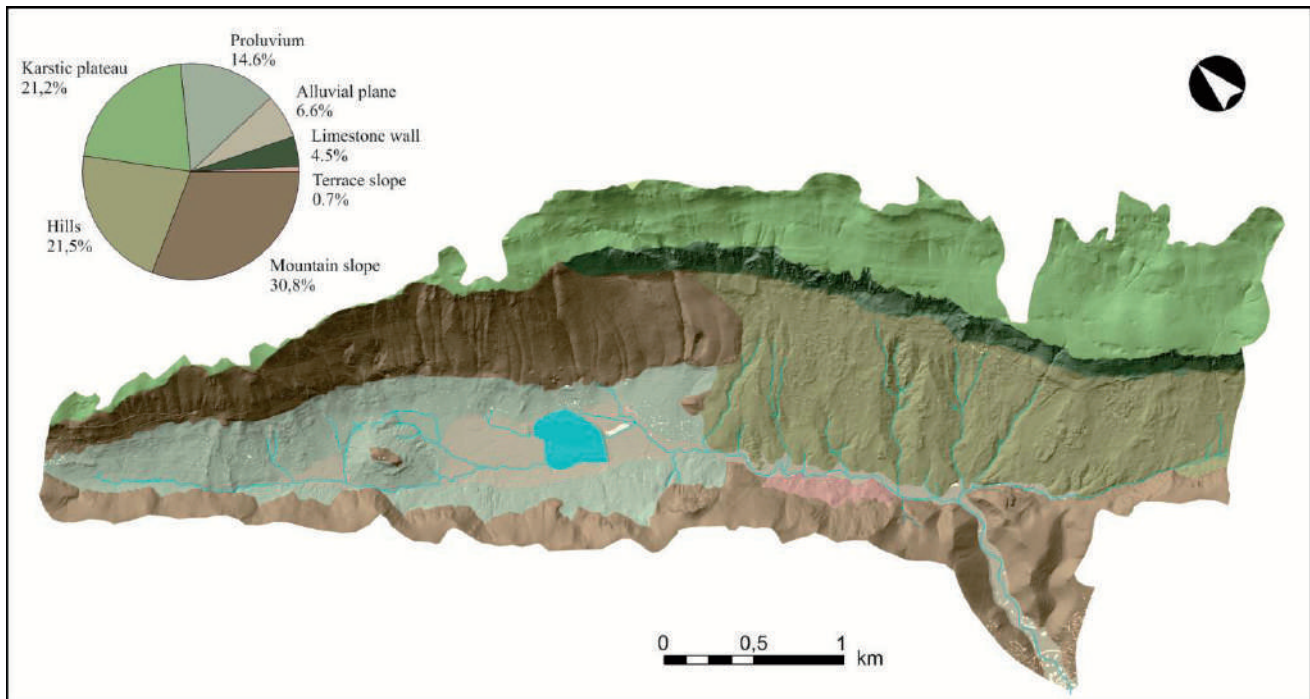


Figure 3 Landform classification map of the Dubračina River Basin representing seven different landform units determined on the basis of visual interpretation of stereo-pairs of aerial photographs and images derived by high resolution DEM.

In this early phase of geomorphological mapping, the aim was primarily to identify all present types of slope movements which are characteristic for all landform unit types in the Dubračina River Basin. This resulted in the landform map depicting seven different landform unit types in the Dubračina River Basin, but yet without outlined geomorphological processes (Fig. 3). Seven outlined landform unit types are the following: mountain slope (30.8%); limestone wall (4.5%); karstic plateau (21.2%); hills (21.5%); terrace slope (0.7%); proluvium (14.6%); and alluvial plain (6.6%).

Landform unit of mountain slope has the largest area and it occupy almost one third of the basin. It is represented by the northern part of the NE carbonate slopes and by the SW carbonate slopes of the Dubračina River Basin. Together with landform unit of the karstic plateau and landform unit of the limestone wall, it occupy more that one half of the basin area (56.5%). This area is characterized by the relief forming processes belonging to the carbonate rock masses. Landform unit of hills, covering 21.5% of investigated area, is represented by moderate inclined slopes of SW aspect. They are built of siliciclastic rock masses mostly covered by superficial deposits of variable thickness. Hills are situated between the landform unit of limestone wall in the NE and the units of alluvial plane and mountain slope in the SW. In the foothill of the southern part of SW mountain slope, the very small landform unit of terrace slope (area of 0.7%) is situated, built of lithified and semi-lithified talus breccias. Landform unit of proluvium stretches beneath the NE and SW carbonate mountain slopes, in area of 14.6% of the basin. It is built of heterogeneous mixture of

various clastic sedimentary deposits, mostly originating from the hypsometrical higher areas of the landform unit of mountain slope, transported by gravitational and torrential processes from the source carbonate material. The landform unit of alluvial plane (area of 6.6%) is situated in the lowland of the valley and it stretches along the stream of the Dubračina River. The width of the landform unit of alluvial plane is very variable, and the maximum width is in central part of the Dubračina River Basin.

Distinguished landform units in the Dubračina River Basin can be grouped into two genetic types, depending on denudational or fluvial characteristics. The alluvial plane is the only one landform unit without prevailing geomorphological processes which are not related to slope instabilities. Processes of river erosion and accumulation (sedimentation) in flat area of the basin differ significantly from the same processes in landform units in hilly and mountain areas. Flooding in flat areas is also limited to the small unit of aluvial plain.

Identification of active geomorphological processes in the Dubračina River Basin

Several types of slope movements and erosional phenomena are identified that are characteristic for delineated landforms of the Dubračina River Basin. In this phase of investigation, the aim was only to identify all types of slope movement processes that are characteristic for each landform unit. All types of identified active and historical geomorphological

Table 1 Identified landform units with attributive historical and active geomorphological processes in the Dubračina River Basin.

Landform type	Definition	Material	Processes
Alluvial plane	A largely flat landform created by the deposition of sediment over a long period of time by one or more rivers	Alluvial sediments	No processes causing slope instabilities
Proluvium	Loose formations that are the products of rock fragmentation and that are carried by streams of water to the foot of highlands	Mixture of fine-grained and course-grained soils	Historical and active sliding
Terrace slope	The inclined surface in the foot of mountain slope where karstified rock masses are covered by thicker superficial deposits	Mixture of fine-grained and course-grained soils	Historical and active sliding
Hills	A naturally raised area of land, not as high or craggy as a mountain	Paleogene siliciclastic sedimentary rocks (flysch)	Excessive erosion Gully erosion Historical and active sliding and mudflows
Mountain slope	The inclined surface that forms a mountainside	Karstified carbonate rocks (mostly Upper Cretaceous and Paleogene limestone)	Gully erosion Instabilities in scree deposits Historical and active sliding, debris flows
Limestone wall	A continuous vertical rock masses that encloses or divides an area of land	Karstified carbonate rocks (mostly Upper Cretaceous)	Gully erosion Historical and active rockfalls and topplings
Karstic plateau	An area of fairly level high ground	Karstified carbonate rocks (mostly Upper Cretaceous)	Gully erosion

processes and phenomena are listed in the Table 1: active and historical slides, creeping phenomena, active gully erosions, screes, rockfalls, topplings, and traces of historical debris flows.

Landslides of different types and state of activity, and also erosion phenomena, are the most significant processes in the landform unit of hills. Excessive erosion is dominant in the sub-basin area of the Salt Creek catchment (Fig. 1b) resulting in badland relief (Aljinović et al., 2010), which is also one of the main landslide causal factors in this part of the study area. There are numerous active landslides around the zones of erosion, which are dominantly small and mostly shallow movements of superficial deposit composed of a mixture of silty clay and fragments of sandstones and limestone originating from the flysch rock mass. In the landform unit of hills, there is a second landslide type represented by generally larger and old dormant landslides on gently inclined slopes. Morphological indications of soil creeping are also identified in the landform unit of hills. Small and periodical mudflows occur in steep gullies and on concave slopes without vegetation cover which was removed due to the excessive erosion. Activation of these mudflows is specific in the periods after a long dry season followed by heavy rains.

Evidences of historical and active landslides are also identified in the area of the landform units of mountain slope (SW part of the landform unit), terrace slope and the unit of proluvium. In the landform unit of proluvium there are especially expressed indicators of active sliding processes. In the landform unit of mountain slope there are also identified periodically active process

of gully erosion and gravitational talus (scree) moving. In the NE part of the unit of mountain slope, indices of historical debris flow are identified. In the landform unit of limestone wall there are indications of small rockfalls, gully erosion and toppling. Rock fall processes are dominant along steep slopes composed of carbonate rock masses. Top parts of the most erosional gully channels are situated and identified in the landform unit of karstic plateau. No active processes related to slope instabilities are present in the landform unit of alluvial plane, because of horizontal to very gently inclined relief.

Discussion and conclusion

A landform classification map was created for the area of the Dubračina River Basin (43.5 km²) based on visual interpretation of stereo-pairs of aerial photographs in medium scale (1:20.000). Seven landform unit types are: mountain slope; limestone wall; karstic plateau; hills; terrace slope; proluvium; alluvial plain. The criteria applied for identification of specific landform type were morphological settings (relief type), geological settings (lithology of base rock and superficial deposits) and hydrological conditions. Each of seven landform unit types is characterized by set of active and historical geomorphological processes and phenomena. Further identification of active geomorphological processes and traces of historical geomorphological processes was based on the visual interpretation of maps derived from the high resolution DEM obtained by airborne LiDAR survey. However, in this phase of investigations, the objective was primarily to distinguish different landforms unit

types and specific hazardous phenomena and processes, related to slope instabilities.

The most significant active, but also historical, geomorphological processes in the Dubračina River Basin are represented by several types of landslides identified in the landform units of hills, mountain slope, proluvium and terrace slope. Excessive erosion phenomena are significant for the landform unit of hills, where also gully erosion and mudflow are present. Geomorphological processes typical for landforms created in carbonate rock masses are small rock falls, active gravitational movements of talus (i.e., scree) and toppling. In the NE part of the landform unit of mountain slope, features of historical large scale debris flow are also identified.

The applied visual interpretation of stereo-pairs of aerial photographs proved to be useful for the identification of landform topography and for the delineation of landform units. On the other hand, the scale of used aerial photographs is too large, in relation to the size of all geomorphological processes in the Dubračina River Basin. Although some of the larger geomorphological phenomena (e.g. large active/historical landslides, gully erosion phenomena) still can be recognized by the visual inspection of stereo-pairs, the interpretation of aerial photographs however can not be efficiently used as a method of systematic geomorphological mapping in large scale. Outlining of each identified geomorphological phenomena is not possible without using high resolution DEM, which enable visual identification of morphological features characteristic for slope instability processes. During this study, it was confirmed that the high resolution of the DEM and of derivative topographic maps result in a high level of visibility of the main topographical features of identified geomorphological processes. It is concluded that airborne LiDAR imagery presents a very valuable tool for further investigation and geomorphological mapping in large and detailed scale. Methodology of visual interpretation of morphological features indicative for active/historical geomorphological phenomena is necessary for the creation of the geomorphological map of the Dubračina River Basin in large scale.

Acknowledgments

The authors acknowledge the financial support from JST/JICA's SATREPS Program (Science and Technology Research Partnership for Sustainable Development).

References

- Aljinović D, Jurak V, Mileusnić M, Slovenec D, Presečki F (2010) The origin and composition of flysch deposits as an attribute to the excessive erosion of the Slani Potok valley („Salty Creek“), Croatia. *Geologia Croatica*. 63(3): 313-322.
- Benac Č, Jurak V, Oštrić M, Holjević D, Petrović G (2005) The phenomenon of excessive erosion in the area of Slani potok (Vinodol valley). Abstract book of the 3rd Croatian Geological Congress, 29 September-1 October 2005. Zagreb, Croatia. pp. 173-174. (In Croatian)
- Benac Č, Mihalić S, Vivoda M (2010) Geological and geomorphological conditions in the area of Rječina river and Dubračina river catchments (Primorsko-goranska County, Croatia). Proceedings of 1st Workshop of the Japanese-Croatian SATREPS FY2008 Project, 22-24 November 2010. Zagreb, Croatia. pp. 39-39.
- Blašković I (1983) Distribution and placement of Pliocene and Quaternary deposits in Vinodol. *Geološki vjesnik*. 36: 27-35. (In Croatian)
- Blašković I (1991) Arrangement of strike-slip, reverse and normal faults and forms development and depth of the subduction plains. *Geološki vjesnik*. 44: 247-256. (In Croatian)
- Blašković I (1997) The helicoidal fault systems of Vinodol and their genesis. *Geologia Croatica*. 50(1):49-56.
- Blašković I (1999) Tectonics of part of the Vinodol Valley within the model of the continental crust subduction. *Geologia Croatica*. 52(2): 153-189.
- Blašković I, Tišljarić J (1983) Promina deposit and Jelar deposit in the Vinodol area (Hrvatsko Primorje, Croatia). *Geološki vjesnik*. 36: 37-50. (In Croatian)
- Jurak V, Petraš J, Gajski D (2002) Research into excessive erosion of bare flysch slopes in Istria by use of terrestrial photogrammetry. *Hrvatske vode – Časopis za vodno gospodarstvo*. 38: 49-58. (In Croatian)
- Jurak V, Petraš J, Aljinović D, Gajski D (2003) Field intensity measurements of erosion instability in flysch deposits in Istria, Croatia. Proceedings of the International Symposium on Geotechnical Measurements and Modeling, 23-25 September 2003. Lisse, Netherlands. pp. 283-289.
- Jurak V, Slovenec D, Mileusnić M (2005) Excessive flysch erosion - Slani potok. Excursion Guide-Book of the 3rd Croatian Geological Congress, 29 September-1 October 2005. Zagreb, Croatia. pp. 51-55. (In Croatian)
- Jurak V, Slovenec D, Mileusnić M, (2006) Excessive flysch erosion – Slani Potok. Field Trip Guidebook of the MECC'06, 18-23 September 2006. Zagreb, Croatia. pp. 48-51.
- Mihalić S, Arbanas Ž (2032) The Croatian-Japanese joint research project on landslides: activities and public benefits. In: Sassa et al. (eds) *Landslides: Global Risk Preparedness*. Springer, Berlin Heidelberg (ISBN 978-3642220869), pp. 333-349.
- Miluesnić M, Slovenec D, Jurak V (2004) Thenardite-efflorescence indicating cause of the excessive flysch erosion, Slani Potok, Croatia. *Acta Mineralogica-Petrographica Abstract Series*. pp. 75-75.
- Rubinić J, Ožanić N (2010) Hydrology of Dubračina River catchment area. *Zbornik radova Građevinskog fakulteta Sveučilišta u Rijeci*. XIII: 33-68. (In Croatian)

Landslide Occurrence Prediction in the Rječina River Valley as a Base for an Early Warning System

Martina Vivoda, Sanja Dugonjić Jovančević, Željko Arbanas

University of Rijeka, Faculty of Civil Engineering, Rijeka, Croatia, Radmile Matejčić 3, +385 51 265933

Abstract This paper presents deterministic 3D stability analyses using LS-Rapid software applied on the wider area of the Grohovo Landslide at the north-eastern slope of the Rječina River Valley near the city of Rijeka, Croatia. Results of these analyses in combination with results of existing monitoring data are necessary for the future landslide behavior prediction as a base for an early warning system establishment at the Grohovo Landslide.

Keywords landslide, early warning system, stability analyses

Introduction

The Grohovo Landslide is a reactivated complex landslide in the outback of the City of Rijeka, Croatia. Several historical episodes of landslide movements and their consequences demonstrate the need for a landslide behavior forecasting and an early warning system establishment in order to reduce the landslide risk and to protect human lives. The part of the Rječina River Valley between the Valiči Lake and the Pašac Bridge (Fig. 1) is the most unstable part of the wider area of the City of Rijeka, with the highest landslide hazard and possible sliding risk (Benac et al. 2006).

Numerous historical descriptions, figures and maps those describing landslides were found in the Croatian State Archive in Rijeka (Fig. 2). The last large landslide reactivation occurred on 5th December 1996 at the same location of the landslide from the 19th century on the north-eastern slope of the Rječina River Valley.

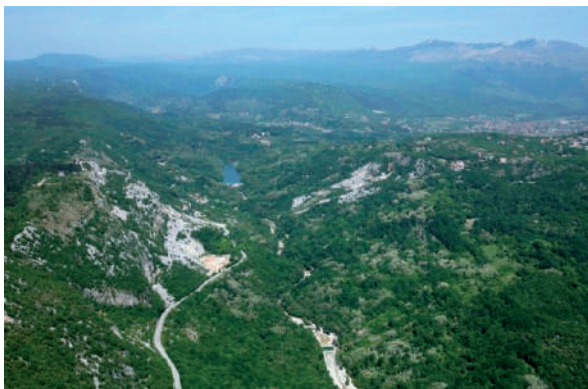


Figure 1 Investigated area of the Rječina River Valley (Photo: Ž. Arbanas).

Significantly smaller volume of sliding mass was activated than the volume affected by older sliding. Long rainy period was preceded this reactivation in autumn and early winter 1996.

As part of the research activities in the Croatian–Japanese Bilateral Project Risk Identification and Land-Use Planning for Disaster Mitigation of Landslides and Floods in Croatia, a comprehensive integrated real-time monitoring system was installed at the Grohovo Landslide. Geodetic monitoring includes geodetic surveys with a robotic total station, and displacement measurements of GPS points. Geotechnical monitoring consists of pore pressure gauges, inclinometers and wire extensometers (Arbanas et al. 2011a). The monitoring system enables real time transmission of the data to the control centre and the presentation to the public. This real time transmission will aid in establishing of an early warning system for landslide hazard when the measured values exceed defined limits (Mihalić and Arbanas 2013). The deterministic 3D stability analyses of the wider zone of the north-eastern slope of the Rječina River Valley were carried out as a base for an early warning system defining and establishment (Arbanas et al. 2011b).

Early warning system

An early warning can broadly be defined as a timely advice before a potentially hazardous phenomenon occurs. An efficient early warning system comprises identification and estimation of hazardous processes, communication of warnings and adapted reaction of local population. Moreover, early warning systems have to be embedded into local communities to ensure effectiveness of the entire system (Thiebes 2012).

An early warning system in the Rječina River Valley should be established based on prediction of movements and instabilities appearances in the zones where the monitoring equipment is installed. Prediction of possible movements was carried out on the basis of the results of 2D or 3D landslide stability analyses of wider landslide area in combination with the results of existing monitoring data. Critical limit values were defined to indicate new sliding appearances and starting up the alarm. Critical limit value determination was based on the monitoring results and accuracy of installed monitoring equipment.

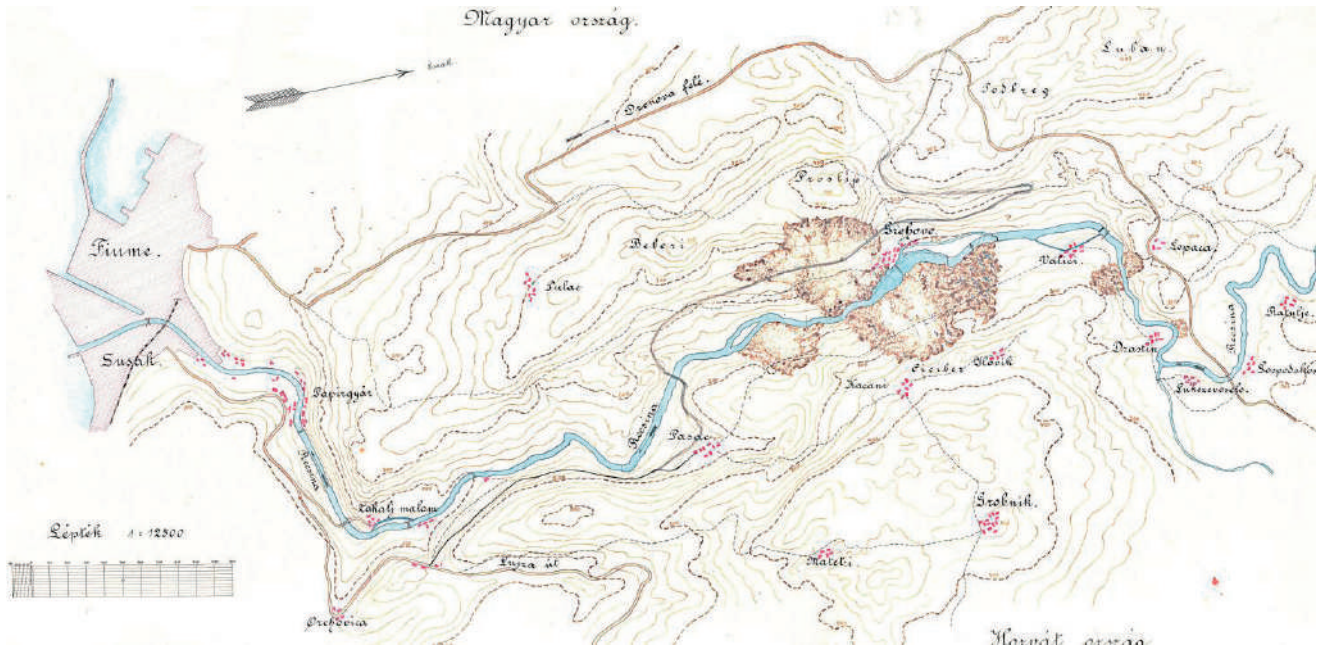


Figure 2 Topographic map of the Rječina River Valley showing landslides occurred in 1894 (Anon 2011).

Deterministic 3D stability analyses

Landslide modelling is, along with experimental subsoil exploration and experience driven safety assessment, one of the main tasks of slope stability analysis practice (Janbu 1996). Models are applied to analyze current stability status and to predict slope behavior under certain conditions such as rainfall events or scenarios for environmental change.

The intent of deterministic models usage in landslide hazard analyses is not to define the safety factor in an absolute and precise way at each point in the analyzed area. The high spatial variability of geotechnical parameters is a serious limitation of deterministic model. The final stage in deterministic landslide hazard zonation consists of the failure probability calculation and converts the factor of safety maps into the failure probability maps.

The deterministic 3D landslide stability analyses of the most unstable part of the Rječina River Valley (Fig. 1) enable indication of possible sliding zones under unfavorable groundwater conditions. The deterministic 3D stability analyses were carried out using landslide simulation model software LS-Rapid (Sassa et al. 2010). LS-Rapid software could integrate the initiation of the landslide process triggered by rainfalls and/or earthquakes and the development of sliding due to strength reduction and the entrainment of deposits in the run out path. Stability analyses are based on strength parameters obtained from laboratory tests on soil samples taken from the slip zones.

Soil testing

Soil testing was conducted on representative samples in a portable ring shear apparatus ICL-1 designed for testing the residual shear resistance mobilized along the sliding surface at large shear displacements under static and/or dynamic local conditions. The results of the ring shear tests are necessary to enable input data for analyses of the development and propagation of the sliding mass in LS-Rapid software.

Testing apparatus

No other laboratory apparatus than the ring shear apparatus has so far been able to provide an integrated simulation of the natural landslide process. Ring shear apparatus has two important purposes: it can be used as the basic soil test to obtain soil strength parameters and as a landslide simulation test.

The developed Portable Ring Shear Apparatus, ICL-1 (Fig. 3), was developed in 2010, as an activity of Croatian-



Figure 3 Portable Ring Shear Apparatus, ICL-1 (Photo: M. Vivoda).

Japanese bilateral project Risk identification and land-use planning for disaster mitigation of landslides and floods in Croatia, SATREPS (Science and Technology Research Partnership for Sustainable Development) project financed by Japan International Cooperation Agency (JICA) and Japan Agency for Science and Technology (JST) and donated to Croatian research group in 2012. Compared to similar existing apparatus, the new apparatus is smaller in its dimensions but with higher performances; it can keep undrained condition up to 1.0 MPa of pore water pressure and normal stress that makes it suitable for investigations of large-scale and deep-seated landslides with high values of normal stresses applied to the slip surface.

Samples, testing conditions and results

The soil samples from the Grohovo landslide were taken from the flysch outcrop in the central part of the landslide body. Speed control test was conducted under constant shear speed of 0.002 cm/sec in undrained conditions. Sample was sheared until the shear displacement reached 1.0 m and the steady state conditions were obtained. As a results of this test, the basic parameters values (peak, mobilized and apparent friction angle, so as cohesion) as well as steady state normal and shear stress of soil sample were obtained (Fig. 4). The straight line fitting the stress path gave values of the friction angle as $\phi_m=25.4^\circ$, cohesion as $c=15.2$ kPa and apparent friction angle $\phi_a=20.4^\circ$ (Oštrić et al. 2012).

The integrated model of landsliding simulation for the north-eastern slope of the Rječina River Valley

The LS-Rapid software is the first landslide simulation model possible to integrate the whole process of stable state, failure, post-failure strength reduction, motion and deposit of sliding mass (Sassa 2010). In the simulation, the friction angle and cohesion will be reduced from their peak values to the normal motion time values within the source area in the determined distribution of the unstable mass (reducing from $\tan\phi_p$ to $\tan\phi_m$ and from c_p to c_m). The strength reduction will be started in the moment when the travel length will become equal to shear displacement at the start of strength reduction (DL, mm). The strength reduction will be completed and the normal motion simulation will start when the travel length will reach the value of shear displacement at the end of strength reduction (DU, mm).

The topography of the Rječina River Valley (Fig. 5a) was determined using original DEM data. The limestone rock mass is situated at the top of the slopes, while the siliciclastic rocks and flysch are situated on the lower slopes and the bottom of the valley. Depth of the sliding mass varies from 3 to 10 m over the flysch bedrock and from 0.0 to 0.5 m over the limestone rock mass (Fig. 5b). This assumption is based on knowledge that the existing slip surface is positioned at the contact between superficial slope deposits and flysch bedrock (Benac

2005). The long-term rainfalls and consequent ground water level rising were the main triggering factor for the existing landslide occurrences in the Rječina River Valley. This ground water level rising in the model was expressed by excess of the pore pressure ratio until the value of $r_u=0.60$, which is correspondent to the ground water level equal to terrain surface. The time period of ground water level rising in the model was set up as 60 seconds and one second in the model was correspondent to one day real time period.

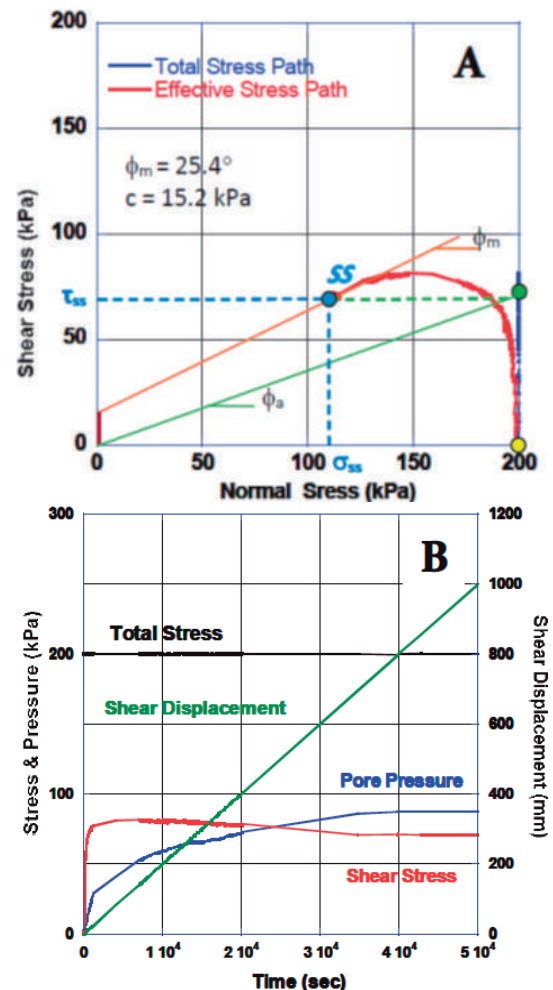
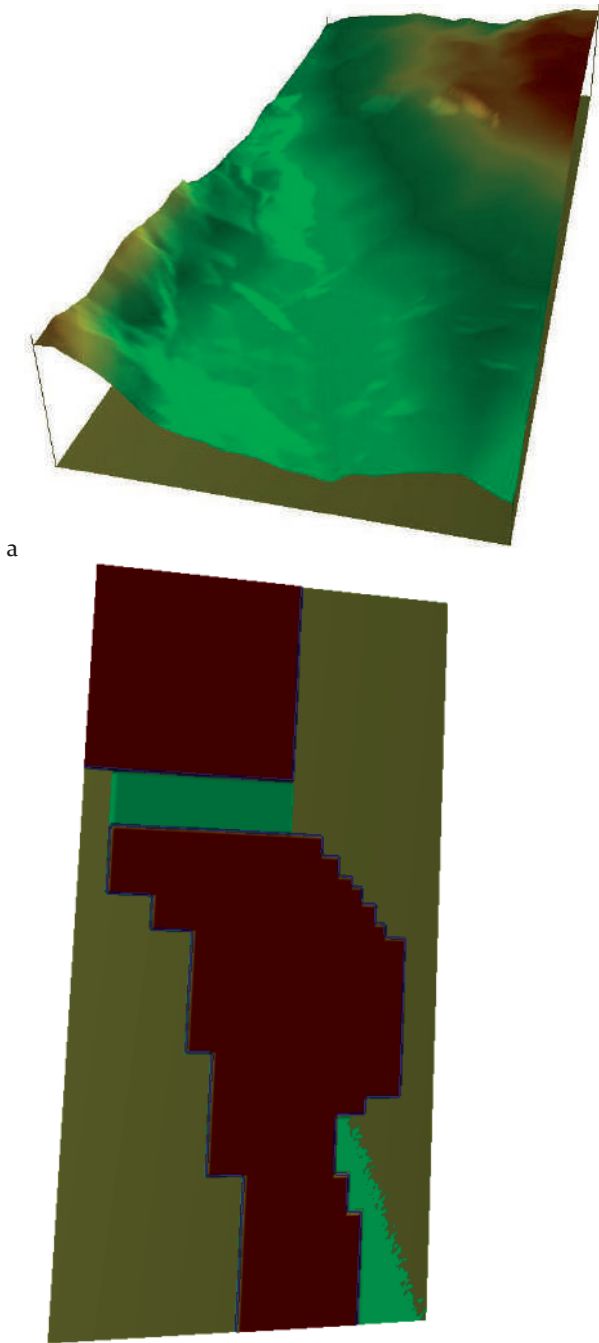


Figure 4 Undrained speed control test on saturated clayey sample from the Grohovo landslide: a Stress path; b Time series data for stress, pressure and shear displacement (Oštrić et al. 2012).

Parameters used for the computer simulation

Important parameters for the integrated landslide computer simulation are the steady state shear resistance (τ_{ss}), the lateral pressure ratio ($k=\sigma_h/\sigma_v$) and the critical shear displacements (DL, DU). The most of the soil parameters used in conducted computer simulation (Tab. 1) were determined from the undrained cyclic loading ring shear test (Fig. 5) and some of them from older laboratory testing results (Benac et al. 2005).



b
Figure 5 Computer simulation area: (a) Slope surface 3D model before the landslide event; (b) Superficial deposits thickness distribution.

Results of the computer simulation

Excess of pore pressures significantly influence on the shear strength reduction and appearance of sliding events on the north eastern slope of the Rječina River Valley (Fig. 6).

The simulation results are shown on Fig. 7a-7f. The blue colored zones represent the stable areas or areas with movement velocity less than 0.1 m/s (Fig. 7b-7f). The orange and red colored zones represent areas where the sliding occurred.

Table 1 Soil parameters used in the computer simulation.

Soil parameters	Value	Source
Total unit weight of the mass (γ_t)	20 kN/m ³	Benac et al. 2005
Steady state shear resistance in the source area (τ_{ss})	65 kPa	Test data Oštrić et al. 2012
Lateral Pressure ratio ($k=\sigma_h/\sigma_v$)	0.7	Estimation from the test data
Friction angle inside landslide mass (ϕ_h)	33°	Benac et al. 2005
Friction angle during motion (ϕ_m)	26°	Test data Oštrić et al., 2012
Peak friction angle at sliding surface (ϕ_p)	34°	Benac et al. 2005
Peak cohesion at slip surface (c_p)	7.5 kPa	Benac et al. 2005
Shear displacement at the start of strength reduction (DL)	30 mm	Test data Oštrić et al. 2012
Shear displacement at the end of strength reduction (DU)	1000 mm	Test data Oštrić et al. 2012
Pore pressure generation rate (B_{ss})	0.7	Estimation
Cohesion inside mass (c_i)	0.0 kPa	Benac et al. 2005
Cohesion at sliding surface during motion (c_m)	0.0 kPa	Benac et al. 2005
Excess pore pressure (r_u)	0.0 – 0.6	Assumption

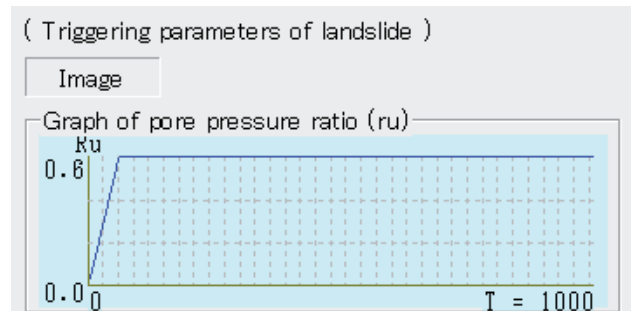


Figure 6 Triggering factor of landslides in the Rječina River Valley (pore pressure ratio $r_u=0.6$).

Figure 7b represents the state of the slope soon after the start of a pore pressure rising and strength reduction. The sliding in simulation was started at the top of the slope in the upper part of the existing Grohovo Landslide. Figures 7c to 7f show development of new sliding as the pore pressure ratio rises. The zone affected by sliding shown in the Figure 7e is very similar to the area of existing landslide (Fig. 8). A new landslide above the Valiči Lake appears in the correspondent time of 23 days and pore pressure ratio of $r_u=0.23$ (Fig. 7d). Fig. 7e shows landslide appearances at the end of the pore pressure rising after 60 days from the process initiation. Landslide movements were continued at the constant ground water level and the process landslide movements were terminated after 100 days of simulation (Fig. 7f).

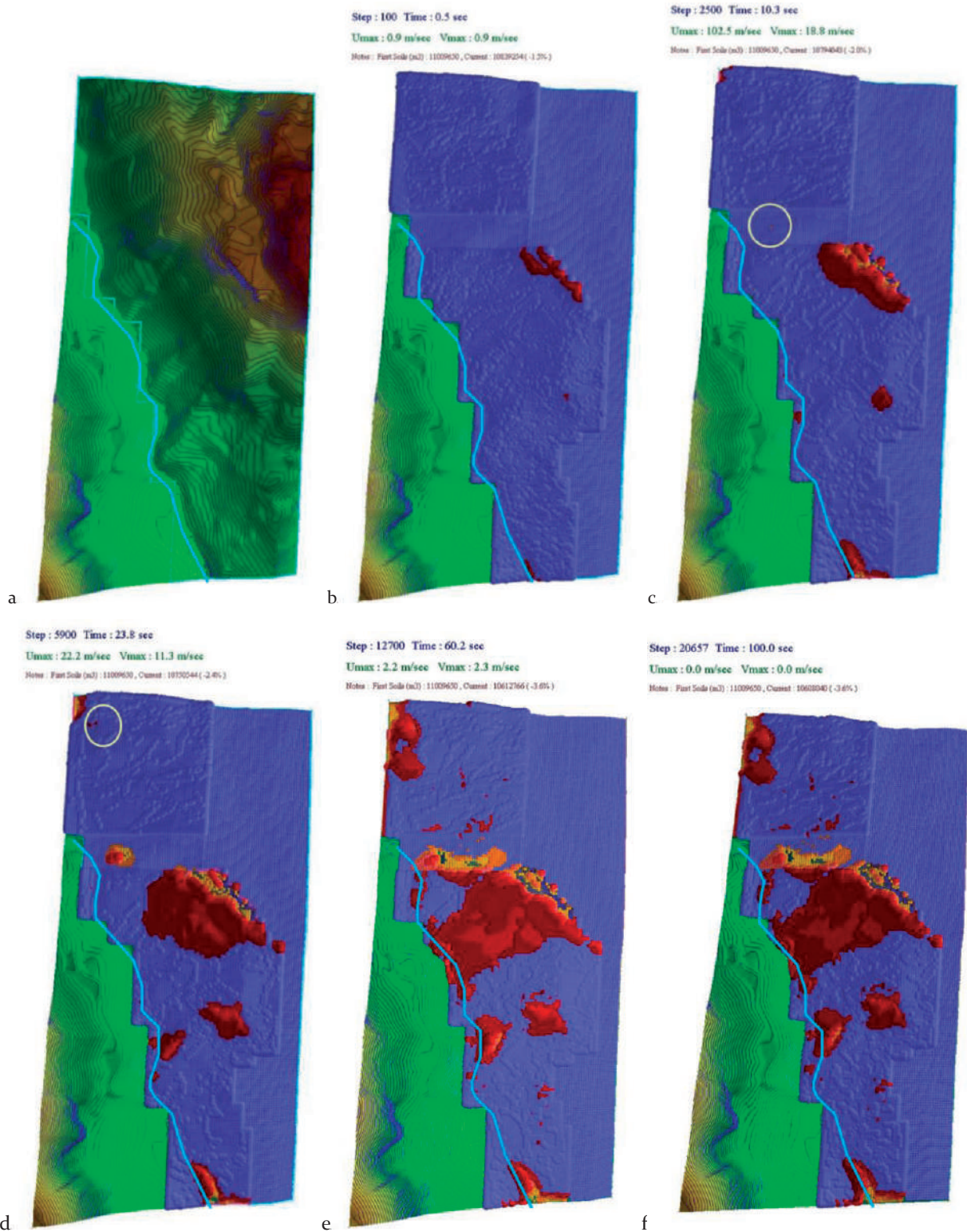


Figure 7 Landslide simulation results for the north-eastern slope of the Rječina River Valley area: a Computer simulation area; b Beginning of pore pressure rising and strength reduction with forming of the Grohovo Landslide; c r_u rising to 0.10 with local failure; d r_u rising to 0.1 with landslide above the Valići Lake; e End of pore pressure rise at $r_u=0.60$; f Landslide areas at the end of the movements.

The results of conducted simulation very clearly suggest that the new slides, caused by future unfavorable hydrogeological conditions, can occur in the area of

existing landslide. The new slides could also be expected at some others locations in the slope as it presented at the Figure 7e. Some of these predictions are confirmed

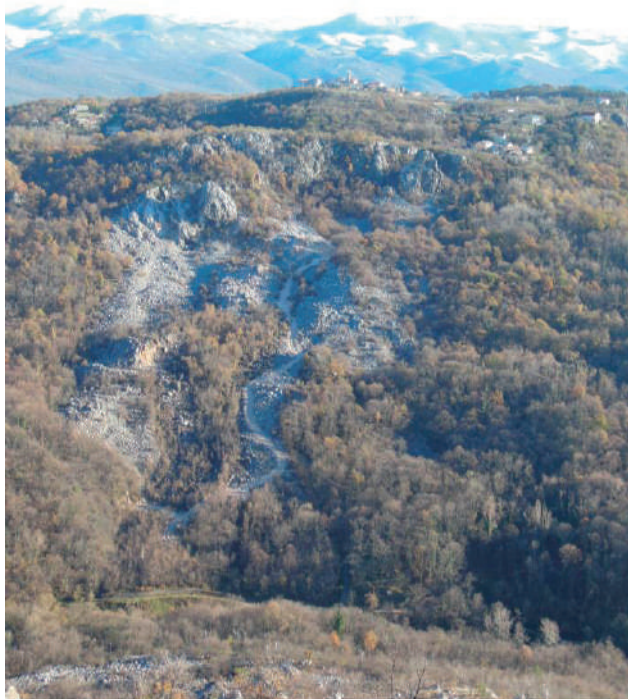


Figure 8 A view at the Grohovo Landslide from the opposite side of the valley (Photo: M. Vivoda).

with scars and small slides registered north western of the existing landslide occurred during the winter and spring 2013.

The most interested and dangerous prediction is the possibility of landslide occurrence on the slope above the Valići Lake (Fig. 7d-7f). This landslide can cause very serious consequences such as filling of the lake with landslide accumulation and possible impulsive wave generation and this possibility should be seriously analyzed as an important hazardous event.

The results of the conducted deterministic slope stability analyses using LS-Rapid software clearly show the critical areas for future landslide appearances in unfavorable hydrogeological conditions. The predicted landslide appearances are validated by existing landslide occurrences or scars those suggest the start of instability processes. So, the results of conducted analyses can be used as landslide prediction and susceptibility maps, and, if it would be possible to connect rainfalls and infiltration with time component of occurrences, as a landslide hazard maps in the Rječina River Valley.

Conclusion

The Grohovo Landslide is a reactivated complex landslide in the Rječina River Valley in the outback of the City of Rijeka, Croatia. The part of the Rječina River Valley between the Valići Lake and the Pašac Bridge is the most unstable part of the Rječina River Valley, with the highest landslide hazard and correspondent sliding risk. All these facts point on the needs for a landslide behavior

forecasting and an early warning system in order to reduce related hazard and risk and to protect human lives.

The deterministic 3D stability analyses were carried out using landslide simulation model software LS-Rapid which can integrate the initiation of the landslide process triggered by rainfalls and/or earthquakes and the development of sliding due to strength reduction and the entrainment of deposits in the run out path. Stability analyses are based on strength parameters obtained from laboratory tests on soil samples taken from slip surface zones. The results of the conducted deterministic 3D slope stability analyses using LS-Rapid software clearly show the critical areas for future landslide appearances in unfavorable hydrogeological conditions and they can be used as landslide prediction, susceptibility and hazard maps in the Rječina River Valley.

The most important indicators for the alarm decision should be measured values, such as displacements and pore pressures, on installed monitoring equipment in the moment when measured values reach proposed critical values.

References

- ANON (2011) City of Rijeka. Technical department (1840-1918) State archive in Rijeka (unpublished documents, in Hungarian)
- Arbanas Ž, Benac Č, Dugonjić S (2011a) Dynamic and Prediction of future behavior of the Grohovo Landslide. Proceedings of the 1st Workshop of the Project Risk identification and Land-Use Planning for Disaster Mitigation of Landslides and Floods in Croatia. Dubrovnik. (in press)
- Arbanas Ž, Vivoda M, Jagodnik V, Dugonjić Jovančević S, Ljutić K (2011b) Consideration of early warning system on the Grohovo Landslide. Proceedings of the 2nd Workshop of the Project Risk identification and Land-Use Planning for Disaster Mitigation of Landslides and Floods in Croatia. Rijeka. pp. 51-54
- Benac Č, Arbanas Ž, Jurak V, Oštrić M, Ožanić N (2005) Complex landslide in the Rječina River Valley (Croatia): Origin and sliding mechanism. Bulletin of Engineering Geology and the Environment 64(4). pp. 361-371.
- Benac Č, Jurak V, Oštrić M (2006) Qualitative assessment of geohazard in the Rječina Valley, Croatia. Proceedings of the 10th IAEG International Congress: IAEG Engineering geology for tomorrow's cities. The Geological Society of London. 658 (1-7).
- Janbu N (1996) Slope stability evaluations in engineering practice. Proceedings Seventh International Symposium on Landslides. Trondheim, Norway. pp. 17-34
- Mihalić S, Arbanas Ž (2013) The Croatian-Japanese joint research project on landslides: activities and public benefits. Landslides: Global Risk Preparedness. Sassa, K., Rouhban, B., Briceño, S., McSaveney, M., He, B. (eds). Heidelberg: Springer. pp. 333-349.
- Oštrić M, Ljutić K, Krkač M, Setiawan H, He B, Sassa K (2012) Undrained Ring Shear Tests Performed on Samples from Kostanjek and Grohovo Landslide. Proceedings of the IPL Symposium. Sassa, K., Takara, K., He, B. (eds). Kyoto. pp. 47-52.
- Sassa K, Nagai O, Solidum R, Yamazaki Y, Ohta H (2010) An integrated model simulating the initiation and motion of earthquake and rain induced rapid landslides and its application to the 2006 Leyte landslide, Landslides 7-3. pp. 219-236.
- Thiebes B (2012) Landslide Analysis and Early Warning Systems. PhD Thesis. The University of Vienna, Austria. Springer, Heidelberg.

Analysis of Historical Landslide Information from the Area of the City of Zagreb and Primorsko-Goranska County

Snježana Mihalić Arbanas⁽¹⁾, Sanja Bernat⁽¹⁾, Slađan Fabijanović⁽¹⁾, Željko Arbanas⁽²⁾

1) University of Zagreb, Faculty of Mining, Geology and Petroleum Engineering, Zagreb, Croatia, Pierottijeva 6, +385 1 5535 765

2) University of Rijeka, Faculty of Civil Engineering, Rijeka, Croatia

Abstract This paper presents the analysis results of historical landslide contours available in Croatia for the certain landslides, collected from various types of sources: geotechnical reports, landslide inventories and unpublished landslide maps. Landslide contours of three landslides from the City of Zagreb of various size (0.03-2.55 ha) and one landslide area with fossil landslides from the Primorsko-Goranska County are presented to show uncertainty of landslide identification by geomorphological field mapping in large and detailed scale caused primarily by subjectivity of interpretations.

Keywords historical landslide information, landslide contours, landslide inventory, field mapping

Introduction

Landslides in Croatia cause significant economic losses, which trend is increasing due to urbanization of hilly areas followed by adverse human activities which cause slope instabilities, such as cutting without adequate support systems, improper drainage systems, creation of dumps of very loose waste, etc. Possibilities for landslide hazard management and generally for mitigation of landslide risk are very limited due to the fact that there is no archive about landslides in the form of reliable landslide inventory maps or landslide databases. Moreover, only few Cities and Counties, or other local permitting authorities in Croatia are obligatory to take into account evaluation of landslide hazard in the planning and development approval processes.

According to the regulations of the City of Zagreb, landslide maps in large scale are part of the document Physical Plan of the City of Zagreb to protect public safety from the effects of landslides. In last 50 years, the City ordered landslide hazard assessment three times which resulted in landslide inventory maps from 1967, 1979 and 2007 and two landslide susceptibility maps from 1967 and 1979 (Šikić 1967, Polak et al. 1979, Miklin et al. 2007). City, as a local permitting authority, must regulate certain development projects within zones of higher landslide hazard by requiring site investigation which will enable design of appropriate mitigation measures. According to the prescribed procedure, there are three

types of users of landslide maps: (i) the owner/ developer seeking approval of specific development projects within zones of required investigation; (ii) the engineering geologists and/or civil engineers who must investigate the site and recommend mitigation of identified hazards; and (iii) the lead agency engineering geologist and/or civil engineer who must complete the technical review, and other lead agency officials involved in the planning and development approval process.

According to the described procedure from the City of Zagreb, this type of use of landslide data requires high reliability of landslide information about evidence of existing landslide phenomena and prognosis of potential landslide processes provided by landslide inventory and landslide zonation maps. The paper Podolszki et al. (in press) shortly describes the main characteristics of historical landslide inventory and susceptibility maps available for the City of Zagreb (Šikić 1967, Polak et al. 1979 and Miklin et al. 2007) together with general comparison of historical landslide data. In this paper, available information about certain landslides are compared. Besides the data from historical landslide inventories, this research also use landslide data collected from published and unpublished landslide maps which are part of technical reports (e.g., geotechnical reports) and diploma thesis. Landslide contours interpreted by different landslide researchers were overlapped to enable evaluation of quality of existing landslide information.

At the beginning of the paper, classification of landslide identification and mapping methods is presented according to Guzzetti et al. (2012). According to the proposed systematisation, all historical landslide data available for the area of the City of Zagreb and in Primorsko-Goranska County were collected by geomorphological field mapping in large and detailed scale. The subjectivity of expert evaluation of landslide contours and limitations of local perspective during ground survey reflects significantly on quality of landslide information in terms of reliability of landslide contours.

General objective of the research is to illustrate all types of available historical information about landslide contours in the Podsljeme area of the City of Zagreb and in Primorsko-Goranska County at the area of the Rječina River Basin. The purpose is to analyse possible sources of errors and uncertainties in landslide mapping in Croatia.

Landslide identification by geomorphological field mapping

The occurrence of a landslide changes the surface topography and leaves a distinct signature. Landslide mapping is the process of identification of landslide features on the ground surface aimed at a cartographic representation of slope movement. The choices of the type and scale of the map depends on many factors, primarily on the requirements of the end user and the ultimate purpose of the landslide research. The primary requirements of the end user can be grouped

into two broad categories: detailed scale landslide maps for engineering purposes are the subjects of site-specific investigations (Fig. 1); and large-, medium- and small-scale landslide inventory maps provide information on where landslides are located and are the subjects of regional studies (Fig. 2).

The objective of landslide identification is the determination of landslide boundaries at the ground surface, including the source area and displaced mass. All of the techniques can be grouped into two broad categories according to Guzzetti et al. (2012): conventional methods and new (innovative) techniques.

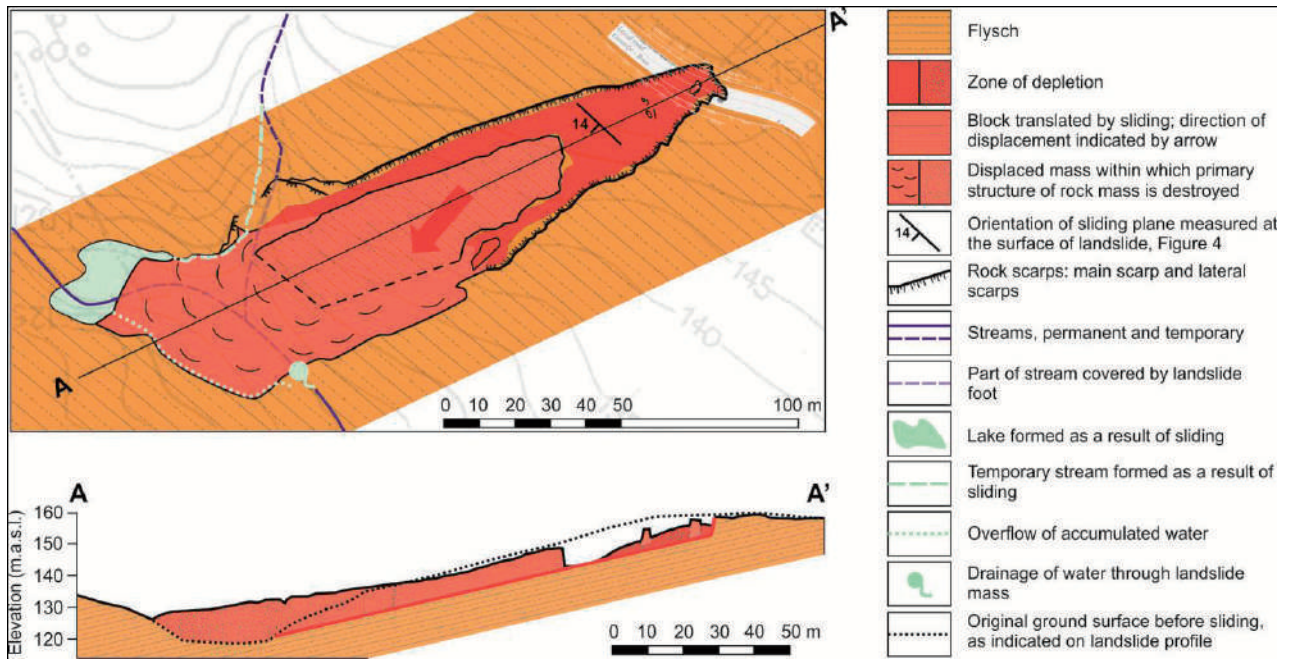


Figure 1. Detailed scale landslide map for engineering purposes (engineering geological map and cross-section of the Brus landslide in Croatia).

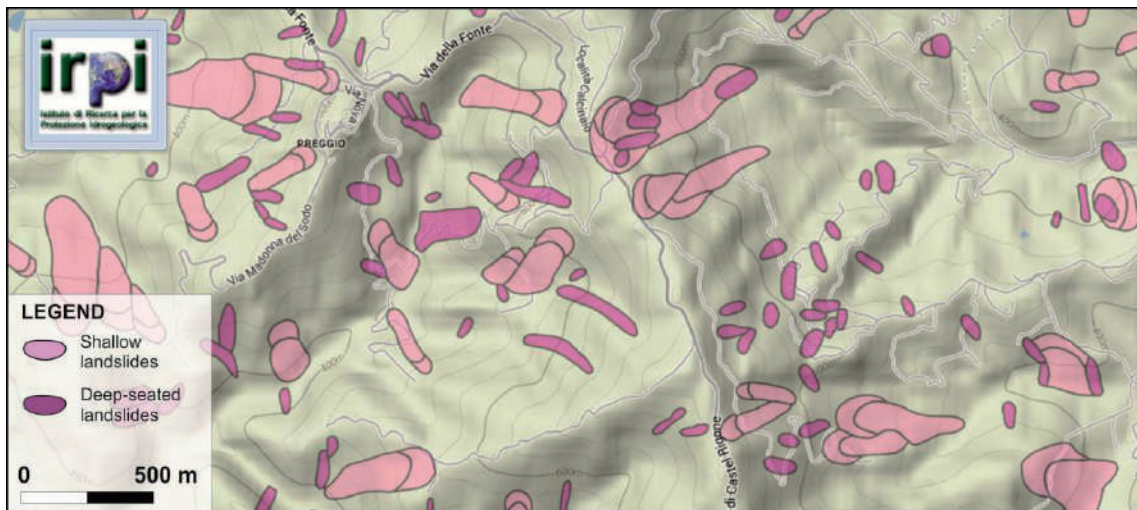


Figure 2. Segment of the medium scale landslide map for inventory of slides of the High Tiber River Basin (Italy). Source: interactive landslide map of the IRPI Geonetwork Catalog published at the <http://webmap.irpi.cnr.it/> (IRPI 2014).

Conventional methods used to identify landslides include: (i) geomorphological field mapping and (ii) visual interpretation of stereoscopic aerial photographs. Guzzetti et al. (2012) grouped recent and new methods and technologies for identification and mapping of landslides over large areas as follows: (i) analysis of surface morphology with high-resolution (HR) digital elevation models (DEMs) and (ii) interpretation and analysis of satellite images, that is, panchromatic, multispectral, and synthetic aperture radar (SAR) images. Regardless of the adopted technique, detection and mapping of landslides is a difficult, time-consuming, and error-prone task (Galli et al. 2008).

Identification of landslides in the field is a component of standard geomorphological mapping (Brunsden 1993) or engineering geological mapping (Keaton and DeGraff 1996). The key features of landslide phenomena at the ground surface are the main scarp, lateral flanks, internal morphology, and landslide toe. However, because considerable topographic details are required to locate many critical landslide elements, a detailed ground survey generally must be included as a major component of landslide identification at the detailed scale, which is economically justified only in the case of site-specific landslide investigation. A disadvantage of field mapping is the limited ability to accurately determine a landslide boundary in the field due to the reduced visibility of the slope failure (a consequence of the local perspective), the size of landslide, and the fact that the landslide boundary is often indistinct or fuzzy (Santangelo et al. 2010). Unlike field mapping of individual landslides, field work aimed at mapping of landslides over large areas should be of rather limited use (Guzzetti et al. 2012).

Comparison of landslide contours from different data sources

Sloge landslide

Fig. 3 shows all historical landslide contours of the Sloge landslide (in the City of Zagreb) from different documentation types, i.e., two landslide inventories and one geotechnical report. The oldest historical data are from landslide inventory map Polak et al. (1979) in the scale 1:10,000 with approximate landslide area of 1.74 ha. The most detailed landslide map in the scale 1:500 was derived in the framework of geotechnical investigation of the Sloge landslide performed in 2007. This map was derived using detailed topographic map derived by ground survey. It depicts two landslides: older landslide no. 1 (landslide area of 2.03 ha) and smaller landslide no. 2 (landslide area of 0.54 ha) which is reactivated in left upper part of older landslide. During identification of older landslide, there was limited ability to accurately determine a landslide boundary in some parts due to the reduced visibility of the landslide features older than 35 years masked and modified by human activities.

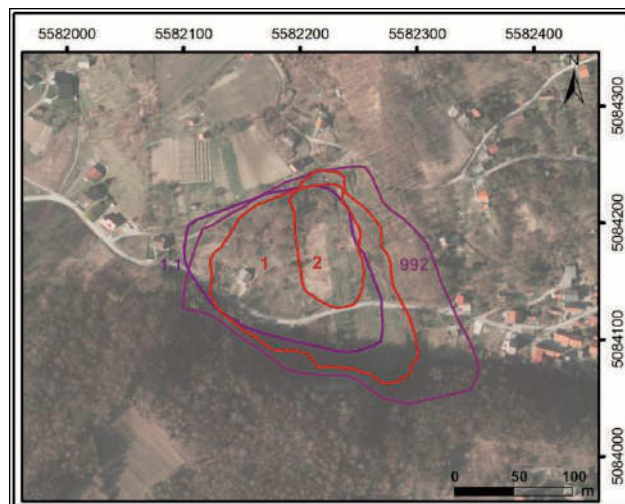


Figure 3 Landslide contours of the Sloge landslide in Zagreb city. Dark violet contour no. 1.1 depicts landslide from landslide inventory Polak et al. (1979). Dark red contours no. 1 and 2 depict two landslides from geotechnical report of the company Geokon-Zagreb Ltd. from 2007. Violet contour no. 992 depicts landslide from landslide inventory Miklin et al. (2007).

Landslide contour of younger landslide was clearly expressed during mapping. From the spatial position of landslide contours of older and younger landslides, it is visible that landslide no. 2 was developed retrogressively. Landslide contour no. 992 (landslide area of 3.25 ha) is from the landslide inventory Miklin et al. (2007) and it is identified on the basis of reconnaissance filed mapping on topographic base map 1:5,000 aimed at landslide inventory mapping.

Comparison of landslide contours from the large scale landslide inventory map Polak et al. (1979) and the detailed landslide map from 2007 clearly shows that landslide older than 35 years was reactivated in eastern part of the displaced mass. Comparison of landslide contours from the large scale landslide inventory map Miklin et al. (2007) and the same detailed landslide map shows unreliability of landslide contour derived by field mapping in 2007 used as a landslide identification method. Area of unreliable landslide contours are ~86% larger than landslide area from 1979 and ~60% larger than landslide area derived by detailed mapping in 2007.

Črešnjevec landslide

All historical landslide contours of the Črešnjevec landslide (in the City of Zagreb) which can be found in different documentation are presented in Fig. 4. The oldest historical information about sliding on the slope south from Črešnjevec Street are from landslide inventory map Polak et al. (1979) in the scale 1:10,000. In the accompanying report there is short description of five small landslides no. 1.2-1.6 (landslide areas of 0.03-0.06 ha) registered in the foot part of the slope. In the report there is explanation that landslides were caused by uncontrolled filling of waste material from excavations.

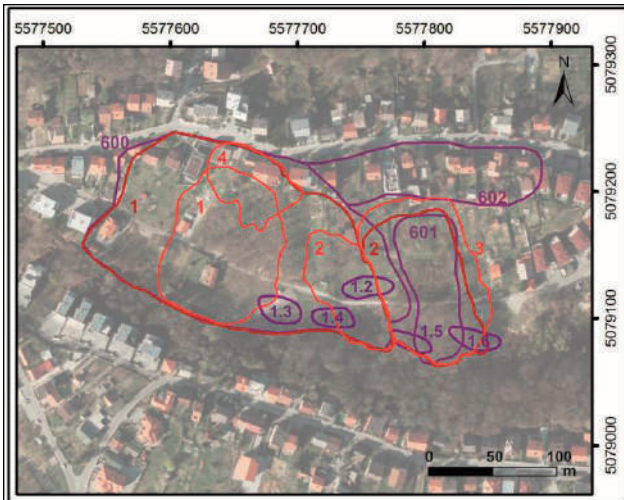


Figure 4 Landslide contours of the Črešnjevac landslide in Zagreb city. Dark violet contours no. 1.2-1.6 depict five landslides from landslide inventory Polak et al. (1979). Dark red contours no. 1 and 2 depict two landslides from geotechnical report of the Civil Engineering Institute of Croatia from 2002. Violet contours no. 600, 601 and 602 depict three landslides from landslide inventory Miklin et al. (2007). Red contours no. 1-4 depict four landslides visually identified on high resolution DEM from 2011. Contour no. 4 is border of landslide active for more than 30 years.

The most detailed landslide map in the scale 1:500 was derived in the framework of site investigation of the Črešnjevac landslide performed in 2001 taking into account considerable topographic details located on the basis of ground survey as well as historical data from geotechnical report from 1982. Detailed landslide map depicts two landslides in the form of landslide contours (landslide no. 1 and 2) and crowns of two older landslides mapped in 1982. Landslide no. 1 (landslide area of 2.55 ha) extends from top to the bottom of the slope. Smaller landslide no.2 (landslide area of 0.78 ha) is successive landslide on the east of the landslide no. 1. Detailed landslide map shows clearly expressed landslide features in upper part of landslide where they exist in the form of open cracks. Flanks and toe part of landslide were masked by human activities in the period of approximately 20 years from landslide initiation. Interpreted model of the landslide no. 1 served as a base for design of remedial works (regulation of the stream in the valley bottom and construction of drainage wells in the valley) which was finished in 2004. Three landslide contours no. 600-602 from the landslide inventory Miklin et al. (2007) are derived on the basis of reconnaissance filed mapping in the scale 1:5,000 and reinterpretation of historical information from described detailed landslide map. In the inventory from 2007 there are identified the same landslides as previously recorded, but with different landslide borders and sizes (landslide area of 2.82 ha and 0.44 ha). There is also one new landslide (landslide area of 0.69 ha) in the upper completely built-up part of the slope. On the basis of visual analysis of high resolution bare-earth DEM from March 2011 and historical data from

geotechnical report, it was possible to derive contours of three landslides (landslide area of 0.92 ha, 0.4 ha and 0.96 ha) as it is described in Mihalić et al (2013). Contour of small active landslide (landslide area of 0.31 ha) in the top part of landslide, described in Ferić et al. (2012), was derived on the basis of the same DEM data and by field checking. Activity of small landslide was detected by continuous damaging of four houses in the Črešnjevac St. at the top part of the slope.

Comparison of landslide contours from the landslide inventory map Polak et al. (1979) and landslide features derived by detailed landslide mapping in 1982 shows incomplete identification of instabilities placed at the same slope, most probably due to indistinct landslide boundaries. It can be concluded that in 1982 only contours in upper part of the landslide were clearly visible. Comparison of landslide contours derived by field mapping and ground surveys in 1982 and 2001 clearly shows retrogressive reactivation of 20 year old landslide. Comparison of landslide contours derived by reconnaissance field mapping for inventory mapping in 2007 (Miklin et al. 2007) and the detailed landslide map from 2001 shows significant changes in borders of two previously identified landslides and identification of one new landslide. Comparison of historical landslide contours with contours derived by visual interpretation of high resolution DEM from 2011 shows the best overlapping with landslide contours derived by detailed mapping in 2001.

Kvaternikova landslide

Fig. 5 shows all historical landslide contours of the Kvaternikova landslide (in the City of Zagreb) from different documentation types, i.e., two landslide inventories and one geotechnical report. The oldest historical data are from the landslide inventory map

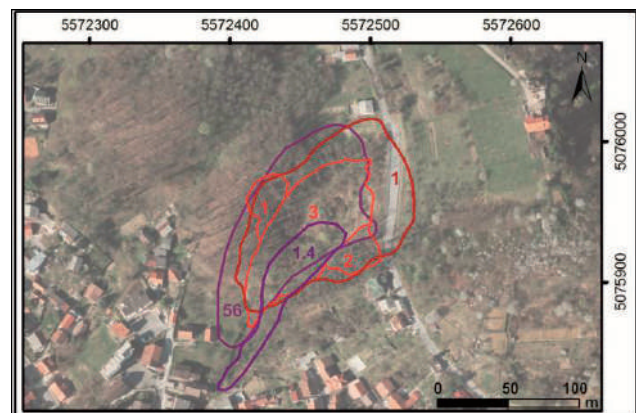


Figure 5 Landslide contours of the Kvaternikova landslide in Zagreb city. Dark violet contour no. 1.4 depicts landslide from landslide inventory Polak et al. (1979). Dark red contour no. 1 depict landslide from geotechnical report of the company Smagra Ltd. from 2006. Violet contour no. 56 depict landslide from landslide inventory Miklin et al. (2007). Red contours depict three landslides (no. 1-3) visually identified on high resolution DEM from 2011.

Polak et al. (1979) in the scale 1:10,000. Landslide no. 1.4 (landslide area of 0.26 ha) was recorded on SE steep slope of the gully. The most upper part of this gully with very steep slopes (30°–40°) has been used as an uncontrolled waste disposal for more than 20 years. The most detailed landslide map in the scale 1:100 was derived in the framework of geotechnical investigation of the Kvaternikova landslide performed in 2003, after reactivation of old landslide. This map was derived using detailed topographic map derived by ground survey. It depicts one landslide with landslide area of 1.08 ha encompassing displaced map in bottom part of the valley and steep slopes. Reduced visibility of the landslide features in some parts was caused by dense vegetation cover and partially due to artificial modifications by multiple fillings. Landslide contour no. 56 (landslide area of 0.92 ha) is from the landslide inventory Miklin et al. 2007 and it is identified on the basis of reconnaissance field mapping on topographic base map 1:5,000 aimed at landslide inventory mapping. On the basis of visual analysis of high resolution bare-earth DEM from March 2011 and historical data from geotechnical report, it was possible to identify contours of the biggest landslide (landslide area of 0.69 ha) and two small landslides (landslide area of 0.07 ha and 0.08 ha) formed on the steep slopes above flanks of the main landslide, which are the most probably active as it is described in Mihalić et al (2013).

Comparison of landslide contours from the landslide inventory map Polak et al. (1979) and the detailed landslide map from 2003 shows that landslide older than 20 years was reactivated by widening along bottom of the gully. Comparison of landslide contours from the landslide inventory map Miklin et al. (2007) and the detailed landslide map from 2003 shows significant changes of landslide contour derived by reconnaissance field mapping in 2007 used as a method of inventory mapping. Comparison of historical landslide contours with contours derived by visual interpretation of high resolution DEM from 2011 shows that historical landslide contours from 2003 and 2007 are both 33–56% larger than the main landslide body in the middle of the valley.

Grohovo landslide

All historical landslide contours of the Grohovo landslide (in the Primorsko-Goranska County) which can be found in different documentation are presented in Fig. 6. The oldest historical information about sliding on the slopes around Grohovo village in the Rječina river valley are from landslide map prepared by the Ministry of Agriculture of the Hungarian Kingdom in 1894 (Anon. 1894) in large scale 1:2,880 as it is described in Mihalić and Arbanas (2013). The map depicts contours of three big landslides no. 1–3 (landslide areas of 8.83, 29.35 and 31.68 ha) registered on both sides of the Rječina river. It was also recorded that a largest landslide occurred in 1893 on the north-eastern slope of the Rječina River causing shifting of the river channel to the south for approx.

50 meters. The most detailed landslide maps in the scale 1:1,000 were derived in the framework of geotechnical investigation of the Grohovo landslide after reactivation of old landslide in 1996. First detailed map was performed in 1998 using detailed topographic map derived by ground survey. It depicts one landslide with landslide area of 6.73 ha developed from the top to the bottom of the slope. Reduced visibility of the landslide features in some parts was a consequence of the local perspective during field mapping caused by the size of landslide and type of landslide cover in the form of limestone boulders. Landslide contour no. 2 (landslide area of 6.30 ha) was also derived in 2009 by field mapping on the same detailed topographic map.

Comparison of landslide contours from large scale landslide map (Anon. 1894) and the detailed landslide map from 1998 shows that landslide older than 100 years was reactivated in the middle part of landslide, from top to the bottom of the old landslide. Comparison of landslide contours in upper part of landslides shows retrogressive widening of reactivated landslide, but this interpretation is uncertain because of low reliability of landslide borders from 1894 due to technique of topographic mapping in this century. Comparison of landslide contours from two epochs of detailed landslide mapping in the period of 11 years (1998–2009) shows minimal changes in landslide contours. Most probably this is consequence of subjectivity of landslide expert intrinsic to visual interpretation of landslide features in the field, especially in case of larger landslides and heavily passable terrains partially covered by dense vegetation.

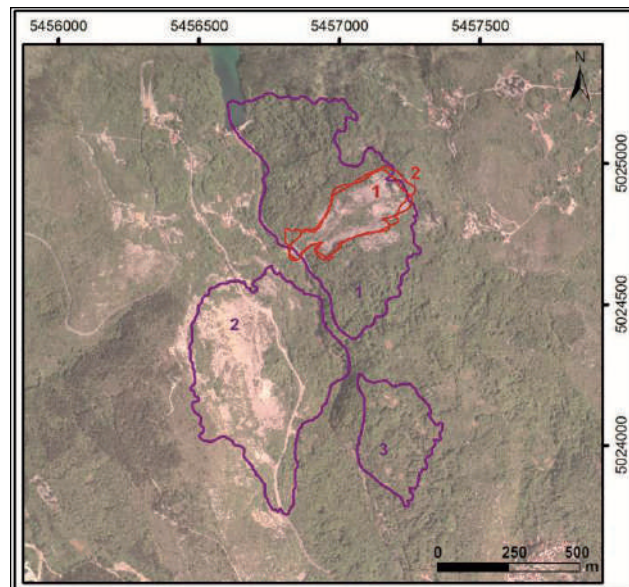


Figure 6 Landslide contours of the Grohovo landslide in Primorsko-Goranska County. Dark violet contours no. 1–3 depict landslides from landslide map from 1894 prepared by the Ministry of Agriculture of the Hungarian Kingdom. Dark red contours no. 1 and 2 depict landslides from geotechnical report and preliminary design of remediation measures of the Civil Engineering Institute of Croatia from 2000 and 2009.

Discussion and conclusions

Analysis of available historical information about landslides in the City of Zagreb shows that results of landslide mapping are archived on detailed scale landslide maps prepared for engineering purposes in the framework of site-specific investigations of individual landslides and on large scale landslide inventory maps of the hilly area of the Medvednica Mt. (i.e., Podsljeme area) for inventory mapping in 1979 and 2007.

Comparisons of landslide inventory from 1979 and site investigations maps of Sloge, Črešnjevci and Kvaternikova landslides (performed in the period 2001-2007) show: (i) usefulness of this historical inventory; and (ii) limitations of landslide field mapping on topographic maps in large scale without ground survey. Smaller landslide areas of Črešnjevci and Kvaternikova landslides depicted on the landslide inventory maps from 1979 can serve for interpretations of positions and approximate sizes of initial landslides. Similar landslide areas of the old Sloge landslide on large scale landslide inventory map from 1979 (1.74 ha) and detailed landslide map from 2007 (2.03 ha) imply uncertainty of reconnaissance field mapping used in 1979.

Comparisons of the landslide inventory map from 2007 and the detailed landslide maps of the Sloge, Črešnjevci and Kvaternikova landslides (created in the period 2001-2007) show necessity of using available information from existing geotechnical reports for compilation of inventory maps. For example, in the landslide inventory from 2007 contours of the Sloge landslide are enlarged for 1.22 ha (~60%) in relation to detailed landslide contours without depicting clearly expressed younger reactivated landslide. Modifications of landslide contours of the Črešnjevci landslide derived by site investigation from 2001 resulted in increase of the total landslide area on the slope below Črešnjevci St. for ~0.62 ha. Moreover, multiple landslide contours disable reinterpretation of complex landslide history important to derive borders of stabilized inactive, dormant and active landslide which are the most important information for potential users of landslide maps (owners/developers, engineers and official involved in the planning and development approval processes).

Overlay of historical landslide contours and visually interpreted landslide borders from high-resolution bare-earth DEM from 2011 enable evaluation of historical landslide identifications in terms of its reliability. Comparison of detailed landslide maps (from the period 2001-2007) based on ground survey with landslides identified from HR DEM shows differences due to subjectivity of interpretations. Comparison of large scale landslide inventory map from 2007 with landslides identified from HR DEM shows erroneous identifications of landslide borders interpreted for the purpose of inventory mapping in 2007.

Analysis of available historical information about landslides on the slopes of the Rječina river valley around

Grohovo village in Primorsko-Goranska County shows usefulness of historical information, even in case of historical maps with questionable topographic data. More than 100 years old landslide map of this area enable approximate determination of landslide ages and interpretations of recent landslide activity in terms of reactivations of very large historical landslides.

References

- Anon. (1894). Recovery of the Rječina River Channel. Unpublished report of the Ministry of Agriculture of the Hungarian Kingdom. Croatian State Archive, Rijeka, Croatia. (In Hungarian).
- Brunsdon D (1993). Mass movements; the research frontier and beyond: a geomorphological approach. *Geomorphology*. 7: 85–128.
- Ferić P, Mihalić S, Krkač M (2012). Visual mapping of landslides from LiDAR imagery, Zagreb, Croatia. In: Proceedings of the 2nd Japanese-Croatian Project Workshop 'Monitoring and analyses for disaster mitigation of landslides, debris flow and floods. Ožanić N et al. (eds). University of Rijeka, Rijeka, Croatia. pp. 130-133.
- Galli M, Ardizzone F, Cardinali M, Guzzetti F, Reichenbach P (2008). Comparing landslide inventory maps. *Geomorphology*. 94: 268–289.
- Guzzetti F, Mondini A C, Cardinali M, Fiorucci F, Santangelo M, Chang K-T (2012). Landslide inventory maps: New tools for an old problem. *Earth-Science Reviews*. 112: 42-66.
- IRPI (2014). IRPI web mapping. URL: <http://webmap.irpi.cnr.it>[Last accessed: 22 February 2014].
- Keaton J R, DeGraff J V (1996). Surface observation and geologic mapping. In: *Landslides - Investigation and Mitigation*. Transportation Research Board Special Report 247. Turner A K and Schuster R L (eds). National Academy Press, Washington D C, USA. pp. 178-230.
- Mihalić S, Arbanas Ž, (2013). The Croatian–Japanese joint research project on landslides : activities and public benefits. In: *Landslides : global risk preparedness*. Sassa K et al. (eds). Springer, Heidelberg, Germany. pp. 333-349
- Mihalić S, Marui H, Nagai O, Yagi H, Miyagi T (2013). Landslide inventory in the area of Zagreb City: Effectiveness of using LiDAR DEM. In: *Proceedings of the 2nd World Landslide Forum 'Landslide Science and Practice'*, Vol. 1. Springer, Heidelberg, Germany. pp. 155-162.
- Miklin Ž, Mlinar Ž, Brkić Ž, Hećimović I, Dolić M (2007). Report of the project 'Detailed engineering geological map of Podsljeme urban area in scale of 1:5.000 (DIKG-Phase I)'. Croatian Geological Survey, Zagreb. (In Croatian)
- Podolszki L, Mihalić Arbanas S, Arbanas Ž, Miklin Ž, Martinčević J (2014). Overview of historical landslide inventories of the Podsljeme Area. In: *Proc of the 1st Reg Symp on Landslides in the Adriatic-Balkan Region*. Mihalić Arbanas S, Arbanas Ž, (eds). Croatian Landslide Group, Zagreb, Croatia. In press.
- Polak K, Klemar M, Nejkova M, Radošević N, Stepan Z, Miroslav M, Križanić Z (1979). Report of the study 'Lithology and categorization according to slope stability of Medvednica Mt. hills at the area of the Zagreb City.' *Geotehnika-Geoexpert*, Zagreb. 102p. (In Croatian)
- Santangelo M, Cardinali M, Rossi M, Mondini A C, Guzzetti F (2010). Remote landslide mapping using a laser rangefinder binocular and GPS. *Nat Hazards and Earth System Sciences*. 10: 2539–2546.
- Šikić V (1967). Report of the study 'Engineering geological study of Zagreb and wider area'. Geological Survey, Zagreb. 131p. (In Croatian)

Hydrologic Data Analysis for the Grohovo Landslide Area

Elvis Žic⁽¹⁾, Ivana Sušanj⁽¹⁾, Igor Ružić⁽¹⁾, Nevenka Ožanić⁽¹⁾, Yosuke Yamashiki⁽²⁾

1) University of Rijeka, Faculty of Civil Engineering, Rijeka, Croatia, Radmile Matejčić 3, +385 51 265 900

2) University of Kyoto, Disaster Prevention Research Institute, Kyoto, Japan

Abstract This paper describes the hydrological analysis of measurement data obtained by measuring instruments that were installed on the Grohovo landslide and Valići accumulation. The hydrological analysis is performed on hydrologic data obtained from the meteorological station on the crown of Valići Dam, which is located immediately upstream of the Grohovo landslide. The meteorological station measures 35 hydrologic parameters; some of these parameters serve as inputs for numerical models of debris flow and mud flow propagation. The hydrological analysis of the Grohovo landslide requires the real-time estimation of storm water discharge and volume in the section of the drainage canal located in front of the gabion retaining wall, which is situated at the bottom of the Grohovo landslide. The data are obtained by Mini Diver instruments installed in the drainage canals, which measure variations in the surface water levels. This paper provides a comparison of 2011 and 2012 hydrologic data, as well as guidelines for future research on the Grohovo landslide area.

Keywords Grohovo landslide, hydrological analysis, meteorological station, Mini Diver instrument

Introduction

The Rječina River, whose composition derives from the Grohovo landslide, is the most important river on the Kvarner coast. Its length constitutes 18.7 km. The spring of the Rječina River is a karst spring that is located at the foot of the Gorski Kotar Mountains and drains water from the vast underground karst. The Valići Dam and the Valići accumulation, which are located in the central area of the river, are situated immediately downstream of the Grohovo landslide. The Rječina River has extremely torrential features with large flow oscillations, which have caused significant damage along the riverbed in the past. The average and maximum spring water discharge rates are 7.17 m³/s and 60.1 m³/s, respectively; however, the Rječina River is frequently dry (Žic et al. 2012). The average annual water discharge rate for the Grohovo station, which is located immediately downstream of the Valići dam, was 9.12 m³/s prior to the construction of the accumulation. Currently, the average annual water discharge rate is 1.66 m³/s (Rubinić and Sarić 2005).

Recent research in the area of the Grohovo landslide indicates that the risk of sliding rock masses has not been eliminated. The area of the valley between the Valići accumulation and the Rječina River near the canyon entrance represents the area with the greatest risk of instability in the vicinity of Rijeka city (Vivoda et al. 2012). Potential consequences include backfilled river beds, the demolition of naturally forming dams and the propagation of water waves to the mouth of the Rječina River.

The Grohovo landslide is located on the northern slope of the Rječina river valley, north of Rijeka city. Although its most recent period of activity occurred in 1996, it is an active landslide. Multiple phenomena of slippage were registered at the end of the 19th century in the area of the landslide, with disastrous consequences. The area in the vicinity of the landslide is relatively unstable (Vivoda et al. 2012). The rearrangements of the river beds due to slides of rock mass represent a significant risk of danger. The total size of the landslide is estimated at approximately 18 ha (300*600 m). Siliciclastic flysch or basic rocks are characterized by substantial lithological heterogeneity due to frequent vertical and lateral alternation of various lithological members, such as marls, siltstones, shales and fine-grained sandstones (Benac et al. 2005, Benac et al. 2006). Flysch rock mass exhibits weak permeability, which causes susceptibility to decomposition and erosion. The entire area is characterized by a network of small streams that erode slopes and significantly enhance the production of sediment in the Rječina basin.

The Croatian-Japanese bilateral scientific research project entitled "Risk Identification and Land-Use Planning for Disaster Mitigation of Landslides and Floods in Croatia" (Mihalić and Arbanas, 2013) monitors the area of the Grohovo landslide with respect to the behavior of landslide bodies, causes of and potential for sliding, hazard and risk assessments of potential surfaces, and the establishment of a monitoring and early warning system for new skating areas. In the hydrological studies, we continuously collect hydrologic data for the development of 2D and 3D numerical models to simulate the propagation of flash floods and debris flow during landslides or rockslides, in which large quantities of debris accumulate in the river bed.

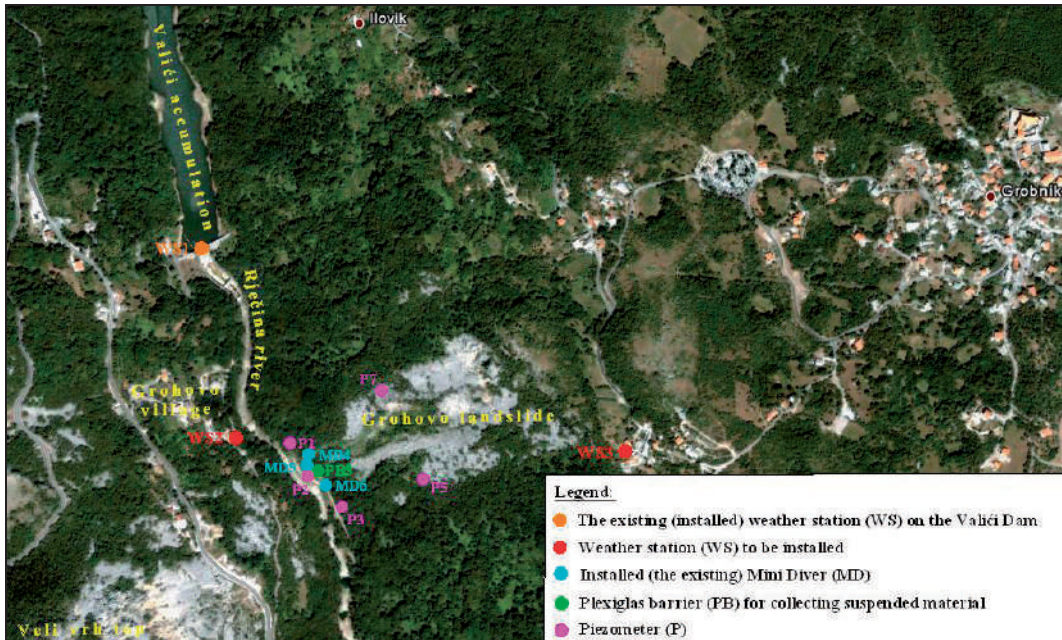


Figure 1 Map of current and proposed installations of the measuring instruments on the Grohovo landslide.

Installation of equipment on the Grohovo landslide

To monitor the Grohovo landslide, several measuring instruments were installed to measure hydrologic and hydraulic parameters. At the end of May 2011, the Vantage Pro2 weather station was installed in the middle of the crown of the Valiči Dam (WS₁, Fig. 1) near the Grohovo landslide (approximately 200 m from the foot of the Grohovo landslide). The weather station measured 35 hydrologic parameters. The time steps (increments) used for the collection of hydrologic data consist of 10-minute intervals. The Vantage Pro2 wireless weather station includes two components: the integrated sensor suite (ISS), which houses and manages the external sensor array, and the console, which provides the user interface, data display and calculations. The ISS and the Vantage Pro2 console communicate via an FCC-certified, licence-free, and frequency-hopping spread spectrum (FHSS) transmitter and receiver. The standard version of the ISS contains a rain collector, temperature sensor, humidity sensor and anemometer. In addition to the standard weather features, the ISS Plus also contains a pre-installed solar radiation sensor and a ultra-violet (UV) radiation sensor. The console displays and records the station's weather data, provides graph and alarm functions, and interfaces to a computer using optional WeatherLink software. The WeatherLink software and data logger connect the Vantage Pro2 weather station directly to a computer, which enables enhanced weather-monitoring capabilities, continuous and preserved data records, and powerful Internet features. The console of the meteorological station, which was installed 70 m from the weather station within the water-protection house, enables downloading of wireless data to the console via a USB cable. The data were collected

beginning on June 13, 2011 and were updated every 16 days. To develop an efficient numerical model (Debris Flow Modelling) of the Grohovo landslide, the installation of two new Davis Vantage Pro2 weather stations and their associated equipment (WS₂ and WS₃ in Fig. 1) will ultimately be required.

We installed three Mini Diver instruments at the foot of the Grohovo landslide to measure the surface water and groundwater that are collected through the gabion retaining wall. Mini Diver instruments have a ceramic pressure sensor, temperature sensor, data recorder and battery, which are placed in a hermetically sealed stainless steel box. This box reduces the sensitivity of the Mini Diver instrument to moisture and electrical influences. The Mini-Diver instrument is equipped with a memory capacity of 24,000 measurements. The first Mini Diver instrument (MD₄) is mounted at the end of the left drainage channel, the second (MD₅) Mini Diver instrument is mounted at the end of the right-hand drainage channel, and the third Mini Diver instrument (MD₆) is placed at the end of the channel that runs parallel to the gabion retaining wall (collects leachate behind the gabion retaining wall), as shown in Figure 2. Data collection using the Mini Diver instrument began on July 11, 2011. The time steps (increment) for the data collection are comprised of 1-minute intervals. Mini Diver instruments 4, 5 and 6 (MD₄, MD₅ and MD₆) are placed in a drilled hole with a depth of 17 cm in the middle drainage channel of the storm water.

Five piezometers were installed in the area of the Grohovo landslide (P₁, P₂, P₃, P₅ and P₇ in Fig. 1). Three piezometers were installed on the lower part of the landslide (at the landslide foot), and two piezometers were installed in the middle of the slide zone. The three lower piezometers (P₁, P₂ and P₃) measure the



Figure 2 Positions of the Mini Diver instruments near the foot of the Grohovo landslide.

groundwater levels, whereas groundwater levels (recharge to the Rječina stream) are measured at the base of the upper piezometers (P5 and P7). Continuous monitoring of groundwater levels began in December 2011 for piezometer P1 and in February 2012 for piezometer P3. The hydrological analysis of fluctuations in groundwater levels in the vicinity of the Grohovo landslide was not discussed in this paper.

The required measurement and research equipment, numerical programs, and systems and equipment for the meteorological and hydrological observations were provided by the Japanese government as part of the Croatian-Japanese bilateral scientific research project (Mihalic and Arbanas 2012). The remaining research equipment was provided by the faculty of the Department of Civil Engineering at the University of Rijeka.

Data analysis for the Grohovo landslide

The research methods are based on hydrologic and hydraulic data that were collected from field measurements in the Grohovo landslide. The database contains real-time data collected with the installed measuring devices: weather station, Mini Diver and Baro Diver instruments, ombrographs, limnigraphs, satellite radar and an ADCP flow meter. The research methods include surface exploration, groundwater exploration (measurement of groundwater levels in the area of the Grohovo landslide), 2D and 3D numerical modelling, and GIS technology; all are dependent on the availability of data at the defined locations. Based on the hydrological and hydrogeological data, 2D and 3D numerical models of debris flow propagation were constructed. The following section includes graphical views and a brief analysis of the most important real-time hydrological parameters for 2011 and 2012, which can serve as parameter inputs for numerical models.

Figure 3 displays the variation in the outside air temperatures in the area near the Grohovo landslide. The maximum air temperature in August 2011 was 33.7 °C, whereas the minimum air temperature in December 2011 was -3.6 °C. The output humidity in 2011 ranged from 24% to nearly 100%. The mean air density on the Grohovo landslide in 2011 was approximately 1.17 kg/m³. Minimum and maximum air density values were 1.123 kg/m³ and 1.228 kg/m³, respectively. The maximum dew point recorded for a given area was 22.3 °C.

Note that no hydrologic data were measured during the period of July 22 to the end of July, as shown in Figure 4, due to certain hydraulic repairs within the crown of the Valići Dam. The maximum and minimum

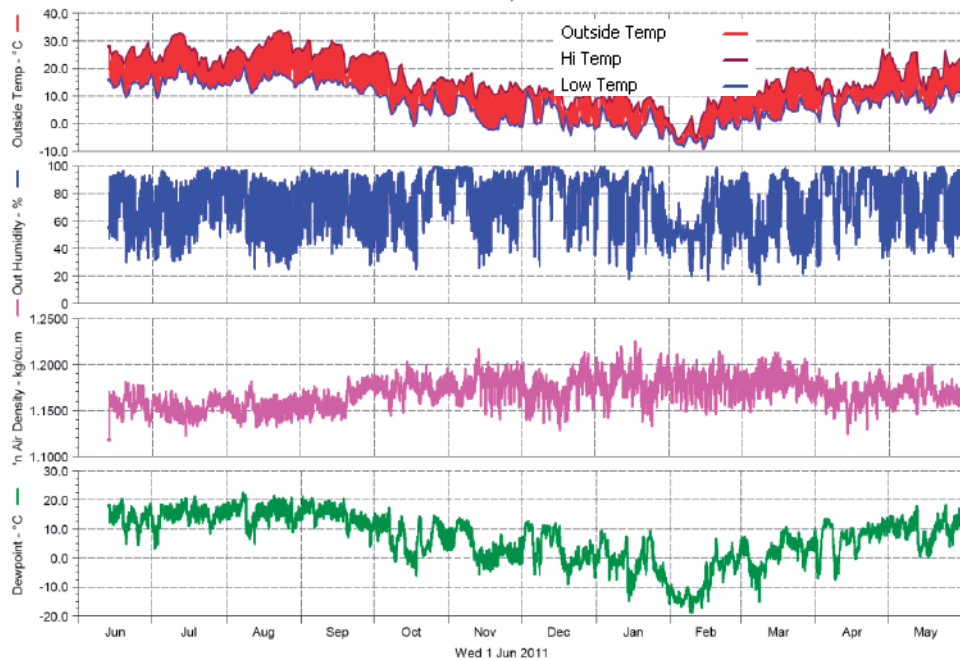


Figure 3 Graphical view of variations in outside temperature, maximum and minimum outside temperatures, outside humidity, air density values and dew point in real time in 2011, Weather station, Valići Dam.

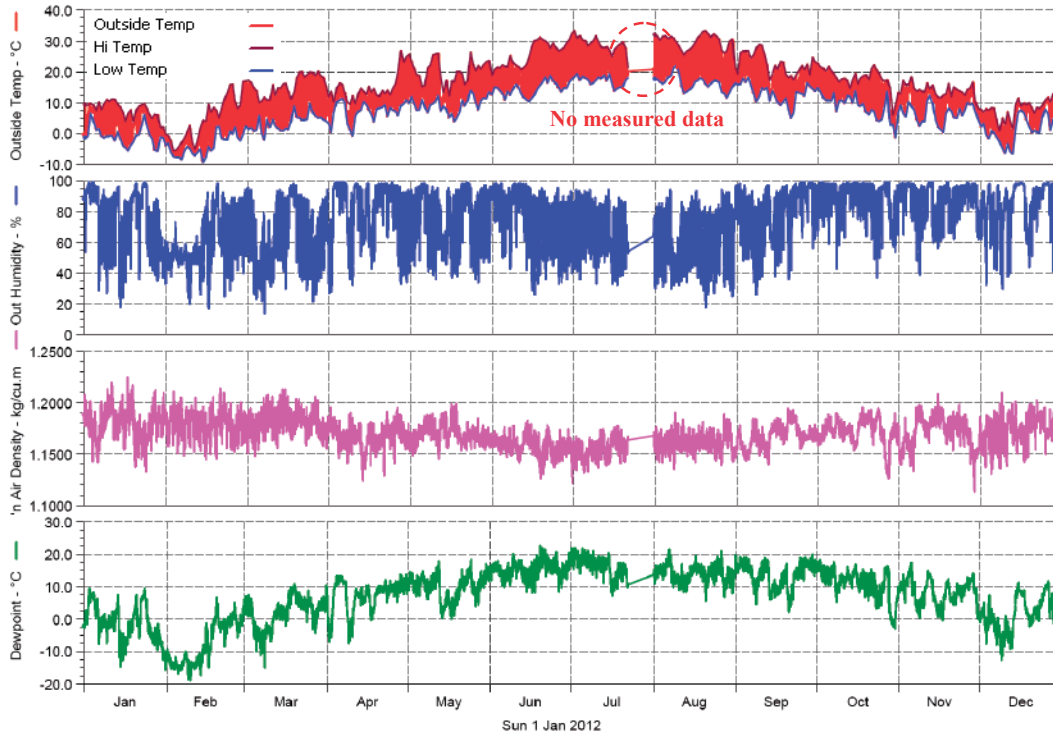


Figure 4 Graphical view of variations in outside temperature, maximum and minimum outside temperatures, outside humidity, air density and dew point in real time in 2012, Weather station, Valići Dam.

recorded outside air temperatures in 2012 were 32.3 °C (in June) and -9.3 °C (in February), respectively. The air humidity ranged 14-100%, whereas the minimum and maximum air densities were 1.112 kg/m³ and 1.225 kg/m³, respectively. The maximum dew point was slightly greater than 21 °C (in June and August), as shown in Figure 4.

Rain intensity is an important parameter for monitoring the occurrence of debris flow propagation, which is closely linked to the saturation of terrain materials and potential landslide triggering. Figure 5a displays the high variability of total monthly rainfall in 2011. The majority of the precipitation, 237 mm, fell during the month of October, whereas the lowest amount of rainfall, 5 mm, was recorded in August. 2012 was a slightly rainy year, in which the maximum monthly precipitation occurred in October (338.6 mm); March and July were the driest months of the year (1.4 mm and 0.4 mm, respectively). The minimum atmospheric pressure corresponded to the greatest rainfall intensities, whereas the maximum atmospheric pressure corresponded to predominantly dry periods (Figs 5a,b). Tables 1 and 2 list the monthly cumulative values for the variations in air temperature, precipitation and wind speed for 2011 and 2012 on the Valići accumulation. In 2011, the Grohovo landslide experienced a total of 672.6 mm of rainfall (from June through December), whereas the total rainfall experienced in 2012 was 1484.9 mm.

This paper provides an overview of the variations in maximum wind speed and evapotranspiration in the Grohovo landslide area for 2011 and 2012, as shown in Figures 6a and 6b. The maximum recorded wind speed in 2011 was 86.9 km/h (in July), whereas the mean value for the entire year was approximately 6.0 km/h. A maximum wind speed of 83.7 km/h was recorded in 2012 (in February), whereas the mean annual wind speed was 6.1 km/h. The north wind was the dominant wind direction in the Grohovo landslide area. Maximum values of evapotranspiration were significant for the period of May to the end of August. In 2011, the maximum monthly amount of evapotranspiration was 87.8 mm (in August), whereas the lowest amount of evapotranspiration was 12 mm (in December). In 2012, similar values were recorded, with a maximum evapotranspiration of 85.8 mm (in August) and a minimum evapotranspiration of 10 mm (in December).

The processing of hydraulic data for the Grohovo landslide area included the collection of hydrological data from the three Mini Diver instruments, which were placed inside the drainage canals to collect rainwater and seepage water from the area of the Grohovo landslide. Based on the measured water levels in the drainage channels in real time and based on the hydraulic geometric parameters (Tab. 3) measured for each cross section by the installed Mini Diver instrument, the maximum monthly flow velocity, water discharge and volume in the drainage channels were easily computed.



Figure 5 Graphical view of variations in atmospheric pressure and rainfall in real time in a) 2011 and b) 2012, Weather station, Valići Dam.

Table 1 2011 annual climatological summary, Weather station, Valići Dam.

TEMPERATURE (°C), HEAT BASE 18.3, COOL BASE 18.3																
YEAR	MONTH	MEAN MAX	MEAN MIN	MEAN	DEP. FROM NORM.	HEAD DEG DAYS	COOL DEG DAYS	HIGH	DATE	LOW	DATE	MAX>=32	MAX<=0	MIN<=0	MIN<=-18	
11	1	-	-	-	-	-	-	-	-	-	-	-	-	-	-	
11	2	-	-	-	-	-	-	-	-	-	-	-	-	-	-	
11	3	-	-	-	-	-	-	-	-	-	-	-	-	-	-	
11	4	-	-	-	-	-	-	-	-	-	-	-	-	-	-	
11	5	-	-	-	-	-	-	-	-	-	-	-	-	-	-	
11	6	25.6	13.9	19.7	0.0	21	45	29.4	29	9.5	20	0	0	0	0	
11	7	25.5	15.2	20.2	0.0	32	90	32.7	12	9.2	3	4	0	0	0	
11	8	28.4	15.7	21.6	0.0	19	122	33.8	23	10.8	11	7	0	0	0	
11	9	25.8	14.3	19.4	0.0	38	71	30.1	3	10.6	25	0	0	0	0	
11	10	16.8	6.5	11.0	0.0	234	9	26.2	2	-0.8	17	0	0	1	0	
11	11	13.6	2.3	6.6	0.0	351	0	18.1	10	-2.4	19	0	0	12	0	
11	12	10.3	2.3	6.0	0.0	381	0	13.7	8	-4.2	21	0	0	13	0	
		20.6	9.8	14.6	0.0	1076	338	33.8	AUG	-4.2	DEC	11	0	26	0	

Table 1 2011 annual climatological summary, Weather station, Valići Dam, continue.

YERR	MONTH	PRECIPITATION (mm)							WIND SPEED (km/hr)						
		TOTAL	DEP. FROM NORM.	MAX. OBS DAY	DATE	DAYS OF RAIN OVER			YERR	MONTH	AVER.	HIGH	DATE	DOMIN. DIREC.	
						0.2	2	20							
11	1	-	-	-	-	-	-	-	11	1	-	-	-	-	
11	2	-	-	-	-	-	-	-	11	2	-	-	-	-	
11	3	-	-	-	-	-	-	-	11	3	-	-	-	-	
11	4	-	-	-	-	-	-	-	11	4	-	-	-	-	
11	5	-	-	-	-	-	-	-	11	5	-	-	-	-	
11	6	11.0	0.0	8.6	19	2	2	0	11	6	5.9	37.0	18	N	
11	7	152.0	0.0	43.0	23	12	9	3	11	7	5.8	86.9	21	N	
11	8	5.0	0.0	3.4	1	4	1	0	11	8	6.2	33.8	10	N	
11	9	103.6	0.0	60.0	19	6	5	2	11	9	5.9	48.3	20	N	
11	10	237.0	0.0	82.0	7	8	5	4	11	10	6.1	45.1	21	N	
11	11	21.2	0.0	12.2	7	6	3	0	11	11	6.7	32.2	12	N	
11	12	142.8	0.0	33.0	14	16	11	3	11	12	5.7	56.3	19	N	
		672.6	0.0	82.0	OCT	54	36	12			6.0	86.9	JUL	N	

Table 2 2012 annual climatological summary, Weather station, Valići Dam.

YEAR	MONTH	TEMPERATURE (°C), HEAT BASE 18.3, COOL BASE 18.3													
		MEAN MAX	MEAN MIN	MEAN	DEP. FROM NORM.	HEAD DEG DAYS	COOL DEG DAYS	HIGH	DATE	LOW	DATE	MAX>=32	MAX<=0	MIN<=0	MIN<=-18
12	1	7.5	-0.9	2.8	0.0	481	0	11.2	11	-5.7	28	0	1	23	0
12	2	4.3	-3.9	-0.0	0.0	531	0	16.8	29	-9.3	14	0	10	25	0
12	3	15.7	3.5	9.5	0.0	274	1	20.1	28	-2.2	8	0	0	1	0
12	4	14.6	7.1	10.7	0.0	234	6	26.8	28	-0.8	10	0	0	1	0
12	5	20.2	9.3	14.5	0.0	138	20	26.4	24	3.9	18	0	0	0	0
12	6	25.5	14.3	19.5	0.0	39	77	31.2	19	10.3	15	0	0	0	0
12	7	28.9	17.2	23.0	0.0	4	107	33.3	2	13.8	17	2	0	0	0
12	8	29.7	16.3	22.9	0.0	14	158	33.2	20	11.6	28	4	0	0	0
12	9	22.6	12.9	17.2	0.0	71	37	28.8	9	4.9	21	0	0	0	0
12	10	17.8	8.8	12.6	0.0	181	4	22.8	1	-1.3	30	0	0	1	0
12	11	13.9	6.6	10.1	0.0	247	0	18.3	5	0.5	17	0	0	0	0
12	12	8.1	0.9	4.3	0.0	433	0	12.8	28	-6.7	13	0	0	12	0
		17.2	7.5	12.0	0.0	2647	410	33.3	JUL	-9.3	FEB	6	11	63	0

YERR	MONTH	PRECIPITATION (mm)							WIND SPEED (km/hr)						
		TOTAL	DEP. FROM NORM.	MAX. OBS DAY	DATE	DAYS OF RAIN OVER			YERR	MONTH	AVER.	HIGH	DATE	DOMIN. DIREC.	
						0.2	2	20							
12	1	79.4	0.0	53.6	3	8	4	1	12	1	6.0	38.6	30	N	
12	2	18.0	0.0	12.6	20	3	2	0	12	2	8.9	83.7	7	N	
12	3	1.2	0.0	0.8	18	3	0	0	12	3	6.7	48.3	10	N	
12	4	109.0	0.0	30.0	11	19	11	1	12	4	5.2	53.2	1	N	
12	5	117.8	0.0	47.0	7	13	8	1	12	5	6.0	64.4	14	N	
12	6	72.0	0.0	29.4	12	11	5	2	12	6	5.4	37.0	13	N	
12	7	0.4	0.0	0.4	15	1	0	0	12	7	6.7	54.7	22	N	
12	8	59.4	0.0	34.8	31	4	2	2	12	8	6.7	53.1	26	N	
12	9	251.0	0.0	113.8	19	15	7	2	12	9	5.3	66.0	14	N	
12	10	338.6	0.0	105.6	15	24	11	4	12	10	5.6	57.9	27	N	
12	11	242.1	0.0	54.6	1	20	11	5	12	11	5.3	64.4	5	N	
12	12	196.0	0.0	67.4	15	16	10	3	12	12	5.3	67.6	8	N	
		1484.9	0.0	113.8	SEP	137	71	21			6.1	83.7	FEB	N	

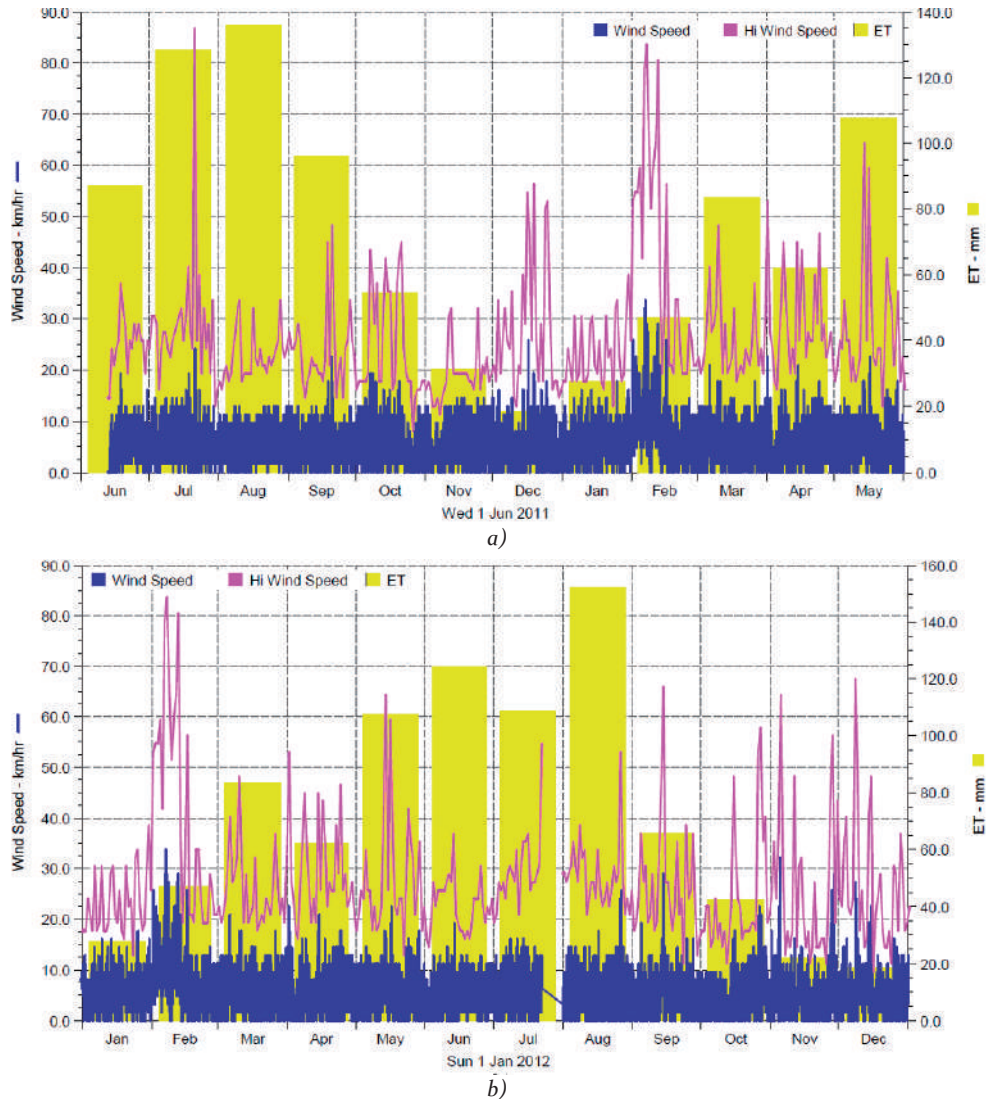


Figure 6 Graphical view of variations in wind speed, high wind speed and evapotranspiration in real time for Weather station, Valići Dam: a) 2011 and b) 2012 year.

Table 3 Geometric and hydraulic characteristics for the channel profile of the positions of the installed Mini Diver instruments, Grohovo landslide.

	MINI DIVER 1	MINI DIVER 2	MINI DIVER 3
Hole depth for Mini Diver instrument [m]	0.170	0.160	0.165
Channel slope [%o]	32.0	6.6	13.6
Slope of the left channel side [°]	30.58	37.88	41.33
Slope of the right channel slope [°]	25.25	47.95	29.18
Manning's roughness coefficient [$m^{-1/3s}$]	0.030	0.030	0.030
Time step [s]	60.00	60.00	60.00
Bottom channel width [m]	0.800	0.510	0.870

Figures 7 to 9 illustrate the variations in maximum monthly water levels, maximum monthly flow velocities in the channel and maximum monthly water discharges

in the channel for the positions of Mini Diver instruments 1, 2 and 3 from July 2011 to December 2012. At the left-hand drainage channel, the maximum flow velocity was 3.34 m/s, as shown in Figure 7. These high speeds are common for a high channel slope of 32%. In August and September 2011, no water levels were recorded by the Mini Diver instruments; thus, the flow velocity, water discharge and volume of storm water were not measured. At the beginning of February 2012, freezing water was discovered in the drainage channels in the area of the Grohovo landslide due to a strong winter and low temperatures (-9.3 °C, 30 cm ice layer). During this period, the Mini Diver instruments incurred damaged to the ceramic membranes, which caused them to be unusable. As a result, new Mini Diver instruments were installed at the end of March. The maximum monthly water volumes in the left-hand drainage channel (position of Mini Diver 1) were the highest in November (14,055.03 m³) and October (11,177.18 m³) of 2011, as shown in Table 4.

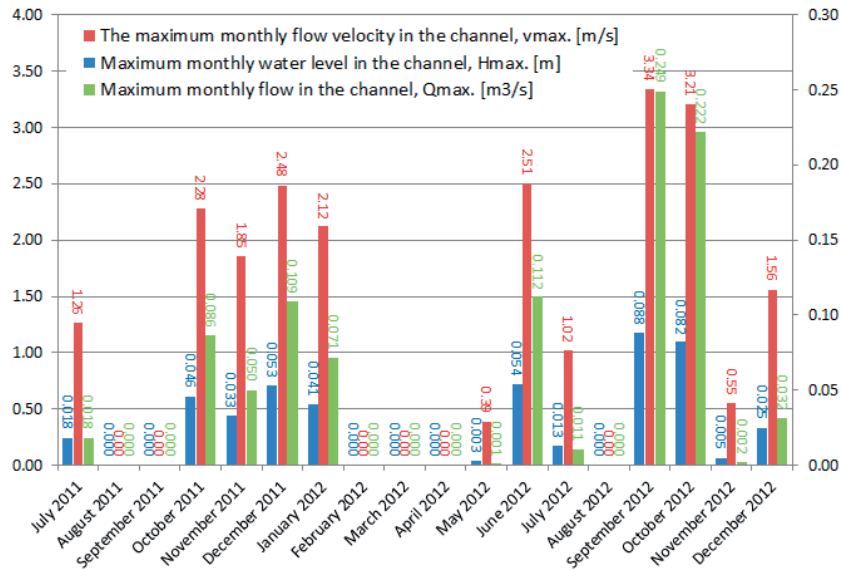


Figure 7 Graphical view of variations in the maximum monthly water levels in the channel, maximum monthly flow velocities in the channel and maximum monthly water discharges in the channel for the period of July 2011 to December 2012, Mini Diver instrument 1, Grohovo landslide.

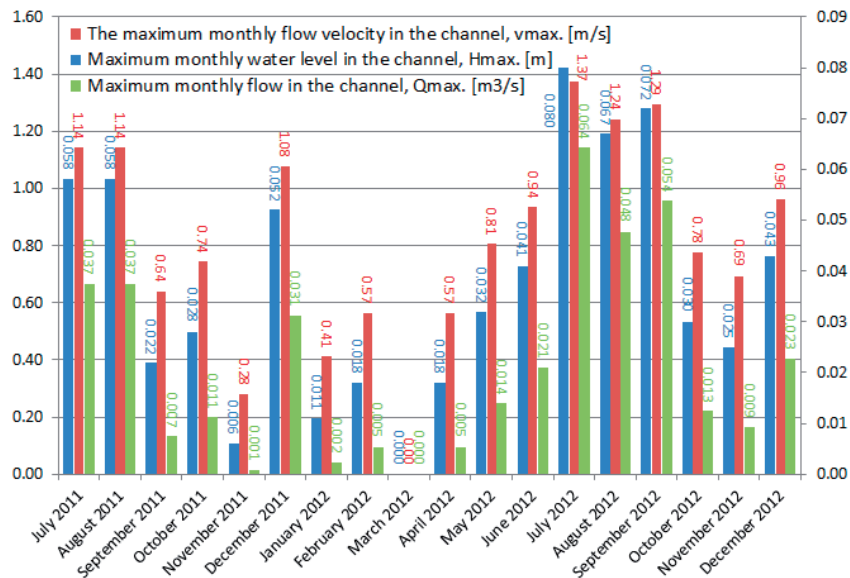


Figure 8 Graphical view of variations in maximum monthly water levels in the channel, maximum monthly flow velocities in the channel and maximum monthly water discharges in the channel for the period of July 2011 to December 2012, Mini Diver instrument 2, Grohovo landslide.

The flow velocity in the main drainage channel (position of Mini Diver instrument 2) consisted of 0.28 to 1.37 m/s, the maximum recorded water discharge was 0.053 m³/s (Fig. 8), and the maximum recorded total monthly volume of water in July and December of 2012 were 13,987.64 m³ and 7,278.55 m³, respectively, as shown in Table 4. The minimum total monthly volume of water was 2.50 m³ in November 2011.

The maximum total monthly water volumes for the

right-hand drainage channel on the Grohovo landslide (position of Mini Diver instrument 3), which is located in front of the gabion retaining wall, were 20,859.77 and 13,329.5 m³ in July 2011 and August 2011, respectively, as shown in Table 4. The maximum monthly water flow velocities for a given channel ranged from 0.12 to 1.80 m/s, the water levels ranged from 8 to 63 mm, and the maximum recorded water discharge was approximately 0.10 m³/s (December 2011), as shown in Fig. 9.

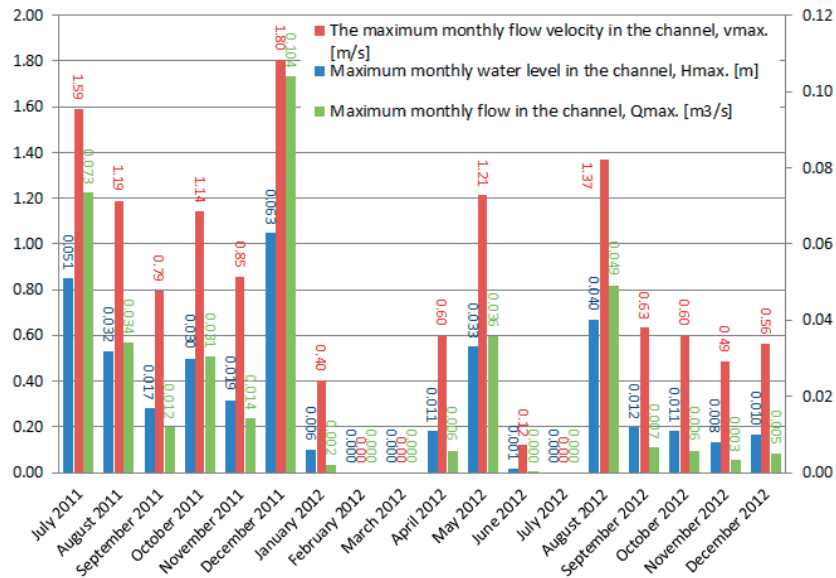


Figure 9 Graphical view of variations in maximum monthly water levels in the channel, maximum monthly flow velocities in the channel and maximum monthly water discharges in the channel for the period of July 2011 to December 2012, Mini Diver instrument 3, Grohovo landslide.

A review of total monthly storm water levels for individual drainage channels in the Grohovo landslide is provided in Table 4. Based on the hydraulic calculations of stormwater runoff for the drainage channels under the Grohovo landslide, the cumulative annual volume of storm water in 2011 and 2012 were calculated as 66,266.71 m³ and 42,931.91 m³, respectively. Although the hydraulic

analysis for 2011 only included the last 6 months of the year (July to December), the total annual storm water volume was significantly higher compared with the entire 2012 year. Although the volume of water during the winter months was anticipated to be significant, the maximum monthly water volumes occurred in July and August.

Table 4 Total monthly water volumes for the period of July 2011 to December 2012. Mini Diver instruments 1, 2 and 3, Grohovo landslide.

Month	Monthly amount of water volume, [m ³],			Total monthly amount of water volume, [m ³], V _{tot.month} , [m ³]
	MINI DIVER 1 V _{month} , [m ³]	MINI DIVER 2 V _{month} , [m ³]	MINI DIVER 3 V _{month} , [m ³]	
July 2011	374.93	1256.32	20859.77	22491.02
August 2011	0.00	746.72	13329.50	14076.22
September 2011	0.00	247.09	370.23	617.32
October 2011	11177.18	212.65	1224.77	12614.61
November 2011	14055.03	2.50	1644.46	15701.99
December 2011	749.56	3.15	12.85	765.55
January 2012	1160.63	3.70	0.23	1164.56
February 2012	0.00	230.75	0.00	230.75
March 2012	0.00	0.00	0.00	0.00
April 2012	0.00	230.75	20.05	250.80
May 2012	0.07	4130.92	259.76	4390.76
June 2012	1095.73	884.69	0.01	1980.42
July 2012	53.07	13987.64	0.00	14040.71
August 2012	0.00	1080.49	291.99	1372.48
September 2012	1609.55	7123.87	6.66	8740.08
October 2012	1174.27	361.98	6.33	1542.58
November 2012	1.08	1848.77	13.16	1863.00
December 2012	57.43	7278.55	19.77	7355.75
			Sum (2011):	66266.71
			Sum (2012):	42931.91

Conclusion

One of the primary goals of the Croatian-Japanese bilateral project is to analyse the input and output parameters associated with the flood wave and landslides. The basic parameters are as follows: terrain morphology and conditions of surface and ground water, the intensity and duration of rainfall, cumulative rainfall, the frequency of rainfall prior to sliding, the impact of the seasons and climate changes, the slope stability (stability of cut slopes) and drainage conditions, density and type of vegetation cover, and seismicity areas. These parameters indicate the causes of sliding on inclines, which were comprised of flysch formation, and the occurrence of debris flow. Based on collected meteorological, hydrological and geological data from the Grohovo landslide, 2D and 3D numerical models of debris flow propagation downstream of the Rječina River were developed. The data results from the established meteorological and hydrological monitoring system indicate the efficiency and adequacy of the established system and reveal any necessary modifications of the system. Continuous monitoring and data collection, as well as future simulation models will enable the establishment of an early warning system for the dangers of flooding.

Acknowledgements

The authors would like to thank the Croatian Ministry of Science, who supported this research on the Croatian-Japanese scientific project entitled “Risk Identification and Land-Use Planning for Disaster Mitigation of Landslides and Floods in Croatia”.

Reference

- Benac Č, Arbanas Ž, Jurak V, Oštrić M, Ožanić N (2005) Complex landslide in the Rječina River valley (Croatia): origin and sliding mechanism. *Bulletin of Engineering Geology and the Environment*. 64(4): 361-371.
- Benac Č, Jurak V, Oštrić M (2006) Qualitative assessment of geohazard in the Rječina Valley, Croatia. *Proceedings of the 10th IAEG International Congress: IAEG Engineering geology for tomorrow's cities*, The Geological Society of London, 658 (1-7).
- Mihalić S, Arbanas Ž (2013) The Croatian–Japanese Joint Research Project on Landslides: Activities and Public Benefits. *Landslides: Global Risk Preparedness*. Sassa K.; Rouhan B.; Briceno S.; He B. (eds). Springer-Verlag Berlin Heidelberg. (ISBN 978-3642220869). pp. 345-361.
- Rubinić J, Sarić M (2005) Hidrologija vodnih resursa u slivu Rječine. *Zbornik radova „Prošlost, sadašnjost i budućnost vodoopskrbe i odvodnje - Iskustva i izazovi“*, Linić A. (ed). Opatija: Vodovod i kanalizacija Rijeka, Rijeka. pp. 199-207.
- Vivoda M, Benac Č, Žic E, Đomlija P, Dugonjić Jovančević S (2012) Geohazard u dolini Rječine u prošlosti i sadašnjosti. *Hrvatske vode*. 20, 81; 105-116.
- Žic E, Palinić N, Čebuhar L, Kajapi I (2012) Brana i akumulacija Valići na vodotoku Rječine. *Proceeding of 5th International conference on industrial heritage thematically related to Rijeka and the industrial building heritage*, Palinić N. (ed.), Rijeka: Pro Torpedo. pp. 48-49.

Analysis of Flash Flood Occurred at Slani Potok Catchment, Croatia

Ivana Sušan⁽¹⁾, Nevenka Ožanić⁽¹⁾, Yosuke Yamashiki⁽²⁾

1) University of Rijeka, Faculty of Civil Engineering, Rijeka, Croatia, Radmile Matejčić 3, +385 51 265 942

2) Kyoto University, Disaster Prevention Research Institute (DPRI), Kyoto, Japan

Abstract Estimation of potential hazard caused by flash flood is important for the design and construction of the structural mitigation elements. Due to this matter, river discharge after short time rain event and its environmental impact are two main parameters that have to be studied in detail. Measurement of water velocity is difficult when short time flash flood occurred and at the same time is crucial for calculation of water discharge. This paper describes the calculation procedure of river discharge after high rain intensity when water level and velocity data are not available. Calculation is based on flash flood water table traces (left after flash flood) and riverbed geometry.

Keywords flash flood, water discharge, water table traces, riverbed geometry

Study area

Location of research area

The Slani Potok catchment area is a part of the Dubračina River catchment area which is located in the central part of the Vinodol valley (Fig. 1). The Vinodol Valley is a separated geographical entity of the eastern Kvarner area and unique spatial unity between Križišće in the northwest and Novi Vinodolski in southeast and the Vinodol Channel.

Geological setting and hydrological characteristics

Slani Potok catchment area may be considered as an example of combined erosion, landslides and torrential impacts and it is known for many years as an area of potential hazard risk. Excessive surface erosion occurs on the area of 600 m in length and 250 m in width. Side effects around the erosion center are landslides, which are the results of weathering of the flysch rock mass. The size of this affected area is about 3 km² and the surrounding the Belgrade, Baretići, Grižane and Kamenjak settlements are at risk as well as the surrounding roads (Benac et al. 2005).

For erosion affected area, local landslides and torrents, reconstruction projects (roads, riverbed regulations, retaining walls, etc.), as well as geological and hydrogeological research have been performed

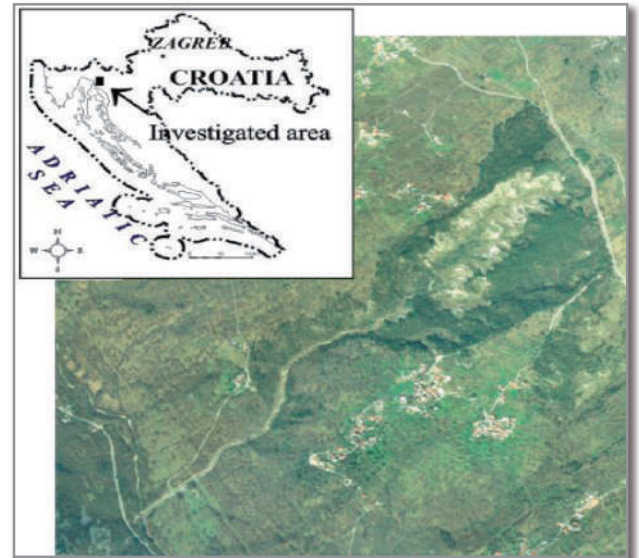


Figure 1 Location of investigated area with air photograph of Vinodol Valley and Slani Potok catchment area (Aljinović et al. 2010).

many times in the last hundred years, unfortunately, without positive outcome and with no prospect in finding the permanent solution of existing problems.

The basin of Slani Potok has an area of approximately 2 km², and its altitude extends from 50 m a.s.l. to 700 m a.s.l. The lower part of the catchment area (0.9 km²) is formed in flysch sediments (mainly siltstones), and it represent the majority of surface runoff (Ružić et al. 2010). The upper part of catchment area is a karstic plateau from which the runoff is insignificant. In the karst and flysch contact zone is more overflow springs that make the majority of water balance in the dry season (Fig. 2).

Catchment area middle slope of the terrain is 22% and the slopes are in scale between 5% and 100% (Fig. 3), which is characterized as a very steep basin. Slope of catchment area determine runoff and the erosion processes. Time of catchment area concentration is 15 minutes, proposed in Kirpich calculation method (Žugaj 1995). If we consider the part of the catchment area on flysch - middle slope is about 19%, and the time of concentration is around 9 minutes.

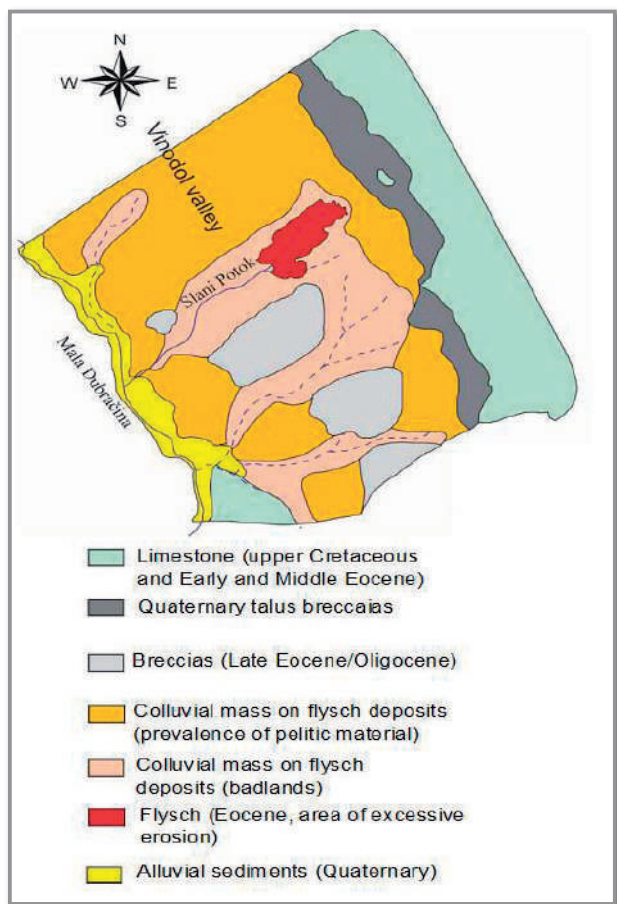


Figure 2 Schematized geologic map of the Vinodol Valley with the Slani Potok catchment area (Aljinović et al. 2010).

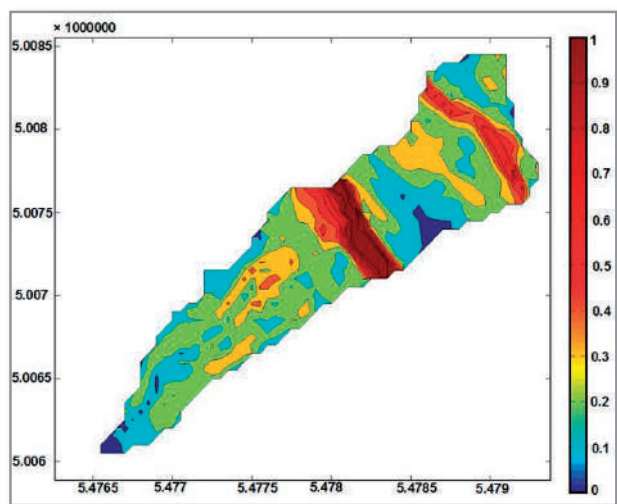


Figure 3 Map of slope gradients in the Slani Potok catchment area.

Data and methods

Data collection

As part of research, it was established the continuous measuring of water levels at four hydrological profiles with minute frequency measurements of water levels. Minute frequency measurement is necessary because of torrential character water flow. Water levels were measured by pressure sensors Mini Diver manufactured by Schlumberger Water Services. Atmospheric pressure is compensated by the data collected from device Baro Diver. Meteorological parameters were measured by two meteorological station Vantage Pro 2 manufactured by Davis Instruments Corporation. Water velocity is measured occasionally by OTT-hydrometrie and RYUKAN WJ7661 (surface current meter).

In a case of flash flood occurrence it is difficult to measure velocity of water. It is also common that collected data are not reliable.

During the night of 19 September 2012 to 20 September 2012 an episode of flash flood occurred at the mouth of Slani Potok into the Dubračina River (Fig. 4). Flash flood was induced by intensive short time rainfall. Meteorological station recorded 79.50 millimeters of rainfall. Recorded monthly rainfall for the September 2012 was 155.7 millimeters. According to recorded data at that particular location, the largest amount of rainfall occurred in September 2012 since the beginning of measurements (April 2011).

Water level and velocity of water are not measured at the place of flash flood occurrence. In the order to calculate maximum water discharge, riverbed geometry and water table traces (remain after flash flood) are measured (Fig. 5) for 28.5 meters long river section.



Figure 4 Riverbed section of Slani Potok where the flash flood occurred with visible water table traces.

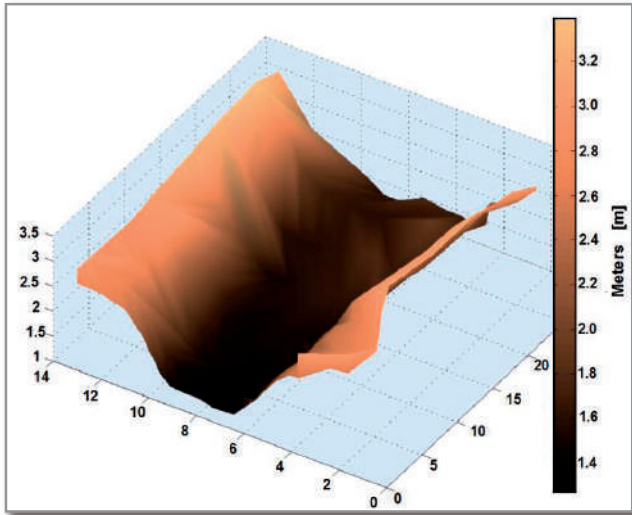


Figure 5 Measured geometry of riverbed section.

Method

Observed section of riverbed is divided into ten cross sections which geometry is precisely measured. Depth of the water is determined according to water table traces left after flash flood for every cross section.

For the purpose of calculation, natural unsteady non-uniform flow is simplified to steady non-uniform flow. Flow of the water is characterized as gradually varied flow and energy and frictional resistance equations are applied. Change of water level between cross sections in this case is caused with change of river bed geometry. Bernoulli equation is used for calculation of change of the water levels and distance between cross sections [1], where z is defined as the elevation above arbitrary datum [m]; h is defined as the flow depth [m]; α is Coriolis coefficient [-]; Q is the discharge of water [m³/s]; g is gravitational acceleration [m/s²]; A is cross sectional area of flow [m²]; I_E is decrease of energy line along the flow [m].

$$\frac{d}{dl} \left(z + h + \frac{\alpha \cdot Q^2}{2g \cdot A^2} \right) - I_E = 0 \quad [1]$$

Decrease of energy line along the flow is described in equation [2] where Q is the discharge of water [m³/s]; n is the Manning's roughness coefficient; A_{sr} is a medium cross sectional area of flow between two cross sections [m²]; R_{sr} is medium Hydraulic radius between two cross sections [m].

$$I_E = \frac{Q^2 \cdot n^2}{A_{sr}^2 \cdot R_{sr}^{4/3}} \quad [2]$$

Discharge of water is obtained by calculation of changes of water levels and distance between cross section for different discharges until calculated water levels become same as measured.

Results

Before calculation the Manning's coefficient and Coriolis coefficient are established. Manning's coefficient value for this type of natural riverbed is 0.035 (Chow 1959), and the Coriolis coefficient common value for this type of calculations is 1.0.

Measured water levels and distance between cross sections and calculated water levels for the discharge of the 15.8 m³/s are shown (Fig. 6).

Results are also presented in the Table 1 showing measured distance between cross sections and levels of water and calculated water levels and cross sections distances for the discharge of $Q=15.8 \text{ m}^3/\text{s}$.

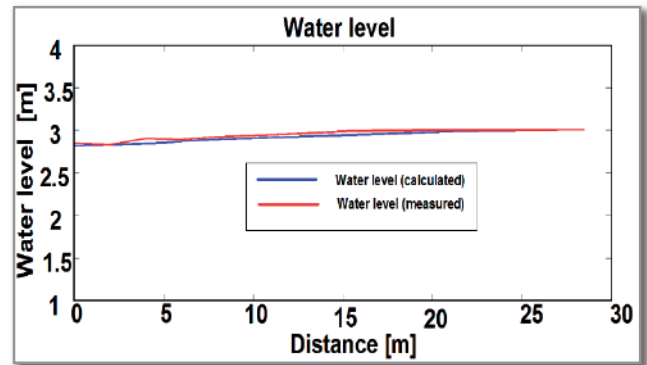


Figure 6 Comparison of measured (red line) and calculated (blue line) water level ($Q = 15.8 \text{ m}^3/\text{s}$) on 28.5 meters riverbed section for the flash flood occurred during the night between 19 and 20 September 2012.

Table 1 Comparison of measured water levels and distances between cross sections and calculated levels and distances for discharge of 15.8 m³/s.

Measured		Calculated	
Distance [m]	Water level [m]	Distance [m]	Water level [m]
0	2.85	0	2.82
2	2.83	2.17	2.83
2	2.9	2.12	2.85
2	2.89	1.2	2.86
2	2.92	0.7	2.87
2.5	2.94	1.56	2.89
5	2.99	4.43	2.92
4.5	3	4.01	2.95
5.5	3	5.34	2.99
3	3	6.21	3

Conclusion

In a case of flash flood occurrence when velocity and depth of water are not measured it is usually impossible to determine water discharge and in this paper an approximate calculation of water discharge was done. Water discharge of the 15.8 m³/s is obtained from measurement of water table traces left after flash flood and riverbed geometry.

Flash flood occurred during the night between 19 September 2012 and 20 September 2012 did not caused any significant material damage while the local road near river was flooded, and the traffic was interrupted. This flash flood didn't initiate a significant erosion process and surrounding settlement and roads were not endangered and stayed intact.

The occurrence of hazard is usually caused by a combination of different factors those could be combined with triggering factors. Monitoring of changes on researched areas in order to determine possible hazard and to define mitigation and prevention measures is extremely important. It is also important to continue the researches in the catchment area of Slani Potok because the erosion processes in combination with intensive short time rainfall can cause new hazardous events and the data of occurred water discharge could be considered as one of crucial elements for the design and construction of the structural mitigation measures to prevent and reduce further erosional processes.

Acknowledgments

This paper is result of research carried out as a part of the Croatian-Japanese science project: Risk identification and land-use planning for disaster mitigation of landslides and floods in Croatia. Many thanks to the students Ms. Ines Gržinić and Ms. Nina Garić for their assistance during the field work.

References

- Aljinović D, Jurak V, Mileusnić M, Slovenec D, Presečki F (2010) The origin and composition of flysch deposits as an attribute to the excessive erosion of the Slani Potok Valley (Salty Creek), Croatia. *Geologia Croatica*. 63/3: 313-322.
- Benac Č, Jurak V, Oštrić M, Holjević D, Petrović G (2005) Extensive erosion phenomenon in the area of the Salt Creek (Vinodol Valley), Abstracts Proceedings of 3rd Croatian Geological Congress (Velić I, Vlahović I, Biondić R, eds.), Opatija, September 2005. Croatian Geological Survey, Zagreb, pp. 173-174. (In Croatian)
- Chow V T (1959) *Open Channel Hydraulics*, Mc Graw – Hill Book Company Inc. New York.
- Ružić I, Sušan I, Ožanić N (2010) Analyses of event runoff coefficients: Slani Potok and Dubračina river, Croatia–Japan Project On Risk Identification And Land-Use Planning For Disaster Mitigation Of Landslides And Floods In Croatia: 1st Project Workshop „International Experience“, Dubrovnik (Croatia).
- Žugaj R (1995) *Hydrology*, Faculty of Mining, Geology and Petroleum Engineering University of Zagreb. (In Croatian).

Validation Study of Debris Flow Movement – Laboratory Experiments and Numerical Simulation

Elvis Žic⁽¹⁾, Yosuke Yamashiki⁽²⁾, Shota Kurokawa⁽²⁾, Shigeo Fujiki⁽²⁾, Nevenka Ožanić⁽¹⁾, Nenad Bićanić^(1,3)

1) University of Rijeka, Faculty of Civil Engineering, Rijeka, Croatia, Radmile Matejčić 3, +385 51 265 900

2) Kyoto University, Disaster Prevention Research Institute, Kyoto, Japan

3) University of Glasgow, Faculty of Civil Engineering, Glasgow, UK

Abstract Experimental physical model for debris flow movement and Hydro-Debris 2D numerical model for its calibration are described. To understand the general behavior of particle segregation in debris flow, a physical model experiments for debris flow with two distinct diameters were conducted. Furthermore, the high-speed video camera (HSVC) results, tracing each particle movement are compared with the solutions of Hydro Debris 2D Model (HD2DM), a Lagrangian sediment particle tracing numerical scheme. The underlying purpose of this study is to ultimately understand the characteristic movements of stony debris flow and to develop an improved and reliable numerical model to predict the debris flow disasters, through laboratory experiments and numerical simulation models. The paper presents comparisons of particle velocities in the two models by varying input data. In the framework of the Croatian-Japanese bilateral scientific project entitled "Risk Identification and Land-Use Planning for Disaster Mitigation of Landslides and Floods in Croatia", a experimental physical model of the debris flow propagation was created at the Faculty of Civil Engineering, University of Kyoto (Japan). Such physical model provided some of the most significant quantitative values of input model parameters used to create numerical models of debris flow.

Keywords debris flow, experimental physical model, Hydro-Debris 2D numerical model, high-speed video camera, particle velocity

Introduction

A debris flow is a mixture of water, poorly sorted sediment and other debris, typically flowing rapidly, with one or more surges and a coarse-grained front, down steep mountain channels to a fan. Both solid and fluid forces strongly influence the motion, distinguishing debris flows from related phenomena such as rock avalanches and sediment-laden floods. A debris flow has a higher solid concentration than normal or hyperconcentrated streamflow on the one end, and higher water content than a landslide or rock avalanche

on the other end of the spectrum (Iverson, 1997; Crosta, 1998). The material involved in debris flows usually includes sediment from the clay size up to boulders, and organic components such as woody debris.

Debris flows, mobilized from numerous small landslides or from a large and individual landslide, are the most common type. They occur when a debris slide or landslide changes into a debris flow. The process of forming debris flows from a static mass of water-laden soil, sediment or rock is called mobilization. Mobilization occurs under three conditions, which are: the failure of the mass, a sufficient amount of water to saturate the mass and a sufficient conversion of the gravitational potential energy to the internal kinetic energy (Blanc 2008). The conversion of the energy changes the type of mass movement from a slide on a failure surface to a flow.

When the initial landslide mass rides on the torrent bed deposits, an undrained loading process may generate a high pore-water pressure within the torrent deposits and this helps incorporate those deposit into moving mass (Coe 2008). This phenomenon is called the liquefaction failure of the torrent deposits which results in the entrainment of the bed material. Thus the volume of the debris flow increases significantly. Theoretically, during initial infiltration during a rainstorm, the dissipation of negative pore-water pressure, or capillary soil suction, reduces the soil strength and could result in shallow landslides which may transform into debris flows. In such circumstances rapid increases in pore water pressures can trigger slope failure and mobilization of landslides.

Debris flow can also initiate from channel bed and bank erosion. A sufficient water discharge is required to start the process of erosion. Rapidly the flow erodes the bed and mixes a large solid volume with the water. It occurs from an irreversible chain of reactions which increases the solid concentration of the mixture (Blanc 2008). Debris flow forms under required conditions which are channel bed and bank erosion capacity, water discharge, slope. Debris flow can be also originated by different mechanisms: like earthquake (may destabilize slope and causes landslides which are a source of

material), natural dam may break and release sufficient material to form a debris flow, human activity (such as mining, may destabilize slopes) and “moraine” phenomena which may break up and deliver a large amount of water and rock (Blanc 2008).

Hydrological and geo-mechanical model parameters for Debris flow modelling

As the previous description of the debris flow phenomena shows, lots of parameters have to be considered to describe such a flow. These parameters can be divided in two categories: terrain properties and flow properties. The terrain properties are the slope and characteristics of the ground surface (mainly the erodibility of the channel bed). The other parameters, which characterize the flow, are the sediment concentration, the particle density, the amount of water, the flow velocity, parameters describing stresses and the initial and final volumes. A numerical model uses data as input parameters to give results as output parameters. The parameters described previously are both input and output parameters. The input parameters may be the following:

- the slope of the terrain is provided generally by a digital terrain model (DTM)
- the erodibility of the channel bed informs on the capacity of the bed to be eroded. The parameters representing the erodibility depend on the erosion law used in the model.
- a hydrograph gives the amount of water
- the initial conditions (initial volume and flow depth) are required to describe the initial state of the flow
- the density of the solid particles (varies from 2500 kg/m³ to 3000 kg/m³)
- the viscosity of the fluid (from 0.001 Pas to 0.1 Pas)

Table 1 The list of parameters which describing debris flow processes (Blanc 2008).

Parameters	Mathematical symbol	Type of parameter
Slope	Z (the elevation)	Input parameter
Erodibility	e_r (The erosion rate)	Calibration parameter
Amount of water (given by hydrograph)	Q_{inp}	Input parameter
Initial volume	Deduce from the initial height: h	Input parameter
Viscosity	μ, ν	Input parameter
Angle of friction of the mixture	$\tan \phi$	Calibration parameter
Volumetric solid fraction	c	Calibration parameter
Turbulence coefficient	ζ (Voellmy coefficient)	Calibration parameter
Flow velocity	\bar{v} Depth integrated velocity	Output parameter
Flow depth	h	Input parameter + Output parameter
Volume	Deduce from the flow depth	Output parameter
Position of the deposit	Deduce from the velocity	Output parameter

- the density of the fluid (from 1000 – 1200 kg/m³)
- the internal angle of friction (between 25° - 45°)
- the solid volume fraction (from 0.5 to 0.8) and the fluid volume fraction (between 0.2 and 0.5).

In case of a mudflow or debris flow with large amount of water, turbulence processes can occur. In this case we use a turbulence coefficient to describe this phenomenon. Generally the output parameters of a debris flow model are the velocity, the flow depth, the volume, and the position of the deposit. The Table 1 described the most important parameters to describe debris flow phenomena.

Hydro-Debris 2D numerical model and debris flow experimental physical model

In what follows a brief description of the Hydro-Debris 2D numerical model and the purpose of its use is given. The main aim of a Hydro-Debris 2D numerical model development is to estimate the particle tracing of 2,5 mm and 10mm particles. The current model development is based on an earlier model developed by Yamashiki et al. (2012a). The particle tracing movement can be analysed by using High speed video-camera (HSVC) images. A numerical model was developed using the Marker and Cell (MAC) Method, which involves a SGS (Subgrid-Scale) model and the PSI-Cell (Particle Source in Cell) Method (Gotoh 1992; Crowe et al. 1977; Yamashiki et al. 2012a). The transportation processes of the debris and air bubbles were simulated in Lagrangian form, by introducing air bubble and debris markers. The MAC grid method discretises the space into cubical cells with width h . Each cell has a pressure p , defined at its centre. It also has a velocity, $u=(u_x, u_y, u_z)$, but the components of the velocity are placed at the centres of three of the cell faces, u_x , on the x-min face, u_y , on the y-min face and u_z on the z-min face. The marker particles are moved through the velocity field and then used to determine which cells contain fluid. The computer code for Hydro-Debris 2D numerical model was written in C language, using the reference “103 Yo/VIFMAC” of the computer library of Kyoto University, created by Takemoto (Takemoto 1983) and developed by Sakai et al. (1987). The systems of governing equations are the grid-filtered time-dependent three-dimensional compressible (with low Mach number) mixed flow Navier-Stokes, liquid phase continuity equations. The effect of Lagrangian sediment particle onto the liquid phase is being considered using PSI-CELL method. The input parameters that describe the numerical model are based on the debris flow experimental physical model, as described below. Some of the most important input parameters that are taken in the numerical model are: kinematic viscosity coefficient of water with the value $\nu=1.307 \cdot 10^{-6}$ m²/s, dynamic viscosity coefficient of water $\mu=1.307 \cdot 10^{-3}$ Pas, friction coefficient $\mu'=0.3$, cohesion coefficient $c=0$ kPa, internal friction angle $\phi=22-35^\circ$ (depending on the material saturation).

Debris Flow Validation study

In order to understand the characteristics of the debris flow routing mechanism and its deposition behavior, it is necessary to validate model predictions by setting up well controlled debris flow experimental physical models. Physical modelling consists of representing phenomena at a small scale which need to be similar to the real scale phenomena. For debris-flows, this requires to use specific model fluids, whose appropriate composition remains an important and open scientific issue. The scale similarity criteria are generally based upon the Froude number and other dimensionless numbers, chosen according to the assessed rheology of the debris-flow material (Yamashiki et al. 2012b). Experimental setup of the debris flow physical model was carried out at the Ujigawa Open Laboratory, Kyoto University. The model has three main parts comprising rectangular flume, deposition board and the water intake tank (Fig. 1).

At the top of the physical model is the water intake tank, 1m long, 0.8m wide and 0.7m high (approximately 0.56 m³ of water). The debris flow rectangular flume has dimensions of 0.2 m in width, 0.2 m in depth and with 5 m effective flow length. The flume is supported with a moveable prop, which could be moved back and forth to adjust the flume slope ranging from 5° to 25°. Sand particles of 3mm were glued to the bottom of the flume, representing surface roughness, later included in the numerical model as the Manning coefficient. Rectangular flume has a transparent sidewall connecting the downstream end of the deposition board. This transparent sidewall proved very useful during observation and image capturing by a high speed video camera (HSVC). The third major part of the model is the debris flow deposition board, each side 2m long and divided into a grid. In the middle of the deposition board, the grid size was smaller than elsewhere because in this area the concentration of the deposited materials is higher. The board and flume were smoothly connected at one end and at on the other end the materials collection

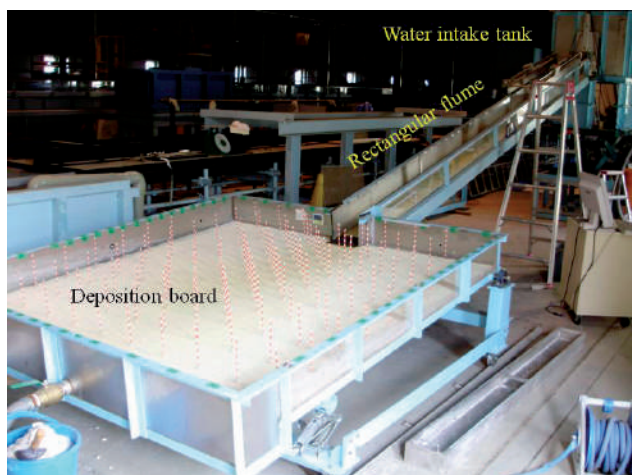


Figure 1 The main parts of the debris flow experimental physical model.

sump is located. The deposition board slope varied from 0° to 7°. As stated earlier, it was also covered by sands of 3 mm in diameter to simulate the roughness coefficient at the bottom of the deposition board (Yamashiki et al. 2012b), Figure 1.

Three cases of laboratory experiments were conducted with slope angles of 15°, 20° and 25°. For all experiments the water discharge was fixed. The debris was placed 3.5 m from the bottom of the rectangular flume (Fig. 2). The debris was a well prepared mixture of smaller and larger materials. For each case, at least three experiments were repeated to study the particle distribution and movements. After a flume and board were set to the prescribed slopes, a constant discharge (3.0 l/s) was supplied from the upstream end of the channel through an electromagnetic valve (gate). During the water supply, HSVC recorded images of particle tracking. The HSVC was positioned at two locations, one near the downstream and the other near the upstream of the rectangular flume. The HSVC captured a video footage during short time intervals time (0-9s). Video recording of the experiments were performed to analyze debris flow characteristics and capture the formation of the debris flow deposition process. The diagram of the experimental procedure is shown in Fig. 2, while the experimental conditions are summarized in Table 2.

Two different material particle sizes were used in the experimental physical model. Each material can be easily differentiated by observing their sizes. The materials mean sizes were 2.5 mm and 10mm respectively. Both particle sizes have the same unit weight are 2.7 g/cm³. For a single run the total weight of each material is 10kg. These materials were mixed well before being used for the experimental study. Material was placed at the top of the flume channel (Fig. 1). The distance of the free surface flow appeared 3.5 m from the deposition board. The part of the bed upstream from this point was unsaturated. The materials lay on the bottom of the channel, with a thickness of 10cm. The roughness

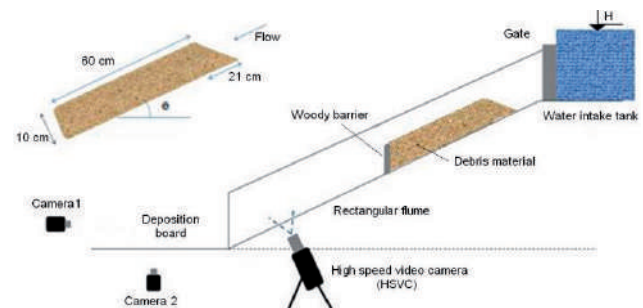


Figure 2 Schematic diagram of the debris flow experimental physical model.

Table 2 Experimental conditions.

Case	Bed length [cm]	Bed thickness [cm]	Water supply	
			Position	Discharge (l/s)
15°	81	10	Upstream end	3.0
20°	81	10	Upstream end	3.0
25°	81	10	Upstream end	3.0

layer on the bottom of the rectangular flume was 0.3 mm.

The experimental data collection can be separated into three parts: (a) sampling of the materials, (b) observation of the material depositions and (c) image capture from the HSVC and camcorder. The main goals of the deposition observation were to understand the particle characteristics, particle distribution and the physical data of the deposition materials. Observation of the deposition processes included (1) measuring a deposit shape and thickness distribution, (2) mapping surface structure, (3) deposition contour sketch and (4) reviewing video and still photographs of the stages of the debris deposition formation. These four processes were repeated several times to ensure more reliable and accurate results.

The objective of the sampling processes was to obtain the percentage of materials at a given grid node, at a different height. This process involved four steps

(Fig. 3). First step included materials collection at a certain grid node that been identified. After that, materials at a given height had been packed and marked.

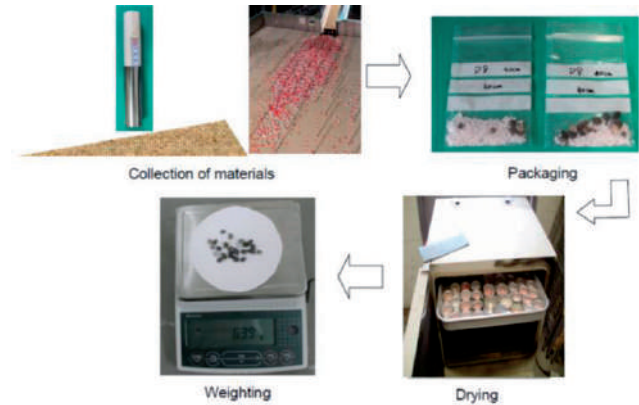


Figure 3 Steps taken during sampling.

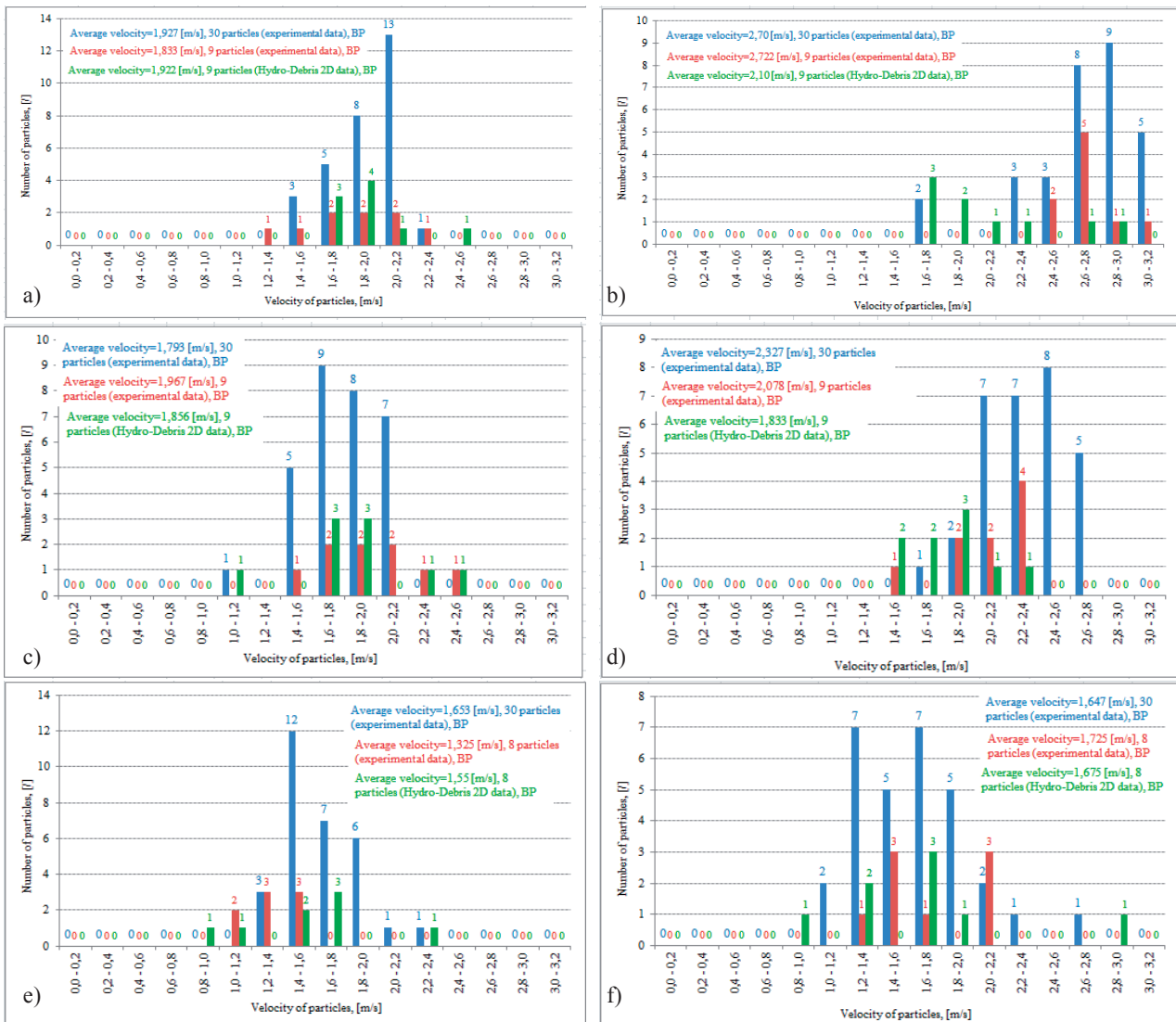


Figure 4 Comparison of experimental and numerical particles velocity frequency distribution at different cases near the downstream part for larger particle (BP), a) channel slope 25° - initial case, b) channel slope 25° - intermediate 2s case, c) channel slope 20° - initial case, d) channel slope 20° - intermediate 2s case, e) channel slope 15° - initial case, f) channel slope 15° - intermediate 2s case.

Each pack was then dried at 105°C for 24 hours (Yamashiki et al. 2012b). Reason for doing this is to make sure that the materials were fully dried to get consistent results. The last step was by to weigh each sample (Fig 3).

Output data analysis

Displacements of the large (BP) and small particles (SP) in a given real-time (at the beginning of the simulation - initial case, after 2s - intermediate 2s case and after 4s - last 4s case) were determined based on the high speed video camera (video recordings). The actual velocity of the particle is determined by dividing the total distance travelled and the time required for that particle to pass from one position to another (Fig. 4, 5).

The average values of velocity for all particles were obtained by averaging the velocity arbitrarily taken for 30 particles and the determination of their actual velocity, especially for the large and small particles (for different slopes of rectangular flume on the experimental physical model).

The average velocity values of large (BP) and small (SP) particles obtained by Hydro-Debris 2D numerical model were compared with the average velocity values of the set of arbitrarily chosen 30 particles (Case 1, experimental model) and another set of arbitrarily chosen 9 particles (Case 2, experimental model). Graphical comparisons of these average velocities are given in Figs 4 and 5. For a rectangular flume slope angle of 25° it can be

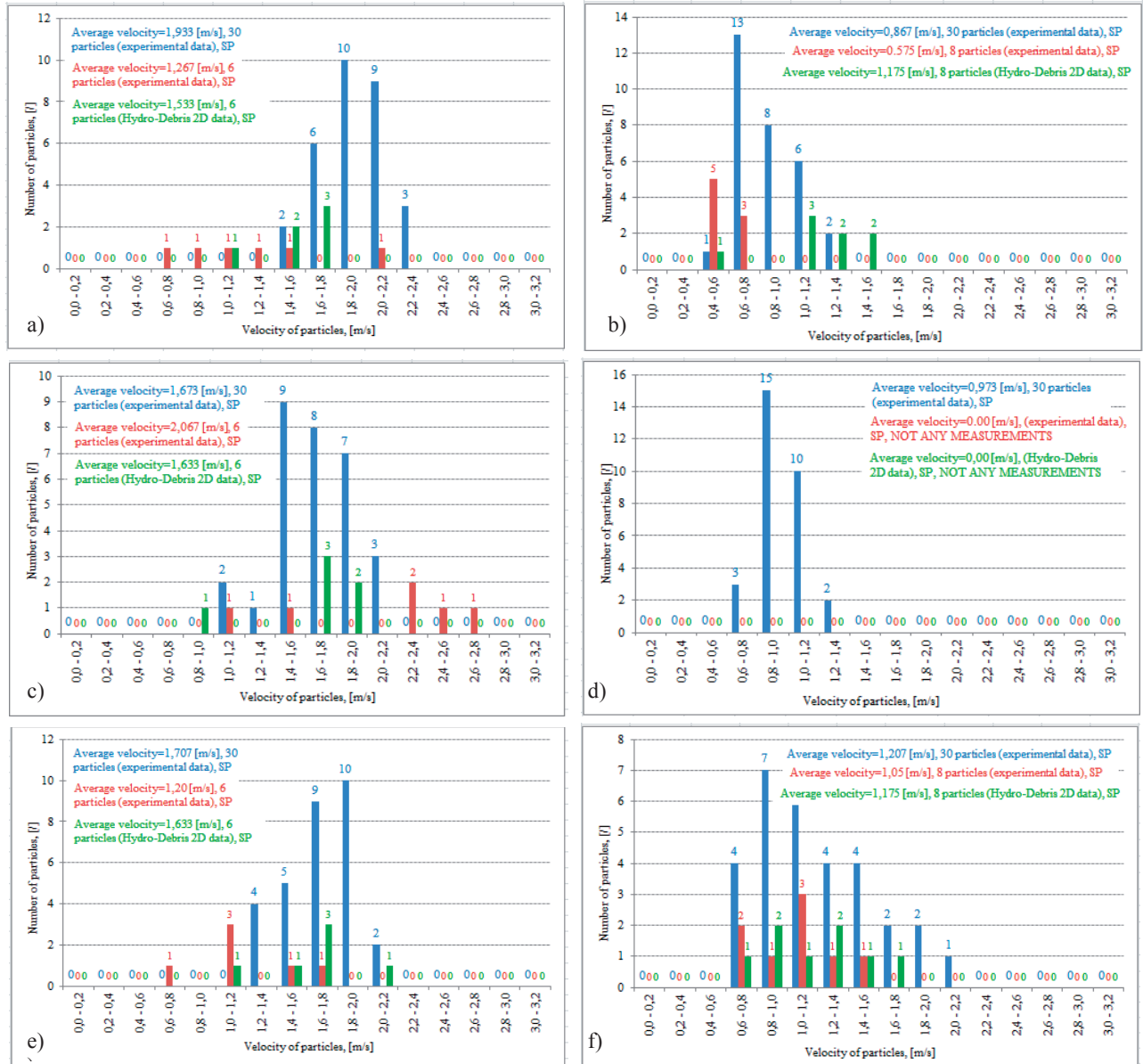


Figure 5 Comparison of experimental and numerical particles velocity frequency distribution at different cases near the downstream part for small particle (SP), a) channel slope 25° - initial case, b) channel slope 25° - last 4s case, c) channel slope 20° - initial case, d) channel slope 20° - last 4s case, e) channel slope 15° - initial case, f) channel slope 15° - last 4s case.

seen that the average velocities of large particles on the experimental physical model (1.927 m/s) and numerical model (1.922 m/s) almost coincide, the difference is only 0.005 m/s. Very good match of average velocities for the large particles were obtained for the other cases of the channel slope of 20° and 15°. In Fig. 4 it can be seen that the average velocity of large particles at the beginning of debris flow propagation are less than the average velocity of large particles in the intermediate stage of the flow (after 2 s), which is valid for all three cases of observed slope for a rectangular flume. This can be interpreted as the fact that the velocity at the head of debris flow is more pronounced in relation to the body and tail of debris flow. With a decrease of the slope of the rectangular flume, the average velocities of large and small particles were reduced (Fig. 4). If one compares the average velocities of fine (small) particles it can be concluded that the deviations were slightly more pronounced than the average velocities of large particles. The largest discrepancies between average velocity values of small particles was observed in a rectangular flume with angle slope of 25° and has value of 0.4m/s in the case of initial state of debris flow propagation. At smaller angles (with 20° and 15°) deviations are negligibly small. The deviations of the average velocity for fine particles on the end of debris flow propagation (after 4 s) between the experimental and numerical model are very significant. With the rectangular flume slope of 25° the average velocity value of 0.867 m/s was obtained (on the experimental model, Case 1), while the value on the HD2DM is almost 1.175 m/s (Fig. 5b). Large particles move upwards and are faster than small particles. The bigger particle movements were concentrated at the upper (high velocity) part of the fluid, while small particles were concentrated near the bottom (low velocity).

Conclusion

Debris flows are complex phenomena. During the event, the flow properties vary and therefore it is really difficult to model such flow. The more numerous are the input parameters used, the more difficult will be the calibration of the model.

Numerical simulations and experimental works were carried out to determine the characteristics of particle routing of debris flow with two different particle sizes. A two dimensional numerical model was developed for computing the characteristics of the particle routing of debris flow, in order to simulate the classification effects by applying the particle tracking method which is the most suitable for qualitative simulation of the two-phase flow. The correct validation study was limited to debris flows composing of two size particles mixture - large and small particles. The numerical simulation frequency distribution results of the velocity shows fairly good agreement with the experimental results. The

particles routing movement of simulated results also shows a good agreement with the experimental results. From the study it can be concluded that the larger particle movements (high average velocity) were concentrated at the upper part of the fluid, while small particles (low average velocity) were concentrated near the bottom. Moreover, the largest particles accumulated at the front part of the debris flow propagation. The surface of debris flow velocity is larger than the average velocity; it means that the debris flow is characterized by its fast velocity near the surface but slow in the bottom.

Acknowledgments

Research for this paper was conducted within the bilateral international Croatian-Japanese project “Risk identification and Land-Use Planning for Disaster Mitigation of Landslides and Floods in Croatia”, as well as a part of the scientific project “Hydrology of sensitive water resources in karst” (114-0982709-2549) financed by Ministry of Science, Education and Sports of the Republic of Croatia. This research was carried out with financial support from the Japan International Cooperation Agency (JICA).

References

- Blanc T (2008) Numerical simulation of debris flows with the 2D-SPH depth integrated model. Doctoral dissertation, Escuela Superior de Ingeniera Informatica (ESII), Universidad Rey Juan Carlos, Madrid, Spain, 115 p.
- Coe J A (2008) Introduction to the special issue on debris flows initiated by runoff, erosion, and sediment entrainment in western North America. *Geomorphology*. 96: 247–249.
- Crosta G (1998) Regionalization of rainfall thresholds: An aid to landslide hazard evaluation. *Env Geology*. 35(2/3): 131-145.
- Crowe C T, Sharma M P, Stock D E (1977) The particle source in cell (PSI-CELL) model for gas droplet flows. *J Fluid Eng*. 99(2): 325–332.
- Gotoh H (1992) Study of sediment particle dynamics and its application for movable bed. PhD Thesis, Kyoto University, Kyoto, Japan.
- Iverson R M (1997) The physics of debris flows. *Review of Geophysics*. 35(3): 245-296.
- Sakai T, Mizutani T, Tanaka H, Tada Y (1987) Numerical simulation of breaking wave on slope, In: *Bulletin of 34 Coastal Engineering Symposium*, JSCE (Japan Society of Civil Engineers), Japan. 71–75.
- Takemoto Y (1983) A computer code for time-dependent, viscous, incompressible fluid flows using the third-order upwind finite-difference scheme called “QUICK 132 y0/QMAC2D”. *J Super Computer*. 17(6).
- Yamashiki Y, Mohd Remy Rozainy M A Z, Matsumoto T, Takahashi T, Takara K (2012a) Simulation and Calibration of Hydro-Debris 2D Model (HD2DM) to Predict the Particle Segregation Processes in Debris Flow. *Journal of Civil Engineering and Architecture*. 6(6) (Serial No. 55): 690–698.
- Yamashiki Y, Mohd Remy Rozainy M A Z, Matsumoto T, Takahashi T, Takara K (2012b) Experimental study of debris particles movement characteristics at low and high slope. *J Global Environment Engineering*. 17: 9-18.

Mošćenička Draga Early Warning Systems Development Using Machine Learning

Igor Ružić, Nevenka Ožanić, Čedomir Benac

University of Rijeka, Faculty of Civil Engineering, Rijeka, Croatia, Radmile Matejčić 3, igor.ruzic@gradri.hr

Abstract The paper presents a machine learning model for predicting Mošćenička Draga torrential stream water levels and discharges based on meteorological and hydrological data. Possible use of machine learning algorithms for early warning system development is presented as well. One of the most important goals of Croatian – Japanese Project Risk Identification and Land-Use Planning for Disaster Mitigation of Landslides and Floods is development of the Early Warning Systems (EWS). The most important task of the EWS in Mošćenička Draga is identification of the critical torrential discharges and precipitations that can cause floods, early enough to inform the authorities and public. The paper describes an artificial intelligence model that has been developed by integrating meteorological and hydrological data. The WEKA Data Mining Software was used for a model development. Model has been validated on measured hydrological and meteorological data from May 2011 till December 2012. Water levels predicted by the model are in accordance with the measured data. Model validation showed that the machine learning algorithms can be used in the EWS development.

Keywords early warning system, machine learning, flood, Mošćenička Draga

Introduction

Main aim of this paper is to examine use of Machine learning algorithms (ML) for small torrential catchments discharges prediction due to develop Early Warning System (EWS).

Mošćenička Draga catchment is very small (~11 km²) and very steep (~50%) catchment in comparison to catchments where EWS has been developed and machine learning algorithms were used for hydrological predictions. Hydrological prediction systems are usually designed for hydrological simulations based one 1 km spatial resolution and 3 hour time resolution (Alfieri et al. 2011).

Early warning (EW) is “the provision of timely and effective information, through identified institutions, that allows individuals exposed to hazard to take action to avoid or reduce their risk and prepare for effective response” (UN ISDR 2006).

Meteorological forecasts have been recently significantly improved, mostly due to more precise model calibration based on a recorded discharge and rain time series (Fundel et al. 2010, Hamill et al. 2006). But stream flow predictions don't use weather forecast results, especially for the flash and torrential floods prediction (Alfieri et al. 2012).

Floods, earthquakes, landslides, volcanic eruptions, and other natural disasters are happening quite frequently. Frequency of natural disasters is increasing due to climate changes. Authorities all around the world are investing into development of Early Warning Systems for environmental applications. Major task of the EWS is to recognize early enough dangerous situation that can jeopardize human lives, properties and environment and to inform the authorities and general public. Research into flood warnings demonstrates the importance of discovering user requirements before designing and launching flood warnings (Parker 2004).

Data Mining Software WEKA 3 (Hall et al. 2009) was used to develop a water level simulation model. Weka is a collection of machine learning algorithms for data mining tasks. It contains tools for data pre-processing, classification, regression, clustering, association rules, and visualization.

Study area and data

Mošćenička Draga torrential catchment is 6 km long and 2 km wide. Catchment area is 11 km², torrential mouth is at a sea level (0 meters above sea) and catchment highest part is at about 1300 meters above sea. It is a very steep catchment with mean slope 47%. Catchment digital elevation model is shown on a Figure 1. Because of catchment characteristics time of concentration is quite short (less than half hour), and maximal discharges are usually reached soon after start of intensive precipitations.

Mošćenička Draga artificial intelligence model development and validation was based on a measured hydrological (water level) and meteorological data from May 2011 until December 2012. Meteorological station (Davis Vantage Pro) is located near torrential mouth (Fig 1, red circle). Meteorological attributes were used: rainfall, air temperature, atmospheric pressure, solar

radiation and evapotranspiration based on Penman formula. Water levels have been measured in a small

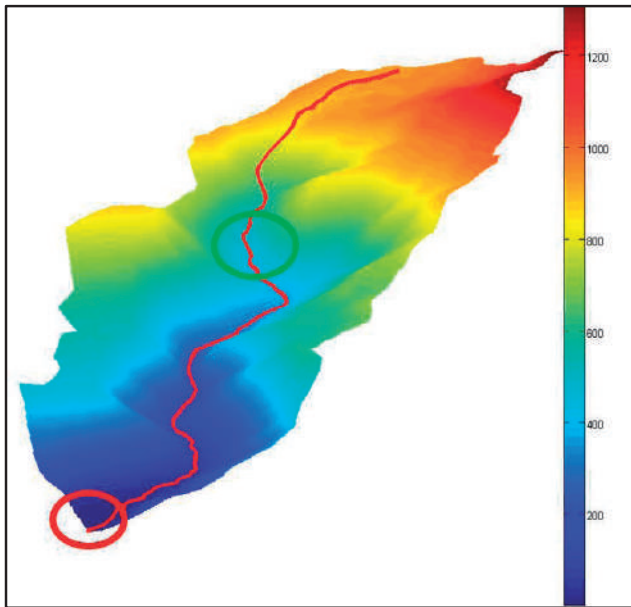


Figure 1 Mošćenička Draga torrential catchment digital elevation model. Color-bar presents meters above sea level.

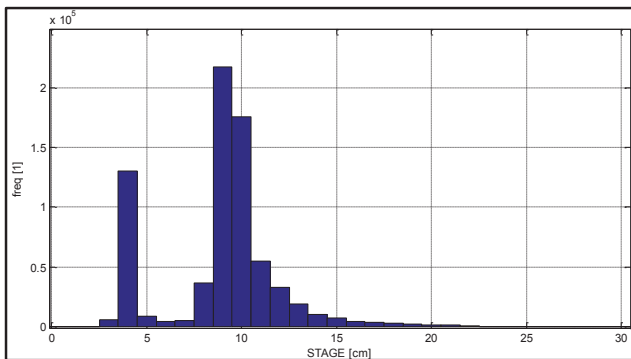


Figure 2 Measured minute water levels frequency distribution Trebišće, May 2011 - December 2012.

village Trebišće (Fig. 1, green circle) near the catchment center.

Data from the downstream hydrological stations were not used because they had frequent recording interruptions. Water level measurement frequency is one minute; models were developed using hourly water levels.

Hydrological analyses and model development were based on water levels, not on discharges because of insufficient number of discharge measurements. Figure 2 shows a measured water levels frequency distribution.

The most frequently recorded water levels were between 8 and 12 cm. Water levels greater than 17 cm are important for flood EWS development, but they were rarely recorded.

Simulated hour water levels are based on previously measured hourly water levels and meteorological data. First AI model used meteorological and previously measured data. Second hourly simulations were based only on meteorological data.

Results

Hourly water level simulations were performed only for recorded water levels greater than 17 cm because of recorded data noise reduction. Majority of the recorded water levels are lower than 17 cm, they are not important for EWS development and can reduce the quality of the AI model results.

Hourly water level predictions based on previous water levels and meteorological data

Artificial intelligence (AI) model used water levels greater than 17 cm, recorded an hour before the predicted water levels and their corresponding meteorological attributes. Water level recorded an hour before the predicted water level may be incorporated in EWS using telemetry data transmission. Hourly water level (WIHr) prediction model delivered by WEKA AI algorithm is simple, hour water levels (WIHr) are a function of recorded water level

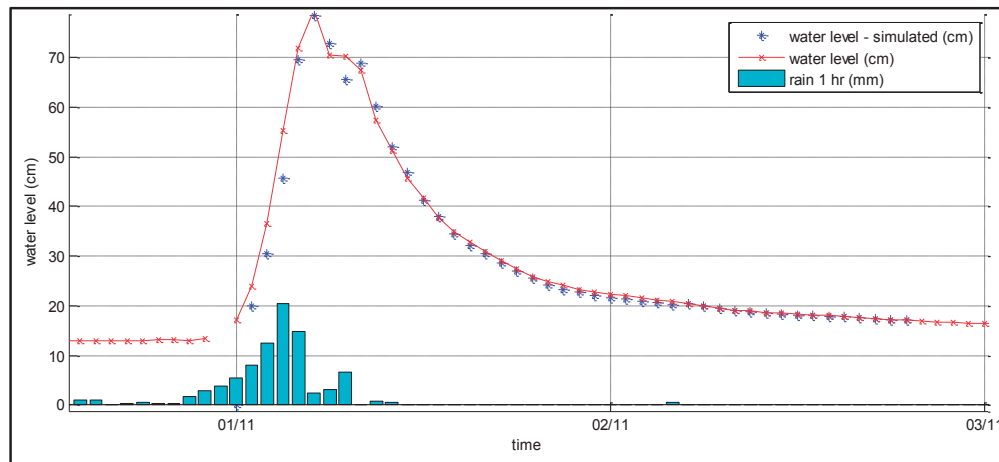


Figure 3 Measured (red) and simulated hourly water levels (blue) based on measured water levels and meteorological perimeters, Trebišće, 1/11/2012.

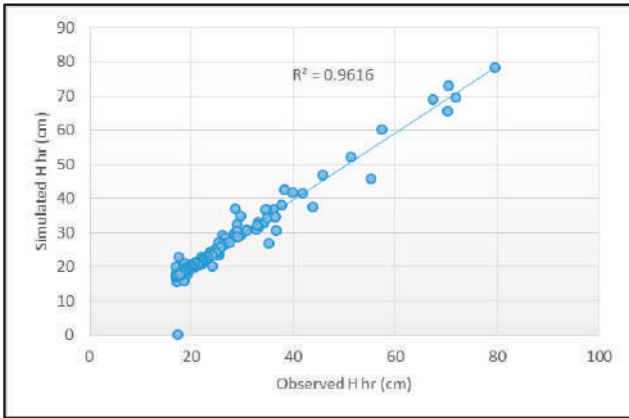


Figure 4 Correlation between measured and simulated hourly water levels, Trebišće, May - December 2012

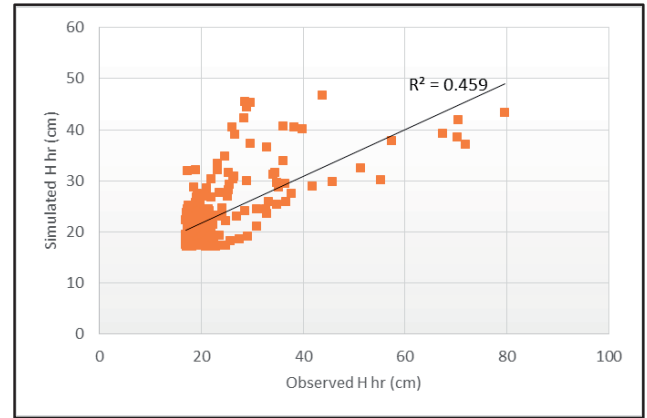


Figure 6 Correlation between measured and simulated hourly water levels, Trebišće, May - December 2012.

before one hour (WlHr_-1hr) and hourly precipitation before one hour (Phr_-1hr) WEKA M5 pruned model tree:

- If water level before one hour (WlHr_-1hr) are smaller than 23.8 equation is:

$$WlHr = 0.537 * Phr_{-1hr} + 0.81 + 3.132 * WlHr_{-1hr}$$

- If water level before one hour (WlHr_-1hr) are greater than 23.8 equation is:

$$WlHr = 0.978 * Phr_{-1hr} + 0.859 + 2.036 * WlHr_{-1hr}$$

Figure 3 shows the observed (red) and simulated water levels (greater than 17 cm - blue) at measuring station Trebišće during 1 November 2012 when were recorded highest water levels.

Correlation between measured and simulated water levels is very good with a correlation coefficient $R_2 = 0.96$ (Fig. 4).

Figures 3 and 4 suggest a good match between measured and simulated water levels if water levels were simulated using precipitation and water level an hour earlier. The model results are very good, especially due to limited number of input data.

Hourly water level predictions based meteorological data

Simulation of hourly water level in WEKA using only meteorological attributes related to water levels greater than 17 cm. A computer program WEKA used M5P decision tree model and as an output set one equation that simulates hourly water levels (WlHr). Hour water level (WlHr) depends on hourly precipitation recorded before two hours (Phr_-2hr) and cumulative rainfall last six (Pcum_6hr) and twelve hours (Pcum_12hr).

WEKA M5 pruned model tree equation:

$$WlHr = 0.27 * Phr_{-2hr} + 0.18 * Pcum_{6hr} + 0.13 * Pcum_{12hr} + 17.14$$

Figure 5 shows the observed and simulated data series at measuring station Trebišće.

Correlation between measured and simulated water levels is quite poor with a correlation coefficient $R_2 = 0.46$ (Fig. 6).

A series of measured and simulated data varies significantly during higher water levels. A predicted water level has similar shape as a recorded one, but significantly lower values.

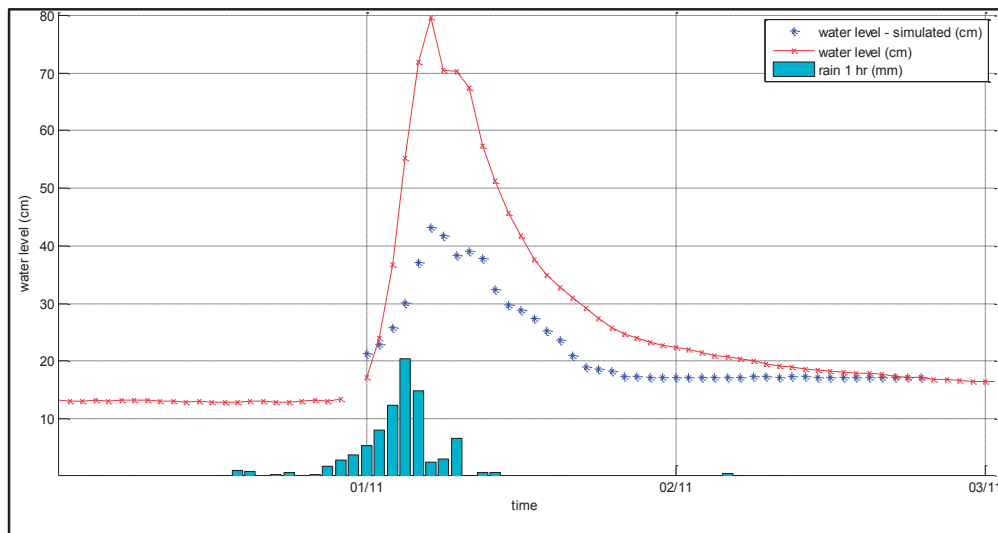


Figure 5 Measured (red) and simulated hourly water levels (blue) based on meteorological perimeters, Trebišće, 1 November 2012.

Conclusion

This paper examines the possibility of using a computer machine learning algorithm WEKA to predict Mošćenička Draga torrential stream water levels, using meteorological and water levels records. The aim of this paper is to examine the possibility of using machine learning algorithms for the development of torrential floods early warning system.

Limitation in this study was a small number of recorded height water levels because of the relatively short measurement time (18 months) and extremely dry period during that time. In this paper were used only one meteorological station data. That can be the cause of the model inaccuracy because of rainfall spatial distributions variability in the catchment.

Results of this study showed that the WEKA artificial intelligence algorithms can predict torrential streams water levels. Further model development may give much better results after processing longer data time series and incorporating more rainfall measurement points in the basin.

Despite the limitations in the input data this study showed that the use of artificial intelligence might be useful for early warning systems development for small torrential catchment.

Simulated hour water levels are well matched with the measured if it was used earlier recorded water levels. If model was developed using only precipitation data simulated runoff hydrograph has a similar shape as a recorded one, but significantly underestimates the observed values.

References

- Alfieri L, Thielen J, Pappenberger F (2012) Ensemble hydro-meteorological simulation for flash flood early detection in southern Switzerland. *Journal of Hydrology*, 424-425: 143–153.
- Alfieri L, Velasco D, Thielen J (2011) Flash flood detection through a multi-stage probabilistic warning system for heavy precipitation events. *Adv. Geosci.* 29: 69–75.
- Fundel F, Walser A, Liniger M, Appenzeller C (2010) Calibrated precipitation forecasts for a limited-area ensemble forecast system using reforecasts. *Mon. Weather Rev.* 138: 176–189.
- Hall M, Frank E, Holmes G, Pfahringer B, Reutemann P, Witten I H (2009) The WEKA Data Mining Software: An Update; *SIGKDD Explorations*, 11(1): 10-18.
- Hamill T, Whitaker J, Mullen S (2006). Reforecasts: an important dataset for improving weather predictions. *B. Am. Meteorol. Soc.* 87(1): 33–46.
- Parker D J (2004) Designing flood forecasting, warning and response systems from a societal perspective, *Meteorologische Zeitschrift*, 13(1): 5-11.

Involving the Public in Flash Flood and Erosion Mitigation

Nevena Dragičević, Barbara Karleuša, Nevenka Ožanić

University of Rijeka, Faculty of Civil Engineering, Rijeka, Croatia, Radmile Matejčić 3, +385 51 265 900

Abstract In this paper, an overview of the research conducted as a part of bilateral Croatian-Japanese project “Risk Identification and Land – Use Planning for Disaster Mitigation of Landslides and Floods in Croatia”, at the Faculty of Civil Engineering, University of Rijeka, about awareness and involvement of local population in the protection of flash flood and erosion in research areas, is given. The study was conducted through the local population and government survey using prepared questionnaires on two research areas: Salt Creek and Mošćenička Draga, and its implementation is planned as well at the research area Grohovo-Rječina. Familiarity of local population regarding above mentioned problems is analyzed, as well as risk awareness and the need for more education of population in this area. The conducted research presents the base for defining the significance of the social factor, as one of the elements that contributes to the consequences of flash flood and erosion, and whose concept and criteria approach will be presented in this paper. Awareness about the problem of local flash flood, as well as knowledge on prevention measures, flood and erosion mitigation, cooperation with local authorities and proper and well timed reaction of local population at the time of the disaster, all together form the social factor, and will be analyzed in this paper.

Keywords social factor, flash flood, torrent, erosion, mitigation, measures

Introduction

Flood is one of the most threatening natural hazards for human societies and can be defined as a temporary covering of land by water outside its normal boundaries (Schanze 2006). Although, a natural phenomenon in most cases, it can often be influenced by man through, for example inappropriate land use, illegal construction, artificial change of natural conditions in the catchment area etc. Damage caused by flood depends on the vulnerability of exposed elements (Schanze 2006), where vulnerability can be defined as the extent of harm, which can be expected under certain conditions of exposure, susceptibility and resilience (Equation 1) [<http://unescoihefvi.free.fr/vulnerability.php>].

Vulnerability = f (exposure, susceptibility, resilience) [1]

There are five different dimensions of vulnerability that need to be taken into consideration in the process of vulnerability assessment: social, physical, economic, institutional and environmental (Vojinović and Abbott 2012). Inability of people, organizations and societies to withstand adverse impacts from flood hazards to which they are exposed, all together describe the social vulnerability. These impacts are closely related to human characteristics (age, gender, income, education, employment, residence type, house and health insurance, etc.) and represent characteristic of a society, but can only provide a partial picture of society's well-being (Vojinović and Abbott 2012).

What makes flash flood significant and important from the aspect of flood management is the fact that they are short-term events that occur within 2 to 6 hours after the beginning of intensive precipitation and are characterized by a sudden increase of water level, flow and velocity which often end with significant material and environmental damage (Colombo et al. 2002).

Even today, with all the worlds' technological achievements, social vulnerability is still the most difficult to assess and measure from a scientific point of view, and requires detailed and extensive investigation (Vojinović et al. 2012). Till today, lot of research has been devoted to natural hazards where triggering factors are water, earth or wind conditions, and not enough emphasis has been given to the social influence on hazard and its effect on people and communities.

Protection measures from flash flood and erosion

Despite rapid technological development, the vulnerability of society to flash flood and their consequences is still great. Better understanding of the interrelations and social dynamics of flood risk perception, preparedness, vulnerability, flood damage and flood management are needed for comprehensive flood damage research, analysis and flood risk management. Till now, only a small scientific community has recognized the relationship between flood damage, its vulnerability and flood risk perception (Messner and Meyer 2006). Nevertheless, successful flood management depends on a systematic and long-term integration of structural and non-structural measures.

Unfortunately, flood risk management is in most

cases widely acknowledged within the short period of time after registered flood disaster in some area, but after some time memories and consequences of a flood disaster tend to fade away. Then, the biggest problem becomes to maintain the political and local population support for flood risk management (Hutter 2006).

Today, non-structural measures are more favored as basic measures, whose purpose is primarily mitigation, and not necessarily prevention of flash floods and erosion. These measures are sustainable; require much less capital investments and their impact on the environment is negligible.

Information and public participation is one of non-structural measures of great significance in protection against erosion and flash flood. It is based on long-term planning and well-timed notification of local population on protection measures against flash flood and erosion (Dragičević et al. 2012).

Public role in flash flood mitigation and prevention

It is known that some human characteristic and characteristic of certain community can contribute to the increase of the risk to life and property damage of those affected by flooding. For example, the presence of elderly or ill people, particular types of property, no previous experience or awareness about flooding, poor community support, the need to evacuate and live in temporary accommodation and etc. (Messner et al. 2006). Because of that, the local government has the task to include planners and decision makers at all levels, as well as the general public, in planned procedures and measures which are aimed to protect people and material assets and to reduce the damage caused by the flood. This contributes to (Messner et al. 2006):

- Easier public acceptance of necessary protection measures,
- Better response of local population at the time of the imminent danger from flash flood and erosion,
- Potential mitigation of human, material and environmental damage at the time of the disaster.

The way people perceive relationship between impacts of a flood and their role in it, for example responsibility to themselves, to others, to nature and material assets, before, during and after flood event, can strongly affect and influence on their personal abilities and efforts in future flood and erosion mitigation strategy. Such example can be found within land use practices that have direct impact on the area's hydrology, so if people are aware of them they are more likely to undertake direct action to prevent or at least mitigate such impacts (Schad et al. 2012).

Local population risk awareness and information exchange about flash flood and erosion on research areas Mošćenička Draga and Slani Potok

The research about involvement and risk awareness of local population about flash floods and erosion was conducted within the international bilateral Croatian-Japanese project "Risk Identification and Land-Use Planning for Disaster Mitigation of Landslides and Floods in Croatia" on two research areas Mošćenička Draga and Slani Potok.

The research area Mošćenička Draga is situated southwest of the city of Rijeka and encompasses the coastal and catchment area of a torrent, passing through the center of the Town Mošćenička Draga. This area is known for frequent floods caused by intensive precipitation as a result of storms (Dragičević et al. 2012, Ružić et al. 2012).

The sub catchment Slani Potok is situated on the northern slope of the Vinodol Valley within Dubračina River catchment area. Information's about problems with erosion in this area date from the late 19th century (Ožanić et al. 2012).

During the past, flash flood and erosion prevention and mitigation measures were conducted several times. They included river regulation, construction and maintenance of structures for prevention and mitigation of erosion and flash flood, as well as reforestation of the catchment area. All of that with not much success in preventing the expansion of erosion affected areas. This area deals with danger from flash flood in combination with erosion sediment transportation by water that could endanger downstream areas, especially the Town of Crikvenica (Bonacci et al. 1999, Dragičević et al. 2012, Ožanić et al. 2012).

The main objective of the research was to define the local population risk awareness about flash floods and erosion that presents a problem at both areas, as well as their interest to be involved in the decision making process aimed at flood and erosion mitigation and prevention strategy.

Public and social criteria needs to be included in the decision-making process for flood management in order to broaden this process beyond the consideration of purely economic factors. Social values and norms are more and more focused on the concern for the environment and well-being of people and not only on economic growth. The success of flood management depends on these social values and norms (Simonović 1999, Karleuša and Beraković 2005).

The need for this kind of research also comes from the necessity to determine which population will be the most vulnerable to floods as well as to improve decision-making process and effectiveness of chosen measures and means of intervening to reduce the vulnerability on



Figure 1 Public presentation of Project aims and objectives to local population at Mošćenička Draga.



Figure 3 Public presentation of Project aims and objectives to local population at Slani Potok.

OPĆINA MOŠĆENIČKA DRAGA
 GRAĐEVINSKI FAKULTET SVEUČILIŠTA U RIJECI
 POZIVAJU VAS NA:
**PREZENTACIJU HRVATSKO-JAPANSKOG ZNANSTVENOG PROJEKTA:
 ISTRAŽIVAČKO PODRUČJE MOŠĆENIČKA DRAGA**

Hidrološka istraživanja bujice Mošćenička Draga
Istraživanja obalnih procesa na žalima Općine MD

Petak 11. Svibnja 2012.
 15.00: Obilazak sliva bujice Mošćenička Draga, Trebišće, Sv. Petar, Draga Centar... (polazak ispred Općine)
 18.00: Javna prezentacija projekta:
 Kongresna dvorana hotela Marina u Mošćenička Draga

Figure 2 Information about public presentation of Project aims and objectives to local population at Mošćenička Draga.

VINODOLSKA OPĆINA – SJEDIŠTE BRIBIR I
 GRAĐEVINSKI FAKULTET SVEUČILIŠTA U RIJECI
 POZIVAJU VAS NA:
**PREZENTACIJU HRVATSKO-JAPANSKOG
 ZNANSTVENOG PROJEKTA:
 ISTRAŽNO PODRUČJE SLANI POTOK**

PROJEKT PREDSTAVLJAJU:
 -Prof. dr. sc. Nevenka Ožanić; dipl. ing. građ.
 -Načelnik Ivica Crnić
 -Yosuke Yamashiki, Dr. Eng.
 -Ivana Sušanji; dipl. ing. građ.

15.05.2012 U 18:00 sati
MJESNI DOM – GRIZANE

Croatia – Japan Project on
 Risk Identification and Land – Use Planning for Disaster
 Mitigation of Landslides and Floods in Croatia

Figure 4 Information about public presentation of Project aims and objectives to local population at Slani Potok.

floods (Guidelines for Socio-Economic Flood Damage Evaluation 2006). Because of that information and public participation is of great significance in protection against erosion and flash flood.

This research was conducted through surveys in May 2012 within public presentations of project aims and objectives in local community on research areas (Figs 1-4).

The survey consisted of 16 questions regarding flash flood and erosion risk awareness, ways of information exchange, knowledge about mitigation and protection measures from floods and erosion, etc. There were 28 participants at research area Mošćenička Draga and 39 at Slani Potok involved in the survey. The target research group was the local population that is not employed by government or some sort of media and are not in a

possibility to be directly at the source of information. So at the end, the number of local residents on which the analysis was made reached the figure of 11 at Moščenička Draga and 25 at Slani Potok.

Participants were asked to define the time period when they last received some information related to local problems of flash flood and erosion. 20% of participants at Slani Potok and only 9.1% of them at Moščenička Draga came upon this kind of information sometime within the last year. A surprising result was that more than 50% at research area Moščenička Draga and 36% at Slani Potok couldn't remember the last time they received information regarding local problems of flash flood and erosion. That itself, is undoubted evidence of lack of information exchange on this areas and within this communities. The local population that remembered the information was asked to name in which form were those information available to them (Fig. 5).

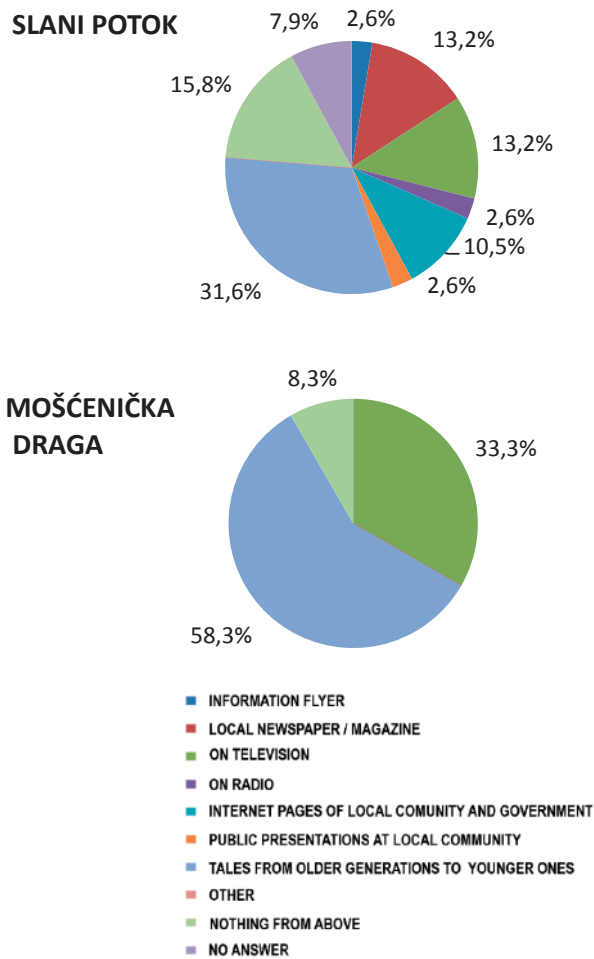


Figure 5 Statistical analysis of answers to the question “In which form were the information about local problems of flash flood and erosion available to local population?” (Dragičević et al. 2012).

Most used way for information exchange were stories and tales passed from older generations to younger ones, mainly within families. At research area Slani Potok all the information sources were present, most of them in same small percent, while at Moščenička Draga only television and stories from generation to generation.

Although, there is a lack of information exchange, the knowledge of local population regarding flash flood and erosion mitigation and prevention measures is pretty good. They were asked to try to recognize some of them and results at both areas showed that the most familiar measures are river regulation and removal of sediment from water bed. Beside these two, all given measures were recognized in some small percent.

The local population still doesn't think they are well informed about these measures and the ones needed to protect their villages and assets (Fig. 6). Approximately, 28% of questioned people at Slani Potok and 9,1% at Moščenička Draga considers they are at same level aware of these measures, but all the rest considers not enough or not at all.

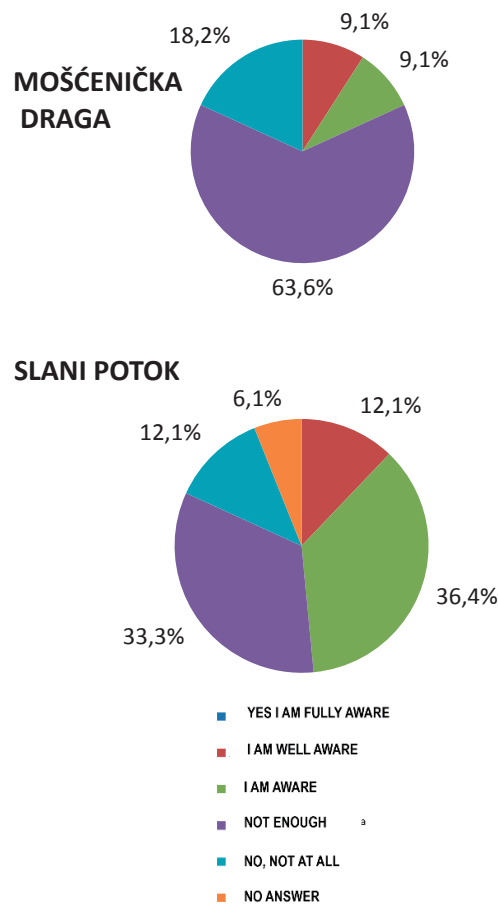


Figure 6 Statistical analysis of answers to the question “Are you as a local resident well informed and aware of risk from flash flood and erosion in this area?”.

One of the most important information that can provide the overall picture of the state of preparedness of local population for hazard events is their awareness on problems and potential hazard risk regarding flash flood and erosion in local area. The results regarding people awareness on research area Mošćenička Draga showed very low level of awareness about mentioned problems. Only 18% of investigated population were in some level aware of the problem, while the rest of participants wasn't. Opposite of that, at research area Slani Potok, little less than 50% of investigated population was aware of the problem in their area, but other 50% was not. The answer to that can be found within the earlier mentioned problem regarding information exchange within the community, local government and local population.

Taking into consideration the lack of awareness regarding earlier mentioned problems of flash flood and erosion, as well as poor or no information exchange regarding these issues, results about coverage of risk management from flash flood and erosion with legislation can hardly be taken as precise and accurate (Fig. 7). Because of that, results have shown that more than 70% of inhabitants at Mošćenička Draga and more than 30% at Slani Potok didn't know the answer to the question, which was expected. Small percent of 27,3% at Mošćenička Draga and 12% at Slani Potok considers the legislation mostly adequate. But this result, as mentioned earlier, should be taken with precaution.

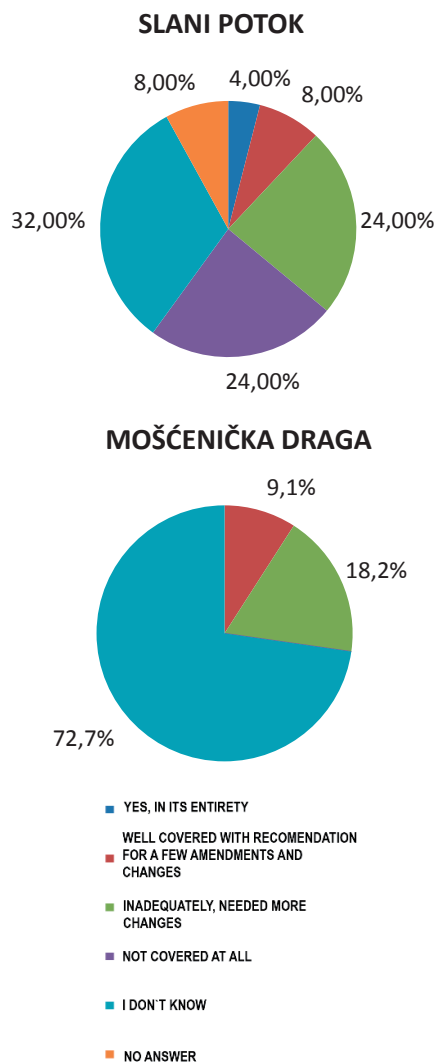


Figure 7 Statistical analysis of answers to the question “Do you consider the problem of risk management from flash flood and erosion is well covered by legislation?”.

Conclusion

There is no such thing as absolute protection from flood, and the only question that needs to be answered is which risk is considered acceptable and which not by the society. Because of that, there is the essential need for public involvement in decision-making processes as well as the need for raising the risk awareness through education, public presentations, local media, etc.

The lack of information exchange can certainly be found in the fact that flood events on that areas are not as often. But at the same time without proper information exchange and mitigation strategy no flood and erosion protection can be fully implemented. Also, the lack of awareness regarding local problems of flash flood and erosion is connected to the deficiency of regularity as well as variety of information exchange that should exist between local government and local population, and is absent in this case. That is why it should be a duty and task of professionals involved in the preparation of flash flood and erosion protection plans and strategies to involve also local communities and encourage information exchange between local government and local population about problems of flash flood and erosion in their areas.

Acknowledgments

The research for this paper was conducted within bilateral international Croatian-Japanese project “Risk identification and Land-Use Planning for Disaster Mitigation of Landslides and Floods in Croatia”, as well as a part of scientific project “Hydrology of Sensitive Water Resources in Karst” (114-0982709-2549) financed by Ministry of Science, Education and Sports of the Republic of Croatia.

References

Bonacci O, Kisić I, Ožanić N (2010) Risk Identification and Land-Use Planning for Disaster Mitigation of Landslides and Floods in Croatia. Croatian National Platform for Disaster Risk Reduction. National Protection and Rescue Directorate Zagreb. pp 72-77.

- Colombo A, Hervas J, Vetere Arellano A L (2002) Guidelines on Flash Flood Prevention and Mitigation, European Commission Joint Research Centre, Institute for the Protection and Security of the Citizen, Technological and Economic Risk management, Natural Risk Sector.
- Dragičević N, Karleuša B, Ožanić N (2012) Involving the Public in erosion and flash flood protection. Croatian Association of Civil Engineers, Cavtat, pp. 775-784.
- Hutter G (2006) Strategies for Flood Risk Management – a Process Perspective, Flood Risk Management: Hazards, Vulnerability and Mitigation Measures. 67: 229-246
- Karleuša B, Beraković B (2005) The Public Participation in the Water Resources Management on the Expert System Basis. Proceedings of IX International Symposium on Water Management and Hydraulic Engineering, Wien, Austria. BOKU - University of Natural Resources and Applied Life Sciences, Vienna, pp 35-42.
- Messner F, Meyer V (2006) Flood Damage, Vulnerability and Risk Perception – Challenges for Flood Damage Research, Flood Risk Management: Hazards, Vulnerability and Mitigation Measures. 67: 149-168.
- Messner F, Penning-Rowsell E, Green C (2006) Guidelines for Socio-Economic Flood Damage Evaluation, T9-06-01.
- Ožanić N, Sušanj I, Ružić I, Žic E, Dragičević N (2012) Monitoring and Analyses for the Working Group II (WG2) in Rijeka Area in Croatian- Japanese Project. Book of Proceedings of 2nd Project Workshop: Risk identification and Land-Use Planning for Disaster Mitigation of Landslides and Floods in Croatia – Monitoring and analyses for disaster mitigation of landslides, debris flow and floods. Rijeka, University of Rijeka.
- Schad I, Schmitter P, Saint-Macary C (2012) Why do people not learn from flood disasters? Evidence from Vietnam's northwestern mountains. Natural Hazards. 62 (2): 221-241.
- Schanze J (2006) Flood Risk Management – a Basic Framework, Flood Risk Management: Hazards, Vulnerability and Mitigation Measures. 67: 1-21
- Simonović S (1999) Social Criteria for Evaluation of flood Control Measures: Winnipeg Case Study, Urban Water 1 (2): 167-175.
- Vojinović Z, Abbott M (2012) Flood Risk and Social Justice – From Quantitative to Qualitative Flood Risk Assessment and Mitigation, IWA Publishing, London.

Citizens' Awareness and Preparedness for Disasters in Zagreb, Croatia

Naoko Kimura⁽¹⁾, Yosuke Yamashiki⁽¹⁾, Ivica Kisić⁽²⁾

1) Kyoto University, Disaster Prevention Research Institute, Kyoto, Japan, Gokasho

2) University of Zagreb, Faculty of Agriculture, Zagreb, Croatia

Abstract This research aims to make a proposal to raise citizens' awareness towards emergency cases, especially floods, through analysis of results from a social survey in Zagreb (Croatia). It also seeks a possible way to build a bridge between past experience and today's life regarding awareness-raising and preparedness in the context of Croatian society. This paper focuses on the status of awareness among youth towards disaster risks, especially floods, in Zagreb through social surveys and analyzes the results in order to propose a tool for raising awareness and preparedness for disaster risks. It also tries to seek applicability of Japanese experiences in disaster risk reduction as well as if computational tool, as way forward, can be effective as educational tool for awareness-raising. It concludes with a proposal of tool development to form a holistic approach regarding education for disaster risk reduction, hopefully taking outcomes of the ongoing bilateral project – the Japanese-Croatian Project – into account.

Keywords disaster risks, flood, awareness, preparedness, youth and children, Zagreb

Background

Protection of people's lives and property from natural disasters is a critical issue. Millennium Development Goals (MDGs) states, "(We must) intensify cooperation to reduce the number and effects of natural and man-made disasters" (UN 2000). International Strategy for Disaster Reduction (ISDR) asserts, "(We should) Ensure that disaster risk reduction is a national and a local priority with a strong institutional basis for implementation"¹, "use knowledge, innovation and education to build a culture of safety and resilience at all levels"², and "strengthen disaster preparedness for effective response at all levels"³ as part of priorities for action. Education for Disaster Risk Reduction (DRR) has more actively been discussed in recent years. Children in international and local societies

alike are important stakeholders who play a vital role in DRR and ISDR prioritizes the inclusion of DRR in all school curricula by 2015 as well as development and implementation of firm action plans for safer schools and hospitals (ISDR 2009).

The City of Zagreb (Croatia) is located between Medvednica Mountain and the Sava River, a tributary of the Danube River. In 1964, due to the characteristic of its location, a large amount of water was flowed into the city both from the breakage of the river bank and the mountain streams when the city had heavy rain. The central part of Zagreb city was flooded and the deepest was about 1m. The city had to be suffered from extensive damages on many of its infrastructures and 17 casualties (ISRBC 2009, Maršić 1998). Having received this bitter experience, the municipality built a modern bank flood protection system along the Sava River, a drainage canal (Sava-Odra Canal), and the retention dams along some of the mountain streams (Trninić 2001). Thanks to them, the city has had no major flood disaster, at the same time, the memory of such disasters have faded away among its citizens. Today the major concerned disaster for Zagreb is earthquake and it seems that the flood has been seem as one of concatenated disaster by the municipality government and their research groups.

Previous studies

The status of education for awareness-raising among young generations toward disaster risks is described in Brief Country Profile "Croatia", the Report "Children and Disasters – building resilience through education" (UNICEF and UNISDR 2011). It remarks some certain practices for raising awareness among young generation toward disaster risks in Croatia. For example, the national government and National Protection and Rescue Directorate (NPRD), the governmental body related to civil protection issues, are now reviewing the official school curricula and trying to include educational items for disaster reduction risk in order to raise awareness among young generation. However, the problem is teachers' capacity, that is, they neither have knowledge nor skills on those topics. The Report states "Knowledge of hazards and risks is included in the school curricula, although not yet at a sufficient level", "NPRD has

¹ Hyogo Framework for Action 2005-2015, Chapter III, Priorities for Action B.1.

² Hyogo Framework for Action 2005-2015, Chapter III, Priorities for Action B.3.

³ Hyogo Framework for Action 2005-2015, Chapter III, Priorities for Action B.5.

partnered the Ministry of Science, Education and Sport to mainstream disaster risk reduction into school curricula”, “The Meteorological and Hydrological Service of Croatia is also providing education and public outreach programmes targeted at increasing awareness of hydro-meteorological hazards”, and “Croatia intensively uses simulation exercises to validate preparedness activities and disaster response operations”.

There have been some activities and practices taken place in Croatia. How is the status of awareness and preparedness among young generations toward disaster risk now? Have the city’s historical disaster experience been used for the purpose of awareness-raising, if so how? This research conducted social survey to find the current status of young generation regarding their awareness towards disaster risks as well as to learn how their past disaster experiences have been used as raising awareness strategy.

Methodology

Historical flood records and document research

This research first collects photo records of the historical flood in 1964 and sees how those have been used for raising awareness of city’s disaster experiences among its citizens. The authors examined photos taken on the occasion of the huge flood in 1964 to specify the exact locations of those photo taken-places. Then, the authors took photos at the same location of those photos in order to make then-current comparison images. These images will be used to see how such historical records can help in awareness-raising, keeping the local disaster experiences, as well as, hopefully, to take over such local knowledge to the future generations.

Social survey - questionnaire

A social survey – questionnaire to children and the youth – was conducted for this research. The targeted groups are the young generation whose age is between 12 to 21 years in Zagreb city (Tab. 1).

The questionnaire was composed in English by the authors and translated into local language (Croatian) by local counterpart in Zagreb. The survey was conducted to the individuals (Tab. 1) of schools and University in Zagreb, September 2011.

Results

Historical flood records and document research

The authors visited the certain places where the photos were taken in 1964 on the occasion of huge flood and took the photos given in Fig. 1. From these photos, it can be learned 1) that majority parts of the city has not been changed much, that is, it would be easy even for young people to compare the old views and current view of each

Table 1 The groups and the number of the respondents.

Targeted groups of questionnaire	n
Children (12-14 years: primary school)	86
Youth (16-21 years old: secondary school, university)	122
Total	208



Figure 1 Comparison images: the photos taken in the same locations where the photos were taken in Zagreb on the occasion of huge flood in 1964 (the ones on the left: 1964; the ones on the right: 2011).

site, and 2) that it is also helpful to grasp some image of the depth of flooded water in case of flood emergency happened in Zagreb even in today.

Regarding these old photos of the historical flood experience in 1964, an exhibition was held at the Zagreb City Museum in 2004 for the purpose of raising awareness and information dissemination. The exhibition showed the audience how such a huge flood engulfed the city by chronologically introducing the then precipitation data and photos (The Zagreb City Museum 2004). There were videos and a display of evacuation goods such as a rubber boat for education purpose. This exhibition was also open to the media such as newspapers and TVs so that it was introduced to the wider population.

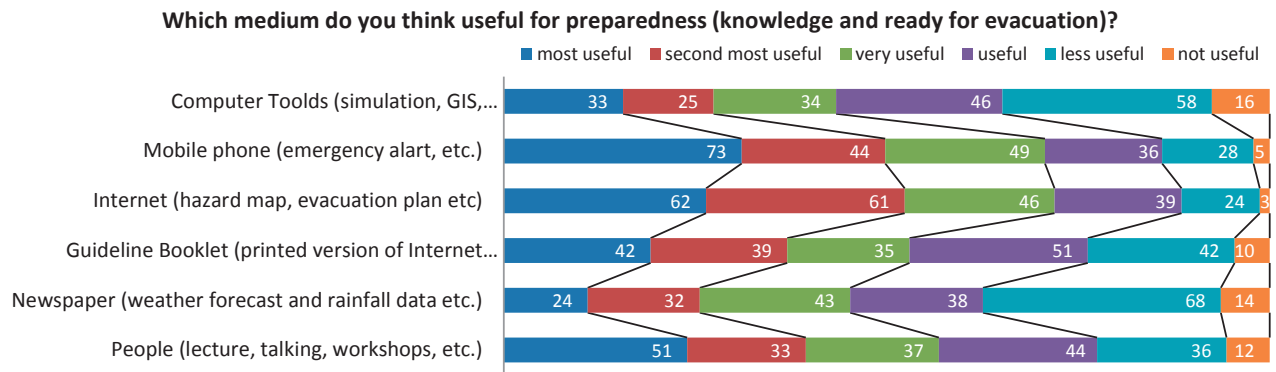


Figure 2 The absolute evaluation by young generation on preference to the means for preparedness.

Social survey

The social survey on the awareness status among young generations clarified the following three things: 1) 47% of the respondents know about the huge flood in Zagreb in 1964 and their information source was family, 2) a dependency on mobile phone or internet was rather high for both preparedness and information on an emergency case, and 3) nearly 74% think that there may be a flood to happen in Zagreb in 10 years' time though they recognize the function of modern flood protection systems such as river banks and canals.

The survey showed the major information source for young generation on the huge flood in 1964 is 'family (62%)' whereas 'school' was chosen by only 7%. Family is a very important information source that children, and this was clearly observed among primary school pupils, and they rely on their family, especially parents, for both preparation and evacuation because they do not know what to do. It was also clarified that many pupils expect a direction from their family when or on a moment a disaster happened. For preparation learning, modern technological tools such as mobile phones and the Internet are the most popular means among the respondents, then traditional means such as 'people' and 'guideline booklets' follow (Fig. 2).

A very interesting finding to draw attention is that 74% of respondents think there may be a flood in Zagreb in 10 years, on the other hand, the ratio of those who has preparation at home was only about 30%. It might tell that their preparation at home or their knowledge about evacuation is not correlated. They may think that a flood is caused only by heavy rain, but actually, this region in Europe has some earthquakes and the possibility of the river bank break or crack cannot be fully denied. The municipality government of Zagreb city has made efforts having produced leaflets on reactions in four types of emergency – earthquake, flood, chemical materials, and radioactive materials – and disseminated to citizens. Yet, it was found that the leaflets are not well recognized and even some university students do not have exact knowledge about evacuation or reaction in emergency case such as earthquake and flood.

Another interesting finding was that there was a similar ratio of respondents who have felt fear of heavy rain or storm and that of those who have preparation at home. The respondents neither have much connection with the Sava River nor spend much time around the River, thus they do not have much time spending in the water environment or any disaster experience thanks to the success of flood protection systems.

At last but not least, a tendency of lower ratio of preparation status in female, compared to male, was observed through an analysis, which might be related to the vulnerability issue of girls/women in emergency cases that is often discussed.

The social survey revealed that young generation in Zagreb is well-aware of the historical flood event and other natural disaster risks. Nearly three-quarter of them answered there may be a flood to happen in Zagreb in 10 years' time, however the result cannot clarify if they really think there will be a flood in the city or they actually assume that it will not happen to them and do not have tangible images of disaster case. In fact, their preparation status and knowledge is quite limited. The survey results showed the ongoing activities on education for disaster risk reduction at public educational arena, in case of Zagreb, may need to be further reinforced so that it comes understood and digested better in young generation so that they can connect their learned knowledge to their own actions to protect themselves and help each other in an emergency case.

Discussion

The survey result showed that the most concerned natural disaster in Zagreb was earthquake and flood follows it. However, again, the flood is a concatenating disaster with a large earthquake, thus its occurrence cannot be overlooked. With this in mind, awareness-raising toward unforeseen flood risks is needed to be further developed and well-structured, especially young generation.

The flood experience in 1964 can be more effectively used in order to raise awareness in public arena of flood

disaster. Although many photos taken on the occasion of flood in 1964 were exhibited in the museum and such history has been taught at school as part of regional history, young generation recognize their own family as information source. This may tell that such disaster experiences come to people's mind with stronger impact when it was provided by a person who is closed to the listener or has actual experiences. The past experiences including those photos and personal stories can be used more effectively and be included in awareness-raising scheme plan by the government. This type of learning may exert non-verbal education helping people build resilience not depending upon infrastructure.

Mobile phones and internet are widely disseminated among young generation; they were popular means for preparation learning and evacuation information source. Yet, this implies that they assume electricity or mobile phone line services are available even in any emergency cases. Many of young generation may have taken their protected life without disaster for granted and cannot imagine that phone lines get down or malfunctioned due to a number of accesses at a time. For the government, it needs to maintain the mobile phone operation system under disaster situation along with their protection and rescue policies. This can be a part from which they can learn from disaster prone country cases, e.g., Japan. In case of North-eastern Great Earthquake and tsunami in March 2011, a chaotic situation happened after the first hits.

Conclusion

There was a huge flood happened in Zagreb in 1964. This event is well-known by even young generation in the city through their family. The government built a modern infrastructure system, and it succeeded in protecting the city center and its citizens. Today, the historical flood event is only knowledge among young generation. Though 74% respondents replied that there may be a flood in Zagreb in 10 years' time, it is yet not sure how seriously they see such flood risks as an issue that might come and related to their life. Many of young generation do not know exactly what to do in order to protect themselves or help each other in case of disaster emergency. Mobile phones and the Internet are popular and they depend much on these tools for learning as well as information source expecting those work in at any time regardless the disaster occurrence.

As the Report from UNICEF and UNSIDR states, it is observed, through the survey in Zagreb, that there are many educational activities for awareness-raising are ongoing in Croatia. However, many of them may have ended as merely events and not yet sure how much impact they left in young generation in terms of learning and building preparedness and resilience. A holistic approach will be necessary in order to build resilience of the whole society by including historical experiences,

learning at public educational arena, reinforcing cohesive community with information dissemination, infrastructure development and maintenance by the government, as well as application of other region/country cases. To train and educate young generation on disaster risk reduction will be the key and a start to build the holistic approach. Flood should be understood a concatenating disaster to earthquake, the most concerned disaster in Zagreb. It is not to scare young generation but to have them prepared so that they react without panicking, thus eventually does it lead to sustainable development of the city in future.

Acknowledgments

We would like to thank Japan International Cooperation Agency (JICA) and Japan Association for Science and Technology (JST) since the surveys were conducted abroad, on the occasion of visit to Croatia for the Project on "Risk Identification and Land-Use Planning for Disaster Mitigation of Landslides and Floods in Croatia." We gratefully acknowledge the assistance of Ms. Darija Bilandžija and Igor Bognović, both from Faculty of Agriculture, University of Zagreb, Principals and teachers of Schol of Agriculture and Elementary school "Antun Gustav Matoš" for their understanding and cooperation, as well as all the pupils and students who cooperated to the survey. Also, we would like to send appreciation to Croatian Waters and Office for Emergency Management, City of Zagreb, Croatia, for their provision of information.

References

- ISDR (International Strategy for Disaster Reduction) (2009) Proceedings – Creating Linkages for Safer Tomorrow. Global Platform for disaster Risk Reduction. Second Session, Geneva Switzerland.
- ISDR (International Strategy for Disaster Reduction) (2005) Hyogo Framework for Action 2005-2015: Building the Resilience of Nations and Communities to Disasters – Extract from the final report of the World Conference on Disaster Reduction (A/CONF.206/6). UN/ISDR. Geneva, Switzerland.
- ISRBC (International Sava River Basin Commission) (2009) Sava River Basin Analysis Report. International Sava River Basin Commission. Zagreb, Croatia.
- Maršić A (1998) 1964 – The City and his river. EROZIJA. JŽ, Belgrade. (In Serbian)
- The Zagreb City Museum (2004) Flood in Zagreb 1964. http://www.mgz.hr/hr/izlozbe/poplava-u-zagrebu-1964-godine_108.html [accessed on 23rd April 2011]
- Trninić D (2001) The Sava River Flood Forecast and Srednje Posavlje Flood Control Efficiency. XXIX IAHR Congress Proceedings. Tsinghua University Press, Beijing, China.
- UNICEF and UNISDR (2011) Children and Disasters – building resilience through education, UNICEF Regional Office, Geneva, Switzerland, UNISDR, Brussels, Belgium.
- UN (United Nations) (2000) United Nations Millennium Declaration. A/RES/55/2. New York. USA.

Seasonal Changes of CO₂ Emissions in Tillage Induced Agroecosystem

Darija Bilandžija, Željka Zgorelec, Ivica Kisić, Milan Mesić, Aleksandra Jurišić, Ivana Šestak

University of Zagreb, Faculty of Agriculture, Zagreb, Croatia, Svetošimunska cesta 25

Abstract Carbon dioxide (CO₂) is the primary greenhouse gas (GHG) emitted throughout human activities which are responsible for the increase of GHGs in the atmosphere since the industrial revolution. It is presumed that increased concentrations of GHG emissions cause the global warming. One part of carbon dioxide is released from soil in the process of soil respiration (soil CO₂ flux, soil CO₂ emission). Due to the lack of research on long term carbon dioxide flux in tillage induced agroecosystem in the Republic of Croatia, the aim of our study is to determine the influence of different tillage treatments on soil carbon dioxide flux.

Field experiment with six different tillage treatments usually used in this area was set up on Stagnic Luvisols in Daruvar, in central, lowland Croatia. Field experiment is characterized by continental climate. Tillage treatments differed in tools that were used, depth and direction of tillage. Field measurements were conducted during one vegetation year (n=8), from May till October 2012, when cover crop was corn (*Zea mays* L.). In this paper the results of determined CO₂ fluxes during one vegetation year are presented.

The treatment with the lowest determined CO₂ flux was black fallow (BF) where average CO₂ flux was 37,99 kg CO₂/ha/day. If we compare the treatments with the cover crop, minimal average CO₂ flux was determined at ploughing up/down the slope to 30 cm treatment (PUDS) where average CO₂ flux amounted 70.09 kg CO₂/ha/day while maximal average carbon dioxide flux was determined at no-tillage (NT) treatment and it amounted 118,78 kg CO₂/ha/day.

We can say that in these agroecosystem conditions, best tillage practice in terms of the lowest carbon dioxide flux is ploughing up and down the slope to 30 cm (PUDS) although the lowest carbon dioxide flux was determined at treatment without any cover crop (BF), and therefore without any yield, but further research in terms of soil conditions is recommended.

Keywords: soil respiration, CO₂ flux, vegetation period, corn, Croatia

Introduction

Carbon dioxide is recognized as a significant contributor to global warming and climatic change, accounting for 60% of global warming or total greenhouse effect (Rastogi et al. 2002). The impact of climate change is obvious in all parts of the world as well as in Republic of Croatia. The period 1991-2000 was the warmest decade of the 20th century in Croatia (Branković et al. 2009).

To reduce the global temperature, Kyoto Protocol has been adopted in Kyoto in 1997, and Republic of Croatia has become the Kyoto Protocol Annex I country in 2007. By adopting the Kyoto protocol, Croatia has made a commitment to reduce the GHG emissions by 5% in the period between 2008 and 2012 compared to the base year 1990 and additional 20% compared to the base year 1990 up to the year 2020. One of the six sectors under the Kyoto Protocol, from which each country has to report their GHG emissions every year, is agricultural sector.

Due to the lack of research and scientific data on long term carbon dioxide emissions (fluxes) in agroecosystem in the Republic of Croatia we started to investigate the influence of different tillage treatments on soil carbon dioxide flux. In this paper, the results of field measurements of carbon dioxide concentrations in tillage induced agroecosystem during one vegetation year when cover crop was corn are presented.

Materials and methods

Field experiment with six different tillage treatments usually used in Croatia was set up in Blagorodovac near Daruvar (N 45°33'937'', E 17°02'056'') in central, lowland Croatia. Field experiment was established in 1994 with the aim of investigation on determination of soil degradation by water erosion and later, in 2011, expanded to the research on soil CO₂ concentration measurements. Soil type at the experimental site is determined as Stagnic Luvisols. Location of the experimental site is situated near village Blagorodovac, in Bjelovarsko-Bilogorska County and is presented at Figure 1 (Google Earth 2013).



Figure 1 Geographical location of the experimental site near Blagorodovac village.

Tillage treatments differed in tools that were used, depth and direction of tillage and planting. Tillage treatments were: black fallow - BF, ploughing up/down the slope to 30 cm - PUDS, no-tillage - NT, ploughing across the slope to 30 cm - PAS, very deep ploughing to 50 cm across the slope - VDPAS and subsoiling to 50 cm plus ploughing to 30 cm across the slope - SSPAS. Investigated tillage treatments are summarized in Table 1.

Table 1 Treatments in field experiment.

Treatment	Tillage direction	Planting direction
Black fallow - BF	Up and down the slope	No crop
Plowed to 30 cm; disked and harrowed - PUDS	Up and down the slope	Up and down the slope
No-tillage, planting into mulch 2-3 cm + total herbicides - NT	Up and down the slope	Up and down the slope
Plowed to 30 cm, disked and harrowed - PAS	Across the slope	Across the slope
Plowed to 50 cm, disked and harrowed - VDPAS	Across the slope	Across the slope
Subsoiled to 50 cm, plowed to 30 cm, disked and harrowed - SSPAS	Across the slope	Across the slope

Field measurements of soil CO₂ concentrations were conducted during one vegetation year (n=8), from May till October 2012. Cover crop at the experimental field was corn (*Zea mays L.*), the main arable crop in Croatia. At the experimental field, corn was seeded on 30. April 2012 and harvest was conducted on 1. October 2012.

In this paper, the official meteorological data from main meteorological station of Meteorological and Hydrological Service of Croatia located in Daruvar for the

interpretation of climate in the climatological period 1961-1990 and studied 2012 at the experimental site are used.

The climate conditions of the experimental site are described by Lang's rain factor and Walter climate diagram. Lang's rain factor represents the ratio of mean annual precipitation amount (mm) and mean annual temperature (°C). The climate classification according to Lang's rain factor is conducted according to Gračanin climate classification (Butorac 1988).

For the measurement of soil carbon dioxide concentrations (ppm), the closed static chamber method was used. The chambers were settled on circular frames that were inserted about 10 cm into the soil. Before the chambers closure, the initial CO₂ concentrations near soil surface were measured. After the chambers closure, the incubation period was 30 minutes after which the CO₂ concentration in closed chambers were measured. *In situ* measurements of carbon dioxide concentrations in the chambers were conducted with portable infrared carbon dioxide detector (GasAlertMicro5 IR, 2011). Measurements of carbon dioxide concentrations were conducted in three repetitions at each treatment and in this paper their average values are presented.

The soil carbon dioxide flux was afterwards calculated according to Widen and Lindroth (2003) and Toth et al. (2005). Field measurement of soil carbon dioxide concentration is shown at Figure 2.



Figure 2 Field measurement of soil carbon dioxide concentration.

Results and discussion

The climate conditions at the experimental site

The experimental field is characterised by continental climate. In the largest part of lowland, continental Croatia there is a prevalent humid climate (Gajić-Čapka and Zaninović 2008).

Mean annual amount of precipitation in Daruvar during 30 - year period (1961-1990) was 878 mm and mean annual temperature was 10.6° C. According to the Lang's rain factor, the 30 - year period (1961-1990) was

characterized by the humid climate. The year 2012 was dryer and warmer compared to 30 - year period (1961-1990) with mean annual precipitation amount of 789 mm and mean annual temperature of 11.8°C. According to the Lang's rain factor, the year 2012 was characterized by semihumid climate in Daruvar. The climate conditions in Daruvar are shown in Tab. 2.

Table 2 Climate conditions at the experimental site.

Period	Precipitation (mm)	Temperature (°C)	Lang's rain factor
1961-1990	878	10,6	82,8
2012	789	11,8	66,9

Dominant climate conditions are without dry period during the 30 - year period (1961-1990) according to Walter climate diagram (Fig. 3) while in studied corn vegetation period in 2012 there was determined a water deficit from June till September (Fig. 4).

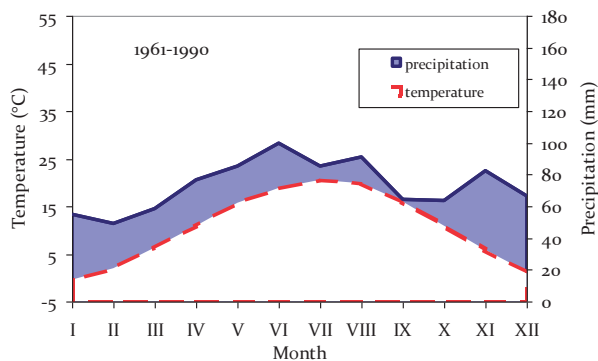


Figure 3 Walter climate diagram: 1961-1990.

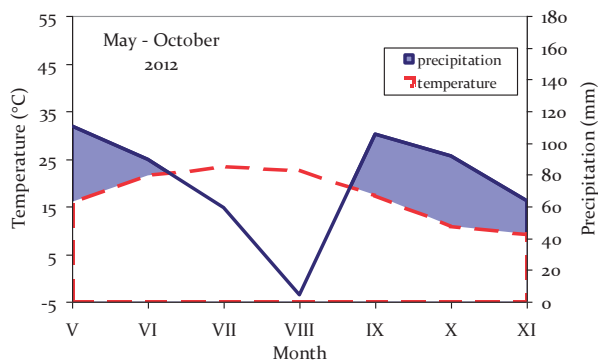


Figure 4 Walter climate diagram: May - October 2012.

Soil carbon dioxide flux

In this paper the results of field measurements of CO₂ concentrations during one vegetation year (May - October 2012) are presented. Fluxes of carbon dioxide were higher in first half of corn growing season than in

the second half of corn growing season what was likely a result of considerable contributions from root and microbial respiration. Lower fluxes were mostly determined in September and higher fluxes in the middle of May.

The lowest flux range had BF treatment where this difference amounted 65.63 kg CO₂/ha/day. The highest flux range had NT treatment where this difference amounted 204.02 kg CO₂/ha/day. Determined carbon dioxide fluxes at experimental field are presented in Table 3 and Figure 5.

Table 3 Minimal, maximal, average and range of CO₂ fluxes.

Treatment	CO ₂ flux (kg CO ₂ /ha/day)			
	Minimal	Maximal	Average	Range
Black fallow - BF	17,12	82,75	37,99	65,63
Plowed to 30 cm; disked and harrowed - PUDS	25,68	128,41	70,09	102,72
No-tillage, planting into mulch 2-3cm + total herbicides - NT	37,10	241,12	118,78	204,02
Plowed to 30 cm, disked and harrowed - PAS	25,68	146,95	91,67	121,27
Plowed to 50 cm, disked and harrowed - VDPAS	32,81	164,07	95,41	131,26
Subsoiled to 50 cm, plowed to 30 cm, disked and harrowed - SSPAS	29,96	222,57	116,46	192,61

The treatment with the lowest measured flux of carbon dioxide was black fallow (bare soil-BF) where average measured carbon dioxide flux was 37.99 kg CO₂/ha/day.

Elder and Lal (2007) assess the impact of tillage on CO₂ emissions on loamy mixed euc under corn and winter wheat. They reported that the CO₂ emissions were not significantly different among conventional tillage, no-tillage and bare soil treatment.

If we look at the treatments with the cover crop, minimal average carbon dioxide flux was determined at ploughing up/down the slope to 30 cm treatment (PUDS) where average CO₂ flux was 70.09 kg CO₂/ha/day while maximal average carbon dioxide flux was determined at no-tillage (NT) treatment (118.78 kg CO₂/ha/day).

Similar results obtained Franzluebbbers et al. (1995) in their research. They determined that soil from no-tillage released more CO₂ than soil under conventional tillage during at least one season of each crop sequence (sorghum-wheat/soybean).

The average carbon dioxide fluxes per treatment at the experimental field during corn vegetation period May - October 2012 are presented at Figure 5.

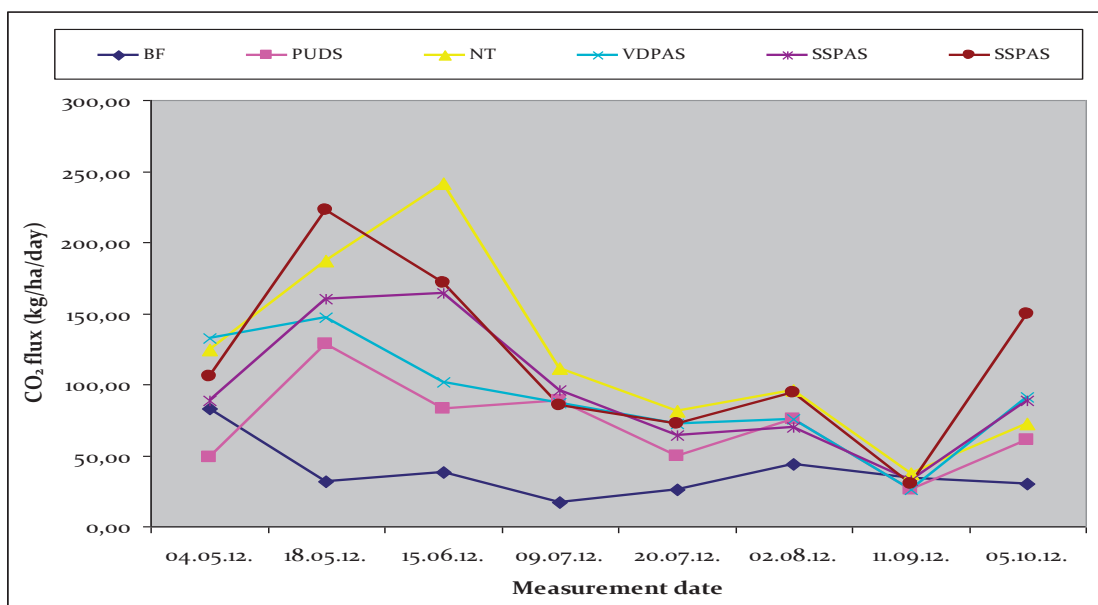


Figure 5 Average values of carbon dioxide flux measured during corn vegetation period from May till October 2012.

Conclusions

Fluxes of carbon dioxide were higher in first half of corn growing season than in the second half of corn growing season. Lower fluxes were mostly determined in September and higher fluxes in the middle of May.

The treatment with the lowest determined flux of carbon dioxide was black fallow (BF) where average measured carbon dioxide flux was 37.99 kg CO₂/ha/day. If we look at the treatments with the cover crop, minimal average carbon dioxide flux was determined at ploughing up/down the slope to 30 cm treatment (PUDS) where average CO₂ flux was 70.09 kg CO₂/ha/day while maximal average carbon dioxide flux was determined at no-tillage (NT) treatment (118.78 kg CO₂/ha/day).

Although the lowest carbon dioxide flux was determined at treatment with black fallow (BF), this treatment cannot be recommended as it serves as the control treatment. We can say that in these agroecosystem conditions, best tillage practice in terms of the lowest average carbon dioxide flux is ploughing up and down the slope to 30 cm (PUDS). Further research extension on the influence of other parameters (soil temperature, soil moisture) on emissions of carbon dioxide from soil is recommended.

Acknowledgments

This research was funded by the projects „Influence of different land management on climate change” (leader: Assistant Professor Željka Zgorelec, PhD) and

“Conservation management of soils exposed to water erosion” (leader: Full Professor Ivica Kisić, PhD).

References

- Branković Č, Bray J, Callaway J, Dulčić J, Gajić-Čapka M, Glamuzina B, Heim I, Japac L, Kalinski V, Landau S, Legro S, Oikon Ortli F, Patačić M, Srnec L, Šimleša D, Zaninović K, Znaor D (2009) A Climate for Change, Climate change and its impacts on society and economy in Croatia, Human Development Report – Croatia 2008. United Nations Development Programme (UNDP) in Croatia, Zagreb. (ISSN: 1332-3989). 284p.
- Butorac, A. (1988) General manufacturing of plants, a practicum. Zagreb. (in Croatian)
- Elder J.W., Lal R. (2007) Tillage effects on gaseous emissions from an intensively farmed organic soil in North Central Ohio. *Soil and Tillage Research*. 98: 45–55
- Franzluebbers A J, Hons F M, Zuberer D A (1995) Tillage-induced seasonal changes in soil physical properties affecting soil CO₂ evolution under intensive cropping *Soil and Tillage Research*. 34: 41-60.
- Gajić-Čapka M, Zaninović K (2008) Climate of Croatia; Climate atlas of Croatia 1961-1990., 1971-2000. Zaninović K. (eds). Meteorological and Hydrological Service of Croatia, Zagreb. (ISBN: 978-953-7526-01-6). 200p.
- Rastogi M, Singh S, Pathak H (2002) Emission of carbon dioxide from soil. *Current Science*. 82: 510–517.
- Widen B, Lindroth A (2003) A calibration system for soil carbon dioxide – efflux measurement chambers: description and application. *Soil Sci Soc Am J*. 67: 327-334.
- Toth T, Forizs I, Kuti L (2005) Data on the elements of carbon cycle in a Solonetz and Solonchak soil. *Cereal Research Communications*. 33: 133-136.

Triggering Mechanism of Shallow Landslides on the Northeast Rim of Mt. Aso Caldera, Japan, in July 2012

Hufeng Yang⁽¹⁾, Fawu Wang⁽²⁾, Yasuhiro Mitani⁽¹⁾, Tomokazu Sonoyama⁽¹⁾

1) Shimane University, Department of Geoscience, Matsue, Japan, Nishikawatsu 1060, yanghufeng@gmail.com

2) Shimane University, Research Center on Natural Disaster Reduction, Matsue, Japan

Abstract In July 2012, Northern Kyushu, Japan was suffered by an intensive rainfall during rainy season. This high precipitation triggered many shallow landslides, especially on the northeast rim of Mt. Aso caldera, which affected many villages and local settlers. One landslide site which is located at Ichinomiya in Kumamoto Prefecture was selected for this study. Field investigation and laboratory tests were conducted to study the triggering mechanism of shallow landslides triggered by intensive rainfall. Several field geotechnical tests including portable cone penetration tests and in-situ permeability tests were conducted on the top soil. Soil samples were collected to study the physical properties of different layers of top soil. Shear strength of the soil above sliding surface was estimated using constant-volume direct shear test. According to the results, it can be observed that the steep slopes of Mt. Aso caldera rim could still be stable under normal precipitation conditions due to the physical properties of the top soil (low permeability and high shear strength). The possible triggering mechanism indicates that initial failure process of the shallow landslides on the rim of Mt. Aso caldera starts with toe erosion caused by surface runoff.

Keywords rainfall, shallow landslides, Mt. Aso caldera

Introduction

In July 2012, Northern Kyushu, Japan was suffered by an intensive rain fall. This high precipitation triggered many shallow landslides, especially on the northeast rim of Mt. Aso caldera, which affected many villages and local settlers. It claimed 30 lives, completely or partially damaged 13,263 houses, with 2 people declared missing. Long-distance lifelines and large area of farmland were also affected (Fire and Disaster Management Agency, Japan 2012).

During rainy seasons or typhoon occurrences, shallow landslides and debris flows are always triggered around the rim of Mt. Aso caldera. Without doubt, intensive rainfall is the main triggering factor of these geo-disasters. Many studies have been carried out to understand the factors contributing to the occurrence of these shallow slope failures. Paudel et al. (2003, 2008) and

Miyabuchi et al. (2011) asserted that top soil is consisted of different layers and slip surfaces of most landslides are formed between upper blackish and lower brownish tephra layers. Paudel et al. (2007) evaluated the spatio-temporal patterns of historical shallow landslides in Mt. Aso caldera based on statistical analysis of shallow landslides which occurred between 1953 and 1998. Besides these research findings discussed above, Kasama et al. (2011) recently tried to clarify the factors which led to the geo-disaster through the geo- and hydro-mechanical evaluation.

In order to understand the triggering mechanism of these shallow landslides, one landslide site was selected for comprehensive study. Several field geotechnical tests were carried out in the landslide site. According to the results obtained from field investigation and laboratory tests, a possible triggering mechanism was proposed for shallow landslides on the rim of Mt. Aso caldera.

Study site

The study site is located at Ichinomiya, northeast of Mt. Aso caldera (Fig. 1). Mt. Aso caldera is one of the largest calderas in the world. It extends 17 km across from east to west, 25 km from north to south, and has an area of about 350 km². The central crater group, referred to as Mt. Aso, incorporates five peaks (Mt. Taka, Mt. Naka, Mt. Eboshi, Mt. Kishima and Mt. Neko). The huge caldera was created by four major eruptive events (Aso-1, Aso-2, Aso-3 and Aso-4). In the study area, it can be found that the geological units include pyroclastic flow and ash fall deposits derived from Aso-1, Aso-2, Aso-3 and Aso-4 eruptions. Gravel, sand and mud were deposited at the toe of slope due to continuous removal of the slope material by erosion over a long period of time. Extensive air-fall volcanic ash covered the top of the slope (outside rim of Aso caldera) (Fig. 2).

From the cross section of Mt. Aso caldera, it can be observed that central cones divide the Mt. Aso caldera into Asodani Valley Nangodani Valley (Figs 1 and 3). The mountain chain and plains surround the outer rim of the caldera and extend to the outer side into a gentle terrain overlain by pyroclastic deposits. Most of all the rainfall-triggered shallow landslides in July 2012 occurred on the inner slope of the northern caldera wall. The study site is

located on the slope of the caldera wall about 700 m asl with slope angle of more than 30° (Fig. 3).

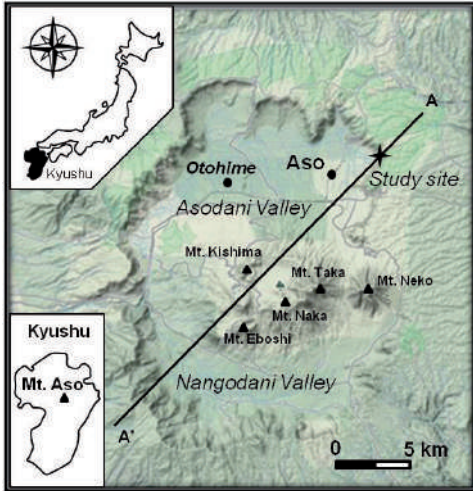


Figure 1 Location map of study site (modified from Google Earth).

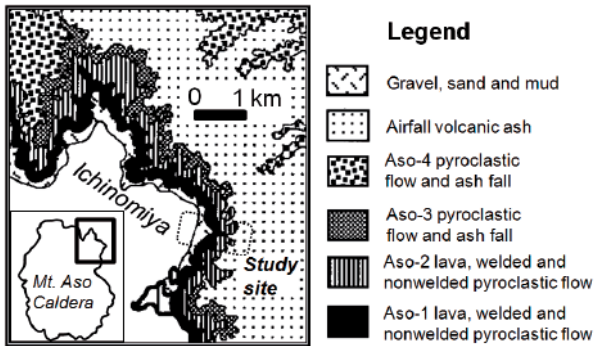


Figure 2 Geological map of study site (after Hunter, 1998).

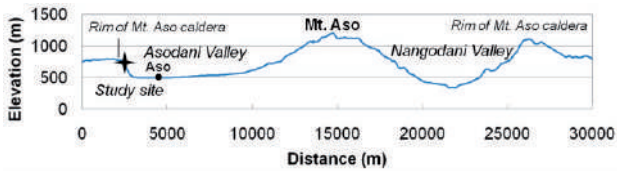


Figure 3 Cross section of the Mt. Aso caldera.

Meteorological data

In contrast to hourly precipitation data collected from all meteorological observatories in Northern Kyushu in the last decade, it was observed that maximum hourly precipitation from seven observatories in July 2012 was the highest local precipitation ever recorded within the area. Among these observatories, collated data shows that accumulated precipitation of the area obtained from five observatories over a four-day period was more than 500 mm (Fig. 4).

In 2012, rainy season of Northern Kyushu was earlier and relatively longer than average period. In order to understand the precipitation characteristics of the study site, daily and accumulated precipitation within the study area were obtained from Otohime Meteorological Observatory (Fig. 5). The Otohime Meteorological Observatory is located 4 km west of Ichinomiya (Fig. 1). From the rainfall distribution plot in Fig. 5, it can be observed that daily precipitation was 493.0 mm in July 12 when the landslide occurred. This precipitation is the highest recorded data from Otohime Meteorological Observatory in the last decade. Before the intensive rainfall in July, accumulated precipitation was over 1200 mm. Obviously, intensive rainfall was the main triggering factor for this geo-disaster.

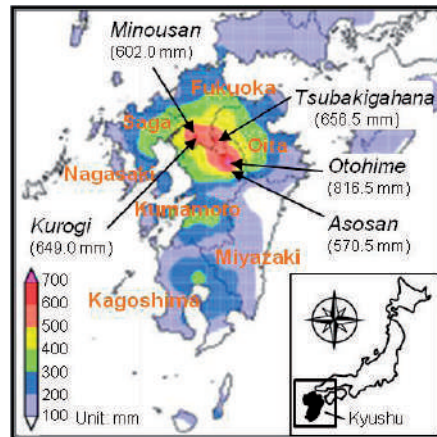


Figure 4 Accumulated precipitation map from July 11 to 14, 2012 (modified from Japan Meteorological Agency).

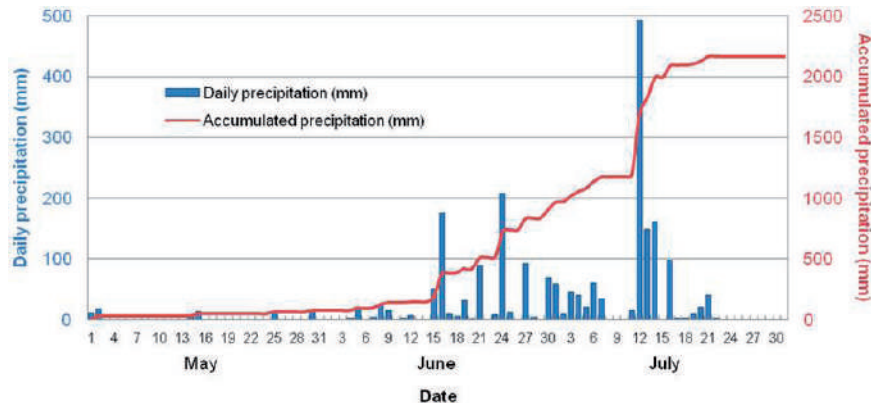


Figure 5 Precipitation of study site in rainy season, 2012.

Filed investigation

In order to understand the geo-disaster caused by this intensive rainfall, a representative landslide was selected to study the triggering mechanism. This landslide site located at Shioi Village in Ichinomiya, Kumamoto Prefecture (Fig. 1). Fig. 6 and Fig. 7 show the photo of slope after failure and cross sections of investigated area, respectively. Several shallow landslides occurred at the grassland at the rim of Mt. Aso caldera. And they were the source of debris flow. The speed of debris flows increased gradually as it traveled through steep slope. The destructive debris flow mixed with rock blocks destroyed two Sabo dams and several houses. Finally, it was deposited on the flat count yard and paddy fields.

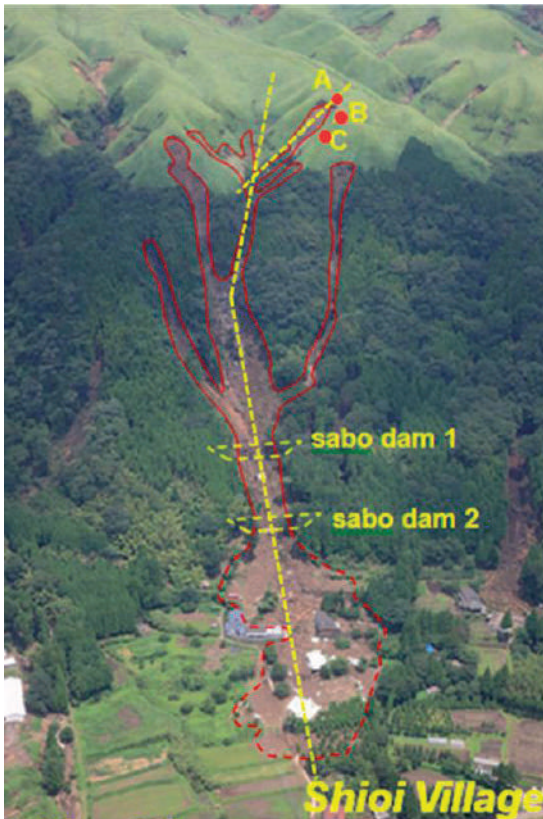


Figure 6 Photo of slope after failure at Shioi Village, Ichinomiya, Kumamoto Prefecture (Photo is taken by Kokusai Kogyo, Japan).

From the exposed main scarp of the shallow landslide, the soil can be divided into three layers (Fig. 8). Layer 1, the top black layer, is composed of volcanic ash, humus and plant roots. Layer 2 consists of clay and sand. Coarse sand and gravels can be found in this layer. The particle size becomes bigger gradually from top to bottom. The maximum particle diameter is about 20 mm. Layer 3, the bottom gravel layer, is residual soil of weathered volcanic tuff. Sliding surface is observed on the surface of layer 3.

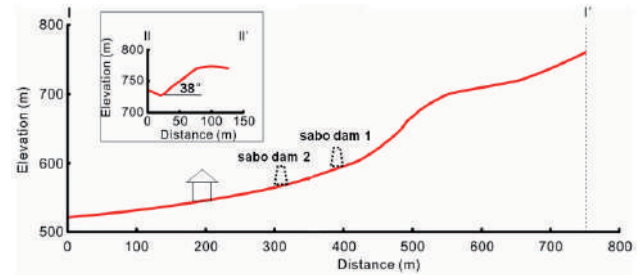


Figure 7 Cross sections of investigated area.

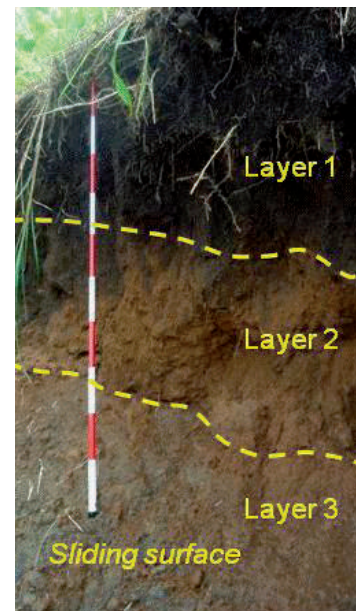


Figure 8 Main scarp of the shallow landslide.

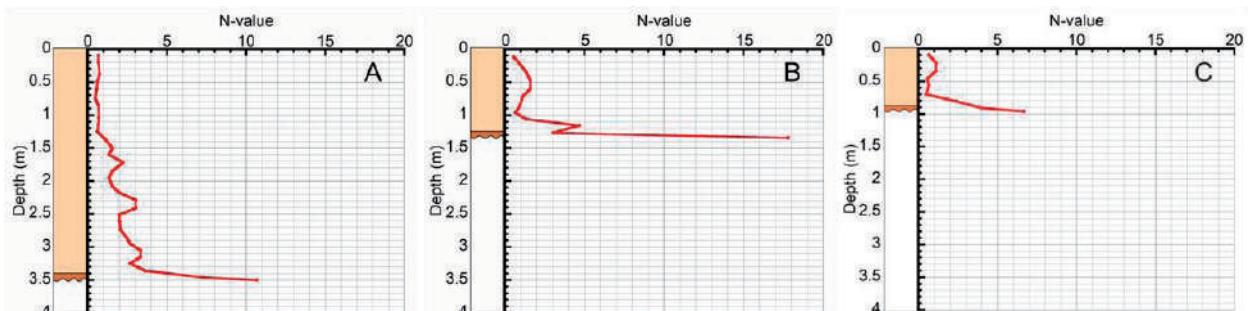


Figure 9 Results of three Portable Dynamic Cone Penetration tests.

Portable Dynamic Cone Penetration Tests

Three Portable Dynamic Cone Penetration tests were conducted to understand the thickness of the top soil. The test locations are shown in Fig. 6.

During the tests, 5 kg hammer from 50 cm height were dropped as free falls. The number of blows was recorded for each 10 cm penetration depth of cone tip, and cycles were repeated. Due to the potential sliding bed has different strengths, the boundaries could be identified and thickness of top soil could be determined. The test results of three locations are shown in Fig. 9. It can be observed that thickness of top soil is about 3.5 m at the upper slope. Gradually, the thickness of top soil became thinner (about 1 m) from upper to lower slope.

In-situ permeability tests

In order to measure infiltration rate of rainfall, in-situ permeability tests were conducted with variations in depth of hand-drilled boreholes on the top of the main scarp of the slope (Fig. 10). Permeability coefficient (*k*) was calculated using Equation 1 (Lambe and Whitman, 1969).

$$k = \frac{\pi D}{11 \Delta t} \cdot \ln \frac{h_1}{h_2} \quad [1]$$

Where *h*₁ and *h*₂ are the two consecutive depths of water in meters; *h*₁ is initial depth and *h*₂ is final depth; *D* is the diameter of pipe, *D*=0.1 m; Δt expresses the time interval between two successive measurements in seconds.

Tests were carried out twice in each borehole to obtain an average value. The test results of in-situ permeability are shown in Tab. 1. It can be observed that permeability coefficient (*k*) is 1.28×10⁻⁶ m/s at shallow depth of 0.25 m. While, permeability coefficient (*k*) is 1.90×10⁻⁷ m/s at a depth of 0.75 m. The results show that the permeability decreases with the increase in depth.

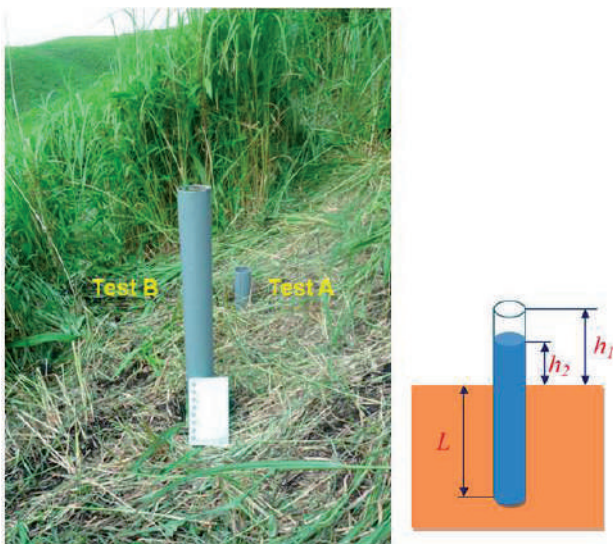


Figure 10 In-situ permeability tests.

Table 1 Results of the in-situ permeability tests.

	Test A		Test B	
	1	2	1	2
<i>h</i> ₁ (m)	0.15	0.15	0.60	0.60
<i>h</i> ₂ (m)	0.14	0.12	0.59	0.58
<i>L</i> (m)	0.25	0.25	0.75	0.75
Δt (s)	1500	5100	2700	4800
<i>k</i> (m/s)	1.31×10 ⁻⁶	1.25×10 ⁻⁶	1.78×10 ⁻⁷	2.02×10 ⁻⁷
Average <i>k</i> (m/s)	1.28×10 ⁻⁶		1.90×10 ⁻⁷	

Laboratory analysis

Physical properties

Soil samples were collected from different layers of the main scarp. The physical properties of the top soil at different layers are shown in Tab. 2. It summarizes specific gravity, natural water content, void ratio, degree of saturation, total and saturated unit weight. Even though, there was no rainfall for several days before the field investigation, it can be observed that layer 1 has kept higher water content and degree of saturation. This phenomenon related to the properties of soil, such as high void ratio and low permeability.

Grain size analysis (sieve and hydrometer analysis) was conducted to understand the grain size distribution (Fig. 11). According to the Unified Soil Classification System (USCS), it can be confirmed that layer 1 is composed of poorly graded tephra clay. Layer 2 is composed of clay with coarse sand and gravels. Layer 3 is gravel (residual soil), and grain sizes are varying from fine to coarse gravel.

Table 2 Physical properties of different layers of soil.

Physical properties	Layer 1	Layer 2	Layer 3
Specific gravity <i>G</i> _s	2.271	2.734	2.672
Water content <i>w</i> (%)	187.0	72.0	54.0
Void ratio <i>e</i>	5.452	2.191	—
Degree of saturation <i>S</i> (%)	78	90	—
Total unit weight γ (kN/m ³)	10.1	14.7	—
Saturated unit weight γ_{sat} (kN/m ³)	12.0	15.4	—

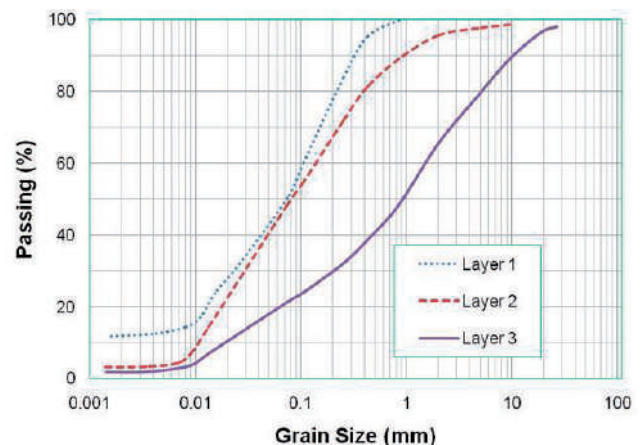


Figure 11 Grain size distributions of different layers.

Direct shear test of sliding zone

In order to evaluate the shear strength of top soil, a series of constant volume direct shear tests were carried out on the samples from the main scarp (Fig. 12). The specimens were prepared using dry soil that was sieved by 2 mm mesh. The soil was filled in three layers into the mold in order to control the uniform density of specimen. The specimen size was 60 mm in diameter and 20 mm in height. Based on the result of portable dynamic cone penetration tests, it could be observed that thickness of topsoil is about 3 meters. In addition, according to the unit weight from Tab. 1, the initial normal stress was applied as 15, 20, 25 kPa respectively. Then, the specimens were sheared up to 7 mm in horizontal direction at a shear speed of 0.2 mm/min according to the Japan Geotechnical Society (JGS) standard. During the shearing, vertical load was adjusted to keep constant volume. From the stress paths of constant-volume direct shear-box tests (Fig. 13), it can be observed that effective stress is decreasing gradually at the beginning of shearing. With the dilatancy effect, shear stress is increased.

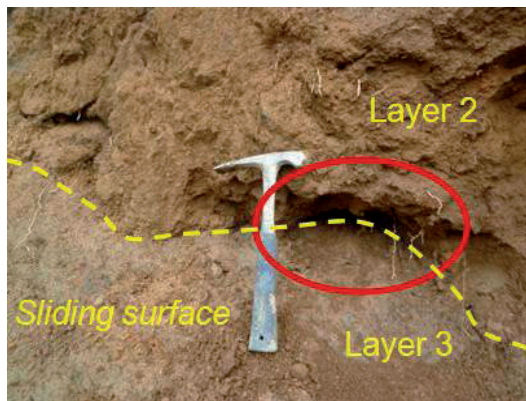


Figure 12 Sampling location of sliding zone.

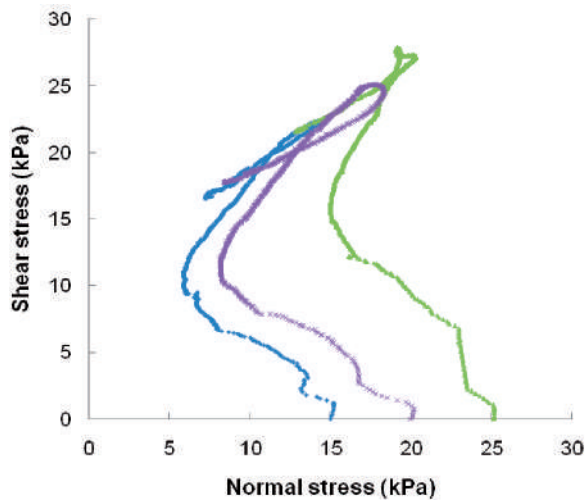


Figure 13 Stress paths during constant-volume direct shear tests.

Discussions

According to the GIS analysis of landslides in Ichinomiya during the intensive rainfall in July 2012, the landslide frequency is the highest for slope angles between 30 and 40° (Geographical Survey and Photography, Japan, 2012). As shown in the cross sections of investigated site (Fig. 7), the relatively steep slope, about 38°, contributes the deformation of top soil under gravity action and movement of water including slope surface runoff and seepage actions in the inner part of the slope. In addition, the steep nature of the slope enhanced the rapid down-slope movement of detached colluviums and debris, which mobilized into a high-speed debris flow that broke two high frame Sabo dams.

Intensive rainfall is the main triggering factor for shallow landslide occurrences in the study area. However, the duration of rainfall is also very important. Before the intensive rainfall in July, accumulated precipitation was over 1200 mm (Fig. 5). Due to the effect of incessant rainfall that lasted for more than one month, the slope surface became saturated and surface water gradually infiltrated into slope. From the result of in-situ permeability test, it can be observed that the permeability of top soil is not so high. Paudel et al. (2008) measured permeability of the soil in the field at ten locations on Mt. Aso caldera area. They also found that the permeability of black layer was quite low (less than 1.0×10^{-6} m/s). With the low permeability top soil, majority of rainfall translated into surface runoff instead of infiltration.

Soil strength is an intrinsic factor for slope stability. From the referred results of shear strength of top soil, it can be observed that the effective friction angle was over 30° and cohesion varied with different soil layers (Paudel et al. 2008). The results were similar with the ones presented in this paper. From the stress path, it can be found that top soil was allowed to own limited deformation before final failure. With the steep slope structure, partial deformation on slope surface may gradually take place. Horizontal cracks, which caused by partial deformation of slope surface, usually serve as flow channels for rainfall infiltration.

Based on the above discussions, possible triggering mechanism was proposed (Fig. 14).

A. With steep terrain (over 35°), partial deformation on slope surface may occur gradually. During the rainy season, rainfall easily infiltrates into the slope through cracks causing the groundwater water table to increase.

B. When intensive rainfall comes, the infiltration rate is far less than the rainfall intensity. Most of rainfall translates into surface runoff. Due to the top soil at the toe of slope is very thin, somewhere, the bedrock is exposed, high-speed surface runoff will easily remove the toe of slope along the gullies gradually.

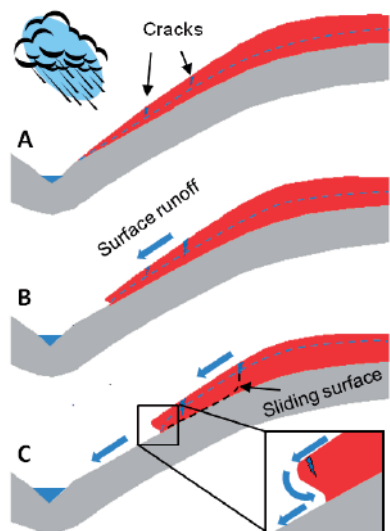


Figure 14 Sketch of triggering mechanism of shallow landslide on inner slope of Mt. Aso caldera.

C. Further, headward erosion may occur combine with surface runoff. Gradually, headward erosion removes the toe of the slope which provides resistance for slope stability. Meanwhile, the water table in the slope may increase gradually due to the rainfall infiltration through cracks. Initially, shallow landslides occur along the gullies. Then, a mass of soil mixed with rainwater has deposited in valley. Finally, disastrous debris flow occurs under continuous intensive rainfall.

Conclusions

Shallow landslides on the northeast rim of Mt. Aso caldera were triggered by intensive rainfall in July 2012. This paper summarizes results of field investigations on a shallow landslide at Ichinomiya, Kumamoto Prefecture. Soil samples were collected to study the physical properties of top soil. And Shear strength of the soil above sliding surface was estimated using constant-volume direct shear test. The conclusions from this study can be summarized as follows:

Under normal precipitation, the steep slopes of Mt. Aso caldera rim can still be stable due to the physical properties of the top soil (low permeability and high shear strength).

During intensive rainfall, the possible triggering mechanisms indicates that initial failure process of the shallow landslides at the rim of Mt. Aso caldera starts

with toe erosion caused by surface runoff. Due to lose the resistance force, the slope finally will be in a critical situation combined with increasing piezometric head in the slope. This is why the shallow landslides frequently occur during rainy season under prolonged rainfall of high intensity.

Triggering rainfall amount for these shallow landslides should be further studied through field monitoring, model tests or numerical simulation.

Acknowledgments

The authors are grateful to Mr. Asano from Kyushu Research Center, Forestry and Forest Products Research Institute and Mr. Araiba from National Research Institute of Fire and Disaster, Japan for their guide and useful contributions during the field investigation. Also, the authors would wish to express their sincere appreciation to Messrs. Austin and Nuwan for editorial comments on the manuscript.

References

- Fire and Disaster Management Agency, Japan (2012) Report of heavy rainfall from 11 July 2012. (No. 20) 7p. (in Japanese)
- Geographical Survey and Photography, Japan (2012) Investigation of debris flows at Mt. Aso caldera triggered by Northern Kyushu intensive rainfall in 2012 using GIS (in Japanese). URL: <http://gpinet.jp/study/aso/aso.html>
- Hunter A G (1998) Intracrustal Controls on the coexistence of tholeiitic and calc-alkaline magma series at Aso Volcano, SW Japan. *Journal of Petrology*. 39(7): 1255-1284.
- Kasama K, Jiang Y, Hiro-oka A, Yasufuku N, Sato H (2011) Geo-and hydro-mechanical evaluation of slope failure induced by torrential rains in northern-Kyushu area, July 2009. *Soils and Foundations*. 51(4): 575-589.
- Lambe W T, Whitman R V (1969) *Soil Mechanics*. John Wiley, New York.
- Miyabuchi Y, Sugiyama S (2011) 90,000-year phytolith record from tephra section at the northeastern rim of Aso caldera, Japan. *Quaternary International*. 246(1-2): 239-246.
- Paudel P P, Moriwaki K, Morita K, Kubota T, Omura H (2003) An assessment of shallow landslides mechanism Induced by rainfall in Hakoishi area. *Kyushu Journal of Forest Research*. 56: 122-128.
- Paudel P P, Omura H, Kubota T, Inoue T (2007) Spatio-temporal patterns of historical shallow landslides in a volcanic area, Mt. Aso, Japan. *Geomorphology*. 88(1-2): 21-33.
- Paudel P P, Omura H, Kubota T, Devkota B (2008) Characterization of terrain surface and mechanisms of shallow landsliding in upper Kurokawa watershed, Mt Aso, western Japan. *Bulletin of Engineering Geology and the Environment*. 67(1): 87-95.

Sliding Causes and Triggering Mechanisms at the Bogatići Landslide

Sabid Zekan, Nedim Suljić

University of Tuzla, The Faculty of Mining, Geology and Civil Engineering, Tuzla, Bosnia and Herzegovina, Univerzitetska 2, ++387 61 562-277

Abstract This paper describes the sliding causes and triggering mechanisms at the Bogatići landslide. It has been found that the low strength of organic silt was one of the main causes of the landslide activation (Elaborate and preliminary project of remediation of the Bogatići landslide, 2012). The Bogatići landslide is located near the Sarajevo-Foča road in Bosnia and Herzegovina, about 15 km south of Sarajevo, on the left bank of the Željeznica River. Activation of the landslide occurred in May 2010, after a heavy rainfall period. Reactivation, which occurred in June 2011, was caused by a new heavy rainfall. This indicates that the landslide has a seasonal occurrence. The Bogatići landslide is approximately 1,400 meters long and 80 to 100 meters wide, with a widening of approximately 300 meters at the toe. Sliding surface is approximately 10-15 meters deep in the upper part and up to 35 meters in the foot. The main causes of the landslide activation were infiltration of water through the cracks at the higher parts of the landslide, and the presence of high plasticity organic silt in the landslide toe. Extreme rainfall caused rising of the groundwater table in the sliding body.

Organic silt was identified in the landslide toe at the depth of 30 meters. The thickness of the layers in the sliding body is variable. There are thinner layers of different soil within the thicker ones. Laboratory tests

have shown extreme plasticity limit values: liquid limit is from 65 to 95%, and plasticity index from 25 to 50%.

Slope stability analysis was performed using the software package GGU by means of the Bishop method. It was concluded that the presence of a high level of groundwater caused the instability of the slope in the layer of organic silt. Lowering of the groundwater level in the landslide body would be one of the main measures of the landslide remediation (Faculty of Mining, Geology and Civil Engineering Tuzla 2012).

Keywords: Bogatići landslide, organic silty soil, extreme rainfall

Introduction

The landslide Bogatići is located 15 km south from Sarajevo, in Bosnia and Herzegovina, on the left bank of the Željeznica River (Fig. 1). Activation of the landslide occurred in June 2010, and reactivation in June 2011. Both cases of triggering occurred during heavy rainfall. The landslide has a periodically discontinued character because there is no sliding without heavy rainfall in June. It has been estimated that there is a fossil part of the landslide marked as F1 and F2, and an active part of the landslide marked as A (Fig. 2).

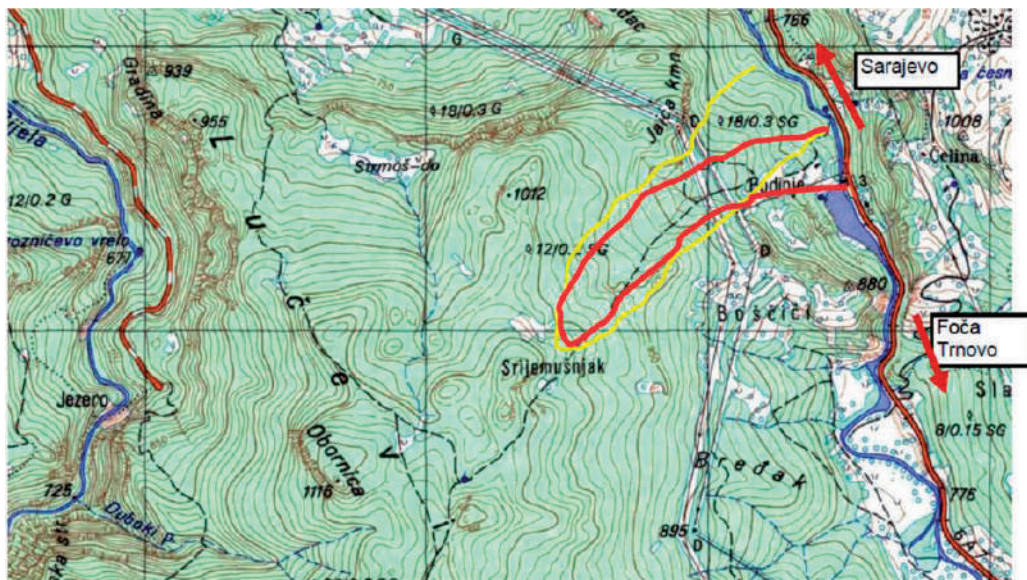


Figure 1 Location of the Bogatići landslide.

A – active landslide F – fossil landslide

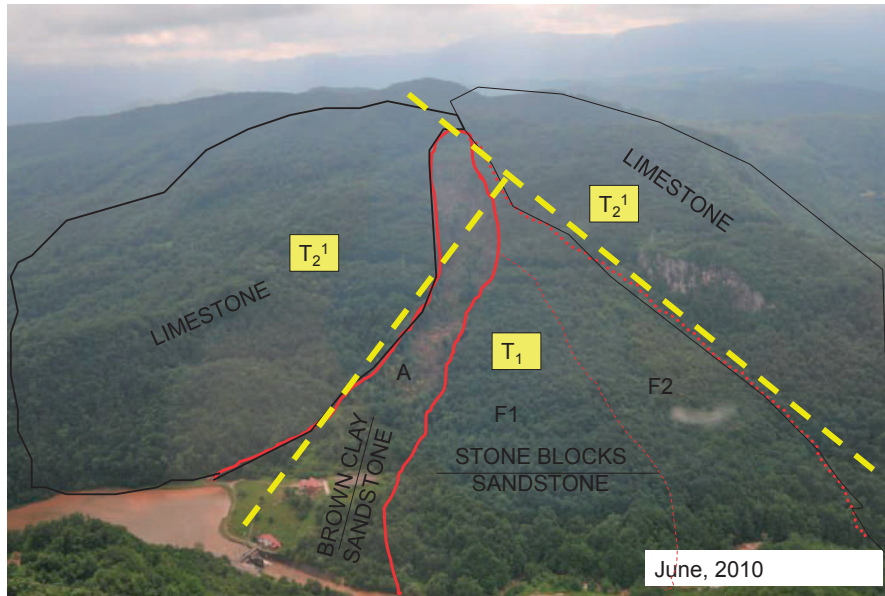


Figure 2 Basic parameters of the slope at the Bogatići Landslide.

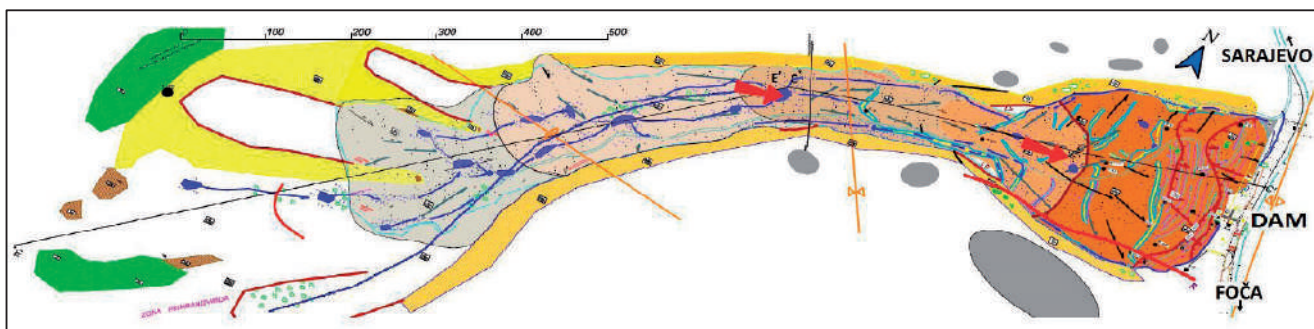
Geotechnical investigation

Geotechnical investigation was started with surveying the Bogatići landslide in 2011 and was finished by the end of 2012. Twelve boreholes of various depths were made in order to carry out the field investigation. SPT experiment was performed and piezometers as well as inclinometers were used at the landslide.

The following landslide parameters, shown in Figures 3, 4 and 5 were estimated on the basis of the geotechnical investigation (RGGF 2012):

- length of 1,410 m
- width at foot: 225 m
- width at transport zone: 100 - 130 m
- landslide area: 160 800 m²
- average depth of the landslide: 13 to 35 m
- head elevation: 1,020.0 m
- toe elevation: 767.0 m
- slope of the landslide: 11°.

At the beginning of the investigation there were a lot of tree trunks lying on the field which made the investigation more difficult.



LEGEND









	Limestone (stable)		Željeznica River
	Sandstone, gray and gray-brown (stable)		Limestone blocks
	Clay, silty-sandy, red-brown with limestone blocks (Accumulation zone)		Surface water
	Clay, silty-sandy, red-brown with limestone blocks (Transport zone)		Active movement

Figure 3 Simplified engineering-geological map.

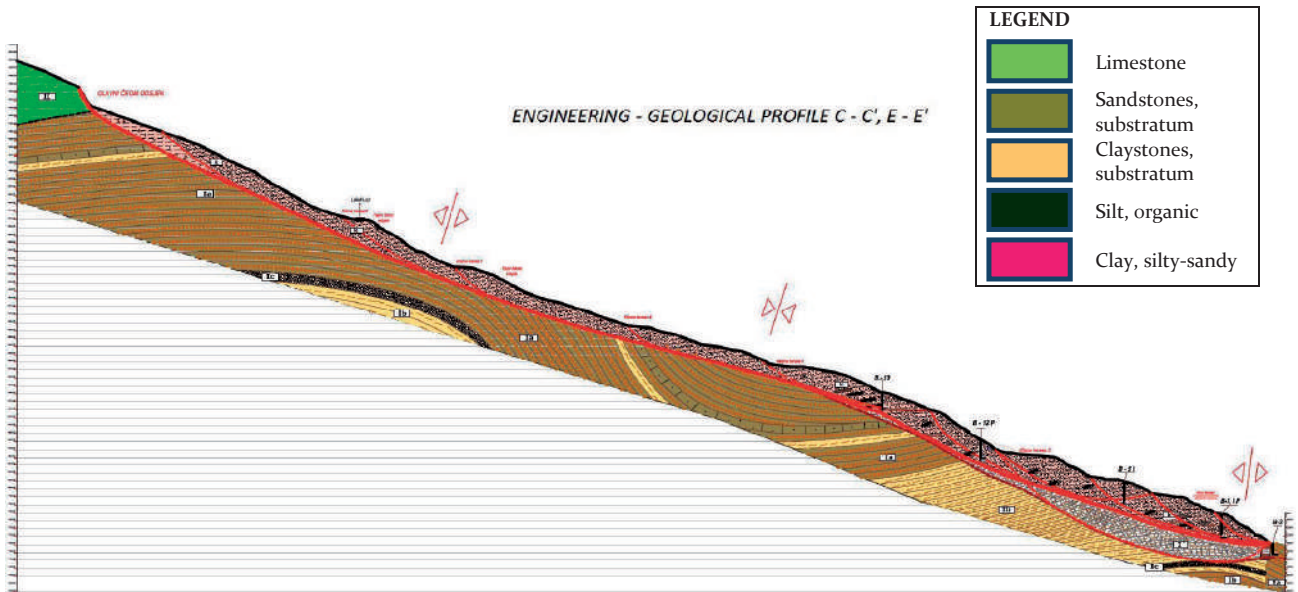


Figure 4 Engineering-geological profiles C-C', E-E'.

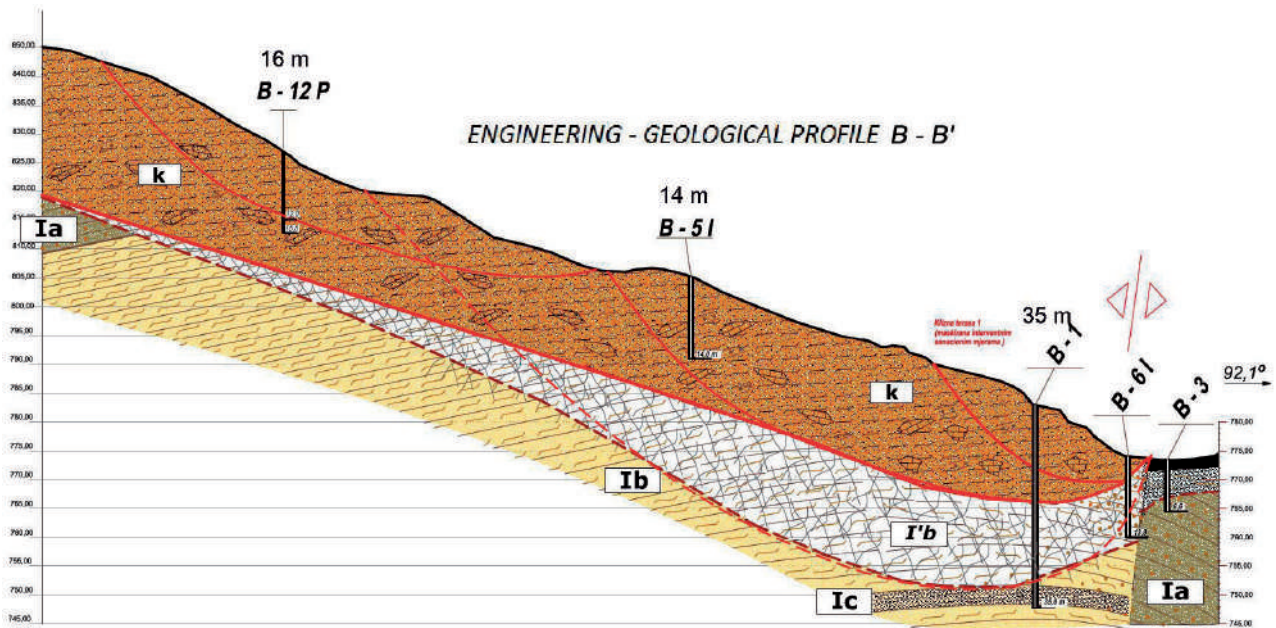


Figure 5 The part of the engineering-geological profile B-B'.

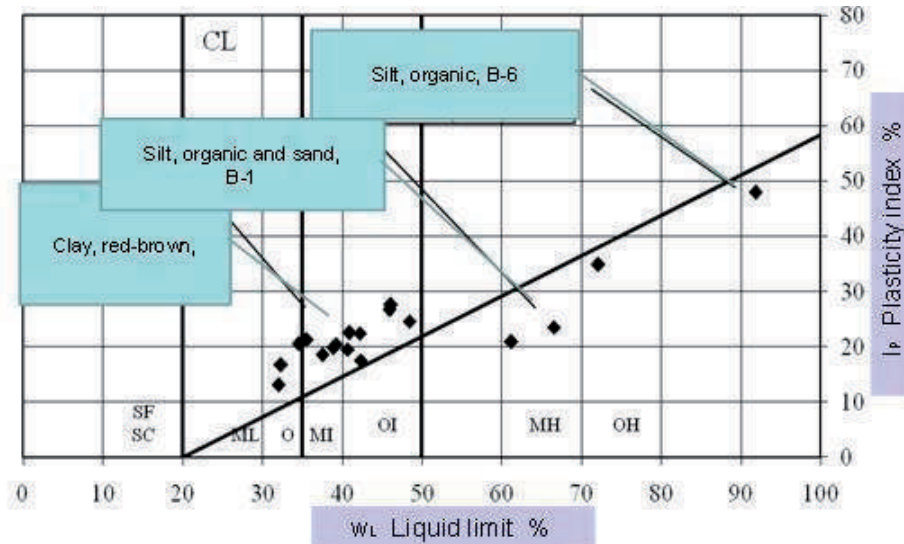


Figure 6 Plasticity index chart.

During the summer of 2012 many of the forest trees were cut down and driven away, so that the investigation was not finished up to the end of summer 2012. On the basis of the research it has been found that the terrain consists of soil and rock mass units, as follows:

a) Clay, silty, sandy, red-brown, with limestone blocks and sandstone, soft to hard;

The general characteristic of clay soils is their poor permeability (Stević 1991). Permeability increases at the central and frontal part of the landslide because they contain a higher percentage of sand and sandstone. However, this clay can have a higher permeability in the sliding cracks, and sandy layers. Movement of the water through this layer is irregular and dependent on the sliding surfaces (Selimović 2000). Due to the presence of silt and sand, the clay has a characteristic of rapid decomposition under the influence of water and air, so that the landslide body turns into a muddy plastic mass during a rainfall period. The strength of the clay is satisfactory. Under natural conditions, without the influence of the hydraulic pressure, it can hold on the slope without slipping.

b) Silt, organic, sandy, gray-brown, soft;

The silt is the main cause of landslides. Organic silt is of a high plasticity. It has the following characteristics: unit weight of 18 kN/m³, liquid limit 60–100% (Fig. 6). It has low shear strength. Due to the sliding process it is partially mixed with clay.

c) Claystones, red-brown, very hard;

Red-brown claystones are defined as the substrate at the landslide. They are characterized by high strength, relatively low moisture content and higher volume weight when compared to clay. They are mostly concentrated in the foot of the landslide. Claystones are waterproof. They are located below the sliding surface

and are stable. However, despite their good qualities, layers of sand or organic silt can be found there as well.

d) Sandstones, gray and gray-brown, hard;

Sandstones are predominantly located in the central and head part of the landslide. They represent the substrate covered with, silty, sandy, red-brown clay. They occur in layers, and are subject to frequent changes. The investigation revealed the presence of local anticlines and synclines which are the result of a geological process of harvesting. Layered structure allows greater permeability because of its discontinuities (Stević 1991). It is considered that they represent the aquifer in the upper part of the slope and provide a year-round watering of the landslide.

e) Limestone;

Limestone's form a "cap" over the sandstone layer. They are located outside the landslide area. On the north, the left wing landslide has no limestone. Limestone's can be found in the distance in the form of large blocks and they are not adjacent to the landslide. Limestone environment is highly permeable, and is susceptible to erosion and karstification. In contact with sandstones, limestone bring a certain amount of water soaking the body of the landslide. There are a lot of limestone blocks and particles which have been transported to and deposited in the landslide body.

Slope stability analysis

The Slope Stability analysis was conducted using GGU software packet and the Bishop Method. Back analysis was used in order to find a potential sliding surface. It has been calculated that the factor of safety increased by approximately 20 %, after the drainage of the landslide and lowering of the groundwater level (Fig. 7, 8).

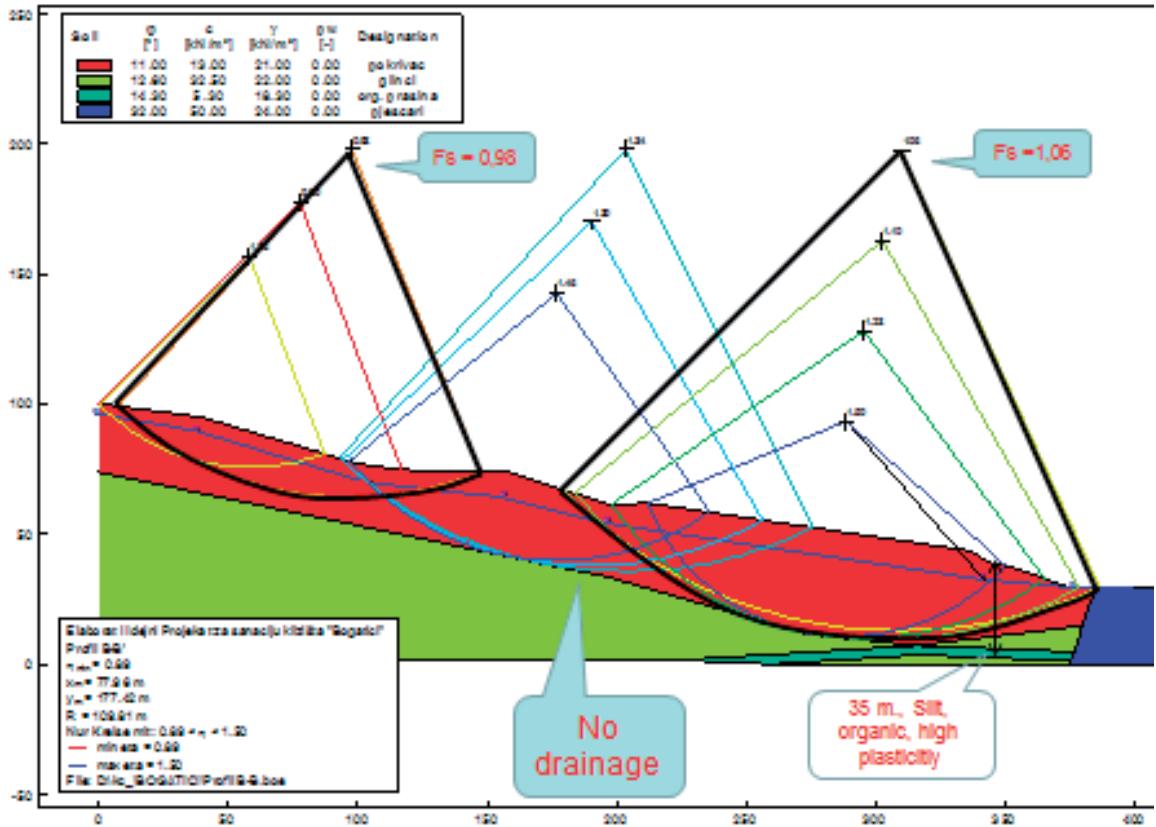


Figure 7 Back analysis without groundwater drainage.

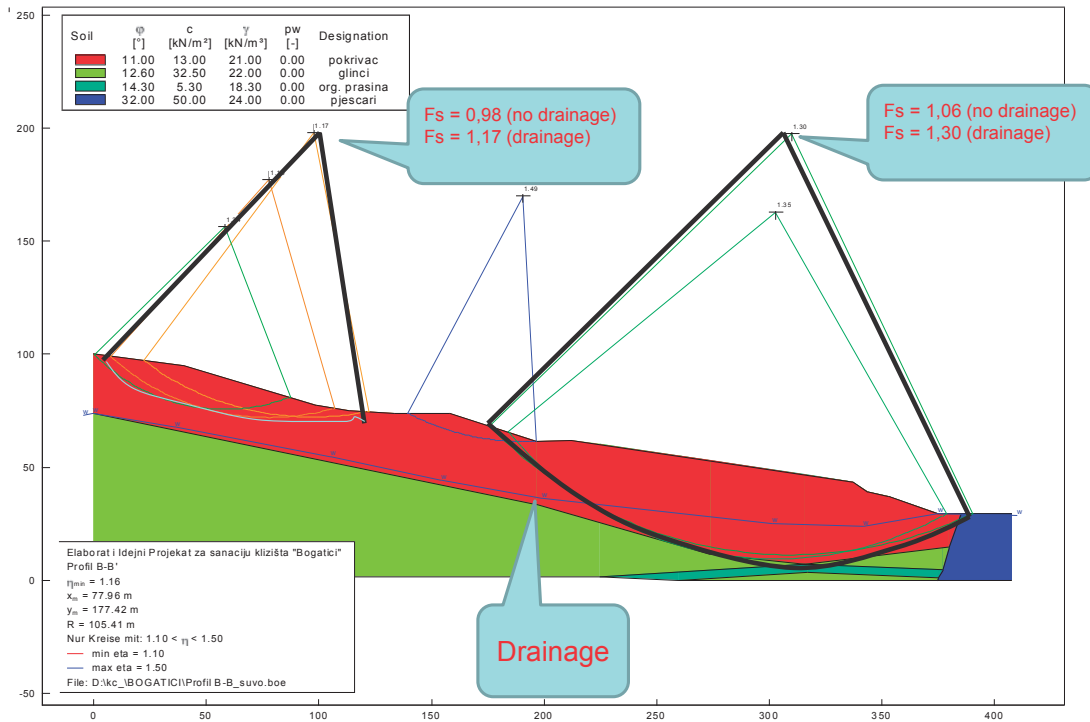


Figure 8 Back analysis, case with groundwater drainage.

Conclusion

The main causes of triggering mechanisms of the landslide activation were: high water content and the presence of organic silt material in the landslide body. The mechanism of triggering was periodically discontinued. The landslide was activated in June during heavy raining periods. The landslide is divided into two parts: A_g –the upper and A_d – the lower part A_g part of the landslide has a translational motion but A_d part has a semi-rotational motion (RGGF 2012).

The slope stability analysis was performed by means of back analysis. It was assumed that the actual safety factor was approximately 1.0. After a calculation with drainage and lowering water level option, a new safety factors were obtained with the increase of about 30-35 %. There was a passive failure at the foot of the landslide, but an active pressure failure occurred at the head and the middle parts of the landslide.

The first remediation measure is a reducing of ground water level in the upper part of the landslide. The second remediation measure is removing the sliding mass out of the landslide body. Reduction of the water level has to be done by digging ditches as a type of surface drainage, by a shallow drainage system and, finally, by a drainage tunnel. Removing sliding mass has to be done at the A_d –lower part of the landslide to prevent semi-rotational sliding.

References

- Faculty of Mining, Geology and Civil Engineering Tuzla (2012) Geotechnical report and preliminary design of remediation of the Bogatići landslide, Tuzla, pp 1-67. (In Bosnian)
- Selimović M (2000) Soil mechanics and foundation. University Džemal Bijedić, Mostar, pp 473-490. (In Bosnian)
- Stević M (1991) Soil and rocks Mechanics, Faculty of Mining, Geology and Civil Engineering, Tuzla, pp 15-21. (In Bosnian)

Instability Phenomena and Mitigation Measures in the Area of the Cluj Ethnographic Museum

Silvaş George-Cătălin

University of Bucharest, Faculty of Geology and Geophysics, Bucharest, Romania, Traian Vuia Str. 6, Sector 2, ++021 318 15 57

Abstract The complexity of the problems and the negative consequences that concern the slope instability phenomena drive some researchers to compare it with „*a demon who laughs at the human competence*” (Stanciu 2006). The Ethnographic museum is situated on the northern side of the Hoia Hill and consists of very old houses that are part of the historical heritage of Romania. The integrity of the historical constructions is endangered by the effects of landslide movements. The cliffs have the S-N orientation, with steep cliffs towards south and a gentle cliff towards north. On the surface of the slope there are numerous rotational landslides, debris flows and creeps. The landslides are shallow with a depth of 4-5 m to the surfaces of rupture. The instability phenomena in the area are old and are generated by the geological and hydrogeological factors. Despite of the influence of these factors there was another factor, the human activity, that in 2008 triggered slope activity that lead to landslides affecting the museum. A big industrial park in construction in the base of the slope needed some cuts to be constructed. The geologic factor is represented by a lithology with poor geotechnical parameters. The geological profile consists of clays with gravel and cobbles and sandy layers (deluvium), clays and silts (loess) and in some areas weathered sandstone. The presence of silts and sandy layers raised some questions about the stability of the slope. As measures of mitigation of the Hoia Hill's northern slope there were proposed retaining walls and drainage systems.

Keywords slope, instability, modelling, analysis, mitigation

Introduction

The Hoia Hill is one of many hills surrounding the Cluj city area. This area is situated in the western part of the Transylvanian Basin, in Romania. The Hoia Hill northern slope bears a big cultural and historical importance to the

Romanian people, namely the Cluj Ethnographic Museum. This museum consists of Romanian houses, churches, barns, etc., taken from various regions of the country. These houses reflect the Romanian way of living between the 16th and 18th centuries. Hence, because of the instability phenomena triggered in this area, the integrity of these constructions is in danger. In 2009 a group of geological engineers and construction engineers started a project concluded in identifying the causes of the instability phenomena, analysis and mitigation measures for ensuring the integrity of the houses at the Cluj Ethnographic Museum.

Study area

The study area is the northern slope of the Hoia Hill. Geographically, geomorphologically and geologically speaking this area is a part of the Transylvanian Basin (Fig. 1). The geological settings of the study area are a result of a sinking of the crystalline-mesozoic relief, which took place from the beginning of the superior cretaceous until the Pliocene. Hence the geology is represented by pre-tertiary bedding structured in the crystalline bedrock and a Mesozoic sedimentary covering, and over them lays the tertiary formations (Mutihac et al. 2004).

The tectonics reveals that Transylvanian Basin is a post-tectogenetic basin and it has formed at the end of the Jurassic (Săndulescu 1984).

The slopes in the Transylvanian Basin are often affected by landslides. The slope's instability factors existing type of soils, the underground water and the human activity at the base of the slope.

The landslides are shallow with slip surface depth of 4-5 m and with rotational and translational movements of a sliding material. They are old and recent, semi-stabilized, reactivated and active landslides (Fig. 2, 3).

The instability phenomena are predominant on the northern slopes; it seems that these slopes are more prone to landslides.

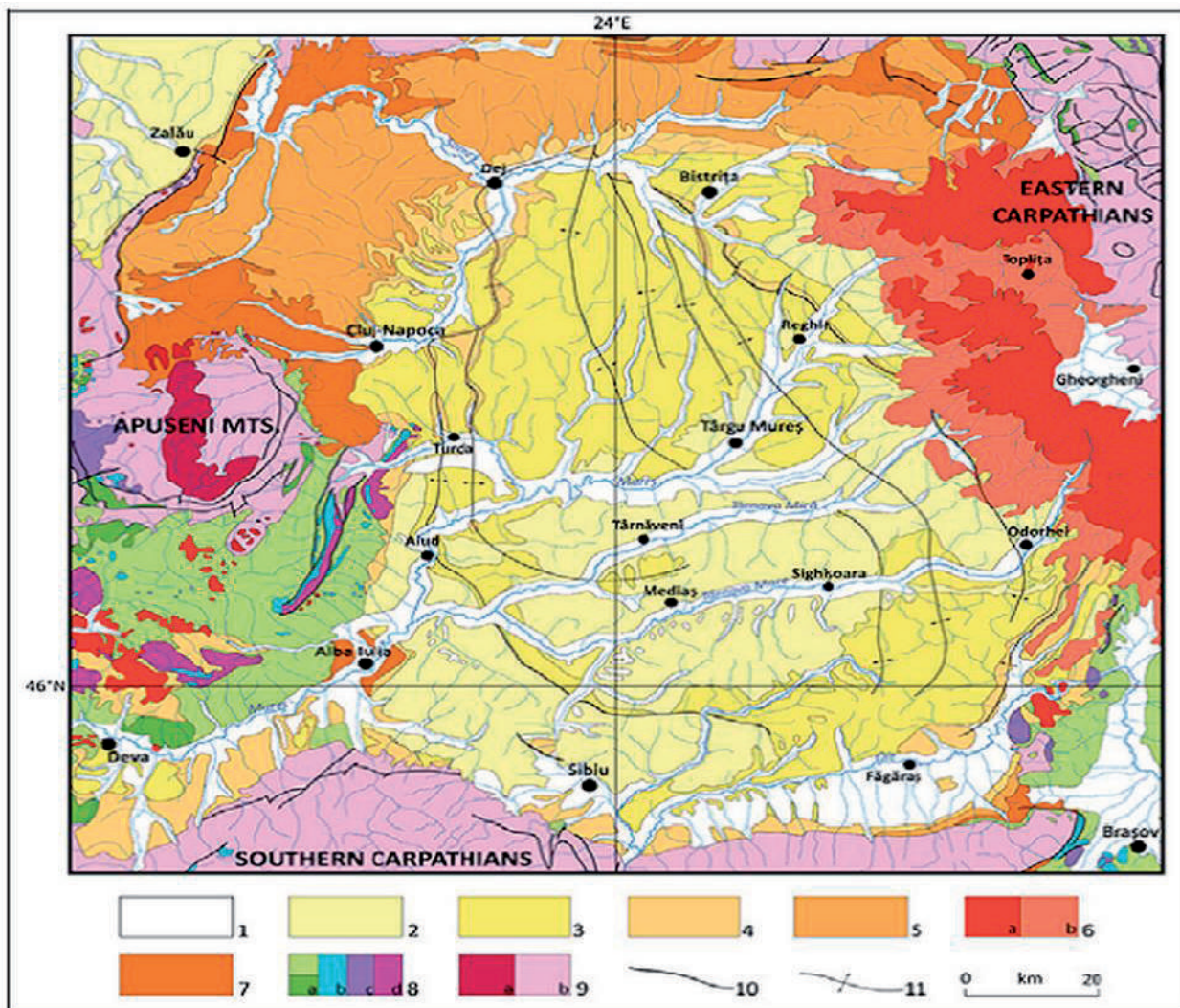


Figure 1 The Transylvanian Basin geological map; 1. Quaternary, 2. Pannonian, 3. Sarmatian, 4. Badenian, 5. Inferior Miocene, 6. Intrusive Neogene (a. Intrusive rocks, b. Intrusive sedimentary deposits), 7. Paleogene, 8. Mesozoic (a. Cretaceous, b. Jurassic, c. Triassic, d. Triassic-Jurassic volcanic arc), 9. Pre-Mesozoic (Filipescu et al. 2009).



Figure 2 Cluj Ethnographic Museum house affected by landslides.



Figure 3 Landslides on the Hoiia Hill northern slope.

Instability phenomena causes

The Hoia Hill northern slope landslides are determined by the low strength characteristics of existing types of soils, high ground water level in the slope and human activity at the base of the slope.

The geological cross section intercepted by the drillings executed throughout the investigation program is represented by clays with gravel and cobbles, silt and silty clays (loess), sand and sandy clays and in some areas weathered sandstone. Undisturbed and disturbed samples were taken from the boreholes for laboratory testing. The results of laboratory testing pointed that the main cause of the landslides was the presence of sandy layers with poor mechanical properties. The further conclusion was that the sandy layers are also prone to liquefaction in rainy seasons. The underground water intercepted in the sand layers with high discharges gave a significant influence on the landslide triggering in the past.

The recent and reactivated landslides were triggered by the human activity in the base of the slope. In 2008 the construction of an industrial park started the base of the slope. Some cuts were executed in different areas of the site that affected the stability of the slopes.

3D Modelling of the study area

The 3D model of the study area was generated using the Rock Works software (Fig. 4). The 3D models were also generated for six landslides in the study area. The 3D models gave information about the orientation of the slopes, degree of slope inclinations and areas where the landslides were triggered. The slope has an inclination between 10° and 30°. The affected areas on the slope surface are marked with circles (Fig. 4).

Stability analysis of the Hoia Hill northern slope

Using the 6 profiles at the slopes most prone areas to landslides, stability analyses were performed. The software used for the stability analysis was GEO 5. This geotechnical software uses an analytical and finite element analysis solution to solve a large number of geotechnical problems commonly encountered.

Using the Bishop slope stability method, the safety factors of the analyzed slopes were calculated. In the Bishop method the rupture takes place at a cylindrical slip surface defined with a rotation axis and radius of slip surface. The shear resistance along the slip surface is not dependent on the realized deformations of the landslide body. The landslide body is divided into a series of vertical slices. The safety factor (F_s) is the ratio between the available shear resistance (τ_{fi}) and the slip share resistance (τ_{ei}), given by equation [1] and [2] (Stanciu 2006).

$$F_s = \frac{\tau_{fi}}{\tau_{ei}} \quad [1]$$

$$F_s = \frac{\sum_1^n (\sigma - u_i) \cdot \operatorname{tg} \varphi_i'' \cdot \Delta_{si} + \sum_1^n c_i'' \cdot \Delta_{si}}{\sum_1^n \tau_i \cdot \Delta_{si}} \quad [2]$$

where:

$\sigma_i = \frac{N_i}{\Delta_{si}}$ [3] - total stress, uniform distributed on the slice surface (i),

$u_i = \frac{U_i}{\Delta_{si}}$ [4] - pore pressure at the middle of the slice base (i),

τ_{fi} - shear stress induced by the soil weight and the external forces at the base of the slice, the shear strength necessary for the assurance of $F_s=1$,

φ_i'', c_i'' - shear strength parameters: friction angle and cohesion,

Δ_{si} - the length of the slice at the slip surface.

The most important information for the stability analysis is: (1) the parameters of existing soil types, and (2) the ground water level. In the process of the stability analysis there were taken in consideration the following hypothesis: (1) the slope in a natural state, (2) the slope in a natural state affected with an earthquake, (3) the slope with a ground water table at a depth of -1,00 m, (4) the slope with a underground water table at a depth of -1.00 m affected with an earthquake, (5) the slope with a ground water drained to the bedrock and (6) the slope with a the ground water drained to the bedrock affected with an earthquake.

Stability analysis results

In hypothesis (1) it can be observed that the safety factors (F_s) of the slope in the natural state are between 1.01 (profile no. 2) and 1.52 (profile no. 3). The water table in this hypothesis is for profile no. 1 at a depth of -6.30 m, for profile no. 2 at -7.00 m, for profile no. 3 at -9.00 m, for profile no. 4 at -9.50 m, for profile no. 5 at -2.50 m and for profile no. 6 at -5.00 m.

In hypothesis (2) with an induced earthquake (horizontal seismic coefficient $k_h=0.20$, vertical seismic coefficient $k_v=0.12$), the F_s values are very low. The F_s has values between 0.58 (profile no. 1) and 1.15 (profile no. 3). In the areas of profile no. 1, 2, 4, 5, 6 the F_s are smaller than 1.00, so the area is affected by instability in case of earthquake occurrence.

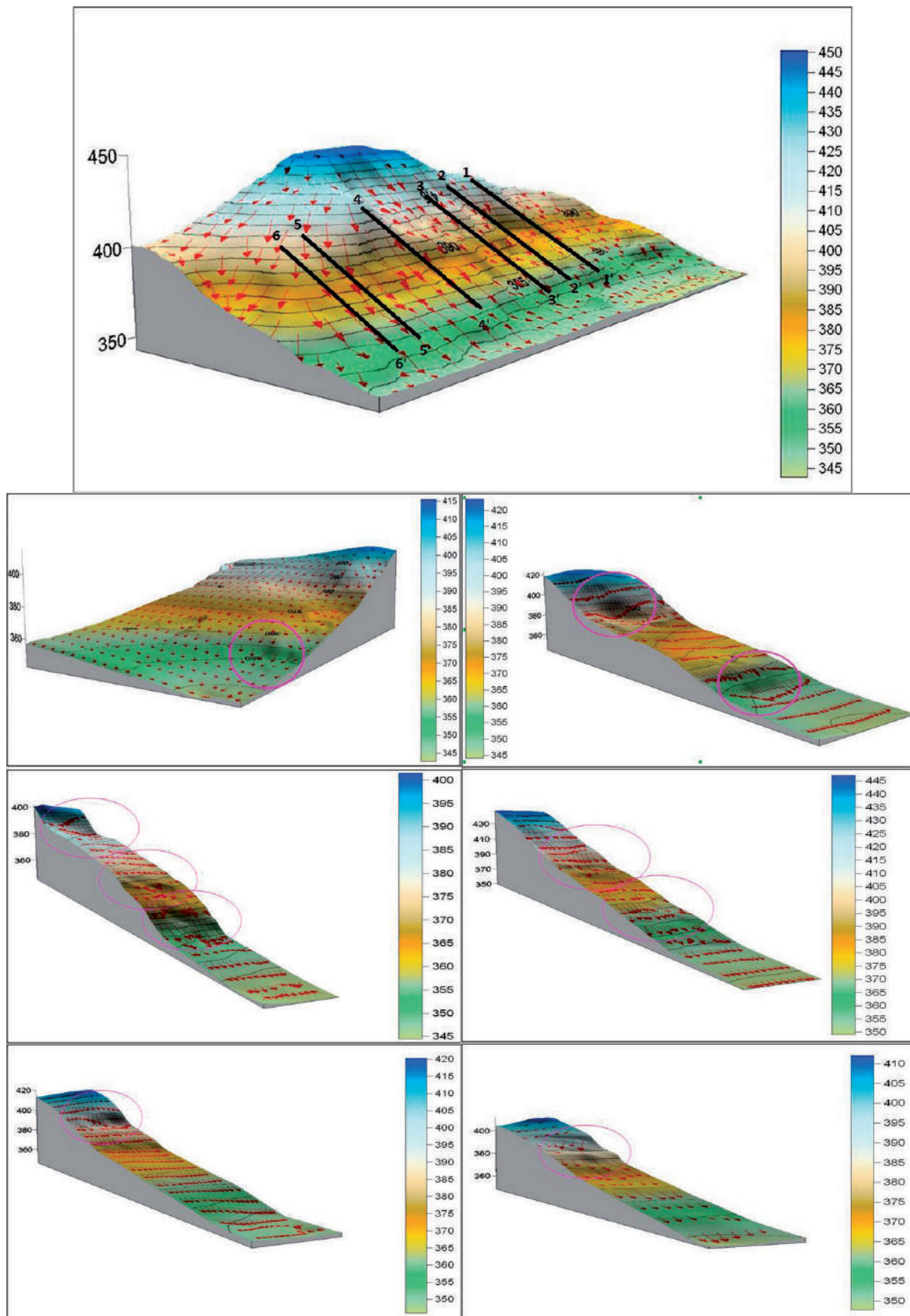


Figure 4 Hoia Hill northern slope, b profile 1-1', b profile 2-2', c profile 3-3', d profile 4-4', e profile 5-5', f profile 6-6' 3D models.

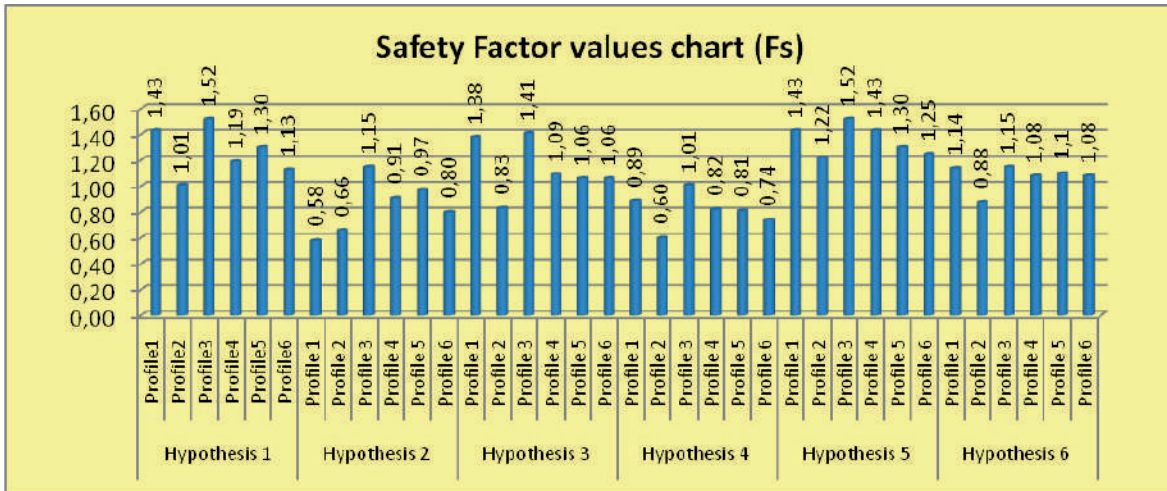


Figure 5 Results of the stability analyses in the area of the Hoia Hill northern slope.

In hypothesis (3) where the ground water table is at a depth of -1.00 m, the F_s has values between 0.83 (profile no. 2) and 1.41 (profile no. 3). Only in the area of the profile no. 2 the F_s value is below 1.00 .

In hypothesis (4) where the underground water table is at a depth of -1.00 m and the possibility of an earthquake the F_s are very low between 0.60 (profile no. 2) and 1.01 (profile no. 3). The areas with F_s lower than 1.00 have stability problems.

In hypothesis (5) where the underground water table is drained until it reaches the bedrock, the F_s values are the biggest of all the rest of the hypothesis. The F_s values are between 1.22 (profile no. 2) and 1.52 (profile no. 3).

In hypothesis (6) where the underground water table is drained and with the possibility of an earthquake (horizontal seismic coefficient $k_h=0.20$, vertical seismic coefficient $k_v=0.12$), the F_s values are between 0.88 (profile no. 2) and 1.15 (profile no. 3). In the case of profile no. 2 the F_s has values below 1.00 , hence the area has stability problems. In Fig. 5 are presented all the stability analysis results for the 6 analysed geological profiles.

Mitigation measures

For assuring the stability of the entire slope in all possible analysed condition it is mandatory to adopt adequate mitigation measures. These mitigation measures must ensure the general and local stability of the slope. The stability analysis gave information about the areas prone to landslide occurrence. To assure stability requests the following mitigation measures were constructed: (1) 16 arrays of drainage systems, (2) 4 arrays of retaining walls with pile foundations, (3) the recovery of the existing ditches and the construction of supplementary ones and (4) the recovery of the existing siphon drainage arrays.

Discussion and conclusions

The instability phenomenon affects the Hoia Hill northern slope. From the results of the stability analyses conducted for six geological profiles, it can be observed that the area of the Hoia Hill northern slope is prone to landslides. The stability condition was that $F_s \geq 1.00$. There are some cases where the stability condition wasn't fulfilled. In the case of hypothesis 5 the stability of the slopes is theoretically assured. So if the ground water is drained to the bedrock the instability issue in the study area will be resolved. Hence the mitigation measures adopted in the case of the Hoia Hill northern slope will assure both the local and general stability.

Acknowledgments

The research was possible with the help of S.C. Proexrom S.R.L. Company.

References

- Filipescu S, Miclea A, De Leeuw A (2009) Microfauna changes around the Sarmatian/Pannonian boundary in the Transylvanian Basin. In Peryt, D., Kaminski, M.A. (eds) Abstracts and Excursion Guide of the 7th Micropaleontological Workshop MIKRO 2009. Grzybowski Foundation Special Publication. pp. 15, 23.
- Mutihaç V, Stratulat I M, Fechet M R (2004) Geologia României. Didactică și Pedagogică. Bucharest.
- SC Proexrom S R L (2009) Geotechnical expertise and geotechnical study regarding the instability of the Hoia Hill slope's, Cluj-Napoca County, Romania.
- Săndulescu M (1984) Geotectonica României. Tehnică. Bucharest.
- Stanciu A, Lungu I, (2006) Fundații. Tehnică. Bucharest.

Instabilities of Open Pit Cut Slopes: Case Study from the Torine Quarry in Croatia

Mirko Grošič⁽¹⁾, Sanja Bernat⁽²⁾, Željko Arbanas⁽³⁾, Snježana Mihalić Arbanas⁽²⁾, Igor Matjašić⁽⁴⁾, Damir Vidović⁽¹⁾

1) Geotech Ltd, Rijeka, Croatia, Moše Albaharija 10a, +385 99 4058 998, mirko.grosic@geotech.hr

2) University of Zagreb, Faculty of Mining, Geology and Petroleum Engineering, Zagreb, Croatia

3) University of Rijeka, Faculty of Civil Engineering, Rijeka, Croatia

4) Calx Ltd, Zagreb, Croatia

Abstract In most cases, once the slope stability analyses of future quarry cuts are completed and mine management accepts results and designs, the geotechnical consulting is outsourced from further activities such as excavation plan design, excavation and mining and necessary activities on engineering geological mapping of excavated cuts, geotechnical supervising and active geotechnical design are not carrying out. This approach often leads to occurrences of local or global instabilities of quarry cuts. This paper presents a case study of global instability of open pit slopes in the Torine open pit that is situated in the Pannonian Basin, near the city of Gradac Našički in Croatia. Exploitation zone of basalt rock mass is underlain by chlorite schist rock mass. Sliding of basalt rock mass was developed along the slip surface at the geological contact with chlorite schist. Exploitation has been continuing even after sliding occurrence, without any previous remediation. On the basis of engineering geological mapping results, three separate landslide phenomena were determined. Despite its fact, the exploitation in the Torine open pit is continued till nowadays.

Keywords open pit, instability, landslide, rock mass

Introduction

The environment of rock slopes in which open pits and other types of cuts are excavated is positioned in an area of low stresses near the surface, and the global stability of slopes is controlled by geological elements such as faults, discontinuities, alteration of different geological units and position of weathering zones. The presence of these elements cannot be controlled and changed, but during the design process the presence of these factors should be considered and taken into account as part of slope design and stability evaluation. Among these major factors, some of minor scale geological elements, such as joint and fissure orientations, may have an influence on slope stability, commonly on a local scale.

In the most of cases, once the slope stability analyses of future quarry slopes are completed and mine management accepts open pit designs, the geotechnical consulting is outsourced from further activities such as excavation plan design, excavation and mining. Additional necessary activities on engineering geological mapping of excavated cuts, geotechnical supervising and active geotechnical design are usually not involved in the excavation process. This irrational, but very often present approach, caused by inadequately control of excavation process commonly leads to local or global instabilities.

This paper presents a case study of global instabilities of open pit walls in the Torine quarry located near the city of Gradac Našički, Croatia (Fig 1). Sliding of basalt cuts was developed along the slip surfaces at the geological contact with chlorite schist rock mass. Engineering geological conditions, instability description and slope stability analysis of occurred instabilities are presented in this paper.

Open pits design

The design of open pits cuts includes a significant number of steps and levels of analyses required to confirm design stability, from the bench geometry and overall stability of the pit walls to the evaluation of the design performance and calibration of parameters (Carvalho 2012). Input data from monitoring that are collected during the initial pit construction phases are often used for optimization of remaining phases of pit construction.

In mining, economic advantages can be obtained in varying the geometry (slope angle and bench geometry) of the cuts, whereas in civil engineering, the possible consequences of a slope failure, especially in urban areas, necessitate a more conservative design. In mining, slopes are sometimes designed with slope angles that often bring the risk of possible instability (Ross-Brown 1972). Stability analyses are carried out depending on the possible failure mechanism, using one of numerous established analysis methods and, as a result of the conducted analysis, the factor of safety is calculated (Arbanas et al. 2007).

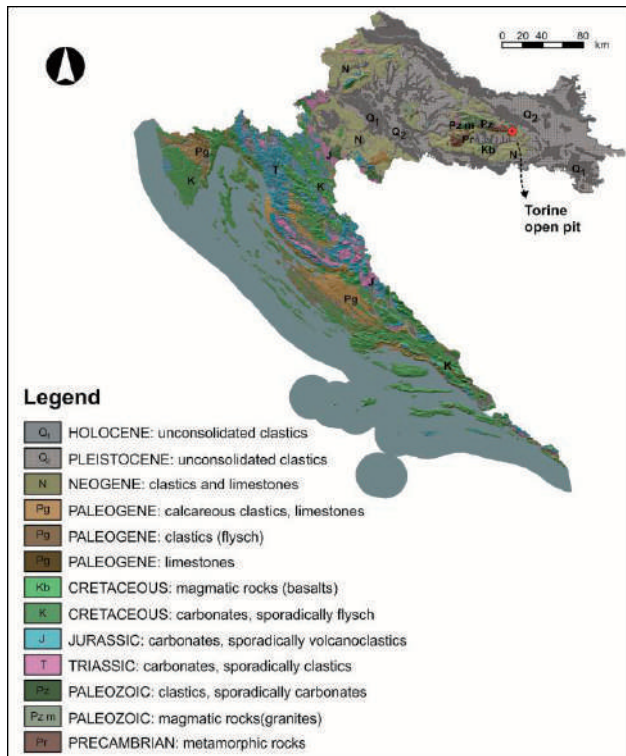


Figure 1 Geological map of Republic of Croatia and position of Torine open pit.

Observation methods and back analyses

The observational method was introduced by Terzaghi and Peck (1967) and Peck (1969) and developed further by Powderham (1998), Nicholson et al. (1999) and others. This method is based on continuous field measurements on installed equipment and conducting back analyses during the cuts construction, the results of which are then compared with numerical modelling predictions.

According to Cividini et al. (1981), there are two different ways to conduct back analyses: the inverse approach and the direct approach. In this case study the direct approach of back-analysis was used. A precondition of performing specified observation methods and back analyses is a quality monitoring system consisted of installed monitoring equipment and continue observations during construction and, at same time, exploitation phase.

Monitoring during exploitation phase

The type of instruments selected for an open pit monitoring program depends on the particular purposes need to be monitored. Monitoring system may include instruments and equipment capable to measure rock mass displacement, ground water parameters, and blast vibration levels. Short descriptions of listed monitoring methods according to Girard (2001) are listed below:

- Survey network consisting from EDM (electronic distance measurements),

- Measuring and monitoring of the changes of crack by tapes, crack-meters, pins, etc.,
- Wire extensometers,
- Inclinator measurements method,
- Time domain reflectometry (TDR),
- Piezometers and
- Tensioned rod extensometers.

The purpose of a monitoring plan (adapted from Call and Savely 1990) is to:

- Maintain safe operational practices for the protection of personnel, equipment and facilities in the quarry,
- Provide warning of instability so action can be taken to minimize the impact of slope displacement and
- Provide crucial geotechnical information to analyze the slope failure mechanism and design the appropriate corrective measures.

General remarks about instability in open pits

Types of instabilities

According to Sjöberg (1996) the factors governing large scale open pit instability are primary:

- The stress conditions in the pit slopes, including the effects of groundwater,
- The geological structure, in particular the presence of large scale features,
- The pit geometry and
- The rock mass strength.

To determine which failure modes are possible at a particular part of an open pit, the geologic parameters in various sectors of the open pit need to be quantified. Collecting of information such as orientation, spacing, trace length, and shear strength with respect to the major structures and other geologic features is an important key to determining failure potential (Girard 2001). The basic failure modes which may occur are:

- Plane shear failures - occur when a geologic discontinuity, such as a bedding plane, strikes parallel to the slope face and dips into the excavation at an angle steeper than the angle of friction,
- Wedge shear failures - occur when two discontinuities intersect and their line of intersection daylight in the face,
- Step path failure - similar to plane shear failure, but the sliding is due to the combined mechanisms of multiple discontinuities or the tensile failure of the intact rock connecting members of the master joint set,
- Raveling - caused by weathering of material and expansion and contraction associated with freeze-thaw cycles. This type of failure generally produces small rockfalls, not massive failures,
- Toppling - occur when vertical or near-vertical structures dip toward the pit and
- Rotational shear failures - occur as general slope failure along a circular arc. Rotational shear failure occurs

in slopes without critically oriented discontinuities or lanes of weakness.

Strength criteria

The strength of a large-scale rock mass is very difficult to assess. At the same time, the required accuracy for the strength parameters which are needed for the design is very high. For large-scale rock mass slopes, back analysis of previous failures proves to be the only practical mean for obtaining relevant strength parameters (Sjöberg 1996).

The difficulty associated with explicitly describing of a rock mass strength based on the actual mechanisms of failure has led to the development of strength criteria that treat the rock mass as an equivalent continuum. A relatively simple and completely empirical failure criterion for shear strength of rock mass is the Hoek-Brown failure criterion commonly used for rotational shear failure analyses (Hoek and Brown 1980a,b; Hoek 1983, Hoek et al. 1995, 2002).

Barton failure criterion for plane shear analysis was developed by Barton (1973, 1976) Barton and Chouby (1977), Barton and Bandis (1990) and Bandis (1992). This criterion studied the behavior of rock mass discontinuities based on the joint roughness coefficient and joint wall compressive strength.

Although failure criterion for rock mass is nonlinear for cases in which the stress state is relatively small the linear approximation with basic models (such as Mohr-Coulomb) could be applied.

The Torine quarry open pit cut instabilities

Study area

The Torine open pit quarry is situated about 9 km southwest of the Našice city in the Slavonia region in the eastern part of the Republic of Croatia. Torine open pit quarry lies in tectonic unit named the Krndija horst characterized by existing of normal faults and radial joint systems.

Materials extracted from the open pit are several types grey to greyish green porous basaltic rocks of Miocene age. In the study area, the basaltic rock mass is extensively fractured by columnar jointing and faulting. The network of vertical joints makes columnar basalt mass especially vulnerable to weathering. Joint systems allow infiltration of precipitation into the ground and enabled rapidly and easily weathering of basalt rock mass. The products of weathering are greenish grey and greenish yellow clays and rock fragments present on ground surface and in open joints of rock mass. Basaltic rock mass overlay Paleozoic chlorite schist, greenish grey folded rocks with schistose texture. In the study area, the Paleozoic chlorite schist is tectonically deformed and folded but permeability of these rocks is still very low.

The open pit mining in Gradec Našički started in 1954 while the modern exploitation of technical stone

using mining, machine excavation and rock crushers started in 1965. Today, the total surface area of the quarry is approximately 38 ha. The field investigations and estimations of technical building stone reserves in the Torine quarry were conducted in 1985, 1990, 2002, 2006 and 2008. During these field investigations totally 67 boreholes were carried out in the quarry area with depth from 8.0 to 50.0 m. Based on results of all these field investigations, the overall sight in geological condition of wider quarry area was established.

Landslide occurrences

In November 2012 the Torine open pit experienced a massive landslide. After the sliding occurrence, the geodetic survey of the broad landslide location was done, where the contours and cracks were instrumentally recorded. In the phase of preliminary geotechnical investigation, three landslides were determined. To determine the geological settings, landslide dimensions and the position of the slip surfaces, the engineering geological mapping was done and data from previous field investigations and laboratory testing were used. Stratigraphic data from 20 boreholes performed from 2000 to 2008 were used to model the subsurface conditions. During the engineering geological mapping of the investigated area, the landslide features such as main scarp (Fig. 2), tension cracks (Fig. 3) and landslide toe were registered. The engineering geological map with borehole locations and highlighted landslide occurrences is presented at Figure 4 and characteristic landslides geological profiles of are presented at Figure 5.

All three landslides form one unique complex landslide in basalt rock mass. The movement type of these landslides are intermediate between rotational and translational slides (Skempton and Hutchinson 1969). Surfaces of rupture have steep main scarps that are flatten with depth and are formed along the contact of basalt rock mass with completely to highly weathered Paleozoic chlorite schist formation in the bedrock zone (Fig.5).



Figure 2 Main scarp of landslide 2 in the Torine Quarry.



Figure 3 One of many secondary tension cracks at landslide 2.

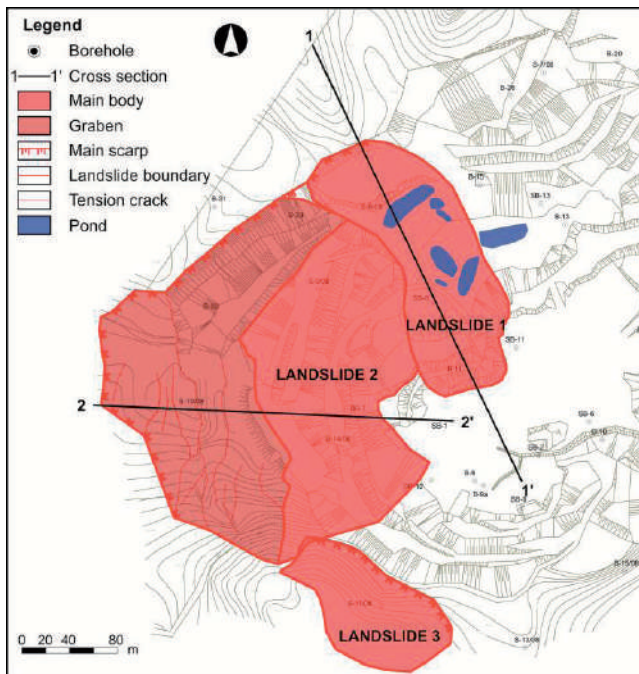


Figure 4 Engineering geological map and landslides in the Torine open pit quarry.

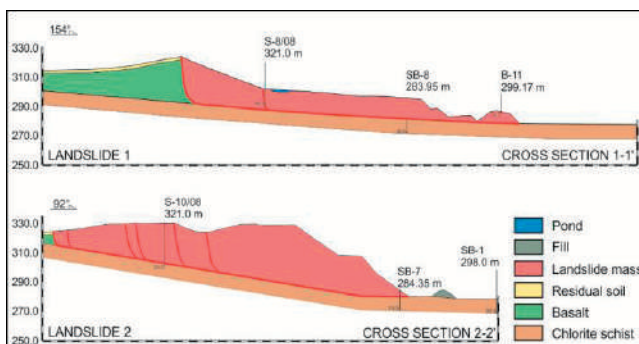


Figure 5 Geological profiles of the landslides in the Torine open pit quarry.

Landslide 1 is located in the north-eastern part of the investigated area. At the time of occurrence in

November 2012, it had a length of about 240 m, width of 78 m in upper part and 90 m in lower part and covered the area of approximately 1.9 ha. Assuming a maximum depth of 26 m at the center of the sliding surface and a flat slip plane, the landslide volume is estimated to be about $5 \times 10^5 \text{ m}^3$. Landslide 1 is reactivated multiple slide; the surface of rupture is extending in the direction of movement and the slide shows repeated development of the same type of movement.

Landslide 2 in the central part of the investigated area has the length of about 248 m, width of 320 m and cover the area of approximately 6.2 ha. With a maximum depth of 40 m at the center of the sliding surface, the landslide volume is estimated to be about $25 \times 10^5 \text{ m}^3$. Landslide 2 is characterized with uphill-facing scarp in displaced mass and the subsidence of blocks of displaced material to form depressed area, graben. Landslide 2 is enlarging, multiple reactivated slide; the surface of rupture is extending in two directions and it shows repeated development of the same type of movement.

Landslide 3 in the southern part of the investigated area has a length of about 70 m, width of 150 m and covered an area of approximately 0.9 ha. Maximum depth of slide was 5 m and the landslide volume is estimated to be about $0,75 \times 10^5 \text{ m}^3$. Landslide 3 is extending reactivated slide; the surface of rupture is extending in two directions.

High permeability of basalt rock mass in the landslide body enhances infiltration of precipitation water to the surface of rupture, which affects increase of the ground water table and pore pressures at the slip surface with consequently decreasing of effective stresses and material strength at the slip surface. Increasing of ground water level additionally accelerates the sliding process. During the engineering geological mapping, the presence of water was registered on the surface of landslide 1 in the form of lakes and large ponds (Fig 4).

The most commonly measured discontinuities are columnar joints. Fractured rock mass in open pit has a low RQD value, which indicates on very low physical and mechanical rock mass properties. The stability of man-made rock slopes in the Torine open pit quarry is greatly dependent on the orientation and shear strength of the discontinuities in the basalt rock mass.

Slope stability analysis

The back-analysis is a more effective method of estimating the shear strength of the material than any in-situ or laboratory tests. Back-analysis method is consist of defining the representative cross section and varying the shear strength of material until the factor of safety equals approximately unity ($F_S \approx 1.0$). The back-calculated shear strength of material is then used for further analysis of mitigation measures.

The slope stability back-analyses were performed for engineering geological profile 3-3' that represents landslide 2 (Figs 4 and 5). Analyses were conducted using FLAC Slope 7.0 software (Itasca 2002) that is used

Table 1 Geotechnical parameters of geotechnical units obtained from back-analysis.

Description	Symbol	Value	Unit
Geotechnical unit 1 - Basalt			
<i>Rock mass characteristics</i>			
Internal friction angle	φ_k	40	°
Cohesion	c_k	350	kN/m ²
Unit weight	γ_k	23	kN/m ³
<i>Characteristics of discontinuities</i>			
Internal friction angle	φ_k	40	°
Cohesion	c_k	350	kN/m ²
Dip of discontinuities	α	110	°
Geotechnical unit 2 – Chlorite schist CW/HW			
Internal friction angle	φ_k	25	°
Cohesion	c_k	10	kN/m ²
Unit weight	γ_k	21	kN/m ³
Geotechnical unit 3 – Chlorite schist SW/F			
Internal friction angle	φ_k	32	°
Cohesion	c_k	50	kN/m ²
Unit weight	γ_k	21	kN/m ³

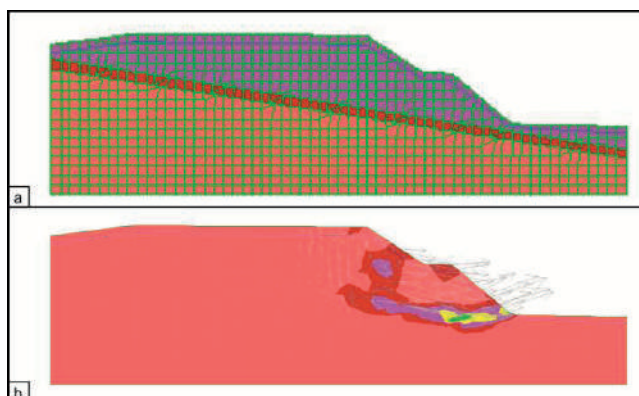


Figure 6 Numerical model and results of representative geological cross section 3-3': (A) Numerical model; (B) Results of stability back-analysis.

strength reduction method to calculate factor of safety. This numerical method is widely used and accepted in geotechnical engineering (Dawson and Roth 1999, Griffiths and Lane 1999).

Engineering geological profile was divided into 3 different geotechnical units: basalt (modeled as Ubiquitous-joint model) and chlorite schist that is divided according to the weathering stage as completely weathered/highly weathered (CW/HW) and slightly weathered/fresh (SW/F) (modeled as Mohr-Coulomb model). Characteristic input geotechnical parameters for each of geotechnical units, obtained from back-analysis, are presented in Tab. 1.

Although the Ubiquitous-joint model is more appropriate for numerical modeling of layered sedimentary rocks, in this case study it is applied to model the basalt rock mass unit using the possibility to model the presence of vertical weakness orientation within a basalt rock mass. Using this model it is possible to model the formation of vertical tensile cracks that

corresponds to the real circumstances in the basalt rock mass in the field.

Stability back-analyses were performed for representative geological cross section 2-2' (Fig. 6a). Numerical model and results of stability back-analysis are presented in Fig. 6b where is clearly visible the yielding zone in basalt rock mass which is correspondent to position of initial surface of rupture in the field.

Conclusions

In the most of cases the instabilities occurred on the open pit cuts in quarries in Croatia are consequence of inadequately carried out slope stability analyses or lack of monitoring, engineering geological mapping of excavated cuts, geotechnical supervising and active geotechnical design during the excavation process.

Instability presented in this paper occurred during exploitation phase of the Torine quarry in Slavonia. During the exploitation and forming of open pit cuts, the monitoring system was not applied and back analyses based on real structural elements of rock mass identified in cuts after excavation were not performed. The exploitation after the first landslide occurrence was continued and excavation activities were moved on the other parts of the quarry caused new instabilities. Geological and geotechnical experts were included in the problem in the moment when instabilities were enlarged over the border of the quarry and endangered wider area.

In current practice in Croatia, when the field investigations, slope stability analyses and open pit design are completed and accepted, the geotechnical consulting is outsourced from further activities such as excavation plan design, excavation and mining. The present regulations those concern the procedures of quarry's slope stability control during the open pit excavation, should be updated by rules those include advanced practice in rock slope stability using observational methods and active design procedures. By the proper monitoring systems and applying of observational method and active design as a part of the open pit excavation process, these global failures could be prevented or reduced in time.

References

- Arbanas Ž, Grošić M, Kovačević M S (2007) Rock Mass Reinforcement Systems in Open Pit Excavations in Urban Areas, Proc. Int. Symp. on Rock Slope Stability in Open Pit Mining and Civil Engineering, 12.-14. September 2007, Perth, Australia, Ed. Y. Potvin, Australian Centre for Geomechanics, Perth, pp. 171-183.
- Barton N R (1973) Review of a New Shear Strength Criterion of Rock Joints. Engineering Geology. 7: 287-332.
- Barton N R (1976) A Review of the Shear Strength of Filled Discontinuities in Rock, Norwegian Geotech. Inst. Publ. No. 105, Oslo: Norwegian Geotech. Inst.
- Barton N R, Chouby V (1977) The Shear Strength of Rock Joints in Theory and Practice. Rock Mech. 10(1-2): 1-54.

- Bandis S C (1992) Engineering Properties and Characterization of Rock Discontinuities, In: J.A. Hudson ed. *Comprehensive Rock Engineering*, Vol. 1, Oxford: Pergamon Press, pp. 155- 183.
- Barton N R, Bandis S C (1990) Review of Predictive Capabilities of JRC – JCS Model in Engineering Practice, In *Rock Joints*, Proc. Int. Symp. on Rock Joints, Loen Norway, (Eds: N. Barton and O. Stephansson), Rotterdam: A.A. Balkema, pp. 603-610.
- Call R D, Savely J P (1990) *Open Pit Rock Mechanics*. Surface Mining, 2nd ed. Society for Mining, Metallurgy and Exploration, (Ed: B.A. Kennedy), pp. 860-882.
- Carvalho J L (2012) Slope stability analysis for open pit, URL: <http://www.rocsience.com> [Last accessed: April 2013].
- Cividini A, Jurina L, Gioda G (1981) Some Aspects of Characterization Problems in Geomechanics. *Int J Rock Mech Min Sci & Geomech Abstr.* 18: 487-503.
- Dawson E M, Roth W H (1999) Slope Stability Analysis by Strength Reduction. *Geotechnique.* 49(6): 835-840.
- Girard J M (2001) Assessing and Monitoring Open Pit Mine Highwalls, Proceedings of the 32nd Annual Institute on Mining Health, Safety and Research, Salt Lake City, Utah, August 5-7, 2001. Jenkins FM, Langton J, McCarter MK, Rowe B, eds. Salt Lake City, UT: University of Utah, pp. 159-171.
- Griffiths D V, Lane P A (1999) Slope Stability Analysis by Finite Elements. *Geotechnique.* 49(3): 387-403.
- Hoek E (1983) Strength of jointed rock masses, 23rd. Rankine Lecture. *Géotechnique.* 33(3): 187-223.
- Hoek E, Brown E T (1980a) *Underground Excavations in Rock*. London: Institution of Mining and Metallurgy, 527 p.
- Hoek E, Brown E T (1980b) Empirical strength criterion for rock masses. *J. Geotech. Engng Div. ASCE* 106(GT9): 1013-1035.
- Hoek E, Kaiser P K, Bawden W F (1995) *Support of underground excavations in hard rock*. Rotterdam: Balkema.
- Hoek E, Carranza-Torres C T, Corkum B (2002) Hoek-Brown failure criterion – 2002 edition. Proc. North American Rock Mechanics Society meeting in Toronto in July 2002.
- Itasca Consulting Group Inc. (2002) *FLAC version 7.0, User Manual*. Minneapolis: Itasca Consulting Group Inc.
- Nicholson D P, Tse C M, Penny C (1999) *The Observational Method in Ground Engineering: Principles and Applications*, Report 185, CIRIA, London.
- Peck R B (1969) Advantages and limitations of the observational method in applied soil mechanics. *Géotechnique.* 19(2): 171-187.
- Powderham A J (1998) The observational method–application through progressive modification. *Civil Engineering Practice, Journal of the Boston Society of Civil Engineers Section/ASCE.* 13(2): 87-110.
- Ross-Brown D M (1972) *Design Considerations for Excavated Mine Slopes in Hard Rock*, Research Report No. 21, Departments of Civil Engineering, Geology and Mining and Mineral Technology, Imperial College of Science and Technology, London, 21 p.
- Sjöberg J (1996) *Large Scale Slope Stability in Open Pit Mining – A Review*, Technical Report 1996; 10T, Lulea University of Technology, 215 p.
- Skempton A W, Hutchinson J N (1969) *Stability of Natural Slopes and Embankment Foundations*, Proceedings of the Seventh International Conference of Soil Mechanics and Foundation Engineering, Sociedad Mexicana de Mecanica de Suelos, Mexico City, State of the Art Volume, pp. 291-340.
- Terzaghi K, Peck R B (1967) *Soil Mechanics in Engineering Practice*. John Wiley, New York.

Experimental Study on the Motion Mechanism of Submarine Landslides and the Impact Force on Communication Cables

Yohei Kuwada⁽¹⁾, Fawu Wang⁽²⁾, Tomokazu Sonoyama⁽¹⁾, Mitsuki Honda⁽¹⁾

1) Shimane University, Graduate School of Geoscience, Matsue, Japan

2) Shimane University, Department of Geoscience, Matsue, Japan, Nishikawatsu 1060, +81 852 32 9878

Abstract Globally, fiber optic cables are important communication equipment used in transmission of information, but these cables are damaged by submarine landslides. When cable failure occurs, the economic loss is vast for cable restoration coupled with temporary or permanent breach in information transmission. Submarine landslides are usually triggered by many factors which include rapid sedimentation, retrogressive failure, earthquake and tectonic activity, gas hydrate dissociation and wave loading. These activities cause severe damage to transocean fiber optic cables. Direct observation of this phenomenon has not been successfully carried out because these events occur deep beneath the sea surface, and direct observation of submarine landslide would be extremely expensive and difficult because of its unpredictability. The aim of this study is to use experimental approach to analyze and understand the motion mechanism of submarine landslides and its effect on communication cables. An experimental apparatus to study submarine landslides was developed for this purpose. Soil and water can be put in the apparatus and a model cable is fixed in the rotatory part, so the relative motion of the landslide and cable can be measured and evaluated. Using this apparatus, normal stress, shear stress, pore water pressure on the bottom of the apparatus and impact force on a communication cable model were measured. From data obtained from series of experiments, friction angle of submarine landslides and impact force on a communication cable were obtained. In addition, small plastic balls which have specific gravity similar to silica sands were used as tracers to observe the characteristic bulk movement of soil masses during the experiments. Result obtained from the experiments show that four critical values of velocities of soil mass flow evolution conditions exist in these experiments, and impact force on the communication cable model and friction coefficient shows different tendencies of increment before and after the critical value of velocity.

Keywords Submarine landslides, internal friction angle, soil type, cable, impact force

Introduction

All over the world, communication cables cross oceans between continents. These cables may be damaged by

submarine landslides, causing interruption in data transmission, and abrupt breach in international communications. The economic loss is vast when cables are cut, due to the cost of cable restoration and loss of valuable information. For instance, many communication cables were cut in the south sea of Taiwan after an earthquake in December 2006. Based on broken time records of the cables, it was concluded that a submarine landslide was triggered by the earthquake, and the cables were cut by the landslide motion from the continental shelf towards the deeper part of the sea floor (Hsu 2008). According to a report by ICPC (2009), 2,162 cable breaks were recorded between 1960 and 2006. Of these, at least 20% were directly influenced by submarine landslides or turbidity currents.

Submarine landslides were initially studied for the needs of resource development in the ocean (Shanmugam 2000). For the purpose of clarifying the mechanisms of geo-hazards such as tsunami, many investigations and exploration have been conducted in the North European oceans, especially in Norway, and the United States of America. Geophysical approaches have been employed during field investigations, which have contributed immensely to the understanding of the topographic features of the ocean floor. It has been observed that common features of submarine landslides are that: (1) the movement covers large areas; (2) the motion can continue even at very gentle slopes, as low as 0.1 degrees (Kokusho and Takahashi 2008). Mohrig et al. (1998) conducted model tests in the laboratory and confirmed that the mechanism of submarine landslides involve a hydroplaning phenomenon. Hydroplaning phenomenon leads to low shear resistance of submarine landslides, causing long run out movement even at gentle slopes.

Many features of submarine landslides and damages they cause to communication cables are unclear, because these events occur beneath the sea's surface. Direct observation of submarine landslides is extremely expensive, and their unpredictability makes it difficult and relatively impossible. Our interest in submarine landslides lies in disaster mitigation of communication cables. In our study, we seek to understand: (1) the motion mechanism of submarine landslides, and (2) the mechanism of submarine landslide damage on communication cables. For these purposes, an apparatus to simulate the relative motion of submarine landslides

and impact on communication cables was developed in the laboratory, and series of experiments were conducted. Although it is difficult to simulate the flow conditions which occur in deep waters, we hope the test results provide some hints for communication cable design and cable positioning in the ocean.

Submarine landslides apparatus

The apparatus has the shape of a car-wheel, with an axle in the centre, and a trough in its inner circumference (Fig. 1). The axle is connected to a motor so the apparatus can rotate on the vertical plane. Soil and water that are used to simulate the submarine landslide are placed in the trough. Under the action of gravity, water and soil settle in the lower part of the apparatus. When the frame of the apparatus is rotated, the water and soil mixes, and motion relative to the bottom of the frame occurs in a similar way to a submarine landslide or gravity flow. In this paper, we use the term “landslide” to refer to mass motion, and use the term “gravity flow” to refer to the motion of a flowing mixture, through observation.



Figure 1 Photo of the apparatus to simulate a submarine landslide and damage of a communication cable.

Fig. 2 is a sketch showing water and soil in the apparatus and position of sensors. The height of the apparatus is 1.9 m, while the diameter and thickness of the rotatory part are 1.8 m and 0.4 m respectively. The maximum height of water and soil in the lower part of the apparatus is 0.3 m. Three types of sensors were set at the base of the rotatory frame. These are: (1) shear stress sensors to measure the shear resistance at the bottom of the landslide model. Six main sensors were set at equal intervals, and three additional sensors were added in one interval; (2) Normal stress sensor. This is used to measure

the normal stress generated by water and soil when the sensor comes to the lowest point; (3) Pore water pressure transducer. This is used to measure the maximum water pressure when the sensor reaches the lowest point. In point A of Fig. 2, the normal stress sensor, pore water pressure transducer, and one of the six main shear stress sensors are located along one line parallel to the axle, so that the three sensors can reach the lowest point at the same time. Using the pore water pressure data, it is easy to find the lowest point. Using the data at the lowest point, the apparent friction coefficient can be obtained by dividing the shear resistance by normal stress. This parameter can be used to evaluate the mobility of the model landslide.

A model cable is set above point A to measure the force of impact of the soil-water mixture. Comparison between the impact force and landslide mobility can be conducted because the cable and the set of sensors are located at the vertical line when point A comes to the lowest point. The height and diameter (size) of the cable can be changed for different tests.

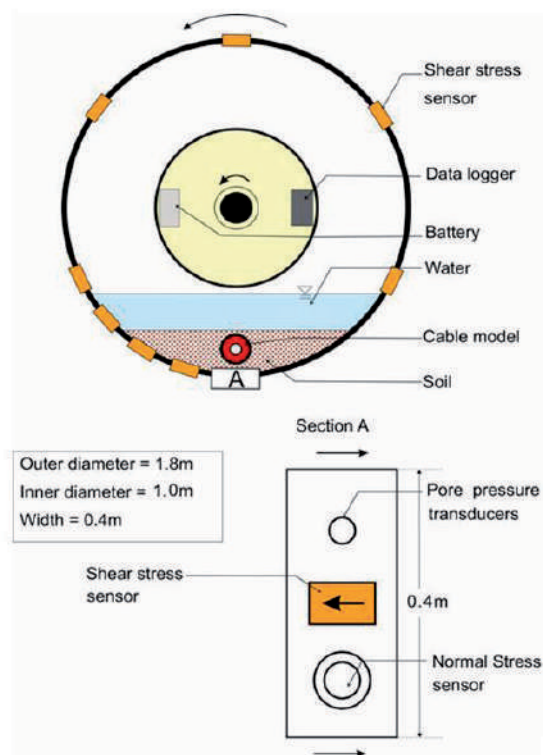


Figure 2 Sketch showing water and soil in the apparatus and sensor setting.

Rotation speed of the rotatable part is controlled by a motor. The speed at the bottom of the rotatable part ranges from 0.013 and 0.78 m/s. A data logger and battery were fixed in the axial part of the apparatus, so that data collection is carried out in an independent unit.

The main purpose of the apparatus is to simulate the movement of landslides relative to the ocean bottom

and communication cables. In actual cases, the ocean bottom is fixed and the landslide moves on the ocean floor. In our apparatus, the landslide body is kept in the lower part while the frame is rotated. For communication cables, in actual cases, the length is always hundreds of thousands of km, and axial deformation along the cable is not permitted. In the model test, the two ends of the model cable are fixed, and the impact force from moving water and soil can be measured.

Properties of the soil sample used in the test

Silica sand no. 7 and no. 8 were used in this test. Silica sand is a construction material usually used for industrial purposes. It is made of weathered silica sand, and has a uniform grain size distribution. Grain shapes are generally angular. It consists of 92-98% quartz, and a small amount of feldspar. Table 1 shows the properties of the two samples.

Because it is difficult to directly observe soil particles inside the moving soil mass, two kinds of plastic balls are used as tracers to make soil mass movement observable (Fig. 3). Table 2 shows properties of the tracers. Tracer 1 has almost the same specific gravity with saturated density of very loose sand, so it moves inside soil mass. On the other hand, tracer 2 is relatively lighter than the soil mass, therefore it flows up only when turbidity current occurs above the soil mass.

Table 1 Properties of the testes soil samples.

Properties	Silica sand no. 7	Silica sand no. 8
Specific gravity	2.64	2.64
Maximum void ratio	1.30	1.594
Minimum void ratio	0.71	0.778
Mean grain size (mm)	0.16	0.045
Effective grain size D10 (mm)	0.09	0.018
Uniformity Coefficient (Uc)	2.1	3.17



Figure 3 Photos of the tracer 1 (left) and the tracer 2 (right).

Table 2 Properties of the tracers

Properties	Tracer 1	Tracer2
Diameter (mm)	6.0	6.0
Weight (g)	0.25	0.20
Specific gravity	1.78	1.06

The motion mechanism of submarine landslides

The situation of the mixture of water and soil in the tests

The change in behavior of the soil-water mixture during rotation at different velocities was observed. Figure 4 shows a set of tests conducted with different velocities that ranged from 0.26 m/s to 0.78 m/s.

As can be seen from the front side of the apparatus, the soil-water mixture is divided into two layers: an upper muddy layer where suspended particles are entrained and carried down-current, and a lower layer of gravity flow with accompanying drag forces on the sand particles, tracking and saltation. It was observed that the height of the lower layer increased with increase in rotation velocity. This is due to increase in current energy which mobilizes the soil mass into turbulent flow, thus forming a uniforming sediment-mix as the interface between the two layers disappears.

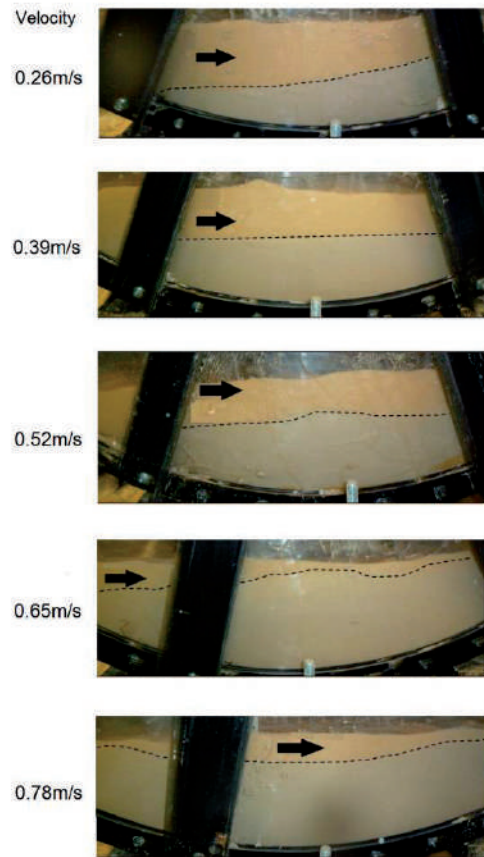


Figure 4 Photo of submarine landslide showing hydraulic behavior of the soil-water mixture at different travelling velocities (black arrow shows motion path while indented line indicates soil-water interface).

Critical values of velocity

We defined critical values of velocities at which the behavior of the tracers change so as to classify the change in behavior of the mixture. In this study, four critical

values of velocity (velocity I to velocity IV) were observed, and are explained further:

- (1) Velocity I is the velocity at which the surface of the soil mass becomes turbulent (Fig. 5);
- (2) Velocity II is the velocity at which the yellow tracers float and drift with the current (Fig. 6);
- (3) Velocity III is the velocity at which the white tracers disappear from the proximal part of soil mass (Fig. 7);
- (4) Velocity IV is the velocity at which the white tracers roll on the flume bed (Fig. 8).

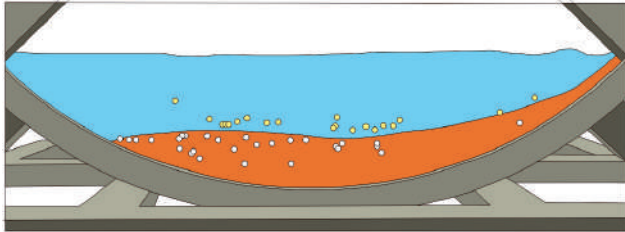


Figure 5 Schematic figure of the mixture at velocity I

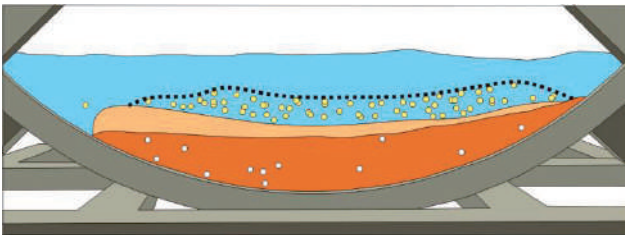


Figure 6 Schematic figure of the mixture at velocity II.

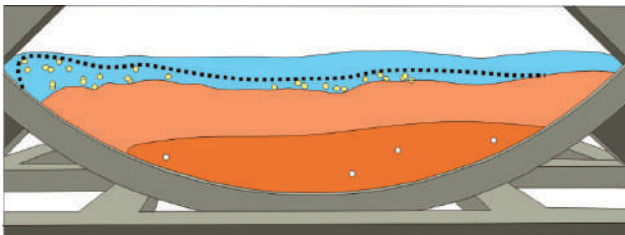


Figure 7 Schematic figure of the mixture at velocity III.

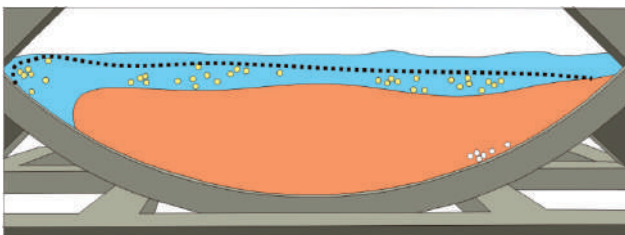


Figure 8 Schematic figure of the mixture at velocity IV.

Initially, liquefaction occurs within the soil mass at velocity I, and then turbidity current appears above the mixture at velocity II, at which the front part of the soil mass turns into turbidity flow, and finally, the soil mass completely changes into turbidity flow at velocity IV. These critical values obtained were compared with silica

sand no. 7 and silica sand no. 8. The results are shown in Fig. 9 and 10, respectively.

Figure 9 shows that the critical values increase with increase in soil mass volume in the tests with SS8. However, these values are almost constant with soil mass volume in the tests with silica sand no. 7 (Fig. 10). The difference observed is due to different properties of the two sand samples.

Generally, submarine sediments are relatively finer, and are moderately to very well graded in contrast to continental slope sediments which sometimes are poorly graded; indicating that the test result with silica sand no. 8 which consists of silt has unique similarity with grain particles of submarine landslide sediments.

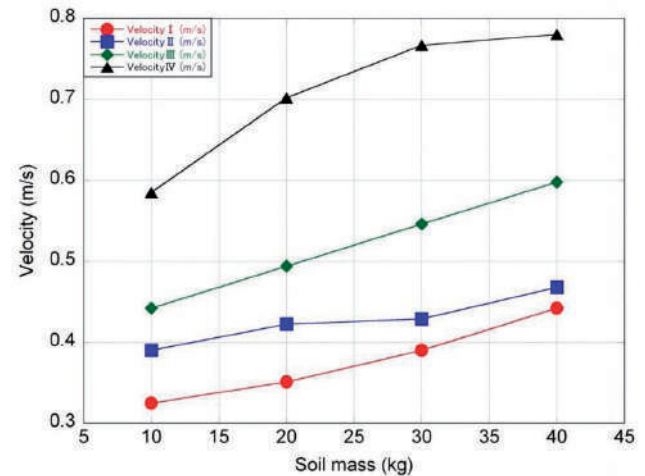


Figure 9 Relation between soil mass volume and critical values of velocity with silica sand no. 8.

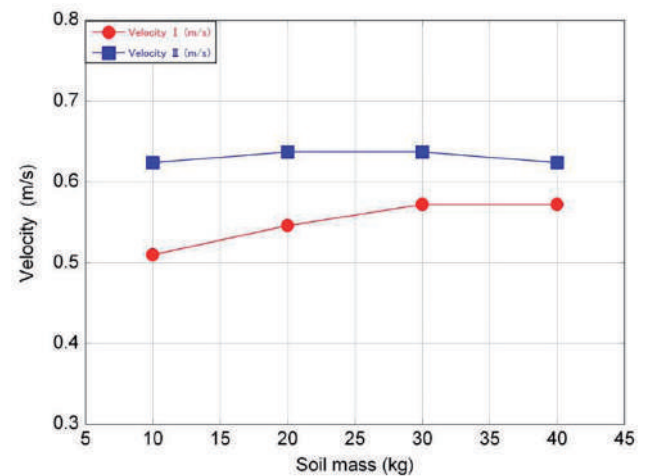


Figure 10 Relation between soil mass volume and critical values of velocity with silica sand no. 7.

Internal friction angle

Normal stress, pore water pressure and shear stress generated by the mixture are measured with silica sand no. 8. As an example, the data of normal stress, pore water pressure and shear stress by one rotation are shown in Fig. 11. Using these data, friction coefficient of the

mixture of soil and water is calculated by the following formula.

$$\tau = (\sigma - u) \tan \phi$$

where, τ is shear stress, σ is normal stress, u is pore water pressure and ϕ is internal friction angle.

Figure 12 summarizes the test results with 20 kg of silica sand no. 8. In Figure 12, each blue line represents critical values of velocity. Figure 12 shows that friction coefficient is positively correlated with velocity of soil mass, but shows different tendency before and after the critical value of velocity.

In particular, a noticeable change in tendency after velocity IV was observed. Before this stage, about 90% of the soil mass moved as gravity flow. This stage is preceded by relatively high energy turbidity flow due to gradual loss of friction between particles of the liquefied soil and bottom of the flume bed.

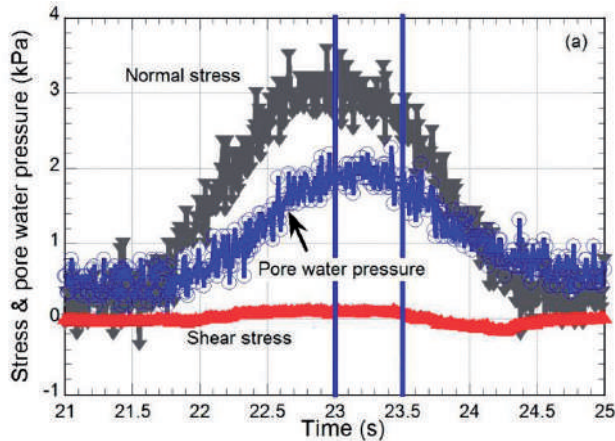


Figure 11 A test results with silica sand no.8.

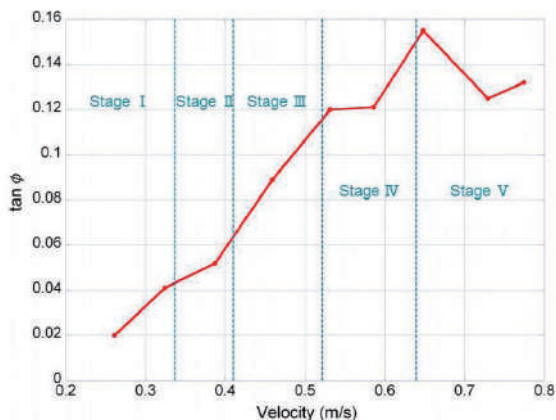


Figure 12 Test result of internal friction angle with silica sand no. 8 and the critical values of velocity.

Test results with the cable model

Thick cables are used in shallow waters near coastlines to prevent damage from fish and human activities, whereas

thinner cables are used in water depths deeper than about 1,500 m (ICPC 2009). Most landslides occur in the deep ocean, and hence thin cables are generally those cut by such events. For example, submarine cables were cut at depth range of 1,500 to 4,000 meters during the 2006 Pingtung earthquake in Taiwan (Hsu 2008). In our tests, vinyl chloride cables, 21 mm in diameter was used as models. This diameter is similar to cables used in the deep sea, and is almost the same as those cut in the 2006 earthquake and submarine landslide in Taiwan.

The length of the model cable is 0.378 m. Two screw holes were made at both ends to fix the cable to the frame of the apparatus. To measure the impact force, strain gauges were fixed onto the model cable as shown in Figure 13. Five strain gauges were located at equal intervals on the front and back sides of the model cable, forming three channels (ch). There were two gauges in ch₁, four gauges in ch₂, and four gauges in ch₃, respectively. When deformation caused by the impact force of the landslide model is generated in the cable, the strain gauges can measure the deformation. Through calibration with known load, the impact force can then be obtained.

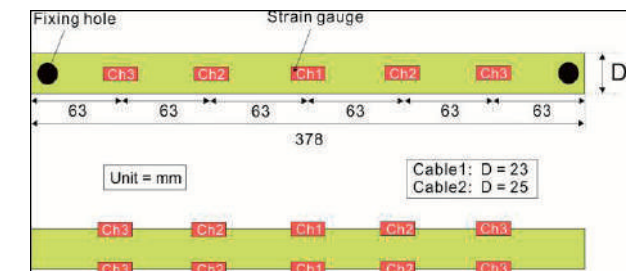


Figure 13 Strain gauge installed cable model.

Figure 14 shows the measurements of ch₁ when the cable model was hit by the landslide model. The impact force generated on the cable increased to the maximum value when it entered the landslide, and then decreased as it exited the landslide. The peak value of the distributed load was defined as the impact force. In Figure 14, it can be seen that the landslide entry and exit points do not have the same value. This result is caused by deformation due to the deadweight of the cable itself. To eliminate the effect caused by deadweight, a line is drawn to connect the entry and exit points, and the impact force is obtained by measuring the difference between the peak value and the lowest value between these points. Considering a case scenario, only sediments move on the seafloor, while sea-water flows parallel to the seafloor. It is then necessary to obtain the impact force caused by the sediment motion only. For this purpose, the impact forces caused by water were obtained by the water-only-test at different rotating velocities with different cables. By subtracting the impact force caused by water only from the measured impact force caused by mixture of sediments and water, the impact force caused by sediments only was obtained.

Figure 15 summarizes the test results with silica sand no. 8, with 40kg at different rotating speed, and a blue vertical line in Figure 15 is Velocity I. Figure 15 shows that impact force on the communication cable model is high for submarine landslides with low motion velocity, but decreases until the velocity gets to a critical value where liquefaction occurs, and subsequently increases in a linear fashion with velocity.

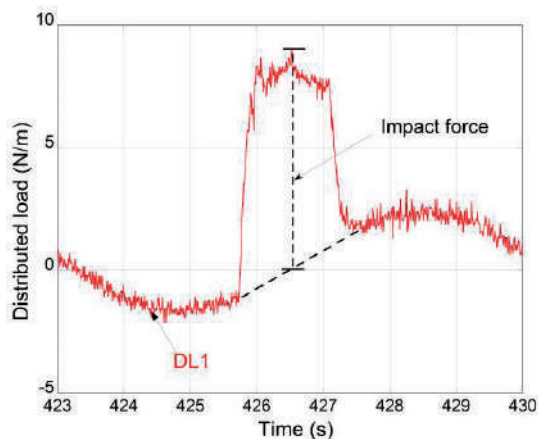


Figure 14 Method to obtain impact force from the measured data.

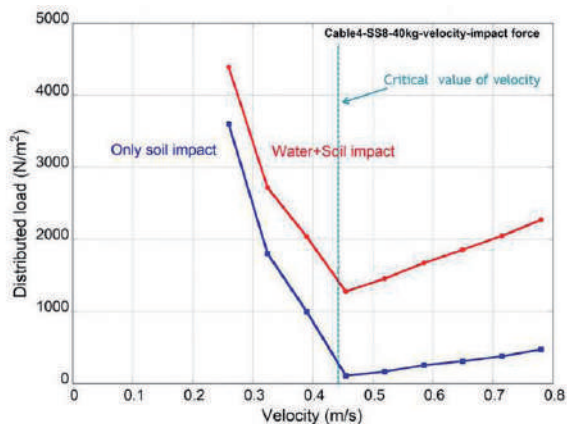


Figure 15 Test result of impact force with silica sand no. 8 and the critical value of velocity.

Conclusions

Our preliminary test results have been presented in this paper. Although the dimension of the test apparatus are relative small compared to actual submarine landslides, and it is also difficult to obtain quantitative results from these experiments, some qualitative tendencies related to the motion mechanism of submarine landslides and its impact on cables were obtained. Conclusions from the model tests are given below.

- (1) Depending on the mechanical properties of the materials, submarine landslides show different trends of change in behavior.
- (2) Friction coefficient is positively correlated with velocity of the soil mass.
- (3) The rate of increase in friction coefficient shows different tendencies before and after the change in behavior of submarine landslides.
- (4) Impact force on the communication cable is high for submarine landslides with low motion velocity.
- (5) Impact force decreases until liquefaction occurs, and subsequently increases in a linear fashion with velocity.

Acknowledgments

This study was conducted with the financial support of the Japanese scientific research grant (No. 20310109). The authors are indebted to Austine Okeke of Shimane University who reviewed the paper.

References

- Hsu SK (2008) Turbidity Currents, Submarine Landslides and the 2006 Pingtung Earthquake off SW Taiwan. *Terr. Atmos. Ocean Sci.* 19(6): 767-772.
- ICPC (2009) Submarine cables and the oceans: Connecting the world. 11-25, 29-53.
- Kokusho T, Takahashi T (2008) Earthquake-induced submarine landslides in view of void redistribution. *Geotechnical Engineering for Disaster Mitigation and Rehabilitation* (Eds: Liu HL, Deng A, Chu J.), Nanjing, China, 2008. Part 3, pp. 177-188.
- Masson DG (2006) Submarine landslides: processes, triggers and hazard prediction. *Phil, Trans, R, Soc, A15.* 364: 2009-2039.
- Mohrig D, Whipple KX, Hondzo M, Ellis C, Parker G (1998) Hydroplaning of subaqueous debris flows. *Geological Society of America, Bulletin.* 110: 387-394.
- Shanmugam G (2000) 50 Years of the turbidite paradigm (1950s-1990s): deep-water processes and facies models-a critical perspective. *Marine and Petroleum Geology.* 17: 285-342.

Ramina Landslide from a Natural Hazard to Remediation

Josif Josifovski, Spasen Gjorgjevski, Bojan Susinov

University Ss. Cyril and Methodius, Faculty of Civil Engineering, Skopje, Macedonia, Partizanski Odredi 24

Abstract This paper presents the modelling of remedial works of Ramina landslide in highly urbanized hilly area of Veles in R. Macedonia. According to the existing data, the main mass movements occurred during 1963 then after longer period without visible mass movements, a landslide zone was reactivated during 1999 and 2002. The extent of the damage on the individual housing and infrastructure had been estimated as in a magnitude of real natural disaster with potential to endanger even the centre of the town near the river Vardar. The situation asked for immediate intervention where in the beginning large set of investigations including geophysical, geological, geotechnical methods, inclinometer and geodetic measurements took place. The results from the investigations indicated that the landslide character is very complex. The total landslide length has been estimated to about 320 m with 90 m average width, where the landslide thickness on certain places reaches up to 24 m. The volume of the sliding mass is in a range of about 400,000 m³.

After the definition of potential sliding zone and surface, the next phase of landslide modelling had been enabled. The models were first calibrated through the process of so-called back analysis, which gave a clear picture of the sliding potential. Moreover, a (limit equilibrium) stability analyses and simulation the stress-deformation behaviour (finite element method analyses) had been performed, where the stage modelling had helped to understand to sliding mechanism and establish set of different measures to secure further instabilities.

Different types of remediation measures had been planned such as, slope reconfiguration with soil excavation, but main elements in the stabilizing process had been the three retaining soldier pile walls, upper - in the head, middle - and lower - in the toe of the landslide. Additionally, a system for evacuation of rainfall has been planned as well as horticulture. Due to the complexity of the landslide and the wide range of remedial works they have been divided in three construction phases.

In August 2005 the retaining wall at the top of the landslide had been finished. The construction of the second (mid-) retaining wall followed in October 2006. From then on Ramina landslide had been regularly monitored without detection of any significant mass movement.

Keywords: landslide, investigations, modelling, remedial works, soldier piles wall, anchors.

Introduction

On the site Ramina in Veles, located on the left bank of the river Vardar, a complex landslide with a length of 350 m, width of about 80 to 90 m, area of around 25,600 m² and volume of around 400,000 m³ is registered. In December 2002 the landslide had been reactivated again after two known events in 1963 and 1999 and caused significant damage to several buildings on the densely populated slope (Fig. 1).



(a)

(b)

Figure 1 Photos of Ramina landslide: (a) Zone of the main scarp; and (b) Towards the urbanized area.

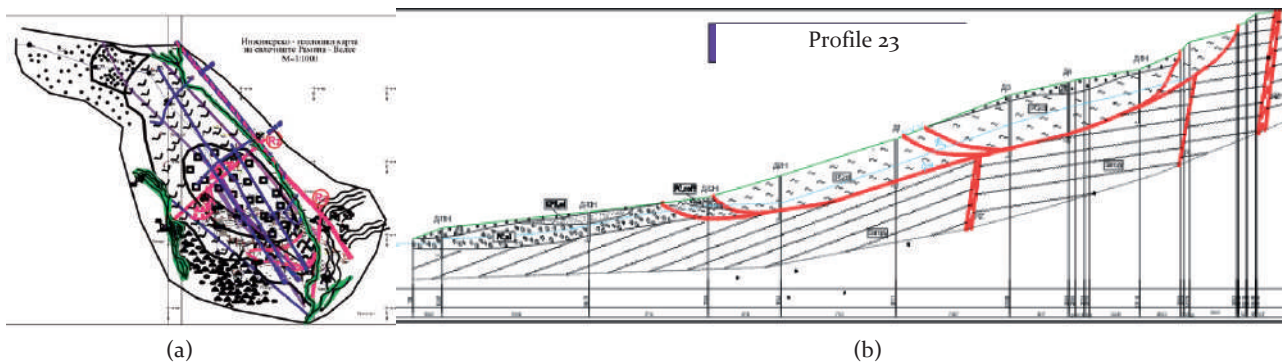


Figure 2 Ramina landslide: (a) Simplified engineering-geological map; and (b) Typical geological profile 23.

Large deformations had been observed on the top of the landslide (head) and in the middle of the landslide mass. There had been a development of open cracks endangering the water supply system. Moreover, all observations had suggested that further development and landslide widening is expected.

All the necessary investigations were performed in two phases. Unfortunately, the results from the first phase of investigations were not used as a basis for the remedial works on time, since the reactivation of the landslide in a period from 2002 had changed the field conditions. So, as a next step, additional investigations were performed in order to define the "new" conditions and changes as a result of the reactivation. An overview of the field investigations Jovanovski et al. (2003) are given in Table 1.

Table 1 Overview of the field investigation at the Ramina landslide.

No.	Investigations (period 1999 -2002)
1	Topographical survey of all area
2	Engineering - geological mapping at a scale 1:1000
3	Rotary drilling (21 boreholes)
4	SPT - test (40 tests)
5	Installing of piezometers (12 piezometers)
6	Installing of inclinometer devices (4 inclinometer boreholes)
7	Geophysical refraction measurements (6 profiles)

Based on the geotechnical investigations a Geological map had been established with all the elements of the landslide (Fig. 2a), according to which geotechnical profiles were developed (Fig. 2b).

The sliding mass (zone) has been detected at great depth on the interface between the two different lithological units. The geotechnical profile is consisted of clayey soil layer over bedrock with an average height of about 8 m in the upper part and up to the maximum observed 25 m in the middle part (Fig. 3).

The bedrock is formed from very stiff and compacted marl (M) with high strength and deformation parameters. Above the stiff rock there is clay like (CH) material with some presence of sand. This material is seen as problematic, namely on the contact with the marl

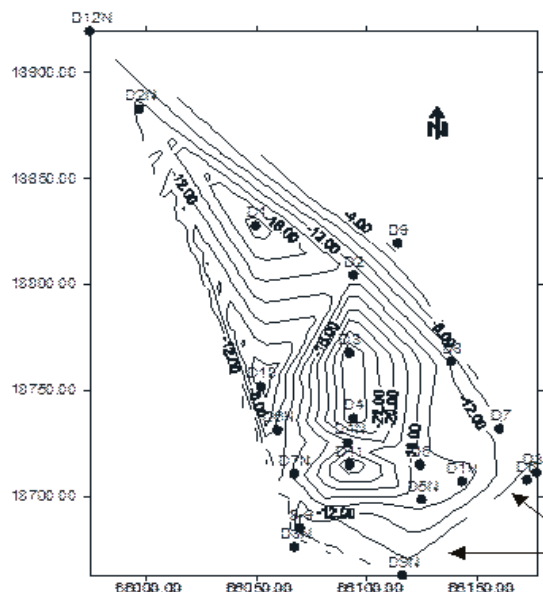


Figure 3 A map of the landslide thickness.

there is presence of water with constant water table. The material on this contact is weathered and with degraded material properties. Therefore, a special attention has been given to the modeling of the slip surfaces. A material with lower material properties depicting the degraded clay has been used. The slip surfaces were predetermined (Fig. 2) from the terrain prospection and analysis of the natural slope. In upper part of the landslide there is additional fill (SfC) on top of the clay layer.

In the upper part of the landslide the ground water level has been detected at depth of 8 m while in the lower part the water level has been 2 m below the terrain.

Planning the remediation a retaining conception which will be able to provide a global stability of such difficult and large landslide had been adopted (Josifovski et al. 2003 a/b). The complexity of the terrain had divided the remediation into three phases. Hence, three pile retaining walls were proposed as main stabilizing elements. The position of the reinforced concrete soldier pile wall had been set according to landslide monitoring and anticipated ground movement (Fig. 4).

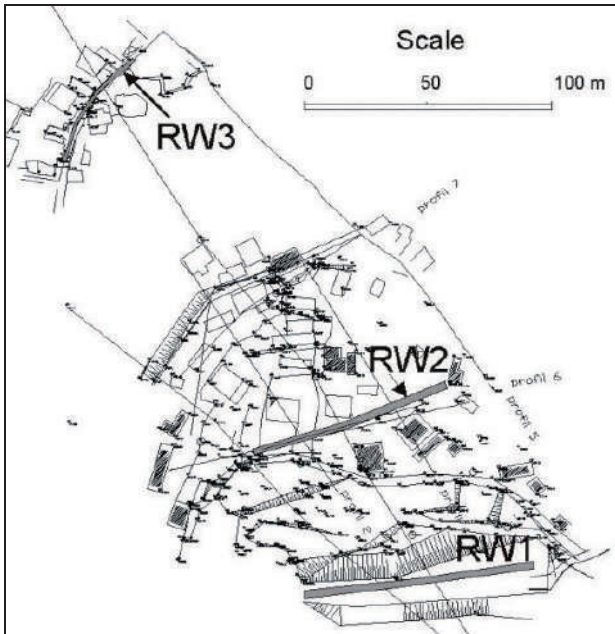


Figure 4 Position of retaining wall structures.

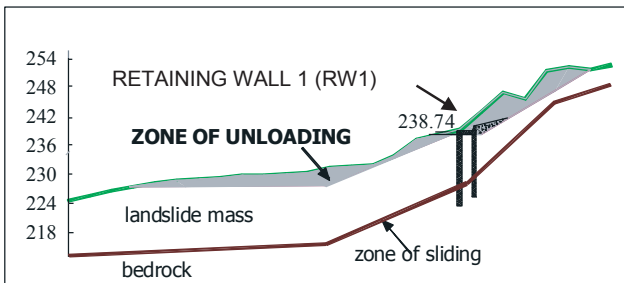


Figure 5 Remedial works on the top of Ramina landslide.

On the top of the landslide a retaining wall (RW₁) is positioned with a task to cut the head of the sliding mass. The position of the second retaining wall (RW₂) is chosen in such way that covers the zone where a part of the landslide is breaking to the ground surface, hence the largest deformations had occurred damaging several houses (Jovanovski et al. 2003). The third retaining wall (RW₃) is placed in the toe of the landslide in highly urbanized area under a roadway-street.

Additional measures such as, partial excavation of the landslide body in the upper zone of the landslide had been seen as favorable reducing the burden of the landslide (Fig. 5), construction of drainage system for evacuation of surface water, as well as afforestation on the ground has been foreseen.

In the first phase Josifovski et al. (2003a) reshaping of the upper part of the landslide was created by excavating 27,712 m³ of landslide body together with the construction of RW₁ with length of L₁=100 m. The RW₁ is comprised of 67 piles with diameter of 90 cm placed in two rows spaced on 3 m. The pile depth is from 6 to 13.5 m with embedment length of 3.8 to 4.2 m in the base rock.

In the second phase (Josifovski et al. 2003b), in the middle of the sliding mass another retaining wall (RW₂) with length of L₂=88 m has been constructed. The RW₂ is comprised of three rows with 89 piles (diameter of 90 cm). The pile depth is between 7.5 and 16.5 m. The sliding mass above the RW₂ is defined with length of about 200 m and maximal depth of 25 m. The piles alone are not sufficient to stabilize the sliding mass in the middle part of the landslide, thus additional stabilizing elements were used in form of 42 pre-stressed geotechnical anchors. The anchored soldier pile wall is joined by a pile cap with width of B=5.95 m and thickness of 50 cm. The total number of anchors is 42. For calculation purposes 12Ø15.2 mm geotechnical anchor has been adopted. The total anchor length is L_a=26-33 m where free length is L_f=20-28 m and bond length is L_b=5-9 m. The distance between the anchors was variable from 1.5 m in the middle part to 3 m on the wall side. According to specification the maximal force P_t=2976 kN and nominal preloading force of P_o=1860 kN (with global safety coefficient factor of F_s=1.6). The anchors are placed in two positions directly connected to the piles in group-1 and group-2 with inclination angles of 60° and 45°, respectively (Fig. 6).

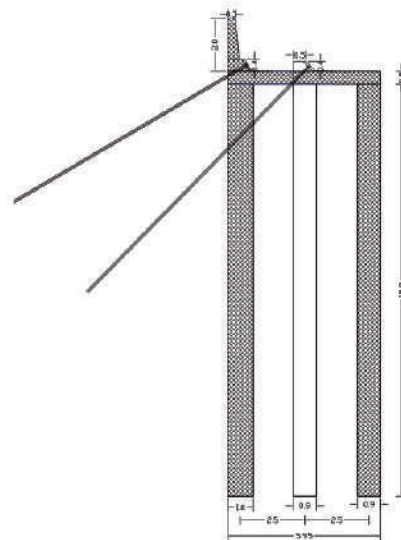


Figure 6 Cross section of retaining wall (RW₂).

In the last (third) phase of construction the retaining wall (RW₃) has been planned to be built in the toe of the landslide. It is equally important in the task to stabilize the sliding mass which ranges from 180 to 200 m length with maximal depth of 18 m. The clay layer in this section averages to about 10 m above the bedrock. Namely, reinforced concrete wall consisting of 45 piles with diameter of 90 cm positioned in two rows spaced on 3 m. The pile length ranges from 3 m to 18 m connected by pile cap with a width of B=3.5 m and thickness of 50 cm (Fig. 7). The total length of the wall is L₃=67.5 m.

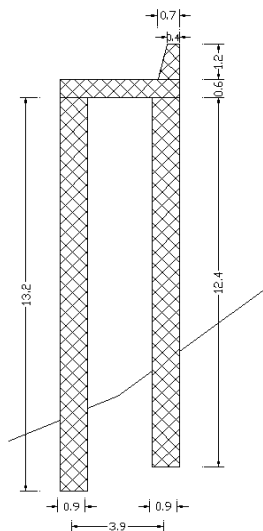


Figure 7 Cross section of retaining wall (RW3).

Modelling and calculation

To assess the effects of the proposed remedial measures the static and seismic stability of the landslide zone has been analyzed in several stages:

- Static slope stability of the natural terrain;
- Static slope stability with retaining walls and unloading of the terrain;
- Seismic slope stability with retaining walls and unloading of the terrain.

The material properties are determined by the numerous laboratory and field investigation which had been performed on several occasions in the period from 1963 to 2002. Beside the field investigations an adequate laboratory tests have been executed, with a special attention on the definition of residual shear strength parameters, which were afterwards compared with the friction angle obtained by the stability back analyses. According to the data Jovanovski et al. (2003) conservative choice of the material characteristics necessary for the modeling process had been made (Tab. 2).

Table 2 Geomechanical properties of the materials on Ramina landslide.

Parameter	Bedrock (Marl)	Clay (CH)	Slip surface material	Fill (SFc)
γ_{unsat} (kN/m ³)	26.0	18.8	18.5	17.7
γ_{sat} (kN/m ³)	26.0	21.3	19.0	21.0
ν (-)	0.250	0.320	0.32	0.30
G_{ref} (kN/m ²)	600000.0	2272.7	1515.1	3846.1
E_{oed} (kN/m ²)	1800000.0	8585.8	5723.9	13461.5
c_{ref} (kN/m ²)	150.0	15.0	0.0	5.0
ϕ (°)	39.0	20.0	16.0	22.0

The stress-strain behavior of three characteristic profiles, namely 22, 23 and 24, represented by two-dimensional models (under assumption of plane-strain state) has been analyzed. The calculation has not taken into account the external load (load of existing buildings), since it has been asses that their impact on general stability is neglectable. The analysis is performed using the finite element method and the PLAXIS program. The finite element solution offers realistic simulation of the soil behavior. The soil is discretized by triangular plane element with 15 nodes while the structures as beam elements with 3 nodes (Fig. 8).

An elastoplastic analysis has been performed where for the soil material a Mohr-Coulomb model is used, while for the reinforced-concrete structure a linear material model is used, Potts and Zdravkovic (1999). Anchors and grouted body are discretized as elastic linear finite elements with only axial rigidity. In the seismic analysis an IX degree earthquake activity after MCS has been assumed with ground acceleration of $\alpha_x= 0.08$ g in the horizontal and $\alpha_y= 0.04$ g in the vertical direction.

The remedial measures had obviously worked since the total displacements are controlled in magnitude and shape splitting the landslide system in two halves (Fig. 9a). The maximal displacement is around 5 cm with only local (surface) manifestations. The global stability is ensured and will be improved by the unloading of the zone bellow the RW2.

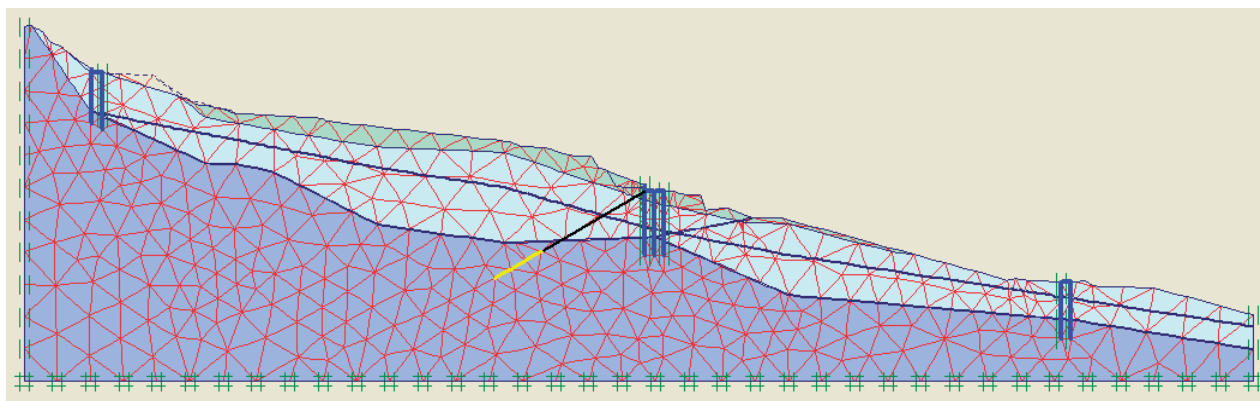


Figure 8 Discretized model of Profile 23 with finite elements.

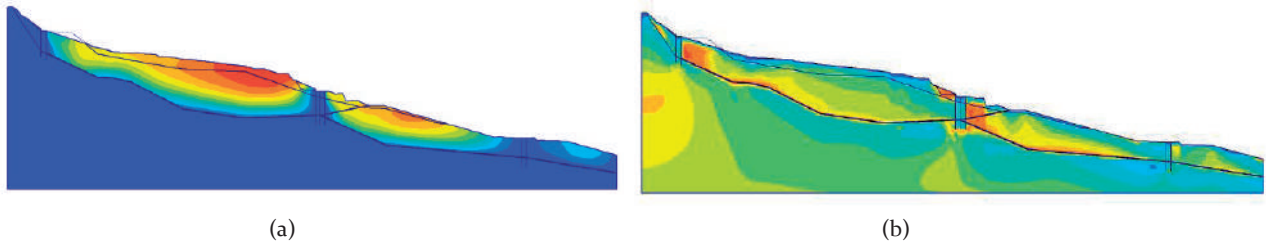
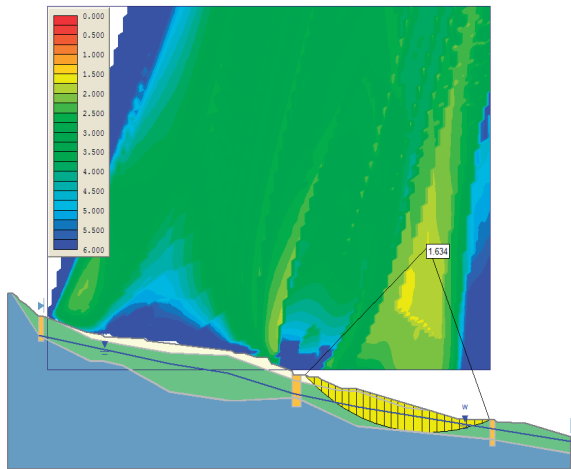
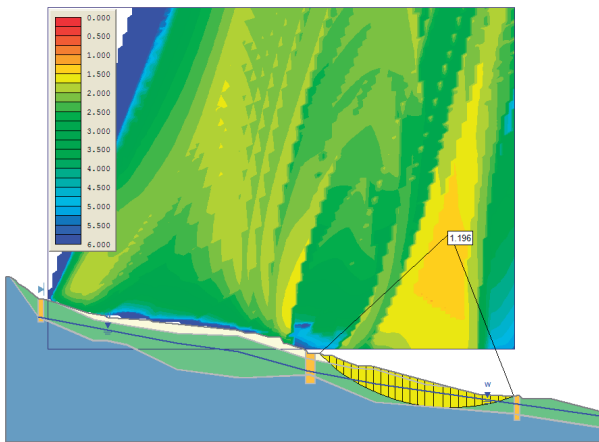


Figure 9 Finite element results of Profile 23: (a) Total displacements; and (b) Shear stresses.



(a)



(b)

Figure 10 Global stability of soil masses in Profile 23: (a) Static; and (b) Seismic.

The shear stresses are largest below the retaining walls and at the contact with the base rock, which has been expected but not large enough to cause new slip surfaces (Fig. 9b). From the above it can be concluded that the measures had been able to reduce the stresses in the potential zones and significantly reduce the displacements. The maximal wall displacements are in the range between 0.2 and 0.5 cm. The activated anchor force in the Profile 23 is calculated to 1150 kN/m'.

Moreover, the global stability of Profile 23 is analysed with the method of limit equilibrium using the program SLIDE. A static and seismic stability has been checked using the Bishop's method determining the safety factors presented in Tab. 3.

Table 3 Factors of safety from Stability analyses of Profile 23.

Global stability	Method Bishop
Static (unloading+RW1+RW2+RW3)	1.63
Seismic (unloading+RW1+RW2+RW3)	1.20

Once again it is confirmed that the retaining structures are able to provides static stability with minimal safety factor of $F_s = 1.6$ which is well above the required 1.3 (Fig. 10a). In the calculation of the seismic stability the minimal safety factor is $F_s = 1.2$ (Fig. 10b) which meets the requirements set in the regulations to be above 1.1.

In both analysis the sliding surface with the minimal safety factor is determined in the lower part of the landslide which is a little unexpected because this part has been quite silent during the sliding from 2002. Nevertheless, the factors are large and are offering confidence for the period ahead.

Conclusion

The numerical modeling can be quite powerful tool which together with good instigations is able to reliable simulate the landslide behavior. From the presented experience in modeling of remedial measures on the Ramina landslide it can be concluded that larger sliding systems are very difficult to be stabilized, thus the solution has to involve a large expensive and complex measures. But if designed and planed well, they will be successful as in this case. The first phase with the wall construction and unloading on the top of the landslide has finished in august 2005. In 2006 the second phase finished when the midsection wall has been constructed. The third phase with the wall at the landslide toe due to insufficient funds had never started. From then on until now the landslide is monitored but no larger deformations are registered.

Finally, based on the observations of the conditions it can be concluded that the unplanned and unurbanized building is exclusively man-made factor which can easily lead to a natural hazard of critical and catastrophic proportions followed with socio-economic influence on the entire region. In such situations often the remediation measures for are very complex and limited as it was in this case with the Ramina landslide in Veles.

References

- Josifovski J, Gjorgjevski Sp, Jovanovski M, Dolanec-Vckova K (2003a) Final design project for remediation of “Ramina” landslide – Veles in first phase. DGR Geotehnika, SDG Pelagonija, Skopje.
- Josifovski J, Gjorgjevski Sp, Jovanovski M, Dolanec-Vckova K (2003b) Final design project for remediation of “Ramina” landslide – Veles in second and third phase. DGR Geotehnika, SDG Pelagonija, Skopje.
- Jovanovski J, Markovski B, Spirovski D (2003) Report from the geotechnical investigation on the “Ramina” landslide location after reactivation in 2002. DGR Geotehnika, SDG Pelagonija, Skopje.
- Potts D M, Zdravkovic L (1999) Finite element analysis in geotechnical engineering: Theory. Imperial College of Science, Technology and Medicine, Thomas Telford Publishing. (ISBN 0-7277-2783-4).
- Potts D M, Zdravkovic L (2001) Finite element analysis in geotechnical engineering: Application. Imperial College of Science, Technology and Medicine, Thomas Telford Publishing. (ISBN 0-7277 2753-2).

Rockfall Hazard Management on Traffic Facilities in Croatia

Dalibor Udovič⁽¹⁾; Željko Arbanas⁽²⁾; Snježana Mihalić Arbanas⁽³⁾; Mirko Grošić⁽⁴⁾

(1) Monterra Ltd., Rijeka, Croatia, Vukovarska 76, dalibor.udovic@monterra.hr

(2) University of Rijeka, Faculty of Civil Engineering, Rijeka, Croatia

(3) University of Zagreb, Faculty of Mining, Geology and Petroleum Engineering, Zagreb, Croatia

(4) Geotech Ltd., Rijeka, Croatia

Abstract Along the Croatian side of the Adriatic Coast some large rockfall on the steep limestone slopes occurred during last decade and caused serious damage on buildings and traffic facilities with injured persons. The main reasons for rockfall in limestone slopes near railways and roads occurring are unfavorable rock mass characteristics, rock mass weathering in combination with heavy rainfalls so as men influence during the facility constructions. The applied technologies of the slopes construction were very conservative and attained safety factors are very low. The technologies of rockfall protections during construction of the new roads in the last decades are significantly improved. The rockfall protection started with using of netting techniques with very low quality of the wire material. After some time, the double twisted netting with galvanic protection occurred as the most common type of the rockfall slope protection. On the more demanding slopes the shotcrete was used and still is regarding the quality of the rock mass in the slope that is needed to be protected. The new technologies are applied throughout construction of the support system including high load bearing meshes with reinforced geotechnical self-drilled anchors in combination with high performance rockfall barriers. After rockfall phenomena occurring on some particular locations, the projects of rockfall protection were conducted to ensure human lives and facilities from further rockfall occurrences. The process of rockfall protection started with rockfall hazard analyses to identify potential of rockfall occurrence so as possible accidental consequences, e.g. rockfall risk. On locations where hazard with related risk was determined the detailed field investigations were provided. Based on identified characteristics of possible unstable rock mass blocks analyses of motion and resulting paths were conducted. Trajectories, impact energy and height of bouncing are depending of slope geometry, slope surface roughness and rockfall block characteristics. Depending on these analyses rockfall protection measures were designed. Two design approaches were

adopted, prevention of rockfall by removing of potentially unstable rock mass or by rock mass support system installation and by suspending of running rock fall mass with rockfall protection barriers. In this paper we will present experiences on rock fall hazard determination and rockfall protection design so as installation of rock fall system protection on some location on limestone slopes near the traffic facilities in Croatia.

Keywords rockfall, hazard, risk, rockfall protection, rockfall hazard management

Introduction

Rockfall protection along the roads and railways in Croatia become very important in all designs of new facilities as well as remediation of old ones. The main reasons for occurring rockfalls in limestone slopes near railways and roads are unfavorable rock mass characteristics, rock mass weathering in combination with heavy rainfalls so as men influence during the facility constructions. After rockfall phenomena occurring (Fig. 1) on some particular location, the projects of rockfall protection were conducted to ensure human lives and facilities from further rockfall occurrences. The deformability and strength properties of the rock mass are determined from geotechnical field investigation and the use of the rock mass classification system. Depending on these analyses, rockfall protection measures were designed. Two design approaches were adopted, prevention of rockfall by removing of potentially unstable rock mass or by rock mass support system installation and by suspending of running rock fall mass with rockfall protection barriers (Arbanas et al. 2012). After adopting one of these approaches it is possible to make the geotechnical model for a rock slope and perform stability analyses. If a low initial factor of safety is obtained, the stability analysis should include a support system.



Figure 1 Rockfall of 700 m³ occurred on the state road Makarska-Vrgorac, Stupica Location, October 2010.

The design support system will thus result from the stability analysis, which provides a satisfactory factor of safety during all phases of excavation. In this paper we will present experiences on rockfall hazard determination and rockfall protection design so as installation of rock fall system protection on some location on limestone slopes near the traffic facilities in Croatia.

Rockfall hazard

A rockfall is defined as a rock mass that has detached from a steep slope or cliff along a surface with little or no shear displacement and descends most of its distance through the air (Hoek and Bray 1981). Once a rock block has detached from the steep slope, it would be occurred as a free fall, topple, bounce, roll or slide along the slope surface at a high speed, which can cause significant damages to the facilities at the foot of the slope (Li et al. 2009). A potential rockfall can be composed of either rock blocks cut by discontinuities and free faces or boulders and rock fragments on a soil or talus slope surface. Rockfalls can be caused by many factors, including unfavorable rock structure (discontinuities), adverse ground water-related conditions, poor blasting practices during original construction or reconstruction, climatic changes, weathering and tree leveling (Brawner 1994).

A rockfall hazard occurs when a rock block falls into an area where there are human activities or construction and causes damages and/or fatalities. The rockfall hazard is a combination of a source, a triggering event and the pathway to the at-risk object (Wyllie 2006). Rockfall is a major cause of landslide fatality, even when elements at risk with a low degree of exposure are involved, such as traffic along highways (Bunce et al. 1997). Although generally involving smaller rock volumes compared to

other landslide types, rockfall events also cause severe damage to buildings, infrastructures and lifelines due to their spatial and temporal frequency, ability to easily release and kinetic energy (Rochet 1987) (Fig. 2). The problem is even more relevant in large alpine valleys and coastal areas, with a high population density, transportation corridors and tourist resorts. Rockfall protection is, therefore, of major interest to stakeholders, administrators and civil protection officers (Hungre et al. 2005). Prioritization of mitigation actions, countermeasure selection and land planning should be supported by rockfall hazard assessment (Raetzo et al. 2002; Fell et al. 2005, 2008) On the other hand, risk analysis is needed to assess the consequences of expected rockfall events and evaluate both the technical suitability and the cost-effectiveness of different mitigation options (Corominas et al. 2005, Straub and Schubert 2008)



Figure 2 Rockfall of 500 m³ occurred on the state road Rijeka-Orehovica, Banska Vrata location, March 2013.

Field investigation and protection design

The rockfall protection projects start with rockfall hazard analyses to identify the potential of rockfall occurrence and the potential consequences, i.e., risk. At the locations where a hazard with related risk was determined, detailed field investigations should be carried out. Based on results of engineering-geological mapping data, the in-situ state of a rock mass can be

adopted and characterized, the geotechnical model can be established and slope stability and stress-strain analyses can be performed. Based on well-known design principles of rock slope engineering (Bieniawski 1992, 1993), the results of the geotechnical field investigation and rock mass classification carried out, the strength criterion and rock mass deformability parameters can be defined.

For a rockfall simulation a two dimensional slope profile or digital elevation slope model is used as a base for an analysis. Slope profiles or slope surface are then divided onto vertical slices or specific areas with different own surface characteristics. The algorithm for simulating rock fall follows an iterative scheme which is governed by a variable time interval. Sliding, rolling, toppling or free fall of a block are possible as an initial movement. All possible types of subsequent movements, such as rolling, sliding, collision and inclined throw are considered in the rockfall simulations. On the occasion of every collision with the slope surface and every transition from one slice or area to the next, the actual rock movement is evaluated as a base for the decision on the type of the subsequent movement. All rock fall paths are according to rock diameter that means the full geometrical representation of the rock, when interacting with slope and/or protection structures.

There are a lot of uncertainties and assumptions during the location mapping, surface parameters determining and other input parameters for rock fall simulations accepting. In simulation software a variation range to any input parameter can be join and thus in a single simulation run a complete statistical study can be conducted and uncertainties and assumptions would be included into calculation.

These simulation and simulation results should be taken as a tool for decision making and as reserve. Rockfall simulations must be carried out on the most critical profiles. Simulations can be carried out as 2D (Pfeiffer and Bowen 1989) or 3D (Guzzetti et al. 2002) simulations and the results of one of the simulation are presented at Fig. 3.

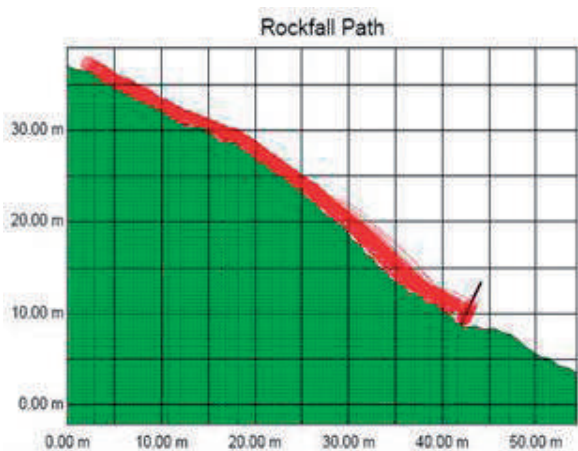


Figure 3 Rockfall simulation results.

On the basis of the results obtained from all of the analyses, it could be decided what kind of the rockfall prevention or rockfall protection measure will be used to reduce rockfall hazard at a particular location. Two design approaches were adopted (Arbanas et al. 2012): (1) the prevention of rockfalls by removing potentially unstable rock mass or by installing rock mass support systems and (2) the reduction of rockfall mass energy and suspension of running rockfall mass using rockfall protection barriers. Where it is possible to detect possible rockfall hazards, rockfall prevention projects are recommended and advisable. The prevention measures should enable the elimination of rockfall occurrence possibility by removing potentially unstable rock mass from the slope or by constructing an adequate rock mass support system. Removing the possible unstable rock mass from the slope could be more expensive than appropriate support construction, especially on steep slopes. In that case, support systems using high-capacity steel meshes or reinforced concrete in combination with rock bolts (Fig. 4) could ensure the appropriate stability of rock slope against rockfall.



Figure 4 Rockfall protection using reinforced shotcrete and stone lining.

When it is not possible to detect or prevent all possible rockfalls, an approach to reduce or/and restrain rockfall consequences should be adopted (Arbanas et al. 2012). Approaches to reduce or/and restrain rockfall energy and suspend running rockfall mass are well known in the geotechnical engineering praxis, using berms and rockheads on the slope, ditches and fills in the toe of the slope and catch fences and protection barriers at different positions of the slope (Wyllie and Norish 1996, Wyllie and Mah 2004, Hoek 2007).

Rockfall protection systems

One of the most often used prevention measure used on high and steep slopes and cuts is the support system consisted of high load bearing wire meshes in combination with selfdrilled rockbolts. The system uses

high tensile steel wire meshes to catch the potentially unstable rock block on his position at the slope (Fig. 5). The whole system of protection meshes around unstable block could be pre-stressed between installed rockbolts positively affecting on local slope stability.



Figure 5 Combination of netting with high load bearing meshes.

Application of high load bearing wire meshes in combination with selfdrilled rockbolts was commonly used in cases where blocks form small areas of a slope or individual bigger blocks are prone to fall or where small zones or rock mass at a slope are susceptible to weathering process and erosion. Combinations of high load bearing wire meshes with shotcrete linings over weathered or highly jointed rock mas are also very often in use. The load transfer in the high load bearing wire meshes system is designed that the loads from the blocks are transferred to the mesh and then using rockbolt load transfer assigned to the deeper zones of the slope. The main role of the system have rockbolts; their surface raster, depth and load distribution along the bolt redistribute loads from the mesh to the stable rock mass in a slope. Pre-stressing of the high tensile protection meshes between the installed can contribute to the surface stress distribution but this impact is still under consideration and it isn't included in slope stability analysis. Installation of selfdrilled rockbolts on high slopes is much challenged operation and requirements on adequate equipment is of high importance (Fig. 6).

Cost price of high load bearing wire protection meshes installation at high slopes and cuts above infrastructure facilities is relatively high and the main part of it is related to the cost of equipment necessary for rockbolt and protection meshes installation, while the costs of protecting meshes and rockbolt is of second importance. In comparison with a cost price of other measures those could be employed to mitigate related rockfall hazard, a cost price of high load bearing wire protection meshes is the most cost effective although has a high requirements on contractors and construction quality.



Figure 6 Installation of geotechnical selfdrilled rockbolts on high steep slopes.

In cases where a rockfall could be triggered in wider potentially unstable zone of a slope a remediation measure would be one of available solution or combination of solutions which can prevent and accept rockfall mass outside of facilities without harmful consequences. Combination of high load bearing meshes and high energy flexible rockfall catch fences and barriers (Fig. 7) was shown as the most efficient system in rockfall hazard mitigation along traffic facilities in Croatia.

Flexible rockfall catch fences or protection barrier fences are designed to have an energy absorption capacity of more than 100 kJ in a common use. This is an equivalent to the mass of 250 kg rock block moving down the slope at the velocity of about 20 m/s in the moment of the rock block hit in a barrier. Much more robust flexible rockfall protection barriers, with an energy absorbing capacity of up to 5000 kJ, higher than 7.0 m have been successfully designed and installed as a rockfall protection at some locations along traffic facilities in Croatia where the rockfall hazard was caused with potentially unstable rock blocks of larger dimensions and with high kinematic energy (Arbanas et al. 2012, Grošić et al. 2009).



Figure 7 Installation of high energy absorption rockfall protection barriers.

Experiences in using high energy absorbing barriers in rockfall protection along traffic facilities have shown that their use is the most effective solution because they are flexible construction those can accept rockfall hits without significant damages and if they are maintained properly would provide the security against rockfalls for a longer period of time. Furthermore, the appropriate designed and installed high energy absorbing barriers can ensure rockfall protection of a wider area of a slope and in these cases represent an economically acceptable solution with much lower cost price than some other conventional technical solutions. Although the installation of high energy absorbing barriers requires well equipped contractor and high trained personnel, application of high energy absorbing barriers became a leading technical solution in rockfall protection in the world.

In cases where enough space in a toe of a slope with possible rockfall appearance is disposed along the facility, some conventional solutions such as ditches, massive retaining constructions and fills are still in use. Ditches and fills are still the most effective solutions in rockfall protection but restriction of disposal space along the facilities, especially along existing roads and railways, conditions constructions of more expensive constructions such as retaining walls, earth reinforced embankments and galleries those need less space for construction. The same problem is also present after construction of new highways in Croatia where rockfall hazard and risk analyses were not conducted through the design process.

Conclusion

Along the Croatian side of the Adriatic Coast some large rockfall on the steep limestone slopes occurred during last decade and caused serious damage on buildings and traffic facilities with injured persons. The main reasons for occurred rockfalls in limestone slopes near railways and roads are unfavorable rock mass characteristics, rock mass weathering in combination with heavy rainfalls so as men influence during the facility constructions.

Although the significant improvement in design considerations and applied techniques in rockfall occurrence prevention during last decade a standard procedure to identify rockfall hazard and risk along infrastructure facilities in Croatia is still not accepted and different approaches to the rockfall risk management are in main highway and railway companies those maintain the most important infrastructure facilities in Croatia are still present. All accepted approaches in rockfall risk management are leaded by experiences of geotechnical designers which are involved in solving of local rockfall appearances on existing, mostly long term present, large rockfall instabilities or local minor rockfall occurrences.

Considering the frequency and volume of rockfall instabilities those were occurred in recent time so as length and importance of traffic and infrastructure

facilities (highways, motorways, roads, railways and pipelines) in areas exposed to the rockfall risk it should be necessary to perceive and accept an unify approach to identifying rockfall hazard and risk along the infrastructure facilities based on modern technologies and good practices. Experiences obtained from long term good practices along facilities in similar geological conditions and applying of local knowledge in rockfall prevention and mitigation would result with an acceptable methodology for rockfall hazard assessment and landslide risk management that could be acceptable in existing facilities maintenance so as new facilities design and construction in Croatia.

References

- Arbanas Ž, Grošić M, Udovič D, Mihalić S (2012) Rockfall hazard analyses and rockfall protection along the Adriatic coast of Croatia. *Journal of Civil Engineering and Architecture*. 6(3): 344-355.
- Bieniawski Z T (1992) Invited paper: Principles of engineering design for rock mechanics. *Proceedings of the 33rd U S Symposium on Rock Mechanics*. Tillerson and Wawersik (eds). Balkema. pp. 1031-1040.
- Bieniawski Z T (1993) Principles and methodology of design for excavations in geologic media, *Research in Engineering Design*, vol. 5, pp. 49-58.
- Brawner C O (1994) Rockfall hazard mitigation methods Participant Workbook. NHI Course No.13219. Publication No. FHWA SA-93-085. U.S. Department of Transportation, Federal Highway Administration.
- Bunce C M, Cruden D M, Morgenstern N R (1997) Assessment of the hazard from rock fall on a highway. *Canadian Geotechnical Journal*. 34(3): 344-356.
- Corominas J, Copons R, Moya J, Vilaplana J M, Altimir J, Amigo J, (2005) Quantitative assessment of the residual risk in a rockfall protected area. *Landslides*. 2: 343-357.
- Fell R, Ho K K S, Lacasse S, Leroi E (2005) A framework for landslide risk assessment and management. *Proceedings of the International Conference on Landslide Risk Assessment and Management*, Vancouver, BC, Canada. AA Balkema, Taylor & Francis Group.
- Fell R, Corominas J, Bonnard C, Cascini L, Leroi E, Savage W Z, (2008) Guidelines for landslide susceptibility, hazard and risk zoning for land-use planning. *Engineering Geology*. 102: 99-111.
- Grošić M, Arbanas Ž, Udovič D (2009) Designing and Constructing Rockfall Barriers – Experiences in Republic of Croatia. *Proceedings of the Regional Symposium of ISRM, Eurock 2009, Rock Engineering in Difficult Ground Conditions - Soft Rock and Karst*, 29-31 October 2009. Vrkljan I (ed.). CRC Press/Balkema, Taylor & Francis Group, Leiden. pp. 703-708.
- Guzzetti F, Crosta G B, Detti R, Agliardi F (2002) STONE: a computer program for the three-dimensional simulation of rock-falls. *Computers & Geosciences*. 28(9): 1079-1093.
- Hoek E, Bray J (1981) *Rock slope engineering*. The Institute of Mining and Metallurgy, London.
- Hoek E (2007) *Practical Rock Engineering*. Rocscience, Toronto (<http://www.rocsience.com>).
- Hungro O, Corominas J, Eberhardt E (2005) Estimating landslide motion mechanism, travel distance and velocity. In: *Landslide Risk Management*. Hungro O, Fell R, Couture R, Eberhardt E (eds). Taylor and Francis, London. pp. 99-128.

- Li Z H, Huang H W, Xue Y D, Yin J (2009) Risk assessment of rockfall hazards on highways. *Georisk*. 3: 147-154.
- Pfeiffer T J, Bowen T (1989) Computer simulation of rockfalls. *Bulletin of Engineering Geology*. 26: 135–146.
- Raetzo H, Lateltin O, Bollinger D, Tripet J P (2002) Hazard assessment in Switzerland – Codes of Practice for mass movements. *Bulletin of Engineering Geology*. 61: 263–268.
- Rochet L (1987) Application des models numeriques de propagation a l'etude des eboulements rocheux. *Bulletin Liaison Pont Chaussee*. 150/151: 84–95. (In French)
- Straub D, Schubert M (2008) Modeling and managing uncertainties in rock-fall hazards. *Georisk*. 2(1): 1-15.
- Wyllie D C (2006) Risk management of rock fall hazards. Wyllie and Norrish Rock Engineers, Seattle (<http://www.wnrockeng.com/presentations.html>).
- Wyllie D C, Mah C W (2004) *Rock Slope Engineering, Civil and Mining*, 4th. Edn. Spon Press, Taylor & Francis Group, New York.
- Wyllie D C, Norrish N I (1996) Stabilisation of rock slopes. In: Landslides: investigation and mitigation. Special Report 247. Turner AK, Schuster RL (eds). Transportation Research Board, National Research Council, Washington, DC. pp. 474–504.

Landslide and Debris Flow Barriers at A83 Rest and be Thankful in Scotland

Vjekoslav Budimir⁽¹⁾, Corinna Wendeler⁽²⁾

1) GEOBRUGG AG, Protection Systems, 31000 Osijek, Croatia, Cvjetkova 63A, +385 91 665 9845

2) GEOBRUGG AG, Protection Systems, Romanshorn, Switzerland

Abstract Rest and be Thankful on the A83 road in northern Scotland has a history of landslides. In 2007 the site was closed for several weeks after shallow landslides, a kind of mudslides deposited 400 t of material on the road. In early September 2009 a further event resulted in 1.070 t of material slipping onto the road at the same place, forcing its closure for 48 hours. No one was hurt in either incident, but these debris flows pose a serious threat to the country's main rural routes (Gibson 2010). This site has been the subject of study and is included in the recent Scottish Roads Network Landslides Study produced by Transport Scotland. The study identified the A83 at Rest and be Thankful as one of the most risk sites for debris flow and/or landslide – a fact confirmed by the events that have occurred. Swiss company Geobrugg AG who is specialised in natural hazard mitigation systems including slope stabilization, avalanche barriers, rock fall catch fences and debris flow barriers is well advanced in the research, development and testing of landslide barriers. While rock falls tend to have discrete blocks falling with high velocities, debris flows tend to have high volumes of materials mobilised by significant water flows. Shallow landslides have compared to debris flows normally smaller volumes but occur suddenly on open hills and are not channelized. Understanding the differences is the key to the provision of suitable tailored catch fences or barriers that work to deal with the type of hazard effectively and in a cost effective manner. Geobrugg has been developing and testing flexible rock catch fences for many years. The development of flexible debris flow barriers is more recent but has reached a point where they may be designed, specified and installed with confidence. Indeed, installations are now quite common in European alpine areas, California, Japan and Korea in particular.

Keywords landslides, debris flow, shallow landslides, natural hazard, barriers, landslides barrier

Introduction

In 2007 the A83 road at Rest and be Thankful was closed for several weeks after a debris flow/landslide event that deposited 400 tons of material on the road. Then in early



Figure 1 Debris blocking the road after event 2009 (picture source Scotland Transport).

September 2009 some further 1070 tons of material slipped onto the road at the same place closing it for 48 hours (Fig. 1). No one was hurt in either incident (Gibson 2010).

This site has been the subject of study and is included in the recent Scottish Roads Network Landslides Study produced by Transport Scotland. The study identified the A83 at Rest and be Thankful as one of the most risk sites for debris flow and/or shallow landslide – a fact confirmed by the events that have occurred (Figs 2, 3).

Following the 2007 event, it had been decided to enlarge the culvert underneath the road to reduce the risk of blockage and the necessary ground investigation was already in the course of procurement when the 2009 event occurred.

However the latest situation, together with the new availability of landslide specific barriers from Switzerland based upon very recent research and development, led to the specification and installation of protection measures up slope of this key public road.

As Transport Scotland's head of network maintenance Graham Edmond said: "While we can't prevent future events, we are working closely with (operating company Scotland Transerv) to keep the A83 road, open as safely as possible."



Figure 2 Shallow landslide events at Rest and be Thankful along the slope 2009 (picture source Scotland Transport).



Figure 4 One of the 20 performed landslide tests in Veltheim.



Figure 3 Small channelized slide occurred like a debris flow.



Figure 5 Completely with mud filled test barrier in Veltheim.

“We are investing £760,000 in this area, helping us to develop early prediction and warning tools” he continued.

Most of the funding is being used to install a landslide barrier and debris flow barrier and bespoke remote monitoring sensing equipment to monitor the movement of the hills and minimize landslide risk.

Research, development and design – Veltheim testing

Swiss company Geobrugg AG who specialized in natural hazard mitigation systems including slope stabilization, avalanche barriers, rock fall catch fences and debris flow barriers are well advanced in the research. The development and testing of landslide barriers is described now in the following section.

The landslide test site in Veltheim community in the Aargau canton of Switzerland has a test slope channel of 8 m wide and 41 long with an average inclination of 30° (Fig. 4). The sides of the channel are about one meter high and the bed surface is made of bedrock covered by sediments. At the top of the slope a release apparatus was built. It consists in a 1.8 m high wall whose 0.8 m lower section is a trap door that can be opened remotely. The lateral sides as well as the bottom surface above the wall are reinforced and made impermeable. The release apparatus has a capacity up to 50 cubic meters of material which could be released at once to model the sudden failure of a shallow landslide.

Barriers are full scale tested by releasing the material at the top, reaching the barrier finally after passing laser sensors, flow measurements, impact forces sensors and force plate with a velocity of up to 11 m/s impacting the barrier. The barrier itself was instrumented with load cells in each cable to be able to do back calculations of acting impact forces (Fig. 5). Maximal measured impact pressures within the tests were almost 200 kPa.

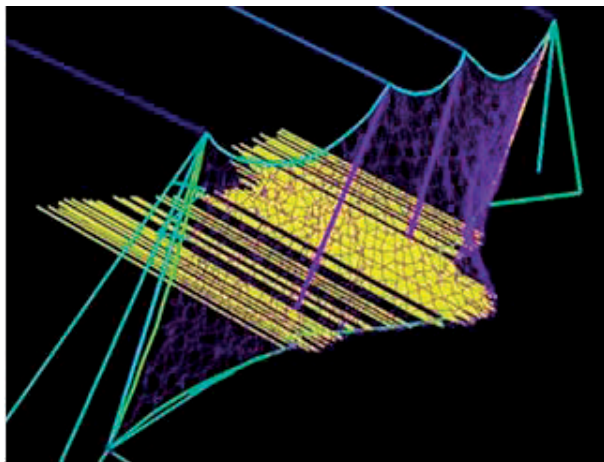


Figure 6 Shallow landslide barrier modeled with finite element software showing mudflow impacting the barrier.

Finally all results of measurements end up in calibration of finite element model which allow us to design flexible barriers against mudslide (Fig. 6). We implemented the acting pressure into our own nonlinear finite element software FARO and compared the results of numerical simulation with measured rope forces. Furthermore rope equation formula was calibrated according to the measured geometry values and the measured rope forces.

Landslide barriers installed at Rest and be Thankful

Following detailed assessments of the circumstances that have occurred at Rest and be Thankful the potential risks have been determined. Following consultation with both barrier supplier and installer, a four meters high and 80 meter long landslide barrier was been specified.

In the stream gully nearby, a debris flow barrier also four meters high and 15 meters span width is required to eliminate the chance of the culvert under the road becoming clogged with debris.

Because of the fine material mobilized in 2009 and based on experiences from field tests, a ROCCO ring mesh with two secondary 50 mm aperture mesh layers was recommended for the debris flow barrier in the gully. This mesh combination was successfully tested for shallow landslide barriers in 1:1 field tests performed in St. Leonard and Veltheim, Switzerland (Bugnion et al. 2010, 2011).

The supporting ropes consist of two lower support ropes of 22 mm diameter with brake rings, along with two upper support ropes also of diameter 22 mm complete with brake rings and abrasion control protection. The debris flow barrier is a standard Geobruigg debris flow barrier designed using in house DEBFLOW online software (Wendeler 2010).

Based upon the research and development carried out in Switzerland the landslide barrier has been designed and manufactured to match the assessed risk

and detailed requirements. Geobruigg's SPIDER mesh is used with secondary 50 mm aperture mesh to retain the finer material. These meshes are held by top and bottom ropes on posts secured by both upslope and lateral rope anchors. The design has been carried out by Geobruigg's Technical Department in Switzerland.

Corinna Wendeler, the leader of Geobruigg's Technical Department, who has been closely involved in the research and development of both debris flow barriers and more recently landslide barriers visited site after the 2009 event, commented "It is very pleasing to see the research and development that I have been so closely involved in Switzerland now being used to the benefit of the Scottish road user.

This project will be the first in the British Isles to use a dedicated flexible debris flow barrier and is particularly interesting in that it will also have the latest flexible landslide barrier – a world first to my knowledge that the two types have been installed on the same site".

Installation of barriers

The barriers are being installed by BAM Ritchies, who with their locally based workforce have experience of the installation of these new generation flexible barriers (Figs 7, 8). Work commenced in late January and is due for completion in March 2009 (Gibson 2010).

With traffic restricted to one lane only by traffic lights, the team have been working in one of the worst winters in recent years. Ground conditions on the 35 degree slope are also challenging with over burden thickness in places being deeper than expected, leading to increases in pile and anchor sizes, depths and drilling times.

The landslide barrier consists of eleven posts at eight meters centres located by upslope restraining ropes without brake rings and top and bottom longitudinal ropes, which carry the SPIDER and secondary mesh facing. These longitudinal ropes are fitted with brake rings which will absorb energy in the event that another landslide occurs.

The posts are hinged onto spheroidal cast iron base plates at ground level secured into the rock by three meter long 35mm anchors. Where there is overburden present the base plates sit on cast in situ concrete blocks secured by a vertical 40 mm galvanized GEWI bar and an inclined 50 mm galvanized GEWI bar acting in tension. The up slope ropes and the ends of the longitudinal ropes are secured by 22.5 mm Geobruigg rope anchors grouted into rock. The advantage of these rope anchors is that they have flexibility to adjust to the changing angles that occur if and when the barrier is loaded.

All the holes for the bars and rope anchors have been drilled using a rope supported Rippamonte drill rig with compressed air rotary head and Down-the-Hole hammer operated by experienced BAM Ritchies' personnel.



Figure 7 Drilling for the anchors.



Figure 9 Installed landslide barrier.



Figure 8 Installation of Landslide barrier.



Figure 10 Landslide barrier near road.

BAM Ritchies' site engineer Rachel Long has been working closely with Scotland Transerv's Engineering Geologist Sarah Walker to realize the project on the ground. Rachel observed: "The weather and the ground conditions on a steep slope have proved difficult but I am really pleased the way the whole project has come together as a result of excellent team work from everyone involved both in Scotland and Switzerland".

Monitoring and instrumentation

Remote sensing equipment will be installed at specific locations on the slope above the road as part of ongoing monitoring to measure the deformations. This monitoring also includes laser scanning to identify any movements or changes of concern. Also additional warning sensors installed on the barriers reacting on vibration are able to send a signal to responsible office of the road authority to check the barriers and the road underneath.

Conclusion

The aim of this paper is to demonstrate and explain new way of solving landslide problems with new generation of flexible barriers. Quickly an introduction about the 1:1 field tests performed in Veltheim was given. The complete design of these barriers is based on the scientific results of these tests. Both rope forces and impact forces were measured with load cells and the results end up in a numerical modelling tool.

The easy and quick way to install this new protection measure even on rough climate conditions like in Scotland can be seen within this paper. Now the customer – Scotland Transerv – is waiting for new slides that the new protection system could start his function and demonstrate his effective performance.

References

Bugnion L, McArdell B, Bartelt P, Wendeler C (2011) Measurements of Hillslope Debris Flow Impact Pressure on Obstacles. Landslides. 9: 179-187, DOI 10.1007/s10346-011-0294-4.

- Bugnion L, Wendeler C (2010) Shallow landslide full-scale experiments in combination with testing of flexible barrier. Debris Flow 2010 Milano, Italy.
- Bugnion L, V. Bötticher, A., Wendeler C (2012) Large scale field Testing of hill slope debris flows resulting in The Design of Flexible Protection Barriers, Abstract of 12th Interprevent Conference, Grenoble, France.
- Gibson D (2010) Landslide Victory, the UK's first flexible debris flow barrier I being installed at the landslide prone Rest and be Thankful site in Scotland, Ground Engineering April 2010.
- Rickli C, Bücher H (2005) Hangmuren ausgelöst durch die Unwetter vom 15.-16.07.2002 im Napfgebiet und vom 31.08-1.09.2002 im Gebiet Appenzell – Projektbericht zuhanden des Bundesamtes für Wasser und Geologie BWG.
- Wendeler C (2010) DEBFLOW – Design tool for flexible ring net barriers against debris flows, Software manual.
- Winter M G, Macgregor F, Shackman L (2008) Scottish Road Network Landslides Study Edinburgh.

Monitoring and Warning Tool for Landslide Risk Prevention

Cristian Marunteanu, Mihaela Roca

University of Bucharest, Faculty of Geology and Geophysics, Bucharest, Romania, Traian Vuia St. 6, +40745041960

Abstract The proposed model is a functional model for permanent monitoring of slope movements in potential unstable areas based on a software tool for risk managers to be able to create warning and civil protection strategies. The monitoring is based on real-time data acquiring from sensor modules (displacements, water level, precipitation, temperature) and transmission of field data through wireless communication to a risk management hub. Following a decisional support solution, the results of measurements on-line are automatically compared with the theoretical curves of critical displacements and the alert (in real time) is triggered via internet.

Keywords landslide risk, probability maps, monitoring, critical displacements, automatic warning.

Introduction

The proposed assessment and methodology of the instability conditions monitoring in potential unstable areas requires three main stages: i) zoning of the instability probability, calculated as a function of critical slope angle, followed by the selection of zone(s) with the highest instability probability, in correlation with incipient movements on the slope or other marks of potential instability; ii) acquisition and storage of monitoring data from the selected slope(s) and iii) warning of sliding.

Zoning of the slope instability probabilities (probability maps)

The zoning of the slope instability probabilities is based on calculation of the critical slope angle and on calculation of the probabilities of sliding in a network of points, according with the following scheme:

1) Storage data:

- coordinates of the observations points in a network (x, y) and
- geomechanical, hydrogeological and geometrical parameters: unit weight (γ), friction angle (ϕ), cohesion (c), groundwater level (h_a) and height of the slope (H);

2) Calculation of the critical slope angle α_c in x, y points using the equation [1] (Sage et al. 1977, Bomboe and Marunteanu 1986):

$$\alpha_c = \frac{445 \cdot c}{\gamma \cdot H} + \bar{\phi} \cdot \left(1,2 - 0,3 \frac{h_a}{H} \right) - 7 \quad [1]$$

Calculation of the statistical parameters: mean and standard deviation of the critical slope angle ($\bar{\alpha}_c$ and S_{α_c});

3) Calculation of the probability of sliding (the probability of the slope angle to reach or exceed the critical angle) in a network of points (x, y), using the equations [2] (Sage et al. 1977):

$$\alpha < (\bar{\alpha}_c - 2S_{\alpha_c}); \quad P_a < 0,05$$

$$\bar{\alpha}_c - 2S_{\alpha_c} < \alpha < \bar{\alpha}_c + 2S_{\alpha_c}$$

$$\alpha > (\bar{\alpha}_c + 2S_{\alpha_c}); \quad P_a > 0,95$$

$$P_a = 0,45 \sin \left\{ \left[\bar{\alpha}_c \left(\frac{S_{\alpha_c}}{45} - 1 \right) + \alpha \right] \frac{45}{S_{\alpha_c}} - \bar{\alpha}_c \right\} + 0,5 \quad [2]$$

The instability probability (P_a) is calculated as a function of critical slope angle (α_c). The monitoring will be performed in the zone(s) with the highest instability probability, correlated with possible incipient movements on the slope;

4) Zoning of the slope instability probabilities (probability maps). Two areas with known instability phenomena have been chosen as model for the application. The probability maps have been realized by zoning the probabilities of instability calculated by the equation [2] in a network of points (Figs. 1 and 2). The two maps are real maps realized by the authors in Suceava Municipality area and Suceava historical citadel area, respectively, (Roca 2012) but they are used only as patterns to apply the proposed methodology;

5) Choice of the monitoring alignments and points (coordinates x_{mon} , y_{mon} , z_{mon}) of the inclinometers locations in the areas with high instability probability (red color on the maps). The selected profiles chosen as examples are drawn in black in Figures 1 and 2.

Monitoring alignments in the field and several installed inclinometers on the two profiles are shown in Figures 3 and 4.

The first stage of the proposed monitoring model was dedicated to zoning the instability probability of a designated area and to assess the highest instability probability (potential sliding) zones. One or more of these zones could constitute the object of monitoring.

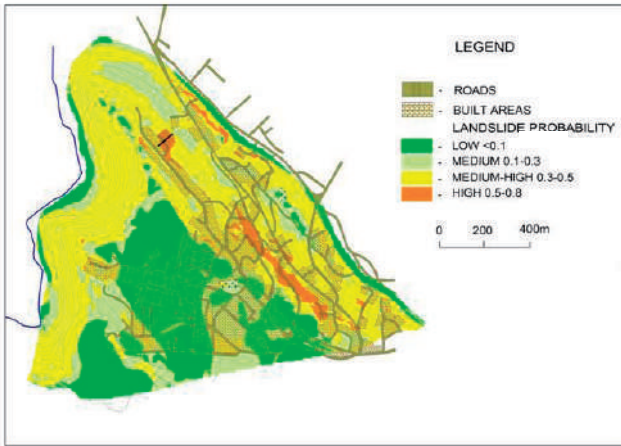


Figure 1 Instability probability map and monitoring alignment (in black) – zone 1 – Suceava Municipality area (Roca 2012).

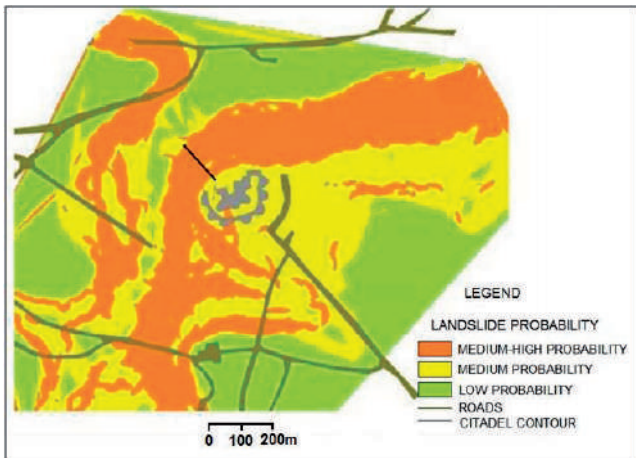


Figure 2 Instability probability map and monitoring alignment (in black) – zone 2 – Suceava historical citadel area (Roca 2012).

The choice of the monitoring profile could be done in correlation with incipient movements or other instability marks on the slope.

If a monitoring profile is imperative required by recognized potential instability conditions, the second and the third stages of the model (monitoring and warning, respectively) can be applied directly, the zoning of the instability probability of the area being no more necessary.

Acquisition and storage of monitoring data

Acquisition and transmission of field data are realized through wireless communication from monitoring points to a risk management center.

Storage of the monitored data from the sensors is attained in sequential files (Tab. 1). The data come from a surface sensor system (P and T) and from an underground sensor system installed on the top and some other depths of the inclinometers (h_w , U_x and U_y) to obtain full information on slope displacements and ground water table.



Figure 3 Monitoring alignment (red line) and installed surface sensor system and inclinometers - zone 1.



Figure 4 Monitoring alignment (red line) and installed inclinometer - zone 2.

Table 1 Model of storage of the monitored data from the sensors in sequential files, where: No – number of the monitoring point; Xmon, Ymon, Zmon – coordinates of the monitoring point; T – air temperature; P - rainfall; ha - ground water level; Ux and Uy - displacements in two orthogonal directions, at different depths on the inclinometer, vertical casing.

No	X _{mon}	Y _{mon}	Z _{mon}	Date:	hour	T	P	h _a	U _x	U _y
				d/m/y						
1										
...										
k										

Table 2 Data base model of the displacement field data received through wireless communication from sensors in one inclinometer, where: No – number of the displacement sensor on the inclinometer; U_x, U_y – horizontal displacements from displacement sensor; U - displacement resultant vector in the dip direction (calculated).

No	Depth of the sensor (m)	U _x	U _y	U	Date
1					
...					
n					

An example of storing of transmitted and received field data through wireless communication is presented in Table 2.

Warning of sliding

Warning of sliding can be put into effect in five stages:

1) Evaluation by deterministic methods of the *critical* horizontal displacements in the monitoring points, at different underground water levels.

The program PLAXIS – Finite code for Soil and Rock Analyses, using the limit equilibrium method and the elastic-plastic model Mohr-Coulomb, allows the determination of the critical horizontal displacements based on elastic and shear parameters of the soils in slope vertical sections. Examples of monitoring profiles (zone 1) showing the distribution of the critical horizontal displacements at two different ground water levels are presented in the Figure 5, together with the critical horizontal displacements distribution on the vertical of two monitoring drillings (A and B, respectively);

2) Storage of the critical displacements values U_{x,critical}, U_{y,critical} - extracted from the output of the PLAXIS program - at different depths in vertical profiles, in the database of a monitoring system (Tab. 3);

3) Comparison between the values of the horizontal displacements provided by the displacements sensors in drillings (U_x, U_y) and the calculated values of the critical displacements corresponding to the installed sensors levels (U_{x,critical}, U_{y,critical}) provides theoretically the starting moment of warning when the below conditions are accomplished:

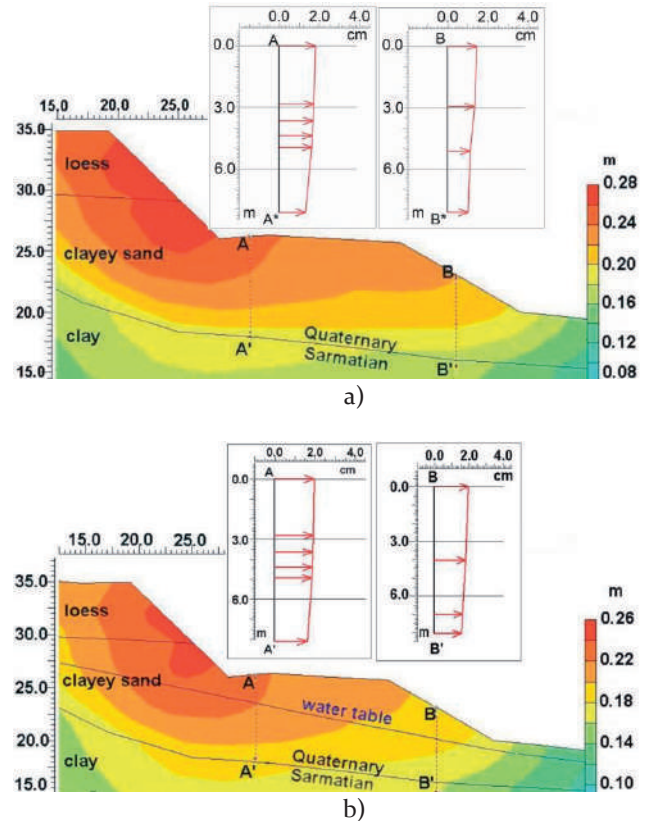


Figure 5 Slope stability profiles in a monitoring alignment and critical horizontal displacements distribution on the profiles (isolines) and on the vertical of two monitoring drillings, A and B (vectors), at two different ground water levels: a) saturated slope; b) 2.0 m depth (sliding surface - at the limit Sarmatian-Quaternary). Vertical, horizontal and displacement scale of the profiles - in meters; horizontal displacements on the vertical of the two inclinometers, A and B - in centimeters.

Table 3 Data base model of critical displacements in a monitoring drilling where: No – number of the displacement sensors in the vertical profiles of the monitoring drilling; Xmon, Ymon – coordinates of the monitoring drilling; Z – depth of the displacement sensors in the monitoring drilling.

No	X _{mon}	Y _{mon}	Z	U _{x,critical}	U _{y,critical}
1					
...					
n					

$$\begin{aligned}
 U_x &\geq U_{x_critical} \\
 U_y &\geq U_{y_critical}
 \end{aligned}
 \tag{3}$$

Practically, for an analyzed vertical profile, the displacement vector in the dip direction (U) must reach or exceed the equilibrium limit displacement (U_{critical}) provided by the data base of critical displacements:

$$U \geq U_{critical}
 \tag{4}$$

Table 4 Critical displacements in the monitoring drilling (A) and stability factor of the monitoring profile from Fig. 5.

Monitoring drilling	Factor of safety Fs	Water table depth (m)	Depth of the sensor		
			0 m	3 m	6 m
U _{critical} (m)					
A	1.134	0	0.246	0.239	0.216
	1.335	2	0.224	0.220	0.201
	1.512	5	0.213	0.210	0.196
	1.636	8	0.209	0.205	0.192

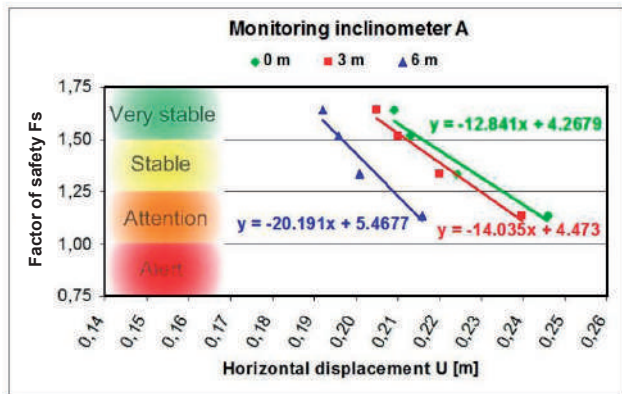


Figure 6 Diagram stability factor - horizontal displacements, inclinometer A (data from Tab. 4).

The data provided by PLAXIS calculation (stability factor for a monitoring profile and critical horizontal displacements on the vertical of the monitoring drillings from the profile, at different levels of underground water) are converted in diagrams factor of safety – critical displacement for each monitoring inclinometer. The stability domains were formally settled function of the factor of safety values in very stable, stable, attention and alert (Marunteanu et al. 2008).

An example of data base structure (Tab. 4) and of diagram factor of safety - critical displacements (Fig. 6) are presented below (Roca, 2012).

4) Following an intelligent decisional support solution (Enache et al. 2007), the results of measurements on-line are automatically compared with the theoretically curves of the displacements from the diagrams stability factor-horizontal displacement.

5) Alert is triggered in the case the monitored displacement values overlaps the values from the critical zones of the curves factor of safety-horizontal displacement (Attention and Alert in Fig. 6). The alert (in real time) is sent via internet from the risk management hub to local authorities.

Conclusions

The proposed model allows:

- locating the potential unstable areas, where normal variation range of the stability parameters is exceeded, and presenting them on digital maps;
- analysis of prone profiles, based on monitoring data, geological - hydrogeological conditions and probabilistic modeling and expressed as theoretical evolution diagrams;
- permanent monitoring of landslides, through online interpretation of data captured from the movement transducers and level sensors of the ground water;
- generating alerts in concordance with the warning assessed conditions.

The developing of a software tool in real time for risk managers so they can create alarming and civil protection strategies represents the most important expected result of our work.

Acknowledgments

The authors thank to the colleagues from the Institute for Computers and from the Research Development, Engineering and Manufacturing for Automation Equipment and Systems from Bucharest, Romania for their contribution to the design of the on-line parameters capture, wireless communication, relational Data Based System and intelligent decisional support solution.

References

- Bomboe P, Marunteanu C (1986) Engineering Geology. University of Bucharest. 802p. (In Romanian)
- Enache A, Olaru V, Stan C, Marunteanu C (2007) Remote decision support system for landslide risk management in a geographical area with high risk of natural disaster – TERRARISC. Revista de automatica: 34-54, Bucharest. (In Romanian)
- Marunteanu C, Stanciu M, Scradeanu D, Roca M (2008) Assessment and monitoring of the instability phenomena in an urban area. II European Conference of International Association for Engineering Geology EUROENGE 2008, Madrid, 15-19 September.
- Roca M (2012) Landslides in urban areas. Case study Suceava area. PhD Thesis, University of Bucharest. (In Romanian)
- Sage R, Toews N, Xu X, Coates D F (1977) Rotational shear sliding. Analysis and computer programs. Supplement 5-2. In Pit Slope Manual, CANMET Report 77-17, Ottawa, Canada.

The Analysis of Landslide Umka Dynamics Based on Automated GNSS Monitoring

Biljana Abolmasov⁽¹⁾, Marko Pejić⁽²⁾, Vladimir Šušić⁽³⁾

1) University of Belgrade, Faculty of Mining and Geology, Belgrade, Serbia, biljana@rgf.bg.ac.rs

2) University of Belgrade, Faculty of Civil Engineering, Belgrade, Serbia

Abstract In the past decade, there has been a gradual introduction of systematic monitoring on the largest landslides in Serbia by establishing a network of monitoring facilities. As the rapid adoption of new technologies continues - the natural evolution of equipment for landslide monitoring has started. The technological evolution of GNSS systems creates the potential for automated remote collection of accurate, high resolution data and represents step forward that will increase speed, precision, cost effectiveness and overall quality of landslide investigations. This paper presents results, features and benefits of three years automated GNSS monitoring of landslide Umka near Belgrade.

Keywords GNSS, monitoring, landslide, landslide dynamics

Introduction

Various professions deal with research and investigation of the landslide processes and landslides as occurrences, but basically the main aim of the greatest part of the research is to design appropriate remedial measures which would enable permanent stability of the slopes or cuts. For that reason, the greatest number of researches is directed to establishing the geometry of the landslides and physical-mechanical characteristics of sliding mass affected by the sliding process and parameters of shear strength in the zone of the sliding surface itself. Monitoring of the landslides is an integral part and very important element of the research process. However, in practice, it most often results in non-continual or observation intervals that are too short, inappropriate or incomplete equipment, which globally leads to insufficient amount of reliable data on parameters that are followed during the monitoring. Apart from traditional survey methods of monitoring (i.e. landmarks, reference points) monitoring systems also imply the use of geotechnical instruments, such as piezometers, inclinometers, or various types of sensors (in rainfall measuring stations, for measuring the moisture content in the soil etc.). In all active landslides they represent the minimum of equipment which enables obtaining various types of data necessary to understand the dynamics and

mechanisms of landslide movement, actually being the basic prerequisite in designing successful remedial measures.

The technological evolution of Global Position System (GPS) technology and sensors for monitoring of landslide activity in real time started not so many years ago. Gili et al. (2000) give a general overview of the GPS principles and discuss its applicability to landslide monitoring on landslide Vallcebre. Using GPS technology to provide differential position information with sub-centimeter level accuracy in structural and land monitoring applications was investigated by Manetti et al. (2002a,b). The motion of the Super-Sauze earthflow is clearly detected by the GPS measurements and the results have been compared with those obtained with conventional geodetic methods (Malet et al. 2002). Seasonal movement of the Slumgullion landslide determined from GPS surveys and field instrumentation from July 1998–March 2002 was presented in Coe et al. (2003). GPS monitoring experiment results from the Ya'an-Xiakou landslide have demonstrated that GPS can provide sufficient accuracy to meet landslide displacement monitoring requirements, leading to the replacement of the conventional geodetic surveying methods (Zhou et al. 2005). Combination of GPS and photogrammetry methods can significantly improve the efficiency of landslide monitoring (Mora et al. 2003, Baldi et al. 2008). Brückl et al. (2006) describes a long experience of monitoring a deep seated mass movement in Gradenbach with GPS. It was concluded that is suitable for measuring relatively large displacements, which cannot be captured by inclinometers or extensometers. Bertacchini et al. (2009) established integrated surveying system for landslide monitoring of the Valoria landslide. The research deals with the integration of surface displacement measurements obtained using geodetic and topographic instruments such as satellite GPS and traditional one, like automatic total station, in a large-scale active earth-slide. Barla et al. (2010) describes monitoring of the Beauregard landslide using advanced and conventional technics. GPS measuring has proved to be an effective and reliable tool, especially for measuring surface deformations on large and slow-moving landslides (Mansour et al. 2011).

This paper presents results, features and benefits of introducing automated GNSS monitoring system on landslide Umka near Belgrade, Serbia in the last three years.

Materials and methods

Case study

Serbia is known for numerous landslide phenomena. This is particularly stressed in the valley banks of rivers Sava and Danube and their respective tributaries. Umka landslide is situated on the right meander of Sava River 25 km South-west from Belgrade in the settlement of Umka (Fig. 1). First written records of the landslide activity date from the beginning of the 20th century.

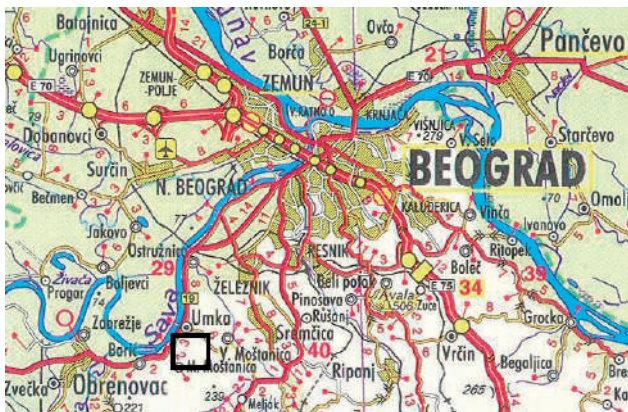


Figure 1 Geographical position of Umka landslide.

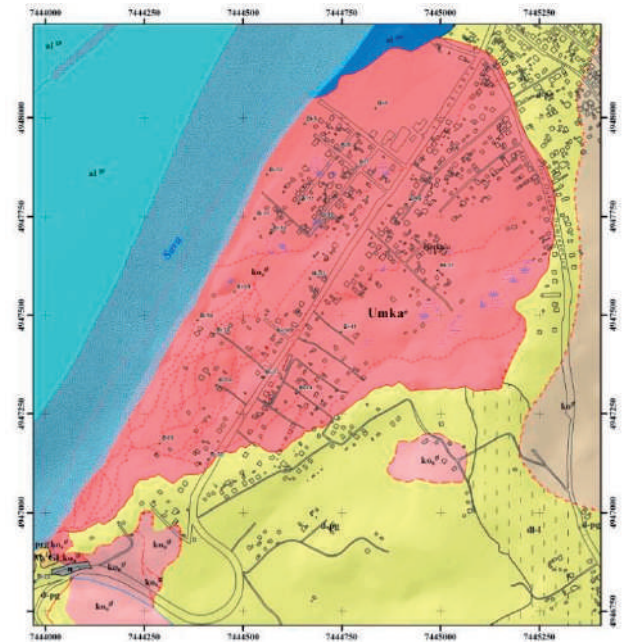


Figure 2 Engineering geological map of Umka landslide.

Pannonian sediments i.e. silty - clayey massive soft rocks have the dominant role in geologic composition of terrain, and these are: marls (M_3^2L), more than 200 m



Figure 3 Deformation on the road M-19.



Figure 4 Deformation on the house.

thick and marly clays (M_3^2GL), 10-25 m thick. Stable landslide underlying stratum is made of grey marls. Under the triaxial test conditions, the shearing strength parameters within the natural moisture amount to $\phi = 18 - 28^\circ$ and $c = 30 - 200$ kPa. This landslide is triangular fan-shaped, with the length along the slope of 900 m, toe width of 1450 m, area of 100 hectares, average depth of 14 m, volume 14.000.000 m³ and average gradient of 9°. Upstream landslide part is surrounding the steep frontal scar with the height from 5 to 25 m, whereas downstream landslide part doesn't have a pronounced leap (Fig 2). Genesis of the landslide is, apart from geological predisposition caused by contact between weathered clay marls and fresh marls, closely connected with erosion of the right bank and evolution of the meanders of the Sava river (Abolmasov et al. 2012).

Landslide area has been investigated over the last 30 years, and the last conventional monitoring has been completed in 2005, at that time the depths of the sliding surfaces in various blocs have been definitively confirmed, based on the numerous inclinometric measurements. During 2005, due to extensive displacements, majority displacements were recorded in

block A - 26 m, while in blocks B and C they amounted to 5 to 15 m. Displacements as a rule have translational pattern along slightly inclined parting planes. Displacement speed is increasing during the diminution of Sava river level.

After 2005, research and monitoring were not performed, nor were there any remedial measures undertaken. Landslide Umka is still an active landslide with visible deformations on the M-19 road and local residential buildings (Fig. 3, 4).

System architecture

In March 2010, a completely automated monitoring system was installed at the Umka landslide in the body of the landslide in bloc B. Monitoring station was installed on the roof of the house which was estimated to enable the equipment to operate uninterruptedly (Fig. 5). Two reference points, Belgrade and Lazarevac were established as stable points up to June 2011. After June 2011 three reference points (Belgrade, Indjija and Grocka) were established up to now. A double-frequency GPS receiver Leica SR530 and AT502 with monitoring and recording the satellite observations every 30 seconds was installed. Automatic upload/download of files of recorded data has been pre-set at every 12 hours, while GSM modem for communication was used for the remote control and download of data, considering that the internet connection was of poor quality. A calculation of 2D and 3D coordinates of the monitoring station every 12h and 24h were programmed from all reference stations, as well as the control monitoring of all stations.

GNSS Spider and GeoMos software are installed on a central computer located in Belgrade, where it stores and processes all the raw registered data from receivers. Automatic download of raw data in RINEX file format is provided using tempered GSM communication intervals.

In parallel to the displacement monitoring, daily climatological data was collected (amount and type of precipitation, temperature and air humidity), as well as hydrological data: the levels of Sava river at measuring stations Beljin and Belgrade.



Figure 5 GNSS sensor on the site location.

Results and discussion

The aim of establishing the GPS monitoring system was to monitor movements in the bloc B of the Umka landslide at low cost. These movements were already possible to assess visually on the M-19 road and surrounding residential buildings as permanent deformations. There were no possibilities to install more GPS sensors, or to link in additional equipment (inclinometers, extensometers, piezometers or rainfall gauge) in the whole monitoring system.

Analysis of the results obtained by automatic monitoring of the landslide movement during the period from 28 March 2010 until 17 June 2011 showed that the movements were continuous and that they cumulatively amounted to 30 cm (x coordinate) and 44 cm (y coordinate). There are two significant interruptions in measurements from 25 July 2010 until 20 September 2010 and from 30 January 2011 to 20 May 2011. Both times the system was restarted and the measuring equipment was calibrated. First interruption in measurements occurred due to a breakdown of the equipment, and the GSM modem was replaced. Second interruption occurred due to the equipment being turned off because of the internal decorating of the building. Fully automated GPS monitoring system in real time was re-established after 20 May 2011 (Fig. 6).

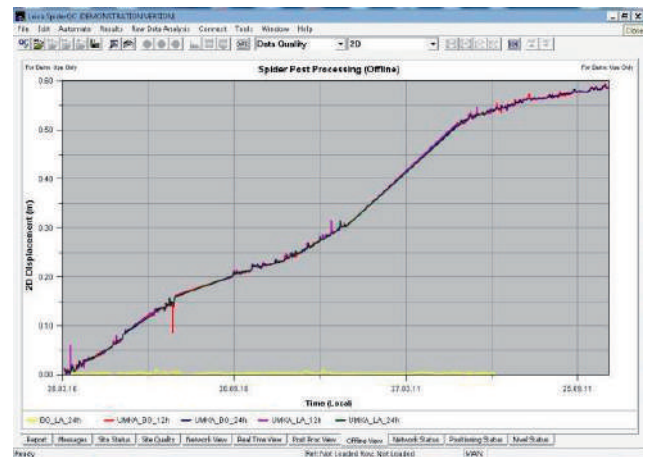


Figure 6 2D displacement plot from March 2010 to September 2011.

During the monitoring, only one leap was recorded when there was a movement of around 2 cm in a single day (25 July 2010). A crack in the staircase in the yard of the building was also recorded then. Calculations of 2D and 3D movements imply that in the period between 30 January 2011 to 20 May 2011, during which there was no monitoring or measuring, the movement amounted to more than 20 cm. Generally, movement coincided with end of springtime, during which the amount of movement is usually greater than during the other seasons because of the precipitations and the increase in the water level of the Sava river. For the same period

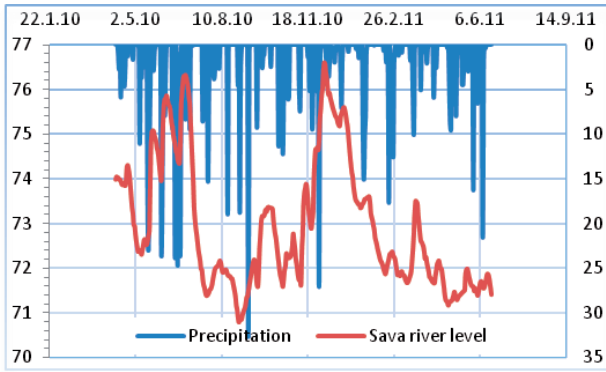


Figure 7 Precipitation and Sava river level (Beljin station) from March 2010 to February 2011.

during which the GPS monitoring was being done, the analysis of the effects of precipitations and the level of Sava was performed. It was obvious that during the period between April and August 2010 sum of precipitation increased as well as the level of the Sava River, especially during June-July 2010 (Fig. 7). After the beginning of July 2010 level of Sava river decrease rapidly - 3 m/ 15 days and movement of 2 cm was recorded on GPS point.

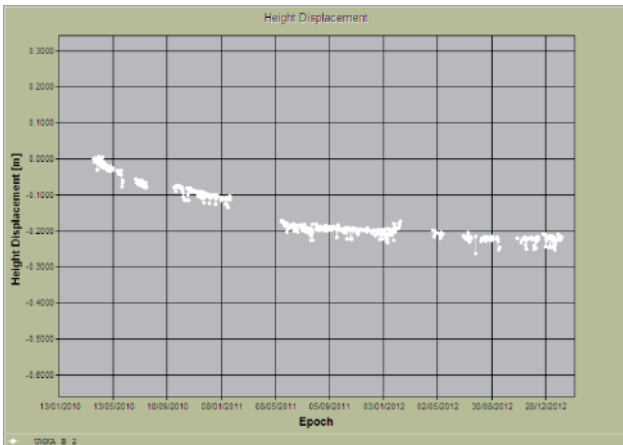


Figure 8 Height displacement plot from March 2010 to January 2012.

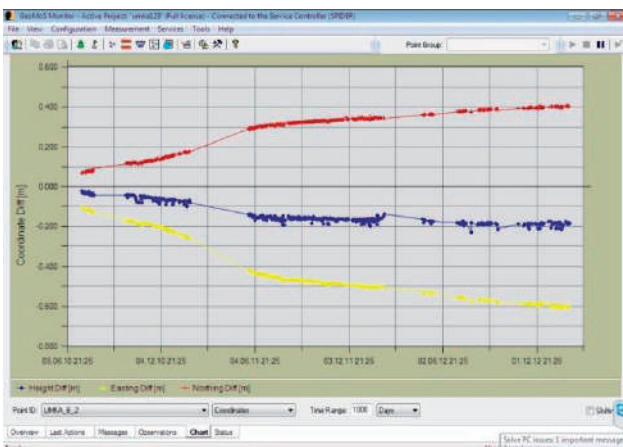


Figure 9 3D displacement plot from March 2010 to January 2013.

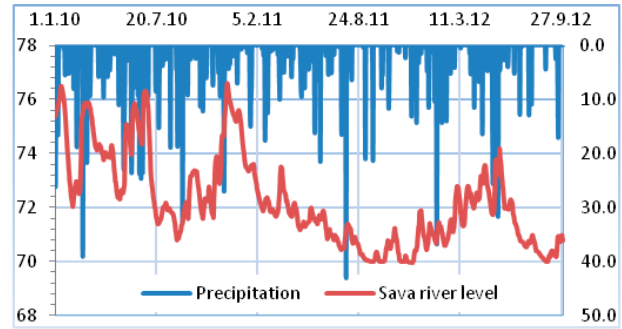


Figure 10 Precipitation and Sava river level (Beljin station) from January 2010 to September 2012.

Analyzing the nature of the 3D movements during March 2010-June 2011, it is clear that trend is close to linear, which confirms that there were no sudden slides in 14 months monitoring period, except movement on 25 July 2010. For the rest of period of monitoring, velocity of movement was slow down and cumulative displacement reached only 20cm E, 10 cm N and 2cm in height (Fig. 8, 9). One can also conclude that Umka landslide has relatively constant velocity of movement towards Sava River, during that period. Precipitation and level of Sava river fluctuated, but in above average level of statistical values (Fig. 10).

During the period June 2011-January 2013 landslide displacement was in the category of very slow velocity. In the same time, it was very dry period and level of Sava river was on absolute minimum for 100y period. It was no significant rising and no significant cumulative precipitation.

Movement in 1D sense shows exponential trend and some short periodic oscillation of estimated positions. Realizing the cause of these oscillations is task for future work; along with implementation of statistical deformation analysis that takes into account the a posteriori errors and size of movement that can be detected. In general, achieved accuracy of site daily GPS positions in this monitoring project is sufficient for Umka landslide.

Conclusion

Performing the automatic GPS monitoring system for the first time in Serbia on the landslide of Umka near Belgrade had a goal to monitor the movements of the landslide during the period when there were no financial possibilities of establishing an integrated monitoring system. Single point GPS unit is not sufficient to track movements of this large bloc landslide. Furthermore, inexperience in operating the GPS real time monitoring systems and sensitivity of the equipment were the cause of some of the interruptions in measurements, which will be avoided in the upcoming period. It was planned to install additional equipment at the landslide – further

two GPS receivers, automatic rainfall gauge, and one more inclinometer, i.e. TDR equipment after first year, but it wasn't financial possibilities.

Establishing a fully integrated and equipped system which would be suitable for Umka landslide is still very expensive. However, the experience gained during the three year of monitoring and measuring clearly indicates the advantages of this type of monitoring system as well as the need to also install standard geotechnical equipment apart from the GPS sensors in extra-large and deep seated slow moving landslides. That is the only way to perform complete monitoring and obtain results that will help us in better understanding of the mechanism and dynamics of landslides.

Acknowledgments

The study would have not been possible without support from VekomGeo,d.o.o., Belgrade, Serbia, Republic Geodetic Authority and Republic Hydrometeorological Service of Serbia. The research was supported by the Ministry of Education, Science and Technology of the Republic of Serbia Project No TR 36009.

References

- Abolmasov B, Milenković S, Jelisavac B, Vujanić V, Pejić M, Pejović M (2012) Using GNSS sensors in real time monitoring of slow moving landslides-a case study. In: Proc. of the 11th Int. and 2nd American Symp. on Landslides and Engineered Slopes, Banff, Canada, 3-8 June, 2012. Taylor & Francis Group, London, pp. 1381-1385.
- Baldi P, Cenni N, Fabris M, Zanutta A (2008) Kinematics of a landslide derived from archival photogrammetry and GPS data. *Geomorphology*. 102 (3-4): 435-444.
- Barla G, Antolini F, Barla M, Mensi E, Piovano G (2010) Monitoring of the Beauregard landslide (Aosta Valley, Italy) using advanced and conventional techniques. *Engineering Geology*. 116 (3-4): 218-235.
- Bertacchini E, Capitani A, Capra A, Castagnetti C, Corsini A, Dubbini M, Ronchetti F (2009) Integrated Surveying System for Landslide Monitoring, Valoria Landslide (Apennines of Modena, Italy). FIG Working Week 2009. Surveyors Key Role in Accelerated Development, Eilat, Israel, 3-8 May 2009. TS 3F – Tectonic Processes, Landslides and Deformation Analysis. URL: www.fig.net/pub/fig2009/ppt/ts03f/ts03f_bertacchini_capra_etal_3343.pdf.
- Brückl E, Brunner F K, Kraus K (2006) Kinematics of a deep-seated landslide derived from photogrammetric, GPS and geophysical data. *Engineering Geology*. 88 (3-4): 149-159.
- Coe J A, Ellis W L, Godt J W, Savage W Z, Savage J E, Michael J A, Kibler J D, Powers P S, Lidke D J, Debray S (2003) Seasonal movement of the Slumgullion landslide determined from Global Positioning System surveys and field instrumentation, July 1998–March 2002. *Engineering Geology* 68 (1-2): pp. 67-101.
- Gili J A, Corominas J, Rius J (2000) Using Global Positioning System techniques in landslide monitoring. *Engineering Geology* 55 (3): 167-192.
- Malet J P, Maquaire O, Calais E (2002) The use of Global Positioning System techniques for the continuous monitoring of landslides: application to the Super-Sauze earthflow (Alpes-de-Haute-Provence, France). *Geomorphology*. 43 (1-2): 33-54.
- Manetti L, Terribilini A, Knecht A (2002a) Autonomous Remote Monitoring System for Landslides. SPIE 9th Annual International Symposium on Smart Structures and Materials. Smart Sensor Technology and Measurement Systems (ss03), 17-21.3.2002 San Diego (CA), USA. Vol 4694, pp. 230-235.
- Manetti L, Frapolli M, Knecht A (2002b) Permanent, autonomous monitoring of landslide movements with GPS. 1st European Conference on Landslides, 24-26.6.2002 Prague, Czech Republic. pp. 245-249.
- Mansour M F, Morgenstern N R, Martin C D (2011) Expected damage from displacement of slow-moving slides. *Landslides*. 8(1): 117-131.
- Mora P, Baldi P, Casula G, Fabris M, Ghirottia M, Mazzini M, Pesci A (2003) Global Positioning Systems and digital photogrammetry for the monitoring of mass movements: application to the Ca' di Malta landslide (northern Apennines, Italy). *Engineering Geology*. 68 (1-2): 103-121.
- Zhou P, Zhou B, Guo J, Li D, Ding Z, Feng Y (2005) A Demonstrative GPS-aided Automatic Landslide Monitoring System in Sichuan Province. *Journal of Global Positioning Systems*. 4(1-2): 184-191.

Landslides in Vietnam and the JICA - JST Joint Research Project for Landslide Disaster Reduction

Khang Quang Dang⁽¹⁾, Kyoji Sassa⁽¹⁾, Do Minh Duc⁽²⁾, Dinh Van Tien⁽³⁾

1) International Consortium on Landslides, Kyoto, Japan

2) VNU University of Science, Hanoi, Vietnam

3) Institute of Transport Science and Technology, Hanoi, Vietnam

Abstract Vietnam has a ratio of mountainous terrain up to ¾ area of its territory, which has very complex geological settings. It is also influenced by the monsoon climate with the average annual rainfalls from 2,000–2,500 mm/year. Due to its geological, geographical conditions and climate characteristics, Vietnam is subjected to frequent slope disasters, those causing annual damage of nearly 100 million USD (Duc 2009). Landslides often take place extensively during the rainy seasons. Therefore, it is required to develop methodologies and models to help reducing the vulnerability of the country with respect to landslide disasters. The project “Development of landslide risk assessment technology along transport arteries in Vietnam” was approved and supported by the Science and Technology Research Partnership for Sustainable Development (SATREPS) which is under the auspices of the Japan Science and Technology Agency (JST) and the Japan International Cooperation Agency (JICA). The goal of the Project is to contribute to geo-disaster reduction along main transport arteries and residential areas through developing of new landslide risk assessment technology, its application to forecast, monitoring and

disaster preparedness of landslides in Vietnam. This paper presents the state of landslide activity and the ability of application of the new ring shear apparatus ICL-2 for landslide study in Vietnam.

Keywords landslide risk assessment, ring shear apparatus, ICL-2, ITST

Introduction

Rainfall in Vietnam is very heavy. It can reach 4,000-4,500 mm/year in some particular areas in the Central Vietnam. Every year in the rainy season between June and September, people in the mountainous regions in Vietnam suffer from the consequences of extensive landslides, those causing annual damage of nearly 100 million USD. The transportation routes in the north-western mountains and in the central part of Vietnam have the highest density of landslides. More seriously, landslides along with debris flows can cause severe fatality. As showing in Table 1 the hazards of landslides and debris flows in Vietnam are very severe in the period from 1986 to 2012.

Table 1 Recent recorded severe landslides and debris flow in Vietnam.

Location	Date	Type	No. of deaths and missing	Damages
Nam Cuong, Cho Don, Bac Kan	23/6/1986	Debris flows, landslides	7	120 ha rice fields, 20 km of roads
Lai Chau Town	27/6/1990	Debris flows, Landslides	Over 100	607 houses, 5 bridges, 10km ² of town demolished
Canh, Cam Duong, Lao Cai Province	6/1996	Landslides	7	2 houses
Muong Lay, Lai Chau Province	17/8/1996	Debris flows, Landslides	55	The commune had to move to another place
Highway No. 27, Lam Dong	10/10/2000	Debris flows, landslides	-	37 severe landslides in 55 km, 500 m highway fully destroyed
Ialy Hydropower Plant, Kon Tum Province	since 2002	Landslides	-	causing damage of billions of VND each year
Du Tien and Du Gia, Yen Minh, Ha Giang	19/7/2004	Debris flows, landslides	48	33 houses, 627 ha rice fields
Dai Tu District, Thai Nguyen Province	15/4/2012	Landslides	6	14 houses



Figure 1 Landslide at the National Road No. 6, Hoa Binh Province.



Figure 2 Landslide at the dump site of the Phan Me Coal Mine, Thai Nguyen Province.

According to the Statistics of Ministry of Transport of Vietnam (MOT), total length of landslide regular highways is over 3,000 km and the annual average volume of landslides caused by typhoons on road network is from 300,000 to 600,000 m³. Particularly, the landslide volume was over 1 million m³ per year during the rainy season of 1999-2000 (Doan and Tien 2012).

In Northwest area, there are still 14 moving tectonic faults which impact directly to the stability of talus and make high ability of landslides on basis of the tectonic destruction zone. On mountainous routes in Central Vietnam, the Ho Chi Minh Road has the highest density of landslides, especially in some sections as the Huong Khe - Tan Ap, the Pheo cross - northern Bung bridge, the Khe Gat - U Bo pass, the Dakrong - Ta Rut - Peke, the A Dot - A Tep - Hien - Thanh My, the Xoi bridge - Kham Duc - Dak Zon - Dak Pet - Dak Glei with a total of over 800 sites in varied sizes. Those landslides were activated due to the activities of left faults in the A Luoi town, in the Hue city and others, which have been published in some research results of Vietnamese scientists.

The average loss of people caused by annual landslides in Vietnam is about 25-30 people/year, the loss

by disasters including typhoon and flood is up to 60 people/year.

Recently, there were some severe landslide occurred along the national roads and on residential areas. For example, on February 16, 2012, a landslide about 15,000 - 20,000 m³ occurred at the National Road No. 6, Hoa Binh Province (Fig. 1), killed 2 persons traveling on the road. On April 15, 2012, a landslide at the dump site of the Phan Me Coal Mine, Thai Nguyen Province (Fig. 2) with a volume of about 2 million m³, buried 14 houses and 6 persons.

The JICA - JST joint research project for landslide disaster reduction

In order to contribute to geo-disaster reduction along main transport arteries and in residential areas in Vietnam, the project "Development of landslide risk assessment technology along transport arteries in Vietnam" was adopted by the Science and Technology Research Partnership for Sustainable Development (SATREPS) which is under the auspices of the Japan Science and Technology Agency (JST) and the Japan International Cooperation Agency (JICA). The International Consortium on Landslides (ICL), Tohoku Gakuin University, Forestry and Forest Products Research Institute, and Kyoto University are Japanese partner institutions in the project. The Institute of Transport, Science and Technology (ITST) has been assigned by the Ministry of Transport of Vietnam (MOT) to collaborate with the International Consortium on Landslides (ICL) in implementation of the Project in 5 years period (2011-2016). The goal of the Project will be obtained through developing of new landslide risk assessment technology, its application to forecast, monitoring and disaster preparedness of landslides in Vietnam. The project activities are organized into four work groups (WG): Work Group on Project Coordination, Education and Public Awareness (WG1), Work Group on Landslide Mapping (WG2), Work Group on Risk Assessment (WG3), and Work Group on Landslide Monitoring (WG4).

Work Group 1: Project Coordination, Education and Public Awareness

The aim of Work Group 1 (WG1) includes:

- Application of risk assessment methodology and examination of practical and effective preparedness to mitigate landslide disasters;
- Coordination and implementation of Education activities in Vietnam, the Greater Mekong Sub-region as well as in Japan;
- Coordination and implementation of meetings (symposia, workshops, public awareness, project group meetings, and publication in print and in web);
- All key persons from Japan and Vietnam will

jointly discuss the plan and the process of the project and coordinate the activities.

Work Group 2: Landslide Mapping

The specific objectives of Work Group 2 (WG2) are:

- Identification of landslide topography from air and images over the targeted areas;
- Mapping of topographic types and landslides over the targeted areas;
- Searching locations of slopes with characteristics of precursor stage of landslides.
- Rating risk of identified landslides by Analytical Hierarchy Process method; Field investigation and field observation to evaluate identified landslide areas;
- Integrated landslide mapping over the targeted areas.

Work Group 3: Soil Testing – Computer Simulation of Landslide Initiation and Motion

Major outputs of Work Group 3 (WG3) are:

- Development of landslide testing apparatus suitable for landslides in Vietnam;
- Geomechanical classification of landslide types posing serious effects in Vietnam;
- Elucidation of initiation mechanism and moving dynamics of selected sites by field investigation, sampling and testing;
- Assessment of initiation and motion of precursor stage of landslides and potential landslides by the developed technology.

Work Group 4: Landslide Monitoring

Main activities of Work Group 4 (WG4) are:

- Selection of monitoring sites in cooperation with other two groups and regional conditions;
- Selection of appropriate monitoring methods based on the field investigation and social conditions;
- Installation of monitoring equipment;
- Establishment of continual monitoring and maintenance system;
- Development of suitable data collection, data transfer and web-showing system;
- Establishment of early warning criteria and system applicable for the targeted sites.

Ring shear apparatus ICL-2

One of the most important objectives of Work Group 3 and also of the Project is developing a landslide testing apparatus which will be used and maintained in Vietnam. The undrained dynamic ring shear apparatus ICL-2 (Figs 3, 4), the latest version of the ring shear landslide simulators series, was designed for laboratory soil testing. The apparatuses have been gradually developed by Professor K. Sassa and colleagues in the Disaster Prevention Research Institute (DPRI), Kyoto University

and the International Consortium on Landslides. The first one was DPRI-3 and the last version of this series was DPRI-7 (Sassa et al. 2004). Then a new series of ring shear landslide simulators (ICL-1 and ICL-2) have been developed in the two projects of Japan - Croatia and Japan - Vietnam supported by SATREPS (Science and Technology Research Partnership for Sustainable Development) (Oštrić et al. 2012). The ICL-2 apparatus was designed to test very deep landslides with the capacity of maintaining an undrained state up to 3MPa, namely 100-200 m deep landslides can be simulated.



Figure 3 The main body of ICL-2.

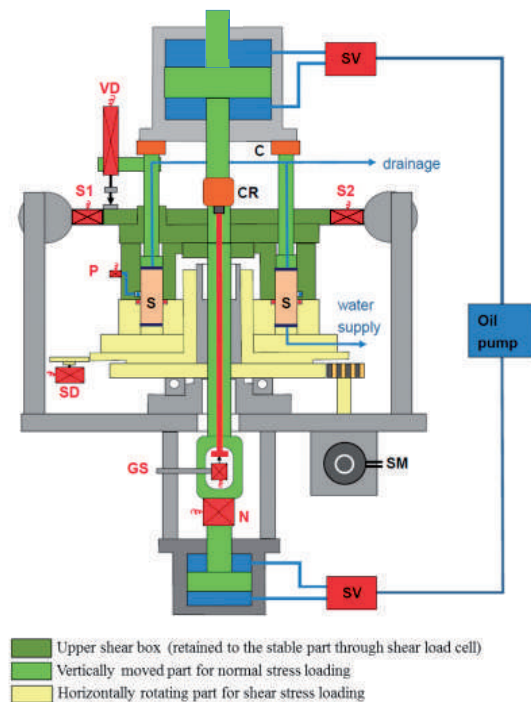


Figure 4. Structure of ICL-2 (central section of main body).

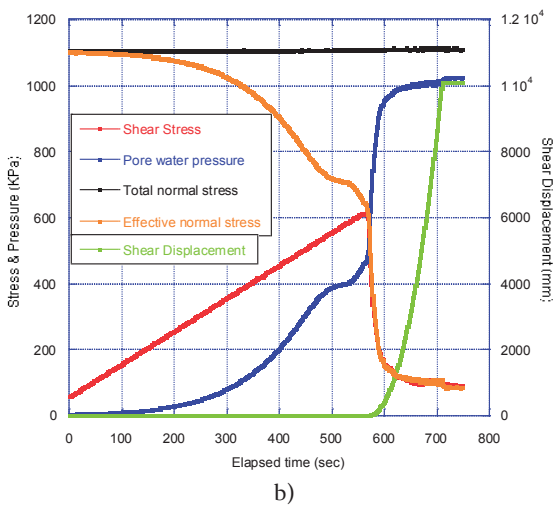
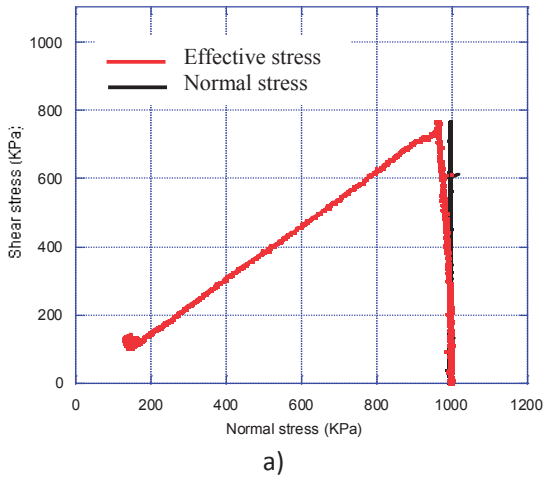


Figure 5. Stress path of undrained monotonic shear stress increment test on volcanic silt (from the Aratozawa landslide): a) Stress path, b) Time series data for stress, pressure and shear displacement.

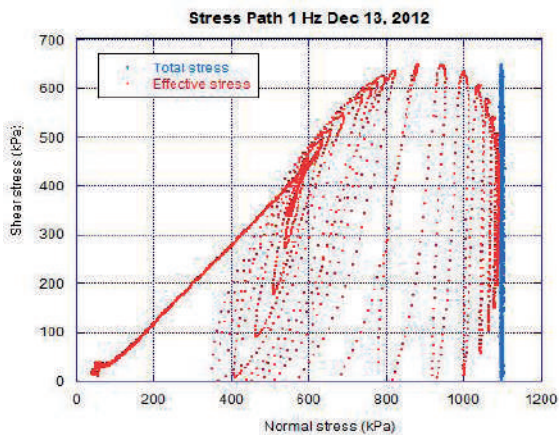


Figure 6. Undrained cyclic loading test on granitic sand.

Figures 3 and 4 present a view of ICL-2. The apparatus is compact comparing to previous version of DPRI-5, 6 and 7. ICL-2 uses the same loading method as ICL-1, with normal stress loaded by tension on the central axis. The ICL series has no tall loading frame as used to provide normal stress in conventional triaxial apparatus and the earlier DPRI series of ring-shear apparatus. The development and testing of the undrained dynamic loading ring shear apparatus is ongoing and it has not been used for testing any sample from Vietnamese landslides. Here we present some results of ring shear test.

Figure 5 shows the stress path of undrained monotonic shear stress increment test on volcanic silt from the Aratozawa landslide, Japan. First, the sample was fully saturated and consolidated at normal stress of 1,000 kPa. Then, it was sheared with monotonic shear stress increment test of 1 kPa/sec. Figure 6 shows the results of cyclic loading test on granitic sand. The sample was also fully saturated and consolidated at normal stress of 1,100 kPa. Then, it was sheared in the shear speed control mode.

Conclusions

This paper has introduced the state of landslide activities in Vietnam and the cooperation project between Japan and Vietnam for landslide disaster reduction. Annually, landslides often take place during the rainy seasons and cause a damage of nearly 100 million USD and about 25-30 people. The JICA-JST SATREPS project “Development of landslide risk assessment technology along transportation arteries in Vietnam” will help to reduce landslides disasters along main transport arteries and on residential areas through development of new technology on mapping, soil testing, computer simulation, monitoring and early warning and capacity development for effective use of this technology in Vietnam.

Acknowledgements

The authors gratefully acknowledge the support of the Science and Technology Research Partnership for Sustainable Development (SATREPS), the Japan Science and Technology Agency (JST), the Japan International Cooperation Agency (JICA), the International Consortium on Landslides (ICL) and the Ministry of Transport of Vietnam (MOT) in implementing the Project.

References

Duc M D (2009) Heavy rainfall induced landslides in Bac Kan and Binh Dinh provinces. VNU Journal of Science, Earth Sciences. 25: 1-9.
 Doan M T, Tien D V (2012) Landslide situation in Vietnam and cooperation with the International Consortium on Landslides in

- enhancement of research and treatment for landslide on road network. Proceeding of ICL Symposium, Kyoto, pp. 134-138.
- Oštrić M, Ljutić K, Krkač M, Setiawan H, He B, Sassa K (2012) Undrained ring shear tests performed on samples from Kostanjek and Grohovo landslides. Proceedings of ICL Symposium, Kyoto, pp. 47-52.
- Sassa K, Fukuoka H, Wang G, Ishikawa N (2004) Undrained dynamic-loading ring-shear apparatus and its application to landslide dynamics. *Landslides*. 1: 7-19.

Landslide Database on the Road Network in Serbia

Svetozar Milenković, Milovan Jotić, Vladeta Vujanić, Branko Jelisavac

The Highway Institute, Geotechnical department, Belgrade, Serbia

Abstract The landslides as one of the most frequent slope gravitational processes not only exert direct influence onto the safety of traffic operation, but at the same time they cause great material damages on the road network in the Republic of Serbia. In the last few decades, very important geotechnical focus and investigation field has been methodological approach regarding landslide dynamics and consequently its damage potential on human life and material goods. Related to that, in the most of the countries, landslide hazard and risk assessment are essential part of geotechnical documentation for planning, design and maintenance of the road network. In Serbia, (also in the neighboring countries) nevertheless absence of the continuity in the landside data collection on road network, adequate analysis and utilization of the data for hazard and risk assessment is missing throughout proper prediction of material losses. Also, as a constant, there is lack of institutions for central gathering, systematization, analysis and proper storage at the state level.

Keywords landslide, database, road network

Introduction

In the last few decades, very important geotechnical focus and investigation field has been methodological approach regarding landslide dynamics and consequently its damage potential on human life and material goods. Related to that, in the most of the countries, landslide hazard and risk assessment are essential part of geotechnical documentation for planning, design and maintenance of the road network. The landslides as one of the most frequent slope gravitational processes (Fig. 1) not only exert direct influence onto the safety of traffic operation, but at the same time they cause great material damages on the road network. In Serbia and also in the neighboring countries nevertheless absence of the continuity in the landside data collection on road network, adequate analysis and utilization of the data is missing throughout proper assessment of the material losses. Also, as a constant, there is lack of institutions for central gathering, systematization, analysis and proper storage at the state level.

Necessity of forming database

Deformations on slopes do not exert direct influence only on the stability and safety of road traffic, but on the security of population living in the close vicinity. Landslides often cause the interruptions of traffic and endanger the lives of people and damaging the structures. The works for reconstruction and reestablishment of previous conditions very often require large financial funds. It is necessary to recognize potential land slips, at the early stage of appearance, through their recording, periodical investigations and inspections, in order to prevent large scale sliding processes. In other words, timely discovery of instability phenomenon would provide for prompt rational repair measures.

The purpose of creating and updating the landslide Database on road network is to provide for prompt, complete and exact information to competent authorities regarding the number and state of occurrences of unstable terrains, level of jeopardy of transport facilities, rating of priorities in undertaking repair measures, as well as information to road users on conditions, passability and safety of road transport facilities.

Review of the database methodology

The preparation of such a complex system as Data Base is crucial for the provision of timely, complete and exact information to competent institutions regarding the number and activity conditions of landslides and unstable occurrences, danger rate on transport facilities, prioritization of repair measures, as well as the information for road users regarding the conditions, serviceability, and safety of transportation.

Basic concept of the database forming is based on the assumption that for each and every landslide, rockslide or road damage, the record sheet should be made. It was assessed that for appropriate, expert interpretation of relevant parameters of every single occurrence of instability, besides the record sheet, one should also present its geographic location within Serbian road network, the sketch of layout and anticipated engineering geologic cross section of terrain, along with adequate photographs.

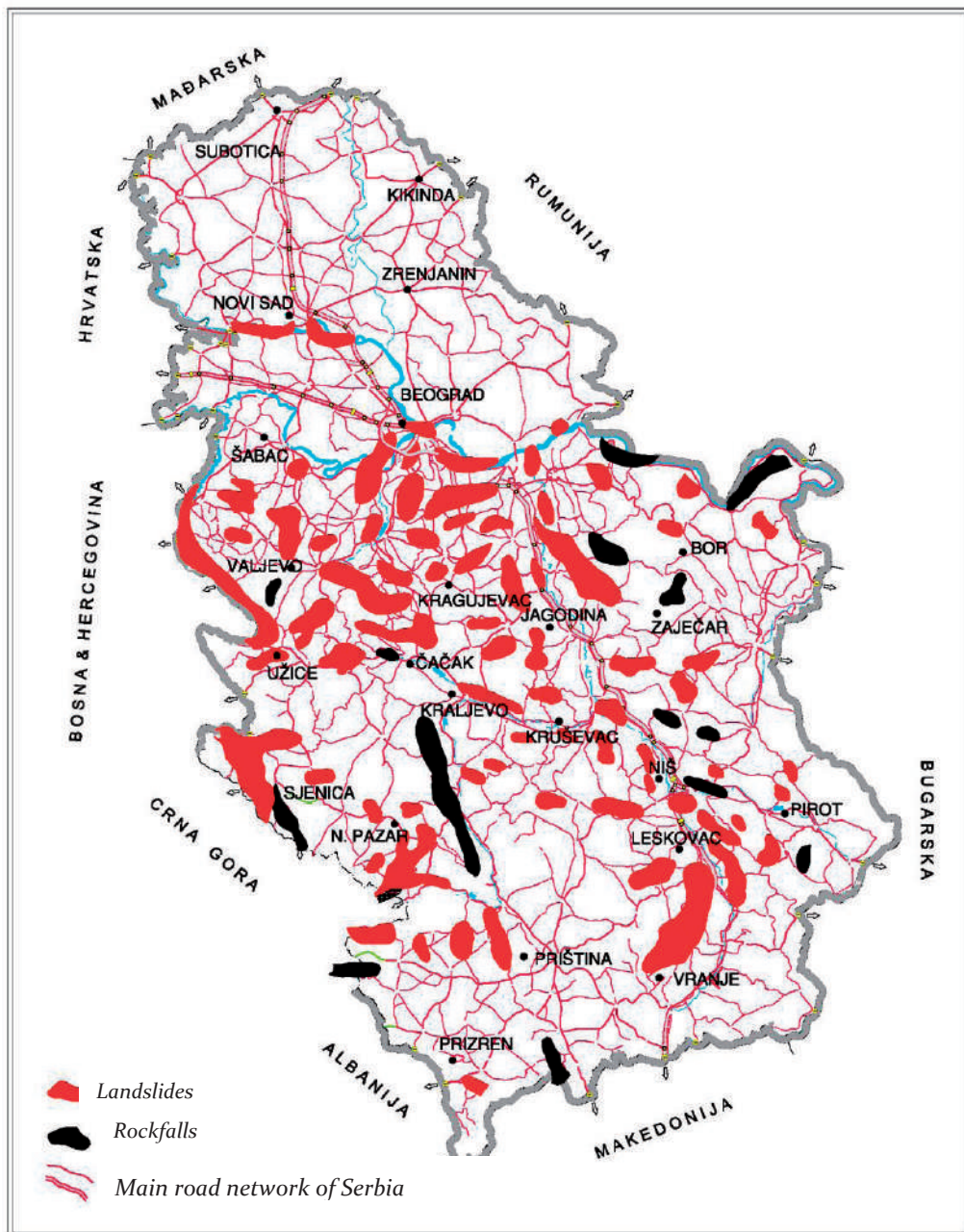


Figure 1 Layout map of Serbia with relevant zones of terrain instability: landslides and rockfalls.

It is anticipated to prepare the record of the every single landslide on the basis of engineering-geologic reconnaissance of terrain, detailed investigation or processing of available geologic and geotechnical documentation. For the purpose of obtaining uniform data gathering and processing of data pertaining to all occurrences of instability in the field, the record is presenting the instructions of filling it out, and it's content as well.

Entry parameters for the Database are classified according to topical entirety grouped in several topics, out of

which every single one has been broken down thoroughly according to certain parameters.

- General data on landslides: one should fill out the road denomination and number, section where the occurrence has been recorded, its change, occurrence number on the section and local denomination of the occurrence according to the nearest settlement and local residents (Fig. 2).

- Elements of the phenomenon: one is filling out the landslide category according to activity, assessed and measured parameters which define elements of the

Figure 2 Typical computer screen for data entry.

phenomenon in space; length of occurrence, its width along the road, surface taken-up by the process, body shape, height and shape of head scarp, location of deformation related to road, vertical and horizontal dislocations, and finally the assessed landslide depth. Geologic structure of terrain: is shown through the sketch of layout and engineering-geologic cross section thus illustrating the geologic structure of terrain. Short text indicates essential engineering-geologic conditions of appearance and development of the phenomenon. Photographs are also attached.

- Assessment of causes pertaining to the phenomenon appearance: causes of the phenomenon are defined, emphasizing natural and anthropogenic impacts. If possible, it is desirable to stress upon the crucial impacts for the landslide formation.

- Forecast of processes and endangered traffic conditions: depending on the acquired knowledge regarding the phenomenon, defined engineering-geologic properties of rock masses and terrain conditions, and through a short analysis, one is able to indicate further propagation of the process and appraise the danger rate of traffic and structures within the road zone, due to the occurrences of instability broadening. One should particularly assess the impact arising from maintenance and other anthropogenic activities onto the phenomena propagation.

- Assessment of intervention urgency: taking into account the road category (State roads of the 1st and the

2nd rank), traffic volume, size of pavement deterioration, danger rate assigned to traffic and structures, one is assessing the urgency to intervene and providing adequate recommendations to the Client.

- Other data: all essential data of recorded phenomenon are filled out, which have not been processed in previous headings, yet are considered to be relevant for establishing overall engineering geologic conditions within the zone of instability.

- Data about the analyst: data regarding the analysts and date of recorded phenomenon are filled out in the final part of the form.

Hazard assessment

Along with Database preparation, the suggestions of the World Road Association are accepted and also the landslide hazard is established according to criteria on the empirical basis and official proposals made by respective national road associations. Technical Committee of PIARC for earth works decided to take into account this issue in order to find out solutions for reducing the damages on roads caused by landslides. Namely, an attempt was made to quantify certain entry parameters and establish the objective level of danger in relation to previously defined conditions of the road network in Serbia, and thus establish priority ratings for repairs. In this procedure of course the subjectivity factor is present, yet with

Table 1 Ultimate value of the landslide hazards.

Hazard categ.	Hazard type	Points		Hazard category description
		without measures	with measures	
I	No hazard	0 - 25	0 - 50	Landslide not foreseen under any expected circumstances
II	Low hazard	26 - 50	51 - 100	Landslide may occur under extremely unfavorable conditions, which have a low probability of appearance (millennium precipitations, high-magnitude earthquakes in the area of low seismic features etc.) or there is a high probability of occurrence, yet with small masses set in motion.
III	Medium hazard	51 - 75	101 - 150	Landslide may occur under the circumstance which one might expect in the period under study, with a slow motion of large volumes of rock masses.
IV	High hazard	76 - 100	151 - 200	Landslide will presumably appear in near future under the circumstance which occur periodically under regular pattern; landslides are expected to take-up large and very large volumes of rock masses; this hazard level encompasses the cases when for the motion of masses there is a coincidence of actions of several unfavorable factors, so that the probability of occurrence is lower, yet potential volumes and areas taken-up by slides are very large and are moving at very high speed.

adequate assessment of parameters herewith, this could be minimized along with realistic perception as regards present conditions and tentative alterations. It is intention to perform the hazard assessment through GIS system, which will considerably speed-up the processing procedures, although there are still some questions about it as regards the objectivity of this procedure for proper quantification of some entry data and realistic assessment of the landslide hazard. Ultimate values according to previously defined criteria are presented in the Table 1.

Emergency response

An important aspect of landslide Database forming is hazard reduction and adequate response. In addition to hazard response, The Highway Institute intends to provide an on-line data collection form to encourage all on- field supervision professionals employed in "Roads of Serbia" to document all sizes of landslides to keep the database up to date and detailed. This form will request information regarding the size and type of landslide, material type, economic damage, etc. While not all the engineers will be able to assess all aspects of landslides, this form will help to keep The Highway Institute experts informed about potentially very large or very damaging events which would require field assessment.

Conclusion

At the moment there are approximately 100 landslides in the database, with growing tendency on a daily basis. It is estimated that at the end of first phase of the database forming, the number of landslides in the database will exceed 2000. Every single landslide will be described and

spatially located. The final goal is for the database to be an open system, which means constant updating of collected data. It is anticipated that the use of the Serbian Road Network Database will bring a large step forward in order to immediate respond to landslide threats and in the field of the landslide prevention. Also many useful scientific data can be collected on the course of analysis of landslide data. All the data, stored in the Database, will be a solid foundation for the better understanding of landslides and will help the experts to provide best possible models of these natural phenomena in the second phase of the project.

All the collected data will further serve for the production of the hazard assessment (Tab. 1), which will gradually improve usability of the data. We hope that presented data base will not end its life, like many times before at the phase of forming description sheet with recording of the present state without clear vision about implementation of the results towards better prediction levels, with regular updating of the database.

References

- WP/WLI (1990) A Suggested Method for Reporting a Landslides, Bulletin of the International Association of Engineering geology. 41: 5-12.
- WP/WLI (1991) A Suggested Method for a Landslide Summary, Bulletin of the International Association of Engineering Geology. 43: 101- 110.
- WP/WLI (1993a) A Suggested Method for Description the Activity of a Landslide Summary, Bulletin of the International Association of Engineering Geology. 47: 53 - 57.
- WP/WLI (1993b) Multilingual Landslide Glossary, Bi.-Tech Publishers, Richmond, British Columbia, Canada, 59p.

Program of the Landslide Database Development of the Republic of Srpska

Cvjetko Sandić, Koviljka Leka

The Republic Institute for Geological Researches of the Republic of Srpska, 75400 Zvornik, Bosnia and Herzegovina, Vuka Karadžića 148b

Abstract This paper presents a program of landslide database development in accordance with Long-term program of basic geological researches in the Republic of Srpska for the period 2013 - 2028. Landslides in the country are the limiting factor for rational land use. According to available data, a large part of the territory was affected by the landslide processes. The landslide database should be the starting point for solving the problem.

Keywords landslides, database, inventory, hazard

Introduction

The process of landslides activation and other phenomena of the terrain instability is complex and complicated problem and it is very common in the territory of the Republic of Srpska. Landslides endanger the population, traffic and construction safety and cause major damage. People with different profiles and professions occupy with problems of slopes stability: geologists, engineers, designers of different types of objects, planners etc., but the population are still the most endangered.

The Republic of Srpska does not have one centralized base of landslides and other geohazards. The establishing of landslide database is necessary, because the data mostly storage on a local level. The establishment of this system for the observation of geohazards provides valuable information for preventing the problems of instability and landslide remediation.

The complete database will be made in the GIS and will consist of:

- General information about the landslides;
- Geomorphological and geological characteristics;
- Hydrological and hydrogeological characteristics;
- The type of the processes and the type of landslides on the slopes;
- Causes of the landslide activation;
- Vegetation covering;
- Data from exploration of the landslides;
- Data on monitoring;
- Reports (text files) and photos.

The landslide database is an integral part of the geological information system, and it will be developed at the Republic Institute for Geological Researches of the Republic of Srpska (Fig. 1).

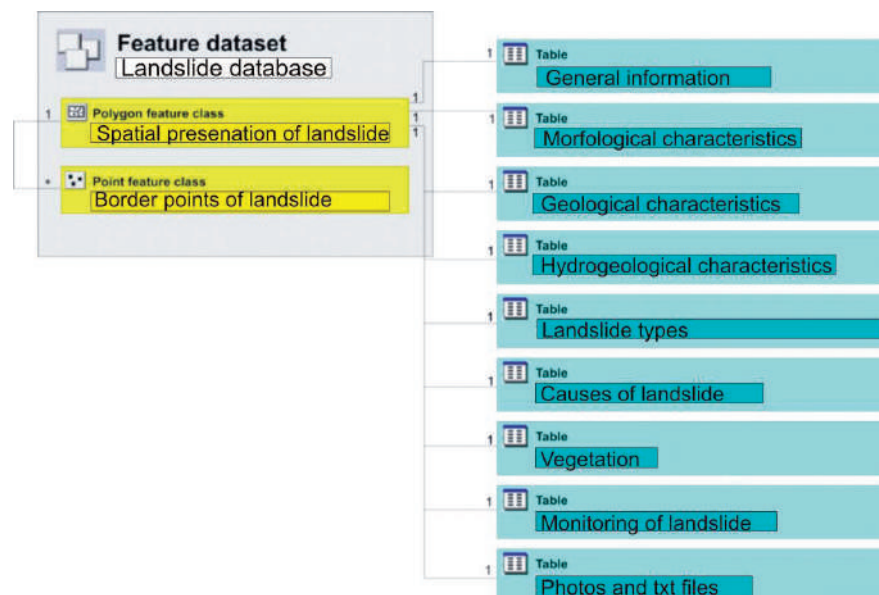


Figure 1 Part of Geological Information System of the Republic of Srpska.

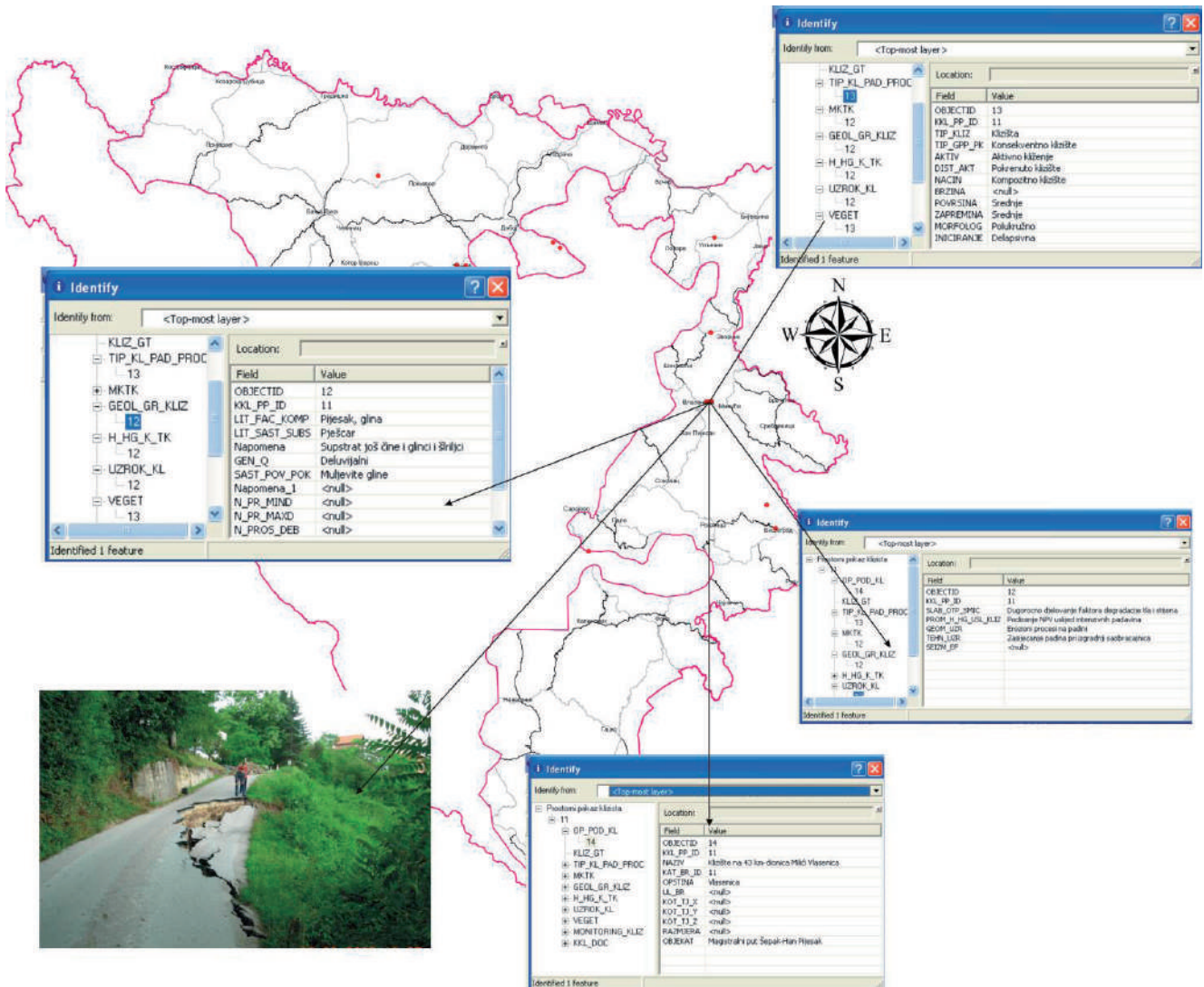


Figure 2 Map of the Republic of Srpska with information about one single landslide from database.

The aim of the landslide database

The main aim of the landslide database (inventory) is to systemize all data about landslides processes in order to fully understand and define the properties of the terrain for planning and rational use. Establishing of the landslide database also aims to:

- Recording of all landslide types;
- Determination of conditions and causes of instability phenomena;
- Assessment of the potential damage;
- Systematic monitoring, control and landslide remediation;
- Gives the quality information to authorities, investors, designers, etc.
- Forming of geological information system;

Hazard and risk assessment of landslides in many countries is an integral part of the geotechnical

documentation for spatial planning, design and construction of facilities. It could not be done without the information obtained from the landslides inventory.

Concept and methodology for landslide database preparation

The landslide database contains a large number of expert information about morphometric, genetic characteristics of landslides, engineering-geological, hydrogeological characteristics, their mechanisms, kinematics of movement and also other important information about endangered facilities which are located on landslides or near them.

For each landslide corresponding database has formed and associated with the graphical data, photographs and tables (Fig. 2).

It is designed that the landslide inventory would be done at several levels:

The first level - collecting existing historical documentation and archive data, making cadastral sheet, preparation of appropriate basis for registration, processing aerial orthophoto images, field reconnaissance and making digital (GIS) database.

This level is crucial for the development and establishment of the overall database. It should include all known information and facts about landslides in the territory of the Republic of Srpska. In the final part of the first level access to the landslide susceptibility assessment.

The second level - detailed engineering-geological mapping of landslides, geotechnical soil testing for determination geotechnical characteristics of the soil and the parameters for stability analysis;

The third level - development of monitoring system, data processing in the real time, in the GIS;

The fourth level - development of priority projects for landslides remediation;

The fifth level - maintaining of the database and continuous input of new data.

Complete landslide database in the GIS will have two levels: level of the individual phenomena; and level for all registered landslide occurrences in the Republic of Srpska.

Each of the registered landslides has its own unique code (FID number). This code allows the spatial location of landslides on the network and quickly searches the database according to the desired criteria.

Inventory sheet

The main part for the development of the database in the territory of the Republic of Srpska makes inventory sheets (Fig. 3).

An inventory sheet is filled on the field and contains all information about a landslide. This information's may be time-constant and variables. Constant information's are geomorphological, geological, tectonic etc., while the variables are the morphometric characteristics, engineering activity and vulnerability of facilities and people.

All data stored in the inventory sheet will be transferred into a digital database and the GIS.

Inventory sheet						
General information						
Inventory number	Name of landslides	Municipality	Site	Coordinates	Map scale	Endangered object
				X		
				Y		
				Z		
Morfological characteristics of terrain and landslides						
Relief	Height of the slope	Length of the slope	Inclination of the slope	Shape of the slope	Exposition	
Length of the landslide	Width of the landslide	The depth of the sliding surface	Velocity (m/s)	Area of landslide (m ²)	Volume of landslide (m ³)	
Landslide types						
Type of landslide				Activity status	Activity of distribution	Way of sliding
According to the mechanism	According to the structure and position of sliding surface	According to the morfology	According to the site initiation			
Geological setting						
Litology of landslide	Badrock	Quaternary cover types	Material composition of the surface cover	Thickness of the surface cover		
Hydrological and hydrogeological characteristics						
Hydrological and hydrogeological characteristics on landslides				Groundwater level		
Causes of landslides						
The weakening of the mechanical properties of materials	Changes of hydrological and hydrogeological conditions	Seizmisc effects	Geomorphological conditions	Antrophogenic causes		
Clasification of slope stability		Vegetation	Monitoring	Remediation meassuers		
Note:						

Figure 3 Inventory sheet.

Organization and dynamics

The landslide database is planned to be implemented over the whole territory of the Republic of Srpska (25,000 km²), for a period of 8-10 years (Tab. 1). Priority areas are determined by the population density, engineering-geological characteristics and the most important anthropogenic (construction) operations.

The priority areas for the development database:

- Urban areas with large number of landslides (Banja Luka, Zvornik, Istočno Sarajevo, Pale, Lopare, Teslić...);
- Traffic roads (national and regional) in the territory of the Republic of Srpska;
- River banks.

Table 1 Phases of organization and dynamics

	Phase I	Phase II	Phase III
	Urban areas	Traffic roads	River banks
Deadline	4 years	3 years	2 years

Conclusion

The landslide database (inventory) is a national project with the aim to identify and map landslides over the

whole territory of the Republic of Srpska, based on the standardized criteria. These database represent the first homogeneous and updated database with collecting the landslides at national level. Information from the database is used for making of the susceptibility maps or hazard and risk maps. These maps are the basis for rational planning and constructing of the Republic of Srpska.

References

- Abolmasov B (2010) Landslides types and processes in Serbia. Abstract Proceedings of the 1st Project workshop "International Experience", 22-24 Nov 2010. Dubrovnik, Croatia. pp. 39-39.
- Hobbs P (2007) BGS landslide data and mapping in Britain. Javier Hervás. Guidelines for Mapping Areas at Risk of Landslides in Europe. Institute for Environment and Sustainability. Joint Research Centre, Ispra, Italy. 11-14.
- Mitrović D, Sandić C (2011) Landslides in the Republic of Srpska, Proceedings of the 2nd Project workshop "Monitoring and analyses for disaster mitigation of landslides, debris flow and floods, 15-17 Dec 2011. Rijeka, Croatia. pp. 138-140.
- WP/WLI (1993) A Suggested method for describing the activity of a landslides. Bulletin of the International Association of Engineering Geology. 47: 53-57.
- WP/WLI (1991) A Simple definition of a landslides. Bulletin of the International Association of Engineering Geology. 43.

Landslide Inventory Map of the Republic of Macedonia: Statistics and Description of Main Historical Landslide Events

Igor Peshevski⁽¹⁾, Milorad Jovanovski⁽¹⁾, Blagoja Markoski⁽²⁾, Silvana Petrusheva⁽¹⁾, Bojan Susinov⁽¹⁾

1) University Ss. Cyril and Methodius, Faculty of Civil Engineering, 1000 Skopje, Macedonia, Blvd. Partizanski odredi 24, 0038923116066, pesevski@gf.ukim.edu.mk

2) University Ss. Cyril and Methodius, Faculty of Science, Institute of Geography, Skopje, Macedonia

Abstract For the first time, landslides in the Republic of Macedonia have been systematically mapped in the past century during the preparation of the Basic Geological Map at scale of 1:100,000. Additional landslides have been registered later during the period of engineering-geological maps preparation for some regions at scales 1:100 000 and 1:200,000. Unfortunately, all these maps were prepared in an analogue form which is a serious drawback in respect to updating with new occurrences and improvement of data. In order to provide a solid database for GIS data, which would serve as a base for preparation of landslide hazard and risk maps in the future, the collection of all existing data of instabilities in the country and creation of landslide inventory is of essential importance. This paper presents the methodology used in creation of the first GIS-based landslide inventory map of the Republic of Macedonia. Systematic approach in data collection and presentation enabled performing of statistical analysis and group the occurrences using different criteria, among the most important being: geological setting, landslide mechanism, depth, location, maximum observed seismic intensity in the area, cause, activity, affected infrastructure, remedial measures, monitoring status, etc.

The most significant landslide events throughout the history are described in detail in order to conceive the socio-economic losses they have brought to the society. Landslides Gradot, Ramina, Germa, Skudrinje, Bogovinje and Velebrdo, Bitushe, Rostushe are taken as the most damaging landslides in Republic of Macedonia. The preparation of the inventory map is considered as a first step in the process of mitigation of landslide consequences in the future. In order to prevent further catastrophes, it was obligation to prepare landslide susceptibility, hazard and risk maps for the most affected regions. The recommendation of the world leading experts and societies in the field of landslide mapping should be certainly taken in consideration.

Keywords data collection, inventory map, statistical analysis, significant events, hazard and risk maps

Methodology of landslide data collection

The total number of landslides in Republic of Macedonia registered, on the basic geological and engineering geological maps, is around 150. Technical reports and other documentation for these occurrences existed but were either kept in archives that have faded and have become unusable or have been lost. Hence, only basic data about landslides from the analogue maps were available (location, regional geological setting, maximum observed seismic intensity in the area, slope aspect). On the other hand, for instabilities that have occurred and have been recorded from 1990 to date, documentation does exist but it was kept in different governmental institutions, private companies or even individuals.

In order to collect all the historical data, in a short period of four months during 2012, many companies who work in the field of geology and geotechnics were contacted and consulted. In addition, museums, national archives and internet sites were thoroughly searched about landslide appearance information. In some cases, even retired civil, geological and geotechnical engineers were contacted. Thanks to this effort, technical documentation in the form of geological and geotechnical reports for over than 150 occurrences were gathered. The data presented in some of these documents were very comprehensive. For the certain number of landslides, whose were considered as relatively recent, notes about activity in the 19 century was found. However, for about 50 cases, data were incomplete or unclear (imprecise location, unmarked change along the road corridor, missing description of geological materials, no geotechnical parameters, no maps, no cause of sliding, etc.). These occurrences were not drawn on the map and further searching had to be performed in order to collect the missing data and include them on the map.

Many historical documents noted the existence of numerous small landslides in the surrounding area of larger occurrences but unfortunately without any data about them. Furthermore, the number of rockfalls is much bigger than the presented number on the maps.

Every year, especially during the winter months, rockfalls are very common on the regional roads in the

north-west and eastern part of the country. From the construction time of these roads, approximately 40-50 years ago, more than 1000 small rockfalls (several cubic meters) have occurred. However, in this phase, it wasn't be possible to reach any technical reports about these occurrences. Other rockfalls have caused damage on local roads, buildings and residential houses. In order to improve the landslide inventory map, collection of historical data should be continued in future.

Landslide data presentation

After collection of the technical documents, for all occurrences with sufficient information, separate landslide information datasheet was prepared. Accepted as the most advanced one similar form the one of the Italian Landslide Inventory (IFFI) was used as a standard datasheet. The main information in the datasheets includes: ID number of landslide, location, local geographic coordinates, date of the first activation, state of activity, type of movement, geology, hydrogeology, speed, dimensions, depth, slope aspect, land use, undertaken remedial measures, monitoring status, etc.

The datasheets are somewhat shortened from the original Italian model due to the deficiency of details for the cost of damage on infrastructure, undertaken remedial measures, monitoring, etc. In order to estimate costs of damage form landslides, additional effort should be made and experts from different scientific institutions should be involved in the future.

Preparation of the landslide inventory map (1:200,000)

In the last two decades, the scientific cartographic presentations in Macedonia were mostly prepared using the AutoCAD software. In order to maintain consistency, the landslide inventory map was also prepared using this computer tools. Exact coordinates of the landslides and rockfalls borders were placed in the software environment with the highest possible precision.

Older engineers who worked in the field helped to define exact locations of some landslides using Google Earth and topographic maps. Due to the informative nature of the map, simple symbols were used for all occurrences. The use of the same symbol for different type of occurrences is justified with the fact that for most of the landslides were taken from the analogue maps, the type of movement was unknown. This problem can be solved only with detailed field re-mapping and performing of geotechnical investigations.

As the most adequate for presenting of the landslide inventory map, the scale of 1:200 000 was used. This scale is considered as most adequate, having in mind the total area of the Republic of Macedonia of 25,713 km². In future, inventory maps at the scale 1:10,000 to 1:25,000 should be prepared.

Statistical analysis of landslide data

The methodology applied enabled us to perform statistical analysis and group the 255 occurrences by different criteria. Among them, the most important are: geology, landslide mechanism, depth, location and slope aspect, maximum observed seismic intensity in the area, cause, activity, affected infrastructure, remedial measures, monitoring status, etc.

For 150 landslides data is completely taken from analogue geological and engineering geological maps at the scale 1:100,000 and 1:200,000. These instabilities were statistically treated only according to geology, slope aspect and maximum observed seismic intensity in the area.

Geology

In relation to the geological setting, 38% of the landslides have occurred in deluvium or debris which covers schistose or granitic bedrock, 11% in limestone (mostly rockfalls), and 31% in lacustrine sediments. Pyroclastic materials, sandstones, flysch, fluvioglacial and proluvial sediments are less represented lithological units (Fig. 1).

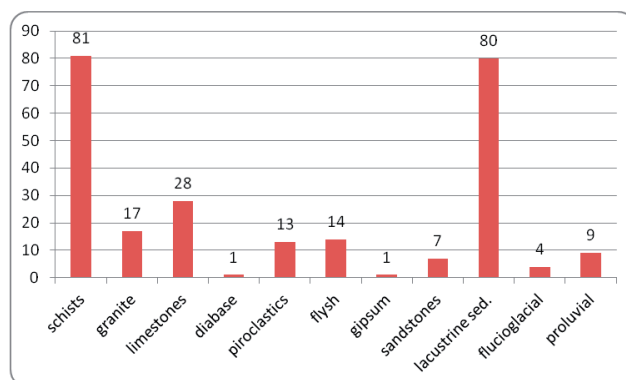


Figure 1 Number of instability occurrences in some of typical lithogenetic units.

Landslide type

According to the landslide type, most of the landslides were defined as translational and rotational slides, debris and rock falls (Fig. 2).

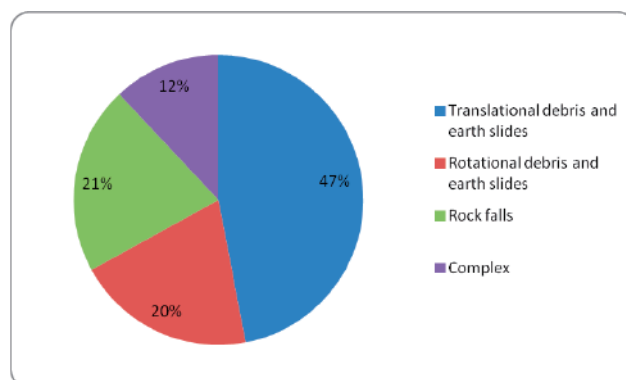


Figure 2 Landslide type of registered occurrences.

Depth

Considering the depth, landslides were grouped as shallow <2 m, intermediate 2-10 m and deep >10 m. Over 60% of the occurrences have been defined as intermediate and deep, and those mostly occurred in debris material overlaying hard rock masses or in fluvioglacial and proluvial sediments. The depth of some of these landslides varies in the range from 5 to over 25-30 meters. Geophysical investigations at some sites indicated existence of several generations of sliding which was confirmed with investigation drill holes. The rest of 40% of the slides are shallow and mostly occurred in sandstones, lacustrine and flysch sediments. Rockfalls are usually classified as shallow slides.

Location

Regarding to the location, rotational and translational debris and earth slides have mostly developed on the transition of steep mountain slopes and river valleys, while rockfalls and rock slides are characteristic in the gorges on the north-west and eastern part of Macedonia. Due to the very developed river network and existence of mountain chains with different strike, there is no dominant orientation of sliding slopes in geographical sense.

Earthquakes

From the historical documents it was found that the several slides are connected with seismic activity. These included the landslides Ramina and Crnik those were among the most damaging. Having in mind the tectonic setting of Macedonia (Fig. 3), the potential for seismically induced landslides is very high.

Due to this, landslides are grouped according to the maximum estimated seismic intensity of the zones in which landslides have occurred (Fig. 4).

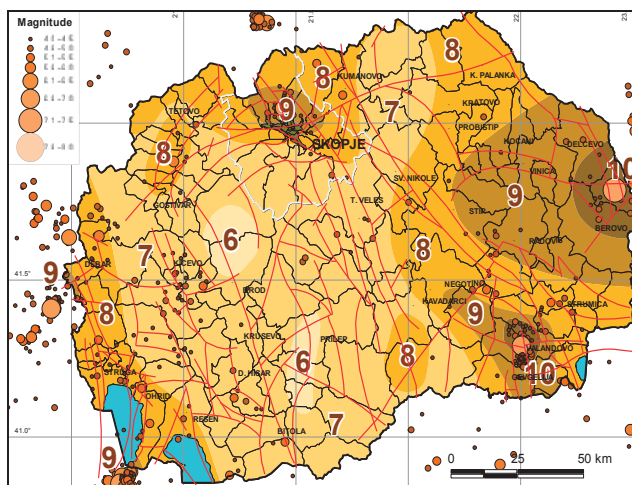


Figure 3 Seismotectonic and maximum estimated seismic intensity map.

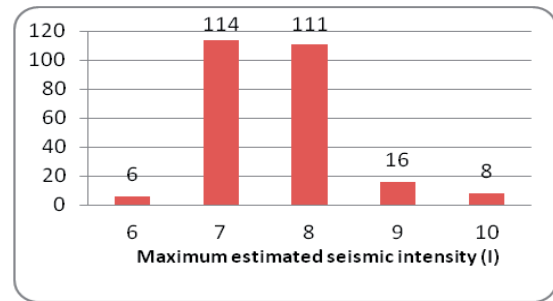


Figure 4 Number of occurrences in zones of Maximum estimated seismic intensity.

Cause

Almost 70% of the landslides have been caused by heavy rainfalls, and the rest have been caused in combination of excavation and water saturation as the main prerequisite. Proluvial sediments are the most sensitive to excavation. For some landslides, combination of several factors contributed to the triggering of instability.

Three large landslides have occurred in active open cast coal mines solely as a result of the process of exploitation.

Activity

On the territory of Macedonia there are currently 21 active landslides, most of those are located in the northwest part of the country. 20 landslides are declared as inactive, but with possibility for reactivation (dormant), and 64 occurrences have been artificially stabilized with undertaking of remedial measures. Landslides from the analogue geological maps were not treated as their state of activity is unknown. Most of them have probably naturally stabilized, but this should be confirmed.

Affected infrastructure and population

Each year landslide events in Macedonia are causing losses in the amount of millions of Euros. Most of this money is usually spent on rehabilitation and cleaning of roads and railways. This is confirmed by the fact that around 60% of the registered landslides have impeded or stopped the traffic on regional or local roads. In periods of prolonged intense rainfalls, whole or parts of settlements had to be moved from the zones of sliding (Jelovjane and Ramina landslides). This also caused additional expenses. For number of cases, extensive geotechnical investigations, designing and remedial works were performed, which also increased the economic losses. Statistics showed that 10% of the landslides have endangered whole settlements, while 30% have damaged individual structures in rural or urbanized area (Fig. 5). Water supply systems, electric power distribution networks and sewage systems have frequently suffered.



Figure 5 House in the City of Tetovo destroyed by rock fall on 9 February 2013.

A lot of people are exposed to constant risk from landslides. The villages Velebrdo, Trebishte, Rostushe, Bitushe, Skudrinje, Mogorce, Jelovjane, with total population of 11,000 residents are directly or indirectly endangered by the landslides.

In several separate events in the past century, 15 people lost their lives as a result of landslides.

Remedial measures and monitoring

Remedial measures have been undertaken for 62 landslides and mostly consist of construction of support walls, road nets, water drainage systems under road and railways, concrete piles etc. For the other landslides remedial works were either not realized or lost function with time.

As far as a monitoring is concerned, 41 landslides are regularly monitored using geodetic measurements and in some cases using inclinometers. The rest of the landslides are periodically checked by visual observation during the supervision and maintaining of roads.

Contemporary real-time monitoring and advanced techniques as InSAR and LiDAR are yet to be introduced in Macedonia, despite the fact that use of this type of instruments is already standard practice in the most of European countries.

Main historical landslide events in Macedonia

Throughout the history of the country, certain landslides have been defined as natural disasters. Crnik, Surnati ridoi and Timjanik landslides changed the appearance of the natural terrain, but because they all occurred in poorly developed rural areas the damage of infrastructure was limited and not a single human life was lost.

The landslide Crnik was activated in 1904 probably as a consequence of the famous Kresna earthquake with magnitude $M=7.8$.

Landslides Surnati Ridoi (1990-ties) and Timjanik (1994) caused damages on the main irrigation channels and ruined vineyards. They were both activated after heavy rainfalls in proluvium and lacustrine sediments

respectively.

Another great disaster including sliding was the rock-tree-snow avalanche in Lukovo pole in 1956, when 52 construction workers of the hydrosystem Mavrovo and local people lost their lives. In 2010 similar type of avalanche blocked the regional road Mavrovo-Debar but fortunately without human losses.

With the growth of population and development of urban settlements in mountainous regions, the socio-economic losses from landslides have been increased. Without analyses of the reasons for poor urban planning in the past, we present the most damaging landslides that have occurred in Macedonia.

The Gradot Landslide

The Gradot slide, near the town of Kavadarci, has been referred to as a rock fall in some literature, and somewhere it is described as earth slide. However, the western slope from the top of the hill to the bottom of the valley of the Luda Mara River was moved for about 150 m with the speed of 6 km/h on 05.9.1956. The width of the landslide was 800 m, length 400 m, while the relative height 200 m, so the mass total amount was estimated at 20,000.000 m³. As a result, the valley of the river was covered up to 70 m height creating landslide dam and artificial lake (Fig. 6). Unfortunately, it was also fatal for 11 people and 1,200 sheep. The investigation showed that existed prefailure long-time creeping with the speed of about 15 mm/year, before reaching the strength of the stiff tuff rock, so as a piping of sand particles due to long-time period of water infiltration and flowing.



Figure 6 Scar from sliding at hill Gradot where the Luda Mara River was blocked.

The Ramina Landslide

In Veles, a fossil landslide from the XIX century was reactivated in 1963, 1999 and 2002. In the past century the forestation was carried out, but the area was later illegally populated and many houses were built.

This landslide is about 500 m long, the average width is 100 m, and its thickness is 20 m. The hydrogeological conditions indicated that zones with increased water content are related to the sliding zone.



Figure 7 Ruined houses in Ramina.

After a small earthquake in April 1999, reactivation caused large damages on the existing houses and the municipal infrastructure (Fig. 7). The landslide directly endangers 120 houses and indirectly another 500 houses.

The Germo Landslide

First indications for existence of landslide dated from 1962. The emerged deformations developed over time with the opening of new fractures and growth of affected area. During 1979 and 1982, the intense rainfalls activated additional masses. Larger deformations were also noted to the end of the last century, with intense folding in the toe of the landslide near the Porojska River. The total vertical displacement on some places is now over 60 meters. The area of the landslide is 450,000 m² (Fig. 8) and its depth varies from 20-40 meters.

The main prerequisites for the sliding were seismotectonic activities, intense rainfalls, cutting of the toe at the Porojska River etc. Many houses were completely or partially damaged and people were settled in other parts of the village.

The landslide endangers about 1200 people, the road to the village Germo, the water supply system, sewage



Figure 8 Ortho photo of the Germo Landslide with contours.

system and electrical power lines. Remedial works were undertaken in several occasions, with the construction of a system for drainage of surface and underground waters.

The Skudrinje Landslide

Deformations on the terrain in the village of Skudrinje have been registered in 2006. The geological setting of the terrain is presented with heterogeneous rock masses of different physical-mechanical properties and it is subjected to intense seismotectonic activity. The area of the landslide is around 330,000 m² and the main scarp is visible from the satellite images. Geophysical investigations confirmed several generations of sliding and active faults with sharp dip angle of 68-80° towards south. There exist scars from the sliding on the field with height of up to 20 m. Approximately 3,500 people are exposed to danger of this landslide. Remedial measures have been undertaken, but small slides are the regular occurrences in the rainy season.

The Jelovjane Landslide

Geological engineers that performed mapping of the terrain of the municipality of Bogovinje in the 1950 declared that the landslide has elements of “small tectonics”. Today, consequences of permanent slow movements endanger residential houses, retaining walls, roads and other infrastructure facilities in many settlements in this area. More than 100 houses have been ruined, and agricultural surfaces transformed into unusable heaps of earth. 1,200 households of the village of Jelovjane are under constant threat of the landslide. As a result of the snowmelt on the Shara Mountain, groundwater cause earth slides every spring.

Velebrdo, Bitushe and Rostushe Village landslides

Older residents of these villages remembered stories from their grandfathers in which they described the slides as the “land collapses”. Figure 9 presents landslide contour of the Velebrdo Landslide.



Figure 9 Ortho photo of the Velebrdo Landslide with contours.

The landslide was last time reactivated in 1996 and until 1999 its size was gradually increased. The whole infrastructure facilities of 4 villages with 2,500 residents are endangered by this landslide. The main reason for sliding is the presence of deep fluvioglacial sediments which cover stable metamorphic rocks. Groundwater also intensifies the developing of the landslide.

The need of formation of national landslide database

We stress the fact that the landslide inventory map (Fig. 10) is the very first of this kind in the country, and during time it should be constantly updated and improved with new collected historical data and new instabilities occurrences in the country. In this context, it should be followed by formation of official national database in similar form to the one already presented by Kapriveski et al. (2009) This database should be accessible via the internet, where authorized users can follow and change the status of the existing and report new instabilities. It will enable update, elaboration, analysis and connection of the landslide data in cartographic, photographic, tabular and alphanumerical forms. World and European experts should also be consulted regarding the selection of the right format of the database and the tools to be used for its creation in order to provide consistency with other countries and better connection with the global and European networks.

Apart from that, with the aim to perform precise and complex statistical analyses and create susceptibility, hazard and risk maps it is necessary to prepare landslide inventory maps at larger scale (1:25,000) for the most endangered regions. These maps should be certainly prepared by means of more specialized computer software as IDRISI, ILWIS (Eastman 2003), etc.

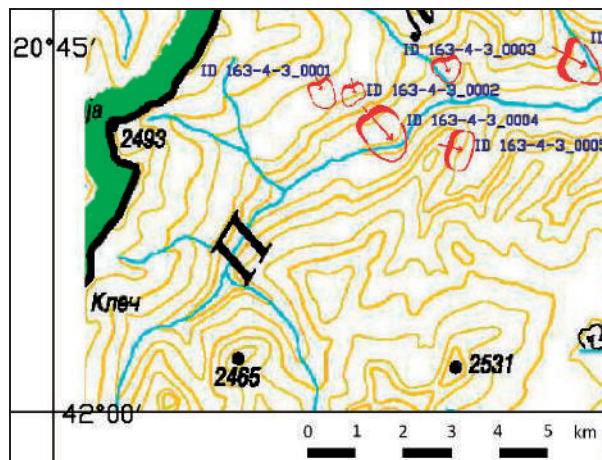


Figure 10 Landslide inventory map of the Republic of Macedonia (detail).

References

- Eastman J R (2003) IDRISI Kilimanjaro, guide to GIS and image processing, user's guide (Ver. 14), Clark University Press, Massachusetts.
- Jovanovski M (2011) Landslides and rockfall occurrences and Processes in R. Macedonia, Croatia-Japan project on Risk identification and land-use planning for disaster mitigation of landslides and floods in Croatia, 1st Project workshop "International experience, Dubrovnik.
- Kapriveski P (2009) Methodology for Creation of Database on landslides of Rockfalls in Republic Macedonia, Master Thesis, Ss. Cyril and Methodius Univ., Skopje, Macedonia.
- Pesevski I, Jovanovski M, Papic J, Markoski B, Milevski I (2012) Approaches in preparation of national landslide and rock fall data base and hazard-maps in R. Macedonia. *Scientific Journal of Civil Engineering*. 1: 49-55.
- Van Westen C J (2003) Statistical landslide hazard analysis. At <http://www.itc.nl/ilwis/applications/application05.asp> [Accessed December 15, 2010]

The Instability Phenomena along the Coasts of the Kvarner Area (NE Adriatic Sea)

Čedomir Benac⁽¹⁾, Petra Đomlija⁽¹⁾, Martina Vivoda⁽¹⁾, Renato Buljan⁽²⁾, Dražen Navratil⁽²⁾

1) University of Rijeka, Faculty of Civil Engineering, 51000 Rijeka, Croatia, Radmile Matejčić 3

2) Croatian Geological Survey, Zagreb, Croatia

Abstract The instability phenomena along the coast of the Kvarner area (channel part of the Northeastern Adriatic Sea, Croatia) generally are predisposed by geological settings and inclination of coastal slopes. Gentle inclined rocky coasts formed in Cretaceous and Palaeogene carbonate rocks are mostly stable, without visible evidences of mass movements. Against that, different types of mass movements are common on very steep and subvertical coasts where geological settings of rocks is similar. Marine erosion caused by wave impact is not very pronounced due to its sheltered position and coastal lithology. In places where the rock mass is tectonically crushed or/and karstified wave notches and cliffs evolve. The destructive impact of waves is more pronounced in the coasts formed in Palaeogene marls and flysch rock mass. The assessment indicates that the most parts of the coast in the Kvarner area generally have low risk wave induced marine erosion. Meanwhile, great parts of those locations are protected by sandy and gravelly beaches. The degree of geological hazard and vulnerability caused by mass movements will be increased to predicted sea-level rise. Many new slope instabilities along the coasts in the Kvarner area have noted after the highest sea-levels in time period from 1 December 2008 to 1 November 2012.

Keywords karst, flysch, marine erosion, mass movement

Introduction

The Kvarner area (the northeastern part of the Adriatic Sea) is located between the Istrian peninsula and the Vinodol-Velebit coast. The island chains Cres-Lošinj and Krk-Rab-Pag divide it into the Rijeka Bay, the Kvarner Bay, the Kvarnerić Bay and the Velebit-Vinodol Channel (Fig. 1).

The coast along the Kvarner area with the most parts of the eastern coast of the Adriatic Sea belong to automorphic coasts or Dalmatian coast type. Coastal processes are known only generally (Juračić et al. 2009, Pikelj and Juračić 2013).

In this paper the complex relationship between the geological settings, resistance of rocks mass and marine erosion induced by sea level rising and wave induced forces have presented. The relation between

marine erosion and stability of coastal slope has also analyzed. The effect of estimated sea-level rising on possible higher degree of coastal erosion susceptibility has been also analyzed. The presented results are based on preliminary investigations and present a base for further, more detailed investigations.

Geological settings

In the terrestrial part of the Kvarner area Cretaceous carbonate sedimentary rocks (limestone, dolomites and carbonate breccia), Palaeogene limestone (foraminiferal limestone and breccia) and Palaeogene siliciclastic rocks (marls and flysch) are present (Velić and Vlahović 2009). Carbonate rocks prevail, whereas siliciclastic outcrops are restricted (Fig. 1). Pleistocene and Holocene cohesive and noncohesive sediments partly cover this bedrock substrate.

At the seafloor of the Kvarner area three main sea bed types are found. Rocky outcrops with or without isolated sediment cover are situated on shallow and wave exposed submarine zone. The bottom covered by coarse grained sandy and gravelly sediments is found in shallow submarine zone where wave action is relatively strong. The deepest parts of bottom and sheltered areas are covered by fine-grained muddy sediments (Juračić et al. 1999).

Oceanographic condition and coastal processes

Wave heights in the channel part of the northern Adriatic Sea are smaller than in western open zone due to relatively short wind fetch. Hence the strongest northeastern wind Bura (or Bora), does not generate the highest waves due to limited fetch. On the other hand, the stormy southeastern wind Jugo (or Scirocco) can generate waves higher than 6 m on western open coast of Cres and Lošinj islands (Leder et al. 1998).

Intensive morphogenetic processes caused by tectonic movements and rapid sea-level changes, as well as climatic changes, caused the present shape of the Kvarner area. Slow sea-level rise during the last 6.000 years (Pirazzoli 2005) created conditions for more intensive marine erosion (Benac and Juračić 1998, Juračić et al. 2009).

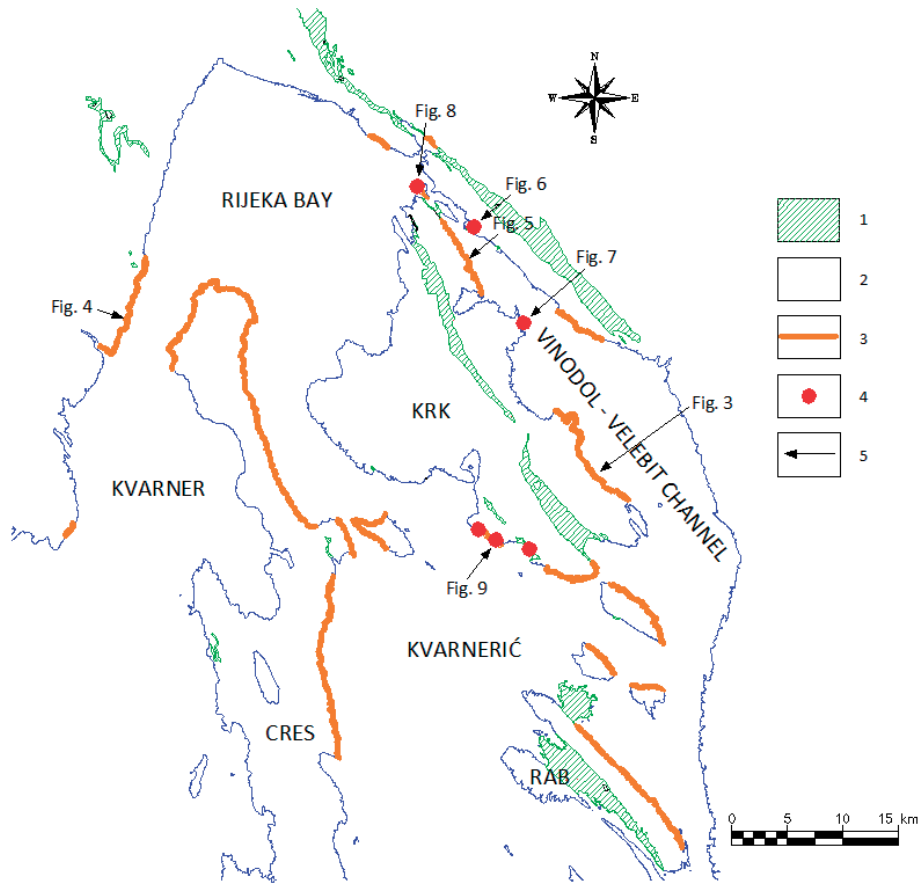


Figure 1 Simplified geological map of the Kvarner area: 1-Palaeogene siliciclastic rocks (marls and flysch); 2- carbonate rocks (Cretaceous limestone, dolomitic limestone and carbonate breccia, Palaeogene limestone and carbonate breccia; 3-steep inclined coast formed in carbonate rocks with common instability phenomena; 4-active landslide (the arrows show the locations of photos; see Figs 3-9).

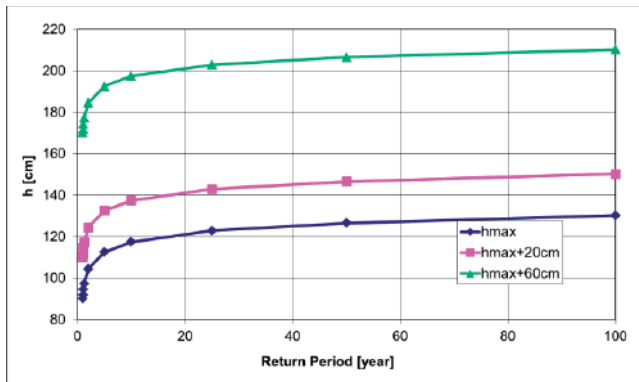


Figure 2 Predicted sea level rise and possibility of extreme high tide (according Benac et al. 2007).

Predicted sea-level rise is 20 to 60 cm during the 21st century in the Mediterranean and the Adriatic Sea (Antonioli and Silenzi 2007). The highest sea-level has been recorded on the mareograph in Bakar during last few years (on 1 December 2008 has been recorded +117 cm above M.S.L and on 1 December 2012 has been recorded +122 cm above M.S.L.). The assesment is that the extreme

high tide will be more frequent in the Kvarner area (Fig. 2).

The sea level is a global boundary with the weathering and erosional processes prevailing above it, whereas the accumulation of sediments occurs below it. In accordance to the sea level changes during the geological history, the intensity and location of erosion, karstification and accumulation of sediments changed too (Bird 2008).

Marine erosion caused by wave impact is not very pronounced on the coasts of the Kvarner area, due to transform direction of winds, sheltered position of coasts and its geologic settings and a resistance on wave forces. At locations where the rock mass is tectonically crushed or/and karstified wave notches and cliffs evolve. The destructive impact of waves is more pronounced in coasts formed in less resistant lithological types of siliciclastic rocks, even in sheltered zones, where wave energy is low. A different effect of wave erosion is observed in many locations. Cliffs are formed in more resistant sandstones, whereas the combination of erosion and mass movements are common in less resistant marls and siltstones.

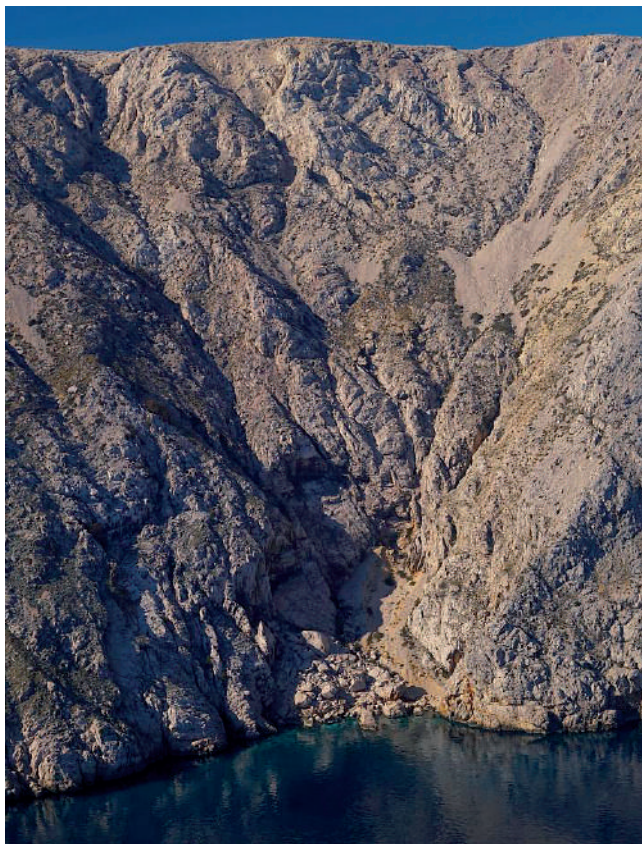


Figure 3 Rockfall and active talus: the northeastern coast of the Island of Krk (Photo: Ž. Gržančić).

Instability phenomena of along the coasts in the Kvarner area

Gentle inclined carbonate rocky coasts are generally stable, without visible evidences of mass movements in all Kvarner area. Destructive influence of waves is small and bioerosion prevails. Against that, different types of mass movements are common on very steep and subvertical coastal parts. These morphodynamic processes are clearly visible along the northeastern coasts of the Krk, Rab and Cres islands, and also along the northeastern coasts of the Prvić, St. Grgur and Goli islands (Fig. 1). These phenomena are also present on western coast of the Rijeka Bay between the Plomin Bay and the Mošćenička Draga Valley, in the Bakar Bay and sporadically along other steep coasts. Active scree and rockfall prevail on rocky scarps (Fig. 3). Remarkable phenomenon is a combination of tectonic subsidence and a huge rocky slide on the western coast of the Rijeka Bay (Fig. 4).



Figure 4 The trace of ancient rock slide: the western coast of the Rijeka Bay, near Brseč (Photo: Č. Benac).

Marine erosion is more pronounced on coasts formed in siliciclastic rocks and cohesive and noncohesive Pleistocene and recent sediments (Benac et al. 2007, Juračić et al. 2009). Narrow gravelly beaches have a role of mitigation from destructive impact of waves. The process of erosion prevail (Fig. 5), but somewhere different types of landslide are found. Different type of active sliding are visible in the Havišće cove, near the Jadranovo settlement (the northeastern part of the Vinodol Channel) (Fig. 6), in the Murvenica cove (the northeastern coast of the Island of Krk) (Fig. 7), on the southwestern coast of the St. Marko Island (Fig. 8), and near Stara Baška as it is shown in Figure 9 (the southwestern coast of the Island of Krk).

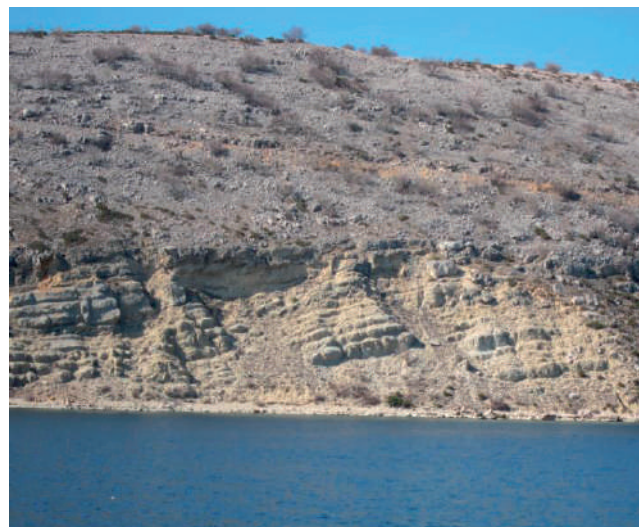


Figure 5 Strong erosion in Palaeogene flysch rocks: the northeastern coast of the Island of Krk (Photo: Č. Benac).



Figure 6 The trace of sliding along the flysch-carbonate rocks contact: Havišće cove near the Jadranovo settlement, northeastern coast of the Vinodol-Velebit Channel (Photo: Ž. Gržančić).



Figure 7 Earthflow in weathered siliciclastic rocks provoked by marine erosion: the Murvenica cove, the northeastern coast of the Island of Krk (Photo: Č. Benac).



Figure 8 Sliding block of talus breccia along the flysch-carbonate rocks contact: the southwestern coast of the St. Marko Island (Photo: Č. Benac).



Figure 9 Debris avalanche provoked by marine erosion: the southeastern coast of the Island of Krk (Photo: Ž. Gržančić).

Discussion and conclusion

The assessment indicates that most parts of the coast in the Kvarner area generally have a low susceptibility of wave induced marine erosion and the bioerosion prevails. Gentle inclined carbonate rocky coasts are generally stable. Against that, the active screens and rockfalls are usually located on rocky scarps. The combinations of extensive erosion and sliding are commonly present on the coasts formed in siliciclastic rocks and Quaternary sediments. Meanwhile, the great parts of those locations are protected by sandy and gravelly beaches. The degree of geological hazard and vulnerability caused by mass movements will be increased due to predicted sea-level rising. The authors of this paper have noted much different types of instability provoked by wave erosion of slopes after extreme high tides (ital. *acqua alta*), in 2008 and 2012. The beach bodies during these extreme tides were flooded, and, consequently, the rule of natural coastal protection was lost. It is possible to expect more frequent instability phenomena along the coast of the Kvarner area in the future in the respect to estimated sea-level rising.

In further investigations it should be necessary to analyze complex relationship between the geological settings, the resistance or strength of rock mass, the coastal slope angle, stability of coastal slopes and the effect of marine erosion.

In the coastal management the different and conflicting interests are present very often, and balanced development is very hard to achieve. In order to develop mitigation and adaptation plans for future coastal changes, an integrated coastal zone management is proposed.

References

- Antonioli F, Silenzi S (2007) Variazioni relative del livello del mare e vulnerabilità delle pianure costiere italiane. Quaderni della Società Geologica Italiana. 2: 1-29. (In Italian)
- Benac Č, Juračić M (1998) Geomorphological indicators of the sea level changes during Upper Pleistocene (Würm) and Holocene in the Kvarner region. Acta Geographica Croatica. 33: 27–45
- Benac Č, Ružić I, Žic E (2007) The vulnerability of coasts in the Kvarner area. Pomorski zbornik. 44: 201-214 (In Croatian)
- Bird E C (2008) Coastal Geomorphology: an introduction. Second edition. John Wiley & sons. Chichester (ISBN 978-0-470-51739-7) 404p.
- Juračić M, Benac Č, Crmarić R (1999) Seabeded and surface sediments map of the Kvarner Bay, Adriatic Sea, Croatia. Geologica Croatica. 52: 131-140.
- Juračić M, Benac Č, Pikelj K, Ilić S (2009) Comparison of the vulnerability of limestone (karst) and siliciclastic coasts (example from the Kvarner area, NE Adriatic, Croatia). Geomorphology. 107(1–2): 90–99.
- Leder N, Smirčić A, Vilibić I (1998) Extreme values of surface wave heights in the Northern Adriatic. Geofizika. 15: 1–13.
- Pikelj K, Juračić M (2013): Eastern Adriatic Coast (EAC): Geomorphology and Coastal Vulnerability of a Karstic Coast. Journal of Coastal Research. 29 (4): 944–957.
- Pirazzoli PA (2005) A review of possible eustatic, isostatic and tectonic contributions in eight late-Holocene sea-level histories from the Mediterranean area. Quaternary Science Reviews. 24: 1989–2001.
- Velić I, Vlahović I (2009) Geologic map of Republic of Croatia 1:300.000. Croatian Geological Survey, Zagreb. (In Croatian)

Landslides Hazard Maps for Mures County Central Area, Romania

Emilia Elena Milutinovici, Simona Corlateanu, Daniel Mihailescu, Raul Iacobescu

Search Corporation, Field Studies Department, Bucharest, Romania, Caderea Bastiliei, no. 65, district no. 1, +40213164018

Abstract Starting from 2006, the Government of Romania showed special interest to the preparation at national level of hazard and risk maps to natural disasters (landslides, floods, earthquakes). It is estimated that almost one third of the Romanian territory is affected by landslides, and their study and recording is still precarious. In Romania, the first attempts to standardize the methods of hazard mapping in general and landslides risk maps in particular were done in 1997 (Benga et al. 1997) and 1998 (Dobre et al. 1998). The Government Decision no. 382/2003 (Anon. 2003a) presented the methodological regulations regarding the requirements for the documentation of the territory arrangement and urbanism in the areas subject for natural risks and the Government Decision no. 447/2003 (Anon. 2003b) establishes the methodological norms regarding the drawing up and content of the landslide hazard and natural risk maps. The main aims of this study are: a) identify all landslides affecting the territory of the central region of Mures County, b) estimate the influence coefficients according to the possibility of landslides formation, c) calculate the hazard average coefficient, based on the values estimated for the influence coefficients, d) preparation of the landslides hazard map.

Keywords landslide, hazard map

Physical, geological and geographical location

This article examines the central area of Mures County, comprising the following localities: Bala, Glodeni, Gornesti, Sincai, Ceausu de Campie, Ernei, Band, Madaras, Panet, Santana de Mures, Sangeorgiu de Mures, Sancariu de Mures, Targu Mures, Iclanzel, Ogra, Sanpaul, Ungheni, Gheorghe Doja, Cristesti, Craciunesti, Corunca, Acatari, Livezeni.

Mureş County is located in the central-northern part of Romania (Fig. 1) and stretches between the Căliman and Gurghiu mountains up to Târnavelor Plateau and Transylvania Plain. The physical - geographic axis of the County is given by the Mureş River which crosses the County from north-east to south-west along 140 km. The central area of the County includes 50 administrative territorial units and is divided into three sub- areas: Sarmasu, Targu Mures si Sovata.

Geologically, in Sarmasu sub-area, located in the central-western region of the County, beyond the right

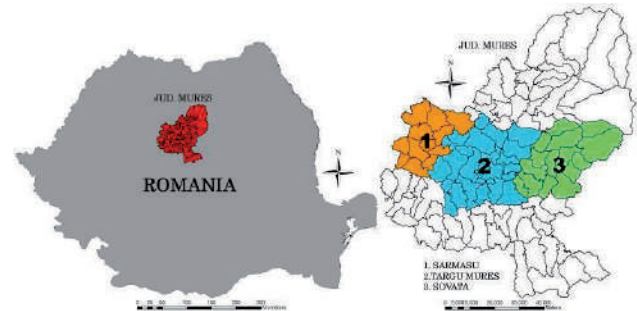


Figure 1 Administrative classification.

bank of Mures River, the predominant deposits are Sarmatian: Volchinian - inferior Bessarabian (Mutihac et al. 2007); in the Targu Mures sub-area located in the center of the County and in the region beyond the left bank of Mures River, the predominant deposits date since the Pannonian age and in the Sovata sub-zone, located in the central-eastern part of the County, the most deposits date since the Pannonian age, except in a series of regions from the western region where volcanogenic-sedimentary formations can be found, represented by Neozoic migmatites (Vasilescu et al. 1968).

Tectonically, the examined area is represented by multiple anticlines and domes. The main structural element in this sector is a normal anticline with the Badenian in axis which bifurcates towards south, the eastern branch becoming a fault-fold, along which the Badenian sometimes superposes towards south-west the Sarmatian, deepening towards Orşova. It is remarked that this fault-fold is an area which delimits the eastern sector, slightly folded, which deepens in the synclinal under eruptive deposits, from the south-western sector, which marks the Zone II, in which the Neogene formations are folded in many anticlines and domes (Raileanu et al. 1967).

Hydro-geologically, the Zone II is represented by alluvia aquifers from the hydrographic basin of Mures, Tarnava Mica and Tarnava Mare Rivers, marked on the map of the Underground Waters of the Romanian territory, scale 1:1000000, as part of the region with «local or discontinuous aquifer strata». In this region, the water is embedded in the Sarmatian and Pannonian formations represented by gravels, sands, conglomerates and clays. The adjacent regions to the hydrographic basins are, in general, regions without underground water, with possible captive depth water (CANUGI 1979).

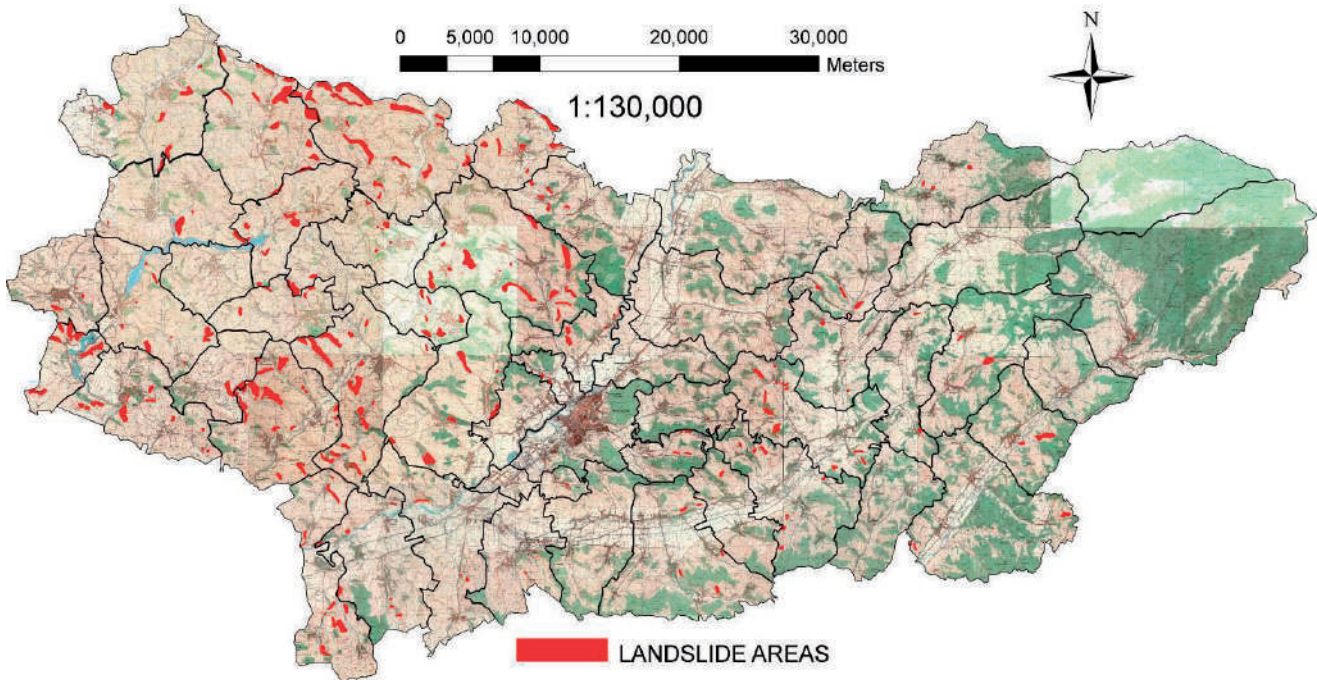


Figure 2 Landslides identification.

The climatologic conditions together with the other factors represent critical processes of the construction of the landslide hazard maps in this region. Precipitations and temperature have a major contribution to the deterioration of the land in this region. The annual average in this area varies between 6-9° Celsius and the average annual precipitations range between 700-800 mm/year. (Maciu et al. 1982)

The studied zone II is included in several categories (Anon. 2001) depending on the risk and manifestation degrees of the erosion processes, landslides and collapses, namely:

- The Sarmasu subzone is included in the category of relatively stable soils, with slight-moderate or insignificant erosion, with reduced risk to landslides and with high risk of erosion increase.
- The Targu Mures subzone is included in the category of moderately stable soils with very reduced stability in certain areas, with moderate-strong erosion, with relatively old, more or less stabilized landslides, but with a high risk of being reactivated during rainy years, or after changing the use of the respective lands (tree clearing, soil turning) or after performing works for destabilizing the slopes (terracing) and after building onto the soil heavy constructions (buildings, roads).
- The Sovata subzone. In the hill section of this territory the predominant lands are relatively stable, with slight to moderate or insignificant erosion, with reduced risk of landslides and with high risk of erosion increase, and in the mountain section the lands are included in the category of relatively instable lands, with high risk of landslides, falls, and collapses.

Landslides identification

A number of 3472 observation points were covered, and a series of vulnerable elements were identified on site. Landslides were identified and consequently 176 landslides identification sheets were prepared (Fig. 2) (Milutinovici et al. 2012a).

The purpose of the geological and geomorphologic mapping was to have an in-depth knowledge of the geological structure and of the geomorphology of the studied area, emphasizing especially the areas with land instabilities, identifying the landslides (Fig. 2), establishing their location and sizes. The following aspects were especially targeted: identification of the instability areas; the geographical coordinates, their sizes, the landslide type (category, material, movements), the preliminary and triggering causes. For each landslide the possible material losses were noted or information was gathered related to body injuries.

The gathered information revealed the following:

- 78% of the localities are affected by landslides, having an average of 5.5 landslides per land. The localities with the most frequent landslides (over 10) are included in the Targu Mures subzone: Band, Iclanzel and Ogra, and in the Sarmasu subzone: Sanpetru de Campie, Raciuc. The fewest landslides occur in the Sovata subzone (only 50% of the localities are affected by landslides); most of the landslides are primary but approximately 40% of them are reactivated;
- Following the geotechnical mapping and after performing the site investigations, it was observed that the identified landslides are included in the following

categories:

- Length: 20-3,000 m;
- Width: 30-2,000 m
- Depth of slip plan: 1.5-5.0 m (medium depth), or <1.5 m (shallow slip);
- Primary and reactivated landslides;
- Slipped material type: soils, rocks, debris;
- Motion type: translation, collapse, extension;
- Motion direction: progressive, sometimes regressive;
- Direction of development: one direction or multiple directions;
- Preparation causes: slope, lithology, spring, moist areas;
- Triggering causes: precipitation, old landslides, earthquakes;
- Material damages: grasslands, buildings; agrarian fields, roads and railroads;
- Human damages: o.

Estimation of the influence coefficients according to the possibility of landslides formation

The influence coefficients were noted during the site visit. For each observation point all the influence coefficients, except the seismic coefficient, were noted depending on the case found on site. (Milutinovici and Nastase 2012) The notes are included, according to the Decision no. 447/2003 in the intervals 0; 0-0.10; 0.10-0.30; 0.31-0.50; 0.51-0.80 and 0.80-1.00. The noting is made based on the quality assessment of the involved factors. For each influence factor, a minimum and a maximum value is considered (Tab. 1). Depending on these two values, the average value of the respective influence coefficient is determined. After calculating this value, the average hazard coefficient will be further calculated.

Table 1 Categories of hazard coefficient (Anon. 2003b).

Criterion (factor)	Probability of landslides occurrence (p)					
	Low	Average	High	Probability of landslides occurrence and corresponding hazard coefficient		
	Practically zero	Low	Average	Average-high	High	Very high
	0	<0.10	0.10-0.30	0.31-0.50	0.51-0.80	>0.80

The influence factors are: Lithologic factor (Ka); Geomorphologic factor (Kb)-(Fig. 3); Structural factor (Kc); Hydrologic and climatic factor (Kd); Hydrogeologic factor (Ke); Seismic factor (Kf); Forest factor (Kg)-(Fig. 4); and Anthropogenic factor (Kh).

The notation and the calculation of the influence coefficients is made using the Table 1, estimating the influence factors in terms of quality and quantity depending on the case found on site.

For each factor a distribution map with isolines was created. The working basis for the thematic maps, for the distribution of the values of the influence thematic coefficients was the topographic map, scale 1:25,000. The processing of the thematic maps, as well as of the final hazard map was made using Bentley (Power Draft) and Esri (GIS) working platforms.

The maps were performed by interpolating the values determined in the measurement points. The interpolation method used was the “Natural Neighbor” method. This is a method of the weighted mean of the determination of the measured values in the points of a grid, the weights being determined based on the position of the data and of the spatial continuity degree present in the data. The weights are determined so that

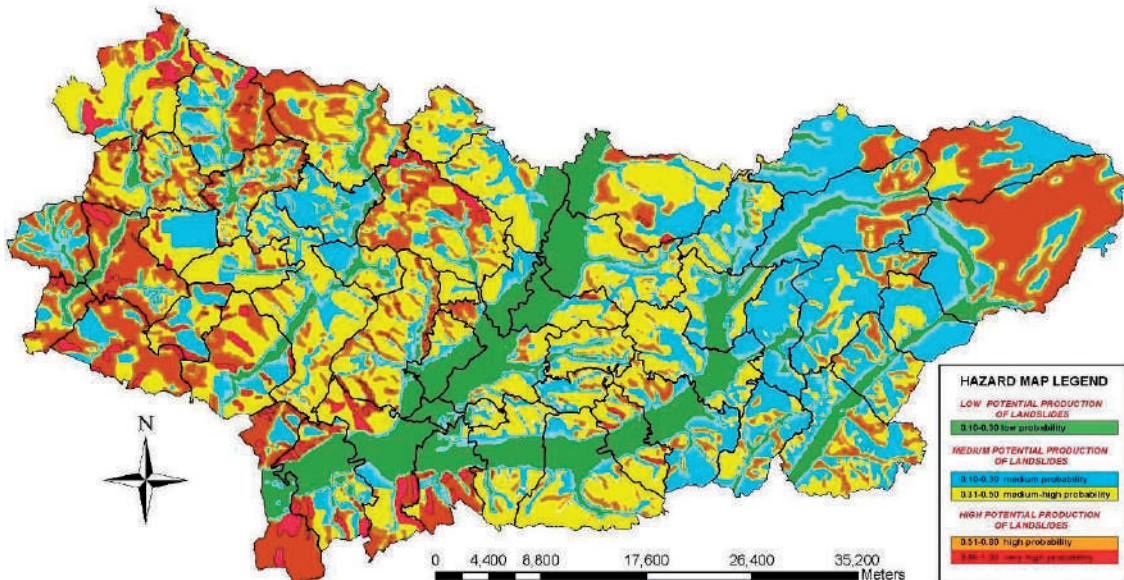


Figure 3 The geomorphologic coefficient distribution.

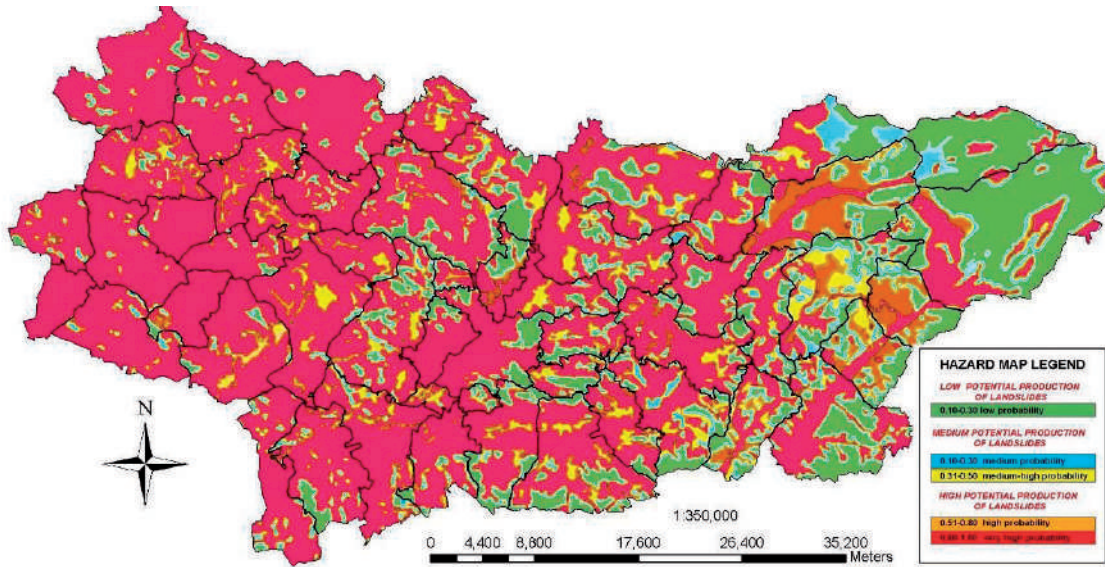


Figure 4 The forest covering coefficient distribution.

the average error of the estimation should be zero and the variant of the estimation should be minimal. The interpolation was performed using the ESRI (GIS – ArcMap) software.

The isolines (the lines which link the points in which a size has the same value) were also traced using the ESRI (GIS – ArcMap) software. The interval of the isolines was of 0.05 for the distribution maps of the influence factors drawn with isolines (Ka-Kh).

Calculation of the average hazard coefficient

After estimating the influence coefficients, the average hazard coefficient, K_m , is calculated. The value of the average hazard coefficient was determined for each

observation point. The minimum and maximum values were determined for the respective points as well as the value of the landslide average hazard coefficient. The average hazard coefficient is calculated according to the methodological norms from the Decision no. 447 (Anon. 2003b), using the formula [1].

$$K_m = \sqrt{\frac{k_a \times k_b}{6} \times (k_c + k_d + k_e + k_f + k_g + k_h)} \quad [1]$$

After calculating the average hazard coefficient it was noticed that the maximal values of the K_m are not higher than 0.8 (Milutinovici et al. 2012b) (Fig. 5), which means that for the entire analyzed territory there are no areas where the probability of landslide should be very high, but it ranges within the practically zero, low, average, average high and high limits (Tab. 1).

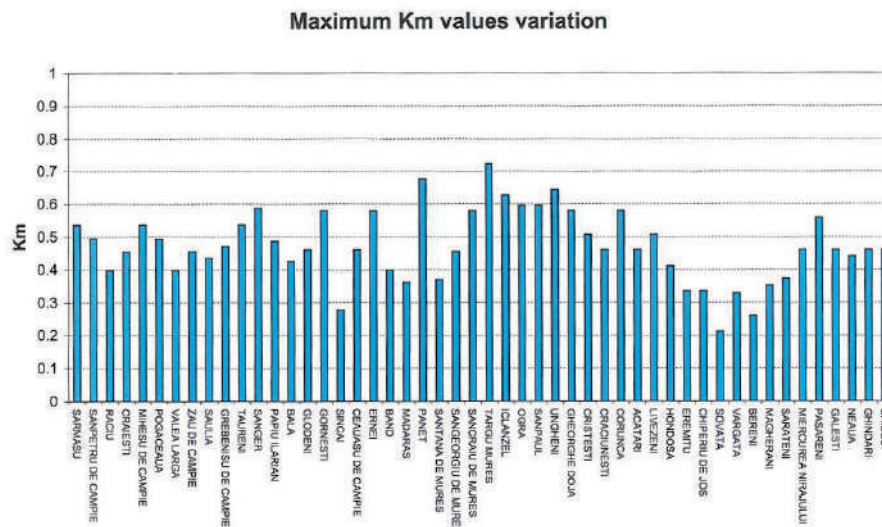


Figure 5 Maximum K_m (hazard coefficient) variation.

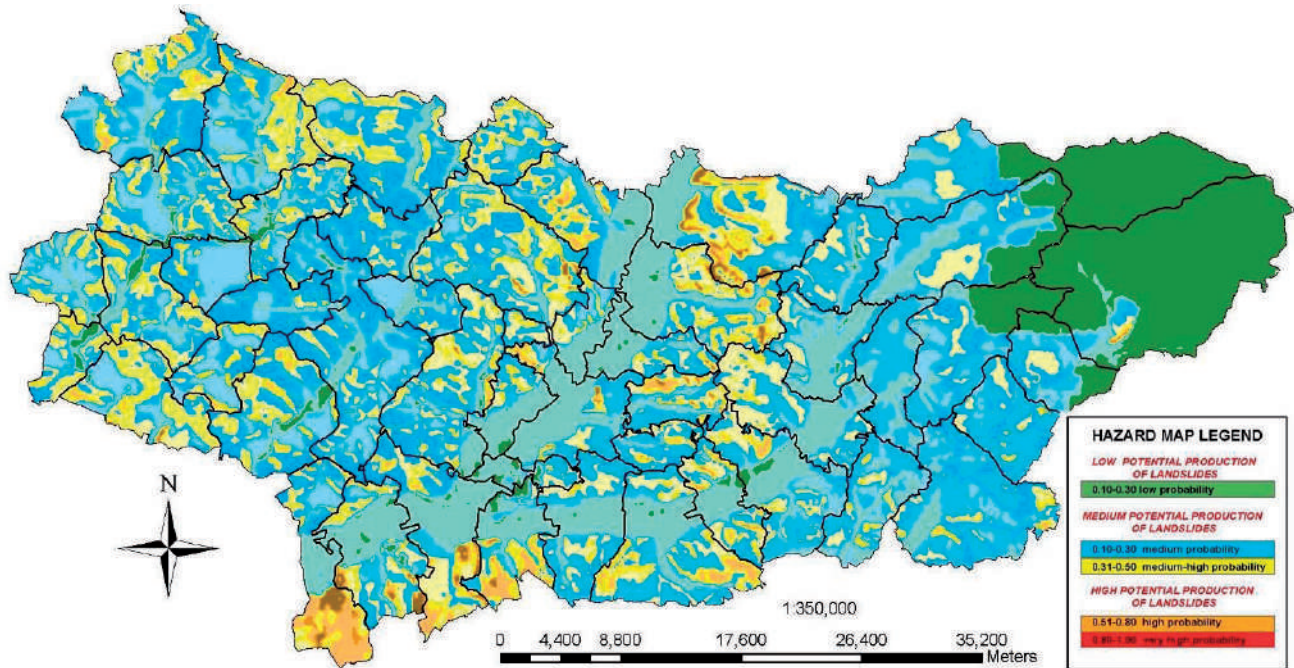


Figure 6 Landslide hazard map for Mures County central area.

Creating the landslide hazard map

For creating the landslide hazard map the average values were used for the calculated landslide hazard coefficients. Similarly to the thematic maps, the interpolation was made using the “natural neighbor” method, and the variation map was made tracing isolines. The equidistance of the isolines was 0.02. The interpolation by the natural neighbor method and the tracing of the isolines were made using the ESRI (GIS – ArcMap) software, based on the topographical map, scale 1:25,000.

The landslide hazard map is made using the STEREO 70 coordinates, and thus it can be used or superposed over any other type of map created using these coordinates, and also its scale of use can be modified to serve the desired purpose (Fig. 6).

Database structure

As an appendix to the project, a data base in GIS – Esri was also performed, thus it comprises all the information used for creating the landslide hazard risk maps, such as the general information (boundaries of the administrative units, boundaries of the inside built-up territories, infrastructure, land improvements; information regarding the geotechnical mapping (mapping points, landslides profile); geotechnical investigations (map of the investigation points and the results of the geotechnical investigations); influence coefficients (their estimation and tracing the variation maps); the landslide hazard maps (urban plans used, the map with the distribution isolines of the average landslide hazard coefficient), to which the significant screens are added (urban plans,

topographical maps, geological maps, orthophotoplans, hydrological maps).

The use of landslide hazard map

The main uses of the landslide hazard maps are the following (Milutinovici et al. 2012):

- The map addresses to the local authorities, helping to raise the awareness regarding the development directions of the inside built-up area or of other objectives of interest (industrial, agricultural, social, touristic growth).
- By using the GIS working system, the maps can be overlapped with the inside built-up area of the localities (GUPs), with the maps presenting the infrastructure or utilities routes, with the touristic objectives or with the objectives of local or national interest, the single condition being that the overlapping maps should be performed in the same coordinates system as the landslide hazard map.
- The acknowledgment of the “sensitive” area and the road and utilities routes leads to a more precise evaluation of the necessary costs for the construction of new roads or for the rehabilitation of the existing ones, for the maintenance of the utilities that have already been introduced or for the performance of new utilities systems;
- The map addresses to natural and legal persons, the acknowledgement of a land or of a real estate position according to a landslide hazard map being able to influence its selling / purchase price, as well as the price of construction insurance.

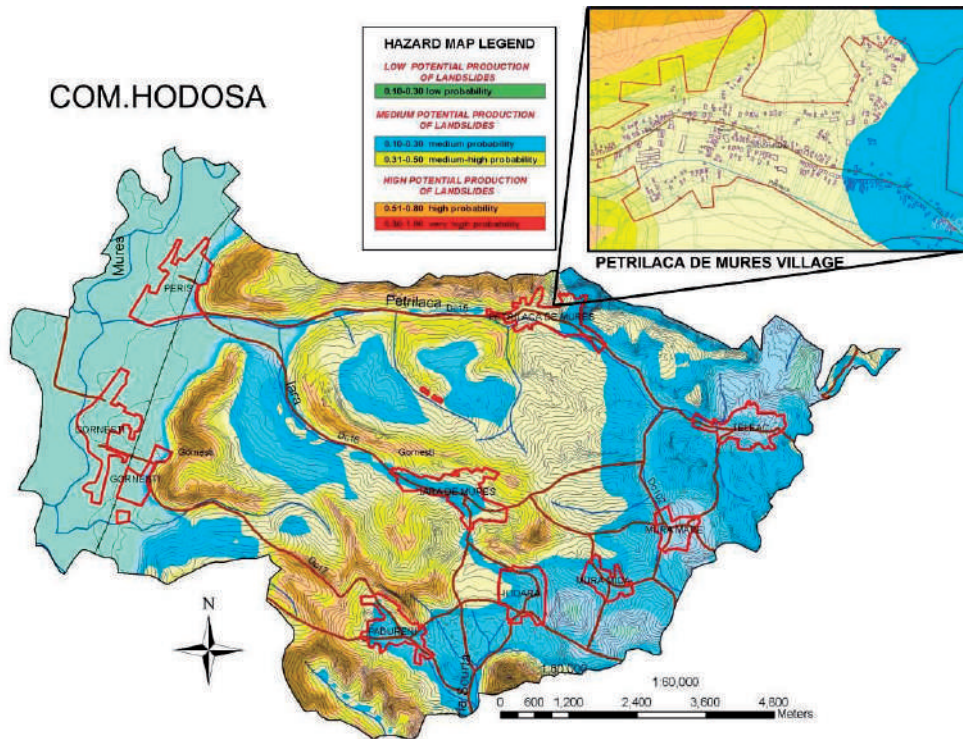


Figure 7 Landslide hazard maps for Hodosa Commune and Petrilaca Village (Milutinovici et al. 2012c).

The landslide hazard maps can be detailed according to the targeted purpose, for other scales, so that details can be further on carried out from an entire studied area to have a better understanding of the status related to the landslide hazard in a township or even in a village located in a township (Fig. 7).

Acknowledgments

Many thanks to Mr. Dan Mihailescu and Mr. Michael Stanciu (Search Corporation) for their proven support within the company in relation to the landslide hazard and risk projects.

References

Anon. (2001) Law 575/2001: The National territory – Section V: Natural hazard areas. Official Journal of Romania, part I, no. 726/14.11.2001, Bucharest, pp. 3-7, 18-19, 31. (In Romanian)

Anon. (2003a) Law 382/2003: Minimum exigencies of document contents for territory arrangement and town-planning for areas with natural hazard problems. Official Journal of Romania, part I, no. 263/16.04.2003, Bucharest, pp. 1-9. (In Romanian)

Anon. (2003b) Law 447/2003, Drawing up and content for landslide natural risk map. Official Journal of Romania, part I, no. 305/07.05.2003, pp. 1-4. Bucharest. (In Romanian)

Benga M, Veliciu D, Serbanescu R (1997) GT006-97/1997: Guide to identify and monitor landslides. Engineering Bulletin. 10: 2-93.

CANUGI (Comisia Atlaselor Nationale si Uniunii Geografice Internationale) (1975) Romanian Atlas, Grounwater map for the

territory of Romania, scale 1:1000000, Editura Academiei. (In Romanian)

Dobre V, Benga M, Veliciu D, Serbanescu R (1998) GT019-98/1998: Guide to draw up the slopes landslides risk maps for assurance building stability. Engineering Bulletin. 6: 116-165.

Maciu M, Chioreanu A, Vacaru V (1982) Romania's geographical encyclopedia. Editura Didactica si Pedagogica, Bucharest. (In Romanian)

Milutinovici E, Corlateanu S, Oculeanu M, Iacobescu R, Nicolaev P (2012a) Risk maps over Mures County, Romania, step 1: Establish territory planning and database structure, Search Corporation, Romania.

Milutinovici E, Nastase A (2012) Risk maps over Mures County, Romania, step 2: Perform in-situ testing and geotechnical laboratory results, Search Corporation, Romania.

Milutinovici E, Corlateanu S, Nicolaev P, Nastase A (2012b) Risk maps over Mures County, Romania, step 3: Calculation of average landslide hazard coefficient and editing the landslide hazard map 1:25.000, Search Corporation, Romania.

Milutinovici E, Corlateanu S, Nicolaev P, Nastase A (2012c) Risk maps over Mures County, Romania, step 4: Calculation of average landslide hazard coefficient and editing the landslide hazard map 1:5.000, Search Corporation, Romania.

Mutihaç V, Stratulat M I, Fechet R M (2007) Geology of Romania. Editura Didactică și Pedagogică, Bucharest. (In Romanian)

Raileanu Gr, Radulescu D (1967) Geological map and book, scale 1:200000, L-35-VII, 11. Bistrita, Romanian Geological Institute. (In Romanian)

Vasilescu AI, Muresan M, Popescu I, Sandulescu J, Popescu A, Brandabur T (1968) Geological map and book, scale 1:200000, L-35-XIV, 20. Odorhei, Romanian Geological Institute. (In Romanian)

Landslide Hazard Forecast in Slovenia – MASPREM

Marko Komac, Jasna Šinigoj, Mateja Jemec Auflič, Magda Čarman, Matija Krivic

Geological Survey of Slovenia, SI-1000 Ljubljana, Slovenia, Dimičeva ulica 14, +386 1 2809 700

Abstract In the past 20 years, intense short and long duration rainfall has triggered numerous shallow landslides worldwide and caused extensive material damage to buildings, infrastructure, roads, and unfortunately also causing deaths. Slovenia was no exception in this regard. But these landslide related problems could be identified and minimized if the knowledge of the landslide occurrence would be upgraded with the more in-depth knowledge of the relation between the triggering factors (rainfalls) and landslides. In the frame of the national project Masprem we aim to develop an automated, online tool for predicting landslide hazard forecast at the national level. The paper presented a design for the system for the modelling a landslide probability through time in Slovenia. The importance of their inclusion in the system will be highlighted.

Keywords landslide hazard, early warning system, real-time rainfall, Slovenia

Introduction

In the last decade over 7,500 people died worldwide due to extreme rainfall events that trigger landslides (EM-DAT 2009). Hence gathering of the knowledge about these dangerous phenomena and the urgency to understand them is a necessity. Society strives towards self-protection and self-preservation, or at least mitigation of the consequences if they cannot be prevented. To manage the hazards associated with shallow landslides, accurate predictive warning system for rainfall induced slope failures is needed.

To analyze rainfall patterns that govern slope failure, it is essential to understand the relationship between rainfall and landslide occurrence. First analysis of the impact of rainfall focused only at the cumulative value of the daily precipitation (Crozier and Eyles 1980, Terlien 1998, Crozier 1999, Wilson 2000) but latter research proved strong affect of antecedent rainfall that trigger slope failures (Kim et al. 1992, Glade et al. 2000, Aleotti 2004, Zezere et al. 2005, Jemec Auflič and Komac 2011). Intensity and period of rainfall that trigger landslides play important role when assessing triggering thresholds values. By using the threshold approach, two major thresholds can be defined: minimum threshold and maximum threshold, which identify the lower and upper boundaries of the threshold's probability range (White et al. 1996). The minimum threshold defines the lowest

level, below which a landslide does not occur. The maximum threshold is defined as the level above which a landslide always occurs. To correlate rainfall and landsliding, detailed information about landslide locations and rainfall data is required (Reichenbach 1998).

In a few places of the world rainfall thresholds are a part of the operational landslide warning systems, in which real-time rainfall measurements are compared with established thresholds, and when pre-established values are exceeded alarm messages are issued (landslide warning system has been designed for San Francisco Bay Region, Hong Kong, Japan, China, Rio de Janeiro, etc.). With respect to numerous landslide occurrences the landslide early warning systems in a real-time mode have been developed also in several countries in the Europe (systems ILEWS, AlpEWAS, INCA, DORIS).

Slovenia has a highly diverse landscape and climate due to its position between the Alps, the Mediterranean Sea, the Dinarides and the Pannonian Basin. Slovenia occupies the territory of the still active boundary of the African and Eurasian plates and, respectively, three large geotectonic units – the Alps, the Dinarides and the Pannonian basin, resulting in a very complex and diverse geology. Within a small area rock of the most diverse origin, composition and age, ranging from Palaeozoic to the Quaternary age, can be found (Fig. 1).

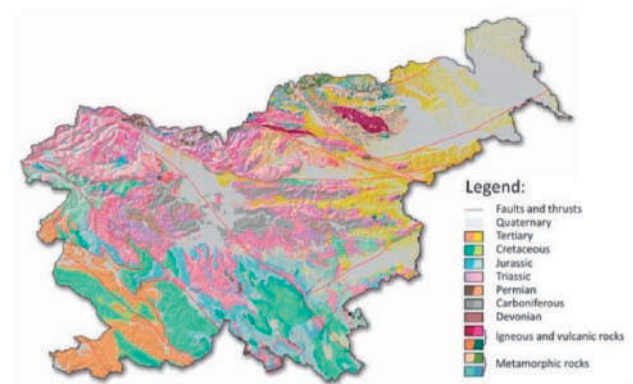


Figure 1 Geological structure of Slovenia. Main faults and thrusts are marked with red lines.

According to Komac and Ribičič (2006) a quarter of Slovenian territory is exposed to landslides. In the past 20 years, intense short and long duration rainfall has triggered numerous shallow landslides and caused extensive material damage to buildings, infrastructure,

roads, and unfortunately also causing deaths. These events could be identified and to some extent also minimized if better knowledge of the relation between landslides and rainfall would be available. A near real-time system for landslide hazard forecast would provide vital information on this issue. The objective of this paper is to present the landslide hazard forecast system and the modelling landslide probability through time using a real-time forecast at regional level. A designed operational system will inform inhabitants of an increased landslide hazard as a consequence of heavy precipitation that would exceed the landslide triggering values.

Methodology

In order to quickly respond to natural calamities or even to be better prepared for them with the goal to avoid casualties, environmental data need to be transmitted and processed in a near-real time. The web-based services can be used to implement a system to predict landslide hazard and to enable easy access to end-users. Considering the latter, the information needs to be provided in an understandable format and at the same time remain scientifically correct. The developed model to predict landslide probability occurrence through time will combine knowledge from geological and also from societal aspect. The general conceptual scheme is present in the Figure 2. The designed system will be based on real-time rainfall data, landslide triggering precipitation values or thresholds, and landslide susceptibility model. Each individual parameter, that plays an important role in the model, is described in the subsections that follow.

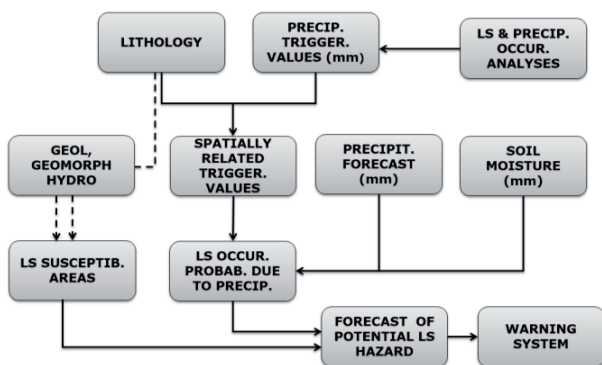


Figure 2 Conceptual model for modelling the landslide hazard forecast system.

Precipitation regime in Slovenia

The interaction of the three major climate systems (Continental, Alpine and Sub-Mediterranean) in the territory of Slovenia strongly influences the country's precipitation regime. The spatial variability of precipitation is high – the annual precipitation sum varies from 800 mm in the NE part of the country to

more than 3500 mm in the NW part of the country, where one of the Alpine precipitation maximum is detected (Fig. 3). The maximum 24-hour rainfall records with a 100-year return period from 100 to 510 mm is shown in Fig. 4. The yearly amount of precipitation decreases with distance from the sea and the Dinaric-Alpine barrier towards the NE part of the country, which is already influenced by the Continental climate. In the outmost NE part of the country (Prekmurje), the mean annual precipitation sum does not exceed 900 mm.

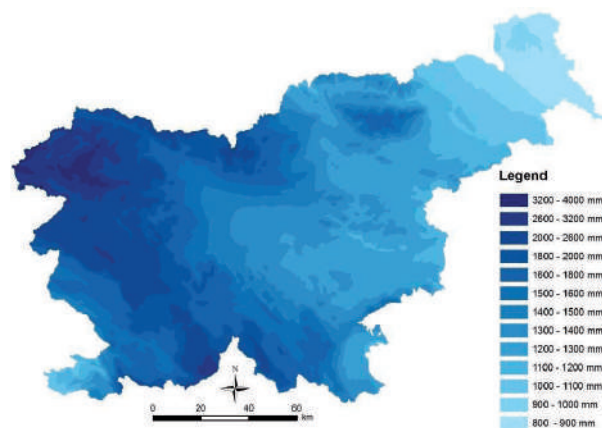


Figure 3 Map of average annual rainfall in Slovenia for the period of 1971–2000 (in mm) (ARSO 2012).

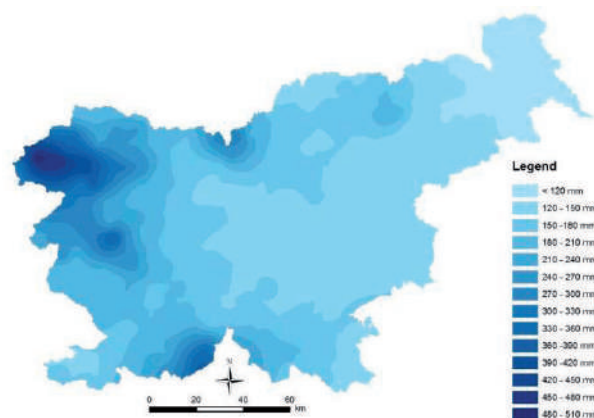


Figure 4 Map of maximum 24-h rainfall with a 100 years return period (in mm/24h) for the period of 1961 – 2000 (ARSO 2012).

The study of daily rainfall patterns (Jemec Auflič and Komac 2011) reveals that precipitation occurs in three peak periods. The first peak is from March to May, the second is characterized by intense summer rainfall storms, and the third is from September to November, of which October and November are usually the wettest months. It is not a surprise that temporal landslide occurrence is in high correlation with highest peak of rainfall. Over the period from 1990 to 2010, twelve individual rainfall events were detected, of which eight occurred during the months of September to November. An analysis of all occurrences on the slopes revealed that

two main factors are required to initiate landslides: (1) intense, short rainstorms exceeding certain levels of intensity for a specified duration and (2) antecedent precipitation at the time of the storm exceeding a minimum threshold.

Real-time rainfall data

Different types of numerical weather forecast models exist: (1) a short-range forecast where weather forecast is made for a time period up to 48 hours; (2) medium range forecasts are for a period extending from about three days to seven days in advance, and (3) long-range forecasts are for a period greater than seven days in advance but there are no absolute limits to the period. Due to the chaotic nature of the atmosphere a short-range forecasts are generally more accurate than the other types of forecasts (Mercogliano et al. 2010).

ALADIN (Aire Limitee Adaptation dynamique Development INternational) is a regional mesoscale model for numerical forecast of weather that simulates events in the atmosphere over much of continental Europe (Bubnová et al. 1995). ALADIN system is used in Slovenia operational weather forecast system since 1997 (Pristov et al. 2012). A regional ALADIN/SI model for Slovenia predicts status of the atmosphere over the area of Slovenia up to 72-hour ahead. A model simulates the precipitation (kg/m^2), snowfall, water in snow pack, and air temperature data. ALADIN/SI is a grid point model ($439 \times 242 \times 43$), where the horizontal distance between the grid points is 4.4 km and it runs in a 6 hours cycling mode for the future 54 by the Environmental Agency of Republic of Slovenia (ARSO).

Rainfall thresholds for landsliding

Analyses of landslide occurrence in the area of Slovenia have shown that in areas where intensive rainstorms occur (maximal daily rainfall for the 100 years period), and where the geological settings are favorable (landslide prone), abundance of landslide can be expected. This clearly indicates the spatial and temporal dependence of landslide occurrence upon the intensive rainfall.

For defining rainfall threshold the frequency of spatial occurrence of landslide per spatial unit was correlated with lithological unit, and 24-hour maximum rainfall data with the return period of 100 years. The result of frequency of landslide occurrence and rainfall data provides a good basis for determining the critical rainfall threshold over which landslides occur with high probability. Thus, the rainfall thresholds were determined using non parametric statistical method chi-square (χ^2) for each lithological unit. In this order we separately cross-analyzed the occurrence of landslides within each unique class derived from the spatially cross-analysis of lithological units and classes of 24-hour maximum rainfall. The critical 24-hour rainfall intensities (thresholds) can be found in the Table 1.

Table 1 Rainfall threshold for lithostratigraphic units. Critical 24-h rainfall intensities are only present for lithostratigraphic unit where a number of observed landslides were statistically higher of number of expected landslides.

Lithostratigraphic unit	Critical 24-h rainfall intensities (mm)
predominantly clay soils (soils)	-
marsh and lake sediments (clay, silt, peat) (soils)	-
alluvium, fluvial loose sediments in terraces (soils)	-
clayey – diluvial, proluvial (soils)	<120
gravely with a clayey component (soils)	150-180
gravely (predominantly thick fraction), moraines (soils)	210-240
clayey (soils)	120-150
alternation of fine and coarse grain soils (soils)	<120
pebbly (soils)	<120
mine tailings – gangues (soils)	120-150
clayey, marly rocks (soft rocks)	120-150
clayey, marly and limestone (soft rocks)	-
alternation of different materials (marl, sand, sandstone, conglomerate pebble, clay) (soft rock)	120-150
conglomerate (soft rock)	120-150
(slaty) claystones with inclusion of other rocks (rocks)	120-150
marl and sandstone (flysch) with inclusions of other rocks (rocks)	210-240
sandstones and conglomerates with inclusionsof other rocks (rocks)	150-180
stratified and cliff limestones (rocks)	-
flat limestones (rocks)	-
limestones and dolomites (rocks)	-
dolomites (rocks)	-
limestones with marls (rocks)	<120
limestones with inclusions of other rocks (rocks)	210-240
limestone conglomerates and breccia (rocks)	150-180
phyllites, schists and slate (rocks)	180-210
amphibolite and gneiss (rocks)	120-150
diabase and other magmatic rocks with tuff (rocks)	120-150
amphibolites, serpentinites, diaphthorites (rocks)	120-150
tonalite, dacite, granodiorite (rocks)	-

Landslides susceptibility model

Landslides in Slovenia occur almost in all parts of the country. Based on the extensive landslide database that was compiled and standardized at the national level, and based on analyses of landslide spatial occurrence, a landslide susceptibility map of Slovenia at scale 1:250,000 was produced (Komac and Ribičič 2006) and (Komac 2012) (Fig. 5). Altogether more than 6,600 landslides were included in the national database, of which roughly half are on known locations. Of 3,241 landslides with known location, random but representative 67% were selected (landslide learning set) and used for the univariate

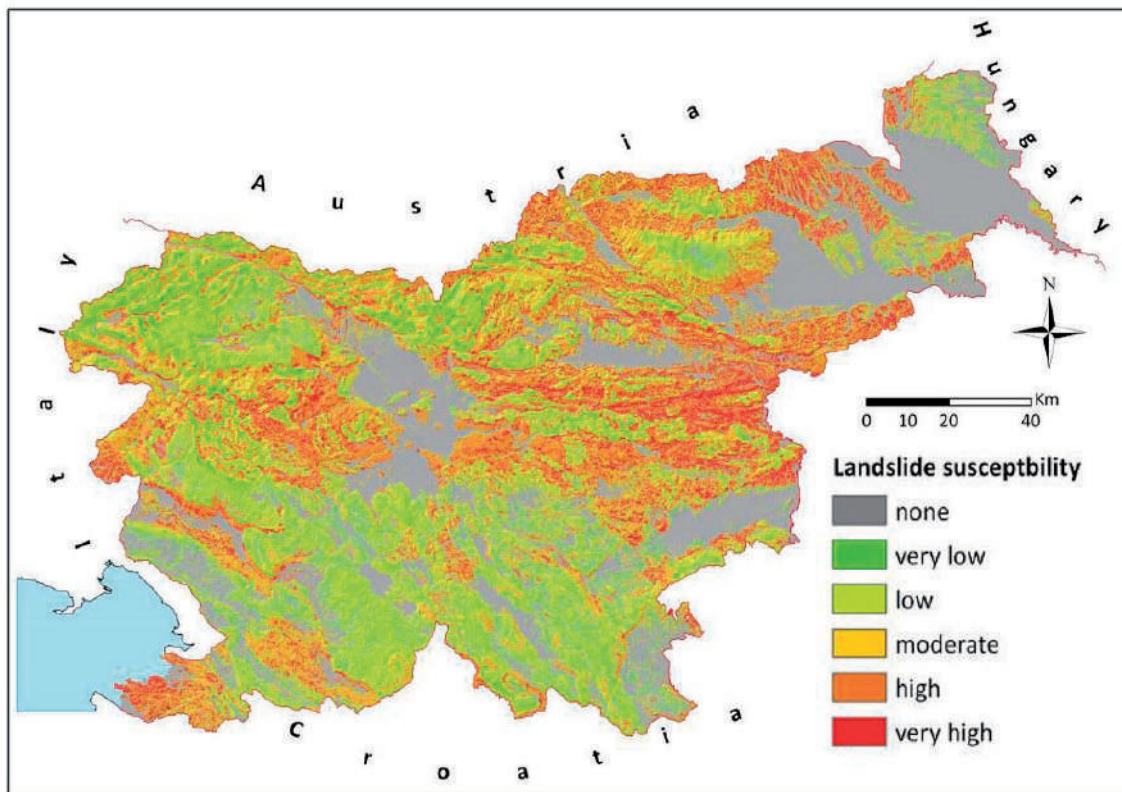


Figure 5 Landslide susceptibility map of Slovenia (Komac 2012).

statistical analyses (χ^2) to analyze the landslide occurrence in relation to the spatio-temporal precondition factors (lithology, slope inclination, slope curvature, slope aspect, distance to geological boundaries, distance to structural elements, distance to surface waters, flowlength, and landcover type). The analyses were conducted using GIS in raster format with the 25x25 m pixel size. The results of the analyses were later used for the development of a weighted linear susceptibility model where more than 156,000 automatically calculated models with random weight combinations were derived. The landslide testing subset (33% of landslides) and representative areas with no landslides were used for the validation of all models developed. The results showed that relevant precondition factors for landslide occurrence are (with their weight in a linear model): lithology (0.33), slope inclination (0.23), land-cover type (0.27), slope curvature (0.08), distance to structural elements (0.05), and slope aspect (0.05).

Roughly 8% of Slovenia is extremely susceptible and consequentially 8% of its population is exposed to potential hazards posed by landsliding. 11% of the population lives in the areas of high landslide susceptibility that spread over 16% of Slovenia. In the areas of moderate landslide susceptibility (10%) lives 5.7% of Slovenia's inhabitants. 6.7% of the population lives in the areas of low landslide susceptibility (20%), 3.7% of the population lives in the areas of insignificant (very low) landslide susceptibility (18%), and the rest of the

population (65%) lives in the areas where landslide occurrence possibility could be neglected (28%).

Landslide hazard forecast model development

The system of modelling a landslide hazard probability through time (landslide hazard forecast) will be designed as an integration of static and dynamic input data. In this regard dynamic input data are represented by a real-time rainfall data that will be provided from the ALADIN model, acquired automatically from the server of Environmental Agency of Republic of Slovenia, transferred to local server, and transformed from ordinary text format into GIS raster format to be prepared for the spatial calculations and modelling part of the system. Static input data are represented by a landslide susceptibility map and by the threshold information related to each location, both will be implemented through separate modules (Fig. 2). Spatial calculations and modelling will be performed on a GIS platform included within the GIS dynamic forecasting modelling module. A landslide hazard forecast model will predict hazards at the level of detail of 4.4 square km as this is the resolution of the rainfall forecast model ALADIN. Updating itself each day (ideally several times per day), the tool will indicate the potential for landslide hazards over the proceeding 24-hour window in a form of five descriptive (instead of numerical representation that

is confusing for non-experts) classes: “very low,” “low,” “moderate,” “high,” and “very high.” Conceptual model of the modelling of landslide probability through time is depicted in Fig. 6. Fig. 7 shows the sample of potential landslide hazard forecast display panel as will be visualized through the website.

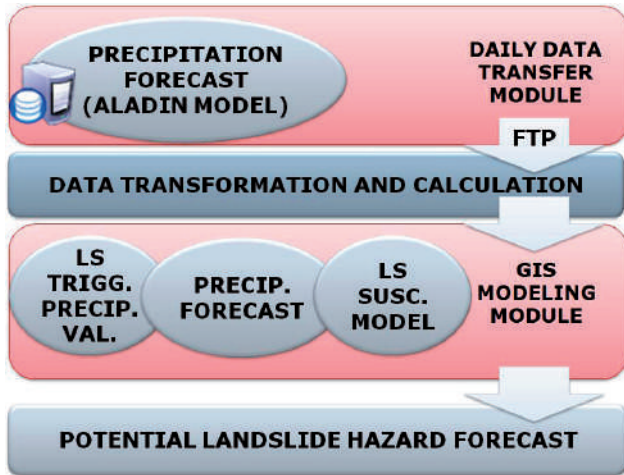


Figure 6 Conceptual model of the operational phase of the modelling landslide probability through time (potential landslide hazard forecast).

Conclusions

In this paper, we presented a design for the system for the modelling a landslide probability through time in Slovenia - MASPREM. A system for landslide hazard forecast will be based on the real-time rainfall data, rainfall threshold values and landslide susceptibility map. The importance of their inclusion in the system was highlighted.

The development of a real-time early warning system landslide hazards that follows for will certainly be beneficial to various stake-holders including the local authorities, relevant government agencies and the public in most exposed and highlighted areas. The developed early warning system, which will be consisted of the static and dynamic input data, data transfer module, landslide hazard forecast calculation module and visualization web module, is hoped to achieve its purpose in providing early warning and alerting the authorities as well as the public in general of the potential high landslide hazard areas within the affected areas once there are incidences of heavy rainfall.

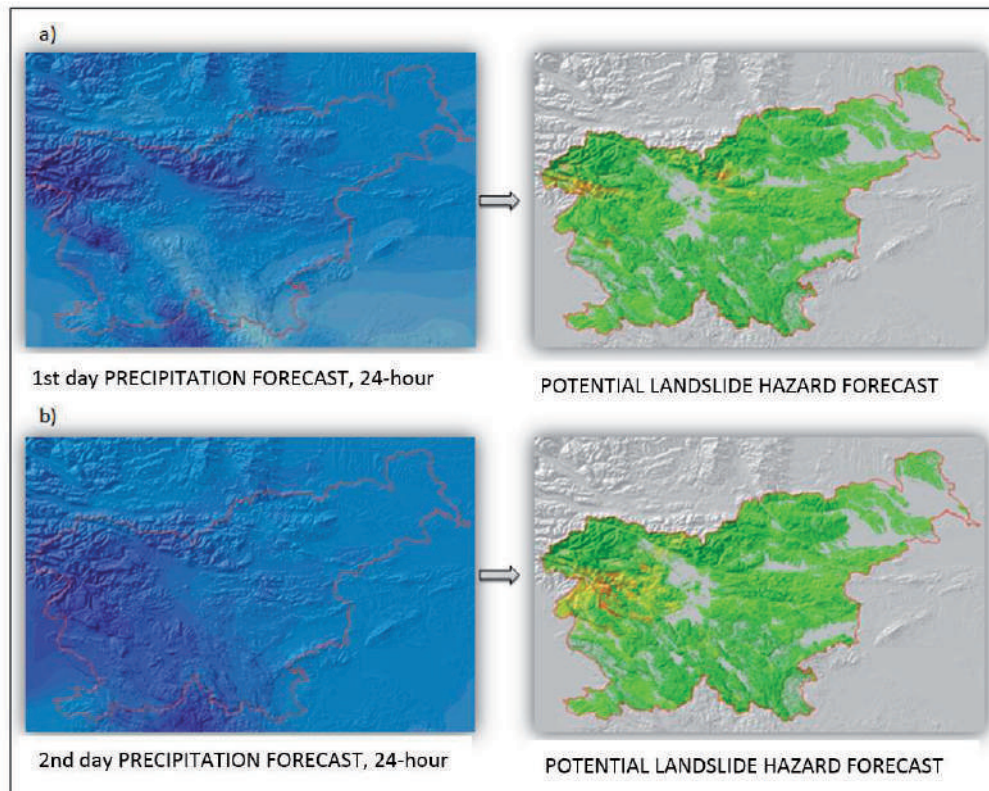


Figure 7 Example of real-time potential landslide hazard forecast display panel as will be visualized through the website. Based on 24-hour rainfall forecast, landslide triggering precipitation values and landslide susceptibility map the potential landslide hazard forecast will be visualized on the website. Example a) shows potential landslide hazard forecast based on the first day of 24-hour rainfall forecast, and b) potential landslide hazard forecast for the next day. Yellow and orange colors indicate areas that are more exposed to landslides occurrence than areas marked with green color.

References

- Aleotti P (2004) A warning system for rainfall-induced shallow failures. *Eng Geol.* 73: 247-265.
- ARSO Ministry for Environment and Spatial Planning, Environmental Agency of the Republic of Slovenia (2012) National Meteorological Service of Slovenia. URL: <http://meteo.arso.gov.si/met/en/app/webmet/> [Last accessed: 20 June 2012].
- Bubnová R G, Hello P, Béenard P, Geleyn J F (1995) Integration of the fully elastic equations cast in the hydrostatic pressure terrain following coordinate in the framework of the ALADIN NWP system. *Mon. Wea. Rev.*, 123: 515–535.
- Crozier M J, Eyles R J (1980) Assessing the probability of rapid mass movement. In: *Proceedings of 3rd Australia-New Zealand Conference on Geomechanics* (Technical Groups, eds). Wellington: New Zealand Institution of Engineers, 6: 247–251.
- Crozier M J (1999) Prediction of rainfall-triggered landslides: a test of the antecedent water status model. *Earth Surf Proc Land.* 24: 825–833.
- Glade T, Crozier M J, Smith P (2000) Applying probability determination to refine landslide-triggering rainfall thresholds using an empirical “Antecedent Daily Rainfall Model”. *Pure Appl Geophys.* 157(6/8): 1059–1079. doi:10.1007/s000240050017
- Jemec Auflič M, Komac M (2011) Rainfall patterns for shallow landsliding in perialpine Slovenia. *Nat. Hazards.* doi: 10.1007/s11069-011-9882-9
- Kim S K, Hong W P, Kim Y M (1992) Prediction of rainfall-triggered landslides in Korea. In: Bell DH (Ed.), *Landslides. Proc. of the 6th Int. Symp. on Landslides*, Christchurch, Balkema, Rotterdam. 2: 989–994.
- Komac M, Ribičič M (2006) Landslide susceptibility map of Slovenia at scale 1:250.000. *Geologija.* 49(2): 295–309.
- Komac M (2012) Regional landslide susceptibility model using the Monte Carlo approach - the case of Slovenia. *Geol. Q.* 56(1): 41-54.
- Mercogliano P, Schiano P, Picarelli L, Olivares L, Catani F, Tofani V, Segoni S, Rossi G (2010) Short term weather forecasting for shallow landslide prediction. *Int. Conf. Mountain Risks: Bringing Science to Society*, Malet JP, Glade T, Casagli N (eds.), Firenze, pp. 525-530.
- Pristov N, Cedilnik J, Jerman J, Strajnar B (2012) Preparation of numerical meteorological forecast ALADIN-SI. *Vetrnica*, pp. 17-23. (In Slovenian)
- Reichenbach P, Cardinali M, De Vita P, Guzzetti F (1998) Regional hydrological thresholds for landslides and floods in the Tiber River Basin (Central Italy). *Environ Geol.* 35(2–3): 146–159.
- Terlien M T J (1998) The determination of statistical and deterministic hydrological landslide-triggering thresholds. *Environ Geol.* 35(2-3): 124–130.
- Zezere J L, Trigo R M, Trig I F (2005) Shallow and deep landslides induced by rainfall in the Lisbon region (Portugal): assessment of relationships with the North Atlantic Oscillation. *Natural Hazards and Earth System Sciences.* 5: 331–344.
- White I D, Mottershead D N, Harrison J (1996) *Environmental Systems*, 2nd edition. Chapman & Hall, London, 616p.
- Wilson R C (2000) Climatic variations in rainfall thresholds for debris-flows activity. In: *Proceedings 1st Plinius Conference on Mediterranean Storms* (Claps P, Siccardi F, eds). Maratea, pp. 415–424.
- EM-DAT (2009) The OFDA/CRED International Disaster Database. URL: <http://www.emdat.be/advanced-search>. [Last accessed: 3 September 2013].

On Perspectives of Semi-Automated Landslide Assessment

Miloš Marjanović^(1,2), Snežana Zečević⁽¹⁾, Irena Basarić⁽¹⁾

1) University of Belgrade, Faculty of Mining and Geology, Belgrade, Serbia, Đušina 7, +381 113 219 224

2) Palacky University Olomouc, Faculty of Science, Olomouc, Czech Republic

Abstract This paper discusses the perspectives of using the state-of-the-art landslide assessment techniques for estimating and predicting spatial distribution of landslides. Driven by the experiences gathered in several case studies, the paper sublimates drawbacks and benefits from using the advanced modelling techniques for predicting landslides or assessing the landslide susceptibility in a semi-automated fashion. This automation particularly entails Machine Learning-based techniques, and for the purpose of this short report on our experiences, the Support Vector Machines technique has been presented. Some particular issues of Machine Learning-based classification tasks, such as sampling strategy, optimization problems, objective model evaluation etc., have been discussed hereinafter. Two separate model types have been distinguished: (i) interpretative and (ii) predictive models. They have both been implemented in three different case studies including: Fruška Gora Mountain (Serbia), Starča basin (Croatia) and Halenkovice area (Czech Republic), all having slightly or fundamentally different landslide typology and ground/environmental conditions. Type (ii) models have been particularly interesting and challenging, and their applicability as auxiliary or preliminary mapping outputs has been discussed. Some of these results have been published as interactive web maps by implementing elements of Web Mapping 2.0 concepts through an open-source R package “plotGoogleMaps”.

Keywords landslide assessment, SVM, model evaluation, web mapping.

Introduction

Landslide assessment has been in a momentum in the past decade. Numerous methodological approaches have been at stake, ranging from heuristic to statistic and deterministic methods. Particular attention has been driven to a group of Machine Learning (ML) techniques which produce spatially predictive models in a semi-automated fashion, i.e. with limited intervention of the field expert. The concept of ML turns out to be very applicable in various spatial prediction scenarios, where landslide assessment is no exception.

ML is a sub-discipline of Computer Science which involves a host of techniques. These can solve various

classification or regression problems through the learning process assisted by the expert – a concept known as supervised learning (Mitchel 1997). In the landslide assessment framework, a supervised classification problem (task) is of relevance. It first implies the training stage, in which a ML algorithm is being introduced with an expert’s interpretation of the landslide classes over a specified portion of the total area, called the training area. Training is then supervised by the testing stage, in which the trained algorithm automatically extrapolates the interpretation (learned in the training stage) to the rest of the area, called the testing area. The ML algorithm thus predicts landslide classes for two spatially related areas (adjacent or interspersed) that are necessarily similar enough in engineering-geological terms, and have a surplus of landslides within (in order to yield appropriately sized statistical sample).

Several ML techniques have been proven successful in landslide assessment framework, including Artificial Neural Networks, Logistic Regression, Decision Trees and Support Vector Machines (Brenning 2005, Yilmaz 2009). Based on the results of numerous researchers, predictable power of such family of algorithms can be speculated. Although the reference overlay (a landslide map or an inventory) usually exists for the testing area, just as it does for the training area, the predictability of the algorithm is being put to test, for the hypothetical case of absence of any landslide reference for the testing area. In current practice of landslide assessment via ML algorithms it has been shown that plausible predictions with the accuracies of over 80%, sometimes even 90% are achievable. Thus, the ML implementation opens further possibilities for applications over terrains which hypothetically do not have a landslide inventory overlay for the testing area or at least not in a suitable scale. One also needs to be aware of the side effects of the ML approach and to be cautious where and when the approach is applicable.

To support and contribute to the above statements and speculations, the authors have been experimenting on several case studies in last couple of years including: NW slopes of Fruška Gora Mountain in Serbia, Starča Basin in Croatia and Halenkovice area in Czech Republic. Most of the mentioned algorithms (Logistic Regression, Decision Trees and Support Vector Machines) have been implemented in each case study, and according to the results, the Support Vector Machines can be singled out

as the most preferable of the techniques, since it performs best in all three case studies. However, the evaluation remains an unsolved problem despite the numerous available statistical measures (Frattini et al. 2010), because the nature of these models can be predictive, meaning that it does not necessarily reflects the present-state of the landslide distribution but perhaps some future time domain.

Materials and methods

Input dataset

It is important to mention that no matter how sophisticated the modelling technique is, it cannot give good results if the input data are not adequate. The latter regards the adequacy of data acquisition methodology, scale, type of the phenomena and of course, the data availability. Furthermore, every attempt of landslide assessment requires a detailed landside inventory (which is actually a crucial piece of information and designates further quality of the analysis) and various thematic data that resemble ground and environmental conditions of the study area (conditioning factors). In the landslide susceptibility framework, it is sufficient to gather such data for one temporal domain (present-state or some earlier states), while hazard and risk frameworks require time-series (van Westen 2004).

There is a common practice in using morphometric, geological and environmental conditioning factors in landslide assessment. Such trend has been followed throughout all three researches in all three study areas. The details on the choice of inputs, their formats, as well as the related preprocessing and feature selection performed in all three cases are given in greater detail in respective publications (Marjanović et al. 2011a,b, Marjanović 2012). From our experiences it could be inferred that a standard input dataset could be comprised of following:

- morphometric data: elevation, slope aspect, slope angle, slope length, slope curvature, topographic wetness index, proximity to drainage network,
- geological data: geological units, proximity to geological boundaries, proximity to faults,
- environmental data: land use/cover, spectral indices (NDVI),
- synthetic data: various statistical derives of given conditioning factors, principal components etc.
- landslide inventory (with sufficient level of detail, gathered by a combination of field and remote sensing techniques, with defined activity).

Scale is another important issue, since the level of detail affects directly the sample sizes for ML techniques, evaluation methods, even visualisation of results. It should be inversly proportional to the study area size, but this also depends on the availability of data. For instance, for Fruška Gora study area, the 30 m resolution of (raster)

inputs was sufficient, while for the Starča and Halenkovice areas it was upscaled to 10 m resolution.

Modelling method

Given the required inputs in appropriate form the ML algorithm can be readily applied. Conditioning factor values have simply become additional coordinates x_i which are defined per each pixel \mathbf{x} , ($\mathbf{x}=[x_1, \dots, x_n]$) in the raster representation of the area. As indicated before, the SVM algorithm has been chosen for performing the supervised classification task, over such coordinate set (represented by the above listed conditioning factors). Herein, a very brief description of the SVM technique will be given, while very detailed explanation, which particularly follows the landslide susceptibility framework are given elsewhere (Marjanović et al. 2011a).

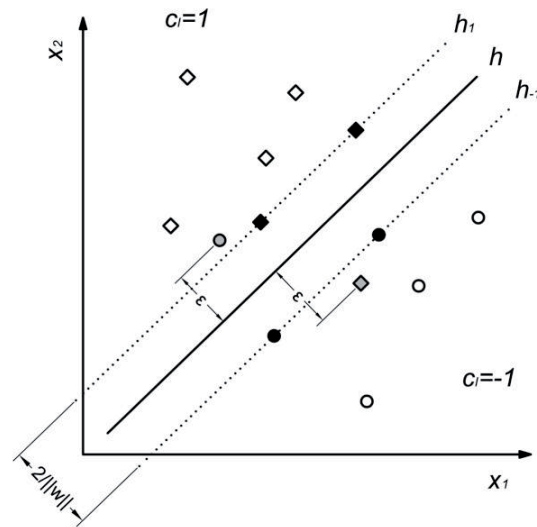


Figure 1 Scheme of the basic variant of SVM classification. Values $x_{1,2}$ represent a random pair of conditioning factors (e.g. slope vs. aspect), c_i represent landslide classes (e.g. landslide=circle and non-landslide=square), ϵ present slack (misclassification error which figures in misclassification penalty C), while \mathbf{w} represents a weight factor of a given margin $M=2/||\mathbf{w}||$ that needs to be maximized. Plane h represents optimal separation (hyper) plane, and instances on M (solid circles/squares) represent Support Vectors.

The SVM is a sub-branch of the Neural Network classifiers (Kanevski et al. 2009), which uses a basic linear binary case of classification, based on so-called quadratic programming problem. Therein a separation plane h between the landslide and non-landslide instances can be fitted in an optimal fashion (Fig. 1), i.e. with the maximal margin of the separation. Thus h becomes a function $f(x_i)=c_j$ which successfully assigns appropriate landslide class c_i to instances \mathbf{x} (in the basic variant $l=2$). However, SVM can deal with the general (non-linear and multi-class) cases. Non-linearity can be handled by introducing the misclassification penalty C and using kernel functions. These functions can transform the original feature-space

(n -dimensional space which has conditioning factors as coordinates) to a higher level feature space, where instances again become linearly separable. The basic variant of SVM is then applied and results are retrieved back to the original space. In addition, SVM can work only with Support Vectors (margin extremes) to obtain the same results as if it has been using all available instances, hypothetically speaking (Vapnik 1995). Multi-class task can be handled by performing a sequence of l one-versus-all or $l(l-1)/2$ one-versus-one binary classification cases, where each of l classes has been classified separately (Belousov et al. 2002).

Evaluation metrics

Standard evaluation metrics for this type of modelling (Frattini et al. 2010) has been proposed, where the available landslide inventories have been used as a reference for modelled high susceptibility classes (model type (i)) or predicted landslides (model type (ii)). It included common accuracy, but also some more advanced parameters that treat the false positives and false negatives errors more cautiously, such as kappa statistics and Receiver Operating Characteristic (ROC) curves, i.e. Area under ROC curve or AUC (Fawcett, 2006). However, the evaluation of the predictive models might not be as straightforward as it first seems. There are several aspects that need to be considered. Firstly, the available reference depicts the present or past states of the spatial landslide distribution, and hence, the evaluation cannot take into account the predictive nature of the model. It would actually penalize the model even though it might not be entirely wrong for some future time domain. Secondly, the population of the landslide class is usually 10-20% of the total, which makes an unbalanced evaluation environment, therefore unjust for penalization in the equal way as the non-landslide class. Finally, there is a conceptual difference between false positive and false negative errors in landslide assessment framework, since the latter should be penalized in the model evaluation much harder than the former (it is much more harmful to make errors in declaring some area safe than vice versa).

Results and discussion

As indicated before, two types of ML-based models have been featured. Type (i) is defined as interpretative model and type (ii) as a predictive model. The major difference lies in the sampling strategy, i.e. in selection of training-testing splits. In type (i) the splits have been separated by random interspersing throughout the entire study area, while in (ii) the splits represent meaningful spatial separations. Hence (i) interprets the landslide susceptibility over the area while (ii) extrapolates the prediction to entirely different (spatially independent) area. Furthermore, predictive models are optimized representation of a single classification output (since

SVM stands for a discrete classifier) and model landslide vs. non-landslide instances, i.e. ones and zeros, while type (i) models have been blended from the iterations during the optimization procedure. These iterative models slightly vary in spatial domain, which means that the model output values can be given in a 0-1 range (SVM is at this point artificially made generative classifier). Thus, type (i) practically resembles the spatial probability of the target class, which is in terms of landslide assessment frameworks defined as landslide susceptibility. Regardless to the model type, the optimization took place over the training area only, by 10-fold cross-validation, where at first nine combinations of C , γ pairs have been tested ($C=1, 10, 100$ and $\gamma=0.1, 1, 10$). Afterwards, fine tuning of the parameters was undertaken.

Each of the case studies has been treated in described way and all three of the model pairs have been discussed hereinafter. For model type (i) the following notation scheme will be used: "case study abbreviation"(i), for instance FG(i) for Fruška Gora, SB(i) for Starča basin, and HA(i) for Halenkovice area. Accordingly, the model type (ii), will be abbreviated as follows: FG(ii), SB(ii), and HA(ii).

1st case study: Fruška Gora Mountain (Serbia)

Both FG models have been generated by 30 m resolution inputs of an area of approximately 100 km², which entailed more than 100.000 instances (pixels), of which some 10% belonged to the landslide class. In statistical terms this is not a very convenient situation, and the disproportion is expected to be very influential. Surprisingly both FG models responded well (model of type (i) most probably because it was balanced, while for the model type (ii) it is still to speculate, but most likely the good prognosis is due to the optimal scale and landslide instances population) and their evaluation parameters seem rather appealing (Tab. 1).

Table 1 Evaluation parameters of each model.

model	accuracy [%]	AUC	kappa index
FG(i)	94.90	0.90	0.43
FG(ii)	90.56	0.71	0.17
SB(i)	91.33	0.79	0.48
SB(ii)	76.49	0.54	0.21
HA(i)	89.09	0.69	0.40
HA(ii)	85.38	0.57	0.38

Both of the models have been fed by the inputs preprocessed in the same fashion. Nominal data (geological units, land cover etc.) have been binarized, and ordinal data (numeric values) normalized to 0-1 span, so that no bias or preference could originate from the data structure. Feature selection has been differently enrolled in each model. In FG(i) it preceded the optimization, so that statistically undesired conditioning factors have been left out. For FG(ii) the feature selection defined the weakest links, and the modelling has been

performed by leave-one-out procedure, wherein the lowest ranked conditioning factor has been removed prior to the next iteration, until the model performance converged to a constant value (i.e. before it started to decrease back). The optimization has been performed by 10-fold cross-validation, with slight differences.

FG(i) model has been split into the training-testing parts by randomly interspersed but balanced sampling, where the size of the training split varied from 5–15%. The optimization further unfolded by iterative generation of models, where number of iterations depended on the size of the training split. The optimal parameters for a Gauss kernel SVM variant have been presented by the parameter pair, $C=100$ and $\gamma=4$. These represent the misclassification penalty and the kernel dimension, respectively. Since each of the iterations has resulted in one variant of the model, the normalized and averaged result could represent the quantitative landslide susceptibility.

In FG (ii) model, no such strategy could have been administered, and the splits have been designed manually. Inspection and selection of the most suitable training-testing splits required a lot of caution, because all of the data inputs, especially nominal ones should have been equally present. Thus, we have tried to near the balanced training sample as much as possible. In turn, the training area, capturing approximately 33% of total area, has been defined (Fig. 2). The optimization then proceeded to 10-fold cross validation ending up with the same optimal $C=100$ and $\gamma=4$, and a single binary output model has been generated after leave-one-out iterative procedure over the input dataset. It has been mapped by using the “plotGoogleMap” (WebMapping 2.0-based) R package (Kilibarda and Bajat 2012). An interactive web map has been temporarily released at: <http://milosmarjanovic.pbworks.com/w/file/fetch/63738284/MyMapFruskaGora.htm>. It is apparent that the model

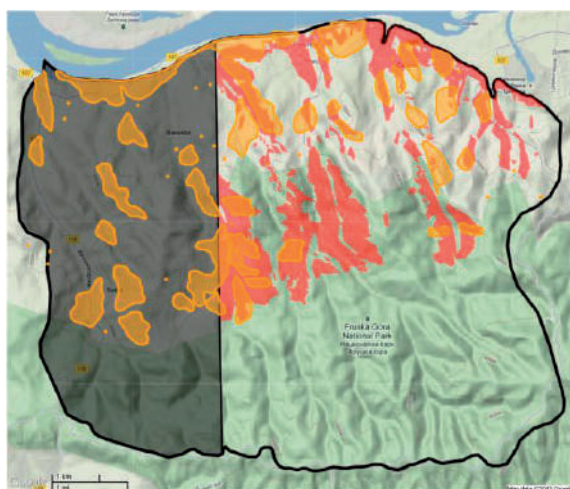


Figure 2 Model FG(ii). Shaded area represents the training split, orange polygons represent the landslides defined by the inventory, and red polygons represent the SVM-predicted landslides (source GoogleMaps).

has slight tendency of overestimation of landslides, but in general it delivers relatively accurate map in a semi-automated fashion.

2nd case study: Starča Basin (Croatia)

The spatial resolution has been upscaled to 10 m, but the area is much smaller (12 km²) leading to the similar number of instances (around 100000) with similarly unbalanced landslide class population as in the preceding case study.

The processing of the inputs as well as the optimization strategy has been completely analogous to the previous case. For SB(i) model $C=100$ and $\gamma=4$, also turned out to be optimal, while for the SB(ii) these equaled $C=10$ and $\gamma=10$. Also in SB(ii) the training split has been slightly bigger (40%). The result has not met the expectations. The performance parameters (Tab. 1) were considerably poorer, especially for (ii) variant, where underestimation of the landslide instances is apparent (Fig. 3). This model is overfitted to make false negative errors (it has learned too many weak relations between non-landslide class and conditioning factors). Otherwise, the visual trends of the proposed landslides are logical and semi-automated landslide mapping is yet viable. The biggest problem toward more successful semi-automated mapping is certainly the class misbalance and disproportion. The results have been also visualized by “plotGoogleMap” script and released at: <http://milosmarjanovic.pbworks.com/w/file/fetch/63741247/MyMapStarca.htm>.

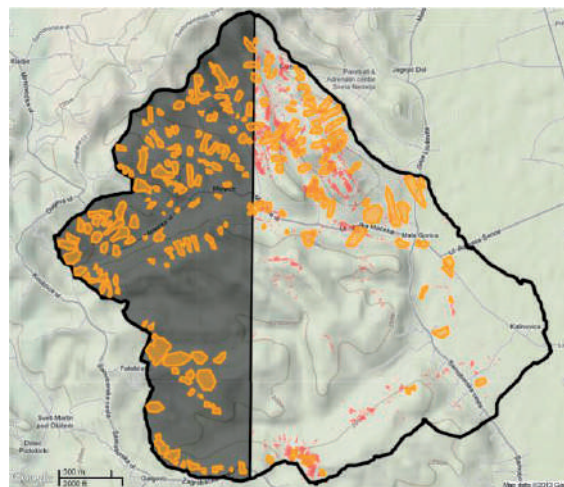


Figure 3 Model SB(ii). Shaded area represents the training split, orange polygons represent the landslides defined by the inventory, and red polygons represent the SVM-predicted landslides (source GoogleMaps).

3rd case study: Halenkovice area (Czech Republic)

The Halenkovice case study has been somewhat specific due to the geological conditions of the landslide occurrences. These are called landslides in flysch and turned out to be challenging in terms of conventional modelling and the general understanding of the process,

for that matter. Expectations of the model have not been raised very high, but some interesting results have been obtained. In addition, the study is a work in progress and further refinements could be appended to the present results.

The assembly and processing protocol of the input dataset has been once again analogue to the procedures adopted and described before. The area is this time around 60 km² and the adopted 10 m resolution has made around 500,000 instances. The proportion of the landslides still remains at around 10%. In model (ii) the training split size remains 40%, and the optimization protocol is exactly the same. The optimization parameters for both variants were: $C=50$ and $\gamma=1$.

Results of HA(i) show similar but slightly lower performance in comparison to the preceding models, though HA(ii) significantly drops in performance (Tab. 1), and parallels the one made in SB(ii). It likewise makes underestimation, i.e. false negative type of errors due to the overfit. Visual trends (Fig. 4) are yet logical but the output remains too scarce even after the majority filter postprocessing. Interactive web display is available at: <http://milosmarjanovic.pbworks.com/w/file/fetch/63739326/MyMapHalenkovice.htm>.



Figure 4 Model HA(ii). Shaded area represents the training split, orange polygons represent the landslides defined by the inventory, and red polygons represent the SVM-predicted landslides (source GoogleMaps).

Conclusion

Semi-automated landslide mapping, as well as quantitative analysis of the landslide susceptibility, has been scrutinized in several case studies. Impressions from these experiences have led to the several conclusions, guidelines and further notices.

The ML-based modelling can generate accurate susceptibility maps and relatively accurate landslide predictions. The major drawback of these predictions is the domination of false negative error due to the overfit-related underestimation of landslides. The problem lays

in unbalanced landslide class sizes in comparison to non-landslide size, which is easily avoided by sampling strategy in type (i) models, but turned unavoidable for type (ii) models. The applicability of both types of models as maps is perspective. They both can augment the landslide specialists in various situations. In the case of type (i) models, the planning and mitigation related to the landslides can benefit from its quantitative estimation of the landslide susceptibility. It is also a valuable input for eventual hazard or risk assessment attempts. The type (ii) models do not literally produce a landslide map in a semi-automated fashion, but rather produce a preliminary mapping product which is to be used as an auxiliary map that underpins the “suspicious” locations. It could then be included in an actual mapping project along with the conventional field methods, remote sensing, field investigation, laboratory and in-situ testing/sampling, logging, etc.

There is also room for improvement of results, primarily via advanced postprocessing, which could reduce the false positive errors significantly (by excluding logical errors). There is also room for redesigning the algorithm optimization, but it is most likely that the data (class balance) limits that possibility. More complex optimization would require even more time and computing capacity, while the method is already time and hardware-consuming.

Acknowledgments

This paper has been supported by the project of the Ministry of science and technological development of Republic of Serbia: “The application of GNSS and LiDAR technology in monitoring of the infrastructure and terrain stability” (TR 36009).

References

- Belousov A I, Verzakov S A, Von Frese J (2002) Applicational aspects of support vector machines. *Journal of Chemometrics*. 16: 482-489.
- Brenning A (2005) Spatial prediction models for landslide hazards: review, comparison and evaluation. *Natural Hazards and Earth System Sciences*. 5: 853-862.
- Fawcett T (2006) An introduction to ROC analysis. *Pattern Recognition Letters*. 27: 861-874.
- Frattoni P, Crosta G, Carrara A (2010) Techniques for evaluating performance of landslide susceptibility models. *Engineering Geology*. 111: 62-72.
- Kanevski M, Pozdnoukhov A, Timonin V (2009) *Machine Learning for Spatial Environmental Data: Theory, Applications and Software*. EPFL Press, Lausanne, (ISBN 9780849382376). 368p.
- Kilibarda M, Bajat B (2012) plotGoogleMaps: The R-based web-mapping tool for thematic spatial data. *Geomatica*. 66(1): 37-49.
- Marjanović M (2012) Advanced landslide assessment of Halenkovice experimental site. *Proceedings of 1st InDog conference October 29 - November 1 2012. Olomouc, Czech Republic*. pp. 38-41.
- Marjanović M, Kovačević M, Bajat B, Voženilek V (2011a) Landslide susceptibility assessment using SVM machine learning algorithm. *Engineering Geology*. 123: 225-234.

- Marjanović M, Kovačević M, Bajat B, Mihalić S, Abolmasov B (2011b) Landslide Assessment Of The Starča Basin (Croatia) Using Machine Learning Algorithms. *Acta Geotechnica Slovenica*. 8(2): 45-55.
- Mitchell T M (1997) *Machine Learning*. McGraw Hill, New York, (ISBN 0070428077). 414p.
- van Westen C J (2004) Geo-information tools for landslide risk assessment: an overview of recent developments. *Proceedings of 9th international symposium on landslides*, June 28 - July 2 2004. Rio de Janeiro, Brazil. pp. 39-56.
- Vapnik V N (1995) *The Nature of Statistical Learning Theory*. Springer, New York, (9781441931603). 316 p.
- Yilmaz I (2009) Comparison of landslide susceptibility mapping methodologies for Koyulhisar, Turkey: conditional probability, logistic regression, artificial neural networks, and support vector machine. *Environmental Earth*. 6(4): 821–836.

Exposure of Inhabitants, Buildings and Different Types of Infrastructure to Potential Landslides in Case of Selected Municipalities in Slovenia

Tina Peternel, Mateja Jemec Auflič, Marko Komac, Jasna Šinigoj, Matija Krivic

Geological Survey of Slovenia, Ljubljana, Slovenia, Dimičeva 14, +386 1 2809 700

Abstract For the five selected Slovenian municipalities exposure maps of inhabitants, buildings and different types of infrastructure to potential landslides were produced in the frame of the project Masprem “Early warning system for potential landslide probability” (Komac et al. 2012). Exposure maps were elaborated based on synthesis of analysis of event-based landslide inventory and field investigations and were developed for the municipalities Bovec, Laško, Slovenj Gradec, Trbovlje and Železniki. Here the term “exposure” should be understood as a term hazard, but without inclusion of the economic loss. Thus, the exposure is the probability that observed objects are located in the hazardous zone. Due to the lack of data that originates from the incomplete landslide database (e.g. frequency of occurrence and magnitude of landslides) the information about exposure of inhabitants, buildings and different types of infrastructure are referred only to the probability of landslide occurrences in a certain area. Exposure of inhabitants, buildings and different types of infrastructure to potential landslides were derived with a cross-tabulation approach using the susceptibility map at scale of 1:25,000 and map of distribution of inhabitants, buildings and different types of infrastructure. All the analyses were conducted in the GIS using ArcGIS software tools. The levels of exposure were classified/ranked into six classes. Level 1 represented areas with negligible exposure to potential landslides and level 6 represented areas with the highest level of exposure to potential landslides. Exposure maps represent areas in the selected municipalities where inhabitants, buildings and different types of infrastructure are more or less exposed to potential landslides and may provide a very good basis for further determination of risk assessments and consequently risk management.

Keywords exposure, exposure maps, Masprem, inhabitants, buildings, different types of infrastructure, potential landslide, Bovec, Laško, Slovenj Gradec, Trbovlje, Železniki

Introduction

The aim of the project Masprem is to develop an early warning system for potential landslide occurrence. One of the project’s main goals was also to make the exposure assessment of the socio-economic elements to potential landslides.

For the study area five municipalities in Slovenia were selected. For this purpose the analytical approach with the method of cross-tabulation was chosen. The susceptibility map at the scale of 1:25,000 served as a basis for the exposure assessment. The analyses were conducted using GIS in raster format with the 5×5 m pixel size. The data of socio-economic elements (inhabitants, buildings and different types of infrastructure) were obtained from The Surveying and Mapping Authority of Republic of Slovenia (Ministry of Infrastructure and Spatial Planning).

Six levels of exposure were defined, ranging from negligible to very high exposure to potential landslides.

Study area

The exposure assessment to potential landslides was developed for the five municipalities (Fig. 1), which were selected in cooperation with Ministry of Defense (Administration for Civil Protect and Disaster Relief).

The first examined municipality Bovec is located in north-western Slovenia in the Soča Valley, close to border with Italy. Municipality Bovec covers an area around 367 km² and has 3,213 inhabitants (The Surveying and Mapping Authority of Republic of Slovenia 2005). The municipality has a well-developed tourist industry and two main road connections between cities Predel – Gorica and between regions Posočje – Carniola. The area of Bovec is characterized by dominantly limestone and dolomites.

The second selected municipality Laško is located in lower Styria in eastern Slovenia. Laško covers a total area of 197 km² and has a population of 13,526 people (The Surveying and Mapping Authority of Republic of

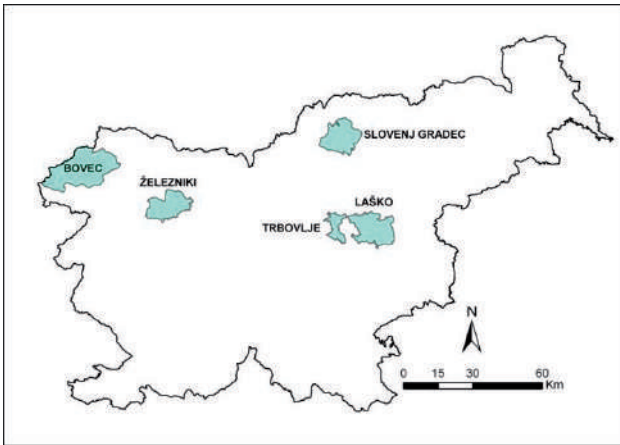


Figure 1 Study area – location map of selected municipalities.

Slovenia 2005). The municipality has a well-developed industry and an important traffic position between cities Celje – Zidani most. Area is composed mainly of sedimentary rocks (marl, sandstone, limestone, etc.), which are folded in Posavske folds.

Municipality Slovenj Gradec is located in Mislinja Valley in Northern Slovenia. The area of Slovenj Gradec is 174 km² and has a population of 16,893 inhabitants. Slovenj Gradec is the administrative and culture centre of the Carinthian region, with important traffic position and tourism industry. The area of municipality is extensively covered with metamorphic and sedimentary rocks.

The fourth selected municipality Trbovlje is located in the valley of the Sava River in the centre of Slovenia. Trbovlje covers an area 58 km² and has a population of 17,134 inhabitants (The Surveying and Mapping Authority of Republic of Slovenia, 2005). The municipality has

well-developed coal industry and an important road connection between cities Zagorje ob Savi – Hrastnik. The area is part of Posavske folds and is composed mainly of sedimentary rocks.

The last selected municipality Železniki is located in North-Western Slovenia in Carniola region. The area of Železniki is 165 km² and has 6,781 inhabitants. The municipality has well-developed electrical, metalwork and wood industries, and important traffic position between Posočje and Carniola region. Area is extensively covered with sedimentary rocks (marl, sandstone, conglomerate, dolomite, etc.).

Theoretical background of exposure assessment

Exposure is a probability that observed objects are located in the landslide hazardous zone. Exposure assessment could represent prior phase of making risk maps and risk assessments. In this case risk is defined as a probability that on specific susceptibility area, elements at risk could be affected (Mikoš et al. 2004).

To define landslide risk assessment for the ultimate goal of the landslide risk management, different approaches or methods can be used. Such methods allow better understanding of landslides and consequently allow more rational decisions within the process of the landslide risk assessment. With using the appropriate approaches we can prevent losses or reduce potential future consequences. Figure 2 represents one possible approach to the whole process of producing the landslide risk maps and the landslide risk management phase at a letter stage. The first stage of assessing landslide risk maps is based on the landslide susceptibility model.

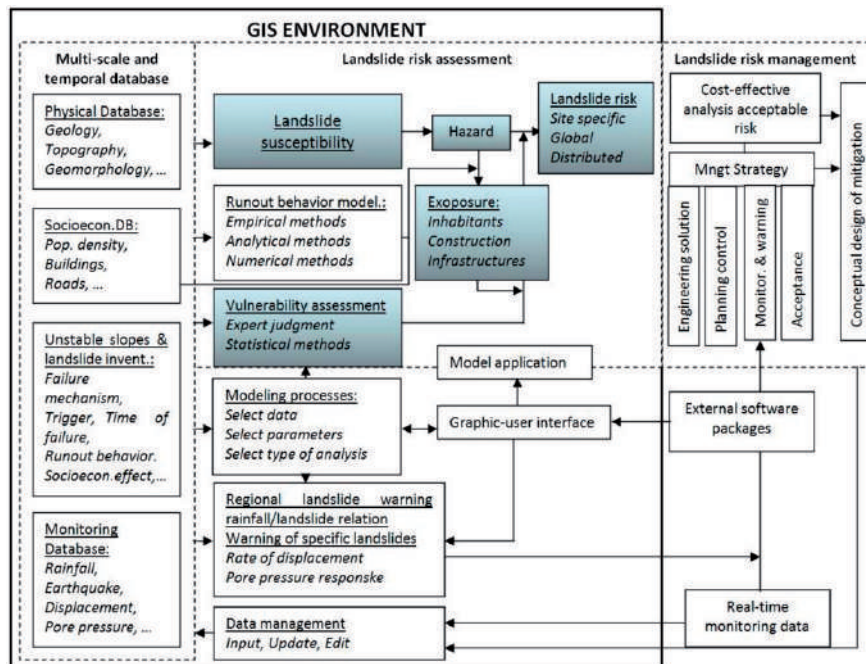


Figure 2 Conceptual model for landslide risk assessment and landslide risk management (Dai et al. 2002).

For the purpose of the model development, the susceptibility model has to be transformed into the hazard model. Hazard model is based on the likelihood of the landslide occurrence within a given period of temporal spatial probability, and is defined as the range and frequency of the historical event. Hazard model should include the location, volume (or areas), classification and velocity of the potential landslides and the probability of their occurrence within given period of time (Fell et al. 2008).

In case that hazard model includes elements of risk (like inhabitants, buildings and different types of infrastructure) and assessment of future extent of losses, it can be considered as an exposure model.

Vulnerability model represents the ratio between the cost of losses and the value of each element at risk. The result of the whole process is a risk model, which is based on exposure, hazard and vulnerability model.

Methods

In comparison to the already described theoretical model in the presented study exposure assessments are referred only to the probability of landslide occurrence in a certain area without inclusion of the calculations of economic loss. It is so due to the lack of data such as the frequency of the occurrences and the magnitude of landslides.

In the study case presented the exposure to potential landslides is based on the municipal landslide susceptibility maps at scale of 1:25,000 (Bavec et al., 2012)

and the socioeconomic data such as the number and the distribution of inhabitants, buildings, the length and the distribution of different types of infrastructure (Fig. 3). For the exposure analysis of different types of infrastructure the following types were included: railway, roads, electric system, sewage system, pipelines, thermal and water supply system.

All analyses were conducted in the GIS, using ArcGIS software, with a raster format of 5 x 5 m. Six levels of exposure were defined, ranging from a negligible to a very high exposure to potential landslides.

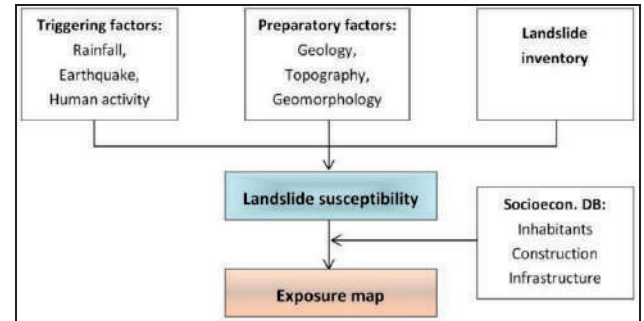


Figure 3 Schematic model for the exposure assessment to potential landslides.

Results and discussion

The results of the exposure analysis and exposure assessment of inhabitants, buildings and different types of infrastructure buildings to potential landslides are graphically presented in the Figures 4, 5 and 6.

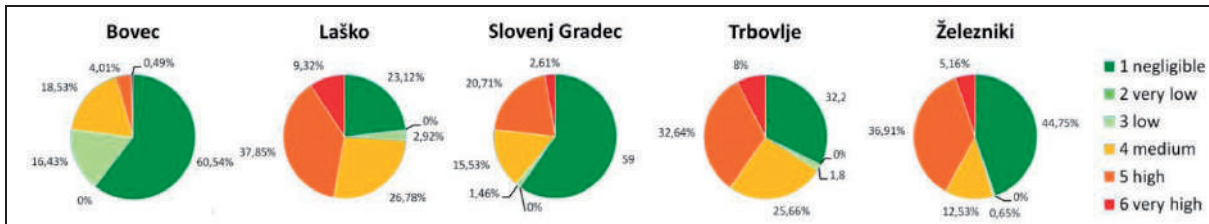


Figure 4 Exposure of inhabitants to potential landslides in the five municipalities.

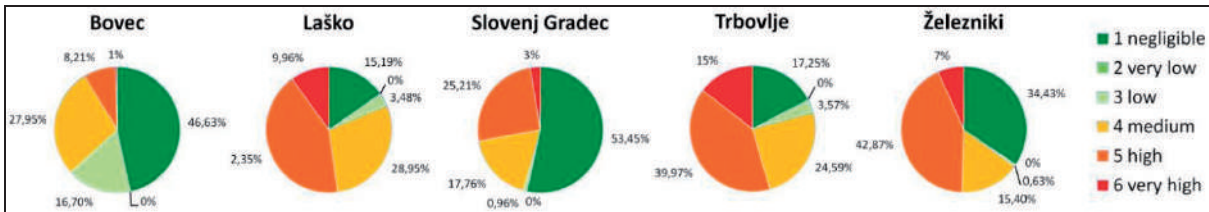


Figure 5 Exposure of buildings to potential landslides in the five municipalities.

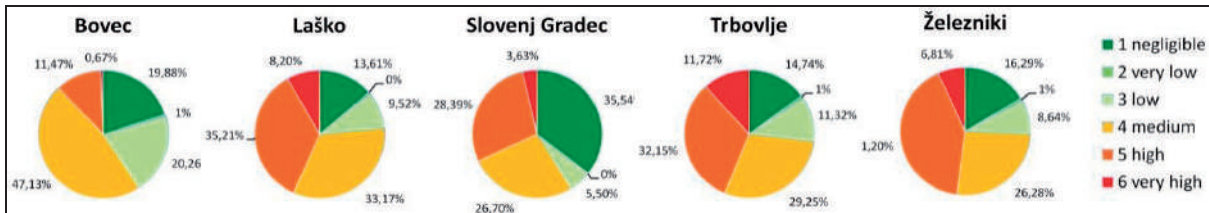


Figure 6 Exposure of different types of infrastructure to potential landslides in the five municipalities.

Figure 4 shows the exposure of inhabitants to potential landslides for the five municipalities. Inhabitants are the most exposed at municipalities Laško and Železniki, where the proportion of inhabitants with a high to a very high level of the exposure is 47.2 % (for the first municipality) and 42 % for second municipality.

The highest proportion of a negligible exposure of inhabitants was estimated for the municipalities Bovec (60.54%) and Slovenj Gradec (59%).

Exposure of buildings (different types of buildings) to potential landslides is presented in Figure 5. Analyses show that the highest exposure of buildings is in the municipalities Trbovlje (15%) and Laško (9.96%).

Buildings are least exposed in the municipalities Bovec and Slovenj Gradec, where the proportion of buildings with a negligible exposure is 53.45% for the municipality Slovenj Gradec and 46.63% for the municipality Bovec.

Results of the exposure analyses of different types of infrastructure (e.g railway, roads, electric system, sewage system, pipelines, thermal system and water supply system) to potential landslides are represented in Figure 6. From graphs it can be concluded that different types of infrastructure are the most exposed (very high level of exposure) in the municipalities Trbovlje (11.72%) and Železniki (6.81%).

The highest proportion of a negligible exposure of inhabitants was estimated for municipality Slovenj Gradec (35.54%).

Conclusions

The results of analyses are exposure maps of inhabitants, buildings and different types of infrastructure to potential landslides in case of the five Slovenian municipalities and represent simplified risk assessment without inclusion of the economic loss. Exposure maps to potential landslides represent basics for the landslide risk assessment and latter for the management of the landslide risk. Exposure maps should be used as guidance in the regional and local spatial planning process and

could represent preliminary warning for the local authorities and the civil population.

Exposure maps are not intended for the direct use in the spatial planning process, as they only represent the current status of potential damages, and lack the information on the spatial distribution of the hazardous zones.

Acknowledgments

The authors would like to thank Ministry for the Defense (Administration for Civil Protect and Disaster Relief) which enabled research through the financing project Masprem.

References

- Bavec M, Čarman M, Durjava D, Jež J, Krivic M, Kumelj Š, Požar M, Komac M, Šinigoj J, Rižnar I, Jurkovšek B, Trajanova M, Poljak M, Celarc B, Demšar M, Milanič B, Mahne M, Otrin J, Čertalič S, Štih J, Hrvatin M (2012) Creating spatial database and web-based information systems-related geologic hazards due processes of slope movement, flooding, erosion charts and maps of avalanches, Pilot Project, Geological Survey of Slovenia Ljubljana (ISBN_P-II-30d/a-1/28). 40p.
- Dai F C, Lee C F, Ngai Y Y (2002) Landslide risk assessment and management: an overview. *Engineering Geology*. 64: 65-87.
- Fell R, Corominas J, Bonnard C, Cascini L, Leroi E, Savageb W Z (2008) Guidelines for landslide susceptibility, hazard and risk zoning for land use planning. *Engineering Geology*. 102: 85-98.
- Komac M, Ribičič M (2006) Landslide susceptibility map of Slovenia at scale 1:250 000. *Geologija*. 49(2): 295-309.
- Komac M, Šinigoj J, Jemec Auflič M, Peternel T, Krivic M, Požar M, Podboj M, Bavec M, Jež J, Čarman M, Otrin J (2012) Early warning system in an emergency landslide triggering – MASPREM – Report at the third milestone. Geological Survey of Slovenia Ljubljana (ISBN_R-II-30d/c-5/6-d). 166p.
- Mikoš M, Batistič P, Đurovič B, Humar N, Janža M, Komac M, Petje U, Ribičič M, Vilfan M (2004) The methodology for identifying hazardous areas and classifying land in classes of landslide hazards – Final Report. University of Ljubljana (ISBN_KSH d-78, Ljubljana). 165p.
- Ministry of Infrastructure and Spatial Planning - The Surveying and Mapping Authority of Republic Slovenia (2005). The cadastre of public infrastructure. The Surveying and Mapping Authority of Republic Slovenia Ljubljana.

The Preliminary Damage Assessment of Properties Based on Massive Appraisal Maps

Branislav Bajat, Milan Kilibarda, Milutin Pejović, Mileva Samardžić Petrović

University of Belgrade, Faculty of Civil Engineering, Department of Geodesy and Geoinformatics, 11000 Belgrade, Serbia, Bulevar kralja Aleksandra 73

Abstract This paper examines a feasible solution for the preliminary assessment of potential damage costs for dwellings in areas prone to the risk of landslides and subsidence. The assessment uses different spatial layers as input parameters and concentrates on the implementation of different spatial databases that are already available as public data. These databases include land-use suitability (LUS), building height typology (BHT) databases and massive appraisal maps that are specifically developed for the real estate market. Massive appraisal maps were produced based on the spatial-econometric hedonic dwelling price model that was developed previously for the Belgrade metropolitan area using cross-sectional and georeferenced transaction data.

The massive appraisal maps were used in combination with LUS and BHT databases to obtain a spatial layer that would indicate potential sites vulnerable to landslides and subsidence with an estimate of damage costs included.

In this study we go one step further by attempting to enhance all the advantages of GIS utilization in risk and mitigation management through the use of the Web 2.0 concept. Web Mapping 2.0 is an important part of the Web 2.0 concept and facilitates the integration and visualization of different geographic information on base maps (such as Google Maps/Earth, Virtual Earth, or Yahoo Map).

Keywords hedonic price modelling, land use suitability, web mapping

Introduction

GIS technology provides suitable tools to support planning and regulation of emergency management activities. These tools have led to the development of risk information systems that can be used to analyze risk and evaluate the consequences of decisions made that mitigate or reduce risk (van Westen 2004). Based on available spatial data, GIS models can be used to combine

a set of input maps or factors to produce an output map that specifies levels of susceptibility and hazard (Fell et al. 2008). Damages caused by landslides and subsidence represent significant risks to buildings and dwelling objects (Fell 1994) and providing estimates of potential damage could be of benefit to economic loss assessment and long term mitigation management.

The contribution of this work to the field is to point out a simple GIS solution that can generate a massive appraisal data layer by integrating the spatial econometric hedonic model (Anselin 1988) with supplementary data layers. The obtained appraisal map could be of interest not only for appraisers, real-estate companies and bureaus, but also for landslide hazard experts and stakeholders that could all gain insight into location prices.

The final results of the GIS solution are portrayed as a thematic map that can be communicated and shared easily through many web map-based services. These thematic maps were achieved using recently developed packages in the R language environment including plotGoogleMaps and plotKML.

Materials and methods

Hedonic price models

The basic hedonic price function can be represented as (Can and Megbolugbe 1997):

$$Y = f(S\alpha, N\gamma) + \varepsilon \quad [1]$$

where Y is a vector of observed housing values, S is the matrix of the structural characteristics of properties, the N matrix characterizes neighborhood characteristics including measures of socio-economical conditions for residential area including environmental conveniences and public accommodations, α and γ are vectors corresponding to S and N, and ε is a vector of random error terms.

The given formula can be expressed as a common regression function:

$$Y = X\beta + \varepsilon \quad [2]$$

where $Y_{n \times 1}$ represents the vector of observed sale prices of n dwellings, $X_{n \times k}$ is a vector of k explanatory variables characterizing housing units. $\beta_{k \times 1}$ is the vector of unknown coefficients and $\varepsilon_{n \times 1}$ is a vector representing error term.

By using ordinary least squares (OLS), the unknown coefficients are solved as:

$$\hat{\beta} = (X^T X)^{-1} X^T Y \quad [3]$$

Recently developed R language packages designed for managing, processing and visualisation of data given in GIS formats facilitate the advanced approach in this field.

R language environment

Preparing and processing of input data were performed in the GIS environment by SAGA GIS (<http://www.saga-gis.org>) and R open-source software packages. R is an open source system for statistical computation and graphics that provides different programming facilities, high-level graphics, interfaces to other languages and debugging facilities.

The newly developed R package *plotGoogleMaps* (Kilibarda and Bajat 2012), based on Asynchronous JavaScript and XML technology (AJAX) and Google Maps Application Programming Interface (API) service produces HTML file map mashups (web maps). These maps combine geographic data from one source with a map from another source (Miller 2006, Gartner 2009, Haklay et al. 2008). In addition, the R package *plotKML* (<http://cran.rproject.org/web/packages/plotKML/plotKML.L.pdf>) was used to visualize spatial and spatio-temporal objects in Google Earth for a more interactive presentation of results.

Case study of Belgrade metropolitan area

The administrative boundary of the Belgrade metropolitan area includes an area of 3,223 km² with a population of 2 million inhabitants. Its territory is divided into 17 municipalities where the urbanized area and the inner part of city accounts for a total area of 360 km² and include 10 urban municipalities that are taken into consideration in this study. There are approximately 420 000 households with 1 200 000 inhabitants in the area of interest according to official census data records (Statistical Office of the Republic of Serbia 2003). The original data set used in this study consists of 747 records of apartment transactions in the year 2010 and were comprised of total transaction value, covered flats size and their corresponding addresses. On the other hand, additional information on internal living space including

the age and availability of garage spaces were not taken into consideration. A geographic information system (GIS) was used to match street addresses of the transactions with the official data set of building geographic coordinates in order to geocode observations into the study area.

Explanatory variables

The determinants of house prices can be divided into four groups when applying the hedonic price model for real estate evaluation (Lake et al. 1998): structural variables (e.g. age, the number of rooms in each house), accessibility variables (e.g. the proximity of schools, bus routes, railway stations, shops, parks, and the Central Business District), neighborhood variables (e.g. local unemployment rates), environmental variables (e.g. road noise and visibility impact). The explanatory variables that refer to accessibility and environment could be considered as spatial determinants that are specifically referred to as the distance variables (Koramaz and Dokmeci 2012). In this study we were confined to accessibility, neighborhood and environmental variables as predictors Table 1.

Table 1 List of explanatory variables and their typology.

Variable	Type
Proximity (Euclidean distance) to: airport; museums; theatres; University/science facilities; elementary/high schools; parks/playgrounds; green markets; big green areas/forest; sport stadiums; station of public transport; shopping centers; main streets; religious facility; kindergarten; ambulance/hospitals.	accessibility
Proximity to: highway; main roads/ boulevards; river banks; railway.	environmental
Percentage of illiteracy habitants; Average income in municipality.	neighborhood

The explanatory variables referring to accessibility and environment were arranged as input maps/grids with 20 m resolution by using a proximity function within the SAGA GIS environment. The values assigned to grid cells are calculated by Euclidean distances between input features (roads, schools, parks, etc.) and each cell in the grid map. Two neighborhood variables (illiteracy and income) are based on census data. The illiteracy layer/map was generated as a factorial variable that is referenced to each municipality, where each cell represents the proportion of illiterate inhabitants in a particular municipality with respect to the whole city of Belgrade. The income variable represents the average income in the municipality so that every grid cell within each municipality area has the same value. Variables that include neighborhood, proximity to markets, schools and rivers were indicated as highly significant predictors (Bajat et al. 2012).

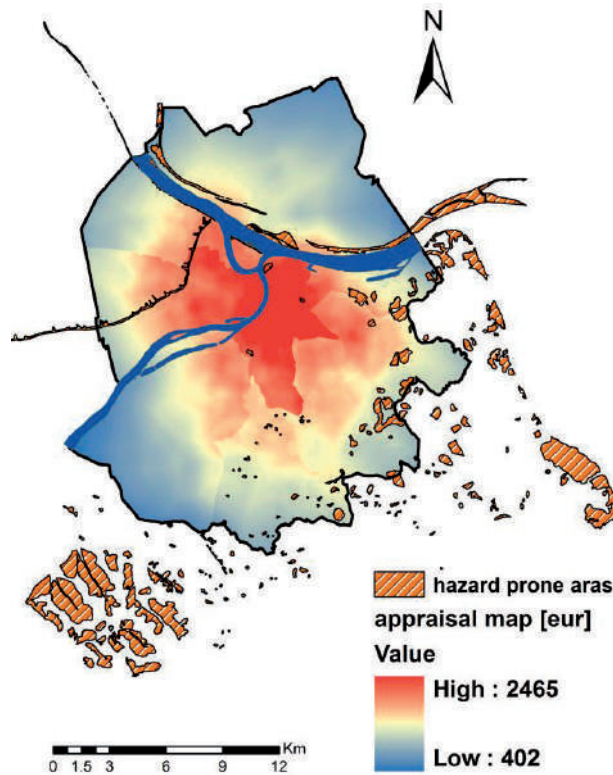


Figure 1 Hazard prone delineated areas over the massive appraisal map of Belgrade urbanized city area.

Data processing and results

The spatial predictors, given as raster maps, were used as auxiliary inputs that are necessary for hedonic regression modelling. The socio-economic data, such as distribution, ages and income of inhabitants were prepared in the same manner enabling their use in the GIS support environment and help achieve a reliable spatial assessment of dwellings prices per square meter. The massive appraisal map was obtained by direct application of the OLS model over the auxiliary grid layers of predictors in the grid format with 20 m resolution Figure 1.

The land-use suitability data layer (given in vector format) was recently prepared for the Master Plan of the city of Belgrade and was used to delineate areas susceptible to the landslide and ground subsidence hazard (Djurić et al. 2013). The other class of input data concerns residential blocks. They are an integral part of planning documents that have already been prepared for the Master Plan of Belgrade from the year 2000 and exist in digital form, readily usable in the GIS environment. The residential blocks are presented in vector format (shp. files) with associated attributes indicating the average number of stores (floors) within the building

block. Obviously, a building block is designated as a residential area clearly delimited by roads.

The hazard-prone areas were delineated by overlaying the produced massive appraisal map raster with LUS layer polygons that refer to unsuitable and very unsuitable land classes Figure 1. Vulnerable objects were identified by applying a polygon intersection function on the layer of delineated hazard-prone areas and the layer depicting building footprints (digital cadaster plan). After joining identified building objects with BHT layer data, the total building areas were calculated for each object by multiplying the building footprint area with the number of total stores. The estimated building values were calculated using the mean price value of enclosed raster cells within the footprint of an object and its multiplied total building area. Identified shape files representing vulnerable buildings with associated estimated price values were embedded in interactive web maps available through web browsers Figure 2. It is possible to obtain details of the total value of specific objects and corresponding area by simply clicking over the object Figure 2 left. The balloon that appears in the Figure 2 left shows the total area of the hazard prone object (2,268 m²) and its estimated value in thousands of Euros (3,237.3 €).

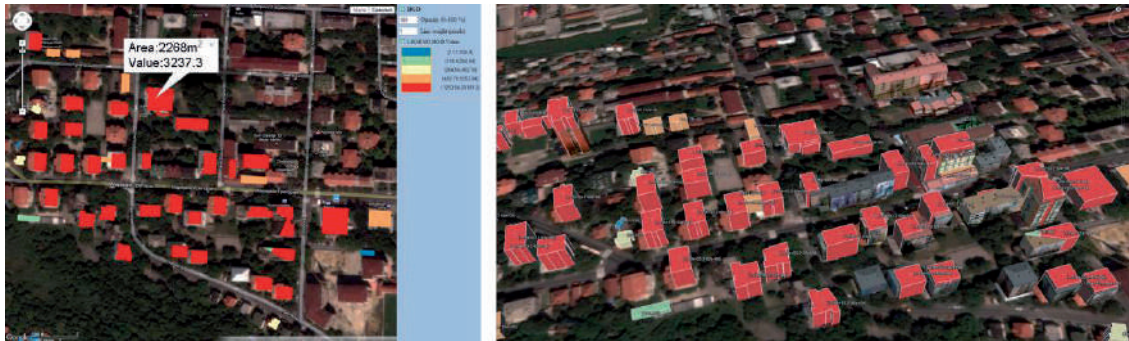


Figure 2 The screenshots of HTML web map (left) produced by plotGoogleMaps package, available at <http://www.grf.bg.ac.rs/~bajat/BGD.htm> and web map in KML format (right) produced by by plotKML package, available at <http://www.grf.bg.ac.rs/~bajat/BGD.kmz>.

Conclusion

Considering that a cross-sectional analysis of house prices involves georeferenced information, GIS tools and spatial statistics are suitable for modelling building price values over an area of interest. The results of spatial prediction were produced as digital maps in raster format. The digital maps could be used to assess potential damage costs when combined with data contained in town planning documentation concerning information on land-use suitability and height of residential buildings. One could then easily calculate potential damage costs of residential buildings due to the risk of landslides over the whole case study area by using simple map algebra of the combined layers. The obtained results were exported in HTML and KML web formats and included some GIS functionality that allowed for the suitable visualization of spatial data and facilitates communication between stakeholders.

A similar methodology could be applied to model the impact of risk hazards on the general population by using a dasymetric population spatial layer (Bajat et al 2011) instead of a massive appraisal map layer.

Acknowledgments

This work was supported by the Ministry of Education, Science and Technological Development of the Republic of Serbia (Contracts No. III 47014, TR36035 and TR 36009).

References

- Anselin L (1988) *Spatial Econometrics: Methods and Models*. Kluwer Academic Publishers, Dordrecht.
- Bajat B, Kilibarda M, Pejović M, Samardžić-Petrović M (2012) Spatial Hedonic Modelling of Dwelling Location Prices Using Auxiliary Maps, CD Proceedings of RSAI 9th Congress, 9-12 May 2012, Timisoara, Romania.
- Bajat B, Krunic N, Bojović, M, Kilibarda M, Kovačević Z (2011) Population vulnerability assessment in hazard risk management: a dasymetric mapping approach, 2nd Project Workshop on Risk Identification and Land-Use Planning for Disaster Mitigation of Landslides and Floods, 15-17 December 2011, Rijeka, Croatia, pp.167-170, ISBN 978-953-6953-30-1
- Can A, Megbolugbe I (1997) Spatial dependence and house price index construction. *Journal of Real Estate Finance and Economics*, 14: 203–222.
- Djurić U, Marjanović M, Šušić V, Petrović R, Abolmasov B, Zečević S, Basarić I (2013) Land-use suitability analysis of Belgrade city suburbs using machine learning algorithm, Symposium GIS Ostrava 2013, CD Proceedings, 21th - 23th January 2013, Ostrava, ISBN 978-80-248-2944-9
- Fell R (1994) Landslide risk assessment and acceptable risk, *Canadian Geotechnical Journal*. 31: 261-272.
- Fell R, Corominas J, Bonnard C, Cascini L, Leroi E, Savage W Z (2008) Guidelines for landslide susceptibility, hazard and risk zoning for land-use planning, *Engineering Geology*. 102(3–4): 83-256.
- Gartner G (2009) Applying Web Mapping 2.0 to Cartographic Heritage, e-Perimtron. pp. 234-239.
- Haklay M, Singleton A, Parker C (2008) Web Mapping 2.0: The Neogeography of the GeoWeb. *Geography Compass*. 2(6): 2011–2039.
- Kilibarda M, Bajat B (2012) plotGoogleMaps: The R-based web-mapping tool for thematic spatial data. *Geomatica* 66(1): 37-49.
- Koramaz TK, Dokmeci V (2012) Spatial Determinants of Housing Price Values in Istanbul. *European Planning Studies*. 20(7): 1221-1237.
- Lake I R, Lovett A A, Bateman I J, Langford I H (1998) Modelling environmental influences on property prices in an urban environment. *Computers, Environment and Urban Systems*. 22(2): 121-136.
- Miller C M (2006) A beast in the field: the Google Maps mashup as GIS/2. *Cartographica*. 41(3): 187–199.
- Statistical Office of the Republic of Serbia (2003) *Population Census, households and housing books 2002*. Belgrade: Statistical Office of the Republic of Serbia.
- van Westen C J (2004) Geo - information tools for landslide risk assessment : an overview of recent developments. Proceedings of the 9th international symposium on landslides, June 28 -July 2, 2004 Rio de Janeiro, Brazil ISBN: 978-0-415-35665-7. pp. 39-56.

Rockslides and Rock Avalanches in the Kokomeren River Valley (Kyrgyz Tien Shan)

Alexander Strom

Geodynamics Research Centre – branch of JSC “Hydroproject Institute”, 125993, Moscow, Russia, Volokolamskoe Shosse 2, +7 910 4553405

Abstract Large-scale bedrock landslides pose an especial threat due to enormous amount of material involved, their high mobility and ability to create natural dams, which result in inundation and catastrophic outburst floods. Long runout rock avalanches, intact and deeply eroded rockslide dams from few millions to more than one billion cubic meters in volume, evidence of inundation and of catastrophic outburst floods have been demonstrated to landslide researchers from 17 countries during field training courses organized annually in the Kokomeren River valley (Tien Shan, Kyrgyzstan) since 2006. Special emphasis is paid on peculiarities indicating rockslide origin and motion mechanisms. This area was selected due to unique concentration of rockslides and rock avalanches of different morphological types within a limited area of about 30×60 km at a one-day trip distance from Bishkek city – capital of Kyrgyzstan, sites attainability and arid climate. Besides landslides, the study area provides expressive manifestations of recent tectonics and of various paleoseismic features.

Keywords rockslide, rock avalanche, outburst flood, paleoseismology

Introduction

Rockslides (bedrock landslides), though being relatively rare in comparison with landslides in non-lithified soils, pose a threat to vast areas due to enormous amount of material involved (sometimes up to billions of cubic meters), high mobility and ability to create large natural dams, which result in inundation of the valleys upstream and catastrophic outburst floods downstream.

Excellent examples of long runout rock avalanches of different morphological types, of intact and deeply eroded rockslide dams, of lacustrine sediments accumulated in the landslide-dammed lakes and of catastrophic outburst floods traces can be found in the Kokomeren River basin (Central Tien Shan, Kyrgyzstan) within a limited area of about 30×60 km (Fig. 1) located at a one-day trip distance from Bishkek city – capital of Kyrgyzstan. Most of these sites are easily attainable by car or require few hours of hiking to reach them. Arid climate and lack of vegetation provide good preservation and visibility of rockslides' morphology and internal

structure.

All these features are demonstrated to the participants of the International Summer School on Rockslides and Related Phenomena - annual field training course supported by the IPL-106-2 Project. Special emphasis is paid on those peculiarities that allow revealing rockslide origin and their motion mechanisms. Some of these case studies are described briefly hereafter.

Morphological types of rockslides and rock avalanches

Morphological analysis of rockslide deposits allows their classification based on various criteria (see, for example, Hermanns et al. 2011). Such classifications are rather complex and strongly depend on the local topography of rockslides' transition-deposition zone.

Simplified classification based on the along-way debris distribution and allowing selection of rockslide types irrespective of the terrain topography (Strom 1996, 2006) was developed by the examples from the Kokomeren basin. Three main types of mobile rock slope failures, likely reflecting different runout mechanisms were proposed (Fig. 2):

- “Primary rock avalanches” characterized by distal debris accumulation. They form either long run-out rock avalanches (Fig. 2-1a) – the Seit one (1 on Fig. 1, Fig. 3) or compact dams with distinct proximal lowering in the relatively narrow valleys (Fig. 2-1b) – the Ak-Kiol (2 on Fig. 1, Figs 4, 5) and Mini-Köfels rockslides (3 on Fig. 1).
- “Jumping rock avalanches” with compact body at the headscarp foot and mobile part. Slope of the compact part rising above the mobile part has convex shape. They are formed when rockslide mass really jumps from a slope like a ski jumper and collides with valley bottom (Fig. 2-2). In the study area this type can be exemplified by the Kashkasu (Strom and Abdrakhmatov, 2009) (4 on Fig. 1), Northern Karakungey (5 on Fig. 1) and, likely, Lower-Aral (12 on Fig. 1) rockslides.
- “Secondary rock avalanches” also with the bipartite debris distribution. Unlike the “Jumping” type, these rock slope failures have distinct concave secondary scarp that marks the boundary between the compact and mobile parts. Such rock avalanches form when rapidly moving debris collides with valley bottom or its opposite slope (Figs 2, 3).

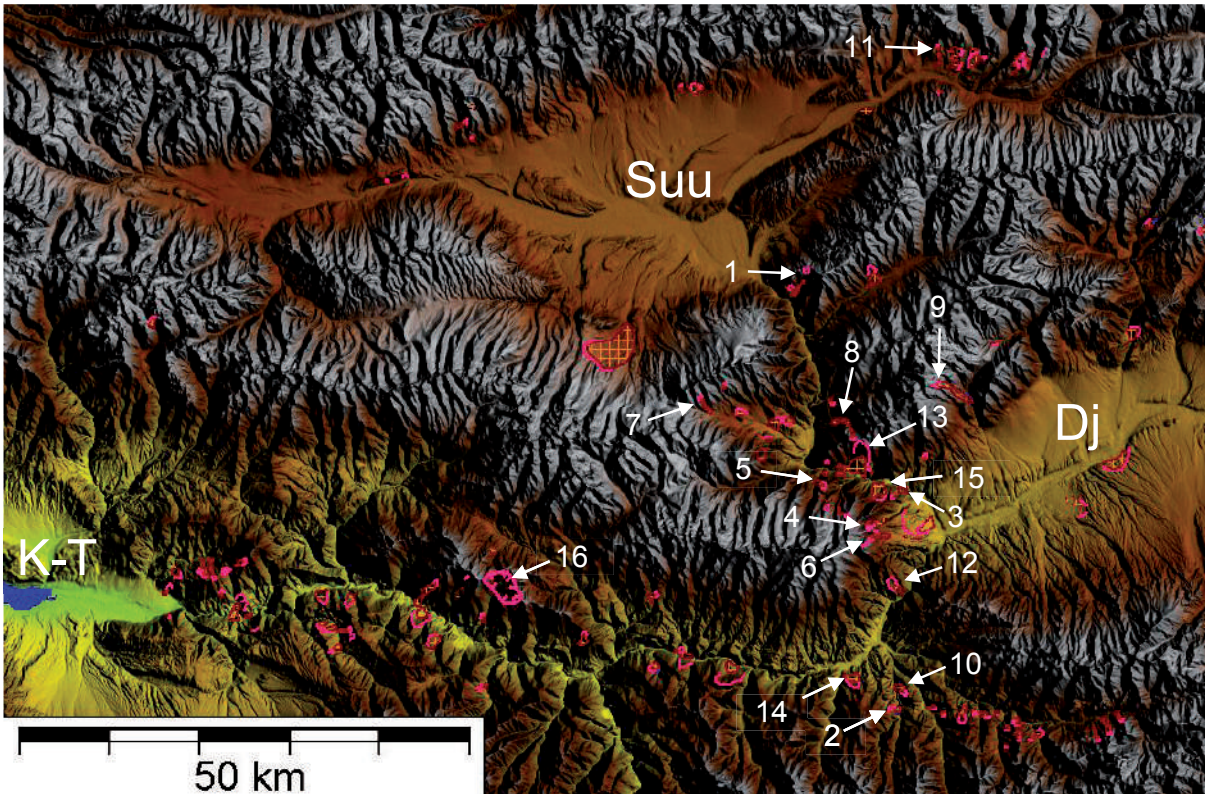


Figure 1 Large-scale landslides rock avalanches and caldera-like collapses in the Kokomeren River basin and adjacent part of the Naryn River basin. Suu, Dj and K-T – the Suusamyr, the Djungal and the Ketmen-Tiube intermountain depressions. Case studies mentioned hereafter: 1 – Seit; 2 – Ak-Kiol; 3 – Mini-Köfels; 4 – Kashkasu; 5 – Northern Karakungey; 6 – Southern Karakungey; 7 – Chongsu; 8 – Sarysu; 9 – Ming-Teke; 10 – Lower Ak-Kiol; 11 – Snake-Head; 12 – Lower-Aral; 13 – Kokomeren; 14 – Ornok; 15 – Displaced Peneplain; 16 – Kyzylkiol.

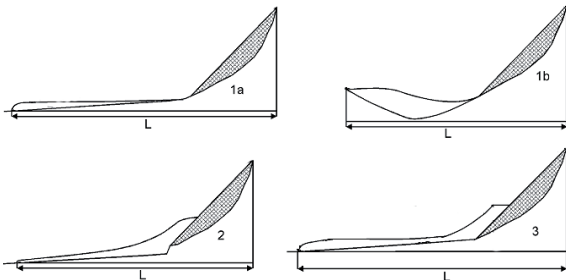


Figure 2 Morphological types of rockslides and rock avalanches based on the along-way debris distribution. L – runout. 1 – “Primary” rock avalanches: 1a – in unconfined environment, 1b – in heavily confined environment; 2 – “Jumping” rock avalanche; 3 – “Secondary” rock avalanche of the “Classical” subtype.

Later on secondary rock avalanches classification was specified and features described by the model shown on Fig. 2-3 were ascribed to the “classical” subtype, while those originated when moving debris enters sharp narrowing on its path – to the “bottleneck” subtype (Strom, 2010). Secondary rock avalanches of “classical” subtype are represented by the Southern Karakungey (6 on Fig. 1), Chongsu (7 on Fig. 1), Sarysu (8 on Fig. 1), Ming-Teke (9 on Fig. 1) and Lower Ak-Kiol (10 on Fig. 1) rock avalanches, while those of the “bottleneck” subtype -

by the abnormally mobile, considering its relatively small volume, Snake-Head rock avalanche (11 on Fig. 1) (Strom 2010).

Primary rock avalanches

The most peculiar feature typical of all rockslides of the “Primary” type is debris accumulation far from the source zone and its absence within the headscarp area and close to it. However, the trimlines marking the debris level during rockslide emplacement can be often traced much above the top of the body or along the transition zone where no debris remain except small patches pasted on the slope (Figs 3 - 5).

They show that rock avalanche debris had moved initially as a thick body and later flowed out like a liquid leaving minor remnants along gully walls. This peculiarity of rockslide debris motion must be considered when performing its numerical modelling.

Similar trimlines have been identified along mobile parts of the Southern Karakungey (6 on Fig. 1, Fig. 6), Sarysu (8 on Fig. 1) and Ming-Teke (9 on Fig. 1) secondary rock avalanches. Distal debris accumulation typical of secondary rock avalanches long runout pasts, along abovementioned trimlines, indicate similarity of their motion mechanism to that of “Primary” rock avalanches.

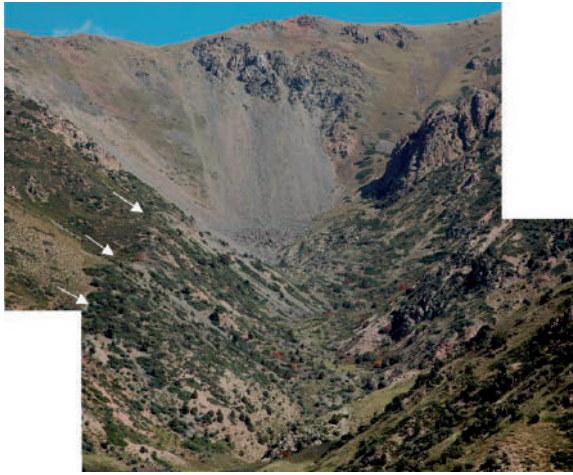


Figure 3 Headscarp of the Seit Primary rocks avalanche and the distinct trimline (white arrows) on the right slope of the dry gully through which its debris passed. Practically nothing remain inside the gully that did not undergo water erosion after rock avalanche formation.

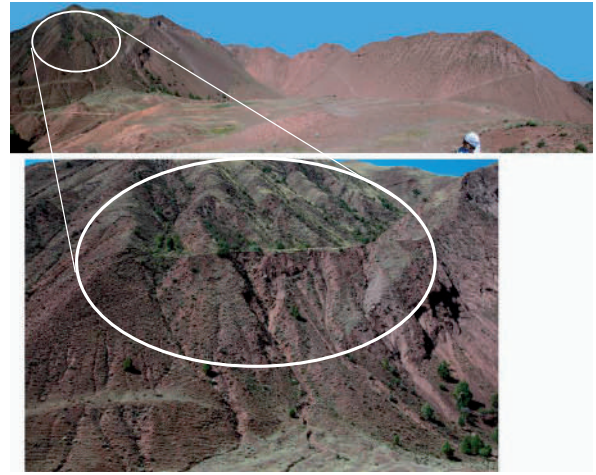


Figure 5 Headscarp of the Ak-Kiol rockslide (above). Below – an old dry gully just outside the headscarp filled by rockslide debris. This remnant is about 50 m above the present day landslide surface.

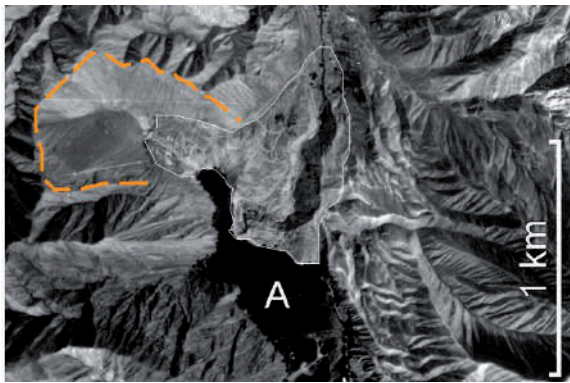


Figure 4 Aerial photograph of the Ak-Kiol rockslide dam and lake (A). Dam's body formed by the primary rock avalanche is outlined by thin white line. Headscarp marked by dashed orange line is almost debris-free. White circle marks area outlined on Figure 4.

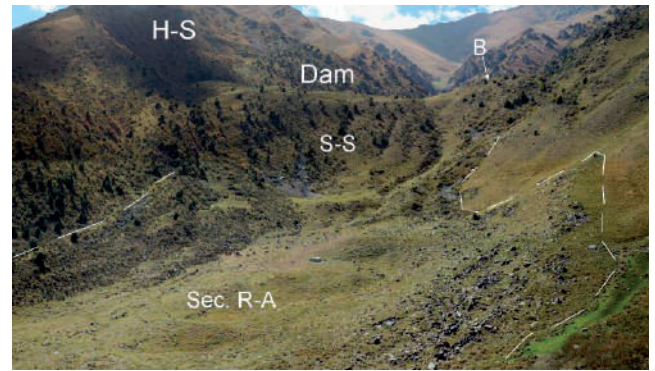


Figure 6 Trimlines (dashed) above the upper part of the secondary rock avalanche of the Southern Karakungey rockslide. H-S – the headscarp; S-S – secondary scar at the downstream part of the dam formed just at the foot of the headscarp; B – the *brandung* rising above the dam's crest.

Jumping rock avalanches

Rock avalanches ascribed to the Jumping type are relatively rare, since their formation requires specific combination of slope topography and rock massif structure due to which sliding surface comes out on the slope much above its foot. Figure 7 presents the sketch model of such rock avalanche formation.

Mobile part of such rockslide could be formed by squeezing of the rockslide frontal part by the tail portion of the sliding mass originated from the upper part of the source zone.

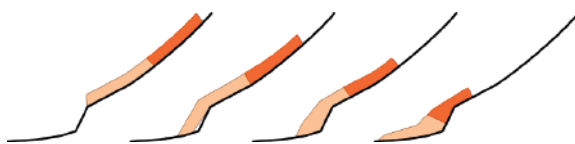


Figure 7 The schematic model of the Jumping rock avalanche formation showing successive relationships of the lower (frontal) and upper (tail) parts of sliding massif.

Rockslides of such type can not be caused by recent stream incision. I want to note that along-way debris distribution typical of "Jumping" type could be observed at the famous Elm rock avalanche caused by artificial slope undercutting by a slate quarry (Heim 1882, Hsu 1975). Rock mass hit over the quarry wall and jumped into the valley.

What about jumping rockslides that occur on natural slopes, they could be triggered, most likely, by seismic shaking, considering well-known effect of strong motion amplification at the upper parts of topographic irregularities (see for example Meunier et al. 2008, Huang 2013).

The most prominent case study of this type, though more complex in comparison with the above mentioned Kashkasu and Northern Karakungey examples, is the Lower-Aral rockslide (Strom 2013a) (12 on Fig. 1, Figs 8, 9). This failure, which seismic origin hypothesis is supported by the presence of liquefaction features in the

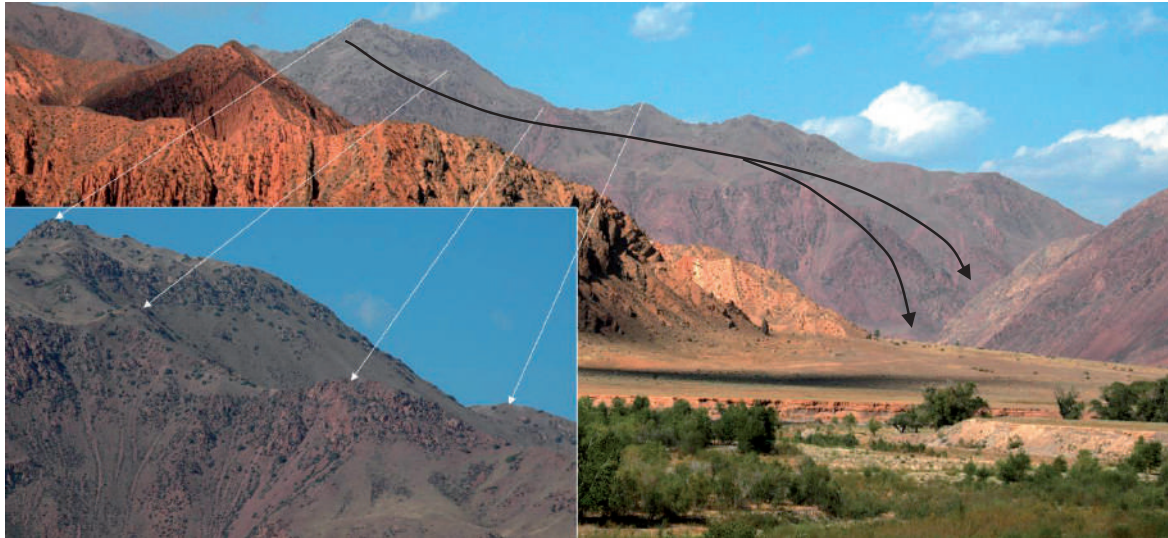


Figure 8 Side view of the Lower-Aral rock avalanche headscarp area (its zoomed view obtained from slightly different viewpoint is shown in the inset) and its transition zone (marked by black arrows).

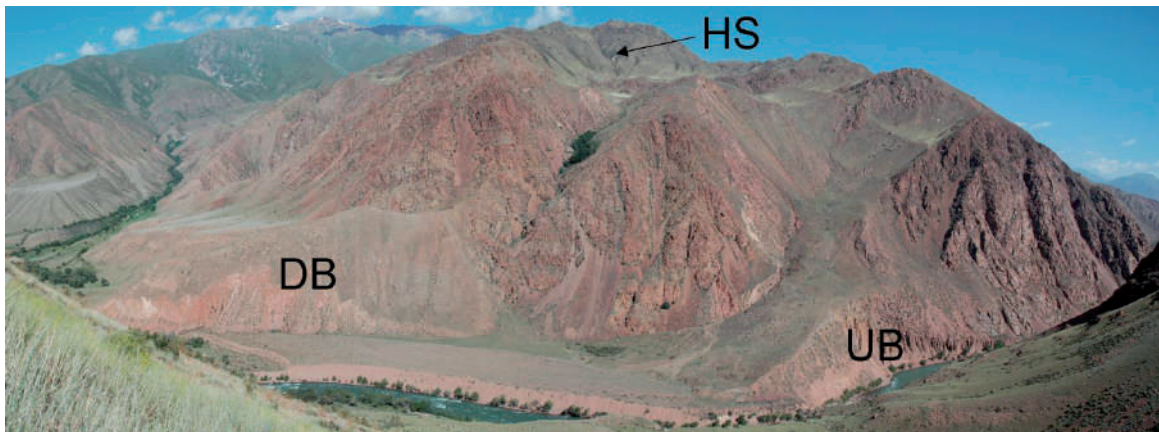


Figure 9 Front view of the Lower-Aral rock avalanche. HS – headscarp area; UB – upstream dam body that had blocked the Kokomeren River; DB – downstream body that had formed partial blockage. Terrace-like flat surface between UB and DB – proximal part of sediments left by outburst flood caused by the upper dam breach.

dammed lake sediments likely triggered by strong aftershock (Strom 2013b) occurred 600-1000 m above the river on top of the ridge and 1.7 km from the edge of the river canyon (Fig. 8). After passing this distance debris had divided into two parts that caved into the valley and formed two separate dam bodies (Fig. 9). The upper one formed the ~70 m high dam, which subsequent catastrophic breach produced the outburst flood with estimated peak discharge of about 30 000 m³/s (Strom 2013a, Strom and Zhirkevich in press).

Secondary rock avalanches

Secondary rock avalanches are most common in the study area. Their morphology and assumed motion mechanism likely associated with momentum transfer from the entire sliding mass to its portion retaining possibility of further motion when rapidly moving debris meets any obstacle were described in details in (Strom 2006, 2010). As mentioned above the mobile “avalanche-like” parts of these rockslides often move similarly to

Primary rock avalanches, forming debris accumulations at their distal parts and leave trimlines on slopes much higher than the final surface of debris (Fig. 10).



Figure 10 Upper part of the Ming-Teke secondary rock avalanche. Black arrow labelled as HS shows the location of the headscarp; white arrows mark the trimlines left by moving debris much above the final top of rock avalanche body.

Additional hazard provided by rock avalanches of secondary type is caused by their ability to change the direction of rapid debris motion abruptly, thus affecting areas that seem to be safe.

Internal structure of rockslide bodies

Some of rockslide deposits in the study area up to 400 m thick have been deeply dissected by erosion providing excellent outcrops where their internal structure could be observed and studied in detail.

Due to presence of different and multi-colour lithologies in the head scarp areas of the Kokomeren (13 on Fig. 1) and Ornok (14 on Fig. 1) rockslides they represent may be the world-best evidence of rock-slide body “stratification” (Fig. 11) when debris originated from different lithologies in the source zone and displaced for several kilometres did not mix but form distinct successive “layers” (Strom 1994, Abdrakhmatov and Strom 2006).

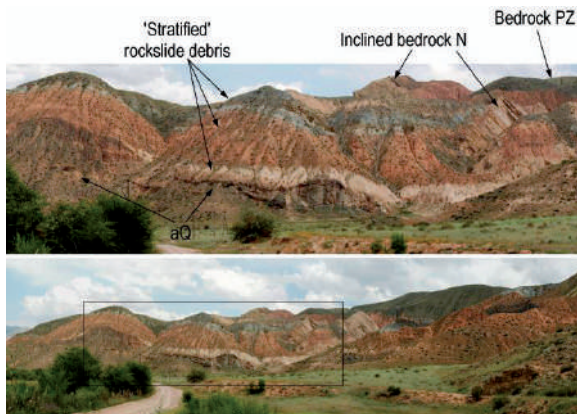


Figure 11 “Stratified” frontal part of the Ornok rockslide body resting over alluvial gravels of the left bank Kokomeren River terrace. Grey “layer” originated from Paleozoic metasediments, pink and reddish “layers” – from Neogene red beds.

Peculiarities of the internal structure of large-scale rockslide deposits – the above mentioned “stratification” and intensive crushing of the internal/lower units contrasting to the coarse outer carapace allow confident identification of old rockslides, which bodies are so strongly reworked by erosion that could be hardly recognised morphologically. In the study region it is exemplified by a gigantic Displaced Peneplain rockslide (15 on Fig. 1), about 0.5 km³, if not larger, in volume. This Late Pleistocene rockslide had blocked the Kokomeren River and forced it to cut a new bypass section through the left bank bedrock massif (Fig. 12).

Such “stratification” and absence of mixing of debris from different lithologies force to exclude turbulence during rapid flow-like debris motion. This limitation must be considered in the software developed for numerical modelling of this process like DAN (Hungar 2011) and similar.

Paleoseismic implications

The study area provides expressive manifestations of Quaternary tectonics and paleoseismic features. Besides numerous surface ruptures indicating recurrent Late Pleistocene and Holocene faulting events likely accompanied by large earthquakes (McCalpin 2009) there are rockslides which seismic origin could be revealed from combination of the indirect evidence - the Kokomeren and Lower-Aral case studies (Strom 2013b). Seismic origin of other rockslides can be assumed as well but to proof or disproof it additional studies, including dating of these features, are necessary.

Along with “typical” paleoseismic features there is an unusual recent structure located west from the Kokomeren River basin on top of the Santash Ridge that forms the right bank of the Naryn River valley. It is the unique caldera-like Holocene (?) depression 3x2 km in size and up to 700 m deep - the so called Kyzylkiol cavity (16 on Fig. 1). Its formation was associated with disappearance of about 3 km³ of rocks in the ridge’s



Figure 12 Participants of the 2008 Summer School at the “entrance” of the abandoned valley of the Kokomeren River immediately upstream from its section that had been blocked by the Displaced Peneplain rockslide. Present day stream passes in front of this outcrop from right to left.

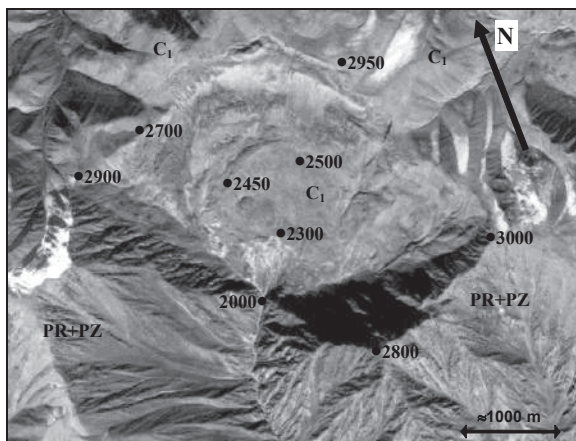


Figure 13 The Kyzylkiol caldera-like cavity. Black dots with numbers – elevations at selected points. Compare elevations inside and outside the cavity.

interior. Strom and Groshev (2009) hypothesized that this really mysterious phenomenon could reflect the final stage of neotectonic detachment anticline evolution. It was proposed that formation of basement anticline under lateral compression produced some spalling of the upper unit of the Earth crust up to several kilometres thick from the underlying unit, its warping and formation of the underground cavity in the anticline core. Subsequently its arch collapsed, either due to tectonic earthquake or producing the collapse earthquake and formed this impressive geomorphic feature. The only one historical analogue is the “Bitut” feature in the epicentral zone of the 1957 M8.2 Gobi-Altai earthquake (Florensov and Solonenko 1965), though the Kyzylkiol one volume is one order larger.

Acknowledgments

I want to express my sincere gratitude to Executive director of ICL Prof. Kyoji Sassa for his permanent support of our activities and to Director of Kyrgyz Institute of Seismology Dr. Kanatbek Abdrakhmatov and his colleagues for multi-year excellent organisation of the field training courses.

References

- Abdrakhmatov K, Strom A (2006) Dissected rockslide and rock avalanche deposits; Tien Shan Kyrgyzstan. In: *Landslides from Massive Rock Slope Failure*. Evans SG, Scarascia Mugnozza G, Strom A, Hermanns RL (eds). NATO Science Series IV: Earth and Environmental Sciences, Springer Dordrecht (ISBN-10 1-4020-4036-9). 49: 551-572.
- Florensov N A, Solonenko V P (1965) The Gobi-Altai Earthquake, Israel Program for Scientific Translations U.S. Department of Commerce, Washington, DC. 424p.
- Heim A (1882) Der Bergsturz von Elm. *Deutsch. Geol. Gesell. Zeitschr*, 34: 74-115.
- Hermanns R L, Hewitt K, Strom A, Evans S G, Dunning S A, Scarascia Mugnozza G (2011) The classification of rockslide dams. In: *Natural and artificial rockslide dams. Lecture Notes in Earth Sciences*. Evans SG, Hermanns R, Strom AL, Scarascia-Mugnozza G (eds) Springer, Heidelberg, London, New York (ISBN 978-3-642-04763-3). 133: 581–593
- Hsü K J (1975) Catastrophic debris streams (sturzstroms) generated by rock falls. *Geological Society of America, Bulletin*. 86: 129-140.
- Huang R (2013) Slope motion response and failure under strong earthquakes: recording, monitoring and modeling. In: *Earthquake-induced landslides*. Ugai K, Yagi H, Wakai A (eds). Springer Heidelberg New York Dordrecht, London (ISBN: 978-3-642-32237-2). pp. 59-73.
- Hungr O (2011) Prospects for prediction of landslide dam geometry using empirical and dynamic models. In: *Natural and artificial rockslide dams*. Evans SG, Hermanns R, Strom AL, Scarascia-Mugnozza G (eds). *Lecture Notes in Earth Sciences*, Springer, Heidelberg New York Dordrecht, London (ISBN 978-3-642-04763-3). 133: 463–477.
- McCalpin J P (2009) *Paleoseismology*. 2nd edition. Elsevier, Amsterdam (ISBN 978-0-12-373576-8). 613 p. & CD ROM
- Meunier P, Hovious N, Haines J A (2008) Topographic site effects and the location of earthquake induced landslides. *Earth Planet Sci Letters*. 275: 221-232.
- Strom A L (1994) Mechanism of stratification and abnormal crushing of rockslide deposits. In: *Proc. 7th International IAEG Congress*. Oliveira R, Rodrigues LF, Coelho A, Cunha AP (eds) Balkema Rotterdam (ISBN 90-5410-506-2). 3: 1287–1295.
- Strom A L (1996) Some morphological types of long-runout rockslides: effect of the relief on their mechanism and on the rockslide deposits distribution. In: *Landslides. Proc. of the Seventh International Symposium on Landslides*. Senneset K (ed) Balkema, Rotterdam. pp. 1977-1982.
- Strom A L (2006) Morphology and internal structure of rockslides and rock avalanches: grounds and constraints for their modelling. In: *Landslides from Massive Rock Slope Failure*. Evans SG, Scarascia Mugnozza G, Strom A, Hermanns RL (eds). NATO Science Series IV: Earth and Environmental Sciences, Springer Dordrecht (ISBN-10 1-4020-4036-9). 49: 305-328.
- Strom A L (2010) Evidence of momentum transfer during large-scale rockslides’ motion. In: Williams AL, Pinches GM, Chin CY, McMorran TG, Massei CI (eds.) *Geologically Active. Proc. of the 11th IAEG Congress, Auckland, New Zealand, 5-10 September 2010*, Taylor & Frensis Group, London. (ISBN 978-0-415-60034-7). pp. 73-86.
- Strom A (2013a) Geological Prerequisites for Landslide Dams’ Disaster Assessment and Mitigation in Central Asia. In: *Progress of Geo-Disaster Mitigation Technology in Asia*, Wang F, Miyajima M, Li T, Fathani TF (eds) Springer-Verlag Berlin Heidelberg. (ISBN 978-3-642-29106-7). 17-53.
- Strom A (2013b) Use of indirect evidence for the prehistoric earthquake-induced landslide identification. In: *Earthquake-induced landslides*. Ugai K, Yagi H, Wakai A (eds). Springer Heidelberg New York Dordrecht, London (ISBN 978-3-642-32237-2). pp. 21-30.
- Strom A L, Abdrakhmatov K E (2009) International summer school on rockslides and related phenomena in the Kokomeren River valley, Tien Shan, Kyrgyzstan. In: *Landslides – Disaster Risk Reduction*. Sassa K, Canuti P (eds) Springer-Verlag Berlin Heidelberg. (ISBN 978-3-540-69970-5). pp. 223-227.
- Strom A, Groshev M (2009) Mysteries of rock massifs destruction. In: *Rock Mechanics: New Research*. Abbie M, Bedford JS (eds) Nova Science Publishers New York (ISBN 978-1-60692-459-4). pp. 211-231
- Strom A., Zhirkevich A. (2013) “Remote” landslide-related hazards and their consideration for the hydraulic schemes design. In: *Proc. Intern. Conf. “Vajont, 1963-2013: Thoughts and analyses after 50 years since the catastrophic landslide”, October 8-10, 2013, Padua, Italy.* (in press)

Torrential Check Dams as Debris-Flow Sources

Jošt Sodnik^(1,2), Andrej Kryžanowski⁽²⁾, Manica Martinčič⁽²⁾, Matjaž Mikoš⁽²⁾

1) Water Management Company, Kranj, Slovenia, Ulica Mirka Vadnova 5, +386 41 288 442

2) University of Ljubljana, Faculty of Civil and Geodetic Engineering, Ljubljana, Slovenia

Abstract In Slovenia, a central European country with a high hydropower potential and intensive torrential processes in mountainous and hilly headwaters, state legislation concerning large dams and spatial consequences of their failure exists. It does not cover torrential check dams as one of the structure types under consideration. When developing a new approach to estimate hazard due to failure of torrential check dams, the before-mentioned existing legislation was taken as the starting point. The evaluation was developed considering the following parameters: basic parameters of a check dam (constructional height, water volume & volume of sediment deposits, design flood/discharge), availability of technical documentation (design documentation, operation instructions, emergency plans in the case of failure, alarming plans), operation parameters (purpose of the structure, monitoring, alarm systems), hazards (collapse, supervision, design system, managing) and state of the structures and hydraulic equipment (construction, sediment deposits, hydraulic equipment).

Each before-mentioned parameter was ranked according to a three-level (large, medium, and low) scale of impact on hazard level, based on a professional judgment (skills, experiences, field expertise). To ensure selectivity of the final evaluation, the rank values of single parameters were scored with increasing steps, and then the ranks were summed up. The final evaluation is based on a 5 hazard level scale (low, medium, large and two intermediate levels). For ranking purposes, also known facts and field conditions were taken into account, gained during previously conducted field inspections of torrential structures and their documentation. The applied rankings of parameters are valid only for the considered structures, and should be further applied on a larger sample of torrential check dams.

The newly proposed qualitative evaluation of the hazard level of failure of torrential check dams was tested for a chain of torrential check dams in a selected torrent (the Suhelj torrential fan in NW Slovenia). The results of mathematical modeling of potential debris flows on the fan using a two-dimensional numerical model (Flo-2D) are presented.

Keywords check dams, dam engineering, dam safety, debris flows, hazard assessment, maintenance, torrent control

Introduction

In the past years and in order to mitigate different torrential hazards, numerous structures were built in headwaters and especially in torrential channels in the Alps and elsewhere in mountainous regions of the world. Channelized debris flows are one type of such hazards, and torrential check dams are typical type of torrential structures. The paper is oriented towards a question whether torrential check dams should be considered as sediment sources when estimating channelized debris-flow scenarios and assessing debris-flow magnitudes. One can assume that large amounts of coarse torrential sediment deposits behind torrential check dams can under circumstances importantly change the debris-flow magnitude and/or debris-flow event scenario. Therefore, plausible estimation of debris-flow magnitudes and debris-flow hydrographs is crucial for reliable hazard assessment along torrential streams and on torrential fans.

Large dams in Slovenia

Definitions for large dams

The ICOLD (International Commission on Large Dams; www.icold-cigb.org; on-line World Register with over 37,000 dams) defined that large dams must have structural dam height above foundation at least 15 m, or that a dam or a weir has:

- the dam crest longer than 150m;
- the dam reservoir volume larger than 1hm³;
- the discharge through the dam cross section is larger than 2,000 m³/s;
- special foundation and construction conditions.

In 2011, ICOLD introduced new large-dam criteria of structural dam or weir height over 5m, and with reservoir volume over 3 hm³.

Inventory of large dams

In Slovenia, 41 large dams are officially registered by the Slovenian National Committee on Large Dams (SLOCOLD 2013; 22 dams for hydropower production, 14 dams for water management; 3 historical dams – so-called Klavže barrages from 18th Century, 2 dumping tailing barrages; Fig. 1) that have fulfilled the old ICOLD criteria.



Figure 1 The locations of 41 large dams in Slovenia.

In Slovenia, the national Construction Act declares for demanding structures (such as dams and weirs) more serious conditions for their locations in the environment as well as for their operation and maintenance. Unfortunately, only technical characteristics of such structures are taken into account, and not also risks that such structures impose on the environment or their vulnerability due to the processes of structure ageing and (material) degradation.

In the list of the existing water infrastructure in Slovenia according to the national Water Act, there are officially 28 dams and weirs, and 9 dry retention reservoirs (UL 2006). The inventory of the state Institute of Waters of the Republic of Slovenia encompasses 58 dams, weirs, and reservoirs.

Research project on safety of dams and weirs

A research project “Earth- and concrete dams of the strategic importance in the Republic of Slovenia” was proposed some years ago by SLOCOLD and financed in 2011 and in 2012 by the Slovenian Ministry of Defense. Altogether, 68 dams and weirs and torrential dams that can be classified into the category of structures of special importance were identified for the task (Fig. 2).



Figure 2 The locations of the enlarged list of 68 dams and weirs in Slovenia.

The main tasks of the project were (Kryžanowski et al. 2012):

- Identification of all problematical structures subjected to the national and ICOLD criteria.
- Survey of condition of the identified structures, based on documentation check and on-site inspection - field work above and under the water surface.
- Analysis of threats posed by the identified structures which includes a review of existing dam-break studies, a review of possible structural and design deficiencies, possible absence of monitoring, maintenance and control, etc.
- Proposal of required remediation measures if necessary and development of basic remedial actions for structures showing deficiencies.
- Preparation of instructions for population downstream – how to react in the emergency case (e.g. observed structure damages or structure failure).

Technical characteristics of the Slovenian dams

Different technical characteristics of 68 dams and weirs and torrential dams under investigation have been collected (height, volume, purpose, construction material, etc.), as an example we show in Figure 3 the relationship between the dam height and reservoir volume (Kryžanowski et al. 2013). The average dam height is 21m, and the average reservoir volume is 5,344 hm³. The dams for hydropower production are mainly higher than 20m, and water management dams are then mainly lower.

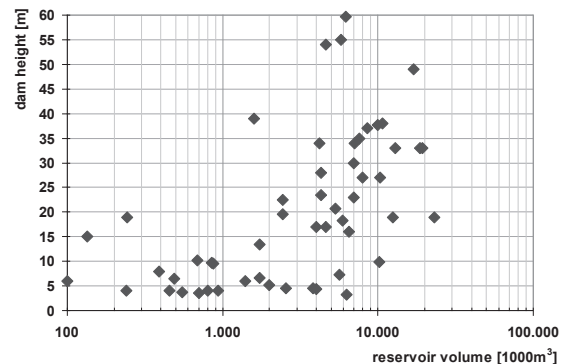


Figure 3 The relationship between the dam height (m) and the corresponding reservoir volume (in 1000 m³) for the 68 dams in Slovenia.

The risk evaluation procedure for dams and torrential structures was developed considering the following parameters (Kryžanowski et al. 2012):

- Basic structure parameters (constructional height, volume of water & sediment deposits, design flood/discharge).
- Availability of technical documentation (design documentation, operation instructions, emergency plans in the case of failure, alarming plans).

Table 1 Marks given for a single hazard (evaluation field) and for the overall hazard.

I. Basic dam parameters	II. Availability of technical documentation	III. Operation parameters	IV. Possible hazards	V. Structure & Hydraulic Equipment conditions	Overall Mark & Hazard Level	
10 - 13	10 - 13	14 - 17	16 - 20	14 - 17	64 - 79	LOW
14 - 18	14 - 18	18 - 23	21 - 26	18 - 23	80 - 105	LOW TO MEDIUM
19 - 24	19 - 24	24 - 31	27 - 36	24 - 31	105 - 140	MEDIUM
25 - 31	25 - 31	32 - 42	37 - 49	32 - 42	141 - 191	MEDIUM TO LARGE
32 - 40	32 - 40	43 - 56	50 - 64	43 - 56	192 - 256	LARGE

- Operation parameters (purpose of the structure, monitoring, alarm systems).
- Possible hazards (collapse, supervision, design system, managing).
- Conditions of structures and hydraulic equipment (construction, sediment deposits, hydraulic equipment).

Each before-mentioned parameter was ranked according to a 3-level scale of impact (large, medium, and low) on the failure risk, based on a professional judgment (skills, experiences, field expertise). The rank values of single parameters were scored with increasing steps, and then the ranks were summed up. The final failure hazard evaluation is based on a 5-level hazard scale (low, medium, large and two intermediate levels – see Table 1).

For ranking purposes, also known (historical) facts and field conditions should be taken into account (due to long life cycle, importance of proper maintenance) that have been gained during previously conducted field surveys of torrential structures and their documentation.

From the hazard-point of view, we also investigated selected torrential check dams within the project framework. Even though no torrential dams are listed in the list of existing water infrastructure in Slovenia, and in vast majority they cannot be defined as large dams according to old ICOLD criteria (i.e. not high enough), they can impose hazard to environment and infrastructure – when they fail. Especially large sediment-retention dams, even more if they are built in a cascade (a chain of check dams), can impose hazard if they fail during torrential flash floods or when destroyed by overtopping by a debris flow initiated on slopes or in natural torrential channels. Using estimates of specific annual sediment yields in torrential watersheds, one can use the area of the watershed and the storage volume of torrential check dams in order to estimate the maximum potential of sediments stored in the retention volume of the check dams – as a first approximation for the magnitude of the debris flows initiated by the dam failure.

Therefore, torrential check-dam as a specific and largely used type of dams has been added to the investigation on dams in Slovenia. When selecting which torrential watersheds should we take into account, we used the inventory of torrential water infrastructure, existing field expert knowledge, estimates of specific annual sediment yields in torrential watersheds (Figs 4,5),

and the recently prepared map of sensitivity of debris flows of Slovenia (in the scale 1:250,000; Komac et al. 2009).

Classification of torrential fans considering Melton's number and fan slope was prepared for the Upper Sava River tributaries. In this regard, two limit values are given in literature: the Melton number = 0.3 and torrential fan gradient = 4° (7%). Both are based on analysis of past events. These limit values should provide a criterion good enough for classification of torrential fans into three groups. In the investigated area, 8 out of 18 torrential fans were recognized as fans prone to debris flow risk, where there is high probability of a debris flow (Sodnik and Mikoš 2006).

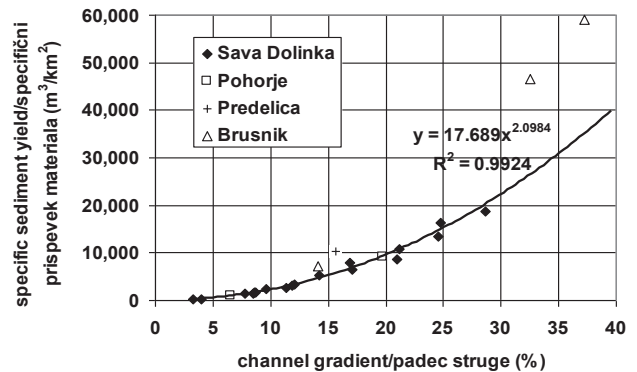


Figure 4 Specific annual sediment yield (m^3/km^2) as a function of torrential channel gradient (%) for selected torrential watersheds in Slovenia (Sodnik and Mikoš 2006).

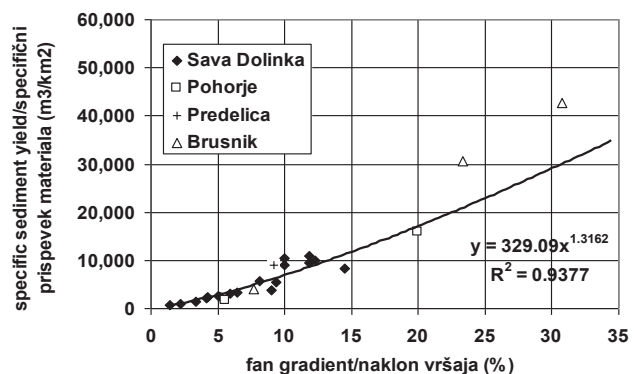


Figure 5 Specific annual sediment yield (m^3/km^2) as a function of torrential fan gradient (%) for selected torrential watersheds in Slovenia (Sodnik and Mikoš 2006).

Other fans were recognized as transitional fans, where debris flows are possible but probability of their occurrence is low (Sodnik and Mikoš 2006).

The Suhelj Torrent in NW Slovenia

A chain of check dams

The Suhelj Torrent was estimated by the field expertise, field evidence and the analysis of watersheds susceptible for possible debris flows in Slovenia, as one of the most hazardous torrential watersheds in Slovenia (Fig. 6). The main reason is an active sediment source in the uppermost part of the watershed, close to the mountain ridge (Fig. 7). The activity of the torrent was handled in the past by a system of over 10 torrential check dams, partially built in a chain – during an extreme event in the watershed a failure of one dam may force the failure of the next downstream dam with a possible initiation of a debris flow generated from the deposited torrential sediments stored behind the check dams.

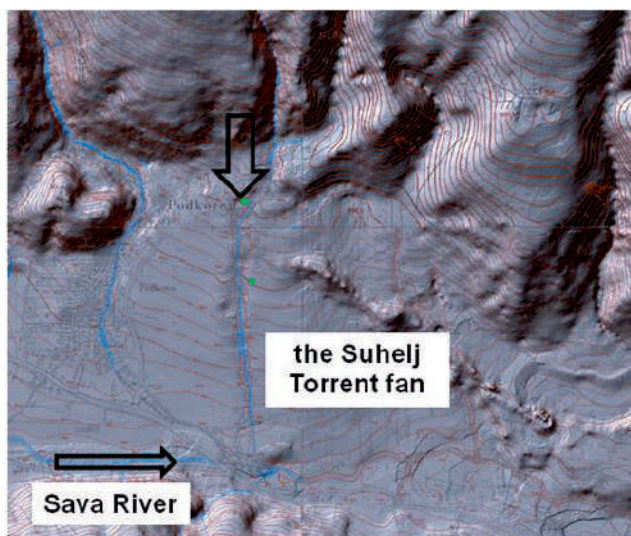


Figure 6 The Suhelj Torrent fan close to the Podkorec Village in NW Slovenia. The torrent is a tributary of the Upper Sava River.

Table 2 Overall hazard levels assessed for Suhelj torrent.

DAM	I.	II.	III.	IV.	V.	MARK	HAZARD LEVEL
SUHELJ	34	24	52	56	44	210	LARGE

The hazard level of the Suhelj torrent check dams is large (Tab. 2). The main problem with this chain of check dams is very poor state of the structures with numerous constructional damages (Fig. 9) in combination with high possible hazards. Poor condition of structures is consequence of low maintenance budget in the last decades. Some structures are threatening to collapse therefore considering failure scenario is justified (Fig. 8).



Figure 7 The uppermost part of the Suhelj Torrent watershed is a source of occasional smaller debris flows or hyper-concentrated sediment-laden flows.



Figure 8 Example of a collapsed check dam.



Figure 9 Example of a filled concrete check dam in the Suhelj Torrent with a filtering function.

For failure of check dams in a cascade, two scenarios were considered:

- Partial failure of a check dam during a torrential flood which results in a hyper-concentrated flow in the downstream channel.
- Complete failure of a check dam. A complete failure results in a channelized debris flow with much greater peak discharge in the downstream channel.

These two different scenarios can be taken as input parameters (inflow hydrograph) for mathematical modeling of potential debris flows in order to assess debris-flow hazard on a torrential fan.

Certainly, also other parameters should be determined, the most problematic are rheological parameters of such a potentially wet or dry debris flow that is hard to determine in advance.

Therefore, only orientation (average) values for rheological properties of debris material may be used – a sensitivity analysis using values in the predetermined interval is to be performed as well in order to get the maximum reach-out zone of a potential debris flow not only due to its magnitude but also due to different material rheological properties (Sodnik et al. 2009, 2012).

Mathematical modeling of potential debris flows

Commercially available model Flo2D was applied for mathematical modeling of potential debris flows on the Suhelj torrential fan. The Flo2D is commercial software for two dimensional mathematical modeling of water flow and fast flowing slope movements including debris flows. Modeling is based on physical laws of the flow and

is applicable under different geographical conditions. For the description of area geometry the model uses numerical grid made out of quadratic cells of the selected size by the user. Model uses interpolation methods to define height of each cell, based on the applied DEM of the surface considered in the model. The main input parameters besides topographic data (DEM) are inflow hydrograph, volumetric concentration (ratio of the debris volume to the total volume of the water-debris mixture), rheological parameters (yield stress and dynamic viscosity), surface roughness coefficients, resistance flow parameter for laminar flow and specific weight of sediment.

A detailed sensitivity analysis with Flo2D showed that the main impact on modeling results has the magnitude (scenario) of a debris-flow event and the quality of topographic data (DEM) (Sodnik et al. 2009).

The importance of the magnitude for a reliable debris-flow hazard assessment put forward the question whether torrential check dams can influence the magnitude of a potential event. When assessing debris-flow hazard and preparing debris-flow hazard maps, most important modeling results are maximum flow depths and maximum flow velocities.

In the Suhelj torrent case study, publicly available DEM5 was used as input topographic data for defining model computational grid 5x5m. Different magnitudes were used as debris flow scenarios and different inflow hydrographs were applied. In Fig.10 results of the model with hydrograph with peak discharge 34 m³/s are presented. Peak discharge of water with 100-year return

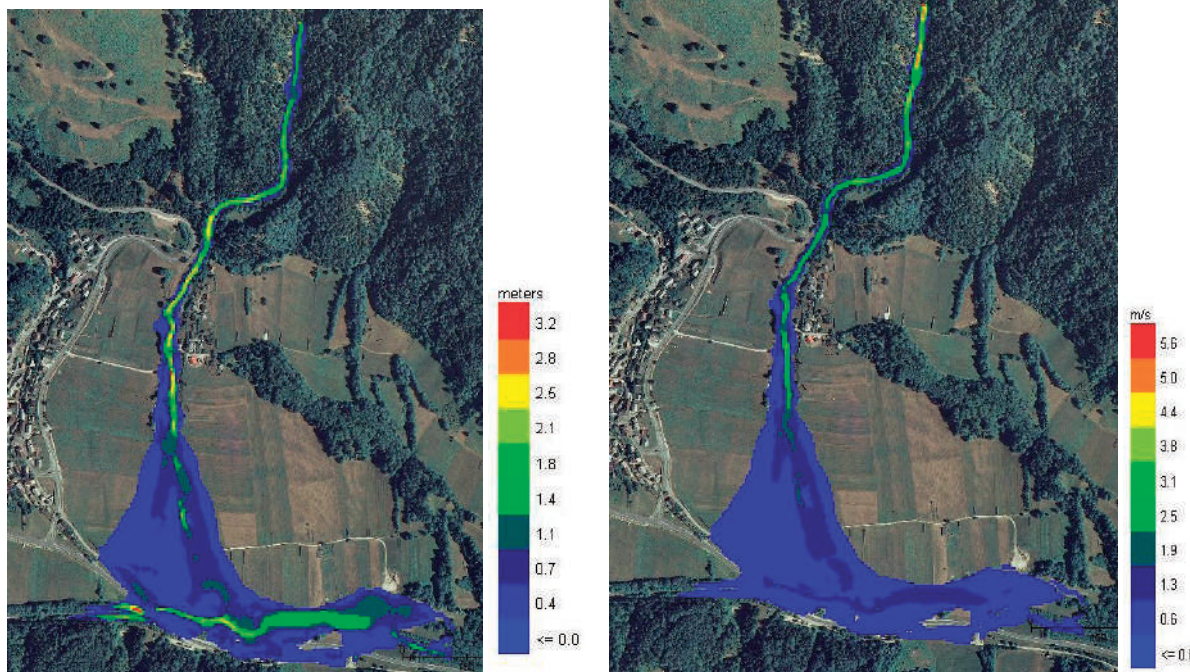


Figure 10 Maximum debris-flow depths (left) and maximum debris-flow velocities (right) on the Suhelj torrential fan. The numerical two-dimensional model Flo-2D used numerical grid 5x5m: debris-flow ($C_v=0.42$) $Q_{max} = 34 \text{ m}^3/\text{s}$, and flash flood $Q_{100} = 24 \text{ m}^3/\text{s}$.

period is $24 \text{ m}^3/\text{s}$. Peak discharge of the hydrograph is the most important parameter when modeling maximum flow depth and maximum flow velocities. Potential failure of a check dam or series of check dams increases peak discharge of channelized debris flow. To assess the quantity of discharge increase precise estimation of sediment budget of torrential check dam must be carried out. With combination of inflow hydrograph defined from the characteristics of the headwaters and sediment budget of potentially failed check dam we get the “new peak discharge”. Further research must be targeted on systematic surveys of existing check dams and their condition and assessment of failure probability. With combining check dams sediment budgets and watershed magnitude worst case scenarios for debris flow events must be defined and applied for debris-flow hazard assessment.

Conclusions

Large dams represent a threat when considering their collapse. Large dams are more visible and consequences are more imaging to broad masses. In Slovenia large dams are covered with legislation and assessment of spatial consequences of their failure exists or should exist. Since Slovenia is an alpine country numerous torrential structures were built in last century. All these structures are considered as easy or less demanding structures and no risk assessment is required when planning and building them. That fact lead to situation where we have over one thousand torrential structures as check dams in Slovenia but no hazard assessment in case of their failure.

The newly proposed qualitative evaluation of the hazard rate due to failure of torrential check dams was tested for a chain of torrential check dams in a selected torrent (the Suhelj torrential fan in NW Slovenia). Case study of the Suhelj torrent shows that also smaller torrential structures can represent a considering threat and that such structures should also be considered with comparable methods as large dams. The results of mathematical modeling of potential debris flows on the fan using a two-dimensional numerical model (Flo2D) confirm that a potential debris flow initiated by a failure of check dams in this torrent truly impose hazard to the torrential fan.

Systematic evaluation of existing torrential structures should be carried out and specific guidelines for designing must be prepared. Our study points out the gap in existing practice and legislation and real situation

on the ground. Numerous structures in poor condition represent a threat to population, settlements and infrastructure that should be evaluated and managed.

Acknowledgments

The authors would like to thank the Ministry of Defense of the Republic of Slovenia that was financing the research project “Earth- and concrete dams of the strategic importance in the Republic of Slovenia (2011-2012)”. To the project the following companies have contributed: Hidrotehnik d.d., Ljubljana, IBE d.d., Ljubljana, and ZAG (Zavod za gradbeništvo), Ljubljana.

References

- Komac M, Kumelj Š, Ribičič M (2009) Debris-flow susceptibility model of Slovenia at scale 1:250,000. *Geologija*. 52(1): 87-104 <http://www.geologija-revija.si/dokument.aspx?id=1056>
- Kryżanowski A, Širca A, Humar N, Ravnikar Turk M, Žvanut P, Mikoš M, Četina M, Rajar R, Polič M (2012) Earthfill and concrete water retention dams of strategic importance in the Republic of Slovenia – VODPREG, Final report, Ljubljana.
- Kryżanowski A, Širca A, Ravnikar Turk M, Humar N (2013). The VODPREG Project: Creation of Dam Database, Identification of Risks and Preparation of Guidelines for Civil Protection, Warning and Rescue Actions. Proceedings of the 9th ICOLD EU Club Symposium, April 2013, Venice, Italy.
- SLOCOLD (2013) Large Dams in Slovenia. URL: http://www.slocold.si/e_pregrade_seznam.htm [Last accessed: March 30, 2013].
- Sodnik J, Mikoš M (2006) Estimation of magnitudes of debris flows in selected torrential watersheds in Slovenia. *Acta geographica Slovenica*. 46(1): 93-123 http://giam.zrc-sazu.si/zbornik/ags46-1-4-SodnikMikos_str-93-123.pdf
- Sodnik J, Petje U, Mikoš M (2009) Terrain topography and debris-flow modelling = Topografija površja in modeliranje gibanja drobirskih tokov. *Geodetski vestnik*. 53(2): 305-318 http://www.geodetski-vestnik.com/53/2/gv53-2_305-318.pdf.
- Sodnik J, Vrečko A, Podobnikar T, Mikoš M (2012) Digital terrain models and mathematical modelling of debris flows. *Geodetski vestnik*. 56(4): 826-837. http://www.geodetski-vestnik.com/56/4/gv56-4_826-837.pdf.
- Sodnik J, Mikoš M (2012) Recent developments in assessing debris-flow hazard in Slovenia. Proceedings of the 2nd Project Workshop of the Croatia - Japan Project on Risk Identification and Land-use Planning for Disaster Mitigation of Landslides and Floods in Croatia, 15-17 December 2011. Rijeka, Croatia. pp. 159-162.
- UL (2006) List of existing water infrastructure. Official Journal of Slovenia, No. 63. URL: <http://www.uradni-list.si/1/content?id=73949> [Last accessed: March 30, 2013]. (In Slovenian)

Hydraulics of Stratified Two-Layer Flow in Rječina Estuary

Nino Kravica, Vanja Travaš, Nenad Ravlić, Nevenka Ožanić

University of Rijeka, Faculty of Civil Engineering, Rijeka, Croatia, Radmile Matejčić 3

Abstract The salinity distributions in the Rječina Estuary, in Croatia, are thoroughly studied through intensive sampling campaigns. Strong vertical stratification was observed throughout the tidal cycle, proving the limited vertical mixing between seawater and freshwater layer, and implying the presence of salt wedge. The salt wedge is developed at the downstream river part, and its length is found to be directly related to Rječina River discharges. The length of the wedge is also dependent, but in smaller intense, to tidal phases. Bathymetry also plays a major role in wedge propagation, especially during small river discharges. A one-dimensional model for two-layer stratified flow, based on Schijf and Schonfeld model, was developed and used. By calibrating the interfacial friction factor, calculated density interface fitted very well to measured data.

Keywords Rječina, estuary, salt wedge, salinity, stratification, regression analysis, numerical model

Introduction

An estuary is typically a transition zone where freshwater from rivers and streams flows into the sea, mixing with the seawater. This zone is subjected to both marine influences (e.g. tides, waves, influx of sea water) and riverine influences (e.g. freshwater and sediment flows).

The interaction between the seawater and freshwater is a highly complex hydraulic problem, which involves a number of physical processes that have not as yet been sufficiently clarified (Van der Tuin 1991). Depending on both marine and riverine influences, estuary can be either fully mixed, partially mixed or a salt wedge can be formed. Salt wedge estuary develops in areas with relatively high river discharges and with very small tidal oscillations, i.e. the micro-tidal seas. It is characterized by a very low turbulent mixing and strong vertical density and salinity stratification.

Many different approaches in analyzing the hydraulics of stratified flow in estuaries have been used: regression methods, empirical expressions, physical models, 1D numerical models of two-layer flow and 2D/3D numerical models. Although there are many different methods, field measurements and model calibration are still essential for accurate description of this process.

In this paper we analyze the hydraulics of stratified

flow in the Rječina Estuary by applying a one dimensional numerical model of two-layer flow and comparing it to measured salinity profiles.

Materials and methods

Site description

Rječina is a typical coastal karst river, located in Croatia near the city of Rijeka, with total length of 18.6 km and catchment area of 246 km². The river enters the Adriatic Sea in the urbanized city center. Length of the estuary is relatively short, approx. 1.0 km from the mouth (Fig. 1).

Water resources from the Rječina River are mainly used for two purposes; hydroelectric power generation (water intake at the Valići Dam, engine room at the city center) and water supply (main sources at the Rječina Spring and the Zvir Spring).



Figure 1 Aerial photo of the Rječina River Estuary.

Based on the analysis from the most downstream hydrological station Sušak tvornica (1999-2011), mean annual discharge is 10.4 m³/s. Rječina River is characterized by strong seasonal oscillations (Fig. 2); maximum mean monthly discharges are usually registered during winter months (51.1 m³/s in December 2010), while minimum mean monthly discharges are observed during summer months (0.14 m³/s in August 2003). Maximum daily discharge, in the same period, was 124.0 m³/s (26 January 2001), while during summer days the channel bed sometimes dries out. Apart from seasonal oscillation, the Rječina River also has daily oscillations, caused by the Hydropower plant Rijeka periodic operation (Kravica et al. 2012).

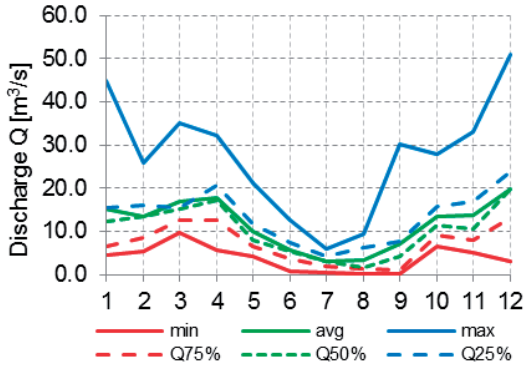


Figure 2 Statistical analyses of minimum, average and maximum discharges of the Rječina River (1999-2011) (Krvavica et al. 2012).

Tidal oscillations of the Adriatic Sea are semi-diurnal (two tidal exchanges during a single day) with the mean daily amplitude of approx. 30 cm. The Adriatic Sea has a relatively high average salinity of 38.3‰ when compared to the average salinity of oceans (35‰).

Field measurements

Field measurements were carried out along the Rječina Estuary in the period from February to August 2012. Eight sampling sites were defined in the study area measuring 730 m in total length from the river mouth. The CTD Diver (Schlumberger DI263) was used to measure depth, temperature and conductivity (Fig. 3).

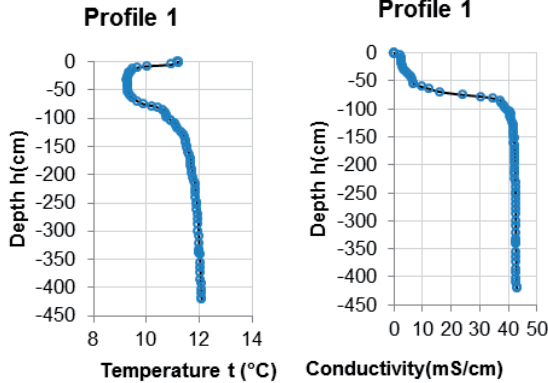


Figure 3 Typical example of measured depth distribution of temperature and conductivity in the Rječina Estuary near the river mouth.

The practical salinity and water density was calculated using UNESCO’s empirical equations (Fofonoff and Millard 1983) based on measured depth, temperature and conductivity data. Measured vertical profiles confirmed that the Rječina Estuary is a salt wedge type under all hydraulic conditions.

Numerical model

The numerical model is based on one-dimensional two-layer flow of homogeneous fluid separated by a sharp

interface. The approach of Schijf and Schonfeld (1953) was extended by allowing for variations in bed slope and cross sections. The equations of continuity and momentum in the upper and lower layer respectively, are:

$$\frac{\partial A_1}{\partial t} + \frac{\partial Q_1}{\partial x} = 0 \tag{1}$$

$$\frac{\partial A_2}{\partial t} + \frac{\partial Q_2}{\partial x} = 0 \tag{2}$$

$$\frac{\partial v_1}{\partial t} + v_1 \frac{\partial v_1}{\partial x} + g \frac{\partial}{\partial x} (h_1 + h_2) = gS_o - g' S_{f1} \tag{3}$$

$$\frac{\partial v_2}{\partial t} + v_2 \frac{\partial v_2}{\partial x} + g \frac{\partial}{\partial x} \left(\frac{\rho_1}{\rho_2} h_1 + h_2 \right) = gS_o - g' S_{f2} \tag{4}$$

Where t and x are time and space coordinates, A_i is layer cross section area, Q_i is layer discharge, v_i is layer velocity, h_i is layer depth, ρ_i is layer density, S_o is bed slope and S_{fi} is layer friction slope, with $i=1,2$ indicates upper and lower layer, respectively (Figs 4, 5).

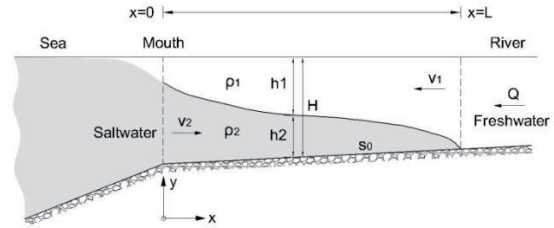


Figure 4 Longitudinal section of the estuary.

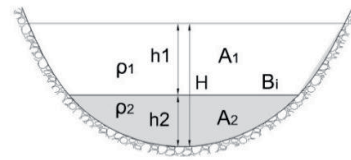


Figure 5 Cross section

We assume that the density difference between layers is sufficiently small that the Boussinesq approximation applies. The relative density difference between the layers is

$$\varepsilon = \frac{\rho_2 - \rho_1}{\rho_2} \approx \frac{\rho_2 - \rho_1}{\rho_1} \tag{5}$$

and $g' = g\varepsilon$ is reduced gravity.

When one is interested in modeling only the arrested salt wedge it is justifiable to assume steady state flow conditions, whereas the lower layer dynamics can be neglected. The friction slope S_{fi} consists of wall friction

slope and interfacial friction slope, which are defined by wall and interfacial shear stress. With these approximations and by replacing the Equations 3 and 4 set of equations [1-4] is reduced to a single equation:

$$\frac{\partial h_1}{\partial x} = \frac{Q_1^2}{g' A_1^2 h_1 - Q_1^2} \frac{h_1}{A_1} \left[f_i B_i \left(\frac{A_1}{A_2} (1 - \varepsilon) + 1 \right) + f_w O_w \right] \quad [6]$$

As the shear stress is defined by layer density, velocity and friction factor, f_w is wall friction factor, and f_i is interfacial friction factor. O_w is wetted perimeter for the upper layer.

The downstream boundary condition is set by defining the upper layer depth h_1 which is calculated iteratively for a given discharge:

$$h_1 = \frac{Q_1^2}{g' A_1^2} \quad [7]$$

A finite difference method was used to obtain numerical approximation of Equation 6. The Dorman-Prince method (1980) with adaptive spatial step was implemented in the MATLAB in order to solve the BVP defined by Equations 6 and 7.

Results

Regression analysis

Several regression equations were obtained based on measured salinity values along the estuary profile; one equation describing the functional relationship between river discharge and density interface at the mouth (Fig. 6)

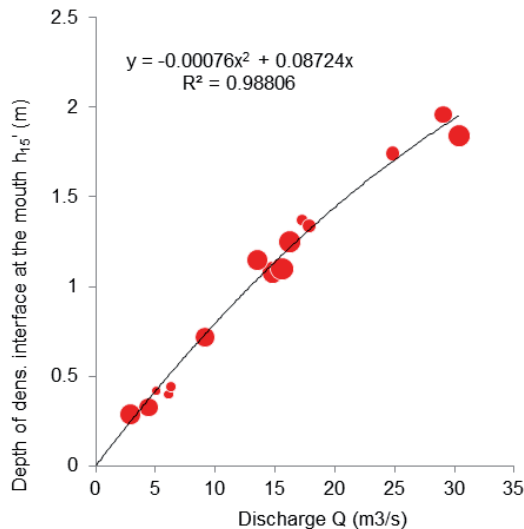


Figure 6 Regression function of measured river discharge and density interface at the mouth (size of the dots are proportional to the sea level).

and two equations describing the functional relationship between the river discharge and salt wedge length, separately for conditions during high tides and low tides (Fig. 7) (Krvavica et al. 2012).

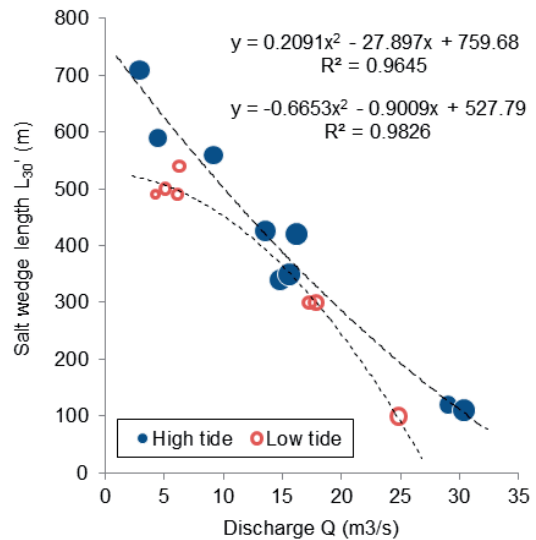


Figure 7 Regression function of measured river discharge and salt wedge length (size of the dots are proportional to the sea level).

The regression analysis shows that the depth of the density interface at the mouth (Fig. 6) is strongly related to the Rječina River discharge (correlation factor $R^2=0.988$). Furthermore, the salt wedge length is also strongly dependent on the Rječina River discharge (Fig. 7), but also to the Adriatic Sea level. Although the correlation is strong in both cases, some data scattering around the regression line can be observed, which can be explained by uneven bed channel and tidal influences (Krvavica et al. 2012).

Numerical model

Previously described model was applied to actual events for which all the relevant data was measured, i.e. upstream river discharge, sea level, density of seawater and freshwater and depth of density interface at the river mouth.

The wall friction factor was calculated for each step by Colebrook-White equation for open channel flow (Chanson 2004), while the interfacial friction factor is averaged along the wedge and calibrated to best-fit the measured data, i.e. determined through a number of repeated, varied attempts.

Several results of calculated salt wedge shape (density interface line between two layers of lower saltwater and upper freshwater) with several points of measured density interface at different distance from the mouth are presented in Figure 8a,b,c,d.

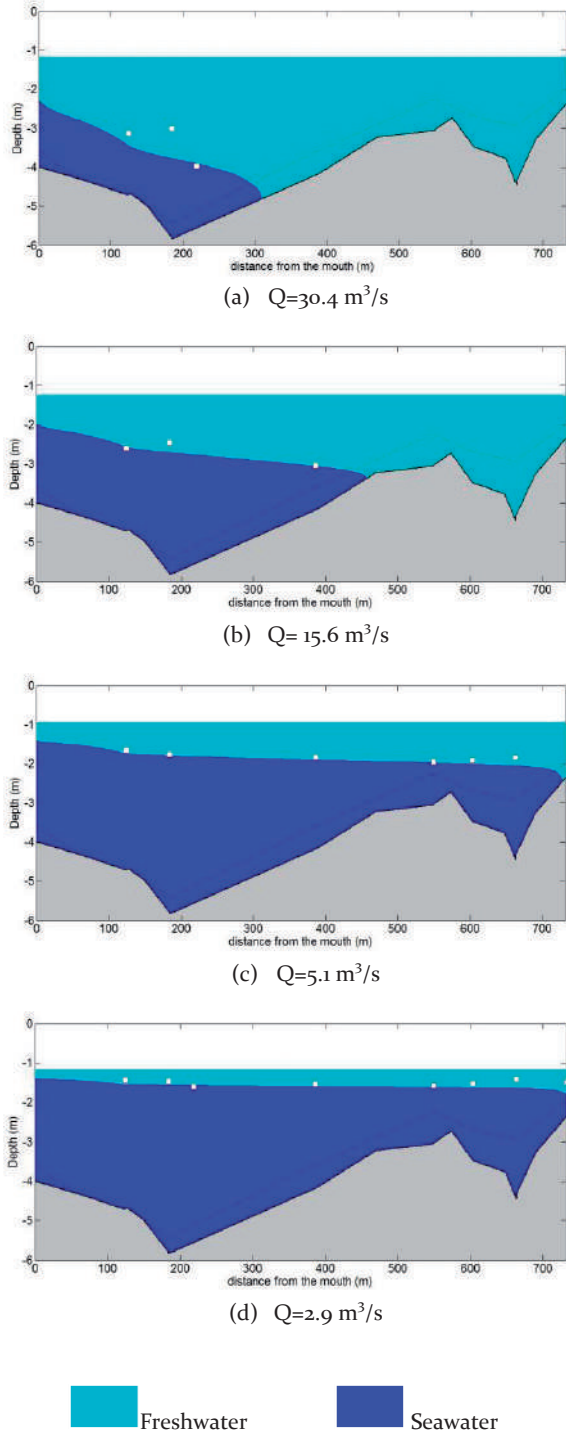


Figure 8 Longitudinal section of the Rječina Estuary – calculated shape of salt wedge with measured points of density interface for several different hydraulic conditions, i.e. river discharges.

Discussion

Findings present in this paper suggest that salt wedge geometric characteristics along the Rječina Estuary are influenced by both the rate of river discharge and the level of Adriatic Sea. As the freshwater discharge changes seasonally and daily the position of the tip of the salt wedge moves up and down the estuary. Although, the estuary is located in micro-tidal sea environment, it was also found that the salt wedge tip moves upstream during the flood tide, and downstream during the ebb tide.

A numerical model was developed by extending the Schijf and Schonfeld two-layer model (1953) to include uneven bottom and cross-sections. Only the arrested salt wedge case is considered herein, which is based on the assumption of a two-layer homogenous steady flow, without any mixing across the interface, negligible lower layer dynamics and bottom shear stress.

There are many studies that have proven the validity of this type of mathematical description applied to laboratory size models (Dermissis and Partheniades 1984, 1985, Arita and Jirka 1987a and 1987b). However, in field conditions, with much higher Reynolds numbers and stronger interfacial shear stress, the stability of density interface is compromised and local vertical mixing and entrainment seems to take place. (Arita and Jirka 1987a)

Furthermore, the interfacial shear stress is expressed by interfacial friction factor. Although, there are many studies that have tried to develop universal interfacial friction diagram (Tamai 1976, Dermissis and Partheniades 1984, 1985, Arita and Jirka 1987a,b, Grubert 1989), the discrepancies between laboratory and field data are too extensive (Arita and Jirka 1987b). None of the existing interfacial friction factor diagrams or expressions could be successfully applied for the case of the Rječina Estuary, so the factor was calibrated to fit the measured data.

Conclusion

Salinity distribution in the Rječina River Estuary was thoroughly analyzed based on a number of measurements taken from February to August 2012. Vertical salinity and density stratification survived all major external hydraulic influences, i.e. tidal phases and river discharges, which suggest the salt wedge type of estuary.

By using regression analysis it was found that both density interface at the mouth and salt wedge length are strongly dependent on the Rječina River discharge rate. Tidal phases have certain influence in case of salt wedge length as well.

To study the interaction of salt water and fresh water in more detail a 1D numerical model of two-layer steady flow was developed. By calibrating the interfacial

friction factor, calculated density interface along the estuary fitted excellent with the measured data.

Future work will be focused on developing numerical model of 1D unsteady two-layer flow, aimed to study the dynamics of salt wedge – i.e. formation and flushing out of the salt wedge, as well as the flood wave propagation through the estuary.

Acknowledgments

Research presented in this paper is a part of the scientific project “Hydrology of Sensitive Water Resources in Karst” (114-0982709-2549), funded by the Ministry of Science, Education and Sports of the Republic of Croatia. A part of the research was also conducted with the help from the international bilateral Croatian-Japanese project “Risk Identification and Land-use Planning for Disaster Mitigation of Landslides and Floods in Croatia”.

References

- Arita M, Jirka G H (1987a) Two-Layer Model of Saline Wedge. I: Entrainment and Interfacial Friction. *Journal of Hydraulic Engineering*. 113(10): 1229-1248.
- Arita M, Jirka G H (1987b) Two-Layer Model of Saline Wedge. II: Prediction of Mean Properties. *Journal of Hydraulic Engineering*. 113(10): 1249-1263.
- Chanson H (2004) *Hydraulics of Open Channel Flow: An Introduction*. Elsevier Butterworth Heinemann, Oxford. (ISBN 0 7506 5978 5). 650p.
- Dermissis V, Partheniades E (1984) Interfacial Resistance in Stratified Flow. *Journal of Waterway, Port, Coastal and Ocean Engineering*. 110(2): 231-250.
- Dermissis V, Partheniades E (1985) Dominant Shear Stresses in Arrested Saline Wedges. *Journal of Waterway, Port, Coastal and Ocean Engineering*. 111(4): 733-752.
- Dormand J R, Prince P J (1980) A Family of Embedded Runge-Kutta Formulae. *Journal of Computational and Applied Mathematics*. 6(1): 19-26.
- Fofonoff N P, Millard Jr. R C (1983). Algorithms for Computation of Fundamental Properties of Seawater. UNESCO Technical Papers in Marine Science, Paris. 53p
- Grubert J P (1989) Interfacial Stability in Stratified Channel Flows. *Journal of Hydraulic Engineering*. 115(9): 1185-1203.
- Schijf J B, Schonfeld J C (1953) Theoretical Considerations on the Motion of Salt and Fresh Water. *Proceedings: Minnesota International Hydraulics Convention, Minnesota. USA.* pp 321 – 333
- Krvavica N, Mofardin B, Ružić I, Ožanić N (2012) Measurement and Analysis of Salinization at the Rječina Estuary. *Građevinar*. 64(11): 923-933.
- Tamai N (1976) Friction at the Interface of Two-layered Flows. *Coastal Engineering*. 15. 3169-3188
- Van der Tuin H (1991) *Guidelines on the Study of Seawater Intrusion into Rivers*. UNESCO, Paris. (ISBN 92-3-102765-4). 137p.

Author Index

Abolmasov, Biljana	187
Arbanas, Željko	11, 27, 39, 45, 57, 73, 85, 91, 153, 171
Bajat, Branislav	241
Basarić, Irena	231
Baučić, Martina	33
Belić, Nikola	63
Benac, Čedomir	117, 213
Bernat, Sanja	17, 79, 91, 153
Bićanić, Nenad	111
Bilandžija, Darija	131
Budimir, Vjekoslav	177
Buljan, Renato	213
Corlateanu, Simona	219
Čarman, Magda	225
Dang, Khang Quang	193
Dragičević, Nevena	121
Duc, Do Minh	193
Dugonjić Jovančević, Sanja	39, 45, 73, 85
Đomlija, Petra	79, 213
Fabijanović, Slađan	91
Fujiki, Shigeo	111
Fukuoka, Hiroshi	51
Furuya, Gen	67
Gajski, Dubravko	63
George-Cătălin, Silvas	147
Gjorgjevski, Spasen	165
Gradiški, Karolina	11
Grošić, Mirko	153, 171
He, Bin	1, 5, 11
Honda, Mitsuki	159
Iaobescu, Raul	219
Jagodnik, Vedran	39, 45
Jelisavac, Branko	199
Jemec Auflič, Mateja	225, 237
Josifovski, Josif	165
Jotić, Milovan	199
Jovanovski, Milorad	207
Jurišić, Aleksandra	131
Kalajžić, Jakov	23
Karleuša, Barbara	121
Kilibarda, Milan	241
Kimura, Naoko	127
Kisić, Ivica	127, 131
Komac, Marko	225, 237
Krivic, Matija	225, 237
Krkač, Martin	11, 17, 23, 27, 33
Krvavica, Nino	257
Kryžanowsk, Andrej	251
Kurokawa, Shota	111
Kuwada, Yohei	159
Kvasnička, Predrag	11
Leka, Koviljka	203
Ljutić, Kristijan	1, 39, 45

Marjanović, Miloš	231
Markoski, Blagoja	207
Martinčević, Jasmina	17, 57
Martinčić, Manica	251
Marui, Hideaki	67
Marunteanu, Cristian	183
Matjašić, Igor	153
Mesić, Milan	131
Mihailescu, Daniel	219
Mihalić Arbanas, Snježana	11, 17, 27, 33, 57, 63, 67, 79, 91, 153, 171
Miklin, Željko	17, 57
Mikoš, Matjaž	251
Milenković, Svetozar	199
Milutinovici, Emilia Elena	219
Miščević, Predrag	51
Mitani, Yasuhiro	135
Nagai, Osamu	5, 27, 73
Navratil, Dražen	213
Oštrić, Maja	1, 11
Ožanić, Nevenka	97, 107, 111, 117, 121, 257
Pejić, Marko	187
Pejović, Milutin	241
Peranić, Josip	39
Peshevski, Igor	207
Peternel, Tina	237
Petrusheva, Silvana	207
Podolszki, Laszlo	17, 57
Ravlić, Nenad	257
Roca, Mihaela	183
Rubinić, Josip	23
Ružić, Igor	97, 117
Samardžić Petrović, Mileva	241
Sandić, Cvjetko	203
Sassa, Kyoji	1, 5, 11, 73, 193
Sodnik, Jošt	251
Sonoyama, Tomokazu	135, 159
Strom, Alexander	245
Suljić, Nedim	141
Susinov, Bojan	165, 207
Sušanj, Ivana	97, 107
Šestak, Ivana	131
Šinigoj, Jasna	225, 237
Šiško, Darko	63
Špehar, Kristijan	27
Šušić, Vladimir	187
Udovič, Dalibor	171
Vidović, Damir	153
Vivoda, Martina	1, 39, 45, 85, 213
Vlastelica, Goran	51
Vujančić, Vladeta	199
Takara, Kaoru	1, 5
Tien, Van Dinh	193

Travaš, Vanja	257
Wang, Chunxiang	67
Wang, Fawu	135, 159
Watanabe, Naoki	67
Wendeler, Corinna	177
Yamashiki, Yosuke	97, 107, 111, 127
Yang, Hufeng	135
Zečević, Snežana	231
Zekan, Sabid	141
Zgorelec, Željka	131
Žic, Elvis	97, 111



geotech 

Geotechnical field investigations
Rock slope and rockfall protection
Monitoring and landslide mitigation
Reinforced walls
Foundations

Geotech d.o.o. | Moe Albaharija 10a | Hr-51000 Rijeka | + 385 (0) 51 343 020, 343 062
+ 385 (0) 51 343 018 | info@geotech.hr | www.geotech.hr



Geotechnical engineering is our main field of expertise and our core business. Monterra d.o.o. was founded in 2011. and was recognised as reliable and flexible business partner. Our policy is to ensure quick and high quality of construction works in geotechnical engineering: from geotechnical investigation works and their implementation to the complete project designs, we perform construction works of the highest quality and within the timeframe requirements.

We offer our knowledge and expertise incorporated with the solutions and the supervision of geotechnical needs and beyond those, the best material with the best price/quality ratio on the market, but also ensure the best service and fast, yet top quality install.

All the members of our team are highly qualified and trained. All of our field personell is trained and certified for slope protection works from the safety point of view plus they have all the machinery education needed to perform the geotechnical works.

We offer first class service of experienced professionals and specialists from our operations team to provide a superior service to our clients.

Our CEO, Dalibor Udovič B.S.C.Civ.Eng. was the Chief Engineer and Executive Project Manager on the most important slope protection projects on all of the sections of the Zagreb - Split motorway. His vast field experience in the geotechnical area of civil engineering includes all the types and slope protection systems plus his knowledge and experience in the geotechnical design makes him one of the best experts in Croatia today.

We are the representatives of various production lines and the world leader companies and can offer the best selection of their top-quality products - from the slope stabilisation systems, slide protection systems, traffic equipment and retaining constructions as well as for fotoluminescent materials and signs that have an important role in securing our work and free time environment.

We will design, provide the material and construct various geotechnical projects, especially slope protection solutions. List of our references is quite long and impressive.

www.monterra.hr

Shallow landslide: Geobrigg barriers withstand the highest dynamic and static loads

On unstable slopes, flexible shallow landslide barriers provide protection against landslips:

- lightweight construction cuts costs
- easy installation
- can also withstand multiple impacts
- effectiveness proven in large-scale field tests
- dimensionable using FARO simulation software



Scan and watch our movie on www.geobrigg.com/youtube/debris_flow



Geobrigg AG
Geohazard Solutions
CH-8590 Romanshorn • Switzerland
Phone: +41 71 466 81 55 • Fax: +41 71 466 81 50
www.geobrigg.com



TECCO® SYSTEM³ – Your slope made stable

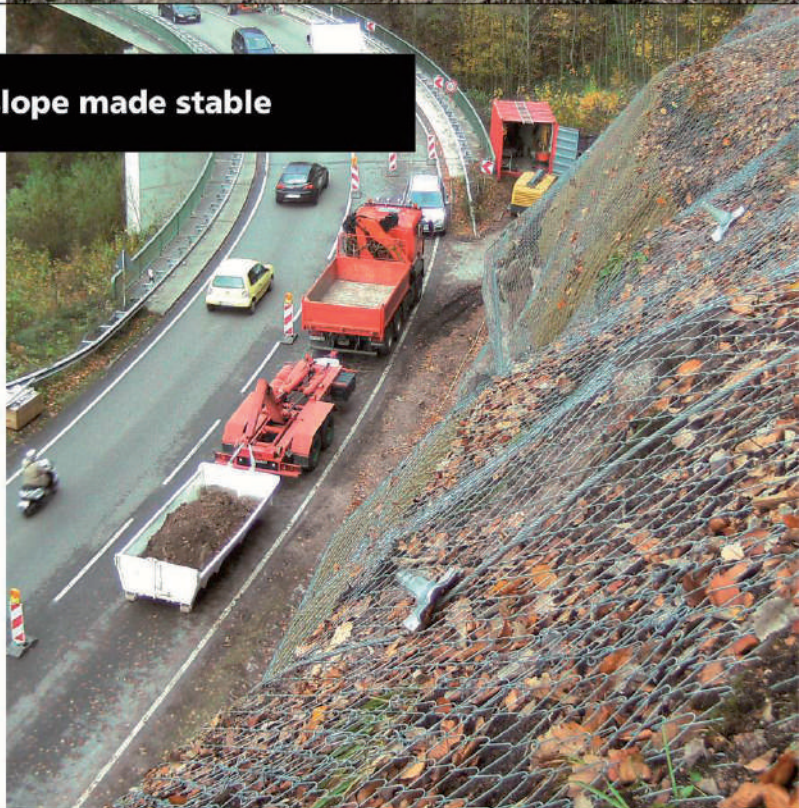
- TECCO® SYSTEM³ can be optimized depending on the subsoil with several mesh types
- meshes made of 2 mm, 3 mm and 4 mm diameter high-tensile steel wire
- optimization of anchor spacing thanks to two new spike plate sizes
- RUVOLUM® dimensioning software based on large-scale field and model tests
- small CO₂ footprint and option to cover with natural vegetation



Scan and watch our movie on www.geobrigg.com/youtube/TECCO-fullscale



Geobrigg AG
Geohazard Solutions
CH-8590 Romanshorn • Switzerland
Phone: +41 71 466 81 55 • Fax: +41 71 466 81 50
www.geobrigg.com



Snježana Mihalić Arbanas · Željko Arbanas

Landslide and Flood Hazard Assessment

This book contains peer-reviewed papers from the 1st Regional Symposium on Landslides in the Adriatic-Balkan Region with 3rd Workshop of the Croatian-Japanese SATREPS FY2008 Project 'Risk Identification and Land-Use Planning for Disaster Mitigation of Landslides and Floods in Croatia' organized by members of the International Consortium of Landslides (ICL) and members of the Croatian-Japanese SATREPS FY2008 project, that took place in Zagreb (Croatia) in March 2013.

Assoc. Prof. Snježana Mihalić Arbanas is professor of engineering geology at the Faculty of Mining, Geology and Petroleum Engineering of the University of Zagreb and Coordinator of the regional ICL Adriatic-Balkan Network.

Assoc. Prof. Željko Arbanas is professor of geotechnical engineering at the Faculty of Civil Engineering of the University of Rijeka, Co-coordinator of the regional ICL Adriatic-Balkan Network and Assistant Editor in Chief of the Landslides journal.

ISBN 978-953-6923-27-4



9 789536 923274

Faculty of
Mining, Geology
and Petroleum
Engineering,
University of Zagreb

A CIP catalogue record
for this book is available
in the Online Catalogue of
the National and University
Library in Zagreb as 895370.